Selected Topics in Superconductivity

Nonequilibrium Electrons and Phonons in Superconductors

Armen M. Gulian
and
Gely F. Zharkov

Nonequilibrium Electrons and Phonons in Superconductors

SELECTED TOPICS IN SUPERCONDUCTIVITY

Series Editor: Stuart Wolf
Naval Research Laboratory
Washington, D. C.

CASE STUDIES IN SUPERCONDUCTING MAGNETS: DESIGN AND OPERATIONAL ISSUES
Yukikasu Iwasa

ELECTROMAGNETIC ABSORPTION IN THE COOPER OXIDE SUPERCONDUCTORS
Frank J. Owens and Charles P. Poole, Jr.

INTRODUCTION TO HIGH-TEMPERATURE SUPERCONDUCTIVITY
Thomas Sheahen

THE NEW SUPERCONDUCTORS
Frank J. Owens and Charles S. Poole

NONEQUILIBRIUM ELECTRONS AND PHONONS IN SUPERCONDUCTORS
Armen M. Gulian and Gely F. Zharkov

QUANTUM STATISTICAL THEORY OF SUPERCONDUCTIVITY
Shigeji Fujita and Salvador Godoy

STABILITY OF SUPERCONDUCTORS
Lawrence Dresner

Nonequilibrium Electrons and Phonons in Superconductors

Selected Topics in Superconductivity

Armen M. Gulian
USRA / Naval Research Laboratory, Washington, D. C. 20375, USA
and
Gely F. Zharkov
P. N. Lebedev Physics Institute, Moscow 117333, Russia

KLUWER ACADEMIC PUBLISHERS
NEW YORK, BOSTON, DORDRECHT, LONDON, MOSCOW

eBook ISBN: 0-306-47087-X
Print ISBN: 0-306-46075-0

Created in the United States of America

Visit Kluwer Online at: http://www.kluweronline.com
and Kluwer's eBookstore at: http://www.ebooks.kluweronline.com

Foreword

Superconductivity occupies a special, unique place in the 20th century physics. Just think of it: its microscopic mechanism was understood only in 1957—46 years after the discovery of superconductivity in 1911. In contrast, the theory of normal metals behavior (or, to be more precise, the theory of metals in normal state) was formed as early as the twenties, immediately following the creation of quantum mechanics. Moreover, when I took up the theory of superconductivity in 1943, not only microscopic theory was non-existent, but even macroscopic superconductivity theory was quite incomplete. The problem is that the Londons equations, introduced in 1935, allow only a quantitative description of superconductors in magnetic fields weak in comparison with the critical field. Also, even in weak fields, the Londons theory is strictly applicable only to Type-II superconductors—although the division of superconductors into Type-I and Type-II materials was not suggested until much later, in early 1950's. As far as nonequilibrium phenomena are concerned, then until 1943 the most remarkable, yet proved to be fault afterwards, implication was that of a complete absence of all thermoelectric effects in superconducting state.

Look how radically the picture has changed in only 55 years! Perhaps for younger generation this would seem a whole lot of time. Is it? Indeed, it is just an average human life-span. And if the same pace is maintained then what will we have 55 years later, in 2053? I am not capable of an extrapolation of this magnitude, without risking being caught in the act of daydreaming. I could only assume that the development would take two major directions.

The first direction—exploration of high temperature superconductors. Clearly, their application in technology, the possibilities of which were vastly overestimated when they were initially discovered 10 years ago, will sharply increase in this period. There can hardly be any doubt that a microtheory of superconducting cuprates, still lacking, will be fully understood by then. The most interesting yet, are trials aimed at raising critical temperature to create room-temperature superconductors. There is no recipe for success here. However, the existing theoretical grounds, do not contradict this possibility in any way. The situation here reminds

the one with the high-temperature superconductivity between 1964, when this problem had received exposure, and 1986–1987, when it got its well-known solution. I remember very well the grinning faces of those skeptics who would ask me sarcastically, "Whatever happened to your heat-resistant superconductivity?" It is quite possible that as far as the room-temperature superconductivity goes, the skeptics would this time prove to be right. Still, it is imperative to keep searching for that kind of superconductivity, and I for one, believe in it.

The second avenue of development that I mentioned above, is nonequilibrium superconductivity. Even for "usual" or, more specifically, isotropic and weakly anisotropic superconductors, much less has been done in this area than for superconductors in equilibrium. It is especially vivid in the case of thermoelectric effects. Despite the faultiness of the statement of complete absence of all thermoelectric effects in superconducting state was clarified as early as in 1944, it was ignored for many years, and even today the picture is still not very clear. The reader will learn about it in Chapters 13–14 of this book. We have many questions here, both in theory and experiment. I am inclined to think that they will find the answers in near future. This is only right in case of "ordinary" superconductors. As far as strongly anisotropic high temperature superconductors and "*unconventional*" ones in general are concerned, the satisfying theory of nonequilibrium phenomena for them has not been developed. The authors of this book point out that only isotropic superconductors are discussed. It is obviously a forced limitation. Besides, even in case of nonequilibrium processes in isotropic superconductors there is plenty of material, which is presented in the book. Other contemporary monographs, to the best of my knowledge, do not exist.

In the light of the aforementioned there is little doubt that the monograph by A. M. Gulian and G. F. Zharkov is actual and desired. I have to admit that I would like to have seen the book more physics-minded, less formal, more transparent and more accessible to a wider physicist audience. Though, and it is a common knowledge, "*better is the enemy of good.*" The authors have done an enormous amount of work to the benefit of the physical community at large, and I believe the book will provide a stimulus for further experimental and theoretical investigations.

V. L. Ginzburg
Moscow, 1998

Preface

"*I wanted most to give you some appreciation of the wonderful world and the physicist's way of looking at it, which, I believe, is a major part of the true culture of modern times.*"

Feynman's Epilogue
(Courtesy of Addison-Wesley)

The appearance of any new book raises several questions. What contents are included under the title? What benefit can I get out of here? What motivated the authors to write this book?

It is about nonequilibrium superconductivity. Typically, articles are written for the professionals in a field, while books serve a wider audience. In part they seek to share the excitement of the work, to attract more individuals to the field, and thereby create more professionals.

So how do we explain the essence of "nonequilibrium superconductivity" to the potential readers of this book? The following discussion has always been helpful even for the people far from superconductivity. Human beings themselves are a system containing large number of atoms in a nonequilibrium state. The equilibrium state of such a system is a plain mixture of atoms. It is the nonequilibrium state that reveals all the wonders of life! The same large qualitative difference exists between superconductivity in thermodynamic equilibrium and in its nonequilibrium state.

What ideas unify the content of this book? Superconductors are inherently quantum mechanical object despite their macroscopic physical scale. The microscopic theory of superconductivity generated by Bardeen, Cooper, and Schrieffer provided a firm basis for the ψ-theory of superconductivity, earlier postulated by Ginzburg and Landau. Further generalization of the ψ-theory provide a method of dealing the time-dependent problem, the TDGL-equations. Chapter 2 reviews the development of the arguments that TDGL-equations strictly apply only in the case of gapless superconductors—an old statement, which is wrong nowadays: after passing through Chapters 3-6 the readers will recognize in Chapter 7 that there is

a modified TDGL scheme which is unequivocally valid for the much more general case of finite-gap materials! This derivation combines the very general equations applicable to equilibrium (Chapter 1) and nonequilibrium (Chapter 3) superconductivity. Both the Keldysh and Eliashberg-Gor'kov analytical continuations technique are exploited to prove the same results are achieved.

It is really amazing how nicely these two mathematically very different tools yield precisely the same results! Given this equivalence of the results, the reader might wonder which is preferable from a practical point of view. We conclude that for the phenomena which have already been treated in equilibrium in the Matsubara technique it is faster to apply the analytical continuation method. In general, Keldysh's method is more straightforward.

Since nonequilibrium superconductivity exploits some concepts which do not occur in equilibrium case, such as the longitudinal electric field penetration depth and branch imbalance potential, we devoted a special discussion (Chapter 8) to collective oscillations. These are formally out of the range of applicability of TDGL. The kinetic equations, which follow from the general nonequilibrium equations (Chapter 4), provided the mathematical basis to discuss various nonequilibrium effects in superconductors. We tried everywhere to treat nonequilibrium electrons and phonons on an equal footing. Thus in parallel to enhancement of the order parameter (Chapter 5), we considered the accompanying phonon deficit effect (Chapter 6). In this two chapters the collision integrals, which traditionally serve to describe the relaxation processes, were used also to describe the sources of nonequilibrium deviation of both electrons and phonons.

The behavior of nonequilibrium Josephson junctions and the more novel but closely related phase-slip centers are treated in detail in Chapters 10 and 9 respectively. Attention is paid to both the phonon and electron components.

Irradiation by lasers is a traditional method for creating a nonequilibrium superconducting state (see Chapter 11). In Chapter 12 we considered the inverse problem: the ability of a superconductor in a nonequilibrium state to act as a coherent phonon or photon generator. This laser-like source behaviors have not yet been experimentally confirmed. However, we hoped our discussion will encourage their demonstration.

The final chapters of the book, 13 and 14, discuss thermoelectricity. This topic is one of the most complex, subtle featured and thus intellectually captivating in solid state physics. The addition of superconductivity to the discussion creates even more opportunity to be excited by thermoelectricity.

The book's initial chapter includes an introduction to the theory of superconductivity for those readers not already acquainted with it. The treatment is very concise but covers the most important physical concepts which will later be assumed to be familiar to the reader. The mathematical constructs of quantum field theory are assumed to need no explanation.

We should apologize for all the possible drawbacks the book may have and encourage any reader's response. We have restricted ourselves to discussions of the phenomena mainly in conventional, low temperature superconductors. This is less a disadvantage than one might assume since our book is focused exclusively on the theory. Experimental facts referred to only for some illustrative purposes. Hopefully, in the third millennium the mechanism of equilibrium phenomenon in high-temperature superconductors will be completely understood, and many new nonequilibrium phenomena and their theoretical explanations will enlarge superconductivity. To assist this process we have written this book. Actually, while an apology may be due for the purely theoretical focus, we note the ancients' belief that "nothing is more practical than a good theory."

In general, studying nonequilibrium phenomena, we feel ourselves to be climbing onto the "shoulders of giants." We now invite the readers to come enjoy with us what we have seen of nonequilibrium superconductivity from this elevated perch. If the readers can see more than we did, we will consider our tasks fulfilled.

Finally, we would like to use this opportunity to acknowledge numerous fruitful discussions with our teachers, students, colleagues, and friends—these discussions assisted greatly to the appearance of this book in its present form.

Armen M. Gulian
Gely F. Zharkov

Washington, D. C., USA - Moscow, Russia
1998

Contents

Chapter 5. Microwave-Enhanced Order Parameter

Chapter 6. Phonon-Deficit Effect

Chapter 7. Time-Dependent Ginzburg–Landau Equations

Chapter 8. A Longitudinal Electric Field and Collective Modes

1

Basic Equilibrium Properties

1.1. INTRODUCTORY CONCEPTS

The first main property of superconductors—the flow of electric current without resistance—was discovered by Kamerlingh-Onnes[1] in 1911. For more than 20 years this phenomenon was interpreted as superfluidity, or lossless motion of the electron liquid in metals. The second main property—the total expulsion of the magnetic field out of the bulk superconductor's interior—was discovered by Meissner and Ochsenfeld in 1933. Their half-page report[2] immediately led to very deep insights into the nature of the phenomenon, which eventually allowed the equilibrium properties of superconductors to be fairly well understood. We start with a brief discussion of these main superconducting properties. In this section, we sacrifice the historical chronology of superconductivity in favor of introducing some major concepts which will be used in later parts of the book without special explanation.

1.1.1. Infinite Conductivity

In an attempt to understand *ideal* (*infinite*) *conductivity,* one can first refer to Ohm's law $\mathbf{j} = \sigma\mathbf{E}$, and try to handle the infinitely large values of σ. To reach this goal, it is necessary to go back to Ohm's law and eliminate the dissipative term at the initial stage of its derivation. Then one would get Newton's law describing the lossless motion of the charge carrier: $m\mathbf{V} = e\mathbf{E}$. Combining it with the relation $\mathbf{E} = -(1/c)(\partial\mathbf{A}/\partial t)$, and performing the integration, we find:

$$m\mathbf{V}(\equiv\mathbf{p}) = -\frac{e}{c}\mathbf{A} \tag{1.1}$$

(here the constant of integration is chosen to be zero owing to the appropriate initial condition). To avoid for the moment the difficulties related to the arbitrariness of the gauge for $\mathbf{A}$ in Eq. (1.1), one should make a rotation, bearing in mind the relations curl $\mathbf{A} = -\mathbf{H}$, $\mathbf{j} = en\mathbf{V}$, where n is the carrier density. From this follows the gauge-invariant relation ($\Lambda = m/e^2n$):

$$c \operatorname{curl} \Lambda \mathbf{j} = -\mathbf{H}, \tag{1.2}$$

first introduced by F. and H. London,[3] which should replace Ohm's law for superconductors.

1.1.2. Ideal Diamagnetism

Let us now move to the second main property of the superconducting state, namely, to ideal diamagnetism, which is frequently called the *Meissner effect.* At first glance there is nothing especially surprising in this phenomenon: we know that the applied magnetic field causes the screening currents, which shunt the interior of the conductor and can persist indefinitely if the conductivity is ideal. However, the experiment with magnetic field repulsion may be performed in a different way: the magnetic field is applied initially at sufficiently high temperatures (in the normal state) and after the screening currents have died out, the temperature is lowered below the superconducting transition point $T = T_c$. Such experiments have shown that in superconductors the screening currents arise again after cooling down through T_c and this distinguishes superconductors from ideal conductors. Thus these currents cannot be explained on the basis of classical concepts because the static magnetic field of classical electrodynamics cannot perform work, and consequently cannot produce the circulating screening currents. Formally the Meissner effect can be explained by the relation (1.2). The derivation is given in Section 1.2, but the justification of Eq. (1.2) itself is a problem: actually, both ideal conductivity and the Meissner effect are related to the proportionality of the current $\mathbf{j}$ to the vector potential $\mathbf{A}$, as expressed by (1.1), since $\mathbf{j} \propto \mathbf{V}$. This somehow contradicts the classical electrodynamics* in which the current is proportional to the electric field $\mathbf{E}$, and provides grounds to look for answers in quantum theory.

1.1.3. Energy Gap

In 1935 F. London published insightful arguments elucidating how the Meissner effect is coupled with the possible existence of the gap in the energy spectrum of the charge carriers.[7] Namely, within the quantum mechanical description the current

$$\mathbf{j} = \frac{\hbar e}{2im} (\psi \nabla \psi^* - \psi^* \nabla \psi) - \frac{e^2}{mc} \mathbf{A} |\psi|^2 \tag{1.3}$$

*Classical electrodynamics is based on Faraday's concept of local influence of electromagnetic fields on charges. Meanwhile, for a long enough solenoid (one can even release an "infinitely long" option in toroidal geometry—we will discuss an example related to the "gigantic" thermoelectric response in Chaps. 13 and 14) the magnetic field $\mathbf{H}$ outside of the solenoid is absent, although in a wire looping the solenoid, a current will start to flow when the loop is cooled down to the superconducting state! As pointed out by Aharonov and Bohm[4] (see also Refs. 5 and 6), the quantum objects can "sense" the field potentials $\mathbf{A}$ and φ when the values of $\mathbf{E}$ and $\mathbf{H}$ are zero.

(here $\hbar$ is Planck's constant h divided by 2π) consists of two components: the term containing $\nabla\psi$ (the "paramagnetic" term) and the term explicitly proportional to A (the "diamagnetic" term). If $\mathbf{A} \neq 0$, the ψ-function in normal metals acquires dependence on $\mathbf{A}$ as well, so these two components are of the same order and usually cancel each other to a large extent, so that a weak dia- or paramagnetism occurs, depending on the details of the electronic structure. If one assumes that is a gap in the energy spectrum associated with the transition to the superconducting state, then the electronic spectrum of the system will not be changed; the wave function ψ of the state will behave as rigid: $\psi = \psi_0 = \psi(\mathbf{A} = 0)$, so that the paramagnetic term should continue to be zero (as in the case of $\mathbf{A} = 0$), while the diamagnetic term should provide the main response. The presence of a gap in the energy spectrum will make the creation of single-particle excitations impossible, providing the nondissipative motion alike of described by Eq. (1.1).

In normal metals the spectrum of elementary excitations of electrons with momenta in the vicinity of p_F has the form

$$\xi_{\mathbf{p}} = v_F(p - p_F), \tag{1.4}$$

which follows straightforwardly in the parabolic band approximation $\xi_{\mathbf{p}} = p^2/2m - \varepsilon_F$, where ε_F is the Fermi energy: $\varepsilon_F = p_F^2/2m = mv_F^2/2$ [the same type of relation as Eq. (1.4) can be justified in more general cases]. Evidently, for normal Fermi liquids there is no gap in the energy spectrum. However, let us suppose that in the superconducting state the excitation spectrum possesses a gaplike singularity:

$$\varepsilon_{\mathbf{p}} = \sqrt{\xi_{\mathbf{p}}^2 + |\Delta|^2}. \tag{1.5}$$

In the presence of the gap $|\Delta|$, the birth of single excitations with small energies is impeded. In Sect. 1.3 we will see that the microscopic theory indeed leads to the spectrum of the type in (1.5). Here we discuss some of the consequences that follow from Eq. (1.5).

1.1.4. Analogy with Relativistic Quantum Theory

The spectrum (1.5) has an analog in relativistic quantum theory,[8] where the electron energy is $E_p = (\mathbf{p}^2 + m_0^2)^{1/2}$ (m_0 is the electron rest mass, $c = 1$). One can try to reconstruct the wave function of the particle having the spectrum (1.5) by writing down the stationary Schrödinger equation (using the equivalent Hamiltonian method; this is sometimes called the *equivalent mass approach*[9]):

$$\hat{\varepsilon}(-i\hbar\nabla)\,\psi = \varepsilon\psi. \tag{1.6}$$

According to the prescriptions of quantum theory (see, e.g., Ref. 10), one can extract the square root from the operator by linearizing it (here and below $\hbar = 1$):

$$\hat{\varepsilon}(-i\nabla) = \hat{\alpha}\left(-\frac{1}{2m}\nabla^2 - \varepsilon_F\right) + \hat{\beta}|\Delta| \tag{1.7}$$

where $\hat{\alpha}$ and $\hat{\beta}$ are some mathematical objects to be identified by squaring the operator (1.7). In the absence of external fields we should obtain the spectrum (1.5). This leads to the relation

$$\hat{\alpha}^2 = 1, \quad \hat{\beta}^2 = 1, \tag{1.8}$$

$$\hat{\alpha}\hat{\beta} + \hat{\beta}\hat{\alpha} = 0. \tag{1.9}$$

In the simplest case $\hat{\alpha}$ and $\hat{\beta}$ are not numbers, but they may be expressed as superpositions of the Pauli matrices [the unity matrix $\hat{1}$ does not participate in these linear combinations, as is seen from Eq. (1.9)]:

$$\hat{\alpha} = \sum{}' a_i \hat{\sigma}_i; \quad \hat{\beta} = \sum{}' b_k \hat{\sigma}_k, \tag{1.10}$$

where the prime denotes $i \neq k$ according to Eq. (1.9), and Eq. (1.8) gives

$$\sum a_i^2 = \sum b_k^2 = 1. \tag{1.11}$$

Thus the wave function in (1.6) is a one-column matrix:

$$\hat{\psi} = \begin{pmatrix} u \\ v \end{pmatrix}, \tag{1.12}$$

One can demand now that in the case of normal metal ($\Delta = 0$) the components u and v should become disconnected. This means that in the composition (1.10) for $\hat{\alpha}$ only the coefficient at the matrix

$$\hat{\sigma}_z = \begin{pmatrix} 1 & 0 \\ 0 & -1 \end{pmatrix} \tag{1.13}$$

will not vanish. In view of relations (1.10) and (1.11), this leads to

$$\hat{\beta} = \begin{pmatrix} 0 & e^{i\theta} \\ e^{-i\theta} & 0 \end{pmatrix}, \tag{1.14}$$

where θ is the (real) phase factor. Introducing the notation

$$\Delta = |\Delta| e^{i\theta} \tag{1.15}$$

we represent Eq. (1.6) in the form

$$\varepsilon u = -\left(\frac{\nabla^2}{2m} + \varepsilon_F\right) u + \Delta v, \tag{1.16}$$

$$\varepsilon \mathcal{V} = \left(\frac{\nabla^2}{2m} + \varepsilon_F \right) \mathcal{V} + \Delta^* \mathcal{U}. \tag{1.17}$$

In the presence of a magnetic field* these equations become

$$\varepsilon \mathcal{U}(\mathbf{r}) = \left[\frac{1}{2m} \left(-i \frac{\partial}{\partial \mathbf{r}} - \frac{e}{c} \mathbf{A} \right)^2 - \varepsilon_F \right] \mathcal{U}(\mathbf{r}) + \Delta \mathcal{V}(\mathbf{r}), \tag{1.18}$$

$$\varepsilon \mathcal{V}(\mathbf{r}) = - \left[\frac{1}{2m} \left(-i \frac{\partial}{\partial \mathbf{r}} + \frac{e}{c} \mathbf{A} \right)^2 - \varepsilon_F \right] \mathcal{V}(\mathbf{r}) + \Delta^* \mathcal{U}(\mathbf{r}), \tag{1.19}$$

which coincides with the Bogolyubov–De Gennes equations.[12]

1. 1 .5. Andreev Reflection

For stationary states we consider the wave function in the Schrödinger representation, which includes the factor $\exp(-i\varepsilon t)$. Separating out the fast-oscillating factors in the wave function:

$$\hat{\psi}(\mathbf{r}, t) = \exp(-i\varepsilon t) \hat{\psi}_{p_F}(\mathbf{r}) \exp(i\mathbf{p}_F \cdot \mathbf{r}) = \hat{\psi}_{p_F}(\mathbf{r}, t) \exp(i\mathbf{p}_F \cdot \mathbf{r}) \tag{1.20}$$

and restoring the time-differentiation operators, one can transform Eqs. (1.18) and (1.19) into the form:

$$\left(i \frac{\partial}{\partial t} - \hat{\alpha} e \varphi \right) \hat{\psi}_{p_F}(\mathbf{r}, t) = \left(-i \hat{\alpha} \mathbf{v} \cdot \frac{\partial}{\partial \mathbf{r}} + \frac{e}{c} \mathbf{v} \cdot \mathbf{A} \right) \hat{\psi}_{p_F}(\mathbf{r}, t) + |\Delta| \hat{\beta} \hat{\psi}_{p_F}(\mathbf{r}, t). \tag{1.21}$$

Thus the analogy between the particle spectra has led to an apparent parallel between Eqs. (1.18) and (1.19) and the Dirac equation.[8,10] There are numerous consequences from Eq. (1.21) [or, equivalently, from Eqs. (1.18) and (1.19)] that are analogous to relativistic quantum effects.† We consider only one of them: the so-called *Andreev reflection.*

*The magnetic field may be introduced by generalization of the standard method.[11] One can start from the Lagrangian $\hat{L}(\mathbf{r},\dot{\mathbf{r}}) = \hat{\alpha} m \dot{\mathbf{r}}^2/2 - \hat{\beta}|\Delta| + \hat{\alpha} e \dot{\mathbf{r}} \cdot \mathbf{A}/c$, The scalar potential φ may be included in ε_F. This Lagrangian gives the correct expression for the Lorenz force acting on the electron in a normal metal (when $\Delta = 0$). In the presence of a magnetic field, we obtain the Hamiltonian $\hat{H} = \mathbf{p} \cdot \dot{\mathbf{r}} - \hat{L}$, where $\mathbf{p} = \partial \hat{L}/\partial \dot{\mathbf{r}} = \hat{\alpha}(m\dot{\mathbf{r}} + e\mathbf{A}/c)$, so $\hat{H} = \hat{\alpha}(\hat{\alpha}\mathbf{p} - \hat{1} e\mathbf{A}/c)^2/2m - \hat{\alpha}\varepsilon_F + \hat{\beta}|\Delta|$, which leads to Eqs. (1.18) and (1.19).

†We note that there is no one-to-one correspondence between effects in superconductors described by the Bogolyubov–De Gennes equations and the physics of the Dirac equation. Even formally there are pronounced differences between these equations. According to them, for example, the quasi-particle does not have a magnetic moment associated with the "zitterbewegung"[13] of electrons in superconductors.

In the absence of external fields, the $\hat{\psi}$-function may be taken as real (without loss of generality), and using the normalization

$$\mathrm{Tr}\,\hat{\psi}^2 = \mathcal{U}^2 + \mathcal{V}^2 = 1, \tag{1.22}$$

one finds from (1.22), (1.16), and (1.17):

$$\mathcal{U}^2 = \frac{1}{2}\left(1 + \frac{\xi}{\varepsilon}\right), \quad \mathcal{V}^2 = \frac{1}{2}\left(1 - \frac{\xi}{\varepsilon}\right). \tag{1.23}$$

According to Eq. (1.22), the charge carrier with spectrum (1.5) is in a superposition of states, having the probability amplitudes $\mathcal{U}$ and $\mathcal{V}$. As follows from Eq. (1.23), this superposition is essential in the energy range $\xi \sim |\Delta|$. For $\xi >> |\Delta|$ we have from (1.22) and (1.23), $\psi^2_{p>p_F} \approx \mathcal{U}^2$; this is an electronlike excitation. For $\xi << -|\Delta|$, we have $\psi^2_{p<p_F} \approx \mathcal{V}^2$; this is a holelike excitation. Because the charges of these excitations have the opposite signs, one has for the charge of quasi-particles, described by the $\hat{\psi}$-function (1.12), the expression[14]:

$$q_* = \mathcal{U}^2 - \mathcal{V}^2 = \xi/\varepsilon \tag{1.24}$$

(the electron charge is unity). It follows that the quasi-particle charge, as well as its group velocity

$$\mathbf{v}_g = \frac{\partial \varepsilon}{\partial \mathbf{p}} = \frac{\xi}{\varepsilon}\frac{\mathbf{p}}{m} = q_* \mathbf{v}, \tag{1.25}$$

vanishes (and reverses its sign) at $p = p_F$.

Consider now the propagation of such a particle in a medium where $|\Delta(\mathbf{r})|$ is a spatially inhomogeneous function. For instance, $|\Delta(\mathbf{r})|$ may increase smoothly from zero to Δ_0 at the boundary between normal and superconducting phases. Let the particle be moving from a normal to a superconducting region, with its energy ξ_p obeying the relation $0 < \varepsilon_p = \xi_p < \Delta_0$ in the normal region. In the superconducting region, as can be seen from Eq. (1.5), somewhat smaller values of $\xi_{p'}$ and consequently smaller values of p', correspond to the same energy ε_p. At the point where $|\Delta(\mathbf{r})| = \varepsilon_p$, we have $p = p_F$, and according to Eqs. (1.24) and (1.25), the particle should stop and be reflected. The group velocity in this case reverses its sign, but the momentum may be retained. This means that the reflected particle reverses its charge [see Eq. (1.24)], i.e., the reflected electron excitation becomes a hole. In the relativistic theory, this phenomenon is known as the Klein paradox.[15] In the superconductivity theory, it corresponds to the Andreev reflection.[16]

The Andreev reflection takes place when a current flows across the boundary between a normal metal and a superconductor. This process was demonstrated experimentally by the radio-frequency size effect.[17] As can be seen from Fig. 1.1, the specifics of such a reflection allow one to place the electron's trajectory (having

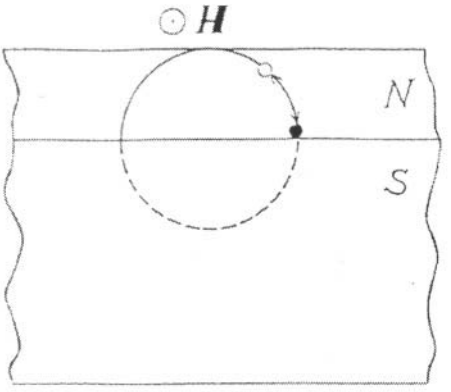

Figure 1.1. Experimental evidence for the Andreev reflection: scattering on the normal-metal (N)—superconductor (S) boundary transforms the "electron" into the "hole" and vice versa. Closed trajectories are possible at half amplitudes of the applied magnetic field **H** compared with the case of a free-standing single film.

a diameter D in the presence of a magnetic field H_0) within the normal metal layer of thickness $d = D/2$. Evidently if the film borders a vacuum, the minimal value of the field is $H = H_0$, but for a film deposited on a superconductor (see Fig. 1.1), the closed trajectory is achievable in the field $H = H_0/2$.[17] This example demonstrates one of the remarkable kinetic properties caused by the nature of superconductivity.*

1.1.6. Electron Density of States

There are two additional points. The first relates to the density of the energy levels of quasi-particles having the spectrum of Eq. (1.5). In a description of normal metals, the density of the levels can be obtained when one passes from the momentum summation to the energy integration:

$$\Sigma(\ldots) \to \int (\ldots) \frac{d^3\mathbf{p}}{(2\pi)^3} \approx \frac{mp_F}{2\pi^2} \int (\ldots)\, d\xi \equiv N(0) \int (\ldots) d\xi, \tag{1.26}$$

so for the momenta $p \approx p_F$, the levels density is a constant $N(0) = mp_F/2\pi^2$. However, in superconductors, the levels density is a singular function

*It is recognized today that the Andreev reflection plays a major role in "our ability to insert current into a superconductor."[18] The related physics is very important for various fundamental and applied problems of superconductivity.[19–28]

$$N(0)\int(\ldots)d\xi \to N(0)\int(\ldots)\frac{\partial\xi}{\partial\varepsilon}\,d\varepsilon = N(0)\int(\ldots)\frac{\varepsilon\theta(\varepsilon^2-|\Delta|^2)}{\sqrt{\varepsilon^2-|\Delta|^2}}\,d\varepsilon. \qquad (1.27)$$

Thus, when there is a gap in the excitation spectrum, the energy levels of quasi-particles are pushed out from the intragap into the gap-edge region of energies $|\varepsilon| \gtrsim |\Delta|$. This singularity of superconducting energy levels will play an important role in further discussions.

1.1.7. Coherence Factors

The second point relates to the coherence factors. The form of the wave function (1.12) indicates that in calculations of the matrix elements connected with the transition of quasi-particles from level ε to level ε', combinations of the type

$$\mathcal{U}(\varepsilon)\mathcal{V}(\varepsilon') \pm \mathcal{V}(\varepsilon)\mathcal{U}(\varepsilon'),\ \mathcal{U}(\varepsilon)\mathcal{U}(\varepsilon') \pm \mathcal{V}(\varepsilon)\mathcal{V}(\varepsilon') \qquad (1.28)$$

would appear, depending on the form of the interaction operator. The squared quantities (which define the corresponding transition probabilities) would be, for example, $(\mathcal{U}\mathcal{U}' + \mathcal{V}\mathcal{V}')^2$. For the last quantity one obtains, after a simple calculation taking into account Eq. (1.23):

$$\left[\mathcal{U}(\varepsilon)\mathcal{U}(\varepsilon') + \mathcal{V}(\varepsilon)\mathcal{V}(\varepsilon')\right]^2 = \frac{1}{2}\left(1 + \frac{\xi\xi'}{\varepsilon\varepsilon'} + \frac{|\Delta|^2}{\varepsilon\varepsilon'}\right). \qquad (1.29)$$

Other combinations in Eq. (1.28) lead to analogous relations, differing only in the signs in the parentheses in Eq. (1.29). These factors are called *coherence factors*. They renormalize the transition matrix elements in superconductors relative to those in normal metals.

For the processes that are symmetric over the electron-hole excitation branches, the odd terms $\xi\xi'$ in (1.29) disappear and the coherence factors are of only two types:

$$(1 + |\Delta|^2/\varepsilon\varepsilon') \text{ and } (1 - |\Delta|^2/\varepsilon\varepsilon'). \qquad (1.30)$$

Note that for $\varepsilon, \varepsilon' \sim |\Delta|$, the transition probability doubles for the first factor and vanishes for the second one. This is important, because the states with $\varepsilon \sim |\Delta|$ play an essential role in kinetic processes, as is seen from Eq. (1.27).

1.2. PHENOMENOLOGICAL GINZBURG–LANDAU THEORY

The Ginzburg-Landau (GL) theory permits a deep insight into the phenomenon of superconductivity in the case of thermodynamic equilibrium and provides

the most transparent technique for investigating this phenomenon. We continue our discussion with the presentation of this theory.[29]

In formulating this theory, the experimental knowledge that the superconducting transition is a second-order phase transition was used. It was assumed that below the phase transition temperature T_c all the electrons of the superconducting metal can be characterized by a superconducting order parameter $\Psi \neq 0$ at $T < T_c$ and $\Psi = 0$ at $T > T_c$. On intuitive grounds, the order parameter Ψ was considered as the "effective wave function of superconducting electrons."

1.2.1. Free Energy Functional

According to the theory of second-order phase transitions,[30] the free energy of the superconducting state in the vicinity of T_c may be presented as a functional of the complex variable Ψ, permitting the expansion (we make for a moment $\mathbf{H} = 0$):

$$F_s^0 = F_n^0 + \alpha|\Psi|^2 + \frac{\beta}{2}|\Psi|^4 + \cdots \tag{1.31}$$

(the terms proportional to Ψ and Ψ^* do not enter this expansion in view of the gauge invariance of the free energy). In expression (1.31) F_n^0 is the free energy of the normal phase. At fixed temperature $T < T_c$, the free energy (1.31) is minimized by the value of $|\Psi(T)|$, which can be found from the equation

$$\frac{\partial F_s^0}{\partial|\Psi|^2} = 0, \tag{1.32}$$

subject to the condition

$$\frac{\partial^2 F_s^0}{\left(\partial|\Psi|^2\right)^2} > 0. \tag{1.33}$$

From Eq. (1.32) and (1.31) one finds

$$|\Psi|^2 \equiv |\Psi_0|^2 = -\frac{\alpha}{\beta}, \tag{1.34}$$

i.e., the factors α and β have opposite signs at $T < T_c$. From the condition (1.33) it follows that

$$\beta_c = \beta(T_c) > 0 \tag{1.35}$$

and combining this with Eq. (1.34), we find

$$\alpha_c = \alpha(T_c) = 0. \tag{1.36}$$

According to this for temperatures near T_c it could be written

$$\alpha(T) = \left(\frac{d\alpha}{dT}\right)_{T_c}(T - T_c), \tag{1.37}$$

$$\beta(T) = \beta_c. \tag{1.38}$$

Based on these expressions one can conclude that in the case of thermodynamic equilibrium at $T \le T_c$

$$|\Psi_0|^2 = -\frac{1}{\beta_c}\left(\frac{d\alpha}{dT}\right)_{T_c}(T - T_c), \tag{1.39}$$

$$F_s^0 = F_n^0 - \frac{\alpha^2}{2\beta} = F_n^0 - \frac{1}{2\beta_c}\left(\frac{d\alpha}{dT}\right)^2_{T_c}(T - T_c)^2 \ . \tag{1.40}$$

Let us now consider a superconductor that is placed in a static magnetic field $\mathbf{H}(\mathbf{r})$. The free energy F_s^H must have an additional term that is equal to the field energy $\mathbf{B}^2/8\pi$. Accordingly, the critical magnetic field in a spatially homogeneous case may be found from the equation

$$\frac{H_c^2}{8\pi} = F_n^0 - F_s^0 = \frac{\alpha^2}{2\beta}. \tag{1.41}$$

Generally, one must also take into account the energy, which is proportional to the inhomogeneity of the wave function $|\nabla\Psi|^2$. Thus at small gradients,

$$F_s^H = F_s^0 + \frac{\mathbf{B}^2}{8\pi} + \text{const}\,|\nabla\Psi|^2. \tag{1.42}$$

The last term in (1.42) corresponds to quantum-mechanical kinetic energy. Hence there are reasons to represent it in the form

$$\frac{\hbar^2}{2m_*}|\nabla\Psi|^2 = \frac{1}{2m_*}|-i\hbar\nabla\Psi|^2, \tag{1.43}$$

where m_* is some coefficient having the dimensionality of a mass. To include the magnetic field in the scheme, it is necessary to make in Eq. (1.43) the usual quantum-mechanical substitution

$$-i\hbar\nabla \to -i\hbar\nabla - \frac{e_*}{c}\mathbf{A}, \tag{1.44}$$

which enables one to obtain the gauge-invariant equations. Here **A** is the magnetic field's vector potential and e_* is the charge of the carrier, represented by the wave function Ψ. Thus the free energy density may be written in the form

$$F_s^H = F_s^0 + \frac{\mathbf{B}^2}{8\pi} + \frac{1}{2m_*}\left|-i\hbar\nabla\Psi - \frac{e_*}{c}\mathbf{A}\Psi\right|^2. \tag{1.45}$$

Demanding the minimum for the total free energy

$$\mathcal{F}^H = \int_{V_0} F_s^H d^3\mathbf{r} \tag{1.46}$$

(V_0 is the system's volume), one can obtain the equation for Ψ. Varying (1.46) by Ψ^* gives

$$\delta\mathcal{F}^H = \int_V \left\{\frac{1}{2m_*}\left(-i\hbar\nabla - \frac{e_*}{c}\mathbf{A}\right)^2 \Psi + \alpha\Psi + \beta|\Psi|^2\Psi\right\}\delta\Psi^* d^3\mathbf{r}$$
$$+ \frac{\hbar^2}{2m_*}\int_S \delta\Psi^*\left(\nabla\Psi - \frac{ie_*}{\hbar c}\mathbf{A}\Psi\right)d\mathbf{s} \tag{1.47}$$

(S is the metal's surface). Because $\delta\Psi^*$ is arbitrary, we find from (1.47) an equation for the order parameter

$$\frac{1}{2m_*}\left(-i\hbar\nabla - \frac{e_*}{c}\mathbf{A}\right)^2 \Psi + \alpha\Psi + \beta|\Psi|^2\Psi = 0 \tag{1.48}$$

and also the boundary condition

$$\mathbf{n}\cdot\left(-i\hbar\nabla\Psi - \frac{e_*}{c}\mathbf{A}\Psi\right) = 0 \tag{1.49}$$

(here **n** is a vector normal to the metal surface). The variation of (1.46) by **A** yields the Maxwell equation

$$\operatorname{curl}\operatorname{curl}\mathbf{A} = \frac{4\pi}{c}\mathbf{j}, \tag{1.50}$$

where the current

$$\mathbf{j} = -\frac{ie_*\hbar}{2m_*}(\Psi^*\nabla\Psi - \Psi\nabla\Psi^*) - \frac{e_*^2}{m_* c}|\Psi|^2\mathbf{A} \tag{1.51}$$

has a typical quantum-mechanical form [cf. (1.3)].

Expressions (1.48) and (1.51) comprise the Ginzburg–Landau system of equations describing the behavior of superconductors in a static magnetic field. Presenting the complex function Ψ in the form

$$\Psi = |\Psi| e^{i\theta}, \tag{1.52}$$

one can rewrite the expression for the current:

$$\mathbf{j} = \frac{\hbar e_*}{m_*} |\Psi|^2 (\nabla\theta - \frac{e_*}{\hbar c}\mathbf{A}) = e_* N_s \mathbf{v}_s. \tag{1.53}$$

Here $|\Psi|^2$ is the density of superconducting electrons in the Ginzburg–Landau normalization, $|\Psi|^2 \equiv N_s$, and the superconducting velocity $\mathbf{v}_s$ is equal to

$$\mathbf{v}_s = \frac{\hbar}{m_*}(\nabla\theta - \frac{e_*}{\hbar c}\mathbf{A}). \tag{1.54}$$

Putting $\mathbf{B}$ = curl $\mathbf{A}$, one can easily prove that Eq. (1.53) coincides with the London equation [ef. (1.2)]

$$\text{curl}\, \mathbf{j} = -\frac{e_*^2 N_s}{m_* c}\mathbf{B}. \tag{1.55}$$

Substituting into (1.55) the Maxwell equation

$$\text{curl}\, \mathbf{B} = \frac{4\pi}{c}\mathbf{j} \tag{1.56}$$

and taking into account that

$$\text{div}\, \mathbf{B} = 0, \tag{1.57}$$

we obtain the equation

$$\nabla^2 \mathbf{B} = \frac{4\pi e_*^2 N_s}{m_* c^2}\mathbf{B}. \tag{1.58}$$

1.2.2. London Penetration Depth

Equation (1.58) subject to condition (1.57) describes the expulsion of a magnetic field from superconductor's interior (the Meissner effect). Let us consider the distribution of a magnetic field in a superconductor near its surface, assuming the latter to be a plane. The characteristic parameter, which has the dimension of a length, in this situation is

$$\lambda_L = \left(\frac{4\pi e_*^2 N_s}{m_* c^2} \right)^{-1/2}, \tag{1.59}$$

as may be seen from expression (1.58). In the case considered here, the field distribution depends on one (say, *x)* coordinate only. Then

$$\frac{d^2\mathbf{B}}{dx^2} = \frac{\mathbf{B}}{\lambda_L^2} \tag{1.60}$$

with the boundary condition

$$\frac{d\mathbf{B}_x}{dx} = 0, \tag{1.61}$$

which follows from Eq. (1.57). From the expressions (1.61) and (1.57) one can conclude that the vector of induction **B** in the depth of the superconductor has the form

$$\mathbf{B}(x) = \mathbf{B}_0 e^{-x/\lambda_L}, \tag{1.62}$$

where $\mathbf{B}_0$ is a tangential component of the external field. The characteristic length λ_L (1.59) is called the *London penetration depth.*

1.2.3. Coherence Length

The Ginzburg-Landau set of equations has one more characteristic scale, which has the dimensionality of the length. Its value [usually marked $\xi(T)$] as may be seen from Eq. (1.48), characterizes the scale of spatial evolution of the Ψ-function and is given by

$$\xi^{-2}(T) = \frac{2m_* |\alpha(T)|}{\hbar^2}. \tag{1.63}$$

The temperature dependence of $\xi(T)$ in the vicinity of T_c is found using the formula (1.37):

$$\xi(T) = \hbar \left\{ 2m_* \left(\frac{d\alpha}{dT} \right)_{T_c} (T_c - T) \right\}^{-1/2}. \tag{1.64}$$

We are able also to obtain the temperature dependence of $\lambda_L = \lambda_L(T)$. Indeed, in the vicinity of T_c one can substitute Eq. (1.39) into (1.59) with the result:

$$\lambda_L(T) = \left\{ \frac{m_* c^2 \beta_c}{4\pi e_*^2 (d\alpha/dT)_{T_c} (T_c - T)} \right\}^{1/2}. \tag{1.65}$$

The ratio of these two characteristic lengths

$$\kappa = \frac{\lambda_L(T)}{\xi(T)} = \frac{m_* c}{\hbar e_*} \frac{\beta_c^{1/2}}{(2\pi)^{1/2}} \tag{1.66}$$

is temperature independent and, as we will now see, is an important parameter of a superconductor, defining its behavior in a magnetic field.

1.2.4. Sign of Surface Energy

Let us consider the surface energy of the flat boundary between normal and superconducting phases, which may exist in a magnetic field. In the normal phase, the free energy density, including the field energy, is equal to $F_n^0 + H_c^2/(8\pi)$. In the region where $\Psi \neq 0$, the free energy density is F_s^H [Eq. (1.42)]. Near the boundary one must take into account the energy associated with the magnetization of a superconductor

$$\mathbf{M} = \frac{\mathbf{B} - \mathbf{H}}{4\pi}. \tag{1.67}$$

In the depth of the normal phase, the equation $\mathbf{B} = \mathbf{H} = \mathbf{H}_c$ holds (the second of these equations is also valid in the superconducting region, because $c\ \mathrm{curl}\ \mathbf{M} = \mathbf{j}$).

Thus the surface energy

$$\sigma_{ns} = \int \left\{ F_s^H(z) - \frac{B(z) - H_c}{4\pi} H_c - F_n^0 - \frac{B^2}{8\pi} \right\} dz \tag{1.68}$$

taking into account Eq. (1.45), is equal to

$$\sigma_{ns} = \int \left\{ \alpha\Psi^2 + \frac{\beta\Psi^4}{2} + \frac{\alpha^2}{2\beta} + \frac{\hbar^2}{2m_*} \left(\frac{\partial \Psi}{\partial z} \right)^2 + \frac{e_*^2}{2m_* c^2} A^2 \Psi^2 + \frac{B^2}{8\pi} - \frac{H_c B}{4\pi} \right\} dz \tag{1.69}$$

[according to Eq. (1.41), $\alpha^2/2\beta = H_c^2/(8\pi)$] In Eq. (1.69), the Ψ-function was assumed to be real, because the term $i\mathbf{A} \cdot \nabla\Psi$ vanishes owing to the condition $\mathbf{A}_z = 0$. The analogous term also disappears from Eq. (1.48) for the order parameter, so Eq. (1.53) for the current acquires the form

$$\mathbf{j} = -\frac{e_*^2}{m_* c} \Psi^2 \mathbf{A}. \tag{1.70}$$

It is expedient to use the variables

$$\bar{z} = \frac{z}{\lambda_L}, \quad \bar{\Psi} = \Psi \left(\frac{\beta}{|\alpha|} \right)^{1/2}, \quad \bar{A} = \frac{A}{H_c \lambda_L}, \quad \bar{B} = \frac{d\bar{A}}{d\bar{z}} = \frac{B}{H_c}. \tag{1.71}$$

Removing the bars above the symbols to simplify the notation, we present Eq. (1.48) in the form

$$\Psi'' = \kappa^2\left[\left(\frac{1}{2}A^2 - 1\right)\Psi + \Psi^3\right] \tag{1.72}$$

and write expression (1.69) as

$$\sigma_{ns} = \frac{\lambda_L H_c^2}{8\pi}\int_{-\infty}^{\infty}\left[\frac{2}{\kappa^2}(\Psi')^2 + (A^2 - 2)\Psi^2 + \Psi^4 + (A' - 1)^2\right]dz. \tag{1.73}$$

Integrating the first term in (1.73) by parts, using the condition $\Psi'(\pm\infty) = 0$, one can reduce Eq. (1.73) to the form

$$\sigma_{ns} = \frac{\lambda_L H_c^2}{8\pi}\int_{-\infty}^{\infty}[(A' - 1)^2 - \Psi^4]\,dz. \tag{1.74}$$

Expression (1.74) vanishes if the integrand is identical to zero: $A' - 1 = \pm\Psi^2$. Since $B = A'$ and B must decrease with increasing z, then

$$A' - 1 = -\Psi^2. \tag{1.75}$$

From Eqs. (1.50) and (1.70) it follows that

$$A'' = A\Psi^2. \tag{1.76}$$

Taking the derivative of (1.75) and introducing it into (1.76), we find

$$\Psi' = -\frac{1}{2}A\Psi. \tag{1.77}$$

Substituting Ψ'(1.77) and A′(1.75) into Eq. (1.72) shows that Eq. (1.72) is fulfilled identically at $\kappa = 1/\sqrt{2}$. One can also see that the condition (1.75), which was used earlier does not contradict the boundary conditions: $A' = 1$ at $z = -\infty$ and $A = 0$ at $z = \infty$. Thus we arrive at a very important conclusion: at $\kappa = 1/\sqrt{2}$ the solution of the order parameter equation causes the surface energy to vanish (this criterion was established numerically by Ginzburg and Landau[29] and proved analytically[12] by the Sarma method; the alternative method we used here is by Lifshitz and Pitaevski[31]). Generally, σ_{ns} may have an arbitrary sign. To see this we will once again use the expression (1.73), as well as the first integral of Eq. (1.72) subject to (1.76), which has the form

$$\frac{2(\Psi')^2}{\kappa^2} + (2 - A^2)\Psi^2 - \Psi^4 + (A')^2 = \text{const} \equiv 1. \tag{1.78}$$

*The last identity here follows from Eq. (1.76) and boundary conditions $\Psi(-\infty) = 0$, $A'(-\infty) = 1$; $\Psi(\infty) = 1$, $A'(\infty) = 0$.

As a result we find

$$\sigma_{ns} = \frac{\lambda_L H_c^2}{4\pi} \int_{-\infty}^{\infty} \left[\frac{2}{\kappa^2} (\Psi')^2 + A'(A' - 1) \right] dz. \tag{1.79}$$

Note that the second term in (1.79) is always negative, because the field $B = A'$, which penetrates into the superconductor, is always smaller than the critical one: $A' \leq 1$. The first term in Eq. (1.79) is always positive, but its value and consequently the sign of σ_{ns} are determined by the magnitude of κ [see Eq. (1.66)]. Superconductors in which

$$\lambda_L < \xi/\sqrt{2} \tag{1.80}$$

are called Type I superconductors, or Pippard superconductors. In these superconductors, as we have seen, $\sigma_{ns} > 0$. The superconductors in which

$$\lambda_L > \xi/\sqrt{2} \tag{1.81}$$

are called Type II superconductors, or London superconductors.

1.2.5. Superheating in a Magnetic Field

Consider a film of a Type I superconductor $(\kappa < 1/\sqrt{2})$ with a thickness d, placed in the magnetic field **H** parallel to its surface.[29,32] Let the film occupy the space $-d/2 \leq z \leq d/2$ in the appropriate reference frame (so that formally the problem is one dimensional). To simplify calculations we will made $\kappa << 1$. In this case Eq. (1.72) reduces to $d^2\Psi/d_z^2 = 0$. Accounting for the fact that $d\Psi/dz|_{z = \pm d/2} = 0$ (according to Eq. 1.49), one obtains Ψ = const. In addition, integrating the Maxwell equation (1.56) and taking into account that $B(\pm d/2) = H$, one gets

$$H\left(\frac{d}{2}\right) - H\left(-\frac{d}{2}\right) = 0 = \frac{4\pi}{c} \int_{-d/2}^{d/2} j dz, \tag{1.82}$$

i.e., the mean value of the superfluid velocity (averaged over the film's thickness) is zero. Substituting the value of Ψ (still unknown) into Eq. (1.58), subject to the above-mentioned boundary condition for $B(z)$, we find

$$B(z) = H \frac{\cosh(z\psi/\lambda_L)}{\cosh(d_*\psi/2)}. \tag{1.83}$$

Here $d_* = d/\lambda_L$, $\psi = \Psi/\Psi_0 \leq 1$; Ψ_0 denotes the value of Ψ in the absence of the magnetic field (see Eq. 1.39). For the superfluid velocity, we obtain on the basis of Eqs. (1.53), (1.56), and (1.83),

$$v_s = \frac{j}{e_* N_s} = \frac{e_* \lambda_L H}{m_* c \psi} \frac{\sinh(z\psi/\lambda_L)}{\cosh(d_*\psi/2)}. \tag{1.84}$$

Averaging over the film's thickness, we arrive at

$$\overline{v_s^2} = \frac{1}{d} \int_{-d/2}^{d/2} v_s^2 dz = \frac{1}{2} \left(\frac{e_* \lambda_L H}{m_* c \psi} \right)^2 \cosh^{-2} \left(\frac{\psi d_*}{2} \right) \left[\frac{\sinh(\psi d_*)}{\psi d_*} - 1 \right]. \tag{1.85}$$

Omitting in Eq. (1.48) the term with a spatial derivative (because $\kappa << 1$), we find

$$\frac{m_* v_s^2}{2} + \alpha + \beta \Psi^2 = 0, \tag{1.86}$$

or, using Eq. (1.34),

$$\frac{m_* v_s^2}{2\alpha} + 1 = \psi. \tag{1.87}$$

On the basis of Eqs. (1.41), (1.59), and (1.39), the relation (1.87) can be represented in the form

$$4(1 - \psi^2)\psi^2 \frac{\cosh^2(\psi d_*/2)}{[\sinh(\psi d_*)/(\psi d_*) - 1]} = \left(\frac{H}{H_c} \right)^2. \tag{1.88}$$

The critical value of the field H_c is reached when the Gibbs potentials of superconducting and normal states equalize. The Gibbs potential density in a superconducting state is

$$G_s = F_s - \frac{\mathbf{H} \cdot \mathbf{B}}{4\pi}, \tag{1.89}$$

where F_s is expressed by Eqs. (1.40) and (1.31) with the spatial derivatives omitted in view of $\kappa << 1$. Using the relation (1.86), one arrives at

$$G_s = F_n^0 + \frac{B^2(z)}{8\pi} - \frac{H_c^2}{8\pi} \psi^4 - \frac{HB(z)}{4\pi}. \tag{1.90}$$

To proceed further we must integrate Eq. (1.90) over the specimen's volume, which is equivalent to averaging over the film thickness. Using Eq. (1.83) and calculating the averaged values $\overline{B}$ and $\overline{B^2}$,

$$\overline{B} = 2H \frac{\tanh(\psi d_*/2)}{\psi d_*}, \tag{1.91}$$

$$\overline{B^2} = H^2 \frac{(\psi d_*) + \sinh(\psi d_*)}{\psi d_*[1 + \cosh(\psi d_*)]}, \tag{1.92}$$

one finally gets

$$G_s = F_n^0 + \frac{H^2}{8\pi}\left\{\frac{\sinh(\psi d_*) + \psi d_*}{\psi d_*[1 + \cosh(\psi d_*)]} - \frac{4\tanh(\psi d_*/2)}{\psi d_*}\right\} - \frac{H_c^2}{8\pi}\psi^4. \tag{1.93}$$

In the normal phase ($\psi \equiv 0$) $G_n = F_n^0 - H^2/8\pi$. To obtain the critical value of a magnetic field one must equalize G_s and G_n, which leads to the equation

$$\left(\frac{H}{H_c}\right)^2\left[1 + \frac{\sinh\psi d_* + \psi d_*}{\psi d_*(1 + \cosh\psi d_*)} - \frac{4\tanh(\psi d_*/2)}{\psi d_*}\right] = \psi^4. \tag{1.94}$$

Another relation between H/H_c and ψ is supplied by Eq. (1.88). As follows from these equations, the critical field depends on the film's thickness d.

We consider the two limiting cases of thin and thick films. In the case $\psi d/\lambda_L << 1$, Eq.(1.88)is

$$\left(\frac{H}{H_c}\right)^2 = \frac{24}{d_*^2}(1 - \psi^2), \tag{1.95}$$

i.e., the reduced-order parameter ψ decreases monotonically, with the field amplitude H increasing. This behavior corresponds to the second-order phase transition. Evidently the value $\psi = 0$ corresponds to the critical field. Substituting $\psi = 0$ into Eq. (1.95), one finds

$$H_{\text{film}} = 2\sqrt{6}H_c\frac{\lambda_L}{d}, \tag{1.96}$$

where H_{film} is the thin film critical field.

In the opposite limiting case of thick film ($\psi d/\lambda_L >> 1$), Eq. (1.88) reduces to

$$\left(\frac{H}{H_c}\right)^2 = 2\psi^2 d_*(1 - \psi^2). \tag{1.97}$$

Substitution of this into Eq. (1.93) yields the equation

$$2d_*\psi(1 - \psi^2) = \psi^3. \tag{1.98}$$

The presence of a large multiplier on the left side means that $\psi \approx 1$, i.e., the thick-film's critical field is approximately equal to H_c because of Eqs. (1.17) and (1.98). Thus the phase transition in thick films is of the first order, because it occurs abruptly at finite values of $\Psi \approx \Psi_0$.

More detailed study (see, e.g., that in Ref. 32) shows that the first-order transition changes to the second order at the film's thickness $d = \sqrt{5}\,\lambda_L$. The physical reason for the first-order transition is the negative value of the surface energy σ_{ns}. Contrary to this, in Type II superconductors σ_{ns} is positive and this leads to the appearance of the layered structure of superconductors in the external magnetic field (i.e., the coexistence of normal and superconducting regions).

1.2.6. Flux Quantization

In their basic paper[29] Ginzburg and Landau assumed that e_* was equal to the electron's charge e. As was later established microscopically by Bardeen, Cooper, and Schrieffer (BCS)[33] the current in superconductors being transmitted by the Cooper pairs, and Gor'kov was able to prove that $e_* = 2e$ (see Section 1.4). We stress that in contrast to the mass m_*, which in the above system of equations may be changed by simple renormalization of ψ, the charge e_* enters Eqs. (1.48) and (1.51) additively and its magnitude is important. To demonstrate this we consider the phenomenon of magnetic flux quantization.

Let us imagine a massive superconductor with a cylindrical cavity placed in a magnetic field **H**, which is parallel to the cylinder's axis. Consider a contour C (see Fig. 1.2) that encloses the cavity and lies entirely within the depth of the superconductor. Owing to the Meissner effect, the superconducting current vanishes at distances from the surface much greater than the London penetration depth λ_L. Thus, as follows from Eq. (1.51), on the contour C one has

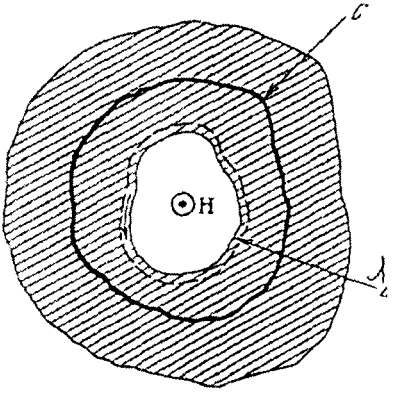

Figure 1.2. A hollow superconducting cylinder in a magnetic field. C, the contour of integration; λ_L, the penetration depth.

$$\mathbf{j} = \frac{\hbar e_*}{m_*} |\Psi|^2 \nabla\theta - \frac{e_*^2}{m_* c} \Psi^2 \mathbf{A} = \mathbf{0}. \tag{1.99}$$

Integrating $\mathbf{j}$ along this contour and using Eq. (1.99), we find

$$\oint \nabla\theta \cdot d\mathbf{l} = \frac{e_*}{\hbar} \oint \mathbf{A} \cdot \mathbf{dl} \tag{1.100}$$

It must be taken into account that

$$\oint \mathbf{A} \cdot d\mathbf{l} = \int \text{curl } \mathbf{A} \cdot d\mathbf{s} = \int \mathbf{H} \cdot d\mathbf{s} = \Phi, \tag{1.101}$$

where Φ is the magnetic flux captured in the cavity. The first of the integrals (1.100) is the phase difference acquired while going around the contour C and it must be a multiple of 2π:

$$\oint \nabla\theta \cdot d\,\mathbf{l} = 2\pi n \tag{1.102}$$

because the Ψ-function is single valued [n is an integer in Eq. (1.102)]. As a result, one finds from Eqs. (1.100) to (1.102)

$$\Phi = \frac{hc}{e_*} n = \phi_0 n, \tag{1.103}$$

or, in other words, the magnetic flux in the cavity of a superconductor is quantized and may change only in portions $\phi_0 = hc/e_*$. This phenomenon was predicted first by F. London[7] and later confirmed experimentally by Deaver and Fairbank[34] and also by Doll and Näbauer,[35] who found the value of e_* in (1.103) to be equal to twice the electronic charge: $e_* = 2e$! Had the doubling of the carrier's charge been known in 1950, the analysis of the Ginzburg–Landau equation for the quantum mechanical function of superconducting electrons might significantly accelerate the subsequent development of the microscopic theory of superconductivity.

1.3. BCS–GOR'KOV THEORY

The basic cornerstone of the microscopic theory of superconductivity was laid down by Cooper[36] in 1956. Cooper considered the indirect (mediated by the phonon exchange) interaction between electrons in metals; this is a process of the second order in electron–phonon interaction. As is known from perturbation theory, the second-order correction to the energy of the ground state is always negative (see, e.g., Ref. 37), i.e., the Cooper interaction is attractive. Because the Fermi sphere at

low temperatures is almost completely occupied, the motion of conducting electrons in the momentum space is quasi-two-dimensional. This means that any weak attraction between electrons produces the bound state, or leads to electron pairing. In the absence of total current, the electrons with opposite momenta have the largest pairing probabilities. The paired electrons become bosons, with the spin equal to 0 or 1. The electron system must have rearranged itself (because the paired state is energetically preferable), forming the Bose condensate of paired electrons (the Cooper or pair condensate). The properties of the Cooper condensate are typical for all the Bose condensates. In particular, at temperatures lower than the condensation temperature T_c, the occupation number of paired states with zero momentum is macroscopically large. This means that in presence of the pair condensate, the anomalous components of Green's functions should be introduced into the theoretical formula. Such a generalization of the theoretical scheme was made by Belyayev[38] in the theory of superfluidity, and the concept of off-diagonal long-range order was developed even earlier (see discussion in Ref. 39). In the theory of superconductivity, this generalization was introduced by Gor'kov[40] and in a slightly different way by Nambu (see, e.g., Ref. 41). The microscopic description of the superconductor in terms of these formulas is fully adequate to the BCS theory and being considerably simpler allows one to avoid all the problems connected with the gauge invariance of the theoretical scheme.

1.3.1. Equations for Ψ Operators

We start with the BCS–Gor'kov model, considering first the case of $T = 0$. The model Hamiltonian has the form ($c = \hbar = 1$):

$$\hat{H} = \sum_{\alpha\beta} \int \left\{ -\left[\Psi_\alpha^\dagger(\mathbf{r}) \left(\frac{\nabla^2}{2m} + \varepsilon_F \right) \Psi_\alpha(\mathbf{r}) \right] \right.$$

$$\left. + \frac{\zeta}{2} \left[\Psi_\alpha^\dagger(\mathbf{r}) \Psi_\beta^\dagger(\mathbf{r}) \Psi_\beta(\mathbf{r}) \Psi_\alpha(\mathbf{r}) \right] \right\} d^3\mathbf{r} \qquad (1.104)$$

where $\Psi(\mathbf{r})$ and $\Psi^\dagger(\mathbf{r})$ are the field operators in the Schrödinger representation (from now on the repeated spin indices imply summation and the sign Σ will be omitted). The BCS potential ζ corresponds to the indirect interaction of electrons. Let us move to the Heisenberg representation, where operators Ψ and $\Psi^\dagger$ are the functions of $x \equiv (\mathbf{r}, t)$ and obey the equations

$$\left\{ i\frac{\partial}{\partial t} + \frac{\nabla^2}{2m} + \varepsilon_F \right\} \Psi_\alpha(x) - \zeta \left(\Psi_\beta^\dagger(x) \Psi_\beta(x) \right) \Psi_\alpha(x) = 0, \qquad (1.105)$$

$$\left\{ i\frac{\partial}{\partial t} - \frac{\nabla^2}{2m} - \varepsilon_F \right\} \Psi_\alpha^\dagger(x) + \zeta \Psi_\alpha^\dagger(x) \left(\Psi_\beta^\dagger(x) \Psi_\beta(x) \right) = 0. \qquad (1.106)$$

Here we have used the usual equations for the field operators

$$-i\frac{\partial\Psi(x)}{\partial t} = [\hat{H},\Psi(x)]_-, \tag{1.107}$$

and the commutation rules for the Schrödinger operators

$$\left[\Psi_\alpha(\mathbf{r}), \Psi_\beta^\dagger(\mathbf{r}')\right]_+ = \delta_{\alpha\beta}\delta(\mathbf{r}-\mathbf{r}'), \tag{1.108}$$

$$\left[\Psi_\alpha(\mathbf{r}), \Psi_\beta(\mathbf{r}')\right]_+ = \left[\Psi_\alpha^\dagger(\mathbf{r}), \Psi_\beta^\dagger(\mathbf{r}')\right]_+ = 0. \tag{1.109}$$

Green's superconductor functions are defined by the familiar[42] expressions

$$G_{\alpha\beta}(x,x') = -i\langle T\left[\Psi_\alpha(x)\,\Psi_\beta^\dagger(x')\right]\rangle, \tag{1.110}$$

and from Eqs. (1.110) and (1.106), and (1.108) and (1.109), we get

$$\left\{i\frac{\partial}{\partial t} + \frac{\nabla^2}{2m} + \varepsilon_F\right\} G_{\alpha\beta}(x,x') + i\zeta\langle\left[\Psi_\gamma^\dagger(x)\Psi_\gamma(x)\right]T\,\Psi_\alpha(x)\,\Psi_\beta^\dagger(x')\right\rangle$$
$$= \delta(x-x')\,\delta_{\alpha\beta}. \tag{1.111}$$

According to Wick's theorem, the T-product of Ψ operators may be presented as the averaged product of binary field operators. Owing to the presence of the pair condensate in the system, the T-product may be written in the form

$$\langle T\left[\Psi_\gamma^\dagger(x)\,\Psi_\gamma(x)\,\Psi_\alpha(x)\,\Psi_\beta^\dagger(x')\right]\rangle \approx$$
$$-\langle T\left[\Psi_\alpha(x)\,\Psi_\gamma(x')\right]\rangle\langle T\left[\Psi_\gamma^\dagger(x)\,\Psi_\beta^\dagger(x')\right]\rangle \tag{1.112}$$

(here the electrons' scattering processes and the renormalization of their chemical potential are neglected).

1.3.2. Off-Diagonal Long-Range Order

We can now introduce the anomalous, nondiagonal Green's functions

$$F_{\alpha\beta}^+(x,x') = \langle T\left[\Psi_\alpha^\dagger(x)\,\Psi_\beta^\dagger(x')\right]\rangle,\ F_{\alpha\beta}(x,x') = \langle T\left[\Psi_\alpha(x)\,\Psi_\beta(x')\right]\rangle, \tag{1.113}$$

which shows that the quantum states with N and $N \pm 1$ paired particles (Cooper pairs) are indistinguishable. The last circumstance is connected with the above-mentioned macroscopic occupation of the paired states, and allows one to neglect the fluctuations in the number of pairs. It is convenient to write the propagators, which describe the superconducting state, in a matrix form

$$\hat{G}_{\alpha\beta}(x,x') = \begin{pmatrix} G_{\alpha\beta}(x,x') & F_{\alpha\beta}(x,x') \\ -F^{+}_{\alpha\beta}(x,x') & \overline{G}_{\alpha\beta}(x,x') \end{pmatrix}, \tag{1.114}$$

where the function $\overline{G}_{\alpha\beta}(x,x') = G_{\beta\alpha}(x', x)$ corresponds to the Feynman diagram with the reversed direction of arrows. The appearance of F-functions, which are nondiagonal in the Hilbert space of single-particle states, is connected with the phase coherence of the superconducting electrons [the off-diagonal long-range order, introduced by Landau (see discussion by Ginzburg[43]) and independently Penrose and Onsager[44]; see also Refs. 29 and 44].

Note that in a spatially homogeneous and stationary state the propagators (1.114) depend on the difference $(x - x')$ only. Introducing in this case the notation

$$F_{\alpha\beta}(0+) = \lim_{\substack{\mathbf{r}\to\mathbf{r}' \\ t\to t'+0}} F_{\alpha\beta}(x - x'), \tag{1.115}$$

one can rewrite Eq. (1.111) in the form

$$\left\{ i\frac{\partial}{\partial t} + \frac{\nabla^2}{2m} + \varepsilon_F \right\} G_{\alpha\beta}(x - x') - i\zeta F_{\alpha\gamma}(0+)\, F^{+}_{\gamma\beta}(x - x') = \hat{1}_{\alpha\beta}\delta(x - x'). \tag{1.116}$$

The equation for $F^{+}_{\alpha\beta}(x - x')$ follows analogously:

$$\left\{ i\frac{\partial}{\partial t} - \frac{\nabla^2}{2m} - \varepsilon_F \right\} F^{+}_{\alpha\beta}(x - x') + i\zeta F^{+}_{\alpha\gamma}(0+)\, G_{\gamma\beta}(x - x') = 0. \tag{1.117}$$

1.3.3. Spin-Singlet Pairing

We can now exclude the dependence on the spin variables (this is permitted in the case of interactions, which do not depend explicitly on the spins of particles). Green's functions may be presented in this case as the products of orbital and spin parts. The diagonal Green's function $G_{\alpha\beta}(x - x')$ is proportional to the unity matrix $\hat{1} \equiv \delta_{\alpha\beta}$:

$$G_{\alpha\beta}(x - x') = G(x - x')\,\delta_{\alpha\beta}, \tag{1.118}$$

whereas the off-diagonal functions F^{+} and F are proportional to the matrix, which is antisymmetric in the spin indices

$$F^{+}_{\alpha\beta}(x - x') = I_{\alpha\beta}F^{+}(x - x'), \tag{1.119}$$

$$F_{\alpha\beta}(x - x') = -I_{\alpha\beta}F(x - x'), \tag{1.120}$$

where $I_{\alpha\beta} = i(\sigma_y)_{\alpha\beta}$ is related to the second of the Pauli matrices:

$$\hat{\sigma}_x = \begin{pmatrix} 0 & 1 \\ 1 & 0 \end{pmatrix}, \hat{\sigma}_y = \begin{pmatrix} 0 & -i \\ i & 0 \end{pmatrix}, \hat{\sigma}_z = \begin{pmatrix} 1 & 0 \\ 0 & -1 \end{pmatrix}. \tag{1.121}$$

This antisymmetry characterizes the singlet pairing of the electrons assumed in the BCS model, and we will adopt it in further analysis. [In the case of triplet pairing, the choice of $I_{\alpha\beta}$ is ambiguous (see, e.g., Refs. 45 and 46) and leads to states with different free energies.] The system of general equations for the superconductors now acquires the form

$$\left\{ i\frac{\partial}{\partial t} + \frac{\nabla^2}{2m} + \varepsilon_F \right\} G(x-x') - i\zeta F(0+)\, F^+(x-x') = \delta(x-x'), \tag{1.122}$$

$$\left\{ i\frac{\partial}{\partial t} - \frac{\nabla^2}{2m} - \varepsilon_F \right\} F^+(x-x') + i\zeta F^+(0+)\, G(x-x') = 0, \tag{1.123}$$

where $F^+(0+) = F(0+)^*$.

1.3.4. Solutions in Momentum Representation

In the momentum space, Eqs. (1.122) and (1.123) may be rewritten as ($P = \mathbf{p}, \varepsilon$):

$$\{\varepsilon - p^2/2m + \varepsilon_F\}\, G(P) - i\zeta F(0+)\, F^+(P) = 1, \tag{1.124}$$

$$\{\varepsilon + p^2/2m - \varepsilon_F\}\, F^+(P) + i\zeta F^+(0+)\, G(P) = 0. \tag{1.125}$$

Or, counting the energy $\xi_{\mathbf{p}}$ from the Fermi energy level ε_F, $\xi_{\mathbf{p}} = p^2/2m - \varepsilon_F \approx v_F(p - p_F)$,

$$\{\varepsilon - \xi_{\mathbf{p}}\}\, G(P) - i\zeta F(0+)\, F^+(P) = 1, \tag{1.126}$$

$$\{\varepsilon + \xi_{\mathbf{p}}\}\, F^+(P) + i\zeta F^+(0+)\, G(P) = 0. \tag{1.127}$$

The solution of Eqs. (1.126) and (1.127) has the form

$$G(\mathbf{p},\varepsilon) = \frac{\varepsilon + \xi_{\mathbf{p}}}{\varepsilon^2 - \xi_{\mathbf{p}} - |\Delta|^2}, \; F^+(\mathbf{p},\varepsilon) = -\frac{\Delta^*}{\varepsilon^2 - \xi_{\mathbf{p}} - |\Delta|^2}, \tag{1.128}$$

where

$$\Delta = -i\zeta F(0+), \quad \Delta^* = i\zeta F^+(0+). \tag{1.129}$$

[One should bear in mind that since the case of $T = 0$ is being considered here, $\Delta = \Delta_0 = \Delta\,(T = 0)$.]

The rules to bypass the poles in Eq. (1.128) are defined by the Landau theorem (see, e.g., Ref. 42), using which one can obtain

$$G\,(\mathbf{p},\varepsilon) = \frac{\varepsilon + \xi_{\mathbf{p}}}{(\varepsilon - \varepsilon_{\mathbf{p}} + i\delta)\,(\varepsilon + \varepsilon_{\mathbf{p}} - i\delta)}, \tag{1.130}$$

$$F^{+}\,(\mathbf{p},\varepsilon) = -\frac{\Delta^{*}}{(\varepsilon - \varepsilon_{\mathbf{p}} + i\delta)\,(\varepsilon + \varepsilon_{\mathbf{p}} - i\delta)}, \tag{1.131}$$

where $\xi_{\mathbf{p}}$ is the excitation spectrum of the superconductor

$$\varepsilon_{\mathbf{p}} = \sqrt{\xi_{\mathbf{p}} + |\Delta|^2} \tag{1.132}$$

with a gap $|\Delta|$. To find the value of the gap, definition (1.129) may be used.

1.3.5. Self-consistency Equation

Substituting Eq. (1.131) into (1.129), one arrives (with $|\Delta| \neq 0$) at the self-consistency equation

$$1 = -\frac{\zeta}{2(2\pi)^3}\int \frac{d^3\mathbf{p}}{\sqrt{\xi_{\mathbf{p}}^2 + |\Delta|^2}}. \tag{1.133}$$

Integration in Eq. (1.133) over the angles and energy leads to divergence of the integral at large energies. Integrating in symmetric limits over $\xi_{\mathbf{p}}$, one finds

$$1 = -\frac{\zeta}{2\pi^2}\, mp_F \ln\frac{2\bar{\varepsilon}}{|\Delta|}, \tag{1.134}$$

where $\bar{\varepsilon}$ is some boundary value of $\xi_{\mathbf{p}}$, which depends on the model's assumptions. From Eq. (1.134) it follows that

$$\Delta_0 = \Delta\,(T = 0) = 2\bar{\varepsilon}e^{-1/\zeta_0}, \tag{1.135}$$

where

$$\zeta_0 = \frac{|\zeta| mp_F}{2\pi^2} = |\zeta|\, N\,(0). \tag{1.136}$$

In Eq. (1.136) $N(0)$ denotes the density of energy levels for the electrons on the Fermi surface in a normal metal.

1.3.6. Isotope Effect

In the model based on the Hamiltonian (1.104), the value of Δ_0 (and as we will see further, the critical temperature of transition, $T_c \propto \Delta_0$) may be arbitrarily large if there is no restriction on the value of $\bar{\varepsilon}$. In the traditional BCS model, it was assumed that only the electrons in the "Debye crust" near the Fermi surface take part in the pairing interaction, since the interaction is mediated by phonons. This assumption is probably the weakest in the BCS picture, if it is considered from the point of view of high-temperature superconductivity. Nevertheless, we will accept this assumption and put $\bar{\varepsilon} = \omega_D$ in the expressions (1.134) and (1.135) and further on. Since $\omega_D \propto M^{-1/2}$, where M is the lattice ion mass, it follows that $T_c \propto \Delta_0 \propto M^{-1/2}$. This leads to the difference in T_c between the same metals of different isotope composition, which is well confirmed experimentally for the usual superconductors.*

1.3.7. Gauge Invariance

Gauge invariance is an important property of Gor'kov's equations. Electromagnetic fields may be introduced into the system of Eqs. (1.122) and (1.123) by the usual operator replacement

$$\nabla \to \nabla - ie\mathbf{A} \quad \text{or} \quad \nabla \to \nabla + ie\mathbf{A}. \tag{1.137}$$

depending on whether the space derivatives apply to the function Ψ or $\Psi^\dagger$, respectively (in the same manner the time derivation operator gains the addition of $\pm ie\varphi$). The equations for G and F^+ may be written as

$$\left\{ i\frac{\partial}{\partial t} + e\varphi + \frac{1}{2m}\left(\frac{\partial}{\partial \mathbf{r}} - ie\mathbf{A}\right)^2 + \varepsilon_F \right\} G(x,x') + \Delta F^+(x,x') = \delta(x - x'), \tag{1.138}$$

$$\left\{ i\frac{\partial}{\partial t} - e\varphi - \frac{1}{2m}\left(\frac{\partial}{\partial \mathbf{r}} + ie\mathbf{A}\right)^2 - \varepsilon_F \right\} F^+(x,x') + \Delta^*(x,x')G(x,x') = 0. \tag{1.139}$$

The functions G, F, and F^+ in the presence of an external field depend on each of the variables x, x', and under the gauge transformation

*We should note that there are exceptions to this rule, even for the case of phonon-mediated pairing, e.g., in the case of the PdH (palladium-hydrogen) alloy, where the effects of phonon anharmonicity are significant.[47] The situation with high-temperature superconductors is more complicated, and both anharmonicity and some additional effects may be important there.[48,49]

$$\varphi \to \varphi - \frac{\partial \chi}{\partial t}, \mathbf{A} \to \mathbf{A} + \nabla\chi \tag{1.140}$$

they transform according to the rules

$$G(x, x') \to G(x, x)e^{ie\{\chi(r) - \chi(r')\}}, F(x, x') \to F(x, x)e^{ie\{\chi(r) + \chi(r')\}}, \tag{1.141}$$

which follow from the transformation rules for the field operators Ψ and.Ψ^+

The transformation rules for $F^+(x, x')$ and consequently for Δ^* and $\Delta_,$ are also defined by expression (1.141). So the gauge invariance of Eq. (1.139) is straightforward. It must be stressed that in certain cases it becomes possible to make the value of Δ real by special choice of the gauge. In such cases this value coincides with the gap parameter in the excitation spectrum, which was introduced in the pioneering BCS theory. But in general, $\Delta = \Delta(x)$ is a complex variable and contains additional physical information. This circumstance is one of the important consequences of the Gor'kov theory, as we will see later in Sect. 1.4.

1.3.8. Description at Finite Temperatures

We now generalize the theory to the case of finite temperatures. To do this, it is necessary to apply the Matsubara technique,[42] which introduces the imaginary time coordinate τ. The emerging equations are analogous to (1.122) and (1.123):

$$\left\{-\frac{\partial}{\partial\tau} + \frac{\nabla^2}{2m} + \varepsilon_F\right\} \mathcal{G}(x - x') + \Delta\mathcal{F}^+(x - x') = \delta(x - x'), \tag{1.142}$$

$$\left\{\frac{\partial}{\partial\tau} + \frac{\nabla^2}{2m} + \varepsilon_F\right\} \mathcal{F}^+(x - x') + \Delta^*\mathcal{G}(x - x') = 0, \tag{1.143}$$

where

$$\Delta = |\zeta|\,\mathcal{F}(0+), \quad \Delta^* = |\zeta|\,\mathcal{F}^+(0+). \tag{1.144}$$

Using discrete imaginary frequencies

$$\varepsilon = \varepsilon_n = i\,(2n + 1)\,\pi T, \quad n = 0, \pm 1, \pm 2, \ldots, \tag{1.145}$$

according to relations of the type

$$\mathcal{F}^+(x - x') = T\sum_n e^{-\varepsilon_n\tau}\int \frac{d^3\mathbf{p}}{(2\pi)3}\, e^{i\mathbf{p}\cdot\mathbf{r}}\mathcal{F}^+_\varepsilon(\mathbf{p}) \tag{1.146}$$

[and analogously for $\mathcal{F}(x - x')$ and $\mathcal{G}(x - x')$], one can find from Eqs. (1.142) and (1.143) the system of equations

$$(\varepsilon - \xi_{\mathbf{p}})\, \mathcal{G}_{\varepsilon}(\mathbf{p}) + \Delta \mathcal{F}^{+}_{\varepsilon}(\mathbf{p}) = 1, \tag{1.147}$$

$$(\varepsilon + \xi_{\mathbf{p}})\, \mathcal{F}^{+}_{\varepsilon}(\mathbf{p}) + \Delta^{*} \mathcal{G}_{\varepsilon}(\mathbf{p}) = 0. \tag{1.148}$$

They have the solutions

$$\mathcal{G}_{\varepsilon}(\mathbf{p}) = \frac{\varepsilon + \xi_{\mathbf{p}}}{\varepsilon^2 - \xi^2_{\mathbf{p}} - |\Delta|^2}, \tag{1.149}$$

$$\mathcal{F}^{+}_{\varepsilon}(\mathbf{p}) = \frac{-\Delta^{*}}{\varepsilon^2 - \xi^2_{\mathbf{p}} - |\Delta|^2}. \tag{1.150}$$

1.3.9. Weak-Coupling Ratio $2\Delta(T=0)/T_C$

The gap value $|\Delta|$ may be defined from any of the relations (1.144) and with the help of Eq. (1.150) one can obtain at $|\Delta| \neq 0$ an equation

$$1 = \frac{|\zeta|\, T}{(2\pi)^3} \sum_{n} \int \frac{d^3\mathbf{p}}{-\varepsilon_n^2 + \xi^2_{\mathbf{p}} + |\Delta|^2}. \tag{1.151}$$

The summation over the frequencies may be carried out using the expression

$$\sum_{n=-\infty}^{\infty} [(2n+1)^2\pi^2 + a^2\,]^{-1} = \frac{1}{2a} \tanh \frac{a}{2}. \tag{1.152}$$

As a result we obtain from (1.151) the self-consistency equation

$$1 = \zeta_0 \int_0^{\omega_D} \frac{d\xi_{\mathbf{p}}}{\sqrt{\xi^2_{\mathbf{p}} + |\Delta|^2}} \tanh \frac{\sqrt{\xi_{\mathbf{p}} + |\Delta|^2}}{2T}, \tag{1.153}$$

which determines the gap at arbitrary temperatures. Note that (1.153) may be presented in more transparent form [$\varepsilon = (\xi^2_{\mathbf{p}} + |\Delta|^2)^{1/2}$]:

$$1 = \zeta_0 \int_{|\Delta|}^{\omega_D} \frac{d\varepsilon (1 - 2n^0_{\varepsilon})}{\sqrt{\varepsilon^2 - |\Delta|^2}}, \tag{1.154}$$

where the distribution function of Fermi excitations is given by the formula

$$n^0_{\varepsilon} = \frac{1}{\exp(|\varepsilon|/T) + 1}. \tag{1.155}$$

Setting $T = 0$, one obtains from (1.154) the relation (1.133) for the gap $|\Delta_0|$. At $T = T_c$ the gap $|\Delta|$ vanishes and Eq. (1.154) reduces to the equation defining T_c:

$$1 = \zeta_0 \int_0^{\omega_D} \frac{d\varepsilon}{\varepsilon} \tanh \frac{\varepsilon}{2T_c}. \tag{1.156}$$

from which one obtains

$$T_c = 2\frac{\gamma}{\pi}\omega_D e^{-1/\zeta_0}, \tag{1.157}$$

where γ is the Euler constant: $\gamma \approx 1.78$.

Comparing the quantities (1.135) and (1.157), we find

$$\frac{2|\Delta(T=0)|}{T_c} = \frac{2\pi}{\gamma} \approx 3.53. \tag{1.158}$$

This relation provides an empirical criterion of the quantitative validity of the BCS model. It is fulfilled for most superconductors with weak electron–phonon coupling, for which

$$\zeta_0 << 1. \tag{1.159}$$

The BCS theory describes quite satisfactorily many phenomena occurring in superconductors at thermodynamic equilibrium, even in cases where the inequality (1.159) is violated. In these phenomena, the BCS interaction potential does not reveal itself directly. The inelastic collisions, which were omitted in the simplified BCS picture, are also not important for this class of phenomena. We note now that the BCS–Gor'kov model may be modified to remove these shortcomings. The Migdal–Eliashberg model, which is more realistic and better applicable to the problems of nonequilibrium superconductivity, is considered in detail in Chap. 3.

1.4. SELF-CONSISTENT PAIR FIELD: MICROSCOPIC DERIVATION OF GINZBURG–LANDAU EQUATIONS

Initially, the idea that the gap in the energy spectrum of superconductors may serve as the superconducting order parameter of the phenomenological Ginzburg–Landau theory was contained in the fundamental work of Bardeen, Cooper, and Schrieffer.[33] This idea was confirmed by Gor'kov,[50] whose work has assigned the status of microscopic theory to the Ginzburg–Landau study. In the next section we follow the derivation presented by Gor'kov.[50]

1.4.1. Iterated Equations

The microscopic equations of superconductivity considered in the preceding section may be written in the form

$$\left\{\varepsilon + \frac{1}{2m}\left(\frac{\partial}{\partial \mathbf{r}} - ie\mathbf{A}(\mathbf{r})\right)^2 + \varepsilon_F\right\} \mathcal{G}_\varepsilon(\mathbf{r},\mathbf{r}') + \Delta(\mathbf{r})\mathcal{F}^+_\varepsilon(\mathbf{r},\mathbf{r}') = \delta(\mathbf{r},\mathbf{r}'), \tag{1.160}$$

$$\left\{-\varepsilon + \frac{1}{2m}\left(\frac{\partial}{\partial \mathbf{r}} - ie\mathbf{A}(\mathbf{r})\right)^2 + \varepsilon_F\right\} \mathcal{F}^+_\varepsilon(\mathbf{r},\mathbf{r}') - \Delta^*(\mathbf{r})\mathcal{G}_\varepsilon(\mathbf{r},\mathbf{r}') = 0. \tag{1.161}$$

The parameter Δ^* (and analogously Δ) is connected with an anomalous Green's function by the relation

$$\Delta^*(\mathbf{r}) = |\zeta| T \sum_\varepsilon \mathcal{F}^+_\varepsilon(\mathbf{r},\mathbf{r}), \tag{1.162}$$

where a summation over the frequencies $\varepsilon = i\pi T(2n + 1)$ spreads up to $|\varepsilon| < \omega_D$. Making iterations over Δ in (1.160) and (1.161), one can obtain the result, which it is convenient to display diagrammatically:

$\mathcal{G}(\mathbf{r},\mathbf{r}') =$ 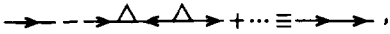 , (1.163)

$\mathcal{F}^+(\mathbf{r},\mathbf{r}') =$ 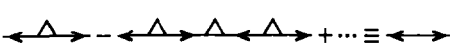 . (1.164)

Here the right arrow corresponds to the normal state function $\mathcal{G}^0$ and the left arrow—to $\overline{\mathcal{G}}^0$; the vertex Δ corresponds to $\Delta(r)$ or $\Delta^*(r)$, depending on the convergence or divergence of neighboring arrows. In addition, the sign of the diagram changes if the vertex Δ enters the diagram twice. This rule should be followed constantly; however, we omit the minus sign on the digram. Taking into account all the terms in the expansions of (1.163) and (1.164) allows us to present Eqs. (1.160) and (1.161) in the integral form:

$$\mathcal{G}_\varepsilon(\mathbf{r},\mathbf{r}') = \mathcal{G}^0_\varepsilon(\mathbf{r},\mathbf{r}') - \int \mathcal{G}^0_\varepsilon(\mathbf{r},\mathbf{r}_1)\Delta(\mathbf{r}_1)\mathcal{F}^+_\varepsilon(\mathbf{r}_1,\mathbf{r}')d^3\mathbf{r}_1, \tag{1.165}$$

$$\mathcal{F}^+_\varepsilon(\mathbf{r},\mathbf{r}') = \int \overline{\mathcal{G}}^0_\varepsilon(\mathbf{r},\mathbf{r}_1)\Delta^*(\mathbf{r}_1)\mathcal{G}_\varepsilon(\mathbf{r}_1,\mathbf{r}')d^3\mathbf{r}_1, \tag{1.166}$$

though only the first terms of this expansion, depicted in (1.163) and (1.164), are needed. The appropriate expressions are

$$\mathcal{G}_\varepsilon(\mathbf{r},\mathbf{r}') = \mathcal{G}^0_\varepsilon(\mathbf{r},\mathbf{r}') - \int \mathcal{G}^0_\varepsilon(\mathbf{r},\mathbf{r}_1)\Delta(\mathbf{r}_1)\overline{\mathcal{G}}^0_\varepsilon(\mathbf{r},\mathbf{r}_2)\Delta^*(\mathbf{r}_2)\mathcal{G}^0_\varepsilon(\mathbf{r}_2,\mathbf{r}')d^3\mathbf{r}_1 d^3\mathbf{r}_2, \tag{1.167}$$

$$\mathcal{F}^{+}_{\varepsilon}(\mathbf{r},\mathbf{r}') = \int \overline{\mathcal{G}}^{\,0}_{\varepsilon}(\mathbf{r},\mathbf{r}_1)\Delta^{*}(\mathbf{r}_1)\mathcal{G}^{0}_{\varepsilon}(\mathbf{r}_1,\mathbf{r}')d^3\mathbf{r}_1$$

$$-\int \overline{\mathcal{G}}^{\,0}_{\varepsilon}(\mathbf{r},\mathbf{r}_1)\Delta^{*}(\mathbf{r}_1)\mathcal{G}^{0}_{\varepsilon}(\mathbf{r}_1,\mathbf{r}_2)\Delta(\mathbf{r}_2)\overline{\mathcal{G}}^{\,0}_{\varepsilon}(\mathbf{r}_2,\mathbf{r}_3)\Delta^{*}(\mathbf{r}_3)\mathcal{G}^{0}_{\varepsilon}(\mathbf{r}_3,\mathbf{r}')d^3\mathbf{r}_1 d^3\mathbf{r}_2 d^3\mathbf{r}_3 . \quad (1.168)$$

For further calculations one must know the function $\mathcal{G}^{0}_{\varepsilon}(\mathbf{r},\mathbf{r}')$. We will find it first in the absence of the magnetic field, putting $\mathbf{A} = 0$ and denoting the corresponding Green's function by $\mathcal{G}^{00}_{\varepsilon}(r)$. Using the definition of $\mathcal{G}^{00}_{\varepsilon}(r)$ and making straightforward calculations, one obtains

$$\mathcal{G}^{00}_{\varepsilon}(r) = \int \frac{d^3\mathbf{p}}{(2\pi)^3} e^{i\mathbf{p}\cdot\mathbf{r}} \frac{1}{\varepsilon - \varepsilon_{\mathbf{p}}} = \int_0^{\infty}\int_{-1}^{1} \frac{p^2\, dp\, d\cos\theta}{(2\pi)^2} e^{ipr\cos\theta} \frac{1}{\varepsilon - \varepsilon_{\mathbf{p}}}$$

$$= -i\int_0^{\infty} \frac{p\, dp}{(2\pi)^2 r}\left(e^{ipr} - e^{-ipr}\right)\frac{1}{\varepsilon - \varepsilon_p} = -\frac{m}{2\pi r}\exp\left\{ip_F r\frac{\varepsilon}{|\varepsilon|} - \frac{|\varepsilon|}{v_F}r\right\}. \quad (1.169)$$

In deriving Eq. (1.169) the relations

$$pdp = md\xi_p, \quad p = p_F + \frac{\xi_p}{v_F} \quad (1.170)$$

were used.

1.4.2. Magnetic Field Inclusion

In the presence of a magnetic field, the function $\mathcal{G}^{0}$ differs from $\mathcal{G}^{00}$ by the phase factor $\varphi(\mathbf{r},\mathbf{r}')$

$$\mathcal{G}^{0}_{\varepsilon}(\mathbf{r},\mathbf{r}') = e^{-\varphi(\mathbf{r},\mathbf{r}')}\mathcal{G}^{00}_{\varepsilon}(|\mathbf{r}-\mathbf{r}'|), \quad (1.171)$$

where $\varphi(\mathbf{r},\mathbf{r}) = 0$. The function $\varphi(\mathbf{r},\mathbf{r}')$ obeys the equation

$$\frac{\partial\varphi}{\partial\mathbf{r}}\cdot\frac{\partial\mathcal{G}^{00}}{\partial\mathbf{r}} = e\mathbf{A}\cdot\frac{\partial\mathcal{G}^{00}}{\partial\mathbf{r}}, \quad (1.172)$$

which may be established from Eqs, (1.171) and (1.160) by taking into account the quasi-classic conditions: $|\mathbf{r}-\mathbf{r}'| >> 1/p_F, p_F >> e\mathbf{A} \sim eH\lambda_L$ (λ_L is the field penetration depth). Because of the spatial homogeneity of $\mathcal{G}^{00}_{\varepsilon}$, the relation follows from (1.172):

$$\mathbf{n}\cdot\frac{\partial}{\partial\mathbf{r}}\varphi(\mathbf{r},\mathbf{r}') = e\mathbf{n}\cdot\mathbf{A}, \quad \mathbf{n} = \frac{\mathbf{r}-\mathbf{r}'}{|\mathbf{r}-\mathbf{r}'|}, \quad (1.173)$$

which would be used further.

1.4.3. Slow Variation Hypothesis

As is evident from Eq. (1.169), the function $\mathcal{G}_\varepsilon^{00}$ (and consequently $\mathcal{G}_\varepsilon^{0}$) decreases over distances on the order of $\xi_0 \sim v_F/|\varepsilon|$. However, the field A near T_c varies over distances greatly exceeding ξ_0: $A(\mathbf{r}) \sim H\lambda_L \sim (1 - T/T_c)^{-1/2}$. This allows us to present the function φ in the form

$$\varphi(\mathbf{r},\mathbf{r}') = e\mathbf{A}(\mathbf{r}) \cdot (\mathbf{r} - \mathbf{r}'). \tag{1.174}$$

Now we are able to derive the equation for parameter Δ. Substituting Eq. (1.168) into (1.162) we find

$$\Delta^*(\mathbf{r}) = |V|\, T\sum_\varepsilon \int \overline{\mathcal{G}}_\varepsilon^{0}(\mathbf{r},\mathbf{r}_1)\Delta^*(\mathbf{r}_1)\, \mathcal{G}_\varepsilon^{0}(\mathbf{r}_1,\mathbf{r})\, d^3\mathbf{r}_1 - |\zeta|\, T\sum_\varepsilon \int \overline{\mathcal{G}}_\varepsilon^{0}(\mathbf{r},\mathbf{r}_1)$$

$$\times \Delta^*(\mathbf{r}_1)\, \mathcal{G}_\varepsilon^{0}(\mathbf{r}_1,\mathbf{r}_2)\Delta(\mathbf{r}_2)\, \overline{\mathcal{G}}_\varepsilon^{0}(\mathbf{r}_2,\mathbf{r}_3)\Delta^*(\mathbf{r}_3)\, \mathcal{G}_\varepsilon^{0}(\mathbf{r}_3,\mathbf{r})\, d^3\mathbf{r}_1\, d^3\mathbf{r}_2\, d^3\mathbf{r}_3 \tag{1.175}$$

Let us suppose that the pair field $\Delta^*(\mathbf{r})$ weakly varies over distances comparable with ξ_0 (this supposition, as we will see, will be confirmed). In the integrand of the first term in (1.175) one can make a series expansion of the parameter $\Delta^*(\mathbf{r})$

$$\Delta^*(\mathbf{r}') = \Delta^*(\mathbf{r}) + \frac{\partial\Delta^*(\mathbf{r})}{\partial\mathbf{r}}(\mathbf{r}' - \mathbf{r}) + \frac{1}{2}\frac{\partial^2\Delta^*(\mathbf{r})}{\partial\mathbf{r}^2}(\mathbf{r}' - \mathbf{r})^2 + \ldots, \tag{1.176}$$

and also keep only the first item in the analogous expansion of the second term in (1.175). Substitution of (1.176) into (1.175) taking into account expressions (1.171) and (1.174), which also could be expanded in powers of the vector potential $\mathbf{A}(\mathbf{r})$, gives the expression

$$\Delta^*(\mathbf{r}) = |\zeta|\, T\sum_\varepsilon \Big\{\Delta^*(\mathbf{r}) \int d^3\mathbf{r}_1\, \overline{\mathcal{G}}_\varepsilon^{00}(r_1)\, \mathcal{G}_\varepsilon^{00}(r_1)$$

$$+ \frac{1}{6}\left(\frac{\partial}{\partial\mathbf{r}} + 2ie\mathbf{A}(\mathbf{r})\right)^2 \Delta^*(\mathbf{r}) \int d^3\mathbf{r}_1\, \overline{\mathcal{G}}_\varepsilon^{00}(r_1)\, \mathcal{G}_\varepsilon^{00}(r_1)\, r_1^2 \tag{1.177}$$

$$- |\Delta|^2\Delta^*(\mathbf{r}) \int d^3\mathbf{r}_1\, d^3\mathbf{r}_2\, d^3\mathbf{r}_3\, \overline{\mathcal{G}}_\varepsilon^{00}(|\mathbf{r} - \mathbf{r}_1|)\, \mathcal{G}_\varepsilon^{00}(|\mathbf{r}_1 - \mathbf{r}_2|)\, \overline{\mathcal{G}}_\varepsilon^{00}(|\mathbf{r}_2 - \mathbf{r}_3|)\, \mathcal{G}_\varepsilon^{00}(|\mathbf{r}_3 - \mathbf{r}|).$$

By direct summation over the discrete frequencies it can be established that

$$T\sum_\varepsilon \overline{\mathcal{G}}_\varepsilon^{00}(r)\mathcal{G}_\varepsilon^{00}(r) = \frac{m^2T}{(2\pi r)^2}\Big/\sinh\frac{2\pi Tr}{v_F}, \tag{1.178}$$

and owing to this, the first of the integrals in (1.177) would diverge, if one does not take into account the "smearing" of the coordinate r over the distances $r \lesssim \xi_0$. In the momentum space one can cut off the summation in (1.177) (at $|\varepsilon| < \omega_D$), which corresponds to this smearing. Using this circumstance, one may write

$$T\sum_{\varepsilon}\int \overline{\mathcal{G}}_{\varepsilon}^{00}(r')\,\mathcal{G}_{\varepsilon}^{00}(r')\,d^3\mathbf{r}' = T\sum_{\varepsilon}\int \frac{d^3\mathbf{p}}{(2\pi)^3}\,\frac{1}{(\xi_{\mathbf{p}}+\varepsilon)(\xi_{\mathbf{p}}-\varepsilon)}$$

$$= \frac{mp_F}{2\pi^2}\,T\sum_{\varepsilon}\int_0^{\omega_D}\frac{d\xi_{\mathbf{p}}}{\xi_{\mathbf{p}}-\varepsilon^2} = \frac{mp_F}{2\pi^2}\int_{-\omega_D}^{\omega_D}\frac{d\xi_{\mathbf{p}}}{\xi_{\mathbf{p}}}\tanh\frac{\xi_{\mathbf{p}}}{2T} = \frac{mp_F}{2\pi^2}\left(1+\ln\frac{T_c}{T}\right). \qquad (1.179)$$

The last equality here is obtained by taking into account Eq. (1.156) for the critical temperature. The second integral in (1.177) may be evaluated using the formula (1.178):

$$T\sum_{\varepsilon}\int r_1^2\,\overline{\mathcal{G}}_{\varepsilon}^{00}(r_1)\,\mathcal{G}_{\varepsilon}^{00}(r_1)\,d^3\mathbf{r}_1 = \frac{7}{8}\,\frac{mp_F}{2\pi^2}\,\frac{\zeta(3)v_F^2}{(\pi T)^2}, \qquad (1.180)$$

where $\zeta(3)$ is the Riemann zeta-function.
The third integral is also not too difficult to evaluate:

$$T\sum_{\varepsilon}\int d^3\mathbf{r}_1\,d^3\mathbf{r}_2\,d^3\mathbf{r}_3\,\mathcal{G}_{\varepsilon}^{00}(\mathbf{r}-\mathbf{r}_1)\,\mathcal{G}_{\varepsilon}^{00}(\mathbf{r}_1-\mathbf{r}_2)\,\mathcal{G}_{\varepsilon}^{00}(\mathbf{r}_2-\mathbf{r}_3)\,\mathcal{G}_{\varepsilon}^{00}(\mathbf{r}_3-\mathbf{r})$$

$$= \frac{mp_F}{2\pi^2}\,T\sum_{\varepsilon}\int d\xi_{\mathbf{p}}\,\frac{1}{(\xi_{\mathbf{p}}^2-\varepsilon^2)^2} = \left(\frac{mp_F}{2\pi^2}\right)\frac{7\zeta(3)}{8(\pi T)^2}. \qquad (1.181)$$

Gathering the results, one obtains after complex conjugation the equation for Δ:

$$\left\{-\frac{1}{4m}\left[-i\frac{\partial}{\partial\mathbf{r}}-2e\mathbf{A}(\mathbf{r})\right]^2 + \left[\frac{7\zeta(3)}{6(\pi T_c)^2}\,\varepsilon_F\right]^{-1}\left[\frac{T-T_c}{T_c}+\frac{7\zeta(3)}{8(\pi T_c)^2}\,|\Delta(\mathbf{r})|^2\right]\right\}\Delta(\mathbf{r}) = 0. \qquad (1.182)$$

The BCS potential disappears from the final result, which has the form of the Ginzburg–Landau equation for the wave function.

1.4.4. Evaluation of Phenomenological Parameters

Microscopic derivation permits one to determine the phenomenological parameters in Eq. (1.48). First, the doubled value of the electron's charge should be noted in (1.182): $e_* = 2e$; this is the consequence of the Cooper pairing. For this

reason $m_* = 2m$ was chosen in (1.182) and as may be found in comparison with (1.37),

$$\left(\frac{\partial \alpha}{\partial T}\right)_{T_c} = \frac{6\pi^2 T_c}{7\zeta(3)\varepsilon_F}. \tag{1.183}$$

The value of the coefficient β is sensitive to the normalization of the Ψ-function. In Sect. 1.2 we have adopted a normalization, with $|\Psi|^2$ corresponding to the density of Cooper pairs [see Eq. 1.53)]:

$$\mathbf{j} = 2eN_s\mathbf{v}_s. \tag{1.184}$$

The microscopic treatment is based on the initial expression for the current

$$\mathbf{j} = \lim_{\substack{\mathbf{r}\to\mathbf{r}' \\ \tau\to -0}} 2\left\{\frac{ie}{2m}\left(\nabla_{\mathbf{r}} - \nabla_{\mathbf{r}'}\right) + \frac{e^2}{m}\mathbf{A}(\mathbf{r})\right\} T\sum_{\varepsilon} \mathcal{G}_{\varepsilon}(\mathbf{r},\mathbf{r}')e^{-\varepsilon\tau}. \tag{1.185}$$

Substituting here $\mathcal{G}_{\varepsilon}(\mathbf{r},\mathbf{r}')$ from (1.167), and using the quasi-classical conditions mentioned above (for details see Ref. 42), one can find:

$$\mathbf{j} = \frac{7\zeta(3)N}{16(\pi T_c)^2}\left\{-\frac{ie}{m}\left(\Delta^*\frac{\partial\Delta}{\partial\mathbf{r}} - \Delta\frac{\partial\Delta^*}{\partial\mathbf{r}}\right) - \frac{4e^2|\Delta|}{m}\mathbf{A}(\mathbf{r})\right\}, \tag{1.186}$$

where N is the total density of electrons, which coincides with the normal state value. Comparing (1.186) with (1.51) one can find a relation between Ψ and Δ:

$$\Psi = \left[\frac{7\zeta(3)N}{8(\pi T_c)^2}\right]^{1/2}\Delta. \tag{1.187}$$

Now the parameter β may be obtained with the help of Eqs. (1.182), (1.187), and (1.48):

$$\beta = \frac{6}{7}\frac{(\pi T_c)^2}{\zeta(3)N\varepsilon_F}. \tag{1.188}$$

Another relation to be noted is

$$N_s = \frac{7\zeta(3)|\Delta|^2}{8(\pi T_c)^2}N, \tag{1.189}$$

which follows from Eqs. (1.184) and (1.187) and connects the density of pairs, N_s, near T_c with the total density of electrons in a normal metal, N.

Thus, the microscopic theory not only laid the foundation for the Ginzburg-Landau theory but also defined the phenomenological coefficients entering it. In particular, the temperature-dependent coherence length $\xi(T)$ and the penetration depth $\lambda_L(T)$ may be calculated. One can ascertain now the self-consistency of the assumptions made earlier, that at temperatures $T \approx T_c$ these lengths greatly exceed the correlation length $\xi_0 \sim v_F/T_c$. For the London superconductors these expressions are still valid for temperatures below T_c, though they fail quickly for the Pippard superconductors if the temperature falls. It must be noted that a large class of a superconducting metals, containing nonmagnetic impurities, may be attributed to the London-type superconductors, as we will see in Chap. 3. Hence, the area of applicability of the Ginzburg–Landau equations actually is rather wide.

1.4.5. Failure of the "Quantum-Mechanical Generalization" for Time-Dependent Problems

In the vicinity of a critical temperature T_c, the solutions of the Ginzburg-Landau equations are fully equivalent to the solutions of the BCS equations. At the same time, the Ginzburg–Landau technique is considerably simpler. As we have seen, the "wave function of superconducting electrons" $\Psi(\mathbf{r})$ is closely connected with the field $\Delta(\mathbf{r})$, which characterizes the Cooper pair condensate. If one ignores the nonlinear term in (1.150), then the equation for $\Psi(\mathbf{r})$ formally coincides with the Schrödinger equation for the particle with the charge $2e$ and the mass $2m$. The simplicity and transparency of such an analogy has led to attempts to use the Schödinger-type equation to describe the dynamic properties of superconductors in nonstationary fields: $\mathbf{A} = \mathbf{A}(\mathbf{r},t)$. At first glance, the "natural" extension of Eq. (1.150) for the nonstationary case may be obtained by the quantum-mechanical generalization:

$$i\frac{\partial\Psi(\mathbf{r},t)}{\partial t} = \left\{-\frac{1}{4m}[\nabla - 2ie\mathbf{A}(\mathbf{r},t)]^2 - \frac{6(\pi T_c)^2}{7\zeta(3)\varepsilon_F}\left[\frac{T-T_c}{T_c} + \frac{1}{N}|\Psi|^2\right]\right\}\Psi(\mathbf{r},t). \tag{1.190}$$

Such a generalization, however, leads to a contradiction. This example is from Eliashberg.[51] Indeed, the "continuity equation"

$$\frac{\partial|\Psi|^2}{\partial t} \propto \operatorname{div}\left\{|\Psi|^2\left(\mathbf{A} - \frac{1}{2e}\nabla\theta\right)\right\} \tag{1.191}$$

follows in the usual manner from (1.190). If now one considers the half-space occupied by a superconductor, where $\mathbf{A}$ and Ψ depend only on the coordinate $\hat{\mathbf{z}}$ normal to the surface, $\Psi = \Psi(z)$, $\mathbf{A} = \mathbf{A}(z)$, and the vector $\mathbf{A}$ is parallel to the surface plane, $\mathbf{A} = \hat{\mathbf{x}}A_x(z) + \hat{\mathbf{y}}A_y(z)$, then from (1.191) an absurd result will follow in an arbitrary time-varying field $\mathbf{A}(t)$, the function $|\Psi|^2$ does not change in time:

$div\mathbf{A}|\Psi|^2 = \{\partial/\partial x[|\Psi(z)|^2 A_x(z)] + \partial/\partial y\,[|\Psi(z)|^2 A_y(z)]\} = 0$. Hence the problem of extending the Ginzburg–Landau-type description to the case of nonstationary external fields is not as simple as might be thought. A deeper analysis of the properties of the superconducting state is required to fully appreciate the difficulties that arise and to solve this problem. The forthcoming chapters, particularly Chaps. 2 and 7, will deal with this problem.

REFERENCES

1. H. Kamerlingh-Onnes, Further experiments with liquid helium. G. On the electrical resistance of pure metals, etc., VI. On the sudden change in the rate at which the resistance of mercury disappears. *Communication from the Physical Laboratory of the University of Leiden,* No. 124c, (1911).
2. W. Meissner and R. Ochsenfeld, Ein neuer Effekt bei Einritt der Supraleitfahigkeit, *Naturwiss.* **21**(44), 787–788(1933).
3. F. and H. London, The electromagnetic equations of the superconductor, *Proc. Roy. Soc. Lond.* **A149**, 71–88(1935).
4. Y. Aharonov and D. Bohm, Significance of electromagnetic potentials in the quantum theory, *Phys. Rev.* **115**(3), 485–491 (1959).
5. E. L. Feinberg, On the "special role" of the electromagnetic potentials in quantum mechanics, *Sov. Phys. Uspekhi* **5**(5), 753–760 (1963) *[Usp. Fiz. Nauk* **78**(1), 53–64 (1962)].
6. S. Olariu and 1.1. Popescu, The quantum effects of electromagnetic fluxes, *Rev. Mod. Phys.* **57**(2), 339–436 (1986).
7. F. London, Macroscopical interpretation of superconductivity, *Proc. Roy. Soc. London* **A152,** 24–34(1935).
8. P. A. M Dirac, *The Principles of Quantum Mechanics,* 4th ed., pp. 253–275, Clarendon Press, Oxford (1958).
9. C. Kittel, *Quantum Theory of Solids,* pp. 286–288, Wiley, New York (1963).
10. J. D. Bjorken and S. D. Drell, *Relativistic Quantum Mechanics,* pp. 1–44, McGraw-Hill, New York (1964).
11. C. Kittel, *Introduction to Solid State Physics,* 4th ed., pp. 727–729, Wiley, New York (1971).
12. P. G. De Gennes, *Superconductivity of Metals and Alloys,* pp. 1–272, W.A. Benjamin, New York (1966).
13. D. Lurié and S. Cremer, Zitterbewegung of quasiparticles in superconductors, *Physica* **50**, 224–240(1970).
14. C. J. Pethick and H. Smith, Relaxation and collective motion in superconductors: A two-fluid *description, Ann. Phys.* **119**(1), 133–169(1979).
15. O. Klein, Die Reflection von Elektronen an einen Potentialssprung nach der relativistischen Dynamic von Dirac, Z. *Phys.* **53**, 157–165 (1929).
16. A. F. Andreev, The thermal conductivity of the intermediate state in superconductors, *Sov. Phys. JETP* **19**(5), 1228–1231 (1964) *[Zh. Eksp. i Teor. Fiz.* **46**(5) 1823–1828 (1964)].
17. I. P. Krylov and Yu. V. Sharvin, Radio-frequency size effect in a layer of normal metal bounded by its superconducting phase, *Sov. Phys. JETP* **37**(3), 481–486 (1973) [*Zh. Eksp. i Tear. Fiz.* **64**(3) 946–957(1973)].
18. P. W. Anderson, When the electron falls apart, *Phys. Today,* October, 42–47 (1997).
19. G. E. Blonder, M. Tinkham, and T. M. Klapwijk, Transition from metallic to tunneling regimes in superconducting microconstrictions: Excess current, charge imbalance, and supercurrent conversion, *Phys. Rev. B* **25**(7), 4515–4532 (1982).

20. S. Sinha and K.-W. Ng, Zero bias conductance peak enhancement in $Bi_2Sr_2CaCu_2O_8/Pb$ tunneling junctions, *Phys. Rev. Lett.* **80**(6), 1296–1299 (1998).
21. Y. Tanaka and S. Kashiwaya, Theory of tunneling spectroscopy of d-wave superconductors, *Phys. Rev. Lett.* **74**(17), 3451–3454 (1995).
22. S. Kashiwaya, Y. Tanaka, M. Koyanagi, and K. Kajimura, Theory for tunneling spectroscopy of anisotropic superconductors, *Phys. Rev. B* **53**(5), 2667–2676 (1996).
23. T. P. Devereaux and P. Fulde, Multiple Andreev scattering in superconductor normal-metal superconductor junctions as a test for anisotropic electron pairing, *Phys. Rev. B* **47**(21), 14638–14641 (1993).
24. C.-R. Hu, Midgap surface states as a novel signature for $d_{x_a^2 - x_b^2}$-wave superconductivity, *Phys. Rev. Lett.* **72**(10), 1526–1529 (1994).
25. J. H. Xu, J. H. Miller, Jr., and C. S. Ting, Conductance anomalies in a normal-metal–d-wave superconductor junction, *Phys. Rev. B* **53**(6), 3604–3612 (1996).
26. J. M. Hergenrother, M. T. Tuominen, and M. Tinkham, Charge transport by Andreev reflection through a mesoscopic superconducting island, *Phys. Rev. Lett.* **72**(11), 1742–1745 (1994).
27. B. J. van Wees, P. de Vries, P. Magée, and T. M. Klapwijk, Excess conductance of superconductor-semiconductor interfaces due to phase conjugation between electrons and holes, *Phys. Rev. Lett.* **69**(3), 510–513 (1992).
28. F. W. J. Hekking and Yu. V. Nazarov, Interference of two electrons entering a superconductor, *Phys. Rev. Lett.* **71**(10), 1625–1628 (1993).
29. V. L. Ginzburg and L. D. Landau, To the theory of superconductivity, *Zh. Eksp. i Teor. Fiz.* **20**(12), 1064–1082 (1950), in Russian.
30. L. D. Landau and E. M. Lifshitz, *Statistical Physics,* 2nd ed., pp. 424–454, Addison-Wesley, Reading, MA (1970).
31. E. M. Lifshitz and L. P. Pitaevskii, *Statistical Physics.* Part 2 (Addison-Wesley Publishing Company, Reading, 1980), pp. 450–468.
32. A. A. Abrikosov, *Fundamentals of the Theory of Metals,* pp. 392–396, North-Holland, Amsterdam (1988).
33. J. Bardeen, L. Cooper, and J. Schrieffer, Theory of superconductivity, *Phys. Rev.* **108**(5), 1175–1204(1957).
34. B. S. Deaver and W. M. Fairbank, Jr., Experimental evidence for quantized flux in superconducting cylinders, *Phys. Rev. Lett.* **7**(2), 43–46 (1961).
35. D. R. Doll and M. Nöbauer, Experimental proof of magnetic flux quantization in superconducting ring, *Phys. Rev. Lett.* **7**(2), 51–52 (1961).
36. L. Cooper. Bound electron pairs in a degenerate Fermi gas, *Phys. Rev.* **104**(4), 1189–1190 (1956).
37. L. I. Schiff, *Quantum Mechanics,* 3rd ed., p. 247, McGraw-Hill, New York (1968).
38. S. T. Belyayev, Application of the methods of quantum field theory to a system of bosons, *Sov. Phys. JETP* **7***(2),* 289–299 (1958) [*Zh. Eksp. i Teor. Fiz.* **34**(2), 417–432 (1958)].
39. P. W. Anderson, *Basic Notions of Condensed Matter Physics,* pp. 229–248, Benjamin/Cummings, London, (1984).
40. L. P. Gor'kov, On the energy spectrum of superconductors, *Sov. Phys. JETP* **7**(3), 505–508 (1964) [*Zh. Eksp. i Tear. Fiz.* **34**(3) 735–739 (1958)].
41. J. R. Schrieffer, *Theory of Superconductivity,* pp. 1–282, W. A. Benjamin, New York (1964).
42. A. A. Abrikosov, L. P. Gor'kov, and I. E. Dzyaloshinskii, *Quantum Field Theoretical Methods in Statistical Physics, 2nd* ed., pp. 42–439, Pergamon, Oxford (1965).
43. V. L. Ginzburg, Superconductivity and Superfluidity (What is done and what is not done) *Sov. Phys. Uspekhi.* **40**(4), 407–432 (1997) [*Usp. Fiz. Nauk* **167**(4), 429–454 (1997)].
44. O. Penrose and L. Onsager, Bose-Einstein condensation and liquid helium, *Phys. Rev.* **104**(3), 576–584(1956).

45. V. P, Mineev, Superfluid ^{3}He: Introduction to the subject, *Sov. Phys. Uspekhi* **26**(2), 160–175 (1963) [*Usp. Fiz. Nauk* 139(2), 303-332 (1983)].
46. G. E. Volovik and L. P. Gor'kov, Superconducting classes in heavy-fermion systems, *Sov. Phys. JETP* **61**(4), 843-854 (1985) [Zh. *Eksp. i Teor. Fiz.* **88**(4), 1412–1429 (1985)].
47. E. G. Maximov, in: *High-temperature Superconductivity,* edited by V. L. Ginzburg and D. A. Kirzhnits, pp. 1–364, Consultants Bureau, New York (1982).
48. V. Z. Kresin and S. A. Wolf, Microscopic model for the isotope effect in high-T_c oxides, *Phys. Rev. B* **49**(5), 3652–3654(1994).
49. A. Bill, V. Z. Kresin, and S. A. Wolf, Isotope effect in high-T_c materials: Role of non-adiabaticity and magnetic impurities, *Z. Phys.* ***B*** **104(4)**, 759-763 (1997).
50. L. P. Gor'kov, Microscopic derivation of the Ginzburg-Landau equations in the theory of superconductivity, *Sov. Phys. JETP* **9**(6), 1364–1367 (1959) [*Zh. Eksp. i Teor. Fiz.* **36**(6), 1918–1923 (1959)].
51. G. M. Eliashberg, Theory of nonequilibrium states and nonlinear electrodynamics of superconductors (Thesis Sov. Doct. Degree, Chernogolovka - Moscow, 1971).

2

Dynamics of Gapless Superconductors

The content of the previous chapter enables us to compare the relatively simple Ginzburg–Landau scheme of description with a much more complex field-theoretical approach. The attractiveness of the GL-type description is even greater for time-dependent problems. We have also seen that the generalization of the GL scheme to include time-dependent fields is not a trivial problem. The simplest case which permits such a generalization is the case of gapless superconductors. This case is considered now.

2.1. SCATTERING ON IMPURITIES

2.1.1. Magnetic and Nonmagnetic Impurities

The interaction Hamiltonian of electrons with impurity atoms may be written as

$$\hat{H}_{\text{int}} = \sum_{\alpha} \int \Psi^{+}(x)\hat{\mathcal{B}}(\mathbf{r} - \mathbf{r}_{\alpha})\Psi(x)d^{3}\mathbf{r}, \tag{2.1}$$

where α indicates the impurity atoms, and the potential $\hat{\mathcal{B}}$ is

$$\hat{\mathcal{B}}(\mathbf{r}) = u_1(\mathbf{r}) + u_2(\mathbf{r})(\mathbf{S} \cdot \hat{\boldsymbol{\sigma}}). \tag{2.2}$$

In expression (2.2) the potentials $u_1(\mathbf{r})$ and $u_2(\mathbf{r})$ stand for the exchange interactions of electrons with nonmagnetic and magnetic impurities, respectively; $\hat{\boldsymbol{\sigma}}$ is the spin matrix of the electron; $\mathbf{S}$ is the magnetic moment of the impurity atom.

2.1.2. Diagram Expansion and Spatial Averaging for Normal Metals

A diagram technique for the scattering of electrons on impurity atoms may be constructed in the usual manner—by the series expansion of the *S*-matrix. We use here the approach developed by Abrikosov and Gor'kov.[1–3] It is convenient to consider the properties of this diagram expansion on a normal metal, using Eq. (2.2) $\hat{\mathcal{B}} = u_1$. Using an × (cross) to mark the interaction vertex of electrons with impurities, we obtain the diagram series

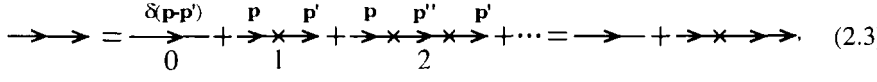

(2.3)

or in analytic form*:

$$G(\mathbf{p}, \mathbf{p}') = \delta(\mathbf{p} - \mathbf{p}')G^0(\mathbf{p}) + \sum_{\alpha} G^0(\mathbf{p}) \int u(\mathbf{p} - \mathbf{p}'')e^{i(\mathbf{p}-\mathbf{p}'')\cdot\mathbf{r}_\alpha} G(\mathbf{p}'', \mathbf{p}') \frac{d^3\mathbf{p}''}{(2\pi)^3} \qquad (2.4)$$

[the combination $u(\mathbf{q})e^{i\mathbf{q}\cdot\mathbf{r}_\alpha}\delta(\varepsilon - \varepsilon')$ with summing over α corresponds to the interaction vertex, where $\mathbf{q}$ is the momentum transferred, and $u(\mathbf{q})$ is the Fourier component of the potential u_1]. Equation (2.4) should be averaged over the impurity coordinates, assuming their chaotic spatial distribution. The averaged values will be denoted by bars above the symbols. Because the averaging procedure is applied to a large volume with many impurity atoms,

$$\overline{G(\mathbf{p}, \mathbf{p}')} = G(\mathbf{p})\delta(\mathbf{p} - \mathbf{p}'). \qquad (2.5)$$

After the averaging, diagram 2 in the series (2.3) becomes proportional to the potential $u(\mathbf{p}'' - \mathbf{p}')u(\mathbf{p} - \mathbf{p}'')e^{i(\mathbf{p}-\mathbf{p}'')\cdot\mathbf{r}_\alpha + i(\mathbf{p}''-\mathbf{p}')\cdot\mathbf{r}_\beta}$, and the averaging yields an expression analogous to the one from diagram 1 in all cases, except when $\mathbf{r}_\alpha = \mathbf{r}_\beta$ and $\mathbf{p} = \mathbf{p}'$. As a result, the averaging of diagram 2 gives

$$\overline{G^{(2)}(\mathbf{p}, \mathbf{p}')} = G^0(\mathbf{p}) \overline{\sum_{\alpha} e^{i(\mathbf{p}-\mathbf{p}')\cdot\mathbf{r}_\alpha}} \int \frac{d^3\mathbf{p}''}{(2\pi)^3} u(\mathbf{p} - \mathbf{p}'')u(\mathbf{p}'' - \mathbf{p}')G^0(\mathbf{p}'')G^0(\mathbf{p}')$$

$$= n \int |u(\mathbf{p} - \mathbf{p}')|^2 G^0(\mathbf{p}') \frac{d^3\mathbf{p}'}{(2\pi)^3} [G^0(\mathbf{p})]^2 \, \delta(\mathbf{p} - \mathbf{p}') \; . \qquad (2.6)$$

where $n = N_i/V_0$ is the density of impurity atoms. Using the explicit expression for $G^0(\mathbf{p}, \varepsilon) = [\varepsilon - \xi_{\mathbf{p}} + i\delta \operatorname{sign} \xi_{\mathbf{p}}]^{-1}$, one can find from Eq. (2.6)

*Because the impurity field is a static one, we omit in this section the variable ε in the propagators $G(\mathbf{p}, \mathbf{p}', \varepsilon)$, $G^0(\mathbf{p}, \varepsilon)$ etc., showing this variable explicitly only when its presence is essential.

$$\overline{G^{(2)}(\mathbf{p}, \varepsilon)} = [G^0(\mathbf{p}, \varepsilon)]^2 \frac{i \operatorname{sign} \varepsilon}{2\tau}, \tag{2.7}$$

where

$$\frac{1}{\tau} = \frac{nmp_F}{(2\pi)^2} \int |u(\theta)|^2 d\Omega \tag{2.8}$$

is the (electron) elastic scattering time. Thus the main contribution arises from the diagrams containing crosses, which correspond to the same atoms. It is convenient to link these crosses by broken lines. The diagrams with three crosses provide nothing new. The fourth order of the perturbation theory generally is represented by the diagram

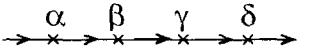

$$= \sum_{\alpha\beta\gamma\delta} \int u(\mathbf{p} - \mathbf{p}_1) e^{i(\mathbf{p}-\mathbf{p}_1)\cdot\mathbf{r}_\alpha} G^0(\mathbf{p}_1)$$

$$\times u(\mathbf{p}_1 - \mathbf{p}_2) e^{i(\mathbf{p}_1-\mathbf{p}_2)\cdot\mathbf{r}_\beta} G^0(\mathbf{p}_2) u(\mathbf{p}_2 - \mathbf{p}_3) e^{i(\mathbf{p}_2-\mathbf{p}_3)\cdot\mathbf{r}_\gamma} G^0(\mathbf{p}_3)$$

$$\times e^{i(\mathbf{p}_3-\mathbf{p}')\cdot\mathbf{r}_\delta} u(\mathbf{p}_3 - \mathbf{p}') \frac{d^3\mathbf{p}_1 d^3\mathbf{p}_2 d^3\mathbf{p}_3}{(2\pi)^9}. \tag{2.9}$$

A comparison of contributions from the diagrams

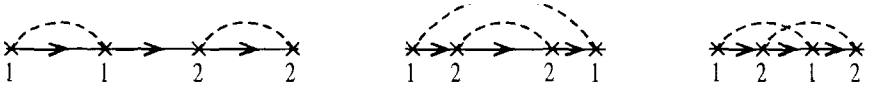

(2.10)

shows that the diagrams with intersected broken lines contain a small parameter $1/(\varepsilon_F\tau) \sim 1/(p_F l)$, where l is the electron's mean-free-path. Indeed, for the first of the diagrams in (2.10) we have

$$G_1^{(4)} \sim \sum_{\alpha,\gamma} \int u(\mathbf{p} - \mathbf{p}_1) e^{i(\mathbf{p}-\mathbf{p}_1)\cdot\mathbf{r}_\alpha} G^0(\mathbf{p}_1) u(\mathbf{p}_1 - \mathbf{p}_2) e^{i(\mathbf{p}_1-\mathbf{p}_2)\cdot\mathbf{r}_\alpha}$$

$$\times G^0(\mathbf{p}_2) u(\mathbf{p}_2 - \mathbf{p}_3) e^{i(\mathbf{p}_2-\mathbf{p}_3)\cdot\mathbf{r}_\gamma} G^0(\mathbf{p}_3) e^{i(\mathbf{p}_3-\mathbf{p}')\cdot\mathbf{r}_\gamma} u(\mathbf{p}_3 - \mathbf{p}')$$

$$\times \frac{d^3\mathbf{p}_1 d^3\mathbf{p}_2 d^3\mathbf{p}_3}{(2\pi)^9}. \tag{2.11}$$

After averaging over the impurity positions, this transforms to

$$\overline{G_1^{(4)}} = \sum_{\alpha,\gamma} \int u(\mathbf{p}-\mathbf{p}_1)\overline{e^{i(\mathbf{p}-\mathbf{p}_2)\cdot\mathbf{r}_\alpha} e^{i(\mathbf{p}_2-\mathbf{p}')\cdot\mathbf{r}_\gamma}} G^0(\mathbf{p}_1)G^0(\mathbf{p}_2)$$

$$\times G^0(\mathbf{p}_3)u(\mathbf{p}_1-\mathbf{p}_2)u(\mathbf{p}_2-\mathbf{p}_3)u(\mathbf{p}_3-\mathbf{p}')\frac{d^3\mathbf{p}_1 d^3\mathbf{p}_2 d^3\mathbf{p}_3}{(2\pi)^9}$$

$$= \frac{(2\pi)^6}{V_0^2}\sum_{\alpha,\gamma}\int |u(\mathbf{p}-\mathbf{p}_1)|^2 G^0(\mathbf{p}_1)G^0(\mathbf{p})G^0(\mathbf{p}_3)|u(\mathbf{p}'-\mathbf{p}_3)|^2\frac{d^3\mathbf{p}_1 d^3\mathbf{p}_3}{(2\pi)^6}$$

$$\times \delta(\mathbf{p}-\mathbf{p}') \sim G^0(p)\frac{1}{\tau^2}\delta(\mathbf{p}-\mathbf{p}') \quad . \tag{2.12}$$

At the same time, the third of the diagrams in (2.10) yields

$$G_3^{(4)} \sim \sum_{\alpha,\gamma}\int u(\mathbf{p}-\mathbf{p}_1)e^{i(\mathbf{p}-\mathbf{p}_1)\cdot\mathbf{r}_\alpha}G^0(\mathbf{p}_1)u(\mathbf{p}_1-\mathbf{p}_2)e^{i(\mathbf{p}_1-\mathbf{p}_2)\cdot\mathbf{r}_\gamma}G^0(\mathbf{p}_2)$$

$$\times u(\mathbf{p}_2-\mathbf{p}_3)e^{i(\mathbf{p}_2-\mathbf{p}_3)\cdot\mathbf{r}_\alpha}G^0(\mathbf{p}_3)e^{i(\mathbf{p}_3-\mathbf{p}')\cdot\mathbf{r}_\gamma}u(\mathbf{p}_3-\mathbf{p}')\frac{d\mathbf{p}_1\, d\mathbf{p}_2\, d\mathbf{p}_3}{(2\pi)^9}, \tag{2.13}$$

or, after averaging over the impurities,

$$\overline{G_3^{(4)}} \sim \frac{(2\pi)^6}{V_o^2}\sum_{\alpha,\gamma}\int \delta(\mathbf{p}-\mathbf{p}_1+\mathbf{p}_2-\mathbf{p}_3)\delta(\mathbf{p}_1-\mathbf{p}_2+\mathbf{p}_3-\mathbf{p}')$$

$$\times G^0(\mathbf{p}_1)G^0(\mathbf{p}_2)G^0(\mathbf{p}_3)u(\mathbf{p}-\mathbf{p}_1)u(\mathbf{p}_1-\mathbf{p}_2)u(\mathbf{p}_2-\mathbf{p}_3)u(\mathbf{p}_3-\mathbf{p}')$$

$$\times\frac{d^3\mathbf{p}_1 d^3\mathbf{p}_2 d^3\mathbf{p}_3}{(2\pi)^9} = \frac{(2\pi)^6}{V_0^2}\sum_{\alpha,\gamma}\int |u(\mathbf{p}_1-\mathbf{p}_2)|^2|u(\mathbf{p}-\mathbf{p}_1)|^2 G^0(\mathbf{p}_1)$$

$$\times G^0(\mathbf{p}_2)G^0(\mathbf{p}-\mathbf{p}_1+\mathbf{p}_2)\frac{d^3\mathbf{p}_1 d^3\mathbf{p}_2}{(2\pi)^9}\delta(\mathbf{p}-\mathbf{p}') \quad . \tag{2.14}$$

Restrictions that follow from the angle integration in Eq. (2.14) require that one of the G-functions be of the order $G \sim 1/\varepsilon_F$. Meanwhile in expression (2.13) the same function is of the order $G \sim \tau$ in the region important for integration. This circumstance confirms the statement on diagrams with intersections. The situation is analogous to the case of the second and third diagrams (2.10).

2.1.3. Born's Approximation

Apart from the diagrams considered (2.10), there is another one of the fourth order:

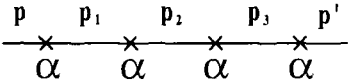

(2.15)

The contribution of such diagrams is essential in the case of non-Born scattering. We consider the opposite situation*

$$P_F^3 \int u(\mathbf{r}) d^3\mathbf{r} \ll \varepsilon_F, \tag{2.16}$$

where one can omit contributions such as Exp. (2.15).

Let us now sum the selected diagrams. We have

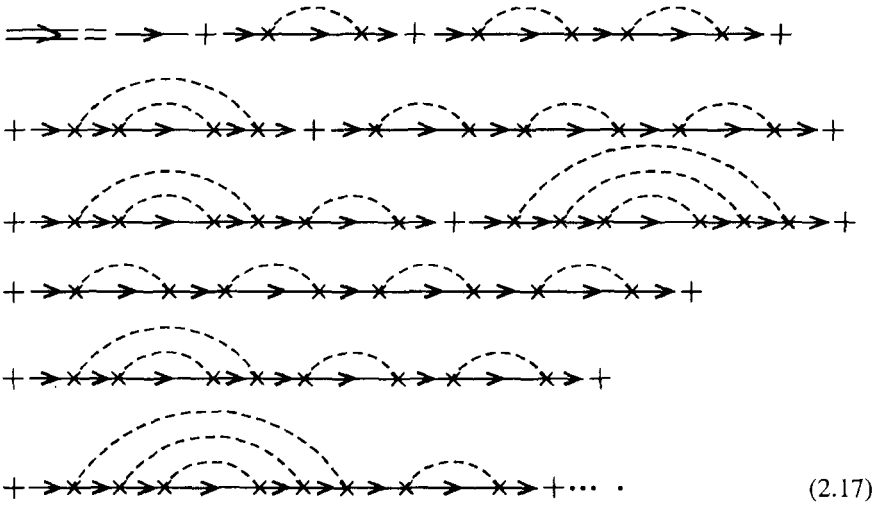

(2.17)

It is not difficult to see that the result of the graphical summation of series (2.17) may be depicted as

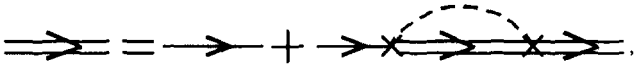

(2.18)

or in analytic form

$$G(\mathbf{p}) = G^0(\mathbf{p}) + nG^0(\mathbf{p}) \int |u(\mathbf{p}-\mathbf{p}')|^2 G(\mathbf{p}') \frac{d^3\mathbf{p}'}{(2\pi)^3} G(\mathbf{p}). \tag{2.19}$$

*This assumption is satisfactory for our immediate purposes. However, when we discuss electron scattering by magnetic impurities later, continuing to make this assumption results in the failure to predict the Kondo effect[4] and its very interesting consequences for transport phenomena in metals, especially in the case of thermoelectricity.[5–10]

The solution of Dyson's equation (2.19), as usual, may be presented in the form,

$$G(\mathbf{p}, \varepsilon) = \frac{1}{[G^0(\mathbf{p}, \varepsilon)]^{-1} - \Sigma^{\text{imp}}} \tag{2.20}$$

where, since it follows from Eqs. (2.19) and (2.20), the self-energy part Σ^{imp} is defined by the equation

$$\Sigma^{\text{imp}} = n \int \frac{d^3\mathbf{p}'}{(2\pi)^3} |u(\mathbf{p} - \mathbf{p}')|^2 \frac{1}{[G^0(\mathbf{p}, \varepsilon)]^{-1} - \Sigma^{\text{imp}}}. \tag{2.21}$$

Assuming Σ^{imp} is purely imaginary, $\Sigma^{\text{imp}} = -i\beta$, we find in analogy with Eq. (2.7):

$$\beta = \frac{\text{sign } \beta}{2\tau}. \tag{2.22}$$

Comparing Eq. (2.22) with the limiting case $G \to G^0$, one finds $\beta = \text{sign } \varepsilon/2\tau$ and, consequently,

$$G(\mathbf{p}, \varepsilon) = \frac{1}{\varepsilon - \xi_{\mathbf{p}} + \dfrac{i}{2\tau} \text{sign } \varepsilon}. \tag{2.23}$$

Moving now from (2.23) to the coordinate representation:

$$G(\mathbf{r}, t) = \int e^{i\mathbf{pr} - i\varepsilon t} G(\mathbf{p}, \varepsilon) \frac{d\varepsilon\, d^3\mathbf{p}}{(2\pi)^4} \tag{2.24}$$

and taking into account formula (1.170), we rewrite (2.24) in the form

$$G(\mathbf{r}, t) = \frac{m}{i(2\pi)^2 r} \int_{-\infty}^{\infty} \frac{d\varepsilon}{2\pi} e^{-i\varepsilon t} \int_{-\infty}^{\infty} \frac{d\xi_{\mathbf{p}}}{\varepsilon - \xi_{\mathbf{p}} + i \text{ sign } \varepsilon/2\tau} \times \left[\exp\left\{ i \left(p_F + \frac{\xi_P}{v_F} \right) r \right\} - \exp\left\{ -i \left(p_F + \frac{\xi_P}{v_F} \right) r \right\} \right]. \tag{2.25}$$

Closing the integration contour over $\xi_{\mathbf{p}}$ in the upper and lower half-planes for the first and second integrals in (2.25), respectively, and noting that the first integral is nonzero at $\varepsilon > 0$ and the second at $\varepsilon < 0$ only, we find

$$G(\mathbf{r}, t) = -\frac{m}{2\pi r} e^{-r/2l} \left\{ \int_0^{\infty} \frac{d\varepsilon}{2\pi} e^{-i\varepsilon t} e^{ip_F r + i\varepsilon r/v_F} + \int_{-\infty}^{0} \frac{d\varepsilon}{2\pi} e^{-i\varepsilon t} e^{-ip_F r - i\varepsilon r/v_F} \right\}$$

$$= e^{-r/2l} \left\{ \int_{-\infty}^{\infty} \frac{d\varepsilon}{2\pi} e^{-i\varepsilon t} \frac{m}{2\pi r} \left[e^{i(p_F + \varepsilon/v_F) r \text{ sign } \varepsilon} \right] \right\} = e^{-r/2l} G^0(\mathbf{r}, t), \tag{2.26}$$

where $l = v_F\tau$ is the electron mean-free-path.

2.1.4. Equations for a Superconducting State

For superconductors we have the system of equations

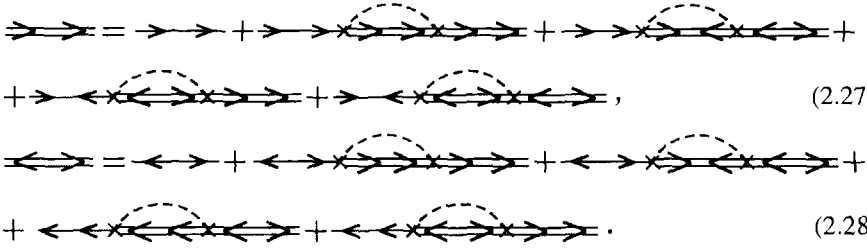

(2.27)

(2.28)

in analogy with (2.18) (here we set $\hat{\mathcal{B}} = u_1$). Let us make the series expansion in (2.27) and (2.28) in powers of the Bose field Δ, for example, in an equation for the G-function:

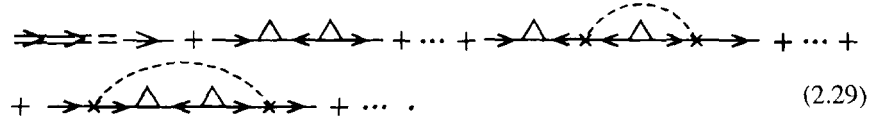

(2.29)

Separating the free line ⟶ in this diagram, we obtain a remaining series

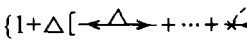

plus a class of diagrams with even numbers of Δ, which enter the sum after the sign of the cross (we do not distinguish here between Δ and Δ^*):

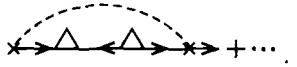

Two options are possible when the external broken line is separated from such a diagram: there is either an even or an odd number of vertices Δ in the inner and in the outer regions of this broken line. Summation of these two classes of diagrams yields

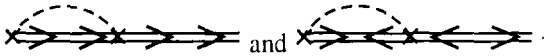

(2.30)

Thus, we get the equation for the G-function

$$G_0^{-1}G = 1 - \Delta F^+ + \Sigma_1^{\text{imp}} G - \Sigma_2^{\text{imp}} F^+ \tag{2.31}$$

(we have used here the rule concerning the diagram signs mentioned in Sec. 1.4).

In the same manner one can obtain for F^+ the expansion

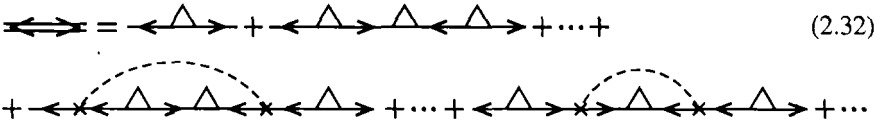

(2.32)

Again, the left free line may be separated, which is followed by the vertex Δ or by a cross. Summing the first class of diagrams, one obtains ΔG. If a vertex

follows an arrow ⟵, one can separate the first external broken line:

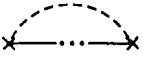

(in the inner part of the diagram series there are broken lines and vertices Δ). If there is an even number of Δ in the inner part, then summation of the diagrams gives the function Σ_1^{imp}, and the function F^+ obviously emerges in the outer part. If the broken line embraces the odd numbers of Δ, then this class of diagrams yields the function $\Sigma_2^{+\text{imp}}$, and the function G emerges in the outer part.

Thus

$$(\overline{G^0})^{-1} F^+ = \Delta^* G + \Sigma_1^{\text{imp}} F^+ + \left(\Sigma_2^+\right)^{\text{imp}} G, \tag{2.33}$$

where $\overline{G^0} = (\varepsilon + \xi_{\mathbf{p}})^{-1}$. Taking into account the definition of functions Σ_1^{imp} and $\Sigma_2^{+\text{imp}}$:

$$\Sigma_1^{\text{imp}} = n \int |u(\mathbf{p} - \mathbf{p}')|^2 G(\mathbf{p}') \frac{d^3\mathbf{p}'}{(2\pi)^3}, \tag{2.34}$$

$$\Sigma_2^{+\text{imp}} = n \int |u(\mathbf{p} - \mathbf{p}')|^2 F^+(\mathbf{p}') \frac{d^3\mathbf{p}'}{(2\pi)^3}, \tag{2.35}$$

and analogously for other two elements of the $\hat{\Sigma}$-matrix (1.114), we obtain the system of equations for superconductors with impurities:

$$\begin{pmatrix} \xi - \varepsilon - \Sigma_1^{\text{imp}} & -(\Delta + \Sigma_2^{\text{imp}}) \\ \Delta^* + \Sigma_2^{+\text{imp}} & \xi + \varepsilon - \Sigma_1^{\text{imp}} \end{pmatrix} \begin{pmatrix} G & F \\ -F^+ & \overline{G} \end{pmatrix}_p = \hat{1}. \tag{2.36}$$

The self-energy matrix here is:

$$\hat{\Sigma}^{\text{imp}} = \begin{pmatrix} \Sigma_1 & \Sigma_2 \\ -\Sigma_2^+ & \Sigma_1 \end{pmatrix}^{\text{imp}} = \frac{1}{2\pi\tau} \frac{2\pi^2}{mp_F} \int \frac{d^3\mathbf{p}}{(2\pi)^3} \hat{G}(\mathbf{p}, \varepsilon), \tag{2.37}$$

as follows from Eqs. (2.34), (2.35), and (2.8).

2.1.5. Anderson's Theorem

The solution of Eqs. (2.36) and (2.37) may be found in the same manner as was done for the normal state. It gives the same formal result: the appearance of exponential factors $e^{-|\mathbf{r}-\mathbf{r}'|/2l}$ in the Green's functions. However, the gap in the energy spectrum of the superconductor is subject to the self-consistency equation (1.144), which includes the superconducting propagator at $\mathbf{r} = \mathbf{r}'$. So evidently nonmagnetic impurities do not influence the thermodynamics of a superconductor.

2.1.6. "Londonization" by Elastic Scattering

Another important consequence follows from the comparison of Eqs. (1.169) and (2.26). At $l < v_F/T_c$, the electron correlation radius in superconductors becomes less than ξ_0. We have mentioned this circumstance in Chap. 1 as the "Londonization" of superconductors by the scattering of elastic impurities. This aspect of the influence of impurities is important for superconductors, making their electrodynamics local.

2.2. MAGNETIC IMPURITIES

When the paramagnetic part of the potential $\hat{\mathcal{B}}(\mathbf{r})$ (2.2) is "switched on," the interaction becomes explicitly dependent on the electrons' spins. Consequently, the spin variables should be preserved in the intermediate calculations of Sect. 2.1. Using the Hamiltonian

$$\hat{H} = -\int \left\{ -\left[\Psi^\dagger(\mathbf{r}) \frac{\nabla^2}{2m} \Psi(\mathbf{r}) \right] + \frac{\zeta}{2} \left[\Psi^\dagger(\mathbf{r}) \left[\Psi^\dagger(\mathbf{r}) \Psi(\mathbf{r}) \right] \Psi(\mathbf{r}) \right] + \left[\Psi^\dagger(\mathbf{r}) \hat{\mathcal{B}} \Psi(\mathbf{r}) \right] \right\} d^3\mathbf{r}, \tag{2.38}$$

*In the theory of superconductivity, this result is sometimes called the *Anderson theorem.*[11]

the following equations of motion for the Heisenberg operators $\Psi(x)$ and $\Psi^{\dagger}(x)$ can be obtained:

$$\left\{ i\frac{\partial}{\partial t} - \frac{\nabla^2}{2m} \right\} \Psi_{\alpha}^{\dagger}(x) + \zeta \Psi_{\alpha}^{\dagger}(x) \left[\Psi^{\dagger}(x)\Psi(x) \right] + \Psi_{\beta}^{\dagger}\sigma_{\beta\alpha} = 0 \tag{2.39}$$

$$\left\{ i\frac{\partial}{\partial t} + \frac{\nabla^2}{2m} \right\} \Psi_{\alpha}(x) - \zeta \left[\Psi^{\dagger}(x)\Psi(x) \right] \Psi_{\alpha}(x) - \Psi_{\beta}\sigma_{\alpha\beta} = 0 \tag{2.40}$$

[as earlier, $x = (\mathbf{r}, t)$; we have included the summation over impurities and the exchange potential in $\sigma_{\alpha\beta}$]. Starting from the definition of Green's functions, taking the derivative of (1.110) and account of (2.38) and using "Gor'kov splitting" (1.112), one obtains the equation

$$\left\{ i\frac{\partial}{\partial t} + \frac{\nabla^2}{2m} + \varepsilon_F \right\} G_{\alpha\beta}(x, x') - \sigma_{\alpha\gamma} G_{\gamma\beta}(x, x') - i\zeta F_{\alpha\gamma}(x, x) F^{+}_{\gamma\beta}(x, x') = \delta_{\alpha\beta}\delta(x - x'), \tag{2.41}$$

where the function $F^{+}_{\alpha\beta}(x, x') = \langle T\Psi_{\alpha}^{\dagger}(x)\Psi_{\beta}^{\dagger}(x') \rangle$ obeys the equation

$$\left\{ i\frac{\partial}{\partial t} - \frac{\nabla^2}{2m} - \varepsilon_F \right\} F^{+}_{\alpha\beta}(x, x') + \sigma^{\dagger}_{\alpha\gamma} F^{+}_{\gamma\beta}(x, x') + i\zeta F^{+}_{\alpha\delta}(x, x) G_{\delta\beta}(x, x') = 0 \tag{2.42}$$

Now, making the series expansion for the functions G and F^{+} on the basis of (2.39) and (2.40), one can see that σ enters into the diagrams  , whereas σ^{tr} enters into the diagrams .

2.2.1. Averaging over Spin Directions

Let us return now to the definition of functions

$\Sigma_1^{imp} =$  , $\Sigma_2^{imp} =$  , $\Sigma_2^{+imp} =$  (2.43)

(see Sect. 2.1). Besides averaging over the spatial distribution of impurities, one must also average over the spin directions, assuming their random orientation. In the absence of impurities it follows that $G_{\alpha\beta} = G\delta_{\alpha\beta}$. If the dashed line is spin dependent, then

$$\overline{G_{\alpha\beta}} = \overline{\sigma_{\alpha\gamma} G_{\gamma\delta} \sigma_{\delta\beta}} = \overline{G}\,\overline{\sigma_{\alpha\gamma}\delta_{\gamma\delta}\sigma_{\delta\beta}} = \overline{G}\delta_{\alpha\beta}. \tag{2.44}$$

Thus, the averaging of diagrams for G-functions adds the term $u_2^2 S(S+1)/3$ to the potential u_1^2. The situation with functions $\overline{F}$ and $\overline{F^{+}}$ is different. The corresponding diagrams contain an additional factor Δ and a line ; for example,

(2.45)

As a result, the part of the diagram represented by a dashed line and containing $\sigma^{tr}\hat{\Delta}\sigma$ will have a sign opposite to $\hat{\Delta}$. Indeed, $\hat{\Delta}_{\alpha\beta} = \Delta I_{\alpha\beta}$ (see 1.119 and 1.120). But $I^{-1}\sigma^{tr}I = -\sigma$, and this causes a chain of relations: $\sigma^{tr}I = -I\sigma; \sigma^{tr}I\sigma = -I\sigma^2 = -I$.

2.2.2 Spin-Flip Time τ_S

The "magnetic" part in the averaged diagrams for F and F^+ has a sign opposite to the part produced by the usual impurities. Accounting for this, the value τ^{-1} in the diagonal components of $\hat{\Sigma}$ in Eq. (2.37) is replaced by

$$\tau_1^{-1} = \frac{nmp_F}{(2\pi)^2}\int\left\{|u_1(\theta)|^2 + |u_2(\theta)|^2\,\frac{1}{3}\,S(S+1)\right\}d\Omega, \tag{2.46}$$

and in nondiagonal components by

$$\tau_2^{-1} = \frac{nmp_F}{(2\pi)^2}\int\left\{|u_1(\theta)|^2 - |u_2(\theta)|^2\,\frac{1}{3}\,S(S+1)\right\}d\Omega. \tag{2.47}$$

The difference in values (2.46) and (2.47) is due exclusively to the magnetic part of the interaction and defines the reciprocal spin-flip time τ_S^{-1}:

$$\tau_1^{-1} - \tau_2^{-1} = 2\tau_S^{-1}. \tag{2.48}$$

2.2.3. Depression of Transition Temperature

Let us now consider the influence of paramagnetic impurities on the thermodynamic properties of superconductors. The initial equations (prior to the impurity averaging) in the representation of the imaginary discrete frequencies $\varepsilon = \varepsilon_n = i\pi T(2n+1)$ have the form

$$\left\{\varepsilon + \frac{\nabla^2}{2m} + \varepsilon_F\right\}\hat{\mathcal{G}}_\varepsilon(\mathbf{r},\mathbf{r}') - \hat{\mathcal{B}}\mathcal{G}_\varepsilon(\mathbf{r},\mathbf{r}') + \hat{\Delta}(\mathbf{r})\hat{\mathcal{F}}_\varepsilon^+(\mathbf{r},\mathbf{r}') = \hat{1}\,\delta(\mathbf{r}-\mathbf{r}'), \tag{2.49}$$

$$\left\{\varepsilon - \frac{\nabla^2}{2m} - \varepsilon_F\right\}\hat{\mathcal{F}}_\varepsilon^+(\mathbf{r},\mathbf{r}') + \hat{\mathcal{B}}^{tr}\hat{\mathcal{F}}_\varepsilon^+(\mathbf{r},\mathbf{r}') + \hat{\Delta}^*(\mathbf{r})\hat{\mathcal{G}}_\varepsilon(\mathbf{r},\mathbf{r}') = 0, \tag{2.50}$$

$$\hat{\Delta}^*(\mathbf{r}) = |\zeta| T \sum_{\varepsilon} \hat{\mathcal{F}}^+_{\varepsilon}(\mathbf{r}, \mathbf{r}'). \tag{2.51}$$

As before, we use the potential $\hat{\mathcal{B}}$ (2.2). It will be shown now that the critical temperature remains unchanged if $u_2 = 0$ and diminishes if $u_2 \neq 0$.

Since the temperatures close to the critical one are of interest, in the expansion of $\mathcal{F}^+$ in powers of the field Δ it is sufficient to retain only the lowest-order diagram:

 (2.52)

Substituting the corresponding analytic expression into the self-consistency equation (2.51), we find

$$\Delta^*_{\alpha\beta}(\mathbf{r}) = |\zeta| T \sum_{\varepsilon} \int \overline{\mathcal{G}}_{\alpha\gamma}(\mathbf{r}, \mathbf{r}') \Delta^*_{\gamma\delta}(\mathbf{r}') \mathcal{G}_{\delta\beta}(\mathbf{r}', \mathbf{r}) d^3\mathbf{r}'. \tag{2.53}$$

The equation for Δ^* must have a nonzero solution at the critical temperature. Averaging (2.53) over the impurity positions and taking into account that $\Delta(\mathbf{r})$ is a smooth function and $\mathcal{G}(\mathbf{r})$ is a rapidly oscillating one, one may write

$$\overline{\Delta^*_{\alpha\beta}(\mathbf{r})} = |\zeta| T \sum_{\varepsilon} \int \overline{\Delta^*_{\gamma\delta}(\mathbf{r}')} \overline{\mathcal{G}_{\alpha\gamma}(\mathbf{r}, \mathbf{r}') \mathcal{G}_{\delta\beta}(\mathbf{r}', \mathbf{r})} d^3\mathbf{r}'. \tag{2.54}$$

The averaging procedure in (2.54) produces the broken lines connecting the crosses not only on the same propagation line, but also on different lines (recall that the potential $\hat{\mathcal{D}}^{\mathrm{I}}$ corresponds to crosses on the G-function's line). In the first case, we have $\sigma_{\alpha\gamma}\sigma_{\gamma\beta} = \delta_{\alpha\beta}$, and a factor $|u_1(\mathbf{q})|^2 + \frac{1}{3} S(S+1)|u_2(\mathbf{q})|^2$ arises for the diagram. This leads to the substitution $l \to l_1 = v_F \tau_1$ in expression (2.26):

$$\overline{\mathcal{G}}_{\varepsilon}(\mathbf{r} - \mathbf{r}') = \mathcal{G}^0_{\varepsilon}(\mathbf{r} - \mathbf{r}') \exp\left(- \frac{|\mathbf{r} - \mathbf{r}'|}{2 l_1} \right). \tag{2.55}$$

Correspondingly, the Fourier component of Eq. (2.55) has the form [compare Eq. (2.23)]:

$$\tilde{\mathcal{G}}_{\varepsilon}(\mathbf{p}) = \frac{1}{\varepsilon \eta_1 - \xi_{\mathbf{p}}}, \qquad \eta_1 = 1 + \frac{1}{2\tau_1 |\varepsilon|}. \tag{2.56}$$

In the second case, one must calculate in (2.54) a "ladder" diagram of "dressed" functions:

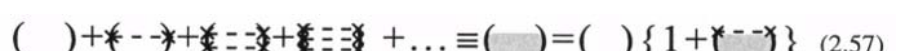 (2.57)

It is expedient to introduce the functions $K_{\alpha\beta}(\mathbf{p}_1, \mathbf{p}_2)$ by the relation

$$\overline{\mathcal{G}_{\alpha\gamma}(\mathbf{r}, \mathbf{r}'')I_{\gamma\delta}\mathcal{G}_{\delta\beta}(\mathbf{r}'', \mathbf{r})} = \int K_{\alpha\beta}(\mathbf{p}_1, \mathbf{p}_2)e^{i\mathbf{p}_1\cdot(\mathbf{r}-\mathbf{r}'')-i\mathbf{p}_2\cdot(\mathbf{r}''-\mathbf{r}')}\frac{d^3\mathbf{p}_1 d^3\mathbf{p}_2}{(2\pi)^6}. \tag{2.58}$$

Then Eq. (2.57) can be presented in the form

$$K_{\alpha\beta}(\mathbf{p}_1, \mathbf{p}_2) = \tilde{\mathcal{G}}_\varepsilon(\mathbf{p}_1)\tilde{\tilde{\mathcal{G}}}_\varepsilon(\mathbf{p}_2)\left\{I_{\alpha\beta} + n\int\frac{d^3\mathbf{p}}{(2\pi)^3}\left[|u_1|^2 + \frac{1}{3}S(S+1)|u_2|^2\sigma_{\alpha\delta}\sigma^{\mathrm{tr}}_{\lambda\beta}K_{\delta\lambda}(\mathbf{p}_1', \mathbf{p}_2')\right]\right\}, \tag{2.59}$$

where $\mathbf{p}_2'$ is defined from the momentum conservation law: $\mathbf{p}_1 + \mathbf{p}_2 = \mathbf{p}_1' + \mathbf{p}_2'$. The spin part of $K_{\alpha\beta}$ can be separated further: $K_{\alpha\beta} = I_{\alpha\beta}K$. After that, a combination of the type $\sigma_{\alpha\delta}\sigma_{\lambda\beta}I_{\delta\lambda}$ appears on the right-hand side of Eq. (2.59), which, as noted earlier, is equal to $(-I_{\alpha\beta})$. So one can write (2.59) in the form

$$K(\mathbf{p}_1, \mathbf{p}_2) = \tilde{\mathcal{G}}(\mathbf{p}_1)\tilde{\tilde{\mathcal{G}}}(\mathbf{p}_2)\{1 + L_\varepsilon\}, \tag{2.60}$$

where

$$L_\varepsilon = n\int\left[|u_1|^2 - \frac{1}{3}S(S+1)|u_2|^2\right]K(\mathbf{p}_1', \mathbf{p}_2')\frac{d^3\mathbf{p}'}{(2\pi)^3}. \tag{2.61}$$

Multiplying Eq. (2.60) by $n\,[|u_1|^2 - \frac{1}{3}S(S+1)|u_2|^2]/(2\pi)^3$ and integrating over $d^3\mathbf{p}_1$, we obtain

$$L_\varepsilon = (1 + L_\varepsilon)n\int\left[|u_1|^2 - \frac{1}{3}S(S+1)|u_2|^2\right]\tilde{\mathcal{G}}(\mathbf{p}_1)\tilde{\tilde{\mathcal{G}}}(\mathbf{p}_2)\frac{d\mathbf{p}_1}{(2\pi)^3}. \tag{2.62}$$

Keeping in mind the self-consistency equation (2.53), we put $\mathbf{p}_1 = \mathbf{p}_2$ in (2.62) and obtain

$$L_\varepsilon = \frac{1}{2\tau_2\varepsilon\eta_S}, \qquad \eta_S = 1 + \frac{1}{2\tau_S|\varepsilon|}, \tag{2.63}$$

taking into account Eqs. (2.48) and (2.56).

We return now to Eq. (2.54) and move the factor $\bar{\Delta}^*$ out from under the integral operator (as in Sect. 1.4, in what follows we will discard the bar above the symbol Δ). Using the expressions (2.58) to (2.63) we find in this way

$$\Delta^*(\mathbf{r}) = \Delta^*(\mathbf{r})|\zeta|T\sum_\varepsilon\int K(\mathbf{p} - \mathbf{p}_1)\frac{d^3\mathbf{p}_1}{(2\pi)^3}$$

$$= \Delta^*(\mathbf{r})|\zeta|T\sum_{\varepsilon}\int\left(1+\frac{1}{2\varepsilon\tau_2\eta_S}\right)\tilde{\mathcal{G}}(\mathbf{p}_1)\tilde{\bar{\mathcal{G}}}(\mathbf{p}_1)\frac{d^3\mathbf{p}_1}{(2\pi)^3}, \tag{2.64}$$

from which the equation for the critical temperature T_c follows:

$$1 = |\zeta|T_c\sum_{\varepsilon}\int\frac{(\eta_1/\eta_S)}{\xi_{\mathbf{p}}^2+(\eta_1|\varepsilon|)^2}\frac{d^3\mathbf{p}}{(2\pi)^3}. \tag{2.65}$$

One can see from this expression that T_c will not change in the absence of magnetic impurities. Indeed, at $u_2 = 0$, $\tau_2 = \tau$, $\eta_S = 1$., Eq. (2.65) transforms to

$$1 = |\zeta|\frac{mp_F}{(2\pi)^2}T_c\sum_{\varepsilon}\int\frac{\eta_1 d\xi_{\mathbf{p}}}{|\varepsilon|^2\eta_1^2+\xi_{\mathbf{p}}^2}. \tag{2.66}$$

Making in (2.66) the replacement $(\xi_{\mathbf{p}}\eta_1) \to \xi_{\mathbf{p}}$, we arrive at Eq. (2.37) determining T_c, which corresponds to a "pure" sample, $\eta_1 = 1$. This verifies the unshifted value of T_c.

The situation is different for $u_2 \neq 0$ when

$$\eta_S = 1+\frac{1}{2\tau_1|\varepsilon|}-\frac{1}{2\tau_2|\varepsilon|} = 1+\frac{1}{\tau_S|\varepsilon|} > 1. \tag{2.67}$$

Restricting ourselves to a crude approximation, we take η_S as a constant.* In this approximation one arrives at the equation

$$1 = \frac{|\zeta|}{\eta_S}T_c\sum_{\varepsilon}\int\frac{\eta_1 d^3\mathbf{p}}{\xi\mathbf{p}^2+(\eta_1|\varepsilon|)^2}, \tag{2.68}$$

which coincides with (2.66), but with a smaller interaction constant and hence [see Eq. (1.157)] with smaller T_c.

2.2.4. Energy Gap Suppression

In the presence of impurities, the single-particle spectrum of the system is not a well-defined quantity, because $\mathbf{p}$ is a bad quantum number. So we will try to determine the value of a gap on the base of reasonings that are slightly different from those used in Sect. 1.3. To solve this problem, we return to the expression for Green's function of a "pure" superconductor at temperature $T = 0$. We present Eq. (1.130) in the form ($\mathcal{P}$ indicates the principal value)

*The exact calculations[2] lead to the following expression for the critical temperature T_c: $\ln(T_{c0}/T_c) = \psi(1/2+\rho/2)-\psi(1/2)$ where ψ is the logarithmic derivative of the Γ-function, $\rho = 1/(\pi\tau_s T_c)$, and T_{c0} is the critical temperature in the absence of impurities.

$$G = \mathcal{P}\frac{\varepsilon + \xi_{\mathbf{p}}}{\varepsilon^2 - \varepsilon_{\mathbf{p}}^2} - i\pi\delta\left(\varepsilon - \sqrt{\Delta^2 + \xi_{\mathbf{p}}^2}\,\operatorname{sign}\xi_{\mathbf{p}}\right). \tag{2.69}$$

The imaginary part of Green's function in (2.69) is determined by the δ-function. The first excited state in the system (at $\xi_{\mathbf{p}} \to 0$) may be found as the minimal positive value of ε: at which Green's function acquires an imaginary part. This conclusion, as was shown by Migdal and Galitzkiy,[12] remains valid in the general case.

Solving the system (2.36) and (2.37) with the help of (2.46) and (2.47), one can find for $G_\varepsilon(\mathbf{p})$ and $F_\varepsilon(\mathbf{p})$ (in a real-order parameter gauge, $\Delta^* = \Delta$) the expressions:

$$G_\varepsilon(\mathbf{p}) = \frac{\bar{\varepsilon} + \xi_{\mathbf{p}}}{\bar{\varepsilon}^2 - \xi^2 - \bar{\Delta}^2}, \qquad F_\varepsilon(\mathbf{p}) = \frac{\bar{\Delta}}{\bar{\varepsilon}^2 - \xi^2 - \bar{\Delta}^2}. \tag{2.70}$$

Here

$$\bar{\varepsilon} = \varepsilon + \frac{i}{2\tau_1}\frac{u}{\sqrt{1-u^2}}, \quad \bar{\Delta} = \Delta + \frac{i}{2\tau_2}\frac{u}{\sqrt{1-u^2}}, \quad u = \frac{\bar{\varepsilon}}{\bar{\Delta}}. \tag{2.71}$$

The equation for the function $u(\varepsilon)$ follows from Eq. (2.71):

$$\frac{\varepsilon}{\Delta} = u\left(1 - \frac{1}{\tau_S\Delta\sqrt{1-u^2}}\right). \tag{2.72}$$

At $\tau_S\Delta > 1$ and for sufficiently small values of ε, both functions u and ε are real. The right-hand side of Eq. (2.72) has the maximum at

$$u_0 = [1 - (1/\tau_S\Delta)^{2/3}]^{1/2} \tag{2.73}$$

at the corresponding value

$$\varepsilon_0 = \Delta\,[1 - (1/\tau_S\Delta)^{2/3}]^{3/2}. \tag{2.74}$$

For larger ε, the solutions u are complex and the quantity $G(\varepsilon)$ acquires an imaginary part. So the quantity ε_0 (2.74) determines the value of the gap in superconductors with paramagnetic impurities.

2.2.5. Gapless Superconductivity

As follows from Eq. (2.74), the value of the gap vanishes at

$$\tau_S\Delta = 1, \tag{2.75}$$

which is possible for $\Delta \neq 0$. This means that for superconductors with paramagnetic impurities, the order parameter Δ does not coincide with the value of the gap.

Let us now determine, at what concentration of impurities Δ vanishes. The self-consistency equation for the order parameter may be written in the form

$$F(0) = \int F_\varepsilon(\mathbf{p}) \frac{d\varepsilon d^3\mathbf{p}}{(2\pi)^4}. \tag{2.76}$$

Integrating (2.76) with the help of (2.71) to (2.73) and (1.129) (for details see Ref. 6), we arrive at the expression (Δ_0 is the gap in a "pure" superconductor):

$$\ln\frac{\Delta}{\Delta_0} = \begin{cases} -\dfrac{\pi}{4\tau_S\Delta} \text{ at } \dfrac{1}{2\tau_S\Delta} \le 1, \\ -\ln\dfrac{1-\sqrt{1-(\tau_S\Delta)^2}}{\tau_S\Delta} - \dfrac{1}{2\tau_S\Delta}\arcsin\tau_S\Delta + \dfrac{1}{2}\sqrt{1-(\tau_S\Delta)^2} \text{ at } \dfrac{1}{2\tau_S\Delta} > 1. \end{cases} \tag{2.77}$$

Setting $\Delta \to 0$ in Eq. (2.77), we have

$$\ln\frac{\Delta}{\Delta_0} = \ln\frac{\tau_S\Delta}{1+\sqrt{1-(\tau_S\Delta)^2}}. \tag{2.78}$$

It follows from Eq. (2.78) that the critical concentration of impurities at which the superconducting order parameter vanishes is determined by the relation

$$\left.\frac{1}{\tau_S}\right|_{\Delta=0} = \frac{\Delta_0}{2}. \tag{2.79}$$

At the same time, as follows from Eqs. (2.77) and (2.75), the gap vanishes when

$$\left.\frac{1}{\tau_S}\right|_{\varepsilon_0=0} = \Delta_0 \exp\left(-\frac{\pi}{4}\right). \tag{2.80}$$

Because $e^{-\pi/4} < 1/2$, one can conclude that superconducting correlations remain in the superconductor while the gap has disappeared. Hence, there is a certain interval of paramagnetic impurity concentration in which gapless superconductivity can be realized. In these gapless superconductors, the quantum correlations in the self-consistent pair field are strong enough to maintain the superfluid nature of the condensate motion (or, in other words, to maintain discussed above "off-diagonal long-range order") despite the absence of the gap in single-electron excitation spectrum.

If the impurity concentration is increased, the gap singularity in a single-particle density of states smears out simultaneously with the vanishing of the gap, as may be seen from Eqs. (2.70) and (2.72) (detailed calculations may be found in Ref. 13 and the corresponding figures in Ref. 14). This property permits us to derive the nonstationary equations of the Ginzburg-Landau type for alloys with magnetic impurities.

2.3. NONSTATIONARY GINZBURG–LANDAU EQUATIONS

As in a stationary case (see Sect. 1.4), the self-consistency equation

$$\Delta_\omega^*(\mathbf{k}) = |\zeta|T \sum_n \int \frac{d^3\mathbf{p}}{(2\pi)^3} \mathcal{F}^+_{\varepsilon\varepsilon-\omega}(\mathbf{p}_1, \mathbf{p}-\mathbf{k}), \qquad \omega = 2n\pi Ti \tag{2.81}$$

may serve as a starting point for derivation of a nonstationary equation for the order parameter $\Delta(\mathbf{r}, t)$. The idea of calculations in a nonstationary situation is to present $\mathcal{F}^+_{\varepsilon\varepsilon-\alpha}$ as a series expansion in powers of Δ_ω and Δ^*_ω and in powers of electromagnetic field potentials, considering all these Bose fields as classical. As a result, an equation will follow from (2.81):

$$\Delta^*_\omega = B^{(1)}(\omega)\Delta^*_\omega + \sum_{\omega'+\omega''+\omega'''=\omega} B^{(3)}(\omega', \omega'', \omega''')\Delta^*_{\omega'}\Delta_{\omega''}\Delta^*_{\omega'''} + \ldots \tag{2.82}$$

where the coefficients $B^{(i)}$ represent the response of the system to the action of the classical field Δ.

2.3.1. Causality Principle and Nonlinear Problems

In nonequilibrium conditions, an equation of the kind (2.81) may be obtained in a real-time representation using the Keldysh technique.[15] The same result may be obtained by the Gor'kov–Eliashberg technique,[16] which is a generalization of the usual procedure of analytical continuation to the nonlinear case. The underlying principle at the base of this technique asserts that the response of system (2.82) in a real-time representation must contain the values of the field Δ in the moments preceding the current time. This demand can be satisfied if the coefficients $B^{(i)}(\omega', \omega'', \ldots, \omega^i)$, which are determined in the Matsubara technique on the imaginary axis, are analytically continued onto the upper half-plane for all the frequencies $\omega', \omega'', \ldots, \omega^i$. One can verify this assertion in a manner analogous to the case of linear response (e.g., in the case of derivation of the Kramers–Krönig relations). In the next section we trace the calculations of Gor'kov and Eliashberg.[16]

2.3.2. Equations on an Imaginary Axis

Allowing for the time dependence of the fields, the Gor'kov equations can be represented in the form [$(\varepsilon = (2n+1)\pi Ti,\ \omega = 2m\pi Ti$]

$$\begin{pmatrix} \dfrac{1}{2m}\left(-i\dfrac{\partial}{\partial \mathbf{r}}\right)^2 + H_1 - \varepsilon_F - \varepsilon & -\Delta_\omega(\mathbf{r}) \\ \Delta^*_\omega(\mathbf{r}) & \dfrac{1}{2m}\left(-i\dfrac{\partial}{\partial \mathbf{r}}\right)^2 + \overline{H}_1 - \varepsilon_F + \varepsilon \end{pmatrix} \begin{pmatrix} \mathcal{G} & \mathcal{F} \\ -\mathcal{F}^+ & \overline{\mathcal{G}} \end{pmatrix} = \hat{1}(2\pi)\delta(\mathbf{r}-\mathbf{r}')\delta(\omega), \tag{2.83}$$

where the function $\Delta^{*}_{\omega}(\mathbf{r})$ is defined by Eq. (2.81). In expression (2.83) the values of H_1 and $\bar{H}_1$ are given by the relations:

$$H_1 = -\frac{e}{c}[(\mathbf{v}\cdot\mathbf{A}_\omega(\mathbf{r})] + e\varphi_\omega(\mathbf{r}), \quad \bar{H}_1 = \frac{e}{c}[\mathbf{v}\cdot\mathbf{A}_\omega(\mathbf{r})] + e\varphi_\omega(\mathbf{r}). \tag{2.84}$$

Equation (2.83) and the expression for the current and the density of particles

$$\mathbf{j}_\omega(\mathbf{k}) = -\frac{2e}{m}T\sum_{\varepsilon}\int\frac{d^3\mathbf{p}}{(2\pi)^3}\,\mathbf{p}\mathcal{G}_{\varepsilon\varepsilon-\omega}(\mathbf{p}_+,\mathbf{p}_-) - \frac{e^2}{mc^2}(N\mathbf{A})_{\omega,\mathbf{k}}, \tag{2.85}$$

$$N_\omega(\mathbf{k}) = -2T\sum_{\varepsilon}\int\frac{d^3\mathbf{p}}{(2\pi)^3}\,\mathcal{G}_{\varepsilon\varepsilon-\omega}(\mathbf{p}_+,\mathbf{p}_-), \quad \mathbf{p}_\pm = \mathbf{p}\pm\frac{\mathbf{k}}{2} \tag{2.86}$$

are basic for further calculations.* Using Eq. (2.83), one can establish the diagram expansions for the functions $\mathcal{G}$ and $\mathcal{F}+$:

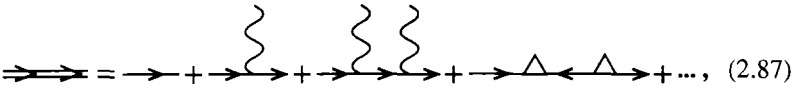

(2.87)

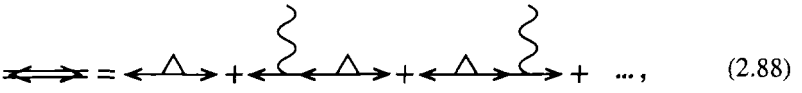

(2.88)

or in analytic form

$$\mathcal{G}_{\varepsilon\varepsilon-\omega}(\mathbf{p},\mathbf{p}') = (2\pi)^4\frac{\delta(\mathbf{p}-\mathbf{p}')\delta(\omega)}{\xi_{\mathbf{p}}-\varepsilon} + \frac{e}{mc}\frac{\mathbf{p}'\times\mathbf{A}_\omega(\mathbf{p}-\mathbf{p}')}{\xi_{\mathbf{p}}-\varepsilon}\frac{1}{\xi_{\mathbf{p}'}-\varepsilon+\omega} + \ldots \tag{2.89}$$

$$\mathcal{F}^{+}_{\varepsilon\varepsilon-\omega}(\mathbf{p},\mathbf{p}') = \frac{1}{\xi_{\mathbf{p}}+\varepsilon}\Delta^{*}_{\omega-\omega'}(\mathbf{p}-\mathbf{p}')\frac{1}{\xi_{\mathbf{p}'}-\varepsilon} - \ldots \tag{2.90}$$

[the summation in Eqs. (2.89) and (2.90) includes all the intermediate energies and integration over all the intermediate momenta]. Note that to derive the nonstationary Ginzburg–Landau equations (as in the static case), one may keep only the first few terms of the decomposition (2.88), with subsequent substitution into (2.81) and

*Note the difference in signs between (2.83) and its static analog (1.142) and (1.143). In both cases we have retained the notation of the original work[17,18] to maintain the connection between these equations and many other original investigations. The difference in the propagators' signs is unimportant here.

(2.85). However, it is expedient to consider the problem from a more general point of view, retaining all terms in Eqs. (2.89) and (2.90).

2.3.3. Analytical Continuation Procedure

In expressions (2.81), (2.85), and (2.86), it is necessary to carry out analytical continuation over ω from the upper half-plane onto the real axis. Note, that the analytical structure of diagrams is insensitive to the directions of arrows and to the presence of vertices Δ_{ω_i} and $H_{1\omega_i}$. Let us consider a general term of the series:

$$T\sum_{\varepsilon} \mathcal{G}_{\varepsilon}\mathcal{G}_{\varepsilon-\omega_1}\mathcal{G}_{\varepsilon-\omega_1-\omega_2}\cdots\mathcal{G}_{\varepsilon-\omega}, \tag{2.91}$$

where the summation is also assumed over the internal frequencies, subject to the condition $\sum \omega_i = \omega$. The procedure of analytical continuation of Eq. (2.89) over all ω_i onto the real axis should not depend on the order in which the continuation over each of the frequencies proceeds. Then the problem of analytical continuation of the whole structure will be solved.

Let us transform the sum in (2.89) into the contour integral

$$T\sum_{n} \mathcal{G}_{\varepsilon_n}\mathcal{G}_{\varepsilon_n-\omega_1}\cdots\mathcal{G}_{\varepsilon_n-\omega} = \oint_C \frac{dz}{4\pi i}\tanh\frac{z}{2T}\mathcal{G}_z\mathcal{G}_{z-\omega_1}\cdots\mathcal{G}_{z-\omega}, \tag{2.92}$$

where the contour C encloses all the poles of the hyperbolic tangent and does not contain the poles of the $\mathcal{G}$-functions (Fig. 2.1). Consider a diagram of the N^{th} power of the field and make the cuts between the singularities of the integrand in (2.92) produced by the functions $\mathcal{G}_z$, $\mathcal{G}_{z-\omega}$ and so on. Transform the integration contour C into a new one, C', which goes along the banks of the cut (Fig. 2.1) and along the arcs of large circles. The contributions from the latter disappear [owing to the factor $(1/z)^{N+1}$] in all the diagrams except the zero-order one for the $\mathcal{G}$-function (which does not depend explicitly on the time variable). On horizontal parts of the integration we have $z = \omega_i + \varepsilon$ where e is a real variable and ω_i is a fixed imaginary frequency. Shifting the integration variable and taking into account that $\tanh(x + i\pi n) = \tanh x$, we can write

$$\oint \frac{dz}{4\pi i}\tanh\frac{z}{2T}\mathcal{G}_z\mathcal{G}_{z-\omega_1}\cdots\mathcal{G}_{z-\omega} = \int_{-\infty}^{\infty}\frac{d\varepsilon}{4\pi i}\tanh\frac{\varepsilon}{2T}\left\{\left(G_\varepsilon^R - G_\varepsilon^A\right)\mathcal{G}_{\varepsilon-\omega_1}\cdots\mathcal{G}_{\varepsilon-\omega}\right.$$

$$+\mathcal{G}_{\varepsilon+\omega_1}\left(G_\varepsilon^R - G_\varepsilon^A\right)\mathcal{G}_{\varepsilon-\omega_2}\cdots\mathcal{G}_{\varepsilon-\omega+\omega_1} + \mathcal{G}_{\varepsilon+\omega_1+\omega_2}\mathcal{G}_{\varepsilon+\omega_2}\left(G_\varepsilon^R - G_\varepsilon^A\right)\mathcal{G}_{\varepsilon-\omega_3}\cdots\mathcal{G}_{\varepsilon-\omega+\omega_1+\omega_2}$$

$$\left. + \mathcal{G}_{\varepsilon+\omega}\mathcal{G}_{\varepsilon+\omega-\omega_1}\cdots\left(G_\varepsilon^R - G_\varepsilon^A\right)\right\}, \tag{2.93}$$

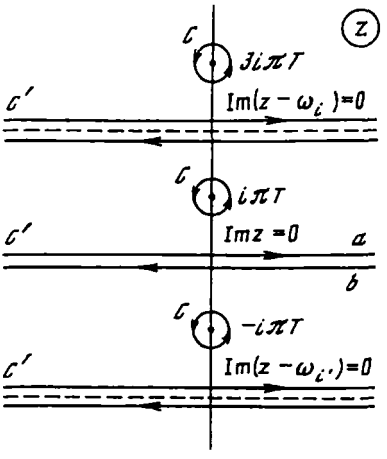

Figure 2.1. Transformation of the integration contour: the dashed lines indicate cuts in the z-plane (in the absence of a cut, e.g., at Im $z = 0$, the total contribution over lines a and b equals zero).

where the functions G^R and G^A have the well-known analytical properties:

$$\overset{(-)^R}{G_\varepsilon} = \left[\xi_{\mathbf{p}^-_{(+)}}(\varepsilon + i\delta)\right]^{-1}, \quad \overset{(-)^A}{G_\varepsilon} = \left[\xi_{\mathbf{p}^-_{(+)}}(\varepsilon - i\delta)\right]^{-1}, \quad \delta \to +0. \tag{2.94}$$

Such representation allows us to determine analytical properties for all factors to the left and to the right of G^R and G^A, if all the frequencies ω_i belong to the same half-plane. In particular, if all the frequencies ω_i belong to the upper half-plane (which corresponds to the general causality principle mentioned earlier), then all the functions in (2.93) to the left of the factor $(G^R_\varepsilon - G^A_\varepsilon)$ would be retarded, and those to the right would be advanced. Indicating these functions by the letters R and A, we can now move to the real frequencies $\omega_i \to \omega_i + i\delta$, $\delta > 0$.

2.3.4. Anomalous Propagators and Dyson Equations

We have formulated the procedure of analytical continuation, which is independent of the ordering in ω_i. The final result may be written after once again shifting the integration variable in the integrands:

$$T\sum_{\varepsilon}\mathcal{G}_{\varepsilon}\mathcal{G}_{\varepsilon-\omega_1}\cdots\mathcal{G}_{\varepsilon-\omega}=\int_{-\infty}^{\infty}4\pi i\left\{-\tanh\frac{\varepsilon}{2T}\,G^A_{\varepsilon}G^A_{\varepsilon-\omega_1}\cdots G^A_{\varepsilon-\omega}\right.$$

$$+G^R_{\varepsilon}G^R_{\varepsilon-\omega_1}\cdots G^R_{\varepsilon-\omega}\tanh\frac{\varepsilon-\omega}{2T}+G^R_{\varepsilon}\left(\tanh\frac{\varepsilon}{2T}-\tanh\frac{\varepsilon-\omega_1}{2T}\right)G^A_{\varepsilon-\omega_1}\cdots G^A_{\varepsilon-\omega}$$

$$+G^R_{\varepsilon}G^R_{\varepsilon-\omega_1}\left(\tanh\frac{\varepsilon-\omega_1}{2T}-\tanh\frac{\varepsilon-\omega_1-\omega_2}{2T}\right)G^A_{\varepsilon-\omega_1-\omega_2}\cdots G^A_{\varepsilon-\omega}$$

$$\left.+\;G^R_{\varepsilon}G^R_{\varepsilon-\omega_1}\cdots G^R_{\varepsilon-\omega+\omega_1}\left(\tanh\frac{\varepsilon-\omega+\omega_1}{2T}-\tanh\frac{\varepsilon-\omega}{2T}\right)G^A_{\varepsilon-\omega}\right\}. \tag{2.95}$$

This expression may be rewritten as

$$T\sum_{\varepsilon}\mathcal{G}_{\varepsilon\varepsilon-\omega}\to\int_{-\infty}^{\infty}\frac{d\varepsilon}{4\pi i}\,G_{\varepsilon\varepsilon-\omega}, \tag{2.96}$$

where

$$G_{\varepsilon\varepsilon-\omega}=G^R_{\varepsilon\varepsilon-\omega}\tanh\frac{\varepsilon-\omega}{2T}-\tanh\frac{\varepsilon}{2T}\,G^A_{\varepsilon\varepsilon-\omega}+G^{(a)}_{\varepsilon\varepsilon-\omega}. \tag{2.97}$$

The regular functions $G^{R(A)}$ in (2.95) and (2.97) are determined from diagram expansions in which all the functions are retarded (or advanced). On the contrary, the analytic structure of the "anomalous" function $G^{(a)}$ is much more complicated. Taking into account the directions of arrows in the diagrams, one can find for $G^{(a)}$ the graphical expression

$G^{(a)}=$ 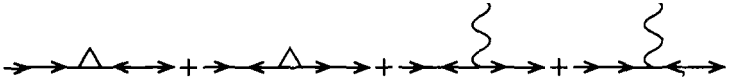

(2.98)

where all the field vertices are multiplied by $[\tanh(\varepsilon-\omega_1/2T)-\tanh(\varepsilon-\omega_1-\omega_2/2T)]$. The retarded propagator corresponds to the line lying to the left of the vertex, and the advanced propagator corresponds to the line lying to the right. In analytic form we have

$$G^{(a)}_{\varepsilon\varepsilon-\omega}(p_1,p-k)=\int\int\frac{d\omega_1 d\omega_2}{(2\pi)^2}\int\int\frac{d^3\mathbf{k}_1}{(2\pi)^3}\frac{d^3\mathbf{k}_2}{(2\pi)^3}\left(\tanh\frac{\varepsilon-\omega_1}{2T}-\tanh\frac{\varepsilon-\omega_1-\omega_2}{2T}\right)$$

$$\times\left\{-G^R\Delta F^{+A}-F^R\Delta^*G^A-G^RH_1G^A+F^R\bar{H}_1F^{+A}\right\}, \tag{2.99}$$

where

$$\left\{G^R\Delta F^{+A}\right\} \equiv G^R_{\varepsilon\varepsilon-\omega_1}(\mathbf{p}_1, \mathbf{p}-\mathbf{k}_1)\Delta_{\omega_2}(\mathbf{k}_2)F^{+A}_{\varepsilon-\omega_1-\omega_2,\varepsilon-\omega}(\mathbf{p}-\mathbf{k}_1-\mathbf{k}_2, \mathbf{p}-\mathbf{k}). \quad (2.100)$$

The expressions for nondiagonal Green's functions may be found analogously. For $F^{+(a)}_{\varepsilon\varepsilon-\omega}$ we obtain

$$F^{+(a)}_{\varepsilon\varepsilon-\omega} = \int\int \frac{d\omega_1 d\omega_2}{(2\pi)^3} \int\int \frac{d^3\mathbf{k}_1}{(2\pi)^3}\frac{d^3\mathbf{k}_2}{(2\pi)^3}\left(\tanh\frac{\varepsilon-\omega_1}{2T} - \tanh\frac{\varepsilon-\omega_1-\omega_2}{2T}\right)$$

$$\times\left\{-\bar{G}^R\bar{H}_1F^{+A} - F^{+R}H_1G^A + \bar{G}^R\Delta^*G^A - F^{+R}\Delta F^{+A}\right\}. \quad (2.101)$$

The Dyson equations may also be found for anomalous functions. A graphic representation is useful for this purpose. Let us present (2.98) in the form

$G^{(a)} =$ 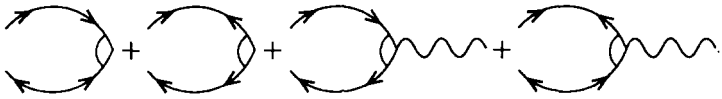 (2.102)

Here the upper lines correspond to the retarded propagator and the lower ones to the advanced propagators; the right vertices are multiplied by $(\tanh\varepsilon/2T - \tanh\varepsilon - \omega/2T)$, where ε, $\varepsilon - \omega$ are the frequencies corresponding to adjacent lines. Specifying these diagrams, say, in the following way

$G^{(a)} =$ 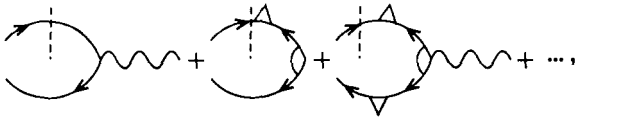 (2.103)

and detaching the upper free line $(\xi_{\mathbf{p}} - \varepsilon - i\delta)^{-1}$ (shown by a dashed line), one obtains the following Dyson-type equation

$$(\xi_{\mathbf{p}} - \varepsilon)G^{(a)}_{\varepsilon\varepsilon-\omega}(\mathbf{p}, \mathbf{p}-\mathbf{k}) = -\int\frac{d^4k_1}{(2\pi)^4}\left\{[H_1(k_1)G^A(p-k_1, p-k) \right. \quad (2.104)$$

$$+ \Delta(k_1)F^{+A}(p-k_1, p-k)]\left(\tanh\frac{\varepsilon}{2T} - \tanh\frac{\varepsilon-\omega_1}{2T}\right)$$

$$\left. + H_1(k_1)G^{(a)}(p-k_1, p-k) + \Delta(k_1)F^{+(a)}(p-k_1, p-k)\right\}.$$

Using the Dyson equations (which the functions $G^{R(A)}$ and $F^{+R(A)}$ obey) and definitions like Eq. (2.97), one can exclude from consideration the anomalous functions obtaining the closed equation for the G-function:

$$(\xi - \varepsilon)G_{\varepsilon\varepsilon-\omega} = -\int \frac{d^4k_1}{(2\pi)^4}\left[H_1(k_1)G_{\varepsilon-\omega_1\varepsilon-\omega} + \Delta(k_1)F^+_{\varepsilon-\omega_1\varepsilon-\omega}\right], \tag{2.105}$$

or in a concise notation

$$(\xi - \varepsilon)G_{\varepsilon\varepsilon-\omega} = -\left\{H_1 G + \Delta F^+\right\}_{\varepsilon\varepsilon-\omega}. \tag{2.106}$$

This equation coincides in form with the equations for retarded and advanced propagators. Being homogeneous, these equations to some extent are deficient without certain additional conditions. We will consider one called a *normalization condition,* in Chap. 3.

2.3.5. Regular Terms

Returning now to the problem of derivation of the Ginzburg–Landau-type dynamic equations, we substitute the expression

$$F^+_{\varepsilon\varepsilon-\omega} = F^{+R}_{\varepsilon\varepsilon-\omega}\tanh\frac{\varepsilon-\omega}{2T} - \tanh\frac{\varepsilon}{2T}F^{+A}_{\varepsilon\varepsilon-\omega} + F^{+(a)}_{\varepsilon\varepsilon-\omega} \tag{2.107}$$

into the self-consistency equation, which now acquires the form

$$\Delta^*_\omega(\mathbf{k}) = |\zeta|\int_{-\omega_D}^{\omega_D}\frac{d\varepsilon}{4\pi i}\frac{d^3\mathbf{p}}{(2\pi)^3}F^+_{\varepsilon\varepsilon-\omega}(\mathbf{p}, \mathbf{p}-\mathbf{k}). \tag{2.108}$$

Because the functions F^{+R} and F^{+A} are analytical in the upper and lower half-planes, respectively, one can move again to the summation over $\varepsilon_n = i\pi T(2n+1)$ in the first two ("regular") terms. As a result we obtain

$$\Delta^*_\omega(\mathbf{k}) = |\zeta|T\left[\sum_{n\geq 0}\int\frac{d^3\mathbf{p}}{(2\pi)^3}\mathcal{F}^+_{\varepsilon_n+\omega\varepsilon_n}(\mathbf{p}, \mathbf{p}-\mathbf{k}) + \sum_{n<0}\int\frac{d^3\mathbf{p}}{(2\pi)^3}\mathcal{F}^+_{\varepsilon_n\varepsilon_n-\omega}(\mathbf{p}, \mathbf{p}-\mathbf{k})\right]$$
$$+ |\zeta|\int_{-\omega_D}^{\omega_D}\frac{d\varepsilon}{4\pi i}\frac{d^3\mathbf{p}}{(2\pi)^3}F^{+(a)}_{\varepsilon\varepsilon-\omega}(\mathbf{p}, \mathbf{p}-\mathbf{k}) \tag{2.109}$$

(ω is real now!). Further manipulations of the regular terms in (2.109) are similar to those considered in Sect. 1.4 for the static case. As follows from that discussion, it is enough to consider only the diagrams

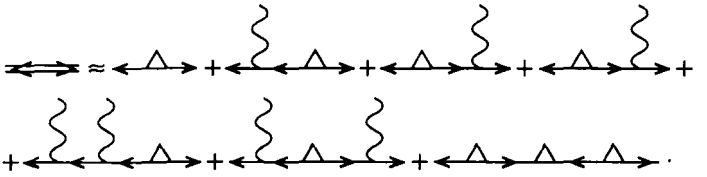

(2.110)

Unlike the static case, the field vertices in Eq. (2.110) are time dependent (e.g., $\Delta = \Delta_\omega$), so the diagrams explicitly depend on time. We will discuss the most simple and important case of alloys with paramagnetic impurities when the impurity concentration is sufficiently high ($\Delta\tau_S << 1$) that $\varepsilon \sim \omega \sim \Delta^2\tau_S << \Delta$. In this case the time dependence may be kept only in the first diagram on the right-hand side of Eq. (2.110), inserting in the others $\omega = 0$ and returning to the static case. Simultaneously, only the first (linear) term may be kept in this selected diagram in its expansion over ω. Substituting these expressions into (2.109), one finds for the regular contribution from the first diagram (2.110):

$$\Delta_\omega^{*(1)}(\mathbf{r}) = |\zeta|T\left[\sum_{n\geq 0}\int d^3\mathbf{r}_1 \{\overline{\mathcal{G}}_{\varepsilon_n+\omega}(\mathbf{r}-\mathbf{r}_1)\Delta_\omega^*(\mathbf{r}_1)\mathcal{G}_{\varepsilon_n}(\mathbf{r}-\mathbf{r}_1)\}\right.$$

$$\left. + \sum_{n<0}\int d^3\mathbf{r}_1 \left\{\mathcal{G}_{\varepsilon_n}(\mathbf{r}-\mathbf{r}_1)\Delta_\omega^*(\mathbf{r}_1)\overline{\mathcal{G}}_{\varepsilon_n-\omega}(\mathbf{r}-\mathbf{r}_1)\right\}\right], \qquad (2.111)$$

where the $\mathcal{G}$-functions are defined according to Eq. (1.169). The series over n arising in (2.111) may be summed, yielding

$$\Delta_\omega^{*(1)}(\mathbf{r}) = |\zeta|T\int d^3\mathbf{r}_1\Delta^*(\mathbf{r}_1)\exp\left\{i\omega\frac{|\mathbf{r}-\mathbf{r}_1|}{v_F}\right\}\frac{m^2}{(2\pi|\mathbf{r}-\mathbf{r}_1|)^2\sinh\dfrac{2\pi T|\mathbf{r}-\mathbf{r}_1|}{v_F}}. \qquad (2.112)$$

As is clear from (2.112), the expansion of the exponent would occur in powers of the factor ω/T_c. In addition to the terms obtained in Sect. 1.4, we will obtain the term

$$\Delta_\omega^{*(1)}(\mathbf{r}) = i\omega\frac{|\zeta|T}{v_F}\Delta_\omega^*(\mathbf{r})\int d^3\mathbf{r}_1\frac{m^2}{(2\pi)^2|\mathbf{r}-\mathbf{r}_1|\sinh\dfrac{2\pi T|\mathbf{r}-\mathbf{r}_1|}{v_F}}, \qquad (2.113)$$

which is integrable in analytic form.

It should be noted that the scalar potential φ escapes from the regular terms' contributions, as one may verify by calculating the second and third diagrams in (2.110). (We will not present here these straightforward but sufficiently tedious calculations.) Note also that the imaginary unit i in (2.113) causes (after the Fourier

transformation) the dynamic equation to be of the diffusion type (thus the difficulty described at the end of Chap. 1 is avoided). In writing down this equation, the presence of impurities makes it necessary to take into account a renormalization of regular terms. This procedure also renormalizes the coefficients* of the static equation (1.182). As a result, the equation for the order parameter acquires the form

$$\frac{\partial\Delta^*}{\partial t}+\frac{\tau_S}{3}\left\{\left[-\pi^2(T_c^2-T^2)+\frac{|\Delta|^2}{2}\right]\Delta^*-\frac{v_F^2\tau_1}{\tau_S}\left(\nabla+\frac{2ie}{c}\mathbf{A}^2\right)\Delta^*\right\}-2ie\Delta^*\Phi=0, \quad (2.114)$$

$$\Phi=-\frac{i}{e\Delta^*\tau_S}\frac{2\pi^2}{|\zeta|mp_F}\int\frac{d^3\mathbf{k}}{(2\pi)^3}\frac{d\omega}{2\pi}e^{ikx-i\omega t}\int_{-\infty}^{\infty}\frac{d\varepsilon}{4\pi i}\int\frac{d^3\mathbf{p}}{(2\pi)^3}F^{(a)}(p,p-k)=0. \quad (2.115)$$

2.3.6. Nonlocal Kernels

We must account now for the contribution to Eq. (2.114) from the anomalous part $F^{(a)}$ in (2.115). In analogy to (2.102), the equation for $F^{(a)}_{\varepsilon\varepsilon-\omega}$ can be written in a form:

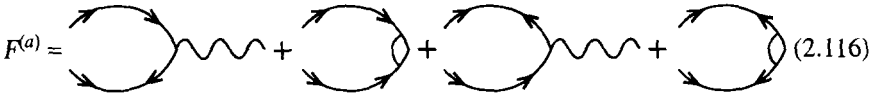

(2.116)

The expression

$$F^{(a)}_{\varepsilon\varepsilon-\omega}=\int\frac{d\varepsilon_1\,d\omega_1}{(2\pi)^2}\left(\tanh\frac{\varepsilon_1}{2T}-\tanh\frac{\varepsilon_1-\omega_1}{2T}\right)F^R_{\varepsilon\varepsilon_1}\Delta_{\omega_1}F^A_{\varepsilon_1-\omega_1,\varepsilon-\omega} \quad (2.117)$$

corresponds to the last diagram in (2.116). For pure superconductors at $\Delta \ll T$, $\omega_1 \ll T$ and $\varepsilon, \varepsilon_1 \ll T$, one may write in (2.117):

$$\tanh\frac{\varepsilon_1}{2T}-\tanh\frac{\varepsilon_1-\omega_1}{2T}\approx\frac{\omega_1}{2T}\cosh^{-2}\frac{\varepsilon_1}{2T}\approx\frac{\omega_1}{2T} \quad (2.118)$$

and consequently:

$$\Phi(t)\sim F^{(a)}(\mathbf{r}_1\mathbf{r};t_1t)\sim\int d^3\mathbf{r}_1\,dt_1\,F^R(\mathbf{r}_1\mathbf{r};t_1t)\Delta(t_1,\mathbf{r}_1)F^A(\mathbf{r}_1\mathbf{r};t_1t). \quad (2.119)$$

*We omit here the details of the calculations, and trace only the principal issues of the derivation of time-dependent Ginzburg–Landau equations (one can find some details in Refs. 2 and 16). The more general case is considered in detail in Chap. 7.

Further transformation of (2.119) seems to be impossible, because the functions $F^{R,A}$ oscillate in time with frequency $|\Delta|$.

In the presence of paramagnetic impurities, the situation differs qualitatively. In this case Green's functions decay exponentially for times $t_1 - t \sim \tau_S$. The kernels of the integral equations for Δ become local in time and that makes it possible to use a technique analogous to the static case. Without further calculations we note only that at a sufficiently high concentration of paramagnetic impurities, the result has the form $\Phi = -\varphi$. Then the equation for Δ may be written as*

$$\left(\frac{\partial}{\partial t} + 2i\varphi\right)\Delta^* + \frac{\tau_S}{3}\left\{\left[-\pi^2(T_c^2 - T^2) + \frac{|\Delta|}{2}\right]\Delta^* - \frac{v_F\tau_1}{\tau_S}\left(\nabla + \frac{2ie}{c}\mathbf{A}\right)^2\Delta^*\right\} = 0. \quad (2.120)$$

The expression for the current in the gapless superconductors has a form characteristic for a two-fluid model:

$$\mathbf{j} = \mathbf{j}_s + \mathbf{j}_n, \qquad \mathbf{j}_s = \frac{2\sigma\tau_S}{c}|\Delta|^2\mathbf{Q}, \qquad \mathbf{j}_n = \sigma\mathbf{E}, \quad (2.121)$$

where $\mathbf{E} = -(1/c)\dot{\mathbf{A}} - \nabla\varphi$ is the electric field strength and $\mathbf{Q} = 2m\mathbf{v}_s$ is the superfluid's momentum, which is related to the superfluid velocity (1.54). In the case of superconductors with a finite gap, some additional terms arise in the current that correspond to the interference of normal and superfluid motions (see Chap. 7).

Thus the dynamic generalization of the Ginzburg–Landau equation for the order parameter has the form of a diffusion-type equation. Clearly, there is an essential difference between (2.120) and the diffusion equation (or the equation for the heat transfer), because in the case of superconductivity Eq. (2.120) is connected with (2.121) and with the Maxwell equations that comprise a strongly nonlinear set of equations. The solutions of these equations (see in particular Chap. 9) can be periodic in space and time, revealing the remarkable properties of nonequilibrium superconductors.

References

1. A. A. Abrikosov and L. P. Gor'kov, On the theory of superconducting alloys, *Sov. Phys. JETP* **8**(6), 1090–1108 (1958) [Zh. *Eksp. i Teor. Fiz.* **35**[6(12)], 1558–1571 (1958)].
2. A. A. Abrikosov and L. P. Gor'kov, Contribution to the theory of superconducting alloys with paramagnetic impurities, *Sov. Phys. JETP* **12**(6), 1243–1253 (1961) *[Zh. Eksp. i Teor. Fiz.* **39[**6(12)], 1782–1796(1960)].
3. A. A. Abrikosov, L. P. Gor'kov, and I. E. Dzyaloshinskiy, *Quantum Field Theoretical Methods in Statistical Physics,* 2nd ed., pp. 323–338. Pergamon, Oxford (1965).
4. J. Kondo, Resistance minimum in dilute magnetic alloys, *Progr. Theor. Phys.* **32**(1), 37–49 (1964).

*A similar equation for superconductors was originally derived on a less rigorous basis by Schmid.[19]

5. J. Kondo, Giant thermo-electric power of dilute magnetic alloys, *Progr. Theor. Phys.* **34**(3), 372–382(1965).
6. A. A. Abrikosov, Electron scattering on magnetic impurities in metals and anomalous resistivity effects, *Physics* **2**(1), 5–20 (1965).
7. K. Fischer, Self-consistent treatment of the Kondo effect, *Phys. Rev.* **158**(3), 613–622 (1967).
8. O.K. C. MacDonald, *Thermoelectricity: An Introduction to the Principles,* pp. 1–133, Wiley, New York (1962).
9. R. D. Barnard, *Thermoelectricity in Metals and Alloys,* pp. 1–259, Taylor and Francis, London (1972).
10. J. Kondo, in *Solid State Physics,* F. Seitz, D. Turnbull, and H. Ehrenreich, eds., Vol. 20, pp. 184–280, Academic Press, New York (1969).
11. P. G. De Gennes, *Superconductivity ofMetals andAlloys,* pp. 157–159, W.A. Benjamin, New York (1966).
12. A. B. Migdal and V. M. Galitzkiy, Application of quantum field theory methods to the many-body problem, *Sov. Phys. JETP* **7**(1), 96–104 (1958) *(Zh. Eksp. i Teor. Fiz* **34**(1), 139–150 (1958)].
13. A, V. Svidzinskii, *Spatially-Inhomogeneous Problems in the Theory of Superconductivity,* pp. 78–83, Nauka, Moscow (1982) (in Russian).
14. A. A. Abrikosov, *Fundamentals of the Theory of Metals,* pp. 502–532, North-Holland, Amsterdam (1988).
15. A.I. Larkin and Yu. N. Ovchinnikov, Nonlinear effects during the motion of vortices in superconductors, *Sov. Phys. JETP* **46**(1), 155–162 (1977) [*Zh. Eksp. iTeor. Fiz.* **73**[1(7)], 299–312(1977)].
16. L. P. Gor'kov and G. M. Eliashberg, Generalization of the Ginzburg-Landau equations for nonstationary problems in the case of alloys with paramagnetic impurities, *Sov. Phys. JETP* **27**(2), 328–334 (1968) [*Zh. Eksp. i Teor. Fiz.* **54**(2), 612–626 (1968)].
17. L. P. Gor'kov, On the energy spectrum of superconductors, *Sov. Phys. JETP* **7**(3), 505–508 (1964) [*Zh. Eksp. i Teor. Fiz.* **34**(3) 735–739 (1958)].
18. G. M. Eliashberg, Inelastic electron collisions and nonequilibrium stationary states in superconductors, *Sov. Phys. JETP* **34**(3), 668-676 (1972) [*Zh. Eksp. i Teor. Fiz.* **61**[3(9)], 1254–1272 (1971)].
19. A. Schmid, A time-dependent Ginzburg-Landau equation and its application to the problem of resistivity in the mixed state, *Phys. Kond. Materie* **5**, 302–317 (1966).

3

Nonequilibrium General Equations

Under the action of alternating external fields, the problem of energy relaxation becomes important since there is energy transfer from the field to the electrons. In the dynamic scheme, developed in Chap. 2, explicit relaxation channels were not involved. The relaxation of the order parameter, which followed from the final expressions, was totally due to the self-consistent nature of the order parameter itself, since the gaplessness decouples the order parameter from single-particle excitations. Meanwhile, the majority of superconductors have finite gaps, and the interaction of Cooper pairs with the electrons and phonons plays an important role in the action of external fields, determining both the behavior of the order parameter and nonequilibrium effects in the electron–phonon system.

3.1. MIGDAL–ELIASHBERG PHONON MODEL

3.1.1. Fröhlich's Hamiltonian

The interaction of electrons with phonons in metals will be considered in this book (except in Chap. 12) within the isotropic model.[1] The oscillations of the ionic lattice produce lattice polarization. The interaction energy of electrons with the lattice is

$$-e\int\int n(\mathbf{r})\,K(\mathbf{r}-\mathbf{r}')\,\mathrm{div}\,\mathbf{P}(\mathbf{r})\,d^3\mathbf{r}\,d^3\mathbf{r}' \tag{3.1}$$

where $n(\mathbf{r})$ is the density of electrons at the point $\mathbf{r}$, $\mathbf{P}(\mathbf{r})$ is the polarization vector, and $K(\mathbf{r}-\mathbf{r}')$ is the interaction having a Coulomb dependence at small distances and vanishing, owing to screening effects, at distances exceeding the lattice parameters of a crystalline cell. Denoting these by a single distance parameter (a), the function $K(\mathbf{r}-\mathbf{r}')$ may be approximated as $K(\mathbf{r}-\mathbf{r}')\approx a^2\delta(\mathbf{r}-\mathbf{r}')$. As to the polarization vector, it is proportional to the displacement $\mathbf{q}(\mathbf{r})$ of crystalline ions*

*Because the interaction energy is proportional to $\mathrm{div}\mathbf{P}\propto\mathrm{div}\mathbf{q}$, one may conclude that (in the isotropic model!) the electrons interact with longitudinal phonons only.

$$\mathbf{P}(\mathbf{r}) = C\mathbf{q}(\mathbf{r}) \equiv Ze\frac{N}{V_0}\mathbf{q}(\mathbf{r}), \tag{3.2}$$

where N/V_0 is the number of ions in a unit volume and Ze is the ionic charge. We expand the displacement vector $\mathbf{q}(\mathbf{r},t)$ in plane waves

$$\mathbf{q}(\mathbf{r},t) = \frac{1}{\sqrt{V}}\sum_{\mathbf{k}}\frac{\mathbf{k}}{|\mathbf{k}|}\{q_{\mathbf{k}}e^{i[\mathbf{k}\cdot\mathbf{r}-\omega_0(\mathbf{k})t]} + q_{\mathbf{k}}^{\dagger}e^{-i[\mathbf{k}\cdot\mathbf{r}-\omega_0(\mathbf{k})t]}\} \tag{3.3}$$

and introduce the operators $b_{\mathbf{k}}$, $b_{\mathbf{k}}^{\dagger}$, connected with $q_{\mathbf{k}}$, $q_{\mathbf{k}}^{\dagger}$ by the relations

$$q_{\mathbf{k}} = \frac{b_{\mathbf{k}}}{\sqrt{2\rho\omega_0(\mathbf{k})}},\ q_{\mathbf{k}}^{\dagger} = \frac{b_{\mathbf{k}}^{\dagger}}{\sqrt{2\rho\omega_0(\mathbf{k})}}, \tag{3.4}$$

where ρ is the mass density of the medium, and $\omega(\mathbf{k})$ is the phonon dispersion law.

Taking into account that $\rho\dot{q}(\mathbf{r},t)$ is the momentum density of the medium, and also the quantum-mechanical commutation rule

$$\rho\,[\dot{q}_i(\mathbf{r},t),\, q_k(\mathbf{r}',t)]_- = -i\delta(\mathbf{r}-\mathbf{r}')\delta_{ik}, \tag{3.5}$$

one can verify that the quantities $b_{\mathbf{k}}$ and $b_{\mathbf{k}}^{\dagger}$ (3.4) are Bose operators. Because the kinetic energy operator is

$$W_{\text{kin}} = \frac{\rho}{2}\int[\dot{q}_t(\mathbf{r},t)]^2\,d^3\mathbf{r} \tag{3.6}$$

and the mean kinetic energy of oscillations is equal to the mean potential energy, we have

$$\overline{H} = 2\overline{W}_{\text{kin}} = \sum_{\mathbf{k}}\omega_0(\mathbf{k})\left(N_{\mathbf{k}} + \frac{1}{2}\right), \tag{3.7}$$

where $N_{\mathbf{k}} = \langle b_{\mathbf{k}}^{\dagger}\, b_{\mathbf{k}}\rangle$. The operator of a free phonon field is defined by the relation

$$\varphi(x) = \frac{1}{\sqrt{V_0}}\sum_{\mathbf{k}}\sqrt{\frac{\omega(\mathbf{k})}{2}}\{b_{\mathbf{k}}e^{i(\mathbf{k}\cdot\mathbf{r}-\omega_0(\mathbf{k})t)} + b_{\mathbf{k}}^{\dagger}e^{-i(\mathbf{k}\cdot\mathbf{r}-\omega_0(\mathbf{k})t)}\}. \tag{3.8}$$

Note that φ is a real quantity [in the Debye model the summation in (3.8) is restricted by the condition $|\mathbf{k}| < k_D$]. The Hamiltonian of the electron–phonon interaction may then be written as

$$H_{e-ph} = g \int \Psi_\alpha^\dagger (\mathbf{r}) \Psi_\alpha (\mathbf{r}) \varphi (\mathbf{r}) d^3\mathbf{r}, \tag{3.9}$$

where the interaction constant g is defined by

$$g = \frac{ea^2C}{u_0\sqrt{\rho}}, \tag{3.10}$$

and $u_0 = \omega_0(\mathbf{k})/k$ is the sound velocity. The Hamiltonian (3.9) in the theory of metals is usually called the *Fröhlich Hamiltonian.*

3.1.2. Migdal Diagram Expansion

The interaction of electrons with phonons in normal metals was considered in a diagram approach by Migdal,[2] who used the Fröhlich Hamiltonian (3.9). In this approach, the Dyson equation for Green's function for electrons has the form

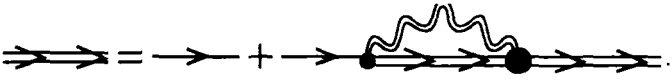

(3.11)

As shown in Ref. 2, even in the case of strong electron-phonon interaction, the vertex remains "bare"*

$$\Gamma = \Gamma_0 \left(1 + O\sqrt{\frac{m}{M}} \right), \tag{3.12}$$

where M is the ionic mass in the crystalline lattice. If one starts from the Green function G_0 for noninteracting electrons and uses for the free phonon field Green's function

$$D_0(x_1 - x_2) = -i \langle T [\varphi (x_1) \varphi(x_2)] \rangle, \tag{3.13}$$

where $\varphi(x)$ is defined by Eq. (3.8), then based on (3.11) and a corresponding equation for the D-function

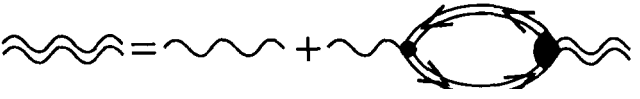

(3.14)

*This point was critically reconsidered by Alexandrov and Ranninger.[3] They have developed an approach (the bipolaron theory of superconductivity), based on violation of Eq. (3.12), which was accepted and developed further by other investigators. We will not consider this possibility (see References in Alexandrov and Mott[4]).

one obtains the renormalized expressions for electron and phonon spectra and also for the damping of electron and phonon excitations. These renormalizations become important when the dimensionless interaction parameter

$$\lambda = \frac{mp_F}{2\pi^2} g^2 \tag{3.15}$$

is of the order of unity. The experiment shows that renormalizations indeed occur in an electron system, whereas they are almost unobservable in a phonon system (at $\varepsilon_F >> \omega_D$). Some doubts were expressed in this connection concerning the adequacy of the Fröhlich Hamiltonian for this problem. As was shown further,[5] the renormalization of the phonon spectrum in the above calculation scheme would correspond to the double counting of interactions between electrons and phonons. Unlike the electron system, the phonons in the "adiabatic approximation" are well defined. The same is valid for the electron system if the parameter λ(3.15) is small.

We will consider further only metals with a weak electron–phonon interaction, assuming that

$$\lambda << 1 \tag{3.16}$$

and neglecting the renormalization effects. Applicability of the results to metals with strong electron–phonon coupling should be analyzed separately. The effects of renormalization are not very essential for the kinetics and can be taken into account in the initial equilibrium state.

3.1.3. *Eliashberg Equations in Weak-Coupling Limit*

All the conclusions concerning the vertex renormalization (Γ) remain valid in the superconducting state, because only the excitations with large energies are essential for renormalization processes. The superconducting scale of energies is much less than these high energies. In the bare vertex approximation (Γ_0) we have the following system for electrons in superconductors

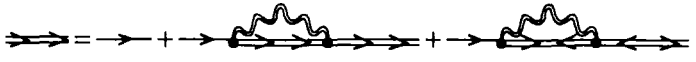

(3.17)

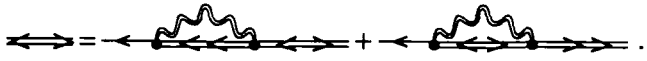

(3.18)

For the phonon Greenfunction  in (3.17) and (3.18), the equation may also be written:

(3.19)

Equations (3.17) to (3.19) were first formulated and solved by Eliashberg.[6]

3.1.4. Comparison with the BCS–Gor'kov Model

One may note a similarity between Eqs. (3.17) and (3.18) and (1.122), (1.123), or (1.147) and (1.148), which can be made more transparent if Eqs. (3.17) and (3.18) are written in the momentum representation $[\varepsilon = \varepsilon_n = 2(n+1)\pi Ti]$:

$$(\varepsilon_n - \xi - \Sigma_{1\varepsilon})\,\mathcal{G}_\varepsilon(\mathbf{p}) + \Sigma_{2\varepsilon}\,\mathcal{F}^+_\varepsilon(\mathbf{p}) = 1,$$

$$(-\varepsilon_n - \xi - \bar{\Sigma}_{1\varepsilon})\,\mathcal{F}^+_\varepsilon(\mathbf{p}) + \Sigma^+_{2\varepsilon}\,\mathcal{G}_\varepsilon(\mathbf{p}) = 0, \tag{3.20}$$

where

$$\Sigma_1(\varepsilon_n, \mathbf{p}) = T\sum_{n'}\int \frac{d^3\mathbf{p}'}{(2\pi)^3}\,\mathcal{G}(\varepsilon_{n'}, \mathbf{p}')\mathcal{D}(\varepsilon_n - \varepsilon_{n'}; \mathbf{p} - \mathbf{p}'), \tag{3.21}$$

$$\Sigma^+_2(\varepsilon_n, \mathbf{p}) = T\sum_{n'}\int \frac{d^3\mathbf{p}'}{(2\pi)^3}\,\mathcal{F}^+(\varepsilon_{n'}, \mathbf{p}')\,\mathcal{D}(\varepsilon_n - \varepsilon_{n'}; \mathbf{p} - \mathbf{p}'). \tag{3.22}$$

The interaction matrix element is incorporated into the definition of the $\mathcal{D}$-function; hence the bare phonon Green function has the form

$$\mathcal{D}_0(\omega_n, \mathbf{q}) = g^2\frac{2\omega_\mathbf{q}^2}{\omega_\mathbf{q}^2 - \omega_n^2} \quad \omega_\mathbf{q} = u|\mathbf{q}|, \quad \omega_n = 2\pi nTi. \tag{3.23}$$

The above-mentioned similarity becomes more complete if one neglects the renormalization of the electron spectrum, letting

$$\xi + \Sigma_1 \approx \xi + \bar{\Sigma}_1 \approx \xi. \tag{3.24}$$

After that, the self-consistency equation (1.144) acquires the form

$$\Delta = \Sigma_2 = T\sum_{n'}\int \frac{d^3\mathbf{p}'}{(2\pi)^3}\,\mathcal{F}(\varepsilon_{n'}, \mathbf{p}')\,\mathcal{D}(\varepsilon_n - \varepsilon_{n'}; \mathbf{p} - \mathbf{p}'). \tag{3.25}$$

Thus it is clear that all the equilibrium results of the BCSr–Gor'kov theory are contained in the phonon model of superconductors. At the same time, the latter

model is much richer and may serve as a basis for the study of electron and phonon kinetics in real superconductors. Besides, in the Migdal–Eliashberg model, the critical parameters of a superconductor are expressed in terms of the parameters of a normal metal. In particular, the critical temperature in the weak coupling phonon model (3.17) and (3.18) is given by the relation, analogous to (1.157), where ζ_0 is replaced by the parameter λ (3.15). The same replacement occurs in the expression (1.135) for the gap at zero temperature, and in addition $\bar{\varepsilon}$ is replaced by ω_D.*

3.2. EQUATIONS FOR NONEQUILIBRIUM PROPAGATORS

3.2.1. Phonon Heat-Bath: Applicability

We continue a theoretical study of nonequilibrium superconductivity with the simplest case, where the phonons play the role of a heat bath for the electron system. In what cases is this phonon heat-bath model applicable? We examine this question in the particular case of a thin film with thickness d. Let us assume $d \sim \xi_0 \sim v_F/T_c$. Because the wavelength of the phonon is $\lambda_{ph} \sim u/T$, where u is the velocity of sound, then at $T \sim T_c$ we have $\lambda_{ph} \ll d$ so that the "geometric-acoustical" approximation could be used to describe the phonon's propagation. (Note that this approximation becomes invalid at $T \to 0$.) If the "acoustical densities" ρu of the film and $\rho' u'$ of its environment coincide, then phonons in the superconductor lose their energy at each collision with the specimen's walls.[7] (Evidently if $\rho u = \rho' u'$, the phonons leave the film without reflection at the boundary.) However, as was shown in Ref. 2, the lifetime of thermal phonons, owing to their interaction with the conduction electrons in the metal, is $\tau_{ph-e} \sim v_F/(uT)$ and consequently the scattering length of the phonon is $L \sim v_F/T$, which has an order of ξ_0. Thus (if $d < \xi_0$) the nonequilibrium phonons emitted during the relaxation processes by electrons have enough time to leave the film without producing an influence on the electron system.

It must be stressed that the phonon heat-bath model can be used in various situations. In each case an analysis of its applicability is required. For example, at $T \ll |\Delta|$ and for weak external pumping, the number of excess electron excitations is small and the electrons shift the phonons from equilibrium only slightly, even in thick films. In the case of a massive superconductor placed in an external electromagnetic field, the picture is spatially inhomogeneous. There diffusion plays the main role in the relaxation processes in single-electron systems. The phonons remain in equilibrium if their scattering length exceeds the diffusion length of electron excitations.

*The expressions for T_c and $\Delta(0)$, as well as their ratio, change significantly in the strong coupling limit $\lambda \gtrsim 1$ (see, e.g., Ref. 7).

3.2.2. Expansion Over External Field Powers

We move now to a formal description of superconductor electrodynamics on the basis of Eliashberg equations in the framework of the phonon heat-bath model. In a static case $[\mathbf{A} = \mathbf{A}(\mathbf{r})]$ the initial equations in the spatial representation have the form

$$\begin{pmatrix} \frac{1}{2m}\left(\hat{\mathbf{p}} - \frac{e}{c}\mathbf{A}\right)_{\mathbf{r}}^2 - \varepsilon_F - \varepsilon - \Sigma_1 & -\Sigma_2 \\ \Sigma_2^+ & \frac{1}{2m}\left(\hat{\mathbf{p}} + \frac{e}{c}\mathbf{A}\right)_{\mathbf{r}}^2 + \varepsilon_F + \varepsilon - \overline{\Sigma}_1 \end{pmatrix} \begin{pmatrix} \mathcal{G} & \mathcal{F} \\ -\mathcal{F}^+ & \mathcal{G} \end{pmatrix} = \hat{1} \cdot \delta(\mathbf{r} - \mathbf{r}'), \quad (3.26)$$

and the self-energy parts are defined by the relations

$$\hat{\Sigma}_{\varepsilon,\mathbf{r},\mathbf{r}'} = \begin{pmatrix} \Sigma_1 & \Sigma_2 \\ -\Sigma_2^+ & \overline{\Sigma}_1 \end{pmatrix}_{\varepsilon,\mathbf{r},\mathbf{r}'} = T\sum_{\varepsilon'} \mathcal{D}_{\varepsilon-\varepsilon'} \begin{pmatrix} \mathcal{G} & \mathcal{F} \\ -\mathcal{F}^+ & \overline{\mathcal{G}} \end{pmatrix}_{\varepsilon',\mathbf{r},\mathbf{r}'}, \quad (3.27)$$

where $\varepsilon = \varepsilon_m \equiv (2m+1)\pi T i$ and the matrix product is understood as a convolution over the internal variables, e.g.:

$$\Sigma\mathcal{G} = \int d^3\mathbf{r}_1\, \Sigma(\mathbf{r}, \mathbf{r}_1)\, \mathcal{G}(\mathbf{r}, \mathbf{r}_1). \quad (3.28)$$

The phonon propagator in Eq. (3.27) is taken as an equilibrium one (3.23):

$$\mathcal{D}(\omega_n, \mathbf{q}) \to \mathcal{D}_0(\omega_n, \mathbf{q}). \quad (3.29)$$

3.2.2.1. Analytical Continuation: Causal Propagators

Using the technique of analytical continuation introduced in Sect. 2.3, we will first obtain the expressions for the functions $\Sigma_\varepsilon^{R(A)}$, analytical in the upper (and, correspondingly, in the lower) half-plane. For this purpose we represent $\hat{\Sigma}_\varepsilon$ (3.27) in the form

$$\hat{\Sigma}_\varepsilon = T\sum_{\varepsilon'} \mathcal{D}_{\varepsilon-\varepsilon'} \hat{\mathcal{G}}_{\varepsilon'} = T\sum_{\omega} \mathcal{D}_\omega \hat{\mathcal{G}}_{\varepsilon-\omega} = \oint_C \frac{dz}{4\pi i} \coth\frac{z}{2T}\, \mathcal{D}_z \hat{\mathcal{G}}_{\varepsilon-z}, \quad (3.30)$$

where the contour C encloses the poles of a hyperbolic cotangent and does not include the singularities of the function $\mathcal{D}_z\, \mathcal{G}_{\varepsilon-z}$ in the z-plane. Making cuts in this plane along the lines $\mathrm{Im}\, z = 0$ and $\mathrm{Im}(\varepsilon - z) = 0$, one can transform the integration

contour C into another one, going along the arcs of large circles and along the banks of these cuts (Fig. 2.1). Taking into account the fact that the integrals along the arcs of large circles vanish when the radii tend to infinity, we obtain, using Fig. 2.1, the result

$$\hat{\Sigma}^{R(A)}_{\varepsilon}(\mathbf{r},\mathbf{r}_1) = \int_{-\infty}^{\infty} \frac{d\varepsilon'}{4\pi i}\left\{\coth\frac{\varepsilon'-\varepsilon}{2T}\,(D^R - D^A)_{\varepsilon'-\varepsilon}\,G^{R(A)}_{\varepsilon'}\right.$$

$$\left. + \; D^{A(R)}_{\varepsilon'-\varepsilon}\tanh\frac{\varepsilon'}{2T}\left(\hat{G}^R_{\varepsilon'} - \hat{G}^A_{\varepsilon'}\right)\right\}_{\mathbf{r}\mathbf{r}'}. \tag{3.31}$$

The hyperbolic tangent appears in (3.31) owing to the shift of the integration variable by the imaginary frequency ε. Because the analytical properties of propagators entering (3.31) are now definite, the variable ε' may be considered as real.

3.2.3. Phonon Heat Bath: Consequences

Let us study the phonon propagators in detail. As follows from Eq. (3.19),

$$\mathcal{D}(q) = \mathcal{D}_0(q) + \mathcal{D}_0(q)\Pi(q)\mathcal{D}(q), \tag{3.32}$$

where $\Pi(q)$ is the polarization operator. We can rewrite (3.32) in the form

$$\mathcal{D}_{\omega}(\mathbf{q}) = \frac{1}{[\mathcal{D}^0_{\omega}(\mathbf{q})]^{-1} - \Pi_{\omega}(\mathbf{q})}. \tag{3.33}$$

The real part of the polarization operator Re $\Pi(q)$ is connected with the renormalization of the sound velocity. It is governed by the total mass of electrons; the range of temperature smearing of the Fermi step gives the correction $\propto T/\varepsilon_F$. The same smallness, $\propto |\Delta|/\varepsilon_F$, have corrections connected with the superconducting transition. This is also true for the renormalization caused by an electromagnetic field. As noted in Sect. 3.1, these renormalizations may be assumed as being already made. However, the imaginary part $\Pi_{\omega}(\mathbf{q})$ is wholly defined by the vicinity of the Fermi surface and thus is very sensitive to the distribution of electron excitations. To realize the assumption concerning the phonon equilibrium, it would be necessary in deriving the dynamic equations to take into consideration in an explicit form a sink for the relaxation of phonons that is stronger than the source producing the deviation of phonons from equilibrium, which is caused by processes in the electron system. However, one can use the following artificial method: maintain the equilibrium distribution of phonons by keeping the initial presentation of discrete phonon frequencies and completely neglecting collisions of phonons with electrons in the equations for the phonon propagator.

Such an approach was proposed by Eliashberg[9] and we outline it here. Note that this approach not only simplifies the calculations, but also opens additional possibilities to be used further (in Chap. 6 in particular). We will generalize the discussion, assuming the external field in Eq. (3.26) and in Green's functions there to depend on $\mathbf{r},t : \mathbf{A} = \mathbf{A}(\mathbf{r},t)$. Consequently, on the right side of Eq. (3.26) the additional factor $\delta(\tau - \tau')$ appears and Green's functions will acquire dependence on τ and τ'.

The modified system (3.26) can be expanded in a series over the external field. The diagrams consist of transit lines with different directions of arrows, containing field vertices  and phonon insertions 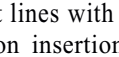 . As in Sect. 2.3, the directions of the arrows are not important for the procedure of analytical continuation.

Consider a diagram of N^{th} power in the external field for Green's function for electrons. Two types of diagrams may arise, depending on whether the diagram contains the phonon insertion (Fig. 3.1). Any diagram will depend on the frequencies of its extreme lines ε and $\varepsilon - \omega$ and of the field vertices ω_l

The analytical structure of $\mathcal{G}^{(N)}$ as a function of the variable ε at fixed ω_l should be found. Owing to the causality principle considered in Chap. 2, the necessary analytical continuation must be made over all ω_l from the upper half-plane, so in all the expressions of the type $\omega_l = 2l\pi Ti$ we will make $\omega_l > 0$. First we will consider the diagrams without Σ-insertions (as in Fig. 3. la). The analytical properties of such diagrams are described by a simple composition:

$$\mathcal{G}^{(N)}_{\varepsilon\varepsilon-\omega}\,\mathcal{G}_{\varepsilon}\,\mathcal{G}_{\varepsilon-\omega_1}\,\mathcal{G}_{\varepsilon-\omega_1-\omega_2}\cdots\mathcal{G}_{\varepsilon-\omega}, \tag{3.34}$$

and their singularities (the poles) lie on the lines Im ε = 0, Im $\varepsilon = \omega_1$, Im $\varepsilon = \omega_1 + \omega_2, \ldots,$ Im $\varepsilon = \omega$, which are parallel to the abscissa. We will ascertain that these lines are singular for the arbitrary type of diagram $\mathcal{G}^{(N)}$. For this purpose it is sufficient to verify that the function $\Sigma^{(N)}_{\varepsilon\varepsilon-\omega}$, as the function of its external argument ε, has the same analytical structure as $\mathcal{G}^{(N)}_{\varepsilon\varepsilon-\omega}$, if the same set of field vertices is included. In other words, the singularities of Σ are determined by the singularities

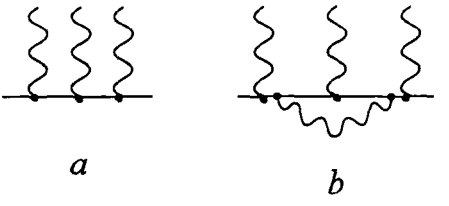

Figure 3.1. Diagrams for an electron propagator (a) without and (b) with the phonon inserted.

of its internal electron Green's function. To see this, we again transform the sum over frequencies in Eq. (3.27) to the contour integral over the singularities of the hyperbolic tangent. Shifting the integration contour along the banks of the cuts, one obtains (in the same manner as in Sect. 2.3) the expression:

$$\Sigma^{(N)}_{\varepsilon\varepsilon-\omega} = \int_{-\infty}^{\infty} \frac{dz}{4\pi i} \left\{ \coth \frac{z}{2T} (D^R - D^A)_z \, \mathcal{G}^{(N)}_{z+\varepsilon, z+\varepsilon-\omega} \right.$$

$$\left. + \tanh \frac{z}{2T} [\mathcal{D}_{z-\varepsilon} \delta_1 (\mathcal{G}^{(N)}) + \ldots + \mathcal{D}_{z-\varepsilon+\omega} \delta_{N+1} (\mathcal{G}^{(N)})] \right\}. \qquad (3.35)$$

In Eq. (3.35) $\delta_l(\mathcal{G}^{(N)})$ is the jump of the function $\mathcal{G}^{(N)}$ at the bank l. Because in (3.35) z is real, one can see that $\Sigma_{\varepsilon\varepsilon-\omega}$ contains ε in the same combinations with ω_l as $\mathcal{G}_{\varepsilon\varepsilon-\omega}$, and this proves the above statement concerning the analytic structure of an arbitrary-type diagram.

3.2.4. Analytical Continuation: Anomalous Functions

Now we can carry out the analytical continuation of Eq. (3.35). Continuing analytically onto the real axis from the upper bank of the uppermost cut, we obtain the function $[\Sigma^{(N)}]^R$, and continuing from the lower bank of the lowermost cut, we get $[\Sigma^{(N)}]^A$. (In these cases all the functions have definite signs of imaginary parts, hence the subsequent continuation over each ω_l does not depend on the value of $\omega_l > 0$.) Thus, making Im $\varepsilon > \omega$ (Im $\varepsilon < 0$), shifting the integration variable to restore the initial notation of the arguments, summing over N and denoting

$$G_{\varepsilon\varepsilon-\omega} = \sum_{N=0}^{\infty} \sum_{l=1}^{N+1} \delta_l (\mathcal{G}^{(N)}) \tanh \frac{\varepsilon_l}{2T}, \qquad (3.36)$$

where $\varepsilon_l = \varepsilon - \omega_1 - \omega_2 - \ldots - \omega_{l-1}$, we arrive at

$$\hat{\Sigma}^{R(A)}_{\varepsilon\varepsilon-\omega} = \int_{-\infty}^{\infty} \frac{d\varepsilon'}{4\pi i} \left\{ \coth \frac{\varepsilon' - \varepsilon}{2T} (D^R - D^A)_{\varepsilon'-\varepsilon} \hat{G}^{R(A)}_{\varepsilon'\varepsilon'-\omega} + D^{A(R)}_{\varepsilon'-\varepsilon} \hat{G}_{\varepsilon'\varepsilon'-\omega} \right\}. \qquad (3.37)$$

The static limit of (3.37) [at $\hat{G}_{\varepsilon\varepsilon-\omega} = 2\pi\delta(\omega)\hat{G}_\varepsilon$, where $\hat{G}_\varepsilon = (\hat{G}^R - \hat{G}^A)_\varepsilon \tanh(\varepsilon/2T)$] coincides with Eq. (3.31). Because all the self-energy functions and propagators composing $\hat{G}^{R(A)}$, are retarded (or advanced), the equation that determines $\hat{G}^{R(A)}$ has the form (see also Sect. 2.3):

$$\left\{\begin{pmatrix} \frac{1}{2m}(\hat{\mathbf{p}}-\frac{e}{c}\mathbf{A})^2_{\omega,\mathbf{r}} - \varepsilon_F - \varepsilon + e\varphi - \Sigma_1 & -\Sigma_2 \\ \Sigma_2^+ & \frac{1}{2m}(\hat{\mathbf{p}}+\frac{e}{c}\mathbf{A})^2_{\omega,\mathbf{r}} + \varepsilon_F + \varepsilon + e\varphi - \bar{\Sigma}_1 \end{pmatrix} \begin{pmatrix} G & F \\ -F^+ & \hat{G} \end{pmatrix} \right\}^{R,A}_{\varepsilon,\varepsilon-\omega}$$

$$= \hat{1}(2\pi)\delta(\omega)\,\delta(\mathbf{r}-\mathbf{r}'), \tag{3.38}$$

where, as earlier,

$$(\Sigma G)_{\varepsilon\varepsilon-\omega,\mathbf{r}\mathbf{r}'} \equiv \int \frac{d\omega_1}{2\pi} \int d^3\mathbf{r}_1\, \Sigma_{\varepsilon\varepsilon-\omega_1}(\mathbf{r},\mathbf{r}_1)\, G_{\varepsilon-\omega_1,\varepsilon-\omega}(\mathbf{r}_1,\mathbf{r}'). \tag{3.39}$$

As for the functions $\hat{G}_{\varepsilon\varepsilon-\omega}$ defined by the relation (3.36), one can obtain the equation for them in a manner used earlier in the Gor'kov model. For this purpose the terms corresponding to the upper bank of the uppermost cut and the lower bank of the lowermost cut must be separated:

$$\hat{G}_{\varepsilon\varepsilon-\omega} = \hat{G}^R_{\varepsilon\varepsilon-\omega} \tanh\frac{\varepsilon-\omega}{2T} - \tanh\frac{\varepsilon}{2T}\hat{G}^A + \hat{G}^{(a)}_{\varepsilon\varepsilon-\omega}. \tag{3.40}$$

For $\hat{G}^{(a)}_{\varepsilon\varepsilon-\omega}$, the diagrams are analogous to Eq. (2.98), although the vertices Δ and Δ^* are replaced now by the functions $\Sigma_2^{(a)}$ and $\Sigma_2^{+(a)}$, and the field vertices

have the additional terms $\Sigma_1^{(a)}$ or $\bar{\Sigma}_1^{(a)}$. Because the functions $\Sigma^{(a)}$ contain the factors $[\tanh(\varepsilon/2T) - \tanh((\varepsilon-\omega)/2T)]$, it is convenient to introduce a function $h_{\varepsilon\varepsilon-\omega} = \{\tanh(\varepsilon/2T) - \tanh[(\varepsilon-\omega)/2T]\}\, H_1(\omega)$. In doing so, $(-h + \Sigma_1^{(a)})$ will correspond to the vertices

and $(-\bar{h} + \Sigma_1^{(a)})$ to

.

Taking into account that the products, such as FF^+ or $\Sigma_2^+ F$, change the sign of the diagram, one can write:

$$G^{(a)}_{\varepsilon\varepsilon-\omega} = \{G^R(-h+\Sigma_1^{(a)})G^A - G^R\Sigma_2^{(a)}F^{+A} - F^R\Sigma_2^{+(a)}\bar{G}^A - F^R(-\bar{h}+\bar{\Sigma}_1^{(a)})F^+\}_{\varepsilon\omega-\varepsilon}, \tag{3.41}$$

where the notation

$$\{ABC\}_{\varepsilon\varepsilon-\omega} = \int\int \frac{d\omega_1 d\omega_2}{(2\pi)^2} A_{\varepsilon\varepsilon-\omega_1} B_{\varepsilon-\omega_1\varepsilon-\omega_2} C_{\varepsilon-\omega_2\varepsilon-\omega} \tag{3.42}$$

is used. In the same manner one has

$$F^{(a)}_{\varepsilon\varepsilon-\omega} = \{G^R(-h+\Sigma_1^{(a)})F^A + G^R\Sigma_2^{(a)}\bar{G}^A + F^R(-\bar{h}+\bar{\Sigma}_1^{(a)})\bar{G}^A - F^R\Sigma_2^{+(a)}F^A\}\{ABC\}_{\varepsilon\varepsilon-\omega}, \tag{3.43}$$

$$F^{+(a)}_{\varepsilon\varepsilon-\omega} = \{\bar{G}^R(-\bar{h}+\bar{\Sigma}_1^{(a)})F^{+A} + F^{+R}(-h+\Sigma_1^{(a)})G^A + \bar{G}^R\Sigma_2^{+(a)}G^A - F^{+R}\Sigma_2^{(a)}F^{+A}\}_{\varepsilon\varepsilon-\omega}, \tag{3.44}$$

$$\bar{G}^{(a)}_{\varepsilon\varepsilon-\omega} = \{\bar{G}^R(-\bar{h}+\bar{\Sigma}_1^{(a)})\bar{G}^A - F^{+R}(-h+\Sigma_1^{(a)})F^A + \bar{G}^R\Sigma_2^{+(a)}F^A - F^{+R}\Sigma_2^{(a)}G^A\}_{\varepsilon\varepsilon-\omega}. \tag{3.45}$$

The elements of $\hat{\Sigma}^{(a)}$ are found from the definition of $\hat{\Sigma}$:

$$\hat{\Sigma}_{\varepsilon\varepsilon-\omega} = \sum_{N=0}^{\infty}\sum_{l=1}^{N+1}\delta_l(\hat{\Sigma}^{(N)})\tanh\frac{\varepsilon_l}{2T}, \tag{3.46}$$

from which, in analogy with Eq. (3.40),

$$\hat{\Sigma}_{\varepsilon\varepsilon-\omega} = \hat{\Sigma}^R_{\varepsilon\varepsilon-\omega}\tanh\frac{\varepsilon-\omega}{2T} - \tanh\frac{\varepsilon}{2T}\hat{\Sigma}^A_{\varepsilon\varepsilon-\omega} + \hat{\Sigma}^{(a)}_{\varepsilon\varepsilon-\omega}. \tag{3.47}$$

3.2.5. Complete Set of Equations

We will find now the explicit form of the dependence between Σ and G. We will use representation (3.35) for $\Sigma^{(N)}_{\varepsilon\varepsilon-\omega}$ and calculate directly the sum (3.46). Taking into account that the phonon propagator has poles at Im $(\varepsilon - \omega_i) = 0$; writing the expression for $\delta_i(\Sigma^{(N)}_{\varepsilon\varepsilon-\omega})$ and shifting the integration variable (subject to $\tanh[(z+\omega_i)/2T] = \tanh[z/2T]$); multiplying the result by $\tanh(\varepsilon_l/2T)$ and taking into account the identity

$$\coth(x-x')\tanh x = -\tanh x\tanh x' + \coth(x-x')\tanh x' + 1 \tag{3.48}$$

and summing first over i and then over all the orders of the perturbation theory, we find the expression

$$\hat{\Sigma}_{\varepsilon\varepsilon-\omega} = \int_{-\infty}^{\infty}\frac{d\varepsilon'}{4\pi i}\left\{\coth\frac{\varepsilon'-\varepsilon}{2T}\hat{G}_{\varepsilon'\varepsilon'-\omega} - \left(\hat{G}^R - \hat{G}^A\right)_{\varepsilon'\varepsilon'-\omega}\right\}(D^R - D^A)_{\varepsilon'-\varepsilon}. \tag{3.49}$$

To complete the set of equations, it is necessary to establish the equation for the $\hat{G}$-function defined by the relation (3.36). The method to be used here was described in Chap. 2. Starting from the diagram expansion for the $\mathcal{G}$-function and separating there the line corresponding to the bare propagator of electrons, we find from the 11-element of the $\hat{G}$-matrix:

$$\left[\frac{1}{2m}\left(\hat{\mathbf{p}}-\frac{e}{c}\mathbf{A}\right)^2+e\varphi-\varepsilon_F-\varepsilon\right]G^{(a)}_{\varepsilon\varepsilon-\omega}$$
$$=\left|(-h+\Sigma_1^{(a)})\,G^A-\Sigma_2^{(a)}\,F^{+A}\right|_{\varepsilon\varepsilon-\omega}+\left|\Sigma_1^R\,G^{(a)}-\Sigma_2^R\,F^{+(a)}\right|_{\varepsilon\varepsilon-\omega}. \tag{3.50}$$

Using the definitions (3.46) and (3.40), and also Eqs. (3.38) for the causal Green's functions, one can obtain on the basis of (3.50) the equation

$$\begin{pmatrix}\frac{1}{2m}(\hat{\mathbf{p}}-\frac{e}{c}\mathbf{A})^2+e\varphi-\varepsilon_F-\varepsilon-\Sigma_1^R & -\Sigma_2^R\\ \Sigma_2^{+R} & \frac{1}{2m}(\hat{\mathbf{p}}+\frac{e}{c}\mathbf{A})^2+e\varphi-\varepsilon_F+\varepsilon-\overline{\Sigma}_1^R\end{pmatrix}\begin{pmatrix}G & F\\ -F^+ & \overline{G}\end{pmatrix}$$
$$=\begin{pmatrix}\Sigma_1 & \Sigma_2\\ -\Sigma_2^+ & \overline{\Sigma}_1\end{pmatrix}\begin{pmatrix}G^A & F^A\\ -F^{+A} & \overline{G}^A\end{pmatrix}, \tag{3.51}$$

or in the integral form:

$$\hat{G}=\hat{G}^R\,\hat{\Sigma}\,\hat{G}^A. \tag{3.52}$$

Thus the closed system of Eqs. (3.37), (3.38), (3.49), and (3.51) is derived for the functions $\hat{G}$, $\hat{G}^R$, $\hat{G}^A$ and Σ, $\hat{\Sigma}^R$, $\hat{\Sigma}^A$, which describes the behavior of nonequilibrium superconductors in the phonon heat-bath model. The temperature enters these equations explicitly only in equations for Σ and $\Sigma^{R(A)}$ as the characteristics of the phonon heat bath.

3.2.6. *Keldysh Technique Approach*

Note that one can obtain the same results by a completely different method developed by Keldysh[10] to describe nonequilibrium states. In that case the electron Green's function is defined in the following way (we use here the notations of Volkov and Kogan[11]):

$$G^{ik}_{\mu\nu}(1,2)=-i\,\langle T\Psi_\mu(1i)\,\Psi^\dagger_\nu(2k)\rangle. \tag{3.53}$$

Here $1=(\mathbf{r}_1,t_1)$ and μ and ν are the Nambu indices of the field operators

$$\Psi_1(1i)\equiv\Psi_\uparrow(1i),\quad \Psi_2(1i)\equiv\Psi^\dagger_\downarrow(1i). \tag{3.54}$$

The Keldysh indices i,k are the signs minus or plus, according to the position of the time coordinate of the Ψ-operators on each of two time axes $(-\infty,\infty$ or $\infty,-\infty)$.[10] The time on the second axis (the index +) is greater than any time on the first axis (the index –). For functions G, G^R, and G^A, which are defined as in the case of a normal metal (see, e.g., Ref. 12),

$$\begin{pmatrix} 0 & G^A \\ G^R & G \end{pmatrix} = \hat{U}^{-1}\,\hat{G}\hat{U},\ \hat{G} = (G)^{ik},\ \hat{U} = \frac{\hat{1} + i\hat{\sigma}_y}{2}, \tag{3.55}$$

one can obtain the equations coinciding with (3.51) and (3.38). This coincidence of the results obtained by the Gor'kov–Eliashberg and the Keldysh techniques will be demonstrated further on, when the phonon kinetics in superconductors are considered.

3.3. QUASI-CLASSICAL APPROXIMATION

The equations obtained in the preceding section may be simplified further when the phenomena occurring in superconductors involve electrons localized in the momentum space near the vicinity of the Fermi surface. (In other words, when microscopic processes of interest may be considered as macroscopic on the atomic scales of space and time.) Such a situation is typical for most of the phenomena occurring in nonequilibrium superconductors. In this case one can use a generalization of the method introduced by Eilenberger[13] for equilibrium superconductors.

3.3.1. Eilenberger Propagators

The essence of this approach may be elucidated in terms of the electron wave function of the superconductor. The wave function of an electron with a momentum in the vicinity of the Fermi surface oscillates rapidly in space and time. Under the influence of external quasi-classical perturbation, the wave function's amplitude becomes weakly modulated. The information of interest is contained in the "enveloping curve" of the modulated signal. This allows us to ignore the "carrying" frequency and to use only the "enveloping curve."* In the Green's functions technique, this procedure is equivalent to integration over the values of $|\mathbf{p}|$ or $\xi = v_F(p - p_F)$.

Consider one of the equations for the self-energy functions, for example, for Σ^R (3.37). In the momentum representation we have

*An analogous procedure is applied in passing from the Bogolyubov–De Gennes equations to the Andreev equations (see Sect. 1.1).

$$\hat{\Sigma}^R(P, P-K) = \int_{-\infty}^{\infty} \frac{d\varepsilon'}{4\pi i} \int \frac{d^3\mathbf{p}'}{(2\pi)^3} \left\{ \coth \frac{\varepsilon' - \varepsilon}{2T} (D^R - D^A)(P' - P) \hat{G}^R(P', P' - K) \right.$$

$$\left. + D^A(P' - P) \hat{G}(P', P' - K) \right\}. \tag{3.56}$$

Here $P = \{\varepsilon, \mathbf{p}\}$, $K = \{\omega, \mathbf{k}\}$. If the external momentum in (3.56) is close to the Fermi surface: $p \sim p_F$, ε and $\varepsilon' < \omega_D$, then the main contribution to integral (3.56) is provided by the region $|\mathbf{p} - \mathbf{p}'| << p_F$ (the integration over $\mathbf{p}'$ in the regions remote from the Fermi surface renormalizes the chemical potential, which is insensitive to details of the electron distribution in the vicinity of p_F. The D-function now depends only on the angle θ between $\mathbf{p}$ and $\mathbf{p}'$: $|\mathbf{p} - \mathbf{p}'|^2 \approx 2p_F^2(1 - \cos\theta)$. Using the chain of equalities

$$\frac{d^3\mathbf{p}}{(2\pi)^3} = \frac{p^2 dp d\Omega_{\mathbf{p}}}{(2\pi)^3} = \frac{d\Omega_{\mathbf{p}}}{2} \frac{pdp^2}{(2\pi)^3} \approx \frac{mp_F}{2\pi^2} d\xi \frac{d\Omega_{\mathbf{p}}}{4\pi}, \tag{3.57}$$

it is easy to establish that $\hat{\Sigma}^R$ is expressed by Green's functions, integrated over the energy variable:

$$\hat{g}^{(R,A)}_{\varepsilon\varepsilon-\omega}(\mathbf{p}, \mathbf{k}) = \int_{-\infty}^{\infty} d\xi \hat{G}^{(R,A)}(P, P - K), \quad \hat{g}^{(R,A)} = \begin{pmatrix} g & f \\ -f^+ & \bar{g} \end{pmatrix}^{(R,A)}. \tag{3.58}$$

Similar conclusions follow for other self-energy functions, so that one has:

$$\hat{\Sigma}^{R(A)}_{\varepsilon\varepsilon-\omega}(\mathbf{p}, \mathbf{k}) = \int_{-\infty}^{\infty} \frac{d\varepsilon'}{4\pi i} \int d\frac{\Omega_{\mathbf{p}'}}{4\pi} \left\{ \coth \frac{\varepsilon' - \varepsilon}{2T} (D^R - D^A)_{\varepsilon'-\varepsilon}(\theta) \hat{g}^{R(A)}_{\varepsilon'\varepsilon'-\omega}(\mathbf{p}', \mathbf{k}) \right.$$

$$\left. + D^{A(R)}_{\varepsilon'-\varepsilon}(\theta) \hat{g}_{\varepsilon'\varepsilon'-\omega}(\mathbf{p}', \mathbf{k}) \right\}, \tag{3.59}$$

$$\hat{\Sigma}_{\varepsilon\varepsilon-\omega}(\mathbf{p}, \mathbf{k}) = \int_{-\infty}^{\infty} \frac{d\varepsilon'}{4\pi i} \int \frac{d\Omega_{\mathbf{p}'}}{4\pi} \left\{ \coth \frac{\varepsilon' - \varepsilon}{2T} \hat{g}_{\varepsilon'\varepsilon'-\omega}(\mathbf{p}', \mathbf{k}) \right.$$

$$\left. - (\hat{g}^R - \hat{g}^A)_{\varepsilon'\varepsilon'-\omega}(\mathbf{p}', \mathbf{k}) \right\} (D^R - D^A)_{\varepsilon'-\varepsilon}(\theta). \tag{3.60}$$

3.3.2. Eliashberg Kinetic Equations

Now let us transform Eq. (3.51). Ignoring the quadratic terms in $\underline{\mathbf{A}}$, and moving to the quantities H_1 and $\overline{H}_1$, one finds by multiplying Eq. (3.52) by $[\overline{G}^R]^{-1}$ from the left and by $[\overline{G}^A]^{-1}$ from the right:

$$\begin{pmatrix} \xi - \varepsilon + H_1 & 0 \\ 0 & \xi + \varepsilon + \overline{H}_1 \end{pmatrix} \hat{G} = \hat{\Sigma}^R \hat{G} + \hat{\Sigma} \hat{G}^A, \tag{3.61}$$

$$\hat{G}\begin{pmatrix} \xi - \mathbf{vk} - \varepsilon + \omega + H_1 & 0 \\ 0 & \xi - \mathbf{vk} + \varepsilon - \omega + \overline{H}_1 \end{pmatrix} = \hat{G}\hat{\Sigma}^A + \hat{G}^R\hat{\Sigma}, \quad (3.62)$$

where $v = P/m$. Subtracting from Eq. (3.62) Eq. (3.61) and integrating the result over ξ, we find the equation for the $\hat{g}$-function (3.58):

$$\begin{pmatrix} (\omega - \mathbf{vk})g & (2\varepsilon - \omega - \mathbf{vk})f \\ (2\varepsilon - \omega + \mathbf{vk})f^+ & -(\omega + \mathbf{vk})\hat{g} \end{pmatrix} = \begin{pmatrix} H_1 & 0 \\ 0 & H_1 \end{pmatrix}\hat{g} - \hat{g}\begin{pmatrix} H_1 & 0 \\ 0 & \overline{H}_1 \end{pmatrix} + \hat{g}\hat{\Sigma}^A - \hat{\Sigma}^R\hat{g} + \hat{g}^R\hat{\Sigma} - \hat{\Sigma}\hat{g}^A. \quad (3.63)$$

The set of arguments of the $\hat{g}$-functions entering this equation is analogous to that of electron distribution function. For this reason Eq. (3.63) may be called the generalized kinetic equation. The quantity

$$\hat{I} = \hat{g}\hat{\Sigma}^A - \hat{\Sigma}^R\hat{g} + \hat{g}^R\hat{\Sigma} - \hat{\Sigma}\hat{g}^A \quad (3.64)$$

is the collision integral (at present between electrons and phonons). The equation for the function $g^{R(A)}$ [which may be obtained from Eq. (3.38) by the procedure used above] is similar to Eq. (3.63), although the quantity $\hat{I}$ must be replaced by $\hat{I}^{R(A)}$:

$$\hat{I}^{R(A)} = \hat{g}^{R(A)}\hat{\Sigma}^{R(A)} - \hat{\Sigma}^{R(A)}\hat{g}^{R(A)}. \quad (3.65)$$

In the equilibrium case, when the field **A** is absent:

$$(\hat{g}^R - \hat{g}^A)_\varepsilon = 2\pi i\begin{pmatrix} \varepsilon & \Delta \\ -\Delta^* & -\varepsilon \end{pmatrix}\frac{\operatorname{sign}\varepsilon}{\sqrt{\varepsilon^2 - |\Delta|^2}}\,\theta(\varepsilon^2 - |\Delta|^2), \quad (3.66)$$

i.e., $(\hat{g}^R - \hat{g}^A)_\varepsilon$ is proportional to the density of single-particle excitation states (for this reason $\hat{g}^R$, $\hat{g}^A$ are called *spectral functions*).

As for the functions $\hat{g}_{\varepsilon\varepsilon-\omega}$, from Eq. (3.58) in the equilibrium case, the relation follows

$$\hat{g}_\varepsilon = (\hat{g}^R - \hat{g}^A)_\varepsilon \tanh\frac{\varepsilon}{2T} = (\hat{g}^R - \hat{g}^A)_\varepsilon\,(1 - 2n_\varepsilon^F)\operatorname{sign}\varepsilon, \quad (3.67)$$

where n_ε^F is the distribution function of the electronlike $(\varepsilon > 0)$ and holelike $(\varepsilon < 0)$ Fermi excitations. In the nonequilibrium case, as we will see, n_ε in general does not necessarily coincide with $n_{-\varepsilon}$. However, the correct generalization of Eq. (3.67) cannot be achieved by the trivial replacement $1 - 2n_\varepsilon^F \to 1 - n_\varepsilon - n_{-\varepsilon}$, as might be thought. Such a replacement would retain g_ε as an odd function in ε, whereas in the general case g_ε can have an even in the ε part also. The necessary generalization can be obtained with the help of the normalization condition for g-functions, as was shown for the equilibrium case by Eilenberger[13] and for the nonequilibrium case by Larkin and Ovchinnikov.[14]

3.3.3. Normalization Condition

In a real-time representation (see Eq. 3.53), this condition has the form*

$$\check{g} * \check{g} = \text{const} \times \check{1}, \tag{3.68}$$

where

$$\check{g} = \begin{pmatrix} \hat{g}^R & \hat{g} \\ \hat{0} & \hat{g}^A \end{pmatrix}, \quad \check{1} = \begin{pmatrix} \hat{1} & \hat{0} \\ \hat{0} & \hat{1} \end{pmatrix}, \tag{3.69}$$

and the symbol * is the convolution in time according to

$$A * B = \int A(t_1, t_3)\, B(t_3, t_2)\, dt_3. \tag{3.70}$$

The normalization condition (3.68) is satisfied identically by the following substitution

$$\hat{g} = \hat{g}^R * \hat{a} - \hat{a} * \hat{g}^A, \tag{3.71}$$

where $\hat{a}$ is an arbitrary 2×2 matrix function of ε, which may be represented as the sum of the Pauli matrices, the diagonal matrices only participating in this decomposition:

$$\hat{a} = f_1 \hat{1} + f_2 \hat{\sigma}_z. \tag{3.72}$$

The functions f_1 and f_2 are linked with the distribution function of electron-hole excitations n_ε. Before showing this relation, we consider some general properties of f_1 and f_2 and establish their gauge transformation laws.

3.3.4. Gauge Transformation

The basic gauge transformation law for a field operator $\Psi(\mathbf{r},t)$ under the transformation of scalar potential $\varphi \to \varphi - \dot{\chi}/2$ is

$$\Psi(\mathbf{r},t) \to \exp[i\chi(\mathbf{r},t)/2]\, \Psi(\mathbf{r},t) \tag{3.73}$$

(where χ is an arbitrary function). From (3.73) and (3.53) it follows that the propagator $\hat{g}$ (as well as the spectral functions $\hat{g}^R$ and $\hat{g}^A$) is transformed according to

*To avoid interrupting the presentation, we will prove this statement in Chap. 7. It is worth noting that in the theory of superconductivity, the normalization condition is proved only at the "physical level" of rigor.

$$\hat{g} \to \exp\,[i\hat{\sigma}_z\,\chi/2\,] * \hat{g} * \exp\,[-i\hat{\sigma}_z\,\chi/2\,]. \tag{3.74}$$

In the quasi-classical limit, when the propagators are fast-varying functions of a difference variable $(t_1 - t_2)$ and slow-varying functions of a sum $t = (t_1 + t_2)/2$, the expression (3.70) may be presented in the form

$$A * B = AB + \frac{i}{2}\{A_{,\varepsilon}\dot{B} - \dot{A}B_{,\varepsilon}\} - \frac{1}{8}\{A_{,\varepsilon\varepsilon}\ddot{B} - 2\dot{A}_{,\varepsilon}\dot{B}_{,\varepsilon} + \ddot{A}B_{,\varepsilon\varepsilon}\} + \ldots\,. \tag{3.75}$$

In Eq. (3.75) the following notations are used: $A_{,\varepsilon} \equiv \partial A/\partial\varepsilon$, $\dot{A} \equiv \partial A/\partial t$, and the frequency ε corresponds to the Fermi transform over the difference argument $(t_1 - t_2)$. From Eqs. (3.74) and (3.75) a transformation law follows for diagonal components of propagators*:

$$\hat{g}^{\text{diag}} \to \hat{g}^{\text{diag}} + \frac{\dot{\chi}}{2}\hat{g}^{\text{diag}}_{,\varepsilon} + \frac{\dot{\chi}^2}{2}\hat{g}^{\text{diag}}_{,\varepsilon\varepsilon}. \tag{3.76}$$

Hereafter the terms proportional to $\ddot{\chi}$ are omitted owing to the assumed quasi-classical character of φ.

At the same time, one can make a gauge transformation of the function defined by expression (3.71). Taking into account that the functions $\hat{g}^R$ and $\hat{g}^A$ transform in analogy to (3.74), one can obtain the coincidence of the corresponding result with (3.76). This provides the transformation laws for the functions f_1 and f_2:

$$f_{1(2)} \to f_{1(2)} + \frac{\dfrac{\dot{\chi}}{2}(f_1 + f_2)_{,\varepsilon} + \dfrac{\dot{\chi}^2}{8}\left[(f_1 + f_2)_{,\varepsilon\varepsilon} + 2\dfrac{N_{1,\varepsilon}}{N_1}(f_1 + f_2)_{,\varepsilon}\right]}{2 + \dot{\chi}\,N_{1,\varepsilon}/N_1 + \dot{\chi}^2\,N_{1,\varepsilon\varepsilon}/4N_1}$$

$$+ (-)\frac{-\dfrac{\dot{\chi}}{2}(f_1 - f_2)_{,\varepsilon} + \dfrac{\dot{\chi}^2}{8}\left[(f_1 - f_2)_{,\varepsilon\varepsilon} + 2\dfrac{\overline{N}_{1,\varepsilon}}{N_1}(f_1 - f_2)_{,\varepsilon}\right]}{2 - \dot{\chi}\,\overline{N}_{1,\varepsilon}/N_1 + \dot{\chi}^2\,\overline{N}_{1,\varepsilon\varepsilon}/4N_1}. \tag{3.77}$$

The functions N_1 and $\overline{N}_1$ in (3.77) are defined by the relations

$$N_1 = \frac{g^R - g^A}{2\pi i},\quad \overline{N}_1 = \frac{\overline{g}^R - \overline{g}^A}{2\pi i}. \tag{3.78}$$

If $\varphi \to \varphi - \chi/2$, we have in accordance with (3.74), (3.71), and (3.78),

*At this stage it becomes clear that expression (3.74) is an equivalent form of the usual relation for Green's function: $G \to G\exp\,[i\chi(t_1)/2 - i\chi(t_2)/2\,]$ in the gauge transformation. Expanding the exponent over the "fast" time $(t_1 - t_2)$ and finding the Fourier transforms over the difference variable, one can obtain expression (3.76) for the appropriate matrix component.

$$N_1 \to N_1 + \frac{\dot{\chi}}{2} N_{1,\varepsilon} + \frac{\dot{\chi}^2}{8} N_{1,\varepsilon\varepsilon}, \tag{3.79}$$

$$\overline{N}_1 \to \overline{N}_1 - \frac{\dot{\chi}}{2} \overline{N}_{1,\varepsilon} + \frac{\dot{\chi}^2}{8} \overline{N}_{1,\varepsilon\varepsilon}. \tag{3.80}$$

Note that, owing to Eqs. (3.77) and (3.79), the functions f_1 and f_2 (in analogy with N_1 and N_2) are functions of a general type. They have definite parity only in the absence of external fields.

3.3.5. Electron and Hole Distribution Functions

In the absence of external fields, as may be seen from the definition of these functions and Eq. (3.63), $f_1(\varepsilon)$ and $N_2(\varepsilon)$ are odd functions of ε, while $f_2(\varepsilon)$ and $N_1(\varepsilon)$ are even functions of ε. Introducing an arbitrary function n_ε (here $-\infty < \varepsilon < \infty$), we can write (making $\varphi = 0$)

$$f(\varepsilon_1) = a_1 (n_\varepsilon + n_{-\varepsilon} - 1), \quad f_2(\varepsilon) = a_2(n_\varepsilon - n_{-\varepsilon}). \tag{3.81}$$

Because the function n_ε should be determined further from the kinetic equations, there is still an arbitrariness in the choice of coefficients a_1 and a_2. It is convenient to choose them in the form

$$a_1 = \operatorname{sign}\varepsilon, \quad a_2 = -u_\varepsilon^{-1} \operatorname{sign}\varepsilon, \tag{3.82}$$

where

$$u_\varepsilon = \frac{|\varepsilon|\, \theta(\varepsilon_{\mathbf{p}}^2 - |\Delta|^2)}{\sqrt{\varepsilon_{\mathbf{p}}^2 - |\Delta|^2}}. \tag{3.83}$$

Then the expressions for $\hat{g}^{R(A)}$ take the form

$$\hat{g}_\varepsilon = -2\pi i \begin{pmatrix} u_\varepsilon \beta_\varepsilon + \alpha_\varepsilon & v_\varepsilon \beta_\varepsilon \\ -v_\varepsilon \beta_\varepsilon & -u_\varepsilon \beta_\varepsilon + \alpha_\varepsilon \end{pmatrix}, \tag{3.84}$$

$$(\hat{g}^R - \hat{g}^A)_\varepsilon = 2\pi i \begin{pmatrix} u_\varepsilon & v_\varepsilon \\ -v_\varepsilon & -u_\varepsilon \end{pmatrix}, \tag{3.85}$$

where

$$v_\varepsilon = \frac{|\Delta|\, \theta(\varepsilon_{\mathbf{p}}^2 - |\Delta|^2)}{\sqrt{\varepsilon_{\mathbf{p}}^2 - |\Delta|^2}} \operatorname{sign}\varepsilon, \tag{3.86}$$

$$\beta_\varepsilon = (n_\varepsilon + n_{-\varepsilon} - 1)\,\theta\,(\varepsilon_p^2 - |\Delta|^2)\,\mathrm{sign}\varepsilon, \tag{3.87}$$

$$\alpha_\varepsilon = (n_\varepsilon - n_{-\varepsilon})\,\theta\,(\varepsilon_p^2 - |\Delta|^2)\,\mathrm{sign}\varepsilon. \tag{3.88}$$

The constant in expression (3.68) may be chosen to be $-\pi^2$. Without a loss of generality, this ensures a limiting transition to expressions (3.66) and (3.67) in the absence of imbalance, and simultaneously assigns to the function n_ε a transparent meaning for the energy distribution function in "pure" superconductors (this will be shown later). At the same time, it might be noted that the description of a superconductor in terms of $\hat{g}$-functions integrated over the ξ-variable is also valid in cases when the concept of the energy spectrum turns deficient and ξ becomes a bad quantum number (e.g., in the case of superconductors containing very many impurities).

3.3.6. Kinetic Equations: Keldysh Option

As shown by Keldysh,[10] in a nonequilibrium system, the Green's function technique allows us to develop kinetic formulas without integrating over energies. In such cases, the energy distribution function of excitations is connected to Green's functions, integrated over the frequency variable. If the energy spectrum is well defined, these two methods are usually adequate.*

For the causal Green's function G_{11}^{--}, using the definition (3.53) and solving at $\varepsilon << \omega_D$ the Dyson equations by analogy to the normal metal case (cf. Ref. 12), we have:

$$G_{11}^{--}(\varepsilon,\mathbf{p}) = \mathcal{U}_\mathbf{p}^2\left(\frac{n_\mathbf{p}}{\varepsilon - \varepsilon_\mathbf{p} - i\delta} + \frac{1 - n_\mathbf{p}}{\varepsilon - \varepsilon_\mathbf{p} + i\delta}\right) + \mathcal{V}_\mathbf{p}^2\left(\frac{n_{-\mathbf{p}}}{\varepsilon + \varepsilon_\mathbf{p} + i\delta} + \frac{1 - n_{-\mathbf{p}}}{\varepsilon + \varepsilon_\mathbf{p} - i\delta}\right), \tag{3.89}$$

where the factors $\mathcal{U}_\mathbf{p}^2$ and $\mathcal{V}_\mathbf{p}^2$ are defined by the relation (1.23), $\varepsilon_\mathbf{p}$ –by (1.132), and $n_\mathbf{p}$ corresponds to the distribution function of electronlike $(\xi_\mathbf{p} > 0)$ and holelike $(\xi_\mathbf{p} < 0)$ excitations.

Following Aronov and Gurevich,[15] one can introduce a spectral representation for the causal function

$$G_{11}^{--}(\varepsilon, \mathbf{p}) = \int_{-\infty}^{\infty} \frac{d\varepsilon'}{2\pi i}\left[\frac{G_{11}^{-+}(\varepsilon', \mathbf{p})}{\varepsilon - \varepsilon' - i\delta} - \frac{G_{11}^{+-}(\varepsilon', \mathbf{p})}{\varepsilon - \varepsilon' + i\delta}\right]. \tag{3.90}$$

*We have noted the advantage of energy-integrated functions for "dirty" superconductors. At the same time, this technique fails when considering processes far from the Fermi surface, e.g., a high-energy particle cascading in superconductors. In such situations usual (Keldysh's) formulation of the kinetic scheme is preferable.

Comparing Eqs. (3.89) and (3.90), one can find

$$G_{11}^{-+}(\varepsilon,\mathbf{p}) = 2\pi i\,[\mathcal{U}_{\mathbf{p}}^2 n_{\mathbf{p}}\,\delta(\varepsilon-\varepsilon_{\mathbf{p}}) + \mathcal{V}_{\mathbf{p}}^2(1-n_{-\mathbf{p}})\,\delta(\varepsilon+\varepsilon_{\mathbf{p}})], \tag{3.91}$$

$$G_{11}^{+-}(\varepsilon,\mathbf{p}) = -2\pi i\,[\mathcal{U}_{\mathbf{p}}^2(1-n_{\mathbf{p}})\,\delta(\varepsilon-\varepsilon_{\mathbf{p}}) + \mathcal{V}_{\mathbf{p}}^2 n_{-\mathbf{p}}\,\delta(\varepsilon+\varepsilon_{\mathbf{p}})]. \tag{3.92}$$

In the same manner

$$G_{12}^{--}(\varepsilon,\mathbf{p}) = \mathcal{U}_{\mathbf{p}}\mathcal{V}_{\mathbf{p}}\left(\frac{n_{\mathbf{p}}}{\varepsilon-\varepsilon_{\mathbf{p}}-i\delta} + \frac{1-n_{\mathbf{p}}}{\varepsilon-\varepsilon_{\mathbf{p}}+i\delta} - \frac{n_{-\mathbf{p}}}{\varepsilon+\varepsilon_{\mathbf{p}}+i\delta} - \frac{1-n_{-\mathbf{p}}}{\varepsilon+\varepsilon_{\mathbf{p}}-i\delta}\right), \tag{3.93}$$

$$G_{12}^{+-}(\varepsilon,\mathbf{p}) = -2\pi i\mathcal{U}_{\mathbf{p}}\mathcal{V}_{\mathbf{p}}\,[\,(1-n_{\mathbf{p}})\,\delta(\varepsilon-\varepsilon_{\mathbf{p}}) - n_{-\mathbf{p}}\,\delta(\varepsilon+\varepsilon_{\mathbf{p}})], \tag{3.94}$$

$$G_{21}^{+-}(\varepsilon,\mathbf{p}) = G_{21}^{-+}(-\varepsilon,-\mathbf{p}). \tag{3.95}$$

Using these relations one can obtain the canonical forms of the collision integrals in superconductors[15] in a manner completely analogous to the case of a normal metal.[12] We will obtain the same kind of collision integrals (in ε–,rather than in ξ– representation) in the next chapter by employing the propagators integrated over energies. When both representations are applicable, these collision integrals are completely adequate.

3.3.7. Expressions for Charge and Current

In general, the technique of the energy-integrated Green's functions is more convenient for those problems where the kinetic processes occur in the vicinity of the Fermi surface. In these cases it provides a powerful tool for the study of both pure and dirty superconductors.

On the contrary, if the main processes occur in the regions remote from the Fermi surface, a straightforward application of this technique may lead to erroneous results. This difficulty may be overcome by properly accounting for the contribution that results from the equilibrium in the Green's function formula. Consider, for example, an expression for the electron charge in a superconductor. In the representation of the discrete imaginary frequencies, one can write an expression (2.86) for the number of electrons in superconductors as

$$N_{\omega}(\mathbf{k}) = -Tr\left\{T\sum_{\varepsilon}\int\frac{d^3\mathbf{p}}{(2\pi)^3}\,\mathcal{G}_{\varepsilon\varepsilon-\omega}(\mathbf{p},\mathbf{p}-\mathbf{k})\right\}. \tag{3.96}$$

We will separate in this expression the contribution supplied by a zero-order Green's function $\mathcal{G}_{\varepsilon}^{0}(\mathbf{p}) = (\xi-\varepsilon)^{-1}$, where $\xi = p^2/(2m) - \varepsilon_F - e\varphi$ includes the quasi-classi-

cal scalar potential in the system. The deviation in the number of particles induced by the potential φ (in the first order in φ) has the form

$$\delta N(\varphi) = 2T \sum_{\varepsilon} \int \frac{d^3\mathbf{p}}{(2\pi)^3} \frac{1}{(\xi - \varepsilon)^2} e\varphi = -\frac{\partial N^{(0)}}{\partial \varepsilon_F} e\varphi = \frac{mp_F}{\pi^2} e\varphi, \tag{3.97}$$

where $N^{(0)}$ is the equilibrium electron density. Thus the electron density in nonequilibrium superconductors is

$$N_\omega(\mathbf{k}) = N^{(0)} (2\pi)^4 \delta(\omega) \delta(\mathbf{k}) - \frac{mp_F}{\pi^2} \left[e\varphi + \int_{-\infty}^{\infty} \frac{d\varepsilon}{4\pi i} \int \frac{d\Omega_{\mathbf{p}}}{4\pi} g'_{\varepsilon\varepsilon-\omega} \right], \tag{3.98}$$

where $g'_{\varepsilon\varepsilon-\omega} = g_{\varepsilon\varepsilon-\omega} - 2\pi i \tanh(\varepsilon/2T)$ [the prime in (3.98) may be omitted if the integration over ε is assumed the principal value sense in symmetrical limits]. From (3.98) the relation follows for a charge in nonequilibrium conditions:

$$\rho_\omega(\mathbf{k}) = e[N_\omega(\mathbf{k}) - N^{(0)} (2\pi)^4 \delta(\omega) \delta(\mathbf{k})]. \tag{3.99}$$

The situation with expression (2.87) for the electric current is analogous. The correct accounting of the contribution supplied by the regions remote from the Fermi surface results in the disappearance of the contribution from the second term in Eq. (2.87), which must be absent if the $\hat{g}$-function technique[9] is used.

References

1. A. A. Abrikosov, L. P. Gor'kov, and I. E. Dzyaloshinskiy, *Quantum Field Theoretical Methods in Statistical Physics,* 2nd ed., pp. 75–76, Pergamon, Oxford (1965).
2. A. B. Migdal, Interaction between electrons and lattice vibrations in a normal metal, *Sov. Phys. JETP* **7**(6), 996–1001 (1958) [*Zh. Eksp. i Teor. Phys.* **34** (6), 1438–1446 (1958)].
3. A. S. Alexandrov and J. Ranninger, Bipolaronic superconductivity, *Phys. Rev.* B24(3), 1164–1169 (1981).
4. A. S. Alexandrov and N. F. Mott, *Polarons and Bipolarons,* pp. 179–187, World Scientific, Singapore (1995).
5. E. G. Brovman and Yu. M. Kagan, Phonons in nontransition metals, *Sov. Phys. Uspekhi* **17** (2), 125–152 (1974) *[Usp. Fiz. Nauk* **112** (3), 369–426 (1974)].
6. G. M. Eliashberg, Temperature Green's function for electrons in a superconductor, *Sov. Phys. JETP* **12**(5), 1000–1002 (1960) [Zh. *Eksp. i Teor. Phys.* **39** [5(11)], 1437–1441 (1960)].
7. E. G. Maximov, in: *High-temperature Superconductivity,* edited by V. L. Ginzburg and D. A. Kirzhnits, pp. 1–364, Consultants Bureau, New York (1982).
8. L. D. Landau and E. M. Lifshitz, *Fluid Mechanics, pp.* 245–310, Pergamon, Oxford (1982).
9. G. M. Eliashberg, Inelastic electron collisions and nonequilibrium stationary states in superconductors, *Sov. Phys. JETP* **34**(3), 668–676 (1972) [Zh. *Eksp. i Teor. Fiz.* **61**[3(9)], 1254–1272 (1971)].
10. L. V. Keldysh, Diagram technique for nonequilibrium processes, *Sov. Phys. JETP* **20**(4), 1018–1026 (1965) [Zh. *Eksp. i Teor. Phys.* **47** [4(10)], 1515–1527 (1964)].

11. A. F. Volkov and Sh. M. Kogan, Collisionless relaxation of the energy gap in superconductors, *Sov. Phys. JETP* **38**(5), 1018–1021 (1974) *[Zh. Eksp. i Teor. Phys.* **65** [5(11)], 2038–2046 (1973)].
12. E. M. Lifshitz and L. P. Pitaevskii, *Physical Kinetics,* pp. 391–412, Pergamon, Oxford (1981).
13. G. Eilenberger, Transformation of Gor'kov equations for type II superconductors into transport-like equations, *Z. Phys.* **214** (2), 195–213 (1968).
14. A.I. Larkin and Yu. N. Ovchinnikov, Nonlinear effects during the motion of vortices in superconductors, *Sov. Phys. JETP* **46**(1), 155–162 (1977) *[Zh. Eksp. i Teor. Fiz.* **73**[1(7)], 299–312 (1977)].
15. A. A. Aronov and V. L. Gurevich, Stability of nonequilibrium Fermi distributions with respect to Cooper pairing, *Sov. Phys. JETP* **38**(3), 550–556 (1974) [*Zh. Eksp. i Teor. Phys.* **65** 3(9), 1111–1124(1973)].

4

Electron and Phonon Collision Integrals

In studies of nonequilibrium phenomena, collision integrals play a unique role. It is well known that they describe the relaxation of excitations toward equilibrium. Less trivial is that they may also be used to describe nonequilibrium excitation sources.

4. 1. COLLISION INTEGRAL DERIVATION

4.1.1. Spatially Homogeneous States

The generalized kinetic equations for integrated Green's functions $\hat{g}_{\varepsilon\varepsilon-\omega}$ provide initial relations for constructing the canonical forms of collision integrals. As was shown in the preceding chapter, the matrix function $\hat{g}_{\varepsilon\varepsilon-\omega}$ obeys Eq. (3.63), which in the spatially homogeneous case can be written as

$$\begin{pmatrix} \omega g & (2\varepsilon-\omega)f \\ (2\varepsilon-\omega)f^{+} & -\omega\bar{g} \end{pmatrix} = \hat{H}_1\hat{g} - \hat{g}\hat{H}_1 + \hat{I}, \tag{4.1}$$

where

$$\hat{I} = \hat{g}\hat{\Sigma}^{A} - \hat{\Sigma}^{R}\hat{g} + \hat{g}^{R}\hat{\Sigma} - \hat{\Sigma}\hat{g}^{A}, \tag{4.2}$$

$$\hat{g}^{R(A)} = \begin{pmatrix} g & f \\ -f^{+} & \bar{g} \end{pmatrix}^{R(A)}, \quad \hat{\Sigma}^{R(A)} = \begin{pmatrix} \Sigma_1 & \Sigma_2 \\ -\Sigma_2^{+} & \bar{\Sigma}_1 \end{pmatrix}^{R(A)}, \tag{4.3}$$

$$\hat{H} = \begin{pmatrix} H_1 & 0 \\ 0 & \bar{H}_1 \end{pmatrix}, \; H_1 = -\frac{e}{c}\mathbf{v}\cdot\mathbf{A} + e\varphi, \; \bar{H}_1 = \frac{e}{c}\mathbf{v}\cdot\mathbf{A} + e\varphi, \quad \mathbf{v} = \mathbf{v}_F. \tag{4.4}$$

The retarded (advanced) functions in Eqs. (4.1) to (4.3) are determined from the diagram expansion in which all the propagators and self-energies are retarded (advanced) (Sect. 3.2). For these functions equations of type (4.1) follow, where $\hat{I}^{R(A)} = \hat{g}^R\hat{\Sigma}^{R(A)} - \hat{\Sigma}^{R(A)}\hat{g}^R$. The self-energy matrices $\hat{\Sigma}^{R(A)}$ in (4.2) are additive functions*:

$$\hat{\Sigma} = \hat{\Sigma}^{(\mathrm{imp})} + \hat{\Sigma}^{(\mathrm{e-ph})} + \hat{\Sigma}^{(\mathrm{e-e})} + \hat{\Sigma}^{(\mathrm{T})}. \tag{4.5}$$

They correspond to the interaction of electrons with impurities, phonons, each other, etc. Some of the self-energy parts are examined in detail in subsequent sections.

4.1.2. Separation of Real and Virtual Processes

Separating in Eq. (4.2) the terms corresponding to the electron–phonon interaction, we will detach the virtual processes. Omitting the renormalization terms $(\Sigma_1^R + \Sigma_1^A)^{(\mathrm{e-ph})}$ and introducing a superconducting order parameter[2]

$$\Delta = \frac{1}{2}(\Sigma_2^R + \Sigma_2^A)^{(\mathrm{e-ph})}, \tag{4.6}$$

one finds for the 11-component of (4.2) the following expression

$$I_{\varepsilon\varepsilon-\omega} = \{-f\Delta^* + \Delta f^+\}_{\varepsilon\varepsilon-\omega} + \{-i(g\gamma + \gamma g) + i(-f\delta^+ + \delta f^+) + g^R\Sigma_1^{(\mathrm{e-ph})}$$
$$-\Sigma_1^{(\mathrm{e-ph})}g^A - f^R\Sigma_2^{+(\mathrm{e-ph})} + \Sigma_2^{(\mathrm{e-ph})}f^{+A}\}_{\varepsilon\varepsilon-\omega} + I'_{\varepsilon\varepsilon-\omega}, \tag{4.7}$$

where the quantities

$$2i\gamma_{\varepsilon\varepsilon-\omega} = (\Sigma_1^R - \Sigma_1^A)^{(\mathrm{e-ph})}, \quad 2i\delta_{\varepsilon\varepsilon-\omega} = (\Sigma_2^R - \Sigma_2^A)^{(\mathrm{e-ph})}, \tag{4.8}$$

as well as $\Sigma_{1,2}^{(\mathrm{e-ph})}$, represent the real interactions between electrons and phonons, which are essential for the kinetics, and $I'_{\varepsilon\varepsilon-\omega}$ no longer contains $\Sigma^{(\mathrm{e-ph})}$ explicitly.

4.1.3. Nondiagonal Channel

The dissipation function γ in Eq. (4.7) (as well as δ and $\Sigma_{1,2}^{(\mathrm{e-ph})}$) has a characteristic magnitude on the order of the energy damping of electron excitations. In normal metals $\gamma \sim T^3/\omega_D^2$; in a superconducting state γ is even smaller, since a significant part of the electron–phonon interaction (the virtual processes) was already taken into account as being responsible for the superconducting transition. The γ-function is less by orders of magnitude than the modulus of the order

*In principle, the interference between different physical processes described by Eq. (4.5) is possible. Such interference has been considered, e.g., by Reizer and Sergeev[1].

parameter Δ almost at all temperatures. Hence, before moving to the kinetic equation in (4.7), we must account exactly for the first expression in braces, using equations for the nondiagonal components of $\hat{g}$-functions following from (4.1) (the nondiagonal channel, cf. Ref. 3). From these equations it follows that

$$(2\varepsilon - \omega)(f - f^+)_{\varepsilon\varepsilon-\omega} = \{i(f\bar{\gamma} + \bar{\gamma}f^+) - i(\gamma f + f^+\gamma) + i(\delta^+ g - g\delta)$$

$$+ i(\bar{g}\delta^+ - \delta\bar{g}) + (g\Delta - \Delta^* g) + (\bar{g}\Delta^* - \Delta\bar{g}) + f^R\bar{\Sigma}_1 + f^{+R}\Sigma_1 - \Sigma_1 f^A$$

$$- \bar{\Sigma}_1 f^{+A} + g^R\Sigma_2 - \Sigma_2\bar{g}^A + \bar{g}^R\Sigma_2^+ - \Sigma_2^+ g^A\}_{\varepsilon\varepsilon-\omega} + I''_{\varepsilon\varepsilon-\omega}. \tag{4.9}$$

As in the derivation of relation (4.7), we have separated in the braces in (4.9) the virtual processes, which explicitly represent the electron–phonon interaction, while $I''_{\varepsilon\varepsilon-\omega}$ contains [in analogy to $I'_{\varepsilon\varepsilon-\omega}$ in (4.7)] all other processes. For the last quantity we have from (4.1):

$$I'' = g\Sigma_2^A + f\bar{\Sigma}_1^A - \Sigma_1^R f - \Sigma_2^R\bar{g} + g^R\Sigma_2 + f^R\bar{\Sigma}_1 - \Sigma_1 f^A - \Sigma_2\bar{g}^A$$

$$+ f^+\Sigma_1^A + \bar{g}\Sigma_2^{+A} - \Sigma_2^{+R} g - \bar{\Sigma}_1^R f^+ + f^{+R}\Sigma_1 + \bar{g}^R\Sigma_2^+ - - \Sigma_2^+ g^A - \bar{\Sigma}_1 f^{+A}. \tag{4.10}$$

(Here all external and internal arguments are omitted; in this notation the order of the co-factors is important.)

4.1.4. Impurities

Here we consider thin-film superconductors with a thickness on the order of the superconducting correlation length. Such specimens always contain a number of electron elastic scattering centers (such as nonmagnetic impurities and lattice defects). If the number of these centers is sufficiently large, the superconducting films would be "dirty" and the mean-free-path of electrons would be shorter than the other lengths, which characterizes their motion in superconductors. This circumstance allows one to make significant simplifications.* In particular, one may ignore anisotropy effects, the nonlocality of electrodynamics, the reflection of electrons from the boundaries, etc.

In the presence of impurities, the self-energy matrix in (4.5) has the form (see Sect. 2.1)

$$\Sigma^{(\mathrm{imp})R(A)}_{\varepsilon\varepsilon-\omega} = \frac{1}{2\pi\tau}\int \frac{d\Omega_{\mathbf{p}}}{4\pi}\hat{g}^{R(A)}_{\varepsilon\varepsilon-\omega}, \quad \Sigma^{(\mathrm{imp})}_{\varepsilon\varepsilon-\omega} = \frac{1}{2\pi\tau}\int \frac{d\Omega_{\mathbf{p}}}{4\pi}\hat{g}_{\varepsilon\varepsilon-\omega}. \tag{4.11}$$

*The case of "pure" superconductors should be studied separately. For example, in Sects. 5.4 and 12.1, some peculiarities will be discussed that arise exclusively in pure superconductors.

If paramagnetic impurities are also present, then (as follows from the analysis in Sect. 2.1) different factors $1/\tau_1$ and $1/\tau_2$ correspond to the functions g, $\bar{g}$ and f, f^+ respectively.

Having in mind the case of nonmagnetic impurities, in Eq. (4.1) we perform averaging over the angular variable, taking into account Eqs. (4.7), (4.9), and (4.10). The self-energy parts, which correspond to the interaction of electrons with impurities, are eliminated owing to the isotropy of this interaction.

4.1.5. *Effective Collision Integral*

Before the derivation of the collision integrals in terms of the distribution function of electron (n_ε) and hole ($n_{-\varepsilon}$)-type excitations, we examine the relation between $n_{\pm\varepsilon}$ and $\hat{g}_\varepsilon$, where

$$\hat{g}_{\varepsilon\varepsilon-\omega} = 2\pi\delta(\omega)\hat{g}_\varepsilon. \tag{4.12}$$

The required relation was established in Sect. 3.2. Using Eqs. (3.64) to (3.70), one finds

$$u(\varepsilon)\dot{n}_\varepsilon = -\frac{1}{8\pi i}\{(\dot{g}_\varepsilon - \dot{g}_{-\varepsilon}) + u(\varepsilon)(\dot{g}_\varepsilon - \dot{g}_{-\varepsilon})\}\operatorname{sign}\varepsilon, \tag{4.13}$$

where the dot designates the time derivative. Thus, the right side of Eq. (4.2) is expressed in terms of the 11-component of Eq. (4.1). Taking into account the nondiagonal channel, the effective collision integral becomes

$$I_{\text{eff}}(\varepsilon) = I_{\text{eff}}^{(\text{e-ph})}(\varepsilon) + I_{\text{eff}}^{(\text{e-e})}(\varepsilon) + I_{\text{eff}}^{(\text{T})}(\varepsilon), \tag{4.14}$$

where the last two terms have the structure

$$\begin{aligned} I_{\text{eff}}(\varepsilon) = I'_{\text{eff}}(\varepsilon) - \frac{|\Delta|}{2\varepsilon} I''_{\text{eff}}(\varepsilon) = {} & g\Sigma_1^A - f\Sigma_2^{+A} - \Sigma_1^R g + \Sigma_2^R f^+ \\ & + g^R\Sigma_1 - f^R\Sigma_2^+ - \Sigma_1 g^A + \Sigma_2 f^{+A} - \frac{|\Delta|}{2\varepsilon}\{g\Sigma_2^A + f\bar{\Sigma}_1^A - \Sigma_1^R f \\ & - \Sigma_2^R\bar{g} + g^R\Sigma_2 + f^R\bar{\Sigma}_1 - \Sigma_1 f^A - \Sigma_2\bar{g}^A + f^+\Sigma_1^A + \bar{g}\Sigma_2^{+A} \\ & - \Sigma_2^{+R} g - \bar{\Sigma}_1^R f^+ + f^{+R}\Sigma_1 + \bar{g}^R\Sigma_2^+ - \Sigma_2^+ g^A - \bar{\Sigma}_1 f^{+A}\}. \end{aligned} \tag{4.15}$$

A similar expression follows for $I_{\text{eff}}^{(\text{e-ph})}$, which contains the quantities γ, δ, etc.

4.2. INELASTIC ELECTRON–ELECTRON COLLISIONS

To find the collision integral in canonical form,[3,4] we will use the general relations (4.13) to (4.15). First, it is necessary to specify the self-energy parts in them.

4.2.1. Diagram Evaluation of Electron-Electron Self-Energy

The diagrams corresponding to intercollisions of two electrons are depicted in Fig. 4.1. The presence of pair condensate in the system, as usual, is responsible for the matrix structure of $\hat{\Sigma}$. The contribution to Σ_1 from the first graph in Fig. 4.1 is shown in Fig. 4.2. In the representation of discrete imaginary frequencies, the elements of matrix $\hat{\Sigma}$ may be written (omitting for a moment unessential indices) in the form

$$\Sigma_1(P,P-K) = T^2 \sum_{\varepsilon_1\varepsilon_2} \int\int \frac{d^3\mathbf{p}_1\, d^3\mathbf{p}_2}{(2\pi)^6} \left\{ A\, \mathcal{G}_1 \mathcal{G}_2 \overline{\mathcal{G}}_3 - B\, \mathcal{F}_1 \mathcal{F}_2^{+} \mathcal{G}_3 \right\}, \tag{4.16}$$

$$\Sigma_2(P,P-K) = T^2 \sum_{\varepsilon_1\varepsilon_2} \int\int \frac{d^3\mathbf{p}_1\, d^3\mathbf{p}_2}{(2\pi)^6} \left\{ B\, \mathcal{G}_1 \overline{\mathcal{G}}_2 \mathcal{F}_3 - A\, \mathcal{F}_1 \mathcal{F}_2 \mathcal{F}_3^{+} \right\}. \tag{4.17}$$

Here the 4-momentum variables of propagators are defined by the "decay" conservation laws $P = P_1 + P_2 + P_3$ and $K = K_1 + K_2 + K_3$. The quadratic forms A and B are related to the scattering amplitudes of two normal excitations on the Fermi surface. Using Fig. 4.1, the following expressions may be derived in Born's approximation:

$$A = -2\,|V_{\mathbf{p}-\mathbf{p}_2}|^2 + V_{\mathbf{p}-\mathbf{p}_2}\, V_{\mathbf{p}-\mathbf{p}_1}, \tag{4.18}$$

$$B = -2\,|V_{\mathbf{p}_1+\mathbf{p}_2}|^2 + V_{\mathbf{p}-\mathbf{p}_1}\, V_{\mathbf{p}-\mathbf{p}_2} + V_{\mathbf{p}_1+\mathbf{p}_2}\, V_{\mathbf{p}-\mathbf{p}_2} + V_{\mathbf{p}-\mathbf{p}_1}\, V_{\mathbf{p}_1+\mathbf{p}_2}, \tag{4.19}$$

where $V_{\mathbf{q}}$ is the interaction potential.

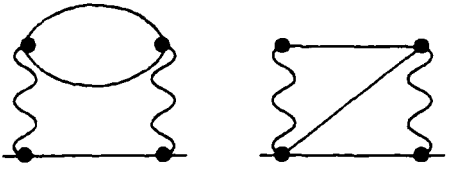

Figure 4.1. Diagrams determining the self-energy functions (4.16) and (4.17). Wavy lines correspond to the electron-electron interaction potential.

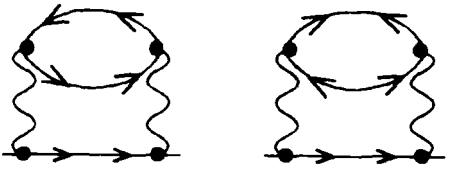

Figure 4.2. Diagrams for 11-component of self-energy matrix (4.16) which corresponds to the first skeleton diagram in Fig. 4.1.

4.2.2. Analytical Continuation

From expressions (4.16) and (4.17), written in the discrete imaginary frequency representation, we move to the expressions on the real axis, using the Gor'kov–Eliashberg technique. To do this, consider the N^{th} order diagram of perturbation theory as the function of the complex variable ε at fixed imaginary frequencies of the field vertices. The analytical continuation over each of the frequencies must be made from the upper half-plane onto the real axis. The cuts lying between the lines $\mathrm{Im}\,\varepsilon = 0$ and $\mathrm{Im}\,(\varepsilon - \omega) = 0$ correspond to this diagram. Assuming that the cuts are

$$\mathrm{Im}\,(\varepsilon_1 - \omega_{1i}) = \mathrm{Im}\,(\varepsilon_2 - \omega_{2k}) = \mathrm{Im}\,(\varepsilon_3 - \omega_{3l}) = 0, \tag{4.20}$$

we transform the sum over frequencies in (4.16) and (4.17) into a double integral. Because the directions of the arrows do not influence the procedure of analytical continuation, one can present (4.16) and (4.17) in the form (omitting temporarily unessential symbols)

$$\Sigma = T^2 \sum_{\varepsilon_1 \varepsilon_2} \mathcal{G}_{\varepsilon_1} \mathcal{G}_{\varepsilon_2} \mathcal{G}_{\varepsilon-\varepsilon_1-\varepsilon_2} = \oint\oint \frac{d\varepsilon_1\, d\varepsilon_2}{(4\pi i)^2} \tanh\frac{\varepsilon_1}{2T} \tanh\frac{\varepsilon_2}{2T} \mathcal{G}_{\varepsilon_1} \mathcal{G}_{\varepsilon_2} \mathcal{G}_{\varepsilon-\varepsilon_1-\varepsilon_2}, \tag{4.21}$$

where the contours of integration enclose all the poles of hyperbolic tangents. Further step-by-step transformation of (4.21) to an integration over the real axis gives the result

$$\Sigma = \int\int \frac{dz_1 dz_2}{(4\pi i)^2} \left\{ \tanh\frac{z_1}{2T} \tanh\frac{z_2}{2T} \sum_{i,k} \delta_i (\mathcal{G}_{z_1+\omega_{1i}}) \delta_k (\mathcal{G}_{z_2+\omega_{2k}}) \mathcal{G}_{\varepsilon-z_2-z_1-\omega_{1i}-\omega_{2k}} \right.$$

$$\left. - \sum_{k,l} \mathcal{G}_{\varepsilon+z_1-\omega_{2k}-\omega_{3l}} \delta_k (\mathcal{G}_{z_2+\omega_{2k}}) \delta_l (\mathcal{G}_{-z_2-z_1+\omega_{3l}}) \coth\frac{z_1}{2T} \tanh\frac{z_2}{2T} \right.$$

$$+\sum_{k,l}\mathcal{G}_{\varepsilon+z_1-\omega_{2k}-\omega_{3l}}\,\delta_k\,(\mathcal{G}_{z_2-z_1+\omega_{2k}})\,\delta_l\,(\mathcal{G}_{-z_2+\omega_{3l}})\coth\frac{z_1}{2T}\tanh\frac{z_2}{2T}$$

$$-\sum_{i,l}\delta_i\,(\mathcal{G}_{z_1+\omega_{1i}})\,\mathcal{G}_{\varepsilon+z_2-z_1-\omega_{1i}-\omega_{3l}}\,\delta_l\,(\mathcal{G}_{-z_2+\omega_{3l}})\tanh\frac{z_1}{2T}\tanh\frac{z_2}{2T}\Bigg\}. \qquad (4.22)$$

Here the external variable ε and the field frequencies remain imaginary. Continuing (4.22) over ε from the region $\mathrm{Im}\,(\varepsilon-\omega)>0$ $(\mathrm{Im}\,\varepsilon<0)$ and next over all the frequencies onto the upper half-plane, one finds for $\Sigma^{R(A)}$ the expression

$$\Sigma^{R(A)}=\int_{-\infty}^{\infty}\frac{d\varepsilon_1\,d\varepsilon_2}{(4\pi i)^2}\Big\{G_1G_2G_3^{R(A)}+G_1G_2^{R(A)}G_3+G_1^{R(A)}G_2G_3$$

$$+G_1^{R(A)}G_3^{R(A)}G_2^{R(A)}-G_1^{R(A)}G_2^{R(A)}G_3^{A(R)}$$

$$-G_1^{R(A)}G_2^{A(R)}G_3^{R(A)}-G_1^{A(R)}G_2^{R(A)}G_3^{R(A)}\Big\}. \qquad (4.23)$$

Using the definition of Σ in a form analogous to (3.46),

$$\Sigma_{\varepsilon\varepsilon-\omega}=\sum_{N=0}^{\infty}\sum_{k=1}^{N+1}\delta_k\left(\Sigma^{(N)}_{\varepsilon\varepsilon-\omega}\right)\tanh\frac{\varepsilon-\Omega_k}{2T}, \qquad (4.24)$$

where Ω_k is some combination of field vertex frequencies, one finds from Eq. (4.22):

$$\Sigma=\int_{-\infty}^{\infty}\frac{d\varepsilon_1\,d\varepsilon_2}{(4\pi i)^2}\Big\{G_1G_2G_3+G_1\,(G^R-G^A)_2\,(G^R-G^A)_3$$

$$+(G^R-G^A)_1G_2(G^R-G^A)_3+(G^R-G^A)_1\,(G^R-G^A)_2G_3\Big\}. \qquad (4.25)$$

The expressions for the quantities $\Sigma^{R(A)}$ and Σ, which define the collision integral, follow from (4.16) and (4.17) and (4.23) and (4.25).

4.2.3. *Transition to Energy-Integrated Propagators*

Before writing down the corresponding results, we will integrate (4.16) and (4.17) over the variables $\xi=v_F(p-p_F)$; this is possible because the effective interaction is short range, so the amplitudes A and B depend on angle variables only. Hence one can write

$$\int\int\frac{d^3\mathbf{p}_1\,d^3\mathbf{p}_2}{(2\pi)^6}\,AG_1G_2G_3$$

$$= \left(\frac{mp_F^2}{2\pi^2}\right) \int\int \frac{d\Omega_{\mathbf{p}_1} d\Omega_{\mathbf{p}_2}}{(4\pi)^2} A \int\int\int d\xi_1 d\xi_2 d\xi_3 \, \delta(\xi_3 - v_F(p_3 - p_F)) \, G_1 G_2 G_3 . \quad (4.26)$$

The δ-function here restricts mainly the angle integration, requiring $p_3 = |\mathbf{p} - \mathbf{p}_1 - \mathbf{p}_2| \approx p_F$ and thus

$$\int\int \frac{d^3\mathbf{p}_1 d^3\mathbf{p}_2}{(2\pi)^6} A G_1 G_2 G_3 = \left(\frac{mp_F}{2\pi^2}\right)^2 \frac{1}{2\varepsilon_F} \int\int \frac{d\Omega_{\mathbf{p}_1} d\Omega_{\mathbf{p}_2}}{(4\pi)^2} \delta\left(\frac{p_3}{p_F} - 1\right) A g_1 g_2 g_3 \quad (4.27)$$

Gathering the results, we have

$$\Sigma_1^R - \Sigma_1^A = \hat{L}\left[A \{g_1 g_2 \bar{g}_3\}^{(R-A)} - B \{f_1 f_2^+ g_3\}^{(R-A)}\right], \quad (4.28)$$

$$\Sigma_1 = \hat{L}\left[A \{g_1 g_2 \bar{g}_3\} - B \{f_1 f_2^+ g_3\}\right], \quad (4.29)$$

$$\Sigma_2^R - \Sigma_2^A = \hat{L}\left[B \{g_1 \bar{g}_2 f_3\}^{(R-A)} - A \{f_1 f_2 f_3^+\}^{(R-A)}\right], \quad (4.30)$$

$$\Sigma_2 = \hat{L}\left[B \{g_1 \bar{g}_2 f_3\} - A \{f_1 f_2 f_3^+\}\right]. \quad (4.31)$$

The notations $\{\ldots\}$ and $\{\ldots\}^{(R-A)}$ are used:

$$\{g_1 g_2 g_3\}^{(R-A)} = g_1 g_2 (g_3^R - g_3^A) + g_1 (g_2^R - g_2^A) g_3 + (g_1^R - g_1^A) g_2 g_3 + (g_1^R - g_1^A)(g_2^R - g_2^A)(g_3^R - g_3^A), \quad (4.32)$$

$$\{g_1 g_2 g_3\} = g_1 g_2 g_3 + g_1 (g_2^R - g_2^A)(g_3^R - g_3^A) + (g_1^R - g_1^A) g_2 (g_3^R - g_3^A), + (g_1^R - g_1^A)(g_2^R - g_2^A) g_3, \quad (4.33)$$

and the operator $\hat{L}$ is defined as

$$\hat{L} = \left(\frac{mp_F}{2\pi^2}\right)^2 \frac{1}{2\varepsilon_F} \int_{-\infty}^{\infty}\int \frac{d\varepsilon_1 d\varepsilon_2}{(4\pi i)^2} \int\int \frac{d\Omega_{\mathbf{p}_1} d\Omega_{\mathbf{p}_2}}{(4\pi)^2} \delta\left(\frac{p_3}{p_F} - 1\right). \quad (4.34)$$

4.2.4. Derivation of the Canonical Form

Substituting expressions (4.16) and (4.17), subject to (4.32) and (4.33) and (3.81) to (3.85), into formula (4.15), we find

$$I_{\text{eff}}(\varepsilon) = 2\pi^4 \hat{L} \{- A(-uu_1 u_2 u_3 \beta\beta_1\beta_2 - uu_2 u_3 \beta\beta_2\alpha_1 - uu_1 u_3 \beta\alpha_2\beta_1$$

$$- uu_3\beta\alpha_1\alpha_2 - uu_1u_2u_3\beta\beta_1\beta_3 - uu_2u_3\beta\beta_3\alpha_1 + uu_1u_2\beta\beta_1\alpha_3$$

$$+ uu_2\beta\alpha_1\alpha_3 - uu_1u_2u_3\beta\beta_2\beta_3 - uu_1u_3\beta\beta_3\alpha_2 + uu_1u_2\beta\beta_2\alpha_3$$

$$+ uu_1\beta\alpha_2\alpha_3 - uu_1u_2u_3\beta - u_1u_2u_3\beta_1\beta_2\alpha - u_2u_3\beta_2\alpha\alpha_1$$

$$- u_1u_3\beta_1\alpha\alpha_2 - u_3\alpha\alpha_1\alpha_2 - u_1u_2u_3\beta_1\beta_3\alpha - u_2u_3\beta_3\alpha\alpha_1$$

$$+ u_1u_2\beta_1\alpha\alpha_3 + u_2\alpha\alpha_1\alpha_3 - u_1u_2u_3\beta_2\beta_3\alpha - u_1u_3\beta_3\alpha\alpha_2$$

$$+ u_1u_2\beta_2\alpha\alpha_3 + u_1\alpha\alpha_2\alpha_3 - u_1u_2u_3\alpha) + B(uu_3v_1v_2\beta\beta_1\beta_2$$

$$+ uu_3v_1v_2\beta\beta_1\beta_3 + uv_1v_2\beta\beta_1\alpha_3 + uv_1v_2u_3\beta\beta_2\beta_3 + uv_1v_2\beta\beta_2\alpha_3$$

$$+ uu_3v_1v_2\beta + u_3v_1v_2\beta_1\beta_2\alpha + u_3v_1v_2\beta_1\beta_3\alpha + v_1v_2\beta_1\alpha\alpha_3$$

$$+ u_3v_1v_2\beta_2\beta_3\alpha + v_1v_2\beta_2\alpha\alpha_3 + u_3v_1v_2\alpha) - B\,(u_1u_2vv_3\beta\beta_1\beta_2$$

$$+ u_2vv_3\beta\beta_2\alpha_1 - u_1vv_3\beta\beta_1\alpha_2 - vv_3\beta\alpha_1\alpha_2 + u_1u_2vv_3\beta\beta_1\beta_3$$

$$+ u_2vv_3\beta\beta_3\alpha_1 + u_1u_2vv_3\beta\beta_2\beta_3 - u_1vv_3\beta\beta_3\alpha_2 + u_1u_2vv_3\beta)$$

$$- A\,(vv_1v_2v_3\beta\beta_1\beta_2 + vv_1v_2v_3\beta\beta_1\beta_3 + vv_1v_2v_3\beta\beta_2\beta_3 + vv_1v_2v_3\beta)$$

$$- A\,(uu_1u_2u_3\beta_1\beta_2\beta_3 - uu_1u_2\beta_1\beta_2\alpha_3 + uu_2u_3\beta_2\beta_3\alpha_1 - uu_2\beta_2\alpha_1\alpha_3$$

$$+ uu_1u_3\beta_1\beta_3\alpha_2 - uu_1\beta_1\alpha_2\alpha_3 + uu_3\beta_3\alpha_1\alpha_2 - u\alpha_1\alpha_2\alpha_3$$

$$+ uu_1u_2u_3\beta_1 + uu_2u_3\alpha_1 + uu_1u_2u_3\beta_2 + uu_1u_3\alpha_2 + uu_1u_2u_3\beta_3$$

$$- uu_1u_2\alpha_3) - B\,(uu_3v_1v_2\beta_1\beta_2\beta_3 + uv_1v_2\beta_1\beta_2\alpha_3 + uu_3v_1v_2\beta_1$$

$$+ uu_3v_1v_2\beta_2 + uu_3v_1v_2\beta_3 + uv_1v_2\alpha_3) + B\,(u_1u_2vv_3\beta_1\beta_2\beta_3$$

$$+ u_2vv_3\beta_2\beta_3\alpha_1 - u_1v_3v\beta_1\beta_3\alpha_2 - vv_3\beta_3\alpha_1\alpha_2 + u_1u_2vv_3\beta_1$$

$$+ u_2vv_3\alpha_1 + u_1u_2vv_3\beta_2 - u_1vv_3\alpha_2 + u_1u_2vv_3\beta_3)$$

$$+ A\,(vv_1v_2v_3\beta_1\beta_2\beta_3 + vv_1v_2v_3\beta_1 + vv_1v_2v_3\beta_2 + vv_1v_2v_3\beta_3)$$

$$- \frac{|\Delta|}{\varepsilon}\Big[- A\,(-u_2u_3\beta\beta_2\alpha_1 - u_1u_3v\beta\beta_1\alpha_2 - u_2u_3v\beta\beta_3\alpha_1 + u_1u_2v\beta\beta_1\alpha_3$$

$$- u_1u_3v\beta\beta_3\alpha_2) + B\,(vv_1v_2\beta\beta_1\alpha_3 + vv_1v_2\beta\beta_2\alpha_3) - B\,(v_3\alpha\alpha_1\alpha_2$$

$$- u_1u_2v_3\beta_3\alpha - u_2v_3\beta_3\alpha\alpha_1 - u_1u_2v_3\beta_2\beta_3\alpha - u_1u_2u_3\beta_1\beta_2\alpha$$

$$- u_2\nu_3\beta_2\alpha\alpha_1 + u_1\nu_3\beta_1\alpha\alpha_2 + u_1\nu_3\beta_3\alpha\alpha_2 - u_1u_2\nu_3\alpha)$$

$$+ A\,(\nu_1\nu_2\nu_3\beta_1\beta_2\alpha + \nu_1\nu_2\nu_3\beta_1\beta_3\alpha + \nu_1\nu_2\nu_3\beta_2\beta_3\alpha + \nu_1\nu_2\nu_3\alpha)$$

$$- A\,(u_2u_3\nu\beta_2\beta_3\alpha_1 + u_1u_3\nu\beta_1\beta_3\alpha_2 - u_1u_2\nu\beta_1\beta_2\alpha_3 - \nu\alpha_1\alpha_2\alpha_3$$

$$+ \nu u_2u_3\alpha_1 + u_1u_3\nu\alpha_2 - u_1u_2\nu\alpha_3) - B(\nu\nu_1\nu_2\beta_1\beta_2\alpha_3 + \nu\nu_1\nu_2\alpha_3)\Big]\Big\}. \quad (4.35)$$

[Here $u = u(\varepsilon)$, $u_1 = u(\varepsilon_1)$, etc.] Reversing the sign of ε in this expression and substituting the values of $I(\varepsilon)$ and $I(-\varepsilon)$ into (4.13), we obtain, subject to the relations (3.86) to (3.88), the following canonical form for the inelastic electron–electron collision integral:

$$J^{(e-e)}(n_{\pm\varepsilon}) = \frac{1}{16\varepsilon_F\sqrt{\varepsilon^2 - |\Delta|^2}} \int_{|\Delta|}^{\infty}\int_{|\Delta|}^{\infty}\int_{|\Delta|}^{\infty} \frac{d\varepsilon_1 d\varepsilon_2 d\varepsilon_3}{\sqrt{\varepsilon_1^2 - |\Delta|^2}\,\sqrt{\varepsilon_2^2 - |\Delta|^2}\,\sqrt{\varepsilon_3^2 - |\Delta|^2}}$$

$$\times \{E_1\delta(\varepsilon - \varepsilon_1 - \varepsilon_2 - \varepsilon_3) + E_2\delta(\varepsilon + \varepsilon_1 - \varepsilon_2 - \varepsilon_3) + E_3\delta(\varepsilon + \varepsilon_2 + \varepsilon_3 - \varepsilon_1)\}\,, \quad (4.36)$$

in which the factors E_i have the form

$$E_1 = M_1^1\Big\{\Big[(1 - n_{\pm\varepsilon})\,n_{\varepsilon_1}n_{\varepsilon_2}n_{\varepsilon_3} - n_{\pm\varepsilon}(1 - n_{\varepsilon_1})\,(1 - n_{\varepsilon_2})\,(1 - n_{\varepsilon_3})\Big]$$

$$+ \Big[(1 - n_{\pm\varepsilon})\,n_{\varepsilon_1}n_{-\varepsilon_2}n_{-\varepsilon_3} - n_{\pm\varepsilon}\,(1 - n_{\varepsilon_1})\,(1 - n_{-\varepsilon_2})\,(1 - n_{-\varepsilon_3})\Big]\Big\}$$

$$+ M_1^2\Big\{\Big[(1 - n_{\pm\varepsilon})n_{-\varepsilon_1}n_{\varepsilon_2}n_{\varepsilon_3} - n_{\pm\varepsilon}\,(1 - n_{-\varepsilon_1})\,(1 - n_{\varepsilon_2})\,(1 - n_{\varepsilon_3})\Big]$$

$$+ \Big[(1 - n_{\pm\varepsilon})n_{-\varepsilon_1}n_{-\varepsilon_2}n_{-\varepsilon_3} - n_{\pm\varepsilon}\,(1 - n_{-\varepsilon_1})\,(1 - n_{-\varepsilon_2})\,(1 - n_{-\varepsilon_3})\Big]\Big\}$$

$$+ 2M_1^3\Big[(1 - n_{\pm\varepsilon})\,n_{\varepsilon_1}n_{-\varepsilon_2}n_{\varepsilon_3} - n_{\pm\varepsilon}\,(1 - n_{\varepsilon_1})\,(1 - n_{-\varepsilon_2})\,(1 - n_{\varepsilon_3})\Big]$$

$$+ 2M_1^4\Big[(1 - n_{\pm\varepsilon})n_{-\varepsilon_1}n_{-\varepsilon_2}n_{\varepsilon_3} - n_{\pm\varepsilon}\,(1 - n_{-\varepsilon_1})\,(1 - n_{-\varepsilon_2})\,(1 - n_{\varepsilon_3})\Big], \quad (4.37)$$

$$E_2 = M_2^1\Big\{\Big[[n_{\varepsilon_2}n_{\varepsilon_3}\,(1 - n_{\pm\varepsilon})\,(1 - n_{\varepsilon_1}) - (1 - n_{\varepsilon_2})\,(1 - n_{\varepsilon_3})n_{\pm\varepsilon}n_{\varepsilon_1}\Big]$$

$$+ \Big[\,n_{-\varepsilon_2}n_{-\varepsilon_3}\,(1 - n_{\pm\varepsilon})\,(1 - n_{\varepsilon_1}) - (1 - n_{-\varepsilon_2})\,(1 - n_{-\varepsilon_3})n_{\pm\varepsilon}n_{\varepsilon_1}\Big]\Big\}$$

$$+ M_2^2\Big\{\Big[\,[n_{\varepsilon_2}n_{\varepsilon_3}\,(1 - n_{\pm\varepsilon})\,(1 - n_{-\varepsilon_1}) - (1 - n_{\varepsilon_2})\,(1 - n_{\varepsilon_3})n_{\pm\varepsilon}n_{-\varepsilon_1}\Big]$$

$$+ \Big[\,n_{-\varepsilon_2}n_{-\varepsilon_3}\,(1 - n_{\pm\varepsilon})\,(1 - n_{-\varepsilon_1}) - (1 - n_{-\varepsilon_2})\,(1 - n_{-\varepsilon_3})n_{\pm\varepsilon}n_{-\varepsilon_1}\Big]\Big\}$$

$$+ 2M_2^3\Big[n_{-\varepsilon_2}n_{\varepsilon_3}\,(1 - n_{\pm\varepsilon})\,(1 - n_{\varepsilon_1}) - (1 - n_{-\varepsilon_2})\,(1 - n_{\varepsilon_3})n_{\pm\varepsilon}n_{\varepsilon_1}\Big]$$

$$+ 2M_2^4\left[n_{-\varepsilon_2}n_{\varepsilon_3}(1-n_{\pm\varepsilon})(1-n_{-\varepsilon_1}) - (1-n_{-\varepsilon_2})(1-n_{\varepsilon_3})n_{\pm\varepsilon}n_{-\varepsilon_1}\right], \tag{4.38}$$

$$\begin{aligned}
E_3 = {} & M_3^1\left\{\left[n_{\varepsilon_1}(1-n_{\pm\varepsilon})(1-n_{\varepsilon_2})(1-n_{\varepsilon_3}) - (1-n_{\varepsilon_1})n_{\pm\varepsilon}n_{\varepsilon_2}n_{\varepsilon_3}\right]\right. \\
& \left. + \left[n_{\varepsilon_1}(1-n_{\pm\varepsilon})(1-n_{-\varepsilon_2})(1-n_{-\varepsilon_3}) - (1-n_{\varepsilon_1})n_{\pm\varepsilon}n_{-\varepsilon_2}n_{-\varepsilon_3}\right]\right\} \\
& + M_3^2\left\{\left[n_{-\varepsilon_1}(1-n_{\pm\varepsilon})(1-n_{\varepsilon_2})(1-n_{\varepsilon_3}) - (1-n_{-\varepsilon_1})n_{\pm\varepsilon}n_{\varepsilon_2}n_{\varepsilon_3}\right]\right. \\
& \left. + \left[n_{-\varepsilon_1}(1-n_{\pm\varepsilon})(1-n_{-\varepsilon_2})(1-n_{-\varepsilon_3}) - (1-n_{-\varepsilon_1})n_{\pm\varepsilon}n_{-\varepsilon_2}n_{-\varepsilon_3}\right]\right\} \\
& + 2M_3^3\left[n_{\varepsilon_1}(1-n_{\pm\varepsilon})(1-n_{-\varepsilon_2})(1-n_{\varepsilon_3}) - (1-n_{\varepsilon_1})n_{\pm\varepsilon}n_{-\varepsilon_2}n_{\varepsilon_3}\right] \\
& + 2M_3^4\left[n_{-\varepsilon_1}(1-n_{\pm\varepsilon})(1-n_{-\varepsilon_2})(1-n_{\varepsilon_3}) - (1-n_{-\varepsilon_1})n_{\pm\varepsilon}n_{-\varepsilon_2}n_{\varepsilon_3}\right]
\end{aligned} \tag{4.39}$$

Coefficients M_i^j, entering (4.37) to (4.39), are given by the following relations:

$$\begin{aligned}
M_1^1 = {} & a(\varepsilon\varepsilon_1\varepsilon_2\varepsilon_3 - |\Delta|^4 - \varepsilon\varepsilon_1\sqrt{\varepsilon_2^2-|\Delta|^2}\sqrt{\varepsilon_3^2-|\Delta|^2} \\
& \pm \sqrt{\varepsilon^2-|\Delta|^2}\sqrt{\varepsilon_1^2-|\Delta|^2}\,\varepsilon_2\varepsilon_3 \mp \sqrt{\varepsilon^2-|\Delta|^2}\sqrt{\varepsilon_1^2-|\Delta|^2}\sqrt{\varepsilon_2^2-|\Delta|^2} \\
& \times \sqrt{\varepsilon_3^2-|\Delta|^2}) + b|\Delta|^2(\varepsilon\varepsilon_3 - \varepsilon_1\varepsilon_2 + \sqrt{\varepsilon_2^2-|\Delta|^2}\sqrt{\varepsilon_3^2-|\Delta|^2} \\
& \pm \sqrt{\varepsilon^2-|\Delta|^2}\sqrt{\varepsilon_1^2-|\Delta|^2}),
\end{aligned} \tag{4.40}$$

$$\begin{aligned}
M_1^2 = {} & a(\varepsilon\varepsilon_1\varepsilon_2\varepsilon_3 - |\Delta|^4 - \varepsilon\varepsilon_1\sqrt{\varepsilon_2^2-|\Delta|^2}\sqrt{\varepsilon_3^2-|\Delta|^2} \\
& \mp \sqrt{\varepsilon^2-|\Delta|^2}\sqrt{\varepsilon_1^2-|\Delta|^2}\,\varepsilon_2\varepsilon_3 \pm \sqrt{\varepsilon^2-|\Delta|^2}\sqrt{\varepsilon_1^2-|\Delta|^2}\sqrt{\varepsilon_2^2-|\Delta|^2} \\
& \times \sqrt{\varepsilon_3^2-|\Delta|^2}) + b|\Delta|^2(\varepsilon\varepsilon_3 - \varepsilon_1\varepsilon_2 + \sqrt{\varepsilon_2^2-|\Delta|^2}\sqrt{\varepsilon_3^2-|\Delta|^2} \\
& \mp \sqrt{\varepsilon^2-|\Delta|^2}\sqrt{\varepsilon_1^2-|\Delta|^2}),
\end{aligned} \tag{4.41}$$

$$\begin{aligned}
M_1^3 = {} & a(\varepsilon\varepsilon_1\varepsilon_2\varepsilon_3 - |\Delta|^4 + \varepsilon\varepsilon_1\sqrt{\varepsilon_1^2-|\Delta|^2}\sqrt{\varepsilon_3^2-|\Delta|^2} \\
& \pm \sqrt{\varepsilon^2-|\Delta|^2}\sqrt{\varepsilon_1^2-|\Delta|^2}\,\varepsilon_2\varepsilon_3 \pm \sqrt{\varepsilon^2-|\Delta|^2}\sqrt{\varepsilon_1^2-|\Delta|^2}\sqrt{\varepsilon_2^2-|\Delta|^2} \\
& \times \sqrt{\varepsilon_3^2-|\Delta|^2}) + b|\Delta|^2(\varepsilon\varepsilon_3 - \varepsilon_1\varepsilon_2 + \sqrt{\varepsilon_2^2-|\Delta|^2}\sqrt{\varepsilon_3^2-|\Delta|^2} \\
& \pm \sqrt{\varepsilon^2-|\Delta|^2}\sqrt{\varepsilon_1^2-|\Delta|^2}),
\end{aligned} \tag{4.42}$$

$$M_1^4 = a(\varepsilon\varepsilon_1\varepsilon_2\varepsilon_3 - |\Delta|^4 + \varepsilon\varepsilon_1\sqrt{\varepsilon_2^2-|\Delta|^2}\sqrt{\varepsilon_3^2-|\Delta|^2}$$

$$\mp \sqrt{\varepsilon^2 - |\Delta|^2}\,\sqrt{\varepsilon_1^2 - |\Delta|^2}\,\varepsilon_2\varepsilon_3 \mp \sqrt{\varepsilon^2 - |\Delta|^2}\,\sqrt{\varepsilon_1^2 - |\Delta|^2}\,\sqrt{\varepsilon_2^2 - |\Delta|^2}$$

$$\times \sqrt{\varepsilon_3^2 - |\Delta|^2}) + b\,|\Delta|^2\,(\varepsilon\varepsilon_3 - \varepsilon_1\varepsilon_2 + \sqrt{\varepsilon_2^2 - |\Delta|^2}\,\sqrt{\varepsilon_3^2 - |\Delta|^2}$$

$$\mp \sqrt{\varepsilon^2 - |\Delta|^2}\,\sqrt{\varepsilon_1^2 - |\Delta|^2}). \tag{4.43}$$

The quantities M_2^j and M_3^j are defined by the expressions

$$M_2^j = -M_1^j(\varepsilon, -\varepsilon_1, \varepsilon_2, \varepsilon_3) - M_1^j(\varepsilon, \varepsilon_2, -\varepsilon_1, \varepsilon_3) - M_1^j(\varepsilon, \varepsilon_3, \varepsilon_2, -\varepsilon_1), \tag{4.44}$$

$$M_3^j = M_1^j(\varepsilon, \varepsilon_1, -\varepsilon_2, -\varepsilon_3) + M_1^j(\varepsilon, -\varepsilon_2, \varepsilon_1, -\varepsilon_3) + M_1^j(\varepsilon, -\varepsilon_3, -\varepsilon_2, \varepsilon_1). \tag{4.45}$$

Factors a and b, entering Eqs. (4.40) to (4.43), are numbers (of an order of unity) and are connected with A and B by relations of the type

$$a = -2\pi\left(\frac{mp_F}{2\pi^2}\right)^2 \int\int\int \frac{d\Omega_{\mathbf{p}} d\Omega_{\mathbf{p}_1} d\Omega_{\mathbf{p}_2}}{(4\pi)^2}\,\delta\left(\frac{|\mathbf{p} - \mathbf{p}_1 - \mathbf{p}_2|}{p_F} - 1\right) A. \tag{4.46}$$

4.2.5. Essence of Elementary Acts

The meaning of the elementary acts described by the collision operator (4.36) is quite transparent. Consider, for example, the term in E_1 that is proportional to M_1^1. With a positive sign of ε, the first component in this term describes the merger of three electron excitations into a single electron-type excitation. With a negative sign of ε, three merging electron excitations create an excitation on the hole branch. Thus in the first case the difference in the number of electrons and holes changes by 2, while in the second case it changes by 4. Analogous processes are described by other items in this term. It vanishes in the case of a normal metal ($M_1^1 = 0$ when $|\Delta| = 0$); hence the channel of homogeneous relaxation of electron-hole imbalance is closed in a normal metal.[5] Note that the collision integral (4.36) has obtained such a transparent meaning, owing to the specific selection of the form of the functions $n_{\pm\varepsilon}$ in the expressions for $\hat{g}^{(R,A)}$ in (3.81) to (3.88).

4.3. KINETIC EQUATION FOR PHONONS

4.3.1. Application of Keldysh Technique

The phonon Green–Keldysh function[4] is introduced in the usual manner*:

*We omit further below the index ν of phonon polarization. It may be restored in the final expressions. As mentioned in Sect. 2.3, in the isotropic model of metals, the electrons interact only with longitudinal acoustic phonons. This interaction is implied in this chapter. In case of transverse phonons, the coherence factors would change their signs (see Chap. 12).

$$\mathcal{D}_{\nu}^{ik}(1,2) = -i\langle T\hat{\varphi}_{\nu}(1i)\hat{\varphi}_{\nu}(2k)\rangle, \quad 1 \equiv X \equiv (r,t). \tag{4.47}$$

The Keldysh indices i, k are the signs minus or plus, according to the location of the time coordinate on each of the two time axes ($-\infty$, $+\infty$ and $+\infty$, $-\infty$). Recall that the time on the second axis (with the sign plus) is greater than any time on the first axis (with the sign minus), and the T-ordering on the second axis proceeds in the reverse order. The free phonon field operators are real ($\hat{\varphi}^{\dagger} = \hat{\varphi}$, see Sect. 3.1):

$$\hat{\varphi}(x) = \frac{1}{\sqrt{V_0}} \sum_{\mathbf{k}} \sqrt{\frac{\omega_0(\mathbf{k})}{2}} \left\{ b_{\mathbf{k}} e^{i[\mathbf{k}\cdot\mathbf{r} - \omega_0(\mathbf{k})t]} + b_{\mathbf{k}}^{\dagger} e^{-i[\mathbf{k}\cdot\mathbf{r} - \omega_0(\mathbf{k})t]} \right\}. \tag{4.48}$$

Here V_0 is the volume of the system; $\omega_0(\mathbf{k})$ is the dispersion of phonons in normal metal; and $b_{\mathbf{k}}^{\dagger}$ and $b_{\mathbf{k}}$ are the phonon creation and annihilation operators.

The "bare" Green-Keldysh functions, defined by Eqs. (4.47) and (4.48), may be easily found in the homogeneous and stationary cases. For instance, the expression for $\mathcal{D}_0^{-+}$ is (cf. Ref. 6):

$$\mathcal{D}_0^{-+}(\mathbf{r},t) = -\frac{i}{2}\int \frac{d^3\mathbf{k}}{(2\pi)^3}\,\omega_0(\mathbf{k}) e^{i\mathbf{k}\cdot\mathbf{r}} \left[N_{\mathbf{k}} e^{-i\omega_0(\mathbf{k})t} + (1 + N_{-\mathbf{k}}) e^{i\omega_0(\mathbf{k})t} \right], \tag{4.49}$$

where $N_{\mathbf{k}} = \langle b_{\mathbf{k}}^{\dagger} b_{\mathbf{k}} \rangle$ is the nonequilibrium phonon distribution function.

In addition, we introduce an operator $\mathcal{D}_{01(2)}^{-1}$, which acts on the first (second) argument of the phonon propagator (u is the phonon velocity):

$$\mathcal{D}_{01(2)}^{-1} = \frac{\partial^2}{\partial t_{1(2)}^2} - u^2 \nabla_{1(2)}^2, \tag{4.50}$$

where

$$\mathcal{D}_{01(2)}^{-1}\,\mathcal{D}_0^{ik}(1,2) = u^2 \hat{\sigma}_z^{ik}\,\delta(t_1 - t_2)\,\nabla_{1(2)}\,\Delta(\mathbf{r}_1 - \mathbf{r}_2), \tag{4.51}$$

and $\hat{\sigma}_z$ is the third of the Pauli matrices $\hat{\sigma}_x$, $\hat{\sigma}_y$, $\hat{\sigma}_z$.

In general the phonon function obeys the Dyson equation

$$\hat{\mathcal{D}}(1,2) = \hat{\mathcal{D}}_0(1,2) + \int \hat{\mathcal{D}}_0(1,4)\,\hat{\Pi}(4,3)\,\hat{\mathcal{D}}(3,2)\,d^4x_3 d^4x_4, \tag{4.52}$$

or

$$\hat{\mathcal{D}}(1,2) = \hat{\mathcal{D}}_0(1,2) + \int \hat{\mathcal{D}}(1,3)\,\hat{\Pi}(3,4)\,\hat{\mathcal{D}}_0(4,2)\,d^4x_3 d^4x_4, \tag{4.53}$$

where all the functions are matrices in Keldysh indices. Note that owing to their definition (4.47), the Green–Keldysh functions are linear dependent ($\mathcal{D}^{--} + \mathcal{D}^{++} - \mathcal{D}^{-+} - \mathcal{D}^{+-} = 0$) and consequently the polarization operators are also linear dependent: ($\Pi^{--} + \Pi^{++} + \Pi^{-+} + \Pi^{+-} = 0$).

The electron Green–Keldysh–Nambu function is defined analogously:

$$G^{ik}_{\mu\nu}(1,2) = -i\langle T\psi_\mu(1i)\psi^\dagger_\nu(2k)\rangle \tag{4.54}$$

as mentioned in Sect. 3.2. Here $\mu = 1, 2$ and $\nu = 1, 2$ are the Nambu indices of the field operators

$$\psi_1(1i) \equiv \psi_\uparrow(1i), \quad \psi_2(1i) \equiv \psi^\dagger_\downarrow(1i). \tag{4.55}$$

The Green's function thus introduced (in the absence of interactions that depend explicitly on spin variables) has the symmetry property

$$(G^{ik}_{\mu\nu})^* = (-1)^{\mu+\nu} G^{\overline{i}\overline{k}}_{\overline{\mu}\overline{\nu}}, \tag{4.56}$$

where the bar above the index indicates its reversion [i.e., $\overline{1} = 2$; $\overline{(-)} = (+)$]. From Eqs. (4.54) and (4.56) it follows that:

$$G^{ik}_{\mu\nu}(1,2) = -\left[G^{ik}_{\nu\mu}(2,1)\right]^* = (-1)^{\mu+\nu+1} G^{\overline{i}\overline{k}}_{\overline{\nu}\overline{\mu}} \quad (\text{for } i \neq j), \tag{4.57}$$

$$G^{ii}_{\mu\nu}(1,2) = -\left[G^{ii}_{\nu\mu}(2,1)\right]^* = (-1)^{\mu+\nu+1} G^{\overline{i}\overline{i}}_{\overline{\nu}\overline{\mu}} \tag{4.58}$$

The functions G, G^R, and G^A are defined according to the relation (3.55):

$$G + G^R + G^A = 2G^{--}, \tag{4.59}$$

$$G + G^R - G^A = 2G^{+-}, \tag{4.60}$$

$$G - G^R + G^A = 2G^{-+}, \tag{4.61}$$

$$G - G^R - G^A = 2G^{++}, \tag{4.62}$$

from which [taking into account Eqs. (4.57) and (4.58)] equalities follow:

$$G_{\mu\nu}(1,2) = -G^*_{\nu\mu}(2,1) = (-1)^{\mu+\nu+1} G_{\overline{\nu}\overline{\mu}}(2,1), \tag{4.63}$$

$$G^R_{\mu\nu}(1,2) = G^{A*}_{\nu\mu}(2,1) = (-1)^{\mu+\nu+1} G^A_{\overline{\nu}\overline{\mu}}(2,1), \tag{4.64}$$

$$G^A_{\mu\nu}(1,2) = G^R_{\nu\mu}(2,1) = (-1)^{\mu+\nu+1} G^R_{\overline{\nu}\overline{\mu}}(2,1). \tag{4.65}$$

4.3.2. Quasi-classical Approximation

In homogeneous and stationary cases, the Green–Keldysh functions depend on the difference of space-time coordinates. If the evolution of the phonon system is taking place sufficiently slowly, one can assume that all the quantities depend only weakly on the summary variable $(1 + 2)$ and are the functions mainly of the difference variable $(1 - 2)$, Separating these variables [we use the notations of type $1 \equiv x_1 \equiv (\mathbf{r}_1, t_1)$, etc.]

$$\hat{\mathcal{D}}(x_1, x_2) = \hat{\mathcal{D}}\left[\frac{x_1 + x_2 + (x_1 - x_2)}{2}; \frac{x_1 + x_2 - (x_1 - x_2)}{2}\right], \tag{4.66}$$

one can perform the Fourier transformation over the difference variables $\mathbf{R} = \mathbf{r}_1 - \mathbf{r}_2$ and $\Theta = t_1 - t_2$:

$$\mathcal{D}^{ik}(\mathbf{q},\omega;\mathbf{r},t) = \int \mathcal{D}^{ik}(\mathbf{r},t;R,\Theta)\, e^{i\mathbf{q}\cdot\mathbf{R}+i\omega\Theta}\, d^3\mathbf{R}d\Theta, \tag{4.67}$$

where obviously, $\mathbf{r} = (\mathbf{r}_1 + \mathbf{r}_2)/2$, $t = (t_1 + t_2)/2$. Acting by the operator $\mathcal{D}_{01}^{-1}$ on Eq. (4.52) and by $\mathcal{D}_{02}^{-1}$ on Eq. (4.53), and subtracting, we obtain the result for the $(- +)$ component:

$$(\mathcal{D}_{02}^{-1} - \mathcal{D}_{01}^{-1})\,\mathcal{D}^{-+}(x_1, x_2) = -\int d^4x_3 d^4x_4 \left\{[\mathcal{D}^{--}(1, 3)\,\Pi^{-+}(3, 4)\right.$$

$$+ \mathcal{D}^{-+}(1, 3)\,\Pi^{++}(3, 4)\,]\,\delta(t_2 - t_4)\,\nabla_2^2\,\delta(\mathbf{r}_4 - \mathbf{r}_2) + [\Pi^{--}(4, 3)\,\mathcal{D}^{-+}(3, 2)$$

$$\left. + \Pi^{-+}(4, 3)\,\mathcal{D}^{++}(3, 2)\,\delta(t_1 - t_4)\,\nabla_1^2\,\delta(\mathbf{r}_1 - \mathbf{r}_4)\right\}. \tag{4.68}$$

Consider first the right side of Eq. (4.68) and transform it with the help of quasi-classical conditions. For the phonon system, these conditions mean that the quantities characterizing its evolution in time (Δt) and space $(\Delta \mathbf{r})$ must be large in comparison with the characteristic phonon reciprocal frequencies $\omega(\mathbf{q})^{-1}$ and wave numbers q^{-1} $(\hbar = 1)$, i.e.:

$$\omega(q)\Delta t >> 1, \quad q\Delta r >> 1. \tag{4.69}$$

This is a good approximation when the perturbation of the phonon system is caused by the superconducting electron system. Condition (4.69) permits us to simplify in the usual manner (cf., e.g., Ref. 6) the left side of (4.68). Taking into account that the operator $(\mathcal{D}_{02}^{-1} - \mathcal{D}_{01}^{-1})$ on the left side of (4.68) may be presented in the form

$$\mathcal{D}_{02}^{-1} - \mathcal{D}_{01}^{-1} = -\frac{\partial^2}{\partial t \partial \Theta} + u^2 \frac{\partial^2}{\partial \mathbf{r} \partial \mathbf{R}}, \tag{4.70}$$

and carrying out the Fourier transformation of (4.68), we obtain the expression

$$2\left(i\omega\frac{\partial \mathcal{D}^{-+}}{\partial t}+iu^2\mathbf{q}\cdot\frac{\partial}{\partial \mathbf{r}}\mathcal{D}^{-+}\right)=-(\mathbf{u}\cdot\mathbf{q})^2\,(\Pi^{-+}\mathcal{D}^{+-}-\mathcal{D}^{-+}\Pi^{+-}). \quad (4.71)$$

(the arguments of all the functions in parentheses are $(\mathbf{q}, \omega; \mathbf{r}, t)$; we have used here the linear interdependence of $\mathcal{D}^{ik}$ and Π^{ik}, mentioned earlier).

4.3.3. Phonon Distribution Function

To obtain the kinetic equation in terms of the distribution function $N(\mathbf{q}, \mathbf{r}, t)$, it is necessary to find a relation between functions N and $\mathcal{D}$. In the quasi-classical case, such a relation may be found rather simply. As noted in Sect. 3.1, the superconducting transition negligibly influences [because $\Delta\omega_0(\mathbf{q})/\omega_0(\mathbf{q}) \sim 10^{-4}$] the bare phonon spectrum: $\omega_0(\mathbf{q}) \approx \omega(\mathbf{q})$. Implying the quasi-classical condition for the phonons, we assume that $N(\mathbf{q}, \mathbf{r}, t)$ and $\hat{\mathcal{D}}(\omega, \mathbf{q}, \mathbf{r}, t)$ obey the relation

$$\mathcal{D}^{-+}(\omega, \mathbf{q}\cdot\mathbf{r}, t)=-\frac{i}{2}\omega(\mathbf{q})\,\{\,[1+N(-\mathbf{q};\mathbf{r},t)\,]\,\delta\,[\omega+\omega(\mathbf{q})]$$

$$+N(\mathbf{q},\mathbf{r},t)\,\delta\,[\omega-\omega(\mathbf{q})]\}. \quad (4.72)$$

For acoustic phonons (only these are important in the isotropic case) and for momenta that are small compared with the extreme value in the crystal, the following relation is valid:

$$\mathbf{q}=\frac{\partial\omega(\mathbf{q})}{\partial\mathbf{u}}\approx\frac{\omega(q)}{u^2}\mathbf{u}. \quad (4.73)$$

Using also the property

$$\mathcal{D}^{+-}(\omega, \mathbf{q}; \mathbf{r}, t)=\mathcal{D}^{-+}(-\omega, -\mathbf{q}; \mathbf{r}, t) \quad (4.74)$$

[which follows from (4.47)], substituting Eqs. (4.72) to (4.74) into (4.71) and integrating over ω within the limits $(0,\infty)$, one obtains the following kinetic equation:

$$\frac{\partial N(\mathbf{q},\mathbf{r},t)}{\partial t}+\mathbf{u}\cdot\frac{\partial N(\mathbf{q},\mathbf{r},t)}{\partial\mathbf{r}}=I(N), \quad (4.75)$$

where the quantity

$$I(N)=i\frac{\omega(\mathbf{q})}{2}\,\{\Pi^{-+}[\mathbf{q},\omega(\mathbf{q});\mathbf{r},t]\,[1+N(\mathbf{q},\mathbf{r},t)\,]$$

$$-\Pi^{+-}[\mathbf{q},\omega(\mathbf{q});\mathbf{r},t\,]\,N(\mathbf{q},\mathbf{r},t)\} \quad (4.76)$$

is the inequilibrium source.

Note that expression (4.76) may also be presented in a somewhat different form if one makes the standard transformation (see Ref. 6) from the Π^{ik} matrix [in analogy with (3.55)] to the linearly independent functions Π, Π^R, and Π^A:

$$I(N) = \frac{i\omega(\mathbf{q})}{2}\left\{(\Pi^R - \Pi^A)\,N - \frac{1}{2}\,[\Pi - (\Pi^R - \Pi^A)]\right\}. \tag{4.77}$$

Now we will specify the polarization operators in Eq. (4.77).

4.3.4. Polarization Operators in Keldysh's Technique

In the Keldysh–Nambu technique, the polarization operator is represented by a diagram expansion:

(4.78)

Regular Feynman rules[7] are applied; the only difference is that all the quantities, including the vertices, are matrices in Keldysh–Nambu indices. Since the transition to the superconducting state (as well as the interaction with an external electromagnetic field) affects only a minor smeared region ($\sim T/\varepsilon_F$, $|\Delta|/\varepsilon_F$ [the bold lines in (4.78)] are considered as exact functions (they contain electrons interacting among themselves, with the external field, phonons, impurities, etc.). Because in this technique the vertices Γ have the matrix structure[8]:

$$\Gamma^{ij,k}_{\alpha\beta} \sim \hat{\sigma}^{ij}_z\,\delta_{jk}\,\hat{\sigma}^{\alpha\beta}_z, \tag{4.79}$$

we obtain (g is the electron-phonon interaction constant)

$$\Pi^{kk'} = -g^2(-1)^{k+k'}\left[G^{kk'}_{11}\,G^{k'k}_{11} - G^{kk'}_{12}\,G^{k'k}_{21} - G^{kk'}_{21}\,G^{k'k}_{12} + G^{kk'}_{22}\,G^{k'k}_{22}\right]. \tag{4.80}$$

However, it is more convenient to deal with the linearly independent quantities G, G^R, and G^A (3.55). Moving simultaneously to Π, Π^R, and Π^A and omitting components like $G^A_{11}(1, 2)\,G^A_{11}(2, 1)$ (which are identically zero), we obtain

$$\Pi^{A(R)}(1, 2) = -\frac{1}{2}\,g^2\Big[G^{A(R)}_{11}(1, 2)\,G_{11}(2, 1) + G_{11}\,G^{R(A)}_{11} + G^{A(R)}_{22}\,G_{22} + G_{22}\,G^{R(A)}_{22} - G^{A(R)}_{12}\,G_{21} - G_{12}\,G^{R(A)}_{21} - G^{A(R)}_{21}\,G_{12} - G_{21}\,G^{R(A)}_{12}\Big] \tag{4.81}$$

and correspondingly

$$\Pi(1,2) = -\frac{i}{2} g^2 \Big[G_{11}(1,2)\, G_{11}(2,1) + G_{22}\, G_{22} - G_{21}\, G_{12} - G_{12}\, G_{21} + G^A_{11}\, G^R_{11}$$

$$+ \; G^R_{11}\, G^A_{11} + G^A_{22}\, G^R_{22} + G^R_{22}\, G^A_{22} - G^A_{12}\, G^R_{21} - G^R_{12}\, G^A_{21} - G^A_{21}\, G^R_{12} - G^R_{21}\, G^A_{12} \Big]. \quad (4.82)$$

Expressions (4.81) and (4.82) allow one to obtain the collision integral for the phonon kinetic equation in a superconducting system. All the influence of the electromagnetic field is contained in Green's functions for electrons, which are exact and also account for impurities and other fields acting on the electron system.

As required by the kinetic equation, written in the form of (4.75), we should move to the *(x,p)* representation. It is clear that the polarization operators can be expressed in terms of the energy-integrated Green's functions. Before making this transformation, we will derive the expressions for the polarization operators in Eq. (4.77), using the analytical continuation technique.

4.3.5. Polarization Operators: Analytical Continuation Technique

In a discrete imaginary frequency representation [$\varepsilon_n = (2n+1)\pi T i$, $\omega_m = 2m\pi T i$] we have the following expression for the polarization operator:

$$\Pi_{\omega\omega-\omega'}(\mathbf{p}, \mathbf{p}-\mathbf{p}') = g^2 T \sum_{\varepsilon_1} \int \frac{d^3\mathbf{p}_1}{(2\pi)^3} \{ \mathcal{G}_{\varepsilon_1} \overline{\mathcal{G}}_{\omega-\varepsilon_1} + \overline{\mathcal{G}}_{\varepsilon_1} \mathcal{G}_{\omega-\varepsilon_1}$$

$$- \mathcal{F}_{\varepsilon_1} \mathcal{F}^+_{\omega-\varepsilon_1} - \mathcal{F}^+_{\varepsilon_1} \mathcal{F}_{\omega-\varepsilon_1} \}. \quad (4.83)$$

For brevity we omit the second arguments of Green's functions ($\mathcal{G}_{\varepsilon_1\varepsilon_2}$, etc.), which may be reconstructed from the "decay" conservation law for internal variables:

$$\varepsilon_1 + \varepsilon_2 = \omega, \quad \omega_1 + \omega_2 = \omega'. \quad (4.84)$$

Rule (4.84) is responsible for the appearance of $\overline{\mathcal{G}}$-functions in (4.83), which differ from $\mathcal{G}$ by the reversed directions of the arrows in the diagrams. In addition, the $\mathcal{F}\mathcal{F}^+$ pair in (4.83) is accompanied (cf. Sect. 1.4.1) by a change in the diagram's sign. Starting the analytic continuation of the polarization operator, we consider each component in (4.83) as the infinite sum of the diagrams of various orders in the external field. The entire procedure is analogous to that used earlier in deriving the analytically continued self-energy parts of electron–electron collisions. The only difference is that the external frequencies here are Bose frequencies (and naturally there are two electron lines). Since the directions of arrows in the diagrams do not influence the analytic continuation process, we will consider only the expression

$$\pi_{\omega\omega-\omega'} = T\sum_{\varepsilon_1} \mathcal{G}_{\varepsilon_1\varepsilon_1-\omega}\,\mathcal{G}_{\omega-\varepsilon_1\omega-\varepsilon_1+\omega_1-\omega'}. \tag{4.85}$$

For simplicity of notation, we omit the signs of internal frequency integration and summation at the vertices of interaction with the external field and phonons. Remember that expression (4.85) corresponds to the diagram series of perturbation theory and contains the sum of the various diagrams up to the infinite order; Green's functions for electrons in the polarization loops contain the phonon self-energy insertions that in turn contain field vertices of an arbitrary order. The diagram of a specific order in the external field (considered as a function of the complex variable ω) has a cut on the line $\mathrm{Im}\,(\omega - \Omega_m) = 0$ for fixed imaginary frequencies of the field vertices, which goes between the uppermost and lowermost banks:

$$0 \le \mathrm{Im}\omega \le \mathrm{Im}\omega'. \tag{4.86}$$

As in the case of the electron–electron self-energy parts, the quantities Ω_m represent certain combinations of the field vertex frequencies; here the set of these combinations and their total number depend on the distribution of vertices along the electron lines. Assuming that the cuts with $\mathrm{Im}(\varepsilon_1 - \omega_{1i}) = 0$, $\mathrm{Im}(\varepsilon_2 - \omega_{2k}) = 0$ correspond to these lines, we transform the frequency sum in (4.85) to the contour integral

$$\pi_{\omega\omega-\omega'} = \oint_C \frac{dz}{4\pi i} \tanh\frac{z}{2T}\,\mathcal{G}_z\,\mathcal{G}_{\omega-z'}, \tag{4.87}$$

where C is the contour shown in Fig. 2.1. Deforming the contour C to C', which goes along the banks of the cut, and noting that for the diagrams of any order the integrals along the big arcs vanish when the corresponding radii tend to infinity, after some straightforward calculations we obtain:

$$\pi_{\omega\omega-\omega'} = \sum_{i,k}\int \frac{dz}{4\pi i}\left\{\delta_i\left(\mathcal{G}_{z+\omega_{1i}}\right)\mathcal{G}_{\omega-z-\omega_{1i}}\tanh\frac{z}{2T}\right.$$

$$\left. - \mathcal{G}_{z+\omega-\omega_{2k}}\,\delta_k\left(\mathcal{G}_{-z+\omega_{2k}}\right)\tanh\frac{z}{2T}\right\}, \tag{4.88}$$

where $\delta_{i,k}(\mathcal{G})$ is the jump in the Green's function at the corresponding cut line. The external variable ω and the field frequencies remain imaginary. Their combination determines the set of cuts for the given diagram. Assuming in all diagrams $\omega > \omega'$ (the upper bank of the upper cut line), shifting the integration variable in all diagram expressions (as was done in Sects. 2.3 and 4.2) and summing over all orders of the perturbation series, we obtain

$$\pi^R_{\omega\omega-\omega'} = \int_{-\infty}^{\infty} \frac{dz}{4\pi i} (G_z G^R_{\omega-z} + G^R_z G_{\omega-z}), \tag{4.89}$$

where the G-function is determined as

$$G_{\varepsilon\varepsilon-\omega} = \sum_{N=0}^{\infty} \sum_{i=1}^{N+1} \delta_i (\mathcal{G}^{(N)}) \tanh \frac{\varepsilon - \omega_{1i}}{2T}, \tag{4.90}$$

while the functions $G^{R(A)}$ are determined directly from the diagram expansion (or the Dyson equation), where all the Green's functions for electrons are retarded (or advanced) and their entire set $\{G, G^R, G^A\}$ coincides with the functions figuring in Sect. 2.3. The expression for $\omega < 0$ also follows from (4.88) for $\omega \leq 0$ (the lower bank of the lower cut line):

$$\pi^A_{\omega\omega-\omega'} = \int_{-\infty}^{\infty} \frac{dz}{4\pi i} (G_z G^A_{\omega-z} + G^A_z G_{\omega-z}). \tag{4.91}$$

Using for $\pi_{\omega\omega-\omega'}$ an expression analogous to (4.90), but with the external frequencies representing now the Bose field, i.e.:

$$\pi_{\omega\omega-\omega'} = \sum_{N=0}^{\infty} \sum_{k=1}^{N+1} \delta_k (\pi^{(N)}) \coth \frac{\omega - \Omega_k}{2T}, \tag{4.92}$$

we obtain after the substitution of (4.88) into (4.92):

$$\pi_{\omega\omega-\omega'} = \sum_{i,k} \left\{ \int_{-\infty}^{\infty} \left[\delta_i (\mathcal{G}_{z+\omega_{1i}}) (\mathcal{G}_{\omega-z-\omega_{1i}}) \tanh \frac{z}{2T} \coth \frac{\omega - \omega_{ik} - \omega_{2k}}{2T} \right.\right.$$

$$\left.\left. - \delta_i (\mathcal{G}_{z+\omega-\omega_{2k}}) \delta_k (\mathcal{G}_{z+\omega_{2k}}) \tanh \frac{z}{2T} \coth \frac{\omega - \omega_{2k} - \omega_{1i}}{2T} \right] \right\}. \tag{4.93}$$

Shifting the integration variable in each of the terms in the first integral $z + \omega_{1i} \to z$ and $z + \omega - \omega_{2k} \to z$ in the second integral, and using the identity (3.48), one gets

$$\pi_{\omega\omega-\omega'} = \sum_{i\,k} \int \frac{dz}{4\pi i} \delta_i (\mathcal{G}_z) \delta_k (\mathcal{G}_{\omega-z}) \left[1 + \tanh \frac{z - \omega_{1i}}{2T} \tanh \frac{\omega - z - \omega_{2k}}{2T} \right]. \tag{4.94}$$

Summing in (4.94) all orders of perturbation theory and accounting for the definition of (4.89), we finally obtain

$$\pi_{\omega\omega-\omega'} = \int \frac{dz}{4\pi i}\left[G_z\, G_{\omega-z} + (G_z^R - G_z^A)\,(G_{\omega-z}^R - G_{\omega-z}^A)\right]. \tag{4.95}$$

Thus, for polarization operator (4.83), the complete set of functions Π, Π^R, Π^A is found, which describes the nonequilibrium case. One can show that they are identical to those obtained earlier on the basis of the Keldysh formula.

4.3.6. Equivalence of Keldysh and Eliashberg Approaches

Consider for this purpose any one of the components in $\Pi_{\omega\omega-\omega'}$, which follow from (4.83), for example,

$$\Pi^1_{\omega\omega-\omega'}(\mathbf{p}, \mathbf{p}-\mathbf{p}') = \frac{g^2}{2i}\left(\int \frac{d\varepsilon_1}{2\pi}\, G_{\varepsilon_1}\, G_{\omega-\varepsilon_1}\right) \equiv \frac{g^2}{2i}\int \frac{d\varepsilon_1 d\omega_1 d^3\mathbf{p}_1 d^3\mathbf{k}}{(2\pi)^8}$$

$$\times\, G_{\varepsilon_1,\varepsilon_1,-\omega}(\mathbf{p}_1, \mathbf{p}_1-\mathbf{k})\, G_{\omega-\varepsilon_1,\omega-\varepsilon_1+\omega_1,-\omega'}(\mathbf{p}-\mathbf{p}_1, \mathbf{p}-\mathbf{p}_1+\mathbf{k}-\mathbf{p}'), \tag{4.96}$$

and make a Fourier transformation to the spatial and temporal variables. As a result, one obtains

$$\Pi^1(x_1, x_2) = -\frac{ig^2}{2}\, G(x_1x_2)\, G(x_1x_2). \tag{4.97}$$

Now we write down all the terms $\Pi(x_1, x_2)$ obtained from the analytical continuation. Taking into account Eqs. (4.83) and (4.97) one finds

$$\Pi(1,2) = -\frac{ig^2}{2}\{G(1,2)\bar{G}(1,2) + \bar{G}G - FF^+ - F^+F$$

$$+ (\bar{G}^R - \bar{G}^A)(G^R - G^A) + (G^R - G^A)(\bar{G}^R - \bar{G}^A)$$

$$- (F^R - F^A)(F^{+R} - F^{+A}) - (F^{+R} - F^{+A})(F^R - F^A)\} \tag{4.98}$$

To compare this with result (4.82) obtained by the Keldysh technique, we must make the substitution $(1, 2) \to (2, 1)$ in the second multiplier of each of the components in braces (or in brackets) either in (4.98) or in (4.82). In the latter case, this should be done using the relations (4.63) to (4.65). We use the first possibility, noting that the Eliashberg functions have the properties

$$G^R(1,2) = \bar{G}^A(2,1), \quad G(1,2) = \bar{G}(21),$$

$$F^R(1,2) = F^A(2,1), \quad F(1,2) = F(2,1) \tag{4.99}$$

[in the absence of the spin-dependent interactions $G_{\alpha\beta} = \delta_{\alpha\beta}G$, $F_{\alpha\beta} = i(\hat{\sigma}_y)_{\alpha\beta}F$]. After removing the parentheses certain components vanish [for example, $\bar{G}^A(1,2)\,\bar{G}^A(2,1) \equiv 0$], so Eq. (4.98) can be reduced to the form

$$\Pi = \frac{ig^2}{2}\,[G(1,2)\,(2,1) + \overline{GG} - FF^{+} - F^{+}F + \overline{G}^{R}\,\overline{G}^{A} + \overline{G}^{A}\,\overline{G}^{R} + G^{R}\,G^{A}$$

$$+ G^{A}\,G^{R} - F^{R}\,F^{+A} - F^{A}\,F^{+R} - F^{+R}\,F^{A} - F^{+A}\,F^{R}]\,. \tag{4.100}$$

Comparing this expression with Eq. (4.82), we see that they coincide if the functions $G^{R(A)}$, $\overline{G}^{R(A)}$, $F^{R(A)}$, and $F^{+R(A)}$ are replaced by $G_{11}^{R(A)}$, $G_{22}^{R(A)}$, $G_{12}^{R(A)}$, and $G_{21}^{R(A)}$. Because these functions coincide up to the sign, the polarization operators (which are quadratic in Green's functions) coincide identically.

4.3.7. Transition to Energy-Integrated Propagators

Consider now an arbitrary component [e.g., the first one in the expression for $\Pi_{\omega\omega-\omega'}(\mathbf{p}, \mathbf{p}-\mathbf{p}')$], which follows from (4.83), taking into account (4.94). In this expression we can move from the integration over $d^3\mathbf{p}_1$ to angle and energy integrations based on the relation

$$\frac{d^3\mathbf{p}_1}{(2\pi)^3} \approx \frac{mp_F}{2\pi^2}\,\frac{d\Omega_{\mathbf{p}_1}}{4\pi}\,d\xi_1. \tag{4.101}$$

Using the auxiliary δ-function $\delta(\xi_2 - \xi_1 - \mathbf{q}\cdot\mathbf{p}_1/m)$, we may integrate with respect to the variable ξ_2. This makes it possible to express the quantity

$$\frac{mp_F}{2\pi^2}\int\frac{d\Omega_{\mathbf{p}_1}}{4\pi}\int\int d\xi_1 d\xi_2\,\delta(\xi_2 - \xi_1 + \mathbf{q}\cdot\mathbf{p}_1/m)\,G_1\,\overline{G}_2 \tag{4.102}$$

in terms of energy-integrated functions determined by a relation of the type

$$g_{\varepsilon\varepsilon-\omega}(\mathbf{p}, \mathbf{k}) = \int_{-\infty}^{\infty} d\xi\; G_{\varepsilon\varepsilon-\omega}(\mathbf{p}, \mathbf{p}-\mathbf{k}), \tag{4.103}$$

since the δ-function in (4.102) restricts mainly the angular integration and hence it may be factored out of the ξ-integral. Thus we have

$$\int\frac{d^3\mathbf{p}_1}{(2\pi)^3}\,G_1\,\overline{G}_2 = \frac{mp_F}{2\pi^2}\,\frac{1}{2qv_F}\int\frac{d\Omega_{\mathbf{p}_1}}{4\pi}\,\delta\left(\frac{\mathbf{q}\cdot\mathbf{p}_1}{qp_1}\right) g_1\bar{g}_2. \tag{4.104}$$

To shorten the notations, we introduce the operator

$$\hat{M} = \frac{g^2}{2i}\,\frac{mp_F}{2\pi^2}\,\frac{1}{2qv_F}\int\frac{d\varepsilon_1 d\omega_1 d^3\mathbf{k}}{(2\pi)^5}\,\frac{d\Omega_{\mathbf{p}_1}}{4\pi}\,\delta\left(\frac{\mathbf{q}\cdot\mathbf{p}_1}{qp_1}\right) \tag{4.105}$$

and the convention

$$[A, B]_+ = A_{\varepsilon_1 \varepsilon_1 - \omega_1}(\mathbf{p}_1, \mathbf{k})\, B_{\omega - \varepsilon_1 \omega - \varepsilon_1 + \omega_1 - \omega'}(\mathbf{p} - \mathbf{p}_1, \mathbf{p}' - \mathbf{k}) + BA, \tag{4.106}$$

obtaining thus the final expressions for the Fourier components of the quantities, which define the inequilibrium source in the phonon kinetic equation:

$$\Pi_{\omega\omega-\omega'} = \hat{M}\left\{\left[g^A \bar{g}\right]_+ - [f, f^+]_+ + \left[g^R - g^A, \bar{g}^R - \bar{g}^A\right]_+ - \left[f^R - f^A, f^{+R} - f^{+A}\right]_+\right\}, \tag{4.107}$$

$$(\Pi^R - \Pi^A)_{\omega\omega-\omega'} = M\left\{\left[g, \bar{g}^R - \bar{g}^A\right]_+ + \left[\bar{g}^A, g^R - g^A\right]_+ - \left[f, f^{+R}\right]_+ - \left[f^+, f^R - f^A\right]_+\right\}. \tag{4.108}$$

Before bringing the equation for phonons to the canonical form, we will obtain the expression for the collision integral of electrons with phonons.

4.4. INELASTIC ELECTRON–PHONON COLLISIONS

The self-energy functions for an electron–phonon interaction were derived in Sect. 3.2 assuming an equilibrium phonon distribution. We will consider now the general case when the phonon system is not in equilibrium.

4.4.1. Electron–Phonon Self-Energy Parts

In the representation of discrete imaginary frequencies [$P = \{\varepsilon, \mathbf{p}\}$, $K = \{\omega, \mathbf{k}\}$, $\omega = 2m\pi Ti$, $\varepsilon = (2n + 1)\pi Ti$, m and n are integers], we have:

$$\hat{\Sigma}(P, P - K) = T \sum_{\varepsilon'} \frac{d^3\mathbf{p}'}{(2\pi)^3} \mathcal{D}(P' - P, P' - P - K' + K)\, \hat{\mathcal{G}}(P', P' - K') \tag{4.109}$$

which corresponds to the diagram of Fig. 4.3. The functions $\hat{\mathcal{G}}$ (as well as $\mathcal{D}$) in (4.109) are assumed to be complete, including both external field and the self-energy parts and polarization operators. Assuming that initially in the absence of an external field the system is in equilibrium, we expand $\hat{\mathcal{G}}$ and $\mathcal{D}$ in a power series over the field and consider the analytical structure of the N^{th}-order diagram as the function of the complex variable ε at fixed imaginary frequencies

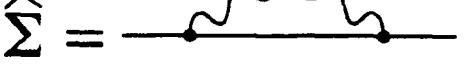

Figure 4.3. Self-energy function of the electron–phonon interaction.

ω_l ($\omega_l = 2m_l\pi Ti$, $\Sigma_l\, \omega_l = \omega$). The manifold of cuts of the object under consideration consists of the cuts of the internal $\mathcal{G}$-function and the $\mathcal{D}$-function. We denote this manifold by Ω_n. These cuts may be considered as situated on the lines $\mathrm{Im}(\varepsilon - \Omega_n) = 0$ in the complex plane ε between the uppermost line $\mathrm{Im}(\varepsilon - \omega) = 0$ and the abscissa (as was assumed earlier in accordance with the causality principle). The combinations of ω_l, which constitute Ω_n, are defined by the distribution of the field vertices over the internal lines of the diagram $\hat{\Sigma}^{(N)}$. Let us assume that manifolds of cuts $\mathrm{Im}(\varepsilon' - \omega_{1l}) = 0$ and $\mathrm{Im}(\varepsilon' - \varepsilon - \omega_{2k}) = 0$ correspond to $\hat{\mathcal{G}}$- and $\mathcal{D}$-functions. Replacing in (4.109) the summation over ε' by contour integration and shifting as usual the integration contour to the banks of the cuts, we find the resulting expression

$$\hat{\Sigma}^{(N)} = \sum_{i,k} \int \frac{dz}{4\pi i} \left\{ \tanh \frac{z}{2T}\, \delta_i (\hat{G}_{z+\omega_{1i}}) \mathcal{D}_{z-\varepsilon+\omega_{1i}} + \hat{\mathcal{G}}_{z+\omega_{2k}+\varepsilon} \coth \frac{z}{2T}\, \delta_k (\mathcal{D}_{z+\omega_{2k}}) \right\}, \tag{4.110}$$

where $\delta_i (\mathcal{G}_{z+\omega_{1i}})$ and $\delta_k (\mathcal{D}_{z+\omega_{2k}})$ are the jumps in Green's functions on the corresponding cuts (hereafter for brevity we omit the second indices of Green's functions). Continuing now analytically in Eq. (4.110) over ε from the upper bank of the uppermost cut (the lower bank of the lowermost cut), we obtain (after returning to real $\omega_{i,k}$, shifting the integration variable, summing over all the orders of perturbation theory, and integrating over the energy ξ) the expression

$$\hat{\Sigma}^{R(A)} = \int_{-\infty}^{\infty} \frac{d\varepsilon'}{4\pi i} \left\{ \hat{g}_{\varepsilon'} \mathcal{D}^{A(R)}_{\varepsilon'-\varepsilon} + \mathcal{D}_{\varepsilon'-\varepsilon}\, \hat{g}^{R(A)}_{\varepsilon'} \right\}, \tag{4.111}$$

in which the $\mathcal{D}$-function is defined as

$$\mathcal{D}_\omega = \sum_{N=0}^{\infty} \sum_{k=1}^{N+1} \coth \frac{\omega - \omega_k}{2T}\, \delta_k (\mathcal{D}^{(N)}). \tag{4.112}$$

Introducing $\hat{\Sigma}_{\varepsilon\varepsilon-\omega}$ as

$$\hat{\Sigma}_{\varepsilon\varepsilon-\omega} = \sum_{N=0}^{\infty} \sum_{k=1}^{N+1} \delta_k (\hat{\Sigma}^N_{\varepsilon\varepsilon-\omega}) \tanh \frac{\varepsilon - \Omega_k}{2T}, \tag{4.113}$$

we obtain, starting from Eq. (4.110), the expressions for the matrix elements of $\hat{\Sigma}$, which may be presented in the form (omitting for simplicity the second arguments)

$$\Sigma_1 = \int_{-\infty}^{\infty} \frac{d\varepsilon'}{4\pi i} \int \frac{d\Omega_{\mathbf{p}'}}{4\pi} [\mathcal{D}_{\varepsilon'-\varepsilon} g_{\varepsilon'} - (g^R - g^A)_{\varepsilon'} (\mathcal{D}^R - \mathcal{D}^A)_{\varepsilon'-\varepsilon}], \tag{4.114}$$

$$\Sigma_1^R - \Sigma_1^A = 2i\gamma = \int_{-\infty}^{\infty} \frac{d\varepsilon'}{4\pi i} \int \frac{d\Omega_{\mathbf{p}'}}{4\pi} [\mathcal{D}_{\varepsilon'-\varepsilon} (g^R - g^A)_{\varepsilon'} - g_{\varepsilon'} (^R - \mathcal{D}^A)_{\varepsilon'-\varepsilon}] , \tag{4.115}$$

$$\Sigma_2 = \Sigma_1 \, (g^{R(A)} \to f^{R(A)}), \, \delta = \gamma \, (g^{R(A)} \to f^{R(A)}). \tag{4.116}$$

In the diagonal over frequencies (quasi-classical) approximation, the phonon propagators may be expressed through the function N_{ω_q}:

$$\mathcal{D}_{\varepsilon'-\varepsilon} = \left(1 + 2N_{\omega_{\mathbf{p}'-\mathbf{p}}}\right) \text{sign} \, (\varepsilon' - \varepsilon) \, (\mathcal{D}^R - \mathcal{D}^A)_{\varepsilon'-\varepsilon}, \tag{4.117}$$

$$\mathcal{D}^{R(A)}_{\varepsilon'-\varepsilon} = \lambda \frac{2\omega^2_{\mathbf{p}'-\mathbf{p}}}{\omega^2_{\mathbf{p}'-\mathbf{p}} - (\varepsilon' - \varepsilon^{(+)}_{(-)} \, i\delta)^2}. \tag{4.118}$$

4.4.2. Canonical Form for Electron–Phonon Collisions

Using the relations (4.114) to (4.118), (3.83) to (3.88), (4.7), (4.9), and (4.13), one arrives at the following form of the electron–phonon collision integral:

$$J^{(\text{e-ph})} (n_{\pm\varepsilon}) = \frac{\pi\lambda}{4(up_F)^2} \int_0^{\infty} \omega_q^2 d\omega_q \int_{|\Delta|}^{\infty} d\varepsilon' \, [p_1 \delta(\varepsilon' - \varepsilon - \omega_q)$$

$$+ p_2 \delta(\varepsilon - \varepsilon' - \omega_q) + p_3 \delta(\varepsilon + \varepsilon' - \omega_q)] , \tag{4.119}$$

where the factors p_{1-3} are

$$p_1 = (u_\varepsilon u_{\varepsilon'} - v_\varepsilon v_{\varepsilon'} \pm 1) \left[n_{\varepsilon'} (1 - n_{\pm\varepsilon}) \, (1 + N_{\omega_q}) - n_{\pm\varepsilon} (1 - n_{\varepsilon'}) \, N_{\omega_q} \right]$$

$$+ (u_\varepsilon u_{\varepsilon'} - v_\varepsilon v_{\varepsilon'} \mp 1) \left[n_{-\varepsilon'} (1 - n_{\pm\varepsilon}) \, (1 + N_{\omega_q}) - n_{\pm\varepsilon} (1 - n_{-\varepsilon'}) \, N_{\omega_q} \right], \tag{4.120}$$

$$p_2 = (u_\varepsilon u_{\varepsilon'} - v_\varepsilon v_{\varepsilon'} \pm 1) \left[n_{\varepsilon'} (1 - n_{\pm\varepsilon}) \, N_{\omega_q} - n_{\pm\varepsilon} (1 - n_{\varepsilon'}) \, (1 + N_{\omega_q}) \right]$$

$$+ (u_\varepsilon u_{\varepsilon'} - v_\varepsilon v_{\varepsilon'} \mp 1) \left[n_{-\varepsilon'} (1 - n_{\pm\varepsilon}) \, N_{\omega_q} - n_{\pm\varepsilon} (1 - n_{-\varepsilon'}) \, (1 + N_{\omega_q}) \right], \tag{4.121}$$

$$p_3 = (u_\varepsilon u_{\varepsilon'} + v_\varepsilon v_{\varepsilon'} \mp 1) \left[(1 - n_{\pm\varepsilon}) \, (1 - n_{\varepsilon'}) \, N_{\omega_q} - n_{\pm\varepsilon} \, n_{\varepsilon'} (1 + N_{\omega_q}) \right]$$

$$+ (u_\varepsilon u_{\varepsilon'} + v_\varepsilon v_{\varepsilon'} \pm 1)\left[(1 - n_{\pm\varepsilon})(1 - n'_{-\varepsilon}) N_{\omega_q} - n_{\pm\varepsilon} n_{-\varepsilon'}(1 + N_{\omega_q})\right]. \qquad (4.122)$$

Having ascertained that the function $N_{\omega q}$ introduced by (4.117) plays the role of a phonon nonequilibrium distribution function, we will now obtain the kinetic equation for this quantity. We start from expression (4.112) for $\mathcal{D}_{\omega\omega-\omega'}$ and (4.92) for a polarization operator $\Pi_{\omega\omega-\omega'}$. Separating the anomalous parts $\mathcal{D}^{(a)}$ and $\Pi^{(a)}$, one obtains

$$\mathcal{D}_{\omega\omega-\omega'} = \mathcal{D}^R_{\omega\omega-\omega'} \coth\frac{\omega - \omega'}{2T} - \mathcal{D}^A_{\omega\omega-\omega'} \coth\frac{\omega}{2T} + \mathcal{D}^{(a)}_{\omega\omega-\omega'}, \qquad (4.123)$$

$$\Pi_{\omega\omega-\omega'} = \Pi^R_{\omega\omega-\omega'} \coth\frac{\omega - \omega'}{2T} - \Pi^A_{\omega\omega-\omega'} \coth\frac{\omega}{2T} + \Pi^{(a)}_{\omega\omega-\omega'}. \qquad (4.124)$$

Regular functions in (4.123) and (4.124) (for example, the advanced function $\mathcal{D}^A$) can be determined by the diagram expansion, in which all the functions (propagators and polarization operators) are advanced ones. Separating in the diagram expansion for $\mathcal{D}^{(a)}_{\omega\omega-\omega'}$ the left free line $\mathcal{D}^R_\omega$, we have the equation

$$(\mathcal{D}^0_\omega)^{-1}\, \mathcal{D}^{(a)}_{\omega\omega-\omega'} = \{\Pi^R\, \mathcal{D}^{(a)} + \Pi^{(a)}\, \mathcal{D}^A\}_{\omega\omega-\omega'}, \qquad (4.125)$$

where the following notation is used

$$\{AB\}_{\omega\omega-\omega'} = \int \frac{d\omega_1}{2\pi} A_{\omega\omega-\omega_1} B_{\omega-\omega_1\omega-\omega'} \qquad (4.126)$$

(an integration over internal momentum or a coordinate variable is also assumed). Separating the right free line in the same manner as $\mathcal{D}^A_{\omega\omega-\omega'}$, subtracting the result from (4.125), and using formulas (4.123) and (4.124) together with the expression for regular $\mathcal{D}^{R,A}$ functions, one obtains the relation

$$\left[(\mathcal{D}^0_\omega)^{-1} - (\mathcal{D}^0_{\omega-\omega'})^{-1}\right]\mathcal{D}_{\omega\omega-\omega'} = \{\Pi^R\, \mathcal{D} - \Pi\, \mathcal{D}^A - \mathcal{D}\, \Pi^A - \mathcal{D}^R\, \Pi\}_{\omega\omega-\omega'}, \qquad (4.127)$$

which is the desired general form of the kinetic equation for phonons. Expressions (4.75) and (4.77) follow from (4.127) after integration over the positive half-axis ω in a quasi-classical limit.

Note that at this stage the "bath" temperature T, which enters into imaginary frequency variables of initial equations, is eliminated both from (4.127) and from (4.114) to (4.116). The situation here is fully equivalent to that obtained by the Keldysh technique. In the technique of analytical continuation, the bath temperature plays the role of the equilibrium density matrix in Keldysh's method—this matrix is also eliminated from the final expressions.

4.4.3. Canonical Form for Phonon–Electron Collisions

The canonical form of the phonon–electron collision integral follows from Eqs. (4.75), (4.77), (4.107), (4.108), and (3.84) to (3.88):

$$I\left(N_{\omega_q}\right) = \frac{\pi\lambda}{8}\frac{\omega_D}{\varepsilon_F}\int_{\Delta}^{\infty}\int_{\Delta}^{\infty} d\varepsilon d\varepsilon' \{\delta(\varepsilon+\varepsilon'-\omega_q)\, s_1 + 2\delta(\varepsilon-\varepsilon'-\omega_q)\, s_2\}, \tag{4.128}$$

$$\begin{aligned} s_1 = {} & (u_\varepsilon u_{\varepsilon'} + v_\varepsilon v_{\varepsilon'} + 1)\left\{[(N_{\omega_q}+1)\, n_\varepsilon n_{-\varepsilon'} - N_{\omega_q}(1-n_\varepsilon)(1-n_{-\varepsilon'})]\right. \\ & \left. + [(N_{\omega_q}+1)\, n_{-\varepsilon} n_{\varepsilon'} - N_{\omega_q}(1-n_{-\varepsilon})(1-n_{\varepsilon'})]\right\} \\ & + (u_\varepsilon u_{\varepsilon'} + v_\varepsilon v_{\varepsilon'} - 1)\left\{[(N_{\omega_q}+1)\, n_\varepsilon n_{\varepsilon'} - N_{\omega_q}(1-n_\varepsilon)(1-n_{\varepsilon'})]\right. \\ & \left. + [(N_{\omega_q}+1)\, n_{-\varepsilon} n_{-\varepsilon'} - N_{\omega_q}(1-n_{-\varepsilon})(1-n_{-\varepsilon'})]\right\}, \end{aligned} \tag{4.129}$$

$$\begin{aligned} s_2 = {} & (u_\varepsilon u_{\varepsilon'} - v_\varepsilon v_{\varepsilon'} - 1)\left\{[(N_{\omega_q}+1)\, n_\varepsilon(1-n_{-\varepsilon'}) - N_{\omega_q}(1-n_\varepsilon)\, n_{-\varepsilon'}]\right. \\ & \left. + [(N_{\omega_q}+1)\, n_{-\varepsilon}(1-n_{\varepsilon'}) - N_{\omega_q}(1-n_{-\varepsilon})\, n_{\varepsilon'}]\right\} \\ & + (u_\varepsilon u_{\varepsilon'} - v_\varepsilon v_{\varepsilon'} + 1)\left\{[(N_{\omega_q}+1)\, n_\varepsilon(1-n_{\varepsilon'}) - N_{\omega_q}(1-n_\varepsilon)\, n_{\varepsilon'}]\right. \\ & \left. + [(N_{\omega_q}+1)\, n_{-\varepsilon}(1-n_{-\varepsilon'}) - N_{\omega_q}(1-n_{-\varepsilon})\, n_{-\varepsilon'})]\right\}. \end{aligned} \tag{4.130}$$

Expression (4.119) describes, besides the energy relaxation of electrons, inelastic collision processes that produce the relaxation of electron-hole population imbalance in superconductors. The situation here is fully analogous to that discussed in Sect. 4.2 and requires no further comments.

References

1. M. Yu. Reizer and A. V. Sergeev, Electron-phonon interaction in impurity-containing metals and superconductors, *Sov. Phys. JETP* **63**(3), 616–624(1986) *[Zh. Eksp. i Teor. Fiz.* **90**(3), 1056–1070 (1986)].
2. G. M. Eliashberg, Inelastic electron collisions and nonequilibrium stationary states in superconductors, *Sov. Phys. JETP* **34**(3), 668–676 (1972) *[Zh. Eksp. i Teor. Fiz.* **61**[3(9)], 1254–1272 (1971)].
3. I. E. Bulyzhenkov and B. I. Ivlev, Nonequilibrium phenomena in junctions of superconductors, Sov, *Phys. JETP* **47**(1), 115–120 (1978) *[Zh. Eksp. i Teor. Fiz.* **74**(1), 224–235 (1978)].
4. A. M. Gulian and G. F. Zharkov, Electron and phonon kinetics in a nonequilibrium Josephson junction, *Sov. Phys. JETP* **62**(1), 89–97 (1985) *[Zh. Eksp. i Teor. Fiz.* **89**(3), 1056–1070 (1985)].
5. M. Tinkham, Tunneling generation, relaxation and tunneling detection of hole-electron imbalance in superconductors, *Phys. Rev. B* **6**(5), 1747–1756 (1972).

6. E. M. Lifshitz and L. P. Pitaevskii, *Physical Kinetics*, pp. 391–412, Pergamon, Oxford (1981).
7. A. A. Abrikosov, L. P. Gor'kov, and I. E. Dzyaloshinskii, *Quantum Field Theoretical Methods in Statistical Physics*, 2nd ed., pp. 63–70, Pergamon, Oxford (1965).
8. L. V. Keldysh, Diagram technique for nonequilibrium processes, *Sov. Phys. JETP* **20**(4), 1018–1026 (1965) *[Zh. Eksp. i Teor. Phys.* **47** [4(10)], 1515–1527 (1964)].

5

Microwave-Enhanced Order Parameter

When a piece of normal metal is put into the high-frequency field, it is heated. This is not surprising from the point of view of physics intuition. What was puzzling and considered a "paradoxical quality" is that metals in superconducting state can behave as if they are being cooled under these circumstances. Enhanced values of critical currents were revealed by initial experimental measurements[1,2] performed on microbridges. It was not until 1970 that Eliashberg[3] recognized that this enhancement has nothing to do with spatial inhomegeneity. Instead, it is caused by the effective cooling of electrons by high-frequency electromagnetic fields. This specific mechanism, which will be described in this Chapter, was then further elaborated for cases where the energy comes from electromagnetic[4–9] and acoustic[10] fields, as well as the tunneling process.[11–14] Experiments[10,15–21] well confirmed these predictions. It was also recognized that this "gap enhancement" effect should be accompanied by a "phonon deficit effect," which will be discussed in the next Chapter.

During many years the enhancement effects looked like "small" and "of no practical significance," though "fascinating from a physical point of view".[22] However, rather recently experimentalists have been able to demonstrate the "microrefrigeration" effect, which relies on physics that is closely related to that of superconductivity enhancement (see Section 10.4).

5.1. SOURCE OF EXCITATIONS

5.1.1. Estimate for Magnetic Field Depairing Effect

An alternating electromagnetic field influences a superconducting order parameter in various ways. We start our discussion with the dynamic suppression of

the order parameter modulus (denoted as Δ in this chapter) by the effective mean square of field amplitude $\mathbf{A}(t)$.

Near T_c the action of $\mathbf{A}^2(t)$ is analogous to the action of a static magnetic field. The time average variation of Δ may be estimated by using the Ginzburg-Landau theory (Sect. 1.2)

$$\frac{\delta\Delta}{\Delta} \approx \left\{ -D\left(\frac{e}{c}\right)^2 \frac{\overline{\mathbf{A}^2}T}{\Delta^2} \right\} < 0, \tag{5.1}$$

where $D = lv_F/3$ is the diffusion coefficient of normal electrons. Second, the field exerts a kinetic influence when the high-frequency quanta are absorbed by electron excitations. That shifts their distribution over energies and changes the value of Δ according to the self-consistency equation.

As we will see in Sect. 5.2, at sufficiently high frequencies

$$\omega_0^2\tau_\varepsilon > \Delta, \tag{5.2}$$

where τ_ε is the characteristic energy relaxation time (to be addressed later) in the single-electron system, the kinetic effect dominates. Moreover, the variation of Δ has a sign that is opposite to that of Eq. (5.1).

5.1.2. Single-Quantum Transitions

We will consider this problem using the results of Eliashberg.[3,23] Because the action of a high-frequency field (5.2) on the oscillating part of the order parameter is negligibly small, the nonequilibrium order parameter Δ may be taken as a stationary one. We assume also that the superconducting film is sufficiently thin (having a thickness d), so the picture does not depend on the z-coordinate, which is perpendicular to the film surface. We assume also that the electron's mean-free-path is small: $l << (\xi_0, \lambda_L, d)$. For orientation, consider first the case of a normal metal, setting $\Delta \equiv \Theta$. In this case the matrix functions $\hat{\Sigma}^{(R,A)}$ and $\hat{g}^{(R,A)}$ are diagonal. The system of equations determining $g^{R(A)}$ reduces to a single equation

$$(\omega - \mathbf{v}_F\mathbf{k})\, g_{\varepsilon\varepsilon-\omega} = (H_1 g - g H_1)_{\varepsilon\varepsilon-\omega} + I_{\varepsilon\varepsilon-\omega}, \tag{5.3}$$

where

$$I_{\varepsilon\varepsilon-\omega} = (g\Sigma^A - \Sigma^R g)_{\varepsilon\varepsilon-\omega} + (g^R\Sigma - \Sigma g^A)_{\varepsilon\varepsilon-\omega}, \tag{5.4}$$

because

$$g^{R(A)}_{\varepsilon\varepsilon-\omega} = \overset{+}{(-)}\, i\pi \cdot 2\pi\delta(\omega) \tag{5.5}$$

(in the case of a normal metal, all the field-containing terms in a diagram expansion for $g^{R(A)}$ vanish after the integration over ξ). For simplicity we assume $d < \lambda_L$; in this case the high-frequency current density and also the vector potential A are constant over the film's cross section. Because the mean-free-path l is small, the

dependence of g on the angle θ between the vectors $\mathbf{p}$ and $\mathbf{A}$ may be approximated by the first spherical harmonic:

$$g = g^{(0)} + g^{(1)} \cos\theta. \tag{5.6}$$

Below we will consider the monochromatic field: $A = A_{\omega_0} \cos \omega_0 t$. As follows from (5.3), the elements

$$g^{(0)}_{\varepsilon\varepsilon} (\equiv g_\varepsilon),\ g^{(0)}_{\varepsilon\varepsilon\pm 2\omega_0}, \ldots, \tag{5.7}$$

containing even powers of the field are nonzero in the equation for $g^{(0)}$, and the elements

$$g^{(1)}_{\varepsilon\varepsilon\pm\omega_0},\ g^{(1)}_{\varepsilon\varepsilon\pm 3\omega_0}, \ldots, \tag{5.8}$$

containing odd powers of the field amplitude A are nonzero in the equation for $g^{(1)}$

5.1.3. Excitation Source in Normal Metals

The collisions with impurities disappear from the equation for $g^{(0)}$. In contrast, impurities play a major role in the equation for $g^{(1)}$. For g_ε one gets from (5.3):

$$0 = \frac{ev_F}{3c}\left\{A_{\omega_0}\left(g^{(1)}_{\varepsilon\varepsilon+\omega_0} - g^{(1)}_{\varepsilon-\omega_0\varepsilon}\right) + A_{-\omega_0}\left(g^{(1)}_{\varepsilon\varepsilon-\omega_0} - g^{(1)}_{\varepsilon+\omega_0\varepsilon}\right)\right\} + I_\varepsilon. \tag{5.9}$$

Because the value of $I_\varepsilon \sim i\tau_\varepsilon^{-1}\,(g_\varepsilon - g_\varepsilon^{eq})$ is small (g_ε^{eq} is the equilibrium value of g_ε), the functions $g^{(0)}_{\varepsilon\varepsilon\pm 2\omega_0}$ (the equations for them contain ω_0 on the left-hand side) are small compared with g_ε in the frequency range (5.2):

$$\left|\frac{g^{(0)}_{\varepsilon\varepsilon\pm 2\omega_0}}{g_\varepsilon}\right| \sim (\omega_0\tau_\varepsilon)^{-1}. \tag{5.10}$$

Hence only g_ε may be retained in the equation for g, and it follows finally from (5.3) and (5.6)*:

$$g^{(1)}_{\varepsilon\varepsilon-\omega_0} = i\tau\frac{ev_F}{c}A_{\omega_0}(g_{\varepsilon-\omega_0} - g_\varepsilon), \tag{5.11}$$

where τ is the elastic scattering time of electrons entering (5.11) in view of (5.9), (4.5), (4.2), (2.37), and (2.8). Substitution of (5.11) into (5.9) gives the equation ($D = v_F^2\tau/3$):

$$0 = 2D\left(\frac{e}{c}\right)^2 A_{\omega_0}A_{-\omega_0}\left[(n_{\varepsilon-\omega_0} - n_\varepsilon)\,\theta(\varepsilon - \omega_0) - (n_\varepsilon - n_{\varepsilon+\omega_0}) + (1 - n_\varepsilon - n_{\omega_0-\varepsilon})\,\theta(\omega_0 - \varepsilon)\right] + J_\varepsilon, \quad \varepsilon \geq 0, \tag{5.12}$$

* As follows from Eqs. (5.9) and (5.10), at $\omega_0 >> \tau_\varepsilon^{-1}$ only single-quantum transitions must be taken into account in the absorption acts of photon by electrons. The n-quanta absorption probability is small in parameter $(\omega_0\tau_\varepsilon)^{-2n}$.

where we have taken into account that $g_\varepsilon = 2\pi i\,(1 - 2n_\varepsilon)\,\mathrm{sign}\varepsilon$, where n_ε is the (even over ε) excitation distribution function.

5.1.4. "Dirty" Superconductors

We turn now to the case of a superconductor.* Retaining in the isotropic part only the diagonal term $\hat{g}^{(0)}_{\varepsilon\varepsilon} \equiv \hat{g}_\varepsilon$, we will consider equations for separate components of $\hat{g}$. From (3.63) it follows immediately that:

$$f = f^+,\ \vec{g} = -g,\ \Sigma_2^+ = \Sigma_2,\ \overline{\Sigma}_1 = -\Sigma_1. \tag{5.13}$$

In this chapter we will consider states that are symmetric in the electron-hole branches. Then the collision integral I_ε takes a simplified form [cf. Eqs. (4.2) and (4.7)]:

$$I_\varepsilon = -(\Sigma_1^R - \Sigma_1^A)_\varepsilon\, g_\varepsilon + (\Sigma_2^R - \Sigma_2^A)_\varepsilon f_\varepsilon - \Sigma_{1\varepsilon}(g^R - g^A)_\varepsilon - \Sigma_{2\varepsilon}(f^R - f^A)_\varepsilon \tag{5.14}$$

and, as earlier, the impurity contributions disappear from (5.14).

In the equations for $\hat{g}^{(1)}_{\varepsilon\varepsilon-\omega_0}$ we can neglect the phonon and electron self-energies, compared with the one related to the impurities. By analogy with the normal state, we will use a zero-field approximation for isotropic spectral functions and a linear approximation for anisotropic spectral functions:

$$g_\varepsilon^{R(A)} = i\pi\frac{\varepsilon}{\xi_\varepsilon^{R(A)}},\ f_\varepsilon^{R(A)} = i\pi\frac{\Delta}{\xi_\varepsilon^{R(A)}}; \tag{5.15}$$

$$g^{(1)R(A)}_{\varepsilon\varepsilon-\omega_0} = i\pi\frac{ev_F}{c}A_{\omega_0}\frac{1}{(\xi_\varepsilon + \xi_{\varepsilon-\omega_0})^{R(A)} + i/\tau}\left[1 - \frac{\varepsilon(\varepsilon-\omega_0)+\Delta^2}{(\xi_\varepsilon\xi_{\varepsilon-\omega_0})^{R(A)}}\right], \tag{5.16}$$

$$f^{(1)R(A)}_{\varepsilon\varepsilon-\omega_0} = -i\pi\frac{ev_F}{c}A_{\omega_0}\frac{1}{(\xi_\varepsilon + \xi_{\varepsilon-\omega_0})^{R(A)} + i/\tau}\frac{2\varepsilon-\omega_0}{(\xi_\varepsilon\xi_{\varepsilon-\omega_0})^{R(A)}}, \tag{5.17}$$

where

$$\xi_\varepsilon^R = -(\xi_\varepsilon^A)^* = \begin{cases}\sqrt{\varepsilon^2-\Delta^2} + i\delta; & \varepsilon > \Delta,\\ i\sqrt{\Delta^2-\varepsilon^2}; & -\Delta < \varepsilon < \Delta,\\ -\sqrt{\varepsilon^2-\Delta^2} + i\delta; & \varepsilon < -\Delta.\end{cases} \tag{5.18}$$

Solving now (3.63) subject to (5.15) to (5.18), we find

$$g^{(1)}_{\varepsilon\varepsilon-\omega_0} = i\tau\frac{ev_F}{c}A_{\omega_0}[\varepsilon(\varepsilon-\omega_0)+\Delta^2]\left[\frac{g_{\varepsilon-\omega_0}}{(\varepsilon-\omega_0)\,\xi_\varepsilon^R} + \frac{g_\varepsilon}{\varepsilon\xi^A_{\varepsilon-\omega}}\right]. \tag{5.19}$$

Introducing, in accordance with Sect. 3.2, the distribution function n_ε:

*The specifics of the problem considered in this chapter permit the use of a gauge with a real order parameter.

$$g_\varepsilon = 2\pi i \frac{\varepsilon}{\sqrt{\varepsilon^2 - \Delta^2}} \theta(\varepsilon^2 - \Delta^2)(1 - 2n_\varepsilon); \; n_\varepsilon = n_{-\varepsilon}, \tag{5.20}$$

we find from (3.63) and (5.14) the kinetic equation

$$0 = 2\left(\frac{e}{c}\right)^2 DA_{\omega_0} A_{-\omega_0} [U_{\varepsilon\varepsilon-\omega_0}(n_{\varepsilon-\omega_0} - n_\varepsilon) - U_{\varepsilon+\omega_0\varepsilon}(n_\varepsilon - n_{\varepsilon+\omega_0}) + V_{\varepsilon\omega_0-\varepsilon}(1 - n_\varepsilon - n_{\omega_0-\varepsilon})] + J_\varepsilon, \tag{5.21}$$

in which

$$U_{\varepsilon\varepsilon-\omega_0} = \frac{\varepsilon(\varepsilon - \omega_0) + \Delta^2}{\sqrt{[(\varepsilon - \omega_0)^2 - \Delta^2](\varepsilon^2 - \Delta^2)}} \theta(\varepsilon - \omega_0 - \Delta), \tag{5.22}$$

$$V_{\varepsilon\omega_0-\varepsilon} = \frac{\varepsilon(\omega_0 - \varepsilon) - \Delta^2}{\sqrt{[(\omega_0 - \varepsilon)^2 - \Delta^2](\varepsilon^2 - \Delta^2)}} \theta(\varepsilon - \Delta)\,\theta(\omega_0 - \varepsilon - \Delta). \tag{5.23}$$

The collision integral in (5.21) corresponds to electron–phonon and electron–electron collisions:

$$J(\varepsilon) = J^{(e-ph)} + J^{(e-e)}, \tag{5.24}$$

and in accordance with (5.14) we should put $n_\varepsilon = n_{-\varepsilon}$ in $J^{(e-ph)}$ (4.119) and $J^{(e-e)}$ (4.36). In the general case, without any restriction on the function n_ε, these integrals were found in Sect. 4.2.

5.2. STIMULATION EFFECT

5.2.1. Nonequilibrium Self-Consistency Equation

The kinetic equations derived in the previous section contain the nonequilibrium gap Δ, connected with $\Sigma_2^{R(A)}$ by the relation (4.6). Using the expressions for $\Sigma_2^{R(A)}$, one can obtain a self-consistency equation

$$1 = \lambda \int_\Delta^{\omega_D} \frac{d\varepsilon}{\sqrt{\varepsilon^2 - \Delta^2}} (1 - 2n_\varepsilon), \tag{5.25}$$

which differs from the equilibrium equation by replacement of $\tanh(\varepsilon/2T) \equiv (1 - 2n_\varepsilon^F)\operatorname{sign}\varepsilon$ by $(1 - 2n_\varepsilon)\operatorname{sign}\varepsilon$, where n_ε is the nonequilibrium distribution function [cf. (1.154)].

We will consider in more detail how the electromagnetic field of frequency $\omega_0 < 2\Delta$ influences the nonequilibrium gap Δ.[3] A formal condition $\Delta << T$ allows one to go far enough analytically. At $\omega_0 < 2\Delta$ the field term in (5.21) [we will denote it $Q(\varepsilon)$] is the difference of some function at the points shifted along the ε-axis by the value ω_0. Substituting in $Q(\varepsilon)$ the equilibrium function $n_\varepsilon^0 = [1 + \exp|\varepsilon|/T)]^{-1}$

instead of n_ε, expanding and keeping only the first, nonvanishing two terms in the series, we obtain:

$$Q(\varepsilon) = 2\left(\frac{e}{c}\right)^2 DA_{\omega_0}A_{-\omega_0}\left\{-\omega_0\frac{\partial n_\varepsilon^0}{\partial\varepsilon}(U_{\varepsilon\varepsilon-\omega_0} - U_{\varepsilon+\omega_0\varepsilon}) + \frac{\omega_0^2}{2}\frac{\partial^2 n_\varepsilon^0}{\partial\varepsilon^2}(U_{\varepsilon\varepsilon-\omega_0} + U_{\varepsilon+\omega_0\varepsilon})\right\}. \tag{5.26}$$

The first term is defined mainly in the region $\varepsilon \sim \Delta$, and the second in the range $\varepsilon \sim T$.

5.2.2. Relaxation-Time Approximation

To find a solution for the linearized equation, we will subdivide the variation of distribution function into parts: $n_\varepsilon^{(1)} = n_\varepsilon - n_\varepsilon^0 = n_{1\varepsilon}^{(1)} + n_{2\varepsilon}^{(1)}$.

For the function $n_{1\varepsilon}^{(1)}$, the collision integral $J(\varepsilon)$ in (5.21) allows us to use the relaxation time approximation. Indeed, substituting $n_\varepsilon = n_{1\varepsilon}^{(1)}$ into (5.24), one can verify that the terms containing $n_{1\varepsilon}^{(1)}$ as integrands are smaller than other terms in which $n_{1\varepsilon}^{(1)}$ is simply a factor. Omitting the smaller terms, we find an approximation (the τ approximation; for more details see Sect. 11.3)

$$J(\varepsilon) \approx -2\gamma n_{1\varepsilon}^{(1)}\frac{\varepsilon}{\sqrt{\varepsilon^2-\Delta^2}}. \tag{5.27}$$

The damping γ may be found using explicit expressions for collision integrals (4.36) and (4.119). It is determined by the range of integration over ε, which is comparable with T and, up to the corrections $(\Delta/T)^2$, has the same value as in a normal state: $\gamma \sim \max(T^3/\omega_D^2, T^2/\varepsilon_F)$.

5.2.3. Solution for Distribution Function at $T \approx T_c$

Introducing the notation $\alpha = D(e/c)^2 A_{\omega_0}A_{-\omega_0}$, we find at $\omega_0 < 2\Delta$:

$$n_{1\varepsilon}^{(1)} = 2\frac{\alpha}{\gamma}\left\{\frac{\omega_0}{4T}\cosh^{-2}\left(\frac{\varepsilon}{2T}\right)(U_{\varepsilon\varepsilon-\omega_0} - U_{\varepsilon+\omega_0\varepsilon})\right\}\frac{\sqrt{\varepsilon^2-\Delta^2}}{\varepsilon},\ \varepsilon \geq \Delta. \tag{5.28}$$

At $\varepsilon \sim \Delta << T$, the value of γ does not depend on ε. Substituting (5.28) into the integral part of $J(\varepsilon)$ (omitted in the τ approximation), one can verify that the correction has the relative smallness Δ/T at $\varepsilon \sim \Delta$, but is nonzero in the region $\varepsilon \sim T$. Subsequent iterations do not change this result.

The correction $n_{2\varepsilon}^{(1)}$, which corresponds to the second term in (5.26), may be investigated in the same manner. This correction has a structure analogous to the above-mentioned correction to (5.28). Thus the full variation of the distribution

function $n_\varepsilon^{(1)}$ consists of the part (5.28), which dominates at $\varepsilon \geq \Delta$, and of a small "tail," diminishing at $\varepsilon \sim T$. To calculate this tail, one must go beyond the τ approximation. The function n_ε enters the expression (5.25) for Δ with the weight $(\varepsilon^2 - \Delta^2)^{-1/2}$. Consequently, the main contribution comes from the region $\varepsilon \sim \Delta$. This allows one to take into account only the part $n_{1\varepsilon}^{(1)}$ (5.28) when determining Δ, and confirms the applicability of the τ approximation in the vicinity of T_c.

5.2.4. Enhancement of the Gap

We substitute now the expression (5.28) into the gap equation (5.25), transforming it preliminarily to the form

$$\delta\Delta = -\frac{T^2}{\Delta}\left(\frac{8\pi^2}{7\zeta(3)}\right)\int_\Delta^\infty \frac{d\varepsilon}{\sqrt{\varepsilon^2 - \Delta^2}}\,\delta n_\varepsilon, \tag{5.29}$$

where now $\delta n_\varepsilon \approx n_{1\varepsilon}^{(1)}$. Accounting for

$$\int_\Delta^\infty \frac{d\varepsilon}{\sqrt{\varepsilon^2 - \Delta^2}}\, n_{1\varepsilon}^{(1)} \approx -\frac{\Delta}{2T_c}\left(\frac{\alpha\omega_0^2}{\gamma\Delta^2}\right)\ln\frac{8\Delta}{\omega_0}, \tag{5.30}$$

we find

$$\delta\Delta \approx a_0 T\left(\frac{\alpha\omega_0^2}{\gamma\Delta^2}\right), \tag{5.31}$$

where

$$a_0 = \frac{8}{7}\frac{\pi^2}{\zeta(3)}\ln\frac{8\Delta}{\omega_0} \sim 1. \tag{5.32}$$

Comparing (5.31) with the dynamic contribution, we can estimate the relative value of the kinetic effect:

$$\left|\frac{\delta\Delta^{kin}}{\delta\Delta^{dyn}}\right| \sim \frac{\omega_0^2}{\gamma\Delta}. \tag{5.33}$$

As $\omega \sim \Delta$, and $\gamma << \omega$ (the latter inequality is the condition of a single-quantum absorption of the field's energy), one may conclude that high-frequency electromagnetic radiation should stimulate superconducting ordering in the film. The enhancement of a superconductor's critical parameters (critical temperature, current, etc.) was indeed observed experimentally.[1,2,24] As follows from (5.31), in weak fields the enhancement effect grows with the intensity of radiation as $\alpha\omega_0^2$. One can expect that the enhancement of Δ by an order of its value ($\delta\Delta \sim \Delta$) may be reached in fields with the intensity

$$\alpha \sim \gamma\frac{\Delta}{T} \tag{5.34}$$

(assuming that the experiment is carried out at optional frequencies $\omega_0 \sim \Delta$). At such intensities, as can be seen from (5.1), the dynamic influence of the field is insignificant. The influence of the field on the superconductor's single-particle electron excitations is also small [i.e., the change of spectral functions (3.66) is small and becomes essential only at significantly higher intensities:[3] $\alpha \sim \Delta$]. Accordingly, the model equation (5.25) remains valid in fields with intensities (5.34). Nevertheless, the experimentally observed values of $\delta\Delta/\Delta$ are only on the order of several percent,[24,25] even in optimal cases. The reason probably is that the "heating" processes in the superconductor's electron subsystem become essential at relatively moderate intensities of the electromagnetic field. Such processes may occur, for example, when the electron with the energy $\varepsilon \geq 3\Delta$ (an energy the electron can obtain by sequential stages of photon absorption) collides with the Cooper pair and decays into three electronic excitations. This mechanism is analogous to the mechanism of "shock ionization" and is described by the electron–electron collision integral (4.36) (by terms that are proportional to the factor E_3). Such processes increase the total number of excitations and lead to the effective damping of the gap Δ (see, e.g., Ref. 26).

5.3. PHOTON–ELECTRON INTERACTIONS

As was established in the preceding section, high-frequency electromagnetic radiation influences a superconductor by the Eliashberg mechanism, effectively redistributing electrons and holes in the momentum space, so that the "center of gravity" of the Fermi distribution function is shifted to higher energies, while the total number of excitations remains constant. As a result, the states near the Fermi surface at the gap edge become unoccupied and this leads to an increase in the superconducting order parameter, according to the self-consistency condition. Even though the enhancement of the order parameter is rather small, the detection of the effect allows us to estimate the characteristic time scales that characterize the microscopic processes in superconductors. For example, the frequency range of electromagnetic radiation, which can produce the enhancement effect, is restricted by the value 2Δ from above and by the value γ from below. Further theoretical analysis of the enhancement mechanism also reveals the existence of other conditions that are important for its realization. One of these conditions is the smallness of an electron's mean-free-path:

$$\Delta\tau \ll 1, \tag{5.35}$$

where τ is the electron's elastic scattering time on impurities. In real superconductors, the condition (5.35) need not be fulfilled. Moreover, the reversed inequality may take place. We will consider now this situation, which would arise in the latter case.

To study the enhancement problem in perfect specimens, it is necessary first to derive the appropriate expression for the nonequilibrium source because the kinetic equation (5.21) describes the case of dirty superconductors. To solve that problem, it is expedient to use the quantum description for the interaction between electrons and photons.

5.3.1. Quantum Description

The Hamiltonian of this interaction in superconductors has the form (the gauge $\varphi = \mathrm{div}\,\mathbf{A} = 0$ is used):

$$\hat{H}_{\mathrm{e-pt}} = -\frac{ie}{2mc}\int_{V_0}[\nabla_i\psi^{\dagger}_{\gamma}(x)\,\psi_{\gamma}(x) - \psi^{\dagger}_{\gamma}(x)\nabla_i\,\psi_{\gamma}(x)]\hat{\mathbf{A}}_i(x)\,d^3\mathbf{r}. \tag{5.36}$$

Introducing the operator

$$\hat{\varphi}_{\mathbf{p}}(\mathbf{k}) = \sum_{\lambda}[\beta^{*}_{-\mathbf{k},-\lambda}(\mathbf{p})\,\hat{C}^{\dagger}_{-\mathbf{k},-\lambda} + \beta_{\mathbf{k},\lambda}(\mathbf{p})\,\hat{C}_{\mathbf{k},\lambda}], \tag{5.37}$$

where $\hat{C}^{\dagger}_{\mathbf{k},\lambda}$ and $\hat{C}_{\mathbf{k},\lambda}$ are the photon creation and annihilation operators ($\mathbf{k}$ and λ correspond to the momentum and polarization of the photon), and

$$\beta_{\mathbf{k},\lambda}(\mathbf{p}) = \frac{e}{m}\left(\frac{2\pi}{V_0\omega_{\mathbf{k}}}\right)^{1/2}(\mathbf{p}\cdot\mathbf{e}_{\mathbf{k},\lambda}). \tag{5.38}$$

Moving to the Nambu representation ($\hat{a}_{\mathbf{p}1} \equiv a_{\mathbf{p}\uparrow}$, $\hat{a}_{\mathbf{p}2} \equiv a^{\dagger}_{-\mathbf{p}\downarrow}$), the Hamiltonian acquires the form:

$$\hat{H}_{\mathrm{e-pt}} = -\sum_{\mathbf{p},\mathbf{k}}\hat{\varphi}_{\mathbf{p}}(\mathbf{k})\left[\hat{a}^{\dagger}_{\mathbf{p},1}\,\hat{a}_{\mathbf{p}-\mathbf{k},1} - \hat{a}_{\mathbf{p},2}\,\hat{a}^{\dagger}_{\mathbf{p}+\mathbf{k},2}\right]. \tag{5.39}$$

For nonequilibrium superconductors, we will use the Keldysh diagram technique (mentioned in Sect. 3.3), in which the electron self-energies are represented by the matrices

$$\check{G} = \begin{pmatrix} \hat{0} & \hat{G}^A \\ \hat{G}^R & \hat{G} \end{pmatrix},\quad \check{D} = \begin{pmatrix} 0 & D^A \\ D^R & D \end{pmatrix},\quad \check{\Sigma} = \begin{pmatrix} \hat{\Sigma} & \hat{\Sigma}^R \\ \hat{\Sigma}^A & \hat{0} \end{pmatrix}, \tag{5.40}$$

where the quantities $\hat{G}$, $G^{R(A)}$, $\hat{\Sigma}$, $\hat{\Sigma}^{R(A)}$ are matrices in the Nambu space. The electron and photon Green's functions are defined by the equations ($i, j = 1, 2$; $\mu, \nu = 1, 2$):

$$G^{ij}_{\mu\nu}(\mathbf{p}t, \mathbf{p}'t') = -i\langle T\hat{a}_{\mathbf{p}\mu}(t_i)\hat{a}^{\dagger}_{\mathbf{p}'\nu}(t')\rangle, \tag{5.41}$$

$$D^{ij}_{\mathbf{p}\mathbf{p}'}(\mathbf{k}t, \mathbf{k}'t') = -i\langle T\hat{\varphi}_{\mathbf{p}}(\mathbf{k},t_i)\hat{\varphi}_{\mathbf{p}'}(\mathbf{k}',t'_j)\rangle. \tag{5.42}$$

For the Fock states of an electromagnetic field, the photon propagators D, $D^{R(A)}$ have the forms

$$D^{R(A)}_{\mathbf{p}\mathbf{p}'}(K) = \sum_{\lambda}\left\{\frac{\beta_{\mathbf{k},\lambda}(\mathbf{p})\beta^{*}_{\mathbf{k},\lambda}(\mathbf{p}')}{\omega - \omega^{+}_{k(-)}i\delta} - \frac{\beta^{*}_{-\mathbf{k},-\lambda}(\mathbf{p})\beta_{-\mathbf{k},-\lambda}(\mathbf{p}')}{\omega + \omega^{+}_{k(-)}i\delta}\right\}, \tag{5.43}$$

$$D_{\mathbf{p}\mathbf{p}'}(K) = -2\pi i\sum_{\lambda}\{\beta^{*}_{\mathbf{k}\lambda}(\mathbf{p})\beta_{\mathbf{k}\lambda}(\mathbf{p}')(1 + 2N_{\mathbf{k}\lambda})\delta(\omega - \omega_k)$$

$$+ \beta_{-\mathbf{k}-\lambda}(\mathbf{p})\beta^{*}_{-\mathbf{k}-\lambda}(\mathbf{p}')(1 + 2N_{-\mathbf{k}-\lambda})\delta(\omega + \omega_k)\}, \tag{5.44}$$

where $N_{\mathbf{k}\lambda} = \langle\hat{C}^{\dagger}_{\mathbf{k}\lambda}\hat{C}_{\mathbf{k}\lambda}\rangle$ is the photon occupation number, $\omega \equiv c|\mathbf{k}|$, $K \equiv (\omega,\mathbf{k})$. The vertices where the energy-momentum transfer takes place are presented in the Keldysh technique[27] by objects of the kind $\Gamma^{mn,l}_{\mu\nu}$, where the two upper and all the lower indices correspond to electrons, while l corresponds to Bosons. In the case of electron–photon interaction, one can find using (5.36):

$$\Gamma^{mn,1}_{\mu\nu} = \frac{1}{\sqrt{2}}\delta_{mn}\delta_{\mu\nu},\ \Gamma^{mn,2}_{\mu\nu} = \frac{1}{\sqrt{2}}(\hat{\sigma}_x)_{mn}\delta_{\mu\nu}. \tag{5.45}$$

Using standard graphic techniques and assuming that the propagator $D_{\mathbf{p}\mathbf{p}'}$ links two vertices with electron momenta $\mathbf{p},\mathbf{p}'$ and those due to the transverse character of electromagnetic field $D_{\mathbf{p}\pm\mathbf{k},\mathbf{p}'\pm\mathbf{k}} \equiv D_{\mathbf{p},\mathbf{p}'}$, we find, taking into account (5.37) and (5.40),

$$\Sigma_{\mu\nu}(P) = \frac{i}{2}\int\frac{d^4p'}{(2\pi)^4}[DG_{\mu\nu} + (D^R - D^A)(G^R_{\mu\nu} - G^A_{\mu\nu})], \tag{5.46}$$

$$(\Sigma^R - \Sigma^A)_{\mu\nu}(P) = \frac{i}{2}\int\frac{d^4p'}{(2\pi)^4}[(D^R - D^A)G_{\mu\nu} + (G^R_{\mu\nu} - G^A_{\mu\nu})]. \tag{5.47}$$

Summing over the photon's polarizations and integrating over $\xi_{\mathbf{p}}$, using also the relation between the $\hat{g}$-function and the distribution function of the electron-hole excitations (see Sect. 3.3), the nonequilibrium source $Q(\pm\varepsilon)$ may be found in the form of the collision integral of electrons with photons:

$$Q(\pm\varepsilon) \equiv J^{(e-pt)}(n_{\pm\varepsilon}(\pm\mathbf{p})) = \left(\frac{\pi e}{mc}\right)^2 N(0) \int_{\Delta}^{\infty} \frac{d\varepsilon'}{2\pi} \int \frac{d\Omega_{\mathbf{p}'}}{4\pi} \rho(\omega_{\mathbf{p}-\mathbf{p}'})$$

$$\times \{q_1 \delta(\varepsilon' - \varepsilon - \omega_{\mathbf{p}-\mathbf{p}'}) + q_2 \delta(\varepsilon - \varepsilon' - \omega_{\mathbf{p}-\mathbf{p}'}) + q_3 \delta(\varepsilon + \varepsilon' - \omega_{\mathbf{p}-\mathbf{p}'})\}, \quad (5.48)$$

where

$$q_1(\pm\varepsilon) = (u_\varepsilon u_{\varepsilon'} + v_\varepsilon v_{\varepsilon'} \pm 1)$$

$$\times \{n_{\varepsilon'}(\mathbf{p}')[1 - n_{\pm\varepsilon}(\pm\mathbf{p})](1 + N_{\mathbf{p}'-\mathbf{p}}) - n_{\pm\varepsilon}(\pm\mathbf{p})(1 - n_{\varepsilon'}(\mathbf{p}'))N_{\mathbf{p}'-\mathbf{p}}\}$$

$$+ (u_\varepsilon u_{\varepsilon'} + v_\varepsilon v_{\varepsilon'} \mp 1)[\ldots \varepsilon', \mathbf{p}' \to -\varepsilon', -\mathbf{p}' \ldots], \quad (5.49)$$

$$q_2(\pm\varepsilon) = (u_\varepsilon u_{\varepsilon'} + v_\varepsilon v_{\varepsilon'} \pm 1)$$

$$\times \{n_{\varepsilon'}(\mathbf{p}')[1 - n_{\pm\varepsilon}(\pm\mathbf{p})]N_{\mathbf{p}-\mathbf{p}'} - n_{\pm\varepsilon}(\pm\mathbf{p})(1 - n_{\varepsilon'}(\mathbf{p}'))(1 + N_{\mathbf{p}-\mathbf{p}'})\}$$

$$+ (u_\varepsilon u_{\varepsilon'} + v_\varepsilon v_{\varepsilon'} \mp 1)[\ldots \varepsilon', \mathbf{p}' \to -\varepsilon', -\mathbf{p}' \ldots], \quad (5.50)$$

$$q_3(\pm\varepsilon) = (u_\varepsilon u_{\varepsilon'} - v_\varepsilon v_{\varepsilon'} \mp 1)$$

$$\times \{[1 - n_{\pm\varepsilon}(\pm\mathbf{p})][1 - n_{\varepsilon'}(-\mathbf{p}')]N_{\mathbf{p}-\mathbf{p}'} - n_{\pm\varepsilon}(\pm\mathbf{p})\, n_{\varepsilon'}(-\mathbf{p}')(1 + N_{\mathbf{p}-\mathbf{p}'})\}$$

$$+ (u_\varepsilon u_{\varepsilon'} - v_\varepsilon v_{\varepsilon'} \pm 1)\{\ldots \varepsilon', -\mathbf{p}' \to -\varepsilon', \mathbf{p}' \ldots\}, \quad (5.51)$$

$$N(0) = \frac{mp_F}{2\pi^2}, \quad \rho(\omega_{\mathbf{k}}) = \frac{(2p_F c)^2}{\omega_{\mathbf{k}}}, \quad N_{\mathbf{k}} \equiv \frac{4c^2}{\omega_{\mathbf{k}}\rho(\omega_{\mathbf{k}})} \sum_{\lambda} N_{\mathbf{k},\lambda} |\mathbf{p} \cdot \mathbf{e}_{\mathbf{k},\lambda}|^2, \quad (5.52)$$

and $|\mathbf{p}| = |\mathbf{p}'| = p_F$. In the "dirty" limit, for the case of a monochromatic field in the absence of branch imbalance ($n_\varepsilon = n_{-\varepsilon}$), expression (5.48) must be converted into the field term of the Eliashberg kinetic equations, obtained by the classical description of an electromagnetic field in Sect. 5.1. We will confirm this now.

5.3.2. *Collision Integral as a Nonequilibrium Single-Electron Source*

In the presence of impurity scattering, the energy-momentum conservation laws [for the relaxation channel in (5.48)] may be presented in the form

$$\varepsilon' - \varepsilon = \pm ck, \quad \mathbf{p}' - \mathbf{p} - \mathbf{q} = \pm \mathbf{k}, \quad (5.53)$$

where $\mathbf{q}$ is a momentum that is transferred to the scattering center (the scattering is assumed to be elastic). In the limiting case of a classical electromagnetic field, one has $N_{\mathbf{k}\lambda} >> 1$. Retaining in (5.48) the terms proportional to $N_{k\lambda}$, and averaging over the directions of $\mathbf{q}$, we find

$$Q(\varepsilon) = \frac{e^2 p_F}{mc^2} \int_{\Delta}^{\infty} \frac{d\varepsilon'}{2\pi} \int \frac{d\Omega_{\mathbf{p}'}}{4\pi} \int \frac{d\Omega_{\mathbf{q}}}{4\pi} \int \rho(\omega_k) N_{\mathbf{k}} d^3\mathbf{k} \{(u_\varepsilon u_{\varepsilon'} + v_\varepsilon v_{\varepsilon'})$$

$$\times [n_{\varepsilon'}(\mathbf{p}') - n_\varepsilon(\mathbf{p})] [\delta(\varepsilon' - \varepsilon - \omega_k) \delta(\mathbf{p}' - \mathbf{p} - \mathbf{q} - \mathbf{k})$$

$$+ \delta(\varepsilon - \varepsilon' - \omega_k) \delta(\mathbf{p} - \mathbf{p}' - \mathbf{q} - \mathbf{k})]$$

$$+ (u_\varepsilon u_{\varepsilon'} - v_\varepsilon v_{\varepsilon'}) [1 - n_\varepsilon(\mathbf{p}) - n_{\varepsilon'}(\mathbf{p}')] \delta(\varepsilon + \varepsilon' - \omega_k) \delta(\mathbf{p} + \mathbf{p}' - \mathbf{q} - \mathbf{k})\} \quad (5.54)$$

Because $|\mathbf{k}| << p_F$, we can write

$$\delta(\mathbf{p}' - \mathbf{p} - \mathbf{q} - \mathbf{k}) \approx \frac{1}{p_F^3} \delta(\mathbf{n}_{\mathbf{p}'} - \mathbf{n}_{\mathbf{p}} - \mathbf{q}/p_F)$$

$$= \frac{1}{p_F q^2} \delta(|\mathbf{n}_{\mathbf{p}'} - \mathbf{n}_{\mathbf{p}}| - q/p_F) \delta(\mathbf{n}_{\mathbf{p}-\mathbf{p}'} - \mathbf{n}_{\mathbf{q}}), \quad (5.55)$$

where $\mathbf{n}_{\mathbf{p}}$ is the unity vector in the direction p. Denoting the angle between $\mathbf{p}'$ and $\mathbf{p}$ as θ, we obtain

$$\delta(|\mathbf{n}_{\mathbf{p}'} - \mathbf{n}_{\mathbf{p}}| - q/p_F) = \delta\left(\sqrt{2(1 - \cos\theta)} - q/p_F\right) = \frac{q}{p_F} \delta(\cos\theta_0 - \cos\theta) \quad (5.56)$$

where $\cos\theta_0 = 1 - q^2/(2p_F^2)$. Dealing in the same manner with other δ-functions, we find

$$\delta(\mathbf{p} \mp \mathbf{p}' - \mathbf{q} - \mathbf{k}) \approx \frac{1}{p_F^2 q} \delta(\cos\theta \mp \cos\theta_0) \delta(\mathbf{n}_{\mathbf{p}\mp\mathbf{p}'} - \mathbf{n}_{\mathbf{q}}). \quad (5.57)$$

This form would be convenient for further angle averaging in the next section.

5.3.3. Classical Field Action in a "Dirty" Limit

Let the external electromagnetic field be a quasi-monochromatic wave having a spectral width $\Delta\omega$ around the "carrying" frequency ω and an angle distribution $\Delta\Omega_{\mathbf{k}}$ around the direction $\mathbf{k}$. Then

$$\int d^3\mathbf{k}' \rho(\omega_{k'}) N_{k'} \approx 64\pi^4 p_F^2 c\omega^2 |\mathbf{S}_{\mathbf{k},\mathbf{e}}| |\mathbf{n}_{\mathbf{p}} \cdot \mathbf{e}|^2, \quad (5.58)$$

where $\mathbf{S}_{\mathbf{k},\mathbf{e}}$ is the Poynting vector of the radiation with the frequency ω and the polarization $\mathbf{e}$. Introducing the free path l by the formula $q = 1/l$, we find

$$Q(\varepsilon) = \alpha \{U_{\varepsilon+\omega\varepsilon}[n_{\varepsilon+\omega}(\cos\theta_0) - n_\varepsilon(\mathbf{p})] + U_{\varepsilon\varepsilon-\omega}[n_{\varepsilon-\omega}(\cos\theta_0) - n_\varepsilon(\mathbf{p})] + V_{\varepsilon\omega-\varepsilon}[1 - n_\varepsilon(\mathbf{p}) - n_{\omega-\varepsilon}(-\cos\theta_0)]\}. \quad (5.59)$$

Here $U_{\varepsilon\varepsilon-\omega}$ and $V_{\varepsilon\omega-\varepsilon}$ are coefficients defined by formulas (5.22) and (5.23) and α is defined by the expression

$$\alpha = \frac{2\pi^2 e^2}{mc} p_F \frac{l}{\omega^2} |\mathbf{S}_{\mathbf{ke}}| |\mathbf{n}_\mathbf{p} \cdot \mathbf{e}|^2. \quad (5.60)$$

Putting $|\mathbf{S}_{\mathbf{ke}}| = (\omega^2/2\pi c)|\mathbf{A}|^2$ and averaging in (5.48) over the directions of an electron's momentum, we obtain (up to the multiplier $\pi/8$) the desired result (5.21).[7]

5.4. ENHANCEMENT IN PERFECT CRYSTALS

5.4.1. Quasi-particle Scattering and Kinematic Conservation Laws

In the case of a pure superconductor, the terms in Eq. (5.59) proportional to the U-factors vanish. To prove this we will carry out a kinematic analysis of the collision integral. Indeed, from (5.53) it follows that:

$$ck = \pm(\varepsilon' - \varepsilon),\ k = [p^2(\varepsilon') + p^2(\varepsilon) - 2p(\varepsilon)\, p(\varepsilon')\cos\theta\,]^{1/2}. \quad (5.61)$$

The second of the expressions in (5.61) shows that all the permitted values of $\mathbf{k}$ obeying the laws of energy-momentum conservation must lie between the lines $k_{\theta=0} \equiv |p(\varepsilon') - p(\varepsilon)|$ and $k_{\theta=\pi} \equiv |p(\varepsilon') + p(\varepsilon)|$. The straight lines $ck = \pm(\varepsilon' - \varepsilon)$ pass at the point $\varepsilon' = \varepsilon$, and in order for the system to possess the solution, they should intersect the region between the lines $k_{(\theta=0)}$, $k_{(\theta=\pi)}$, which is dashed in Fig. 5.1. Hence the following condition must be fulfilled:

$$1/c > \left|\frac{\partial k(\theta=0)}{\partial\varepsilon'}\right|_{\varepsilon'=\varepsilon}, \text{ while } \left|\frac{\partial k(\theta=0)}{\partial\varepsilon'}\right|_{\varepsilon'=\varepsilon} = \left|\frac{\partial p}{\partial\varepsilon'}\right|_{\varepsilon'=\varepsilon} = \frac{1}{|\mathbf{v}(\varepsilon)|}, \quad (5.62)$$

where $\mathbf{v}(\varepsilon)$ is the excitation's group velocity. However, the condition $1/c > 1/|\mathbf{v}(\varepsilon)|$ cannot ever be fulfilled because $c >> |\mathbf{v}(\varepsilon)|$. Analogous reasoning shows that the recombination channel [the terms proportional to $V_{\varepsilon\omega-\varepsilon}$ in Eq. (5.59)] is always open. Hence, if the electromagnetic field falls on a superconductor with a perfect crystalline structure, direct photon absorption is forbidden at photon frequencies $\omega < 2\Delta$.

5.4.2. "Switching on" of Eliashberg Mechanism

Real superconductors always contain a number of elastic scattering centers. It is instructive to estimate the concentration of such centers when the relaxation

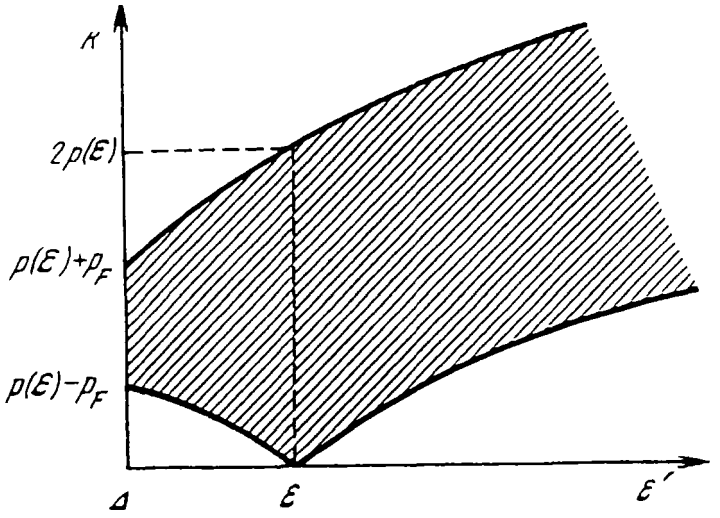

Figure 5.1. Explanation of the solution of kinematic conservation laws.

channel is "switched on." Using the relation (5.53), one can obtain the condition [τ is provided by (2.8), $\tau^{-1} \propto n = N_i/V_0$ is the impurity concentration]:

$$\tau < \frac{2\pi}{\sqrt{\omega\,(\omega + \Delta)}}, \tag{5.63}$$

as a criterion of the appearance of the Eliashberg enhancement effect.

The threshold value of a sample's "pollution" depends on experimental conditions (e.g., on the pumping frequency), but even at allowed minimal frequencies of an external field, the inequality $\tau^{-1} > \gamma$ must be fulfilled. In strong coupling superconductors, the damping of γ is large (e.g., $\gamma \sim 10^{11}$ sec^{-1}) and consequently the critical concentration of impurities n should be $\sim 10^{18}$ cm^{-3} at $\omega_{min} \sim \gamma$. Then the condition (5.63) appears to be sufficiently stringent. In those cases when this condition is not fulfilled, it is necessary to analyze other mechanisms that determine the formation of the nonequilibrium electron-hole excitation distribution function n_ε.

5.4.3. Multiparticle Channels of Photon Absorption

When condition (5.63) is not fulfilled, the photons may be absorbed in a single-electron system of excitations due to multiparticle processes, for example, via the assistance of additional electrons or phonons. We consider below the case of electron-assisted absorption. This process has an analogy with zero-sound absorption in ^{3}He, where a zero-sound quantum is absorbed with the participation of two Fermi particles.[28] The self-energy diagrams that generate the single-particle

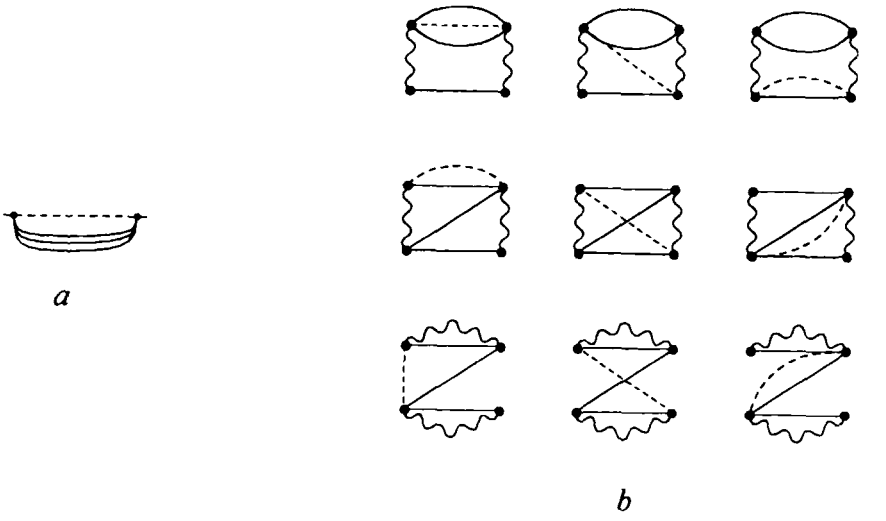

Figure 5.2. (a) Skeleton diagram and (b) specific contributions yielding enhancement in perfect crystals.

electron-hole excitation source (in analogy to the consideration in Sect. 5.3) are shown in Fig. 5.2.

Using the same approach as in the case of acoustic pumping in a superfluid ^{3}He (Ref. 29), one can write down the collision integrals of electrons with photons $J^{(e-e-pt)}$ and derive the source of excitations $Q(\varepsilon)$ for the action of a photon field with the occupation numbers $N_{\mathbf{k}} >> 1$ in the manner demonstrated in Sect. 5.3. In the case of a monochromatic field at frequencies $\omega << \Delta$, we have

$$Q(\varepsilon) \approx \frac{8\pi e^2}{\varepsilon_F} \frac{N_{\mathbf{k}}}{k^3} \frac{v_F^2}{c^3} \int_\Delta^\infty d\varepsilon_1 \int_\Delta^\infty d\varepsilon_2 \int_\Delta^\infty d\varepsilon_3 \mathcal{M}_k [\delta(\varepsilon + \varepsilon_1 - \varepsilon_2 - \varepsilon_3 + \omega)$$

$$+ \delta(\varepsilon + \varepsilon_1 - \varepsilon_2 - \varepsilon_3 - \hbar\omega)]\{(1 - n_\varepsilon)(1 - n_{\varepsilon_1}) n_{\varepsilon_2} n_{\varepsilon_3}$$

$$- n_\varepsilon n_{\varepsilon_1} (1 - n_{\varepsilon_2})(1 - n_{\varepsilon_3})\}, \tag{5.64}$$

where

$$\mathcal{M}_k = \mathcal{M}_k(\varepsilon, \varepsilon_1, \varepsilon_2, \varepsilon_3) = 3x_1 u_\varepsilon u_{\varepsilon_1} u_{\varepsilon_2} u_{\varepsilon_3} + 3x_2 v_\varepsilon v_{\varepsilon_1} v_{\varepsilon_2} v_{\varepsilon_3}$$

$$+ y_1(u_\varepsilon u_{\varepsilon_1} v_{\varepsilon_2} v_{\varepsilon_3} - 2u_\varepsilon v_{\varepsilon_1} u_{\varepsilon_2} v_{\varepsilon_3}) - y_2(v_\varepsilon v_{\varepsilon_1} u_{\varepsilon_2} u_{\varepsilon_3} - 2v_\varepsilon u_{\varepsilon_1} v_{\varepsilon_2} u_{\varepsilon_3}) \tag{5.65}$$

and the coefficients $x_i(y_i)$ are defined as (cf. Ref. 9):

$$x_i(y_i) = \left(\frac{mp_F}{2\pi^2}\right)^2 \int \frac{d\Omega_{\mathbf{p}_1}}{4\pi} \int \frac{d\Omega_{\mathbf{p}_2}}{4\pi} \int \frac{d\Omega_{\mathbf{p}_3}}{4\pi} X_i(Y_i)\, \delta\left[1 - \frac{\mathbf{p}\cdot(\mathbf{p}_1+\mathbf{p}_2+\mathbf{p}_3+\mathbf{k})}{p\,|\,\mathbf{p}_1+\mathbf{p}_2+\mathbf{p}_3+\mathbf{k}\,|}\right] \quad (5.66)$$

Here $X_i(Y_i)$ $(i = 1,2)$ are quadratic forms of the electron–electron interaction potential that are analogous to the coefficients $A(B)$ of Sect. 4.2. The factor $e^2v_F^2/c^3k^3$ in (5.64) is the vertex of electron–photon interaction renormalized by the electron–electron interaction.

It is important to note that in expression (5.64) at the $\varepsilon \sim \Delta$, the function $\mathcal{M}_k$ is negative. One can prove this by considering the collision integral $J^{(e-e-pt)}$. Substituting the photon occupation numbers $N_{\mathbf{k}}$ in this integral as an equilibrium (Bose) distribution, one can ensure that the integral will yield the relaxation of disturbed values of n_ε only at negative values of $\mathcal{M}_k$

Let us consider the properties of (5.64), assuming the parameters Δ/T and ω/T are small, and the distribution function is $n_\varepsilon = n_\varepsilon^0$. In this case $Q(\varepsilon)$ can be represented in the form:

$$Q(\varepsilon) = -\frac{8\pi e^2 v_F^2 N_{\mathbf{k}}(1-n_\varepsilon^0)}{\varepsilon_F \omega^3} \int_\Lambda^\infty d\varepsilon_1 (1-n_\varepsilon^0)\left[2\frac{\omega}{T}(U_- - U_+) - \frac{\omega^2}{T^2}(Z_- - Z_+)\right] \quad (5.67)$$

where the definitions were:

$$U_\mp = \theta(\varepsilon+\varepsilon_1 \mp \omega - 2\Delta) \int_\Delta^{\varepsilon+\varepsilon_1\mp\omega-\Delta} d\varepsilon_2 n_{\varepsilon_2}^0 n_{\varepsilon+\varepsilon_1-\varepsilon_2}^0 \mathcal{M}_k(\varepsilon, \varepsilon_1, \varepsilon_2, \varepsilon \mp \omega + \varepsilon_1 - \varepsilon_2) \quad (5.68)$$

and

$$Z_\mp = \theta(\varepsilon+\varepsilon_1 \mp \omega - 2\Delta) \int_\Delta^{\varepsilon+\varepsilon_1\mp\omega-\Delta} d\varepsilon_2 n_{\varepsilon_2}^0 n_{\varepsilon+\varepsilon_1-\varepsilon_2}^0 \times (1 - 2n_{\varepsilon+\varepsilon_1-\varepsilon_2}^0)\, \mathcal{M}_k(\varepsilon, \varepsilon_1, \varepsilon_2, \varepsilon \mp \omega + \varepsilon_1 - \varepsilon_2). \quad (5.69)$$

The term in (5.67) proportional to $(U_- - U_+)$ is nonzero at $\varepsilon \sim \Delta$; at the same time, the term proportional to $(Z_- - Z_+)$ is defined at a much larger region of $\varepsilon \sim T$. In addition, this second term is small relative to the parameter Δ/T. Taking into account the negativeness of $\mathcal{M}_k(\varepsilon, \varepsilon_1, \varepsilon_2, \varepsilon_3)$ at $\varepsilon_i \sim \Delta$ values of the arguments, one can confirm that $Q(\varepsilon)$ is negative in the immediate vicinity of the overgap region: $\Delta < \varepsilon < \Delta + \omega$.

One can consider now the solution of the kinetic equation

$$0 = O(\varepsilon) + J^{(e-ph)} + J^{(e-e)} \quad (5.70)$$

for the distribution function n_ε of single-particle excitations in a spatially homogeneous and steady state. Since in the problem of stimulation the main role is played by the part of the distribution function that is located in the region of energies

$\varepsilon \sim \Delta$, we will introduce a notation δn_ε, for its localized nonequilibrium addition. To calculate δn_ε, it is enough to use in (5.70) a relaxation time approximation like (5.27). Determining thus the solution δn_ε and substituting it into (5.29), we arrive at

$$\delta\Delta^{(\text{clean})} = \frac{8\pi^5 \mid 3x_1 + 3x_2 - y_1 - y_2 \mid}{7\zeta(3)} \frac{Te^2 v_F^2 W_{\mathbf{k}}}{\gamma\varepsilon_F\omega^2}, \tag{5.71}$$

where $W_{\mathbf{k}} = \omega N_{\mathbf{k}}$ is the energy density of the electromagnetic field. Since $\delta\Delta^{(\text{clean})} > 0$, one can deduce the nonequilibrium gap enhancement in this particular condition. The essence of the enhancement mechanism remains unchanged: the high-frequency field removes the electrons from the gap edge, keeping the total number of excitations constant, and the gap increases owing to the self-consistency condition. It should be noted that in this case the magnitude of the enhancement effect would be smaller compared with the traditional case. Indeed, one can rewrite Eqs. (5.31) and (5.32) in the form

$$\delta\Delta^{(\text{dirty})} \simeq \frac{Te^2 l v_F}{\Delta\gamma\omega} W_{\mathbf{k}}, \tag{5.72}$$

where $l = v_F\tau$ is the electron's mean-free-path ($D = lv_F/3$). Then by an order of magnitude the ratio is:

$$\frac{\delta\Delta^{(\text{clean})}}{\delta\Delta^{(\text{dirty})}} \sim \frac{\Delta}{\varepsilon_F} \frac{1}{\omega\tau}, \tag{5.73}$$

which is small because of the smallness of Δ/ε_F; the second factor in (5.73) could be $\gtrsim 1$, but cannot compensate for the overall smallness in view of (5.63). At the same time, $\delta\Delta^{(\text{dirty})}$ disappears when condition (5.63) is not fulfilled, while $\delta\Delta^{(\text{clean})}$ survives.

References

1. A. F. G. Wyatt, V. M. Dmitriev, W. S. Moore, and F. W. Sheard, Microwave-enhanced critical supercurrents in constricted tin films, *Phys. Rev. Lett.* **16**(25), 1166–1169 (1966).
2. A. H. Dayem and J. J. Wiegand, Behavior of thin-film superconducting bridges in a microwave field, *Phys. Rev.* **155**(2), 419–428 (1967).
3. G. M. Eliashherg, Film superconductivity stimulated by a high-frequency field, *JETP Lett.* **11**(3), 114–117 (1970) *[Pis 'ma v Zh. Eksp. i Teor. Fiz.* **11**(3), 186–188 (1970)].
4. B. I. Ivlev, and G. M. Eliashberg, Influence of nonequilibrium excitations on the properties of superconducting films in a high-frequency field, *JETP Lett.* **13**(8), 333–336 (1971) *[Pis 'ma v Zh. Eksp. i Teor. Fiz.* **13**(8), 464–468 (1971)].
5. B. I. Ivlev, S. G. Lisitsyn, and G. M. Eliashberg, Nonequilibrium excitations in superconductors in high-frequency fields, *J. Low Temp. Phys.* **10**(3/4), 449–468 (1973).
6. J. J. Chang and D. J. Scalapino, Gap enhancement in superconducting thin films due to microwave irradiation, *J. Low Temp. Phys.* **29**(5/6), 447–485 (1977).
7. L. G. Aslamazov, V. I. Gavrilov, On the micropower-induced enhancement of the critical temperature of a superconductor, *Sov. J. Low Temp. Phys.* **6**(7), 877–881 (1980) [*Fiz. Nizk. Temp.* **6**(7), 877–881 (1980)].

8. A.M. Gulian and O. F. Zharkov, Dependence of a superconducting gap on temperature in an UHF field, *JETP Lett.* **33**(9), 454–458 (1981) *(Pis 'ma Zh. Eksp. Teor. Fiz.* **33**(9), 471–474 (1981)].
9. A. M. Gulyan and V. E. Mkrtchyan, Stimulation of superconductivity by electromagnetic radiation, *Sov. Phys. Lebedev Inst. Reports* **2**,40–44 (1989) *[Kratk. Soobsch. po Fiz. FIAN* **2** 31–34 (1989)].
10. T. J. Tredwell and E. H. Jacobsen, Phonon-induced enhancement of the superconducting energy gap, *Phys. Rev. Lett.* **35**(4), 244–247 (1975).
11. A. G. Aronov and V. L. Gurevich, The tunneling of excitations from a superconductor and the increase of T_c, *Sov. Phys. JETP* **36**(5), 957–963 (1972) [*Zh. Eksp. i Teor. Fiz.* **63**(5), 1809–1821 (1972)].
12. S. A. Peskovatskii and V. P. Seminozhenko, Stimulation of superconductivity by constant tunnel currents, *Sov. J. Low Temp. Phys.* **2**(7), 464–465 (1976) [Fiz. *Niz. Temp.* **2**(7), 943–945 (1976)].
13. J. J. Chang, Gap enhancement in superconducting thin films due to quasiparticle tunnel injection, *Phys. Rev. B* **17**(5), 2137–2140 (1978).
14. C. C. Chi and J. Clarke, Enhancement of the energy gap in superconducting aluminum by tunneling extraction of quasiparticles, *Phys. Rev. B* **20**(11), 4465–4473 (1979).
15. Yu. I. Latyshev and F. Ya. Nad', Mechanism of superconductivity stimulated by microwave radiation, *Sov. Phys. JETP* **44**(6), 1136–1141 (1976) [*Zh. Eksp. i Teor. Fiz.* **71**(6) 2158–2167 (1976)].
16. T. M. Klapwijk and J. E. Mooij, Microwave-enhanced superconductivity in aluminum films, *Physica B* + C **81**, 132–136(1976).
17. K. E. Gray, Enhancement of superconductivity by quasiparticle tunneling. *Solid State Comm.* **26**, 633–635(1978).
18. J. A. Pals, Microwave-enhanced critical currents in superconducting *Al* strips with local injection of electrons, *Phys. Let. A,* **61**(4), 275–277 (1977).
19. J. A. Pals and J. Dobben, Observation of order-parameter enhancement by microwave irradiation in a superconducting aluminum cylinder, *Phys. Rev. Lett.* **44**(7), 1143–1146 (1980).
20. Yu. I. Latyshev and F. Ya. Nad', Frequency dependence of superconductivity stimulated by a high-frequency field, *JETP Lett.* **19**(12), 380–382 (1974) *[Pis 'ma v Zh. Eksp. i Teor. Fiz.* **19**(12), 737–741 (1974)].
21. T. M. Kommers and J. Clarke, Measurement of microwave-enhanced energy gap in superconducting aluminum by tunneling, *Phys. Rev. Lett.* **38**(19), 1091–1094 (1977).
22. J. E. Mooij, in: Nonequilibrium Superconductivity, Phonons and Kapitza Boundaries, edited by K. E. Gray (Plenum Press, New York, 1981) pp. 191–229.
23. G. M. Eliashberg, Inelastic electron collisions and nonequilibrium stationary states in superconductors, *Sov. Phys. JETP* **34**(3), 668–676 (1972) [*Zh. Eksp. i Teor. Fiz.* 61[3(9)], 1254–1272 (1971)].
24. V. M. Dmitriev and E. V. Khristenko, Stimulation and enhancement of superconductivity by external electromagnetic radiation, *Sov. J. Low Temp. Phys.* **4**(7), 387–411 [*Fiz. Nizk. Temp.* **4**(7), 821–856(1978)].
25. V. M. Dmitriev, V. N. Gubankov, and F. Ya. Nad', in: *Nonequilibrium superconductivity,* edited by D. N. Langenberg and A. I. Larkin (North-Holland, Amsterdam, 1986), pp. 163–210.
26. A. M. Gulyan and G. F. Zharkov, in: *Thermodynamics and electrodynamics of superconductors,* edited by V. L. Ginzburg (Nova Science, New York, 1988), pp. 111–182.
27. L. V. Keldysh, Diagram technique for nonequilibrium processes, *Sov. Phys. JETP* **20**(4), 1018–1026 (1965) *[Zh. Eksp. i Teor. Phys.* **47** [4(10)], 1515–1527 (1964)].
28. E. M. Lifshitz and L. P. Pitaevskii, *Physical kinetics* (Pergamon Press, Oxford, 1981), pp. 320–324.
29. A. M. Gulyan and O. N. Nersesyan, Phonon-pumped nonequilibrium states in superfluid ^{3} *He, Sov. Phys. JETP* **68**(4), 756–762 (1989) [*Zh. Eksp. i Teor. Fiz.* **95**(4), 1311–1323 (1989)].

6

Phonon-Deficit Effect

We started the discussion of the physics of a phonon heat bath in Sect. 3.2. When applicable, the phonon heat-bath model decouples the kinetics of electron and phonon subsystems. This decoupling is valid if the influence of the nonequilibrium phonons on the nonequilibrium electrons is negligible. In such cases, the phonons play the role of a "heat-bath" only for relaxation processes in the electron system. At the same time, the influence of electrons on phonons cannot be simply regarded as heating. As we will now see, the situation is much more interesting.

6.1. COLLISION INTEGRAL AS A PHONON SOURCE

The principle of a phonon heat-bath is closely tied to the phonon kinetic equation derived in Sect. 4.5. It permits us to find the phonon fluxes from nonequilibrium superconductors using the solutions of Eliashberg kinetic equations (which were considered in Chap. 5 on the basis of the phonon heat-bath model).

6.1.1. Polarization Operators

In applying the analytic continuation method to derive the kinetic equation for the nonequilibrium electrons in the phonon heat-bath model, Green's electron temperature functions were represented by the series expansions in the external field amplitude (Sect. 3.2), and the diagrams of the type shown in Fig. 3.1 were obtained. The physical quantities were defined by corresponding analytic continuation to the upper half-plane with respect to each of the discrete imaginary field frequencies. It is important here that the phonons be in equilibrium. From a formal point of view, this means that in the exact phonon Green's function

$$\mathcal{D}(P - P') = g^2 \frac{2\omega^2(\mathbf{p}' - \mathbf{p})}{\omega^2(\mathbf{p}' - \mathbf{p}) - (\varepsilon' - \varepsilon)^2} \tag{6.1}$$

the initial distribution of the discrete imaginary Bose frequencies is fixed: $(\varepsilon' - \varepsilon) = 2n\pi Ti$, where n is an integer*. Consequently, the cuts in an arbitrary diagram (such as that shown in Fig. 3.1b) coincide with the cuts in a diagram that does not contain the self-energy insertions (although it has the same order in the field's amplitude; see Fig 3.1a). This determines the identical analytic structure for the diagrams of the corresponding order in an external field. Generally when the phonons are not in equilibrium, the phonon Green's function may be presented in the form

$$\mathcal{D}_\omega(\mathbf{q}) = \{[\mathcal{D}_{0\omega}(\mathbf{q})]^{-1} - \Pi_\omega(\mathbf{q})\}^{-1}. \tag{6.2}$$

The real part $\mathrm{Re}\,\Pi_\omega(\mathbf{q})$, which is responsible for the renormalization of the sound velocity, is determined by the total number of electrons, while the temperature blurring region near the Fermi surface produces a correction of the order T/ε_F.[1] As mentioned earlier, the renormalization of the sound velocity due to the superconducting transition has the analogous smallness Δ/ε_F. The influence of the electromagnetic field is small also: it affects primarily the blurring region. Hence we may drop the small corrections and assume that the renormalization has already been carried out in Eq. (6.1). On the contrary, the imaginary part $\mathrm{Im}\,\Pi_\omega(\mathbf{q})$ is determined wholly by the immediate vicinity of the Fermi surface and hence is sensitive to details in the excitation's distribution.

6.1.2. Consequences of Equilibrium Phonon Distribution

The neglect of $\mathrm{Im}\,\Pi_\omega(\mathbf{q})$ in Eq. (6.2) and moving to the initial representation in (6.1) corresponds to the physical assumption that a stronger relaxation source exists in the phonon system than one caused by an electron–phonon interaction. Such a source of phonon absorption (i.e., a sink) may appear if the phonon system is tied to an external medium (the heat bath), causing the phonons themselves to play the role of a thermostat for the electron system. If this coupling were explicitly considered, then the kinetic equations obtained above the right-hand sides would vanish in the limiting case of equilibrium in the phonon system. A different and adequate technique has been used in deriving the kinetic equations in the nonlinear electrodynamics of superconductors (Sects. 3.4, 3.5, 5.1, and 5.2); in the latter case, the coupling of the phonon system to the heat bath would be implemented simply by equating the polarization operator to zero. In both cases an equilibrium phonon system is implied.

*Indeed, making the transformation from the expression for Green's function (6.1) to the phonon distribution function, one may find by direct frequency summation that the resulting distribution function in the case of integer n coincides with the equilibrium Bose distribution.

This discussion helps to clarify the physical meaning of the kinetic equation (4.75). If we assume that the phonon functions (on the right-hand side, as well as in the complete Green's electron functions) are equilibrium ones, then the left-hand side of this equation would correspond to the phonon drift toward the external medium, i.e., it would represent the phonon's emission flux. In situations where this assumption is valid, the Eliashberg kinetic equations obtained for the electron system in the phonon heat-bath model would also be valid.

6.2. NEGATIVE PHONON FLUXES

We discuss here the theory of a phenomenon called the *phonon deficit* effect.[2] The essence of the effect may be summarized as follows. If a thin superconducting film is immersed in a heat-bath and is irradiated by an electromagnetic field of a frequency $\omega_0 < 2\Delta$, then in some spectral interval the film absorbs phonons from the heat-bath, rather than emitting them to it.

In this section we consider only the formal aspects of this effect. We will analyze the solution of the Eliashberg kinetic equations and then classify the phonon sources and study them in detail. The physical aspects of the problem will be discussed in the next section.

The solution describing the steady-state behavior of the nonequilibrium electrons, which is used later, was obtained by Eliashberg[3] in 1970 in connection with the theoretical analysis of the superconductivity enhancement effect in a high-frequency electromagnetic field. In Chap. 5 we reproduced certain important aspects of this solution (Sect. 5.1). We assume that an external electromagnetic wave of frequency ω_0 is incident perpendicular to the film and is described by the vector potential $\mathbf{A}$ lying in the film's plane. For simplicity we assume that the vector potential is constant over the film cross section. This means that the film is thinner than the field's penetration depth. Note, however, that the condition $\mathbf{A}$ = const is not a critical one (from the viewpoint of the resulting homogeneous picture inside the film) due to the typically large diffusion length of the nonequilibrium electron excitations. We assume also a high concentration of nonmagnetic impurities, so that parameter $\tau\Delta$ is small.

6.2.1. Electron Distribution Function

Thus the dynamics of the electron system become simplified (localized in the momentum space); in particular, it is now possible to ignore the electron's reflections off the walls (owing to their short mean-free-path $l = v_F\tau << d$) What is more important is that the relaxation channel of photon absorption is now opened (owing to the condition $\omega_0\tau_\varepsilon >> 1$, where τ_ε is the effective energy relaxation time of excitations), yielding the Eliashberg mechanism. Another source of simplification is the smallness of the imbalance in the electron-hole population (by the parameter

ω_0/ε_F; see below Sect. 8.1). Thus one can put $n_\varepsilon = n_{-\varepsilon}$ in the collision integrals. Recall that in Sect. 5.2 we were interested in the linearized solution of the kinetic equation (5.21), according to which the deviation of the distribution function $n_\varepsilon^{(1)} = n_\varepsilon - n_\varepsilon^{(0)}$ is divided into two parts: the main part, localized at above-the-gap values of ε, and the small "tail," which diminishes with T.

Ignoring this "tail," which contributes insignificantly, we can write the deviation of the distribution function $n_\varepsilon^{(1)} \approx n_{1\varepsilon}^{(1)}$ in the form (see 5.28):

$$n_\varepsilon^{(1)} = \alpha\tau_\varepsilon \left[\frac{\omega_0}{2T}\cosh^{-2}\frac{\varepsilon}{2T}\left(U_{\varepsilon\varepsilon-\omega_0} - U_{\varepsilon+\omega_0\varepsilon}\right)\right]\frac{\sqrt{\varepsilon^2-\Delta^2}}{\varepsilon}, \quad \varepsilon \geq \Delta. \tag{6.3}$$

6.2.2. Phonon Source in Linear Approximation

Let us now consider the phonon sources arising in this way. The emerging features would be of general importance and useful in further analysis. Within the approximations made for the electron system (and in the linear approximation in the amplitude of the external field), the expression (4.75) subject to (4.128) and (6.3) may be written as

$$\frac{dN_{\omega_q}}{dt} = 2\int_\Delta^\infty\int_\Delta^\infty d\varepsilon_1 d\varepsilon_2 L_{\omega_q}(\varepsilon_1,\varepsilon_2)\left[(n_{\varepsilon_1}^{(1)} - n_{\varepsilon_2}^{(1)})N_{\omega_q}^{(0)} - n_{\varepsilon_1}^{(0)}n_{\varepsilon_2}^{(1)} - n_{\varepsilon_2}^{(0)}n_{\varepsilon_1}^{(1)}\right.$$

$$\left. + n_{\varepsilon_1}^{(1)}\right]\left(1 - \frac{\Delta^2}{\varepsilon_1\varepsilon^2}\right)\delta(\varepsilon_1 - \varepsilon_2 - \omega_q) + \int_\Delta^\infty\int_\Delta^\infty d\varepsilon_1 d\varepsilon_2 L_{\omega_q}(\varepsilon_1,\varepsilon_2)$$

$$\times\left[(n_{\varepsilon_1}^{(1)} + n_{\varepsilon_2}^{(1)})N_{\omega_q}^0 + n_{\varepsilon_1}^{(0)}n_{\varepsilon_2}^{(1)} + n_{\varepsilon_2}^{(0)}n_{\varepsilon_1}^{(1)}\right]\left(1 + \frac{\Delta^2}{\varepsilon_1\varepsilon_2}\right)\delta(\varepsilon_1 + \varepsilon_2 - \omega_q), \tag{6.4}$$

where the factor L_{ω_q} is a multiple of the densities of states and the interaction constant:

$$L_{\omega_q}(\varepsilon_1,\varepsilon_2) = \frac{\pi\lambda}{2}\frac{\omega_D}{\varepsilon_F}\frac{\varepsilon_1\theta(\varepsilon_1^2-\Delta^2)}{\sqrt{\varepsilon_1^2-\Delta^2}}\frac{\varepsilon_2\theta(\varepsilon_2^2-\Delta^2)}{\sqrt{\varepsilon_2^2-\Delta^2}}, \tag{6.5}$$

$\omega_q = u|\mathbf{q}|$, $N_\omega^0 = [\exp(\omega_q/T) - 1]^{-1}$ and u is the sound velocity. The expression (6.4), as explained in the preceding section, determines the phonon flux from the superconductor into the external medium.

6.2.3. Phonon Heat-Bath Realization

The reflection of phonons from the superconductor–heat-bath interface plays a significant role here. We assume that the interface is "sufficiently" smooth. Then

the "geometric-acoustical" approximation* can be used to study the phonon's propagation, whose frequency significantly exceeds the quantity u/d (where d is the film's thickness). In this approximation the phonon's behavior at the boundary is determined by the ratio of the "acoustic" densities $\rho_1 u_1/\rho_2 u_2$ of the media ($\rho_{1,2}$ are the densities of the two media). Such phonons will lose all their energy upon each collision with the wall (i.e., they will be freely emitting to the outside) if the phonon "acoustic density" ρu of the external medium coincides with the acoustical density of the film (ρ is the mechanical density). After thus determining the lower limit of the frequencies of the phonons of interest, we select a superconducting film thickness so that the phonon escape time is less than its transit time, which is related to the interaction with the electrons (in a bulk sample it is on the order of $\nu_F/u\omega_q$**). Under such conditions, the feedback of the phonons on the electrons may be ignored and the phonon heat-bath model becomes applicable for the electron system. For example, let the film have a thickness d comparable to the coherence length $\xi_0 \sim \nu_F/T_c$. For such films it would mean that in the frequency range

$$T_c u/\nu_F \leq \omega_q \leq T_c \tag{6.6}$$

the current scheme developed for phonons may be directly employed.

Note that in the preceding discussions phonon damping was ignored, i.e., the phonon lifetime was assumed to be sufficiently long. Assuming that the phonons are being absorbed in each collision with the wall, this time may be estimated as $\tau_{ph} \sim d/u$ and should satisfy the condition $\tau_{ph} >> 1/\omega_q$ for our scheme to be applicable. If we set $d \sim \xi_0$, then this condition takes the form $\xi_0/u \sim \nu_F/uT_c >> \omega_q^{-1}$, which virtually coincides with the applicability condition of the "geometric-acoustical" approximation [see the left inequality in (6.6)]. Thus we may indeed ignore the damping of the phonons with frequencies that lie in the interval (6.6). In general, the problem of boundary conditions is not so simple (see, e.g., the references mentioned in Chang and Scalapino[4]). When the reflection processes are to be taken into account, one can envisage (6.4) as an intrinsic source of phonons.

6.2.4. Induced and Spontaneous Processes

The source [the right-hand side in expression (6.4)] determining phonon kinetics may be classified in the following manner. We will call the first integral in (6.4), which is related to the relaxation processes in the electron system, the

*It implies that the wavelength of the propagating phonon is much less than the characteristic dimensions of the inhomogeneity of the system and consequently one can ignore the diffraction effects (in analogy with the "geometric-optics" approximation for photons).

**Such an estimate is appropriate in the vicinity of critical temperature when $(\Delta/T) << 1$.

relaxation source I^{rel}. The second integral is related to excitation recombination and pair breaking. It may be called the *recombination source* I^{rec}.Each of these sources consists of a set of terms that are proportional to the occupation numbers of the phonons, and of other terms that do not explicitly contain such proportionality. The first set may be called the *induced phonon source* I_{ind}, while the second one may be called the *spontaneous phonon source* I_{sp}. Thus the entire source may be represented in the form

$$I = I^{rel}_{ind} + I^{rel}_{sp} + I^{rec}_{ind} + I^{rec}_{sp}, \tag{6.7}$$

which is convenient for examination.

We emphasize that for frequencies $\omega_q \leq \Delta$ near the transition temperature, the following relation holds

$$N^0_{\omega_q} / n_\varepsilon >> 1. \tag{6.8}$$

Consequently, in this frequency range the spontaneous sources in (6.7) are small and may be neglected. Of interest is the spectral dependence $I = I(\omega_q)$ for various frequencies ω_0 of the external electromagnetic field. It turns out that in the spectral range of primary interest, ω_q, which is comparable to Δ, if $\omega_0 << \Delta$, this dependence can be found analytically. It is expedient to carry out further investigation of the behavior of the relaxation and recombination sources separately.

6.2.5. Properties of the Recombination Channel

We consider first the recombination term I^{rec}_{ind}. It may be represented as

$$I^{rec}_{ind} = 2N^0_{\omega_q} \int_\Delta^\infty \int d\varepsilon_1 d\varepsilon_2 L_{\omega_q}(\varepsilon_1, \varepsilon_2)\, n^{(1)}_{\varepsilon_1} \left(1 + \frac{\Delta^2}{\varepsilon_1 \varepsilon_2}\right) \delta(\varepsilon_1 + \varepsilon_2 - \omega_q). \tag{6.9}$$

Using (6.3) we may write

$$I^{rec}_{ind} = \frac{\alpha \tau_\varepsilon \omega_0}{T} N^0_{\omega_q} \int_\Delta^\infty d\varepsilon_1 L_{\omega_q}(\varepsilon_1, \omega_q - \varepsilon_1) \cosh^{-2}\left(\frac{\varepsilon_1}{2T}\right)$$

$$\times (U_{\varepsilon_1 \varepsilon_1 - \omega_0} - U_{\varepsilon_1 + \omega_0 \varepsilon_1}) \left(1 + \frac{\Delta^2}{\varepsilon_1 \varepsilon_2}\right) \frac{\sqrt{\varepsilon_1^2 - \Delta^2}}{\varepsilon_1}, \tag{6.10}$$

which, after some simple transformations subject to (6.5), reduces to the form

$$I^{rec}_{ind} = \frac{\pi \lambda \tau_\varepsilon \omega_D \alpha \omega_0}{2\varepsilon_F \omega_q} [B_1(\omega_q) - B_2(\omega_q)], \tag{6.11}$$

where

$$B_1(\omega_q) = \int_{\Delta+\omega_0}^{\omega_q-\Delta} d\varepsilon \frac{A(\varepsilon, \omega_0)\,\theta(\omega_q - 2\Delta - \omega_0)}{\sqrt{\omega_q - \varepsilon - \Delta}\sqrt{\varepsilon - \omega_0 - \Delta}\sqrt{\varepsilon - \Delta}}, \tag{6.12}$$

$$B_2(\omega_q) = \int_{\Delta}^{\omega_q-\Delta} d\varepsilon \frac{A(\varepsilon, -\omega_0)\,\theta(\omega_q - 2\Delta)}{\sqrt{\omega_q - \varepsilon - \Delta}\sqrt{\varepsilon + \omega_0 - \Delta}\sqrt{\varepsilon - \Delta}}, \tag{6.13}$$

while the function $A(\varepsilon, \omega_0)$ is determined by the relation

$$A(\varepsilon, \omega_0) = \frac{[\varepsilon(\omega_q - \varepsilon) + \Delta^2][\varepsilon(\varepsilon - \omega_0) + \Delta^2]}{\varepsilon\sqrt{\omega_q - \varepsilon + \Delta}\sqrt{\varepsilon - \omega_0 + \Delta}\sqrt{\varepsilon + \Delta}}. \tag{6.14}$$

Such notations are convenient for revealing the two most important spectral features of the source $I_{\text{ind}}^{\text{rec}}$. First there is the minimum threshold frequency of the nonequilibrium phonons (equal to twice the gap value), above which the source (6.11) becomes nonzero. Second, since the quantity $B_2(\omega_q)$ [which is a positive quantity, as is clear from (6.12) and (6.13)] enters the source (6.11) with a minus sign and is nonzero in a certain frequency range where thequantity $B_1(\omega_q)$ is zero, we may conclude that there exists a frequency range of ω_q where the value of $I_{\text{ind}}^{\text{rec}}$ is negative.

At first glance this is an unexpected result. Hence it would be reasonable to investigate in greater detail the cause of such an anomalous behavior of the recombination source. To do this, we calculate first the integrals (6.12) and (6.13), which may be done by approximately taking into account the smoothness of the function $A(\varepsilon, \pm\omega_0)$ in the integration ranges. This enables one to use the mean-value law and represent (6.12) and (6.13) as

$$B_1(\omega_q) = A(\bar{\varepsilon}, \omega_0)\frac{\theta(\omega_q - 2\Delta - \omega_0)}{\sqrt{\omega_q - 2\Delta}} K\left[\left(\frac{\omega_q - 2\Delta - \omega_0}{\omega_q - 2\Delta}\right)^{1/2}\right], \tag{6.15}$$

$$B_2(\omega_q) = A(\tilde{\varepsilon}, -\omega_0)\frac{\theta(\omega_q - 2\Delta - \omega_0)}{\sqrt{\omega_q - 2\Delta + \omega_0}} K\left[\left(\frac{\omega_q - 2\Delta}{\omega_q - 2\Delta + \omega_0}\right)^{1/2}\right], \tag{6.16}$$

where $\bar{\varepsilon}$ and $\tilde{\varepsilon}$ lie in the regions $(\Delta + \omega_0, \omega_q - \Delta)$ and $(\Delta, \omega_q - \Delta)$, while $K(x)$ is the first-order complete elliptical integral in a normal form, which appears during the transition from (6.12) and (6.13) to (6.15) and (6.16). For this function we have

$$K(x) \approx \frac{\pi}{2}\left(1 - \frac{x^2}{4}\right), x^2 << 1; K(x) \approx \ln \frac{4}{\sqrt{1-x^2}}, x^2 >> 1. \quad (6.17)$$

Of primary interest to us are the frequencies $\omega_q - 2\Delta$ of the scale ω_0. Note that for such frequencies the calculations displayed below, which utilize the mean-value law, are exact in the asymptotic case $\omega_0 << \Delta$. This is precisely the case we have in mind. We set $\bar{\varepsilon} \approx \tilde{\varepsilon} \approx \Delta$ [here $A(\bar{\varepsilon}, \omega_0) \approx A(\tilde{\varepsilon}, -\omega_0) \approx \sqrt{2}\,\Delta^{3/2}$] and find from (6.15) and (6.16) the threshold value of the function $B_2(\omega_q)$ at $\omega_q = 2\Delta$. As a result we obtain

$$B_2(\omega_q = 2\Delta) \approx \sqrt{2}\,\Delta\left(\frac{\Delta}{\omega_0}\right)^{1/2}. \quad (6.18)$$

From this expression, which determines [in combination with (6.11)] the depth of the dip in the spectral curve of the recombination source (Fig. 6. 1a), it follows that the dip will become deeper as the external field frequency ω_0 is increased. The examination of expressions (6.15) and (6.16) shows that $B_2(\omega_q)$ diminishes when the frequency ω_q grows and at $\omega_q - 2\Delta = \omega_0$ takes the value (to an accuracy of ω_0/Δ)

$$B_2(\omega_q = 2\Delta + \omega_0) \approx 0.8\, B_2(\omega_q = 2\Delta) \quad (6.19)$$

(here we use the numerical values of the coefficients).

If ω_q grows further, the contribution from the term $B_1(\omega_q)$ appears, its threshold value coinciding (with accuracy up to ω_0/Δ) with the corresponding value of $B_2(\omega_q)$, i.e.,

$$B_1(\omega_q = 2\Delta + \omega_0) \approx B_2(\omega_q = 2\Delta). \quad (6.20)$$

It follows from this, subject to (6.19), that the difference $B_1(\omega_q) - B_2(\omega_q)$ at $\omega_q = 2\Delta + \omega_0$ is positive and is equal to approximately one-fifth of the value of $B_2(\omega_q)$ at $\omega_q = 2\Delta$. Since a further increase in ω_q causes each of the quantities $B_i(\omega_q)$ and consequently their difference to vanish, we conclude that the function $I_{\text{ind}}^{\text{rec}}$ possesses a "peak" (maximum). A study of the expression

$$B(\omega_q) = B_1(\omega_q) - B_2(\omega_q) = 2\sqrt{2}\,\Delta^{3/2}\left\{\frac{\theta(\omega_q - 2\Delta)}{\sqrt{\omega_q - 2\Delta}} K\left[\left(\frac{\omega_q - 2\Delta - \omega_0}{\omega_q - 2\Delta}\right)\right]^{1/2}\right.$$

$$\left. - \frac{\theta(\omega_q - 2\Delta + \omega_0)}{\sqrt{\omega_q - 2\Delta + \omega_0}} K\left[\left(\frac{\omega_q - 2\Delta}{\omega_q - 2\Delta + \omega_0}\right)^{1/2}\right]\right\}. \quad (6.21)$$

shows that the half-width of the peak is of the order ω_0. The results of the calculations of the source $I_{\text{ind}}^{\text{rec}}$ are illustrated in Fig. 6. 1a.

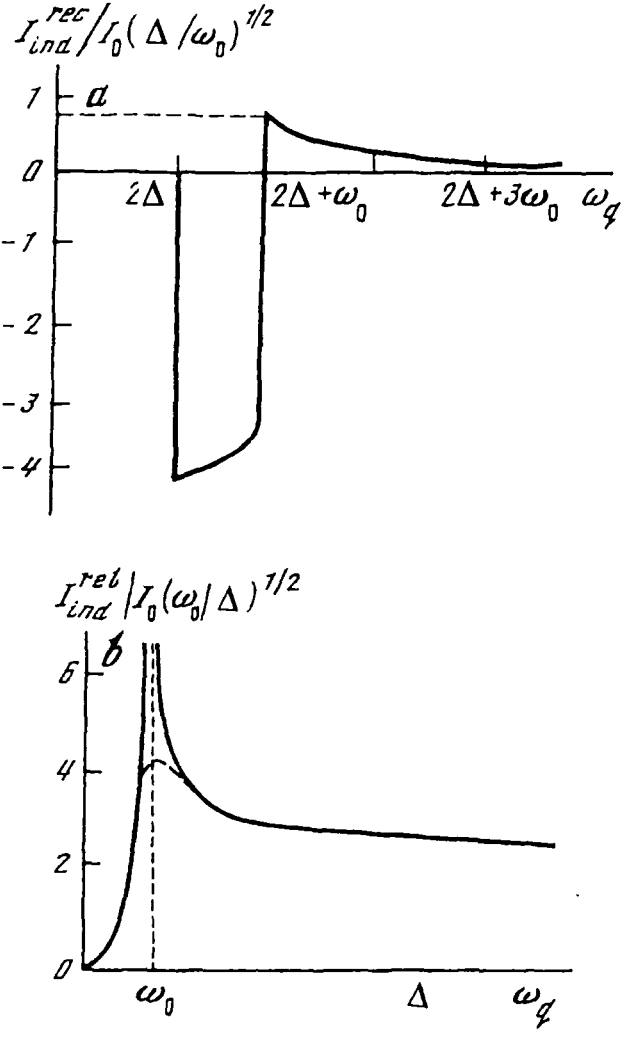

Figure 6.1. Spectral behavior of (a) recombination and, (b) relaxation phonon sources $[I_0 = \pi\lambda\alpha\tau_\varepsilon\omega_D\omega_0\Delta/(2\varepsilon_F\omega_q)]$.

6.2.6. Comparison with Relaxation

We now consider the relaxation source $I_{\text{ind}}^{\text{rel}}$, which is represented in the following form, based on Eq. (6.4):

$$I_{\text{ind}}^{\text{rel}} = 2N_{\omega_q}\left\{\int_{\Delta+\omega_q}^{\infty} d\varepsilon_1 L_{\omega_q}(\varepsilon_1, \varepsilon_1-\omega_q)\, n_{\varepsilon_1}^{(1)}\left[1-\frac{\Delta^2}{\varepsilon_1(\varepsilon_1-\omega_q)}\right]\right.$$
$$\left.-\int_{\Delta}^{\infty} d\varepsilon_2 L_{\omega_q}(\varepsilon_2+\omega_q, \varepsilon_2)\, n_{\varepsilon_2}^{(1)}\left[1-\frac{\Delta^2}{\varepsilon_2(\varepsilon_2-\omega_q)}\right]\right\}. \tag{6.22}$$

Taking into account (6.3) and (6.50) and the relation $\omega_q << T$, as well as some obvious transformations, one can write:

$$I_{\text{ind}}^{\text{rel}} = \pi\lambda\frac{T\omega_D}{\varepsilon_F\omega_q}\int_{\Delta}^{\infty} d\varepsilon_1 \frac{[(\varepsilon_1+\omega_q)\varepsilon_1-\Delta^2]\,(n_{\varepsilon_1+\omega_q}^{(1)}-n_{\varepsilon_1}^{(1)})}{\sqrt{[(\varepsilon_1+\omega_q)^2-\Delta^2](\varepsilon_1^2-\Delta^2)}}. \tag{6.23}$$

Further examination is completely analogous to the case of a recombination source. Omitting the details of calculations, we present the results for the source (6.23). The function $I_{\text{ind}}^{\text{rel}}(\omega_q)$ has no threshold features. It vanishes (being positive) at the beginning of the spectrum ($\omega_q \to 0$). At larger values of the argument, $I_{\text{ind}}^{\text{rel}}(\omega_q)$ increases and when $\omega_q = \omega_0$, it has a logarithmic singularity. Further increasing the argument causes a decrease in $I_{\text{ind}}^{\text{rel}}(\omega_q)$, which initially is logarithmic and then becomes exponential. For example, at values $\omega_q \approx \Delta$, the source takes the value $I_{\text{ind}}^{\text{rel}} \approx 3(\omega_0/\Delta)^{1/2}$ (in units of I_0). This is illustrated in Fig. 6.1b. Thus the behavior of the contributions I^{rec} and I^{rel} is found in the whole range of phonon frequencies of interest.

6.3. VIOLATION OF DETAILED BALANCE

The results obtained in Sect. 6.2 are summarized graphically in Fig. 6.2a. We emphasize that the ranges of the relaxation and recombination sources in the external radiation frequency range considered ($\omega_0 \le \Delta$) factually do not overlap. For this reason the total phonon flux in the narrow frequency range $2\Delta \le \omega_q \le 2\Delta + \omega_0$ has a negative value (the "dip" in Fig. 6.2a). This means that a superconducting film under the influence of a high-frequency electromagnetic field would selectively absorb phonons.

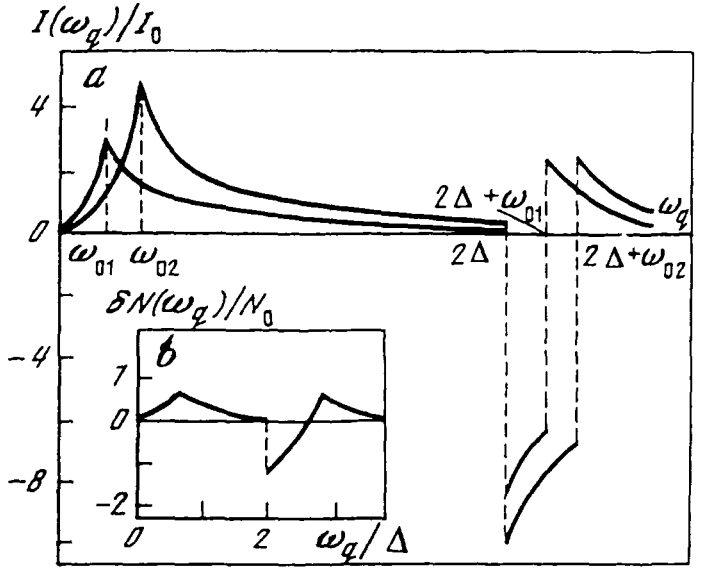

Figure 6.2. (a) Phonon emission spectrum from a thin film and, (b) the behavior of nonequilibrium deviation of the phonon distribution function at $\tau_{es} \neq 0$.

6.3.1. Phonon Deficit and Order Parameter Enhancement

The origin of this effect is closely related to the mechanism that causes the enhancement of superconductivity in a high-frequency electromagnetic field, which was considered in Sect. 5.2. Indeed, at temperatures $T \neq 0$ there are always a certain number of electron excitations above the gap, which are in thermodynamic equilibrium with the phonons. The phonons in the superconductor, having an energy approximately equal to twice the gap value, effectively create quasi-particles that recombine and emit phonons of the same frequency.

Note that according to the detailed balance principle, the probabilities of the direct and reverse processes are identical. The situation changes when an external high-frequency electromagnetic field is applied. As was shown in Chap. 5, if the frequency of the field does not exceed the quasi-particle creation threshold, the action of the high-frequency electromagnetic field is reduced to changing the "center of gravity" of the quasi-particle distribution function toward the higher energies. Then the number of excitations above the gap edge falls below its thermodynamic equilibrium value [the function $n_\varepsilon^{(1)}$ (6.3) is negative at $\Delta \leq \varepsilon \leq \Delta + \omega_0$]. This indicates a violation of the detailed equilibrium in electron–phonon interaction in the presence of an external field. The probability of phonon absorption at frequencies $\omega_q > 2\Delta$ becomes greater than the probability of their

emission. As a result, at some frequency range near $\omega_q \sim 2\Delta$, a deficit of phonons is formed in a nonequilibrium superconductor, which should be compensated from the outside of the system for the entire picture to remain stationary. Thus, phonon fluxes flow from the heat-bath to the superconductor: they could be regarded as negative fluxes.

6.3.2. Comparison with Alternative Approaches

Note in this connection that the experimental detection of phonon absorption could be considered not only as the direct confirmation of the theory developed earlier, but also as an additional proof of the validity of the concepts utilized in formulating the theory of superconductivity enhancement. At this point we offer a comment on the study by Chang and Scalapino.[4] They incorporated an additional term $\delta N_{\omega_q}/\tau_{es}$ in the kinetic equation for the phonons, where τ_{es} is the escape time of the nonequilibrium phonons from the film. This term accounts for the coupling of the phonons to the external medium. Since in free exchange ($\tau_{es} \to 0$) the phonon deficit created by the external field is completely compensated by the flow from the outside ($\delta N_{\omega_q} \to 0$), they noted that the phonon distribution that arises within the film is in equilibrium. However, this equilibrium is dynamic and is directly tied to the existence of phonon fluxes of different signs. In Chang and Scalapino, these phonon fluxes were not calculated. Figure 6.2b reproduces the curve they found by numerical calculation for δN_{ω_q} at $\tau_{es} \neq 0$, from which the existence of negative values of $\delta N_{\omega_q} < 0$ is implied. The form of this curve indicates the presence of a phonon deficit within the film and also implicitly indicates the existence of negative phonon fluxes.

The study by Dayem and Wiegand[5] is also of interest. In their study, the behavior of the nonequilibrium electron–phonon system was investigated under the conditions of phonon pumping. The phonon frequency in the incident flux was considered to be much less than twice the gap value. These authors solved the problem numerically, using their model of discrete levels, in which several dozen levels were used to "construct" the energy region over the gap in the energy space of single-electron states. Electron transitions involving phonon emission and absorption take place between these discrete levels. The authors focused on the possibility of effectively increasing the frequency of the incident phonon flux ("up-conversion," which turned out to be not very effective). It is interesting to note that the curve describing the spectral dependence of the integral phonon flux is negative in a certain frequency range beginning at $\omega_q \geq 2\Delta$. This also indicates the existence of an analog of the phonon-deficit effect under external (in this case, phonon) pumping.

6.3.3. Recombination Peak

As to the peak in the spectral curve (see Fig. 6.2a) at frequencies $\omega_q \approx 2\Delta + \omega_0$, its origin is determined by the recombination of quasi-particles, shifted by an external field far from the gap edge on the energy distance ω_0, with the quasi-particles remaining at the edge. This is quite obvious in our examination. Indeed, as was noted in Sect. 5.1, single-quantum transitions are characteristic of this situation. Consequently, excess quasi-particles are created primarily at energies $\varepsilon \approx \Delta + \omega_0$. As we see from Eq. (6.3), the contribution to the quasi-particle distribution function is singular at such energies. However, since our study is restricted by a linear (in intensity of the external field) approximation, it follows from (6.4) that the main role is played by the recombination of nonequilibrium quasi-particles (at energies $\varepsilon \approx \Delta + \omega_0$) with equilibrium quasi-particles (at energy level $\varepsilon \approx \Delta$) near the gap edge, where the density of electron states is high. As a result of this recombination process, the phonons with energy $\omega_q \approx 2\Delta + \omega_0$ are produced.

6.3.4. Exclusion of Divergence

Concluding this section, we discuss the logarithmic divergence of the relaxation flux at frequencies $\omega_q \approx \omega_0$ (see Figs. 6.1 b and 6.2a). This formal divergence is connected to the singularity in the density of electron levels, which is characteristic for superconductors in the absence of external fields, and appears in the approximations used. This logarithmic divergence vanishes if one accounts for the smearing influence of the electromagnetic field on the electron BCS density of states. Other methods for exclusion of such divergencies also exist [e.g., one can bound Eq. (6.3) using the Pauli principle]. They do not, however, influence the results in any significant way.

References

1. G. M. Eliashberg, Temperature Green's function for electrons in a superconductor, *Sov. Phys. JETP* **12**(5), 1000–1002 (1960) *[Zh. Eksp. i Teor. Phys.* **39** [5(11)], 1437–1441 (1960)].
2. A. M. Gulyan and G. F. Zharkov, Kinetics of phonons in nonequilibrium superconductors at external electromagnetic field, *Sov. Phys. JETP* **53**(1), 756-762 (1989) *[Zh. Eksp. i Teor. Fiz.* **80** (1),303–325(1981)].
3. G. M. Eliashberg, Film superconductivity stimulated by a high-frequency field, *JETP Lett.* **11**(3), 114–117 (1970) *[Pis'ma Zh. Eksp. i Teor. Fiz.* **11**(3), 186–188 (1970)].
4. J.-J. Chang and D. J. Scalapino, Kinetic equation approach to nonequilibrium superconductivity, *Phys. Rev. B* **15** (5), 2651–2670 (1977).
5. A. H. Dayem and J. J. Wiegand, Behavior of thin film superconducting bridges in a microwave field, *Phys. Rev.* **155** (2), 419–428 (1967).

7

Time-Dependent Ginzburg–Landau Equations

7.1. ORDER PARAMETER, ELECTRON EXCITATIONS, AND PHONONS

The external fields acting on a superconductor may lead to nonstationary phenomena that have to be described by dynamic equations. However, as was shown in the previous chapters, the set of nonstationary equations in the general case is very complicated and in addition to the equations for the main parameters characterizing superconductivity (such as $|\Delta|$, μ, $\mathbf{Q}$), it includes generalized kinetic equations for distribution functions (see Sect. 3.3). In the vicinity of the critical temperature (in analogy with the stationary case, Sect. 1.3), one can simplify the general time-dependent Ginzburg-Landau (TDGL) equations by considering the gapless case (Sect. 2.2). For finite-gap superconductors, the attempt to simplify the general scheme encounters serious difficulties connected with the nonlocal kernels of the integral equations governing the order parameter. To derive the equations for such superconductors, one needs to account simultaneously for the condensate, the excitations, and the interaction between them. The success achieved in this direction[1–6] is due to progress in the kinetic description of single-particle excitations in nonequilibrium superconductors (see the review articles in Refs. 7–10). The dynamic equations for the order parameter were obtained in their most complete form by Watts-Tobin et al.[6] But in some respects the theory still had some deficiencies, which we have tried to correct.

In many situations, the possible deviation of the phonon system from equilibrium should be taken into account. The role of phonons in the problem considered is twofold. First, the nonequilibrium in the phonon system may be essential for the dynamics of the order parameter. Second, the time variations of the order parameter modulus might lead to excess phonon generation and to phonon exchange between a superconductor and its environment.

7.1.1. Basic Kinetic Equations

We will use here the generalized kinetic equations[11,12] for energy-integrated Green–Gor'kov functions. As was shown in Chap. 4, these equations are still valid in the case where the phonon system is not at equilibrium. In a real-time approximation,* the equations may be written in a very compact form:

$$i\mathbf{v}\cdot\frac{\partial\check{g}}{\partial\mathbf{r}}+i\check{\sigma}_z\frac{\partial\check{g}}{\partial t_1}+i\frac{\partial\check{g}}{\partial t_2}\check{\sigma}_z=\check{H}(t_1)\,\check{g}-\check{g}\,\check{H}(t_2)$$

$$+\int_{-\infty}^{\infty}dt_3\,\{\check{\Sigma}(t_1\,t_3)\,\check{g}(t_3\,t_2)-\check{g}(t_1\,t_3)\,\check{\Sigma}(t_3\,t_2)\}. \tag{7.1}$$

Here

$$\check{g}=\check{g}(t_1,t_2,\mathbf{r},\mathbf{p}_F),\ \check{g}=\begin{pmatrix}\hat{g}^R & \hat{g}\\ \hat{0} & \hat{g}^A\end{pmatrix},\ \hat{g}^{(R,A)}=\begin{pmatrix}g & f\\ -f^+ & \bar{g}\end{pmatrix}^{(R,A)}, \tag{7.2}$$

$$\check{\Sigma}=\check{\Sigma}(t_1,t_2,\mathbf{r},\mathbf{p}_F),\ \check{\Sigma}=\begin{pmatrix}\hat{\Sigma}^R & \hat{\Sigma}\\ \hat{0} & \hat{\Sigma}^A\end{pmatrix},\ \hat{\Sigma}^{(R,A)}=\begin{pmatrix}\Sigma_1 & \Sigma_2\\ -\Sigma_2^+ & \bar{\Sigma}_1\end{pmatrix}^{(R,A)}, \tag{7.3}$$

$$\check{H}_1(t)=\mathbf{v}\cdot\mathbf{A}(t)\check{\sigma}_z-\check{1}\cdot\varphi(t),\ \check{1}=\begin{pmatrix}\hat{1} & \hat{0}\\ \hat{0} & \hat{1}\end{pmatrix},\ \check{\sigma}_z=\begin{pmatrix}\hat{\sigma}_z & \hat{0}\\ \hat{0} & \hat{\sigma}_z\end{pmatrix}, \tag{7.4}$$

where $\mathbf{p}_F=m\mathbf{v}_F=m\mathbf{v}$ is the Fermi momentum and $\mathbf{r}$ is the quasi-classical coordinate, the Fourier transform of which is denoted by $\mathbf{k}$. In Eq. (7.1) (A, φ) are the electromagnetic field potentials ($e=\hbar=c=1$)

7.1.2. Normalization Condition

Equation (7.1) must be supplied with the normalization condition, which allows us to select the necessary solution of homogeneous (relative to the $\check{g}$-functions) equations (7.1):

*In Eq. (7.1) the integration over the intrinsic spatial coordinate (or, depending on representation, over the momentum variable) is assumed in general.

$$\int_{-\infty}^{\infty} dt_3\, \check{g}\,(t_1, t_3, \mathbf{r}, \mathbf{p}_F)\, \check{g}\,(t_3, t_2, \mathbf{r}, \mathbf{p}_F) = -\pi^2 \check{1} \cdot \delta\,(t_1 - t_2), \tag{7.5}$$

We wrote this condition in Sect. 3.3 (see Eq. 3.68). It may be proven in the following way (see, e.g., Ref. 5). Equation (7.1) may be presented in the form

$$[\,\check{Z}*, \check{g}\,]_- = [\,\check{Z}*\check{g} - \check{g}*\check{Z}\,] = 0, \tag{7.6}$$

where the operator $\check{Z}$, as follows from Eqs. (7.6) and (7.1), is

$$\check{Z} = i\check{\sigma}_z \frac{\partial}{\partial t_1}\delta\,(t_1 - t_2) - \check{H}\,(t_1) + \check{1} i\mathbf{v} \cdot \frac{\partial}{\partial \mathbf{r}} - \check{\Sigma}. \tag{7.7}$$

Since the convolution * is commutative (which follows directly from its definition in 3.70), it is easy to see that the condition

$$\check{g} * \check{g} = \text{const} \cdot \check{1} \tag{7.8}$$

is compatible with the equation

$$\left[\check{Z}*, \check{g}*\check{g}\right]_- = 0, \tag{7.9}$$

which follows from Eq. (7.6). The value of a constant in (7.8) can be obtained by considering Eq. (7.8) either in a superconducting region that is in an equilibrium state, or in a normal area, where $|\Delta| = 0$. The latter option is simpler, and it is possible to calculate the constant immediately. Larkin and Ovchinnikov[12] introduced the normalization in which const = 1. Because a particular value of this constant is of no importance, we will retain the normalization const $= -\pi^2$, used earlier.

7.1.3. Definition of Order Parameter

We will now use the results obtained in Chaps. 3 and 4. The self-energy function Σ is an additive quantity that contains certain terms corresponding to the interaction of electrons with impurities, with phonons, with each other, and so on. The nonequilibrium order parameter Δ in a weak-coupling limit $\lambda << 1$ (λ is the dimensionless electron–phonon coupling parameter) is defined by the formula

$$\Delta = \frac{1}{2}\,(\Sigma_2^R + \Sigma_2^A)^{(\text{e-ph})}, \tag{7.10}$$

where the self-energy function representing the interaction of electrons with phonons is (see Sect. 4.5):

$$(\Sigma_2^{R(A)})^{(e-ph)} = \int_{-\infty}^{\infty} \frac{d\varepsilon'}{4\pi i} \int \frac{d\Omega_{p'}}{4\pi} \{f_{\varepsilon'} D_{\varepsilon'-\varepsilon}^{A(R)} + D_{\varepsilon'-\varepsilon} f_{\varepsilon'}^{R(A)}\}. \tag{7.11}$$

The phonon propagator is expressed in terms of the nonequilibrium phonon distribution function N_{ω_q} by the relations:

$$D_{\varepsilon'-\varepsilon} = \left(1 + 2N_{\omega_{p-p'}}\right) \text{sign}\,(\varepsilon' - \varepsilon)\,(D^R - D^A)_{\varepsilon'-\varepsilon}, \tag{7.12}$$

$$D_{\varepsilon'-\varepsilon}^{R(A)} = \lambda \frac{2\omega_{p'-p}^2}{\omega_{p'-p}^2 - (\varepsilon' - \varepsilon_{(-)}^{+} i\delta)^2}. \tag{7.13}$$

When phonons are in equilibrium, the contribution of the second term in Eq. (7.11) is small by the parameter $(T/\omega_D)^2$, so to find Δ one can use the simplified equation that follows from Eqs. (7.10) to (7.13)

$$\Delta_\omega(\mathbf{k}) = \lambda \int_{-\omega_D}^{\omega_D} \frac{d\varepsilon}{4\pi i} \int \frac{d\Omega_p}{4\pi} f_{\varepsilon\varepsilon-\omega}(\mathbf{p}, \mathbf{k}). \tag{7.14}$$

If the phonon distribution function N_{ω_q} is localized at energies $\omega_q << \omega_D$ and has no singularities as a function of a real argument ω_q (this will be assumed further), Eq. (7.14) may be applied to the situations with nonequilibrium phonons.

7.1.4. Nondiagonal Collision Channel

To obtain the propagator $f_{\varepsilon\varepsilon-\omega}(\mathbf{p}, \mathbf{k})$, one can use the equation that follows from Eq. (7.1) for the nondiagonal "Keldysh" component. Separating in Eq. (7.1) the virtual processes (see Sect. 4.1), which leads to Eq. (7.14), and ignoring the renormalization terms, one finds the expression for the $\hat{I}$-matrix (4.2):

$$\hat{I} = \begin{pmatrix} (-f\Delta^* + \Delta f^+) + K_{11} & (g\Delta - \Delta\bar{g}) + K_{12} \\ (-\bar{g}\Delta^* + \Delta^* g) + K_{21} & (-f^+\Delta - \Delta^* f) + K_{22} \end{pmatrix}, \tag{7.15}$$

where the coefficients K_{ij} are connected with the self-energy functions [the definition of these quantities follows from a comparison of Eqs. (7.15) with (4.2)]. Taking into account the nondiagonal channel in the kinetic equation for the electron-hole distribution function n_ε,[13,14] we get the canonical form of the collision integral. We recall here that the general expression for the $\hat{g}$-function, which satisfies the normalization condition (7.8), was discussed in Sect. 3.3, where the functions f_1 and f_2 were introduced [see Eq. (3.72)]. These functions connect Green's functions with the distribution functions of electronlike (n_ε) and holelike $(n_{-\varepsilon})$ excitations.

7.1.5. Spectral Functions R_1, R_2, N_1, and N_2

According to Eqs. (3.77), (3.79), and (3.80), the functions f_1 and f_2 (as well as $N_1, \overline{N}_1$) are of a general type, i.e., they have definite ε-parity only in absence of an external electromagnetic field. In the latter case they are equal to

$$N_1 = -\overline{N}_1 = \mathrm{Re}\left[\frac{\varepsilon + i\gamma}{\sqrt{(\varepsilon + i\gamma)^2 - |\Delta|^2}}\right], \tag{7.16}$$

$$f_1 = \mathrm{sign}\,\varepsilon\,(1 - n_\varepsilon - n_{-\varepsilon}), \tag{7.17}$$

$$f_2 = -\frac{\mathrm{sign}\,\varepsilon}{N_1}(n_\varepsilon - n_{-\varepsilon}). \tag{7.18}$$

where γ is the energy damping of electrons. Introducing also the functions

$$R_1 = \mathrm{Im}\left[\frac{\varepsilon + i\gamma}{\sqrt{(\varepsilon + i\gamma)^2 - |\Delta|^2}}\right], \tag{7.19}$$

$$R_2 = \mathrm{Re}\left[\frac{|\Delta|}{\sqrt{(\varepsilon + i\gamma)^2 - |\Delta|^2}}\right]. \tag{7.20}$$

$$N_2 = -\,\mathrm{Im}\left[\frac{|\Delta|}{\sqrt{(\varepsilon + i\gamma)^2 - |\Delta|^2}}\right], \tag{7.21}$$

we can express the $\hat{g}$-function as

$$\begin{pmatrix} g & f \\ -f^+ & \overline{g} \end{pmatrix} = 2\pi i \left\{ \begin{pmatrix} N_1 & R_2 e^{i\theta} \\ -R_2 e^{-i\theta} & \overline{N}_1 \end{pmatrix} f_1 + \begin{pmatrix} N_1 & iN_2 e^{i\theta} \\ iN_2 e^{-i\theta} & -\overline{N}_1 \end{pmatrix} f_2 \right.$$
$$\left. + \frac{1}{2}\left[\frac{\partial f_1}{\partial \varepsilon}\frac{\partial}{\partial t}\begin{pmatrix} R_1 & -N_2 e^{i\theta} \\ N_2 e^{-i\theta} & -R_1 \end{pmatrix} - \frac{\partial f_1}{\partial t}\frac{\partial}{\partial \varepsilon}\begin{pmatrix} R_1 & -N_2 e^{i\theta} \\ N_2 e^{-i\theta} & -R_1 \end{pmatrix} \right] \right\}. \tag{7.22}$$

7.1.6. Charge Density

In expression (7.22), only the lowest convolution corrections are kept (the contribution from the f_2-function is negligible).

Using Eqs. (3.99), (3.77), (3.79), and (3.80), one can establish that in superconductors the charge density in the above approximation must have the form

$$\rho = -2N(0)\left\{\varphi + \frac{1}{4}\int_{-\infty}^{\infty} d\varepsilon \left[N_1(f_1+f_2) + \overline{N}_1\,(f_1-f_2)\right]\right\}, \tag{7.23}$$

which is strictly gauge-invariant. [Note that in Refs. 2–6 a slightly deficient expression for ρ is given; it may be obtained from Eq. (7.23) if $N_1 = -\overline{N}_1$, which is not fulfilled at $\varphi \neq 0$.]

Separating in (7.14) the equilibrium part and making standard calculations (see Sect. 1.4), we get an equation for the order parameter near T_c:

$$-\frac{\pi}{8T_c}\left[\frac{\partial}{\partial t} - D\,(\nabla - 2i\mathbf{A}\,)^2\right]\Delta + \left[\frac{T_c - T}{T_c} - \frac{7\zeta(3)}{8(\pi T_c)^2}\,|\Delta|^2\right]\Delta + \kappa(\mathbf{r},t) = 0, \tag{7.24}$$

where $D = lv_F/3$ is the diffusion constant and $\zeta(3)$ is the Riemann ζ-function.

7.1.7. Gap-Control Term

Equation (7.24) for $\Delta(\mathbf{r},t)$ contains a "gap-control" term:

$$\kappa(\mathbf{r},t) = \int_{-\infty}^{\infty} \frac{d\varepsilon}{4\pi i}\,\{[f_1(\varepsilon) - f_1^0(\varepsilon)]\,(f^R - f^A)_\varepsilon - f_2(\varepsilon)\,(f^R + f^A)_\varepsilon\}, \tag{7.25}$$

where $f_1^0(\varepsilon) = \tanh(\varepsilon/2T)$. The nonequilibrium functions f_1 and f_2 should be found from the kinetic Eq. (7.1), where one can assume the phonon system to be initially in equilibrium. Note that the terms generated by $N_{1,\varepsilon}$ make insignificant contributions to Eq. (7.24) because the function $N_{1,\varepsilon}$ is nonzero at $\varepsilon \sim |\Delta|$. Only the values of $\varepsilon \sim T$ play a major role in the integrand of (7.25). For this reason, one can neglect the terms proportional to $N_{1,\varepsilon}/N_1$ in expression (3.77), which then takes the form

$$f_1 \to f_1 + \frac{1}{2}\dot{\chi} f_{2,\varepsilon} + \frac{1}{8}\dot{\chi}^2 f_{1,\varepsilon\varepsilon}, \quad f_2 \to f_2 + \frac{1}{2}\dot{\chi} f_{1,\varepsilon} + \frac{1}{8}\dot{\chi}^2 f_{2,\varepsilon\varepsilon}. \tag{7.26}$$

From the kinetic equations for f_1 and f_2 in the absence of the potential φ in the local equilibrium approximation, it follows that

$$f_1 = f_1^0 - f_{1,\varepsilon}^0 \frac{R_2}{N_1}\tau_\varepsilon \frac{\partial|\Delta|}{\partial t}, \quad f_2 = \frac{N_2\tau_\varepsilon|\Delta|}{N_1 + 2\tau_\varepsilon|\Delta|N_2}\dot{\theta} f_{1,\varepsilon}^0\,. \tag{7.27}$$

We will briefly follow the derivation procedure of these relations to clarify the essence of local equilibrium approximation.

7.1.8. Local-Equilibrium Approximation

If the characteristic frequencies and gradients of the electron system perturbation obey the relations*

$$(Dk^2, \omega) << \gamma, \tag{7.28}$$

where γ is the damping caused by inelastic processes in the electron system, then in the kinetic equations [(7.1) and (3.63)] that define the functions f_1 and f_2, one can neglect the left-hand sides and the terms connected with the Hamiltonian $\hat{H}_1$. This means that the functions f_1 and f_2 do not depend explicitly on the space coordinate $\mathbf{r}$ and time t. Only implicit dependence on $\mathbf{r}$ and t remains through the parameter $\Delta(\mathbf{r},t)$, which enters into (7.1). This means that owing to effective inelastic collisions, the behavior of single-particle electron excitations in an external field is fully determined by the evolution of the order parameter that governs the formation of the distribution function n_ε (and does not depend, e.g., on the diffusion mechanism). In other words, local equilibrium between the system of single-particle excitations and the pair-condensate is taking place.

7.1.9. Determination of the f_1-Function

In this approximation from the diagonal components of (3.63), the equation for the f_1-function follows:

$$\begin{aligned} 0 &= \{-f\Delta^* + \Delta f^+\}_{\varepsilon\varepsilon-\omega} + \{-f^+\Delta + \Delta^* f\}_{\varepsilon\varepsilon-\omega} + K_{11} + K_{22} \\ &\approx -\Delta\omega f^+_{,\varepsilon} - \Delta^*\omega f_{,\varepsilon} + K_{11} + K_{22} \end{aligned} \tag{7.29}$$

[the series expansion of functions $f_{\varepsilon-\omega}$ and $f^+_{\varepsilon-\omega}$ in (7.29) may be restricted to the first terms owing to the quasi-classical conditions]. Inserting expression (7.22) into (7.29) and omitting convolution corrections, one finds

$$0 = f^0_{1,\varepsilon} R_2 \frac{\partial|\Delta|}{\partial t} + \frac{1}{4\pi}(K_{11} + K_{22}), \tag{7.30}$$

where the transformation rule $(i\omega \doteq \partial/\partial t)$ is used and the inequalities

$$(f_1 - f_1^0)_{,\varepsilon} << f^0_{1,\varepsilon}, f_{2,\varepsilon} << f^0_{1,\varepsilon} \tag{7.31}$$

have been taken into account. The functions $K_{11} + K_{22}$ are expressed through the collision operators $J(n_{\pm\varepsilon})$, obtained in Chap. 4:

$$K_{11} + K_{22} = 4\pi \operatorname{sign}\varepsilon\,[J(n_\varepsilon) + J(n_{-\varepsilon})]. \tag{7.32}$$

*We also assume the quasi-classical character of the external fields $\mathbf{A}(\mathbf{r},t)$ and $\varphi(\mathbf{r},t)$.

Furthermore, we will assume that the electron-phonon collisions provide the most effective channel of inelastic relaxation and represent $J(n_{\pm\varepsilon}) \approx J(n_{\pm\varepsilon})^{(e-ph)}$ in the form

$$J(n_{\pm\varepsilon})^{(e-ph)} = \frac{\pi\lambda}{4(up_F)^2} \int_0^\infty \omega_q^2 d\omega_q \int_{|\Delta|}^\infty d\varepsilon' \{ p_1(n_{\pm\varepsilon})\, \delta(\varepsilon' - \varepsilon - \omega)$$

$$+ p_2(n_{\pm\varepsilon})\, \delta(\varepsilon - \varepsilon' - \omega) + p_3(n_{\pm\varepsilon})\, \delta(\varepsilon + \varepsilon' - \omega)\}, \qquad (7.33)$$

where

$$p_1(n_{\pm\varepsilon}) = (u_\varepsilon u_{\varepsilon'} - v_\varepsilon v_{\varepsilon'} \pm 1)\, [n_{\varepsilon'}(1 - n_{\pm\varepsilon})(1 + N_{\omega_q}) - n_{\pm\varepsilon}(1 - n_{\varepsilon'}) N_{\omega_q}]$$

$$+ (u_\varepsilon u_{\varepsilon'} - v_\varepsilon v_{\varepsilon'} \mp 1)\, [n_{-\varepsilon'}(1 - n_{\pm\varepsilon})(1 + N_{\omega_q}) - n_{\pm\varepsilon}(1 - n_{-\varepsilon'}) N_{\omega_q}], \qquad (7.34)$$

$$p_2(n_{\pm\varepsilon}) = p_1(N_{\omega_q} \Leftrightarrow N_{\omega_q} + 1), \qquad (7.35)$$

$$p_3(n_{\pm\varepsilon}) = (u_\varepsilon u_{\varepsilon'} + v_\varepsilon v_{\varepsilon'} \mp 1)\, [(1 - n_{\pm\varepsilon})(1 - n_{\varepsilon'}) N_{\omega_q} - n_{\pm\varepsilon} n_{\varepsilon'}(1 + N_{\omega_q})]$$

$$+ (u_\varepsilon u_{\varepsilon'} + v_\varepsilon v_{\varepsilon'} \pm 1)\, [(1 - n_{\pm\varepsilon})(1 - n_{-\varepsilon'}) N_{\omega_q} - n_{\pm\varepsilon} n_{-\varepsilon'}(1 + N_{\omega_q})]. \qquad (7.36)$$

In Eqs. (7.34) to (7.36), the function N_{ω_q} is the distribution function of phonons, which as yet is assumed to be an equilibrium one:

$$N_{\omega_q} = N^0_{\omega_q} = \exp[(\omega_q/T) - 1]^{-1}. \qquad (7.37)$$

In the vicinity of critical temperature, where $T >> |\Delta|$, for the collision integral the relaxation-time approximation may be used*

*This opportunity occurs because the perturbation of the distribution function n_ε is localized in an energy range smaller than the temperature diffusion scale. Because of this, the term containing the nonequilibrium distribution function n_ε in the integral form is smaller than the "free" term. We stress this circumstance because it remains valid also in derivation of the function f_2 (see later discussion). However, sometimes the τ approximation is criticized and, moreover, negated (see, e.g., Ref. 6) as violating a condition related to the particle number conservation. In our calculation scheme, the missing term automatically appears from the gauge-transformation rules for the functions f_1 and f_2, which were established in Sect. 3.3. (An approach equivalent to that of Ref. 6 is used in Sect. 13.3.4.)

$$J\,(n_{\pm\varepsilon})^{(e-ph)} \approx -2\gamma u_\varepsilon\,(n_{\pm\varepsilon} - n_\varepsilon^0), \tag{7.38}$$

where

$$n_\varepsilon^0 = \exp\left(\frac{|\varepsilon|}{T} + 1\right)^{-1}, \quad 2\gamma = \tau_\varepsilon^{-1} \approx \frac{7\pi\lambda\zeta(3)T^3}{2(up_F)^2}. \tag{7.39}$$

Using Eqs. (7.32), (7.33), and (7.38), we find from (7.30) the first expression in (7.27).

7.1.10. Determination of the f_2-Function

Let us now determine the function f_2. The nondiagonal elements of Eqs. (3.63) and (7.15) are essential, because the first term (proportional to f_1) in Green's functions f and f^+ (7.22) does not contribute to the equation

$$0 = -2f_\varepsilon\Delta^* - 2\Delta f_\varepsilon^+ - \Delta\omega f_{,\varepsilon}^+ + \Delta^*\omega f_{,\varepsilon} + K_{11} - K_{22}. \tag{7.40}$$

Accounting for this, one finds

$$0 = 2\,|\Delta|\,N_2\,(f_2 - \frac{1}{2}\dot\theta f_{1,\varepsilon}^0) + \frac{1}{4\pi}\left(K_{11} - K_{22} + \left[-\frac{\Delta^*}{\varepsilon}K_{12} + \frac{\Delta}{\varepsilon}K_{21}\right]\right). \tag{7.41}$$

The same approximations are used here as in deriving Eq. (7.29). Using the relation

$$K_{11} - K_{22} - \left[\frac{\Delta^*}{\varepsilon}K_{12} + \frac{\Delta}{\varepsilon}K_{21}\right] = \frac{4\pi}{N_1}\,\mathrm{sign}\,\varepsilon\,\{J\,(n_\varepsilon) - J\,(n_{-\varepsilon})\}, \tag{7.42}$$

one obtains from Eqs. (7.38), (7.41), and (7.42) the second part of expression (7.27).

The potential φ may be restored now in (7.27) with the help of Eq. (7.26), where one should make $\dot\chi/2 = -\varphi$. Omitting the term proportional to $\dot\theta\varphi$ [its contribution to Eq. (7.27) is small], one finds

$$f_1 = f_1^0 - f_{1,\varepsilon}^0\frac{R_2}{N_1}\tau_\varepsilon\frac{\partial|\Delta|}{\partial t} + \frac{\varphi^2}{2}f_{1,\varepsilon\varepsilon}^0. \tag{7.43}$$

As for the function f_2, the quadratic in the φ term may be omitted—it is proportional to $f_{1,\varepsilon\varepsilon\varepsilon}^0$. The linear term, which takes into account the transformation rule for θ, gives the equation

$$f_2 = -\frac{\varphi N_1 f^0_{1,\varepsilon} - \tau_\varepsilon |\Delta| N_2 \dot{\theta} f^0_{1,\varepsilon}}{N_1 + 2\tau_\varepsilon |\Delta| N_2}. \tag{7.44}$$

7.1.11. Order Parameter Equation

Utilizing Eqs. (7.43) and (7.44), the equation for an order parameter [Eqs. (7.24) and (7.25)] takes the final form

$$-\frac{\pi}{8T_c}\frac{1}{\sqrt{1+(2\tau_\varepsilon|\Delta|)^2}}\left[\frac{\partial}{\partial t} + 2i\varphi + 2\tau_\varepsilon^2 \frac{\partial |\Delta|^2}{\partial t}\right]\Delta$$

$$+\frac{\pi}{8T_c}[D(\nabla - 2i\mathbf{A})^2]\Delta + \left[\frac{T_c - T}{T_c} - 7\zeta(3)\frac{(|\Delta|^2 + 2\mu^2)}{8(\pi T_c)^2} + P(|\Delta|)\right]\Delta = 0. \tag{7.45}$$

The function $P(|\Delta|)$ in (7.45) is due to the contribution of the nonequilibrium phonon subsystem.

7.1.12. Contribution of Nonequilibrium Phonons

We will now trace the origin of $P(|\Delta|)$. If the phonons are shifted from equilibrium, the collision integral (7.38) acquires the contribution

$$\delta J\,(n_{\pm\varepsilon})^{(e-ph)} = u_\varepsilon \Gamma(\varepsilon), \tag{7.46}$$

which follows from Eq. (7.33). The factor $\Gamma(\varepsilon)$ is the functional and is linked with the deviation of the phonon distribution function from the equilibrium $\delta N_{\omega_q} = N_{\omega_q} - N^0_{\omega_q}$:

$$\Gamma(\varepsilon) = \frac{\pi\lambda}{2(up_F)^2}\int_0^\infty \omega_q^2 d\omega_q \int_{|\Delta|}^\infty d\varepsilon' \delta(\varepsilon' + \varepsilon - \omega_p)(u_\varepsilon u_{\varepsilon'} + v_\varepsilon v_{\varepsilon'})$$

$$\times (1 - n_\varepsilon - n_{\varepsilon'})\,\delta N_{\omega_q}. \tag{7.47}$$

This leads to the redefinition of the function f_1 (7.43), which now has the form

$$f_1 = f_1^0 - f_1^0 \frac{R_2}{N_1}\tau_\varepsilon \frac{\partial|\Delta|}{\partial t} + \frac{\varphi^2}{2} f^0_{1,\varepsilon\varepsilon} - 2\,\mathrm{sign}\,\varepsilon\,\tau_\varepsilon \Gamma(\varepsilon). \tag{7.48}$$

The function f_2 (7.44) remains unchanged. Substituting (7.48) into (7.25), one finds for $P(|\Delta|)$ the form

$$P(\Delta) = -2\tau_\varepsilon \mathrm{Re} \int_0^\infty d\varepsilon \frac{\Gamma(\varepsilon)}{\sqrt{(\varepsilon + i\gamma)^2 - |\Delta|^2}}. \tag{7.49}$$

In the next section we will discuss the contribution to Eq. (7.45) introduced by $P(|\Delta|)$.

7.1.13. Contribution of the Gauge-Invariant Potential

Another peculiarity of (7.45), compared with Refs. 2–6, is the additional term,* which is proportional to μ^2. Such a term was obtained by Galayko[15] in a static limit of the dynamic equations. The presence of the nonlinear μ term in (7.45) is critically important. If $\mu = 0$, the relation for the gap follows from (7.45):

$$|\Delta| = \Delta_{BCS} = \Delta_0,\ \Delta_0 = T_c \left[\frac{8\pi^2}{7\zeta(3)} \left(1 - \frac{T}{T_c} \right) \right]^{1/2}. \tag{7.50}$$

However, if $\mu \neq 0$, the expression for the gap $|\Delta|$ in a spatially homogeneous and stationary case is found from the equation

$$|\Delta| = \sqrt{\Delta_0^2 - 2\mu^2}. \tag{7.51}$$

Hence the initial static pattern cannot exist at $\mu \geq \Delta_0/\sqrt{2}$ (this was first pointed out by Galayko).[16]

Based on the assumption that the behavior of superconductors in a nonstationary steady state has a close analogy with the usual thermodynamics (this principle was discussed in Ref. 17 for superconductors; see also Ref. 18 for more general cases), one can write the free energy functional of the Ginzburg–Landau type for Eq. (7.45) by discarding the first (dynamic) term. Considering μ as a parameter in this functional, it is easy to verify that the absolute minimum of the functional is obtained at $\mu = 0$. Thus in thermodynamic equilibrium, the value of μ vanishes.

7.1.14. Charge Density and Invariant Potential

Since it follows from Eqs. (7.23) and (7.27), the charge density in a local equilibrium approximation is

$$\rho = N(0) \frac{\pi |\Delta|}{T} \frac{\tau_\varepsilon |\Delta|}{\sqrt{1 + (2\tau_\varepsilon |\Delta|)^2}} \mu. \tag{7.52}$$

*This term is presented in a form that guarantees the gauge invariance of Eq. (7.45), i.e., we have replaced φ^2 by μ^2. We have resorted to this procedure because in the derivation of (7.45) the higher time derivatives were not kept. In more consecutive calculations, the term φ^2 might be replaced, for instance, by the operator $[-1/4\,(\partial/\partial t + 2i\varphi)^2]$.

Comparing this value of ρ with the density of electrons in the normal state $\rho_n = 4N(0)\varepsilon_F/3$, one has

$$\frac{\rho}{\rho_n} < \frac{|\Delta|^2}{\varepsilon_F T_c} \frac{\tau_\varepsilon |\Delta|}{\sqrt{1 + (2\tau_\varepsilon \Delta)^2}}. \tag{7.53}$$

Note that $\rho \to 0$ in the gapless limit ($\gamma \to \infty$).

7.1.15. Phonons and Order Parameter Dynamics

Now we return to the definition (7.45) of the function $P(|\Delta|)$, which contains the nonequilibrium addition δN_{ω_q} to the phonon distribution function. Substituting the value $\delta N_{\omega_q} \sim N^0_{\omega_q}$ into (7.45), one would find the value of $P(|\Delta|)$ to be an order of unity that greatly exceeds all other terms in Eq. (7.45). In reality, however, the value of δN_{ω_q} must be determined from the phonon kinetic equation, which has the form

$$\frac{d}{dt}(\delta N_{\omega_q}) = J(N_{\omega_q}) + L(N_{\omega_q}), \tag{7.54}$$

where $I(N_{\omega_q})$ is the phonon-electron collision integral, and $L(N_{\omega_q})$ is the operator describing the phonon exchange of a superconductor with its environment (the heat bath). In the simplest approximation,[19,20] the latter may be defined as

$$L(N_{\omega_q}) \approx -\frac{\delta N_{\omega_q}}{\tau_{es}}, \tag{7.55}$$

where $\tau_{es} \sim d/u$ is the phonon escape time (into the heat-bath) and d is the characteristic dimension of the superconductor. The inelastic collision integral $I(N_{\omega_q}) = I(N_{\omega_q})^{(\text{ph-e})}$ was derived in Sect. 4.5 in the form

$$I(N_{\omega_q})^{(\text{ph-e})} = \frac{\pi\lambda}{8}\frac{\omega_D}{\varepsilon_F}\int_{|\Delta|}^{\infty}\int_{|\Delta|}^{\infty} d\varepsilon d\varepsilon' \{\delta(\varepsilon + \varepsilon' - \omega_q) s_1 + 2\delta(\varepsilon - \varepsilon' - \omega_q) s_2\}. \tag{7.56}$$

Moving in this expression to the functions f_1 and f_2 in the local equilibrium approximations (7.48) and (7.44) (omitting the term with φ^2 in 7.48), and expressing u_ε and v_ε through N_1 (7.16) and R_2 (7.20), respectively, one arrives at

$$I(N_{\omega_q})^{(\text{ph-e})} \approx \frac{\pi\lambda}{2}\frac{\omega_D}{\varepsilon_F}\left\{2N^0_{\omega_q}\left[\frac{\partial|\Delta|}{\partial t}\frac{\tau_\varepsilon}{T}\eta_1 + \eta_3\right] - \eta_2 \delta N_{\omega_q}\right\}, \tag{7.57}$$

where the functions η_1, η_2, and η_3 are defined by the relations

$$\eta_1 = \frac{1}{4}\int_0^\infty d\varepsilon \frac{P(\varepsilon)R_2(\varepsilon)}{N_1(\varepsilon)\cosh^2(\varepsilon/2T)}$$

$$+\frac{1}{4}\int_0^\infty d\varepsilon \left\{ Q(\varepsilon)\frac{R_2(\varepsilon+\omega_q)}{N_1(\varepsilon+\omega_q)\cosh^2[(\varepsilon+\omega_q)/2T]} - \frac{R_2(\varepsilon)}{N_1(\varepsilon)\cosh^2(\varepsilon/2T)} \right\} \quad (7.58)$$

$$\eta_2 = \int_0^\infty d\varepsilon\, P(\varepsilon)\tanh\frac{\varepsilon}{2T} + \int_0^\infty d\varepsilon\, Q(\varepsilon)\left(\tanh\frac{\varepsilon+\omega_q}{2T} - \tanh\frac{\varepsilon}{2T}\right), \quad (7.59)$$

$$\eta_3 = \tau_\varepsilon\left\{\int_0^\infty d\varepsilon\, P(\varepsilon)\,\Gamma(\varepsilon) + \int_0^\infty d\varepsilon\, Q(\varepsilon)\,[\Gamma(\varepsilon+\omega_q) - \Gamma(\varepsilon)]\right\}, \quad (7.60)$$

with

$$P(\varepsilon) = N_1(\varepsilon)\,N_1(\omega_q - \varepsilon) + R_2(\varepsilon)\,R_2(\omega_q - \varepsilon), \quad (7.61)$$

$$Q(\varepsilon) = N_1(\varepsilon)\,N_1(\omega_q + \varepsilon) - R_2(\varepsilon)\,R_2(\omega_q + \varepsilon). \quad (7.62)$$

The behavior of the η_1-function for various parameters of superconductors is illustrated in Fig. 7.1. Under the same conditions the η_2-function is practically linear: $\eta_2 = c\omega_q$, where $c \approx 1$.

These relations taking into account (7.47) in principle allow one to find $\delta N_{\omega_q}(t)$ and to study the interplay between the dynamics of the order parameter and nonequilibrium phonons. We will define a "generalized local equilibrium approximation" (between the pair condensate, electron excitations, and phonons) as the approximation in which (besides the fulfillment of the conditions of the local equilibrium approximation) the characteristic frequencies (and wave vectors) of variations of N_{ω_q} are small compared with $\lambda\omega_D T/\varepsilon_F$, so the left side of Eq. (7.54) may be neglected. In this case the function δN_{ω_q} depends on $\mathbf{r}$ and t implicitly, through $\Delta(\mathbf{r},t)$. From Eqs. (7.54) to (7.62) it follows that

$$\delta N = \left\{\pi\lambda\frac{\omega_D}{\varepsilon_F}N^0_{\omega_q}\left[\frac{\partial|\Delta|}{\partial t}\frac{\tau_\varepsilon}{T}\eta_1 + \eta_3\right]\right\} \Big/ \left(\eta_2\frac{\pi\lambda\omega_D}{2\varepsilon_F} + \tau_{es}^{-1}\right). \quad (7.63)$$

The solution of the integral equation (7.63) may be sought in the form

$$\delta N_{\omega_q} = K(\omega_q)\frac{\partial|\Delta|}{\partial t}. \quad (7.64)$$

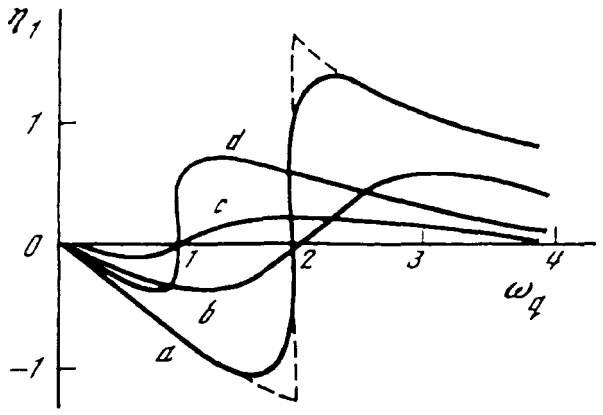

Figure 7.1. Spectral dependence of the $\eta_1(\omega_q)$-function at some parameters of a superconductor: (a) $|\Delta| = 1$, $\gamma = 0.01$; (b) $|\Delta| = 1$, $\gamma = 0.3$; (c) $|\Delta| = 0.5$, $\gamma = 0.3$; and (d) $|\Delta| = 0.5$, $\gamma = 0.01$. Dashed curve indicates the limit $|\Delta| = 1$, $\gamma = 0$. All the values are in $|\Delta|$ units.

In doing this, Eq. (7.63) is transformed into the equation

$$K(\omega_q) = \left\{ \pi\lambda \frac{\omega_D}{\varepsilon_F} N^0_{\omega_q} \left[\frac{\tau_\varepsilon}{T} \eta_1 + \eta_4 \right] \right\} \Big/ \left(\eta_2 \frac{\pi\lambda\omega_D}{2\varepsilon_F} + \tau_{es}^{-1} \right), \tag{7.65}$$

where $\eta_4 = \eta_3$ ($\delta N_{\omega_q} \to K(\omega_q)$). The function $K(\omega_q)$ depends on $|\Delta|$, γ, and τ_{es} parametrically and may be found from (7.65) by numerical methods. Rough estimates based on Eq. (7.65) show that

$$\delta N_{\omega_q} \sim \frac{|\Delta|}{\gamma T} N^0_{\omega_q}. \tag{7.66}$$

Substituting (7.66) into (7.47) and (7.49), one can see that the quantity $P(|\Delta|)$ in Eq. (7.45) significantly renormalizes the term, which is proportional to $\partial|\Delta|/\partial t$ (this term changes by its order of magnitude at $\tau_{es} \to \infty$). The accurate evaluation of this term is outside the scope of this analysis. A detailed investigation is necessary for situations where the conditions of the generalized local equilibrium approximation are violated; in those cases, the value in (7.66) may turn out to be underestimated.

Consider now the limiting case $\tau_{es} \to 0$, when according to Eqs. (7.54) and (7.55) $\delta N_{\omega_q} \to 0$. This condition is fulfilled when $d < \xi_0$; for example, in the case of a superconducting film or filament (see the discussion in Sect. 3.2). The phonon radiation from the superconductor into the surrounding medium (the heat-bath) is then determined by Eq. (7.55).

According to Sect. 6.1, the intensity of the phonon flux emitted by the volume V in a spectral range $d\omega_{\mathbf{q}}$ is

$$dW_{\omega_{\mathbf{q}}} = I\,(N^0_{\omega_{\mathbf{q}}})^{(\mathrm{ph-e})}\,\rho(\omega_{\mathbf{q}})\,d\omega_{\mathbf{q}}, \tag{7.67}$$

where $\rho\,(\omega_{\mathbf{q}}) = V\omega_{\mathbf{q}}^3/(2\pi^2 u^3)$. Using expression (7.55) for $I\,(N_{\omega_{\mathbf{q}}})^{(\mathrm{ph-e})}$, one obtains

$$dW_{\omega_{\mathbf{q}}} = \frac{\pi\lambda}{2}\frac{\omega_D}{\varepsilon_F}\left\{2\,\frac{\partial|\Delta|}{\partial t}\,\frac{\tau_\varepsilon}{T}\,N^0_{\omega_{\mathbf{q}}}\eta_1\right\}\rho\,(\omega_{\mathbf{q}})\,d\omega_{\mathbf{q}}. \tag{7.68}$$

Thus, any variation in the order parameter modulus is accompanied by the exchange of phonons between the superconductor and the heat-bath (i.e., the emission or absorption of phonons is taking place). We will use this circumstance in further analysis (see Chap. 9).

7.2. INTERFERENCE CURRENT

An expression for a nonstationary current enters the set of TDGL equations. As we will see in this section, the current in nonequilibrium superconductors in the vicinity of T_c consists of superfluid, normal, and interference components.

7.2.1. Usadel Approximation

The expression for the current may be derived from Eq. (2.85) by the method of analytical continuation (see the discussion at the end of Sect. 3.3). In our notation it has the form

$$\mathbf{j}(\mathbf{r},t) = -\frac{1}{2}N(0)\int_{-\infty}^{\infty}\frac{d\varepsilon}{4\pi i}\int\frac{d\Omega_{\mathbf{p}}}{4\pi}\,\frac{\mathbf{p}}{m}\,\mathrm{Tr}\left[\hat{\sigma}_z\,\frac{\mathbf{p}}{m}\cdot\hat{\mathbf{g}}_p(\mathbf{r},t)\right]$$

$$= i\,\frac{N(0)p_F^2}{12\pi m^2}\int_{-\infty}^{\infty}d\varepsilon\,\mathrm{Tr}[\hat{\sigma}_z\hat{\mathbf{g}}_p(\mathbf{r},t)], \tag{7.69}$$

where $\hat{\mathbf{g}}_p(\mathbf{r},t)$ is the Keldysh vector part of the energy-integrated matrix Green–Gor'kov $\check{g}$-function (7.2). In the Usadel approximation,[21] the $\check{g}$-function may be assumed to be in the form ($\check{g}_S$ is the isotropic part of $\check{g}$)

$$\check{g} = \check{g}_S + \frac{\mathbf{p}}{m}\cdot\check{\mathbf{g}}_p. \tag{7.70}$$

Because the self-energy parts of the interaction of electrons with impurities may be written as (see Sect. 2.1):

$$\hat{\Sigma}^{R(A)}_{\text{imp}} = \frac{1}{2\pi\tau} \int \frac{d\Omega_{\mathbf{p}}}{4\pi} \hat{g}^{R(A)}, \tag{7.71}$$

where τ is the transport mean-free-path time, one can show that in the adopted normalization (7.8) the solution of kinetic equation (7.1) for the vector harmonic $\check{\mathbf{g}}_p$ is expressed as

$$\check{\mathbf{g}}_p = -\frac{i}{\pi} \tau \, (\check{g}_S * \check{\boldsymbol{\partial}} * \check{g}_S + \pi^2 \check{\boldsymbol{\partial}}), \tag{7.72}$$

where

$$\check{\boldsymbol{\partial}} = \check{1} \frac{\partial}{\partial \mathbf{r}} - i\check{\sigma}_z \mathbf{A}, \tag{7.73}$$

and the isotropic part $\check{g}_S$ in (7.72) obeys the relations

$$\check{g}_S * \check{g}_S = -\pi^2 \check{1}, \tag{7.74}$$

$$[\check{g}_S * , \check{\mathbf{g}}_p]_- = \check{0}. \tag{7.75}$$

On the basis of Eqs. (7.69) to (7.75) we have

$$\mathbf{j} = -\frac{N(0)D}{4\pi^2} \int_{-\infty}^{\infty} d\varepsilon \, \mathrm{Tr} \, \hat{\sigma}_z \{\hat{g}^R * \hat{\boldsymbol{\partial}} * \hat{g}^R * \hat{a} - \hat{g}^R * \hat{\boldsymbol{\partial}} * \hat{a} * \hat{g}^A$$
$$+ \hat{g}^R * \hat{a} * \hat{\boldsymbol{\partial}} * \hat{g}^A - \hat{a} * \hat{g}^A * \hat{\boldsymbol{\partial}} * \hat{g}^A \}, \tag{7.76}$$

where

$$\hat{\boldsymbol{\partial}} = \hat{1} \frac{\partial}{\partial \mathbf{r}} - i\mathbf{A}\hat{\sigma}_z, \tag{7.77}$$

and the spectral functions $\hat{g}^{R(A)}$ (3.66), according to Eqs. (7.16) and (7.19) to (7.21) are*

* In writing the spectral functions (7.78) we have completely ignored the influence of external fields $\mathbf{A}$ and φ; thus the expression (7.78) actually corresponds to the gauge $\varphi = 0$. For an arbitrary gauge with $\varphi \neq 0$, the function $\hat{g}^{(R,A)}$ (and, in particular, N_1) changes (see Sect. 3.3). This, however, produces no substantial changes in the expression for the current in a quasi-classical approximation.

$$\hat{g}^{R(A)} = \overset{+}{(-)} \frac{i\pi}{\sqrt{(\varepsilon^{+}_{(-)} i\gamma)^2 - |\Delta|^2}} \begin{pmatrix} \varepsilon^{+}_{(-)} i\gamma & \Delta \\ -\Delta^* & -(\varepsilon^{+}_{(-)} i\gamma) \end{pmatrix}$$

$$\equiv \overset{+}{(-)} \begin{pmatrix} N^{+}_{1(-)} iR_1 & e^{i\theta}(R^{-}_{2(+)} iN_2) \\ e^{-i\theta}(R^{-}_{2(+)} iN_2) & -(N^{+}_{1(-)} iR_1) \end{pmatrix}. \tag{7.78}$$

In further transformations it is assumed that T is close to T_c, so the following inequalities are held:

$$(\gamma, |\Delta|) << T. \tag{7.79}$$

This means in particular that the function γ does not depend on ε. We also assume that the functions f_1 and f_2 do not explicitly depend on time. The terms with the derivatives $R_{i,\varepsilon}, N_{i,\varepsilon}, \nabla f_{1,\varepsilon}$ and terms with higher- order derivatives and their products (whose contributions to the current are small) are omitted. The symmetry properties of the integrand are taken into account (R_i is an odd function of ε, and N_i is an even function of ε). Note also that in calculating the trace in (7.76) several of the terms can be reduced to total differentials, which vanish upon integration. Furthermore, as follows directly from (7.79), the following identities hold:

$$N_1^2 + N_2^2 - R_1^2 - R_2^2 = 1, \quad R_1 N_1 + R_2 N_2 = 0. \tag{7.80}$$

On the basis of the above arguments, one finds the resulting expression for the significant (even in ε) part of the trace in (7.76):

$$\mathrm{Tr}\,(\ldots) = -4\pi^2 \left\{ \left(\mathbf{A} - \frac{1}{2}\nabla\theta \right) [4R_1 N_1 f_1 - f_{1,\varepsilon} (\dot{R}_2^2 - \dot{N}_2^2)] \right.$$

$$\left. - \left(\dot{\mathbf{A}} - \frac{1}{2}\nabla\dot{\theta} \right) f_{1,\varepsilon} (N_1^2 + R_2^2) + \left(\nabla f_2 - \frac{1}{2} f_{1,\varepsilon} \nabla\dot{\theta} \right) (N_1^2 + N_2^2) \right\}, \tag{7.81}$$

where the upper dot denotes a time derivative, and $\partial \dot{a}^2 \equiv \partial(a^2)/\partial t$. Defining the superfluid momentum by the usual relation

$$\mathbf{Q} = 2m\mathbf{v}_s = \nabla\theta - 2\mathbf{A}, \tag{7.82}$$

the expression for the current can be presented as

$$\mathbf{j} = \sigma_n \int_{-\infty}^{\infty} d\varepsilon \left\{ \mathbf{Q} R_2 N_2 f_1 + \frac{1}{4}\mathbf{Q}(N_1^2 + N_2^2) f_{1,\varepsilon} \right.$$

$$\left. + \frac{1}{2}(N_1^2 + N_2^2)\left(\nabla f_2 - \frac{1}{2} f_{1,\varepsilon} \nabla\dot{\theta}\right) + \frac{1}{4} f_{1,\varepsilon} \frac{\partial}{\partial t} [\mathbf{Q}(R_2^2 - N_2^2)] \right\}, \tag{7.83}$$

where the normal conductivity σ_n is

$$\sigma_n = 2N(0)D = \frac{2}{3} N(0)\, v_F^2 \tau. \tag{7.84}$$

At this stage we see that in the gauge $\dot{\theta} = 0$, expression (7.83) coincides with Schmid's result.[9] The last term in (7.83) with the time derivative (which was omitted in Refs. 2–6) vanishes if the dispersion dependence of $f_{1,\varepsilon}$ is ignored. Substituting the equilibrium value $f_1 = f_1^0(\varepsilon)$ into this term produces a nonzero result, which contains an additional small factor $|\Delta|/T$. Since this term is also proportional to another small parameter ω/T, we omit it below. Expression (7.83) is fundamental for further analysis. Because it has been derived here in an arbitrary gauge, one can be assured that the calculation scheme is self-consistent. The functions $f_1(\varepsilon) = (1 - n_\varepsilon - n_{-\varepsilon})$ sign ε and $f_2(\varepsilon) = -$ sign $\varepsilon\, (n_\varepsilon - n_{-\varepsilon})/N_1$ in (7.83) should generally be determined from the kinetic equation for the distribution of the nonequilibrium electron-hole excitations n_ε. In many cases, however, it is sufficient to substitute the equilibrium function n_ε^0 into (7.83). As was noted in Ref. 22, this procedure was carried out in Refs. 2–6 and 9 insufficiently correctly. Thus, certain terms whose contribution is sometimes not small were omitted from the final equation for the current. We will analyze the situation in more detail below.

To transform the terms containing $\dot{\theta}$ and ∇f_2 in (7.83), we use the definitions of the gauge-invariant potential

$$\mu = \frac{1}{2}\dot{\theta} + \varphi \tag{7.85}$$

and the associated electric field

$$\mathbf{E} = -\dot{\mathbf{A}} - \nabla\varphi = \frac{1}{2}\dot{\mathbf{Q}} - \nabla\mu. \tag{7.86}$$

As follows from (3.77), in the presence of a potential φ, the function f_2 is nonzero and for $\varepsilon >> |\Delta|$ is equal to

$$f_2 = -\varphi f_{1,\varepsilon}. \tag{7.87}$$

Substitution of (7.87) into (7.14) leads to

$$\mathbf{j} = \sigma_n \int_{-\infty}^{\infty} d\varepsilon \left\{ \mathbf{Q} R_2 N_2 f_1 + \frac{1}{2} f_{1,\varepsilon} (N_1^2 + N_2^2)\, \mathbf{E} \right\}. \tag{7.88}$$

In equilibrium theory, the current in dirty superconductors is given by the first term in (7.88), where one should make $f_1 = f_1^0(\varepsilon) = \tanh(\varepsilon/2T)$ (i.e., in an equilibrium situation, the term, which is proportional to $\mathbf{E}$, vanishes). In the nonequilibrium case, two additional groups of terms arise if one inserts the equilibrium

function $f_1^0(\varepsilon)$ into (7.88). The reason for this is the relation (7.89), which follows directly from (7.16) and (7.10) to (7.21):

$$N_1^2 + N_2^2 = \frac{1}{2}\left\{1 + \left[1 - \left(\frac{2\varepsilon|\Delta|}{\varepsilon^2 + \gamma^2 + |\Delta|^2}\right)^2\right]^{-1/2}\right\}. \tag{7.89}$$

The integral (7.88), taking into account (7.89) and inequalities in (7.79), can be evaluated in analytic form. In the time-dependent theory, it is necessary to evaluate this integral for an arbitrary ratio of $|\Delta|$ and γ. [The equilibrium value of $|\Delta|$ in a finite-gap superconductor is large in comparison with γ, but in the dynamic case $|\Delta(\mathbf{r},t)|$ may sometimes vanish at some points!]

We will inspect the integrals in (7.88) in more detail. If $\gamma << |\Delta|$, the factor R_2N_2 acts in fact as the δ-function of the argument $(\varepsilon \pm |\Delta|)$:

$$N_2R_2 \approx \frac{\pi}{2}|\Delta|\,\varepsilon\delta(\varepsilon^2 - |\Delta|^2), \tag{7.90}$$

and thus the first term in (7.88) gives

$$\sigma_n\mathbf{Q}\int_{-\infty}^{\infty} d\varepsilon\, R_2N_2f_1^0 \approx \frac{\sigma\pi}{4T}\mathbf{Q}\,|\Delta|^2 \tag{7.91}$$

(this result does not depend on $\gamma/|\Delta|$ and holds for arbitrary $|\Delta|$ and γ, even if the δ-function becomes "smeared"). The second term in (7.88), taking into account (7.89), takes the form

$$\frac{\sigma_n\mathbf{E}}{2}\int_{-\infty}^{\infty} d\varepsilon\, f_{1,\varepsilon}^0\,(N_1^2 + N_2^2) =$$

$$\frac{\sigma\mathbf{E}}{2T}\int \frac{d\varepsilon\,[\varepsilon^2 + (\gamma^2 + |\Delta|^2)]}{\cosh^2(\varepsilon/2T)\,[\varepsilon^4 + 2\varepsilon^2(\gamma^2 - |\Delta|^2) + (\gamma^2 + |\Delta|^2)^2]^{1/2}}. \tag{7.92}$$

Expression (7.92) can be treated as the sum of two integrals

$$\frac{\sigma_n\mathbf{E}}{2T}\left\{\int_0^{\varepsilon^*} d\varepsilon\, M(\varepsilon) + \int_{\varepsilon^*}^{\infty} d\varepsilon\, M(\varepsilon)\right\}, \tag{7.93}$$

$$M(\varepsilon) = \frac{\varepsilon^2 + \gamma^2 + |\Delta|^2}{\cosh^2(\varepsilon/2T)\,[\varepsilon^4 + 2\varepsilon^2(\gamma^2 - |\Delta|^2) + (\gamma^2 + |\Delta|^2)^2]^{1/2}}, \tag{7.94}$$

where ε^* satisfies the relation (recall that $T >> |\Delta|, \gamma$):

$$(\gamma^2 + |\Delta|^2)^{1/2} << \varepsilon^* << T. \tag{7.95}$$

Using the relation (7.95), one can expand $\cosh^2(\varepsilon/2T)$ in the first integrals in (7.95), keeping only the lowest-order term in a small parameter $\varepsilon/2T$, and use for another integral the approximation

$$\frac{\varepsilon^2+\gamma^2+|\Delta|^2}{[\varepsilon^4+2\varepsilon^2(\gamma^2-|\Delta|^2)+(\gamma^2+|\Delta|^2)^2]^{1/2}}\approx 1, \quad \varepsilon^*\le\varepsilon<\infty. \tag{7.96}$$

Thus the second term in Eq. (7.88) takes the form

$$\frac{\sigma_n\mathbf{E}}{2}\int_{-\infty}^{\infty} d\varepsilon\, f^0_{1,\varepsilon}\,(N_1^2+N_2^2)$$

$$=\frac{\sigma_n\mathbf{E}}{2T}\left\{\int_0^{\varepsilon^*}\frac{d\varepsilon\,[\varepsilon^2+\gamma^2+|\Delta|^2]}{[\varepsilon^4+2\varepsilon^2(\gamma^2-|\Delta|^2)+(\gamma^2+|\Delta|^2)^2]^{1/2}}+\int_{\varepsilon^*}^{\infty}\frac{d\varepsilon}{\cosh^2(\varepsilon/2T)}\right\}. \tag{7.97}$$

One can now integrate (7.97) directly and find for (7.98):

$$\mathbf{j}=\frac{\pi\sigma_n}{4T}\mathbf{Q}|\Delta|^2+\sigma_n\mathbf{E}\left\{1+\frac{\sqrt{|\Delta|^2+\gamma^2}}{2T}\left[\mathrm{K}\left(\frac{|\Delta|}{\sqrt{|\Delta|^2+\gamma^2}}\right)-\mathrm{E}\left(\frac{|\Delta|}{\sqrt{|\Delta|^2+\gamma^2}}\right)\right]\right\} \tag{7.98}$$

where $\mathrm{K}(x)$ and $\mathrm{E}(x)$ are the complete elliptic integrals of the first and second type, respectively. In the limiting case they have the following asymptotic forms:

$$x\ll 1: \quad \mathrm{K}(x)\simeq\frac{\pi}{2}\left(1+\frac{x^2}{4}+\ldots\right),\ \mathrm{E}(x)\simeq\frac{\pi}{2}\left(1-\frac{x^2}{4}+\ldots\right), \tag{7.99}$$

and

$$x\simeq 1: \quad \mathrm{K}(x)\simeq\ln\frac{4}{\sqrt{1-x^2}}+\ldots,\ \mathrm{E}(x)\simeq 1-\frac{1}{2}(1-x)\ln(1-x)+\ldots, \tag{7.100}$$

7.2.2. *Current Components in the Vicinity of T_C*

Expression (7.98) may now be written in the form

$$\mathbf{j}=\mathbf{j}_s+\mathbf{j}_n+\mathbf{j}_{\mathrm{int}}, \tag{7.101}$$

where the superfluid and normal components of the current are given by the standard relations

$$\mathbf{j}_s = \frac{\pi\sigma_n}{4T}\,\mathbf{Q}\,|\Delta|^2, \quad \mathbf{j}_n = \sigma_n \mathbf{E}, \tag{7.102}$$

and the "interference" component is

$$\mathbf{j}_{\text{int}} = \sigma_n \mathbf{E}\,\frac{\sqrt{|\Delta|^2+\gamma^2}}{2T}\left[\mathrm{K}\left(\frac{|\Delta|}{\sqrt{|\Delta|^2+\gamma^2}}\right) - \mathrm{E}\left(\frac{|\Delta|}{\sqrt{|\Delta|^2+\gamma^2}}\right)\right]. \tag{7.103}$$

The quantity $\mathbf{j}_{\text{int}}$ (7.103) has properties of both the superconducting condensate and the normal excitations. In fact, it describes some interference of two types of motion occurring in the electron subsystem of the superconductor.

A comparison of (7.103) with (7.102) shows that the interference component of the current is not always negligible. Using the asymptotic forms (7.99) and (7.100) of the elliptic integrals, one can easily show that (7.98) takes the following forms in the specified limiting cases

$$\mathbf{j} = \frac{\pi\sigma_n}{4T}\,|\Delta|^2\mathbf{Q} + \sigma_n\mathbf{E}\left\{1 + \frac{|\Delta|}{2T}\left(\ln\frac{4|\Delta|}{\gamma} - 1\right)\right\}, \quad \gamma << |\Delta|, \tag{7.104}$$

$$\mathbf{j} = \frac{\pi\sigma_n}{4T}\,|\Delta|^2\,\mathbf{Q} + \sigma_n\mathbf{E}, \quad \gamma >> |\Delta|. \tag{7.105}$$

Equation (7.105) coincides with the expression for the gapless superconductor (see Sect. 2.3); in this case the current consists of the normal and superconducting components only. Thus the interference term in the "finite-gap" superconductor stems from the strong correlation between the system of single-particle excitations and the pair condensate. This correlation vanishes in a gapless regime.

Using (7.104) and (7.105), we can write the following rough approximation, which reflects the behavior of the functions in brackets in (7.103):

$$[\ldots] \approx \left[1 + \frac{|\Delta|}{2T}\ln\frac{4|\Delta|+\gamma}{\gamma}\right]. \tag{7.106}$$

This approximation is convenient for practical calculations.

Note that a logarithmic renormalization of conductivity, analogous to (7.107), appears in the theory of both linear[23,24] and nonlinear[25,26] responses of a superconductor in a time-varying external electromagnetic field of the frequency ω_0; for example,

$$\sigma_*(\omega_0) = \sigma_n\left(1 + \frac{|\Delta|}{2T}\ln\Lambda\right), \quad \Lambda = \max\left(\omega_0\tau_{\text{imp}}, \frac{\omega_0}{|\Delta|}\right). \tag{7.107}$$

Such a logarithmic renormalization of conductivity also reflects the interference between normal and superfluid motions. Although the parameter $|\Delta|/T$ near T_c is small, the corrections might be not negligible, because the logarithmic factor can in principle be large. We should also mention that the interference described above is closely related to the "drag" process investigated by Shelankov.[27]

7.2.3. More Complete Expressions

We used above the equilibrium approximation for the functions f_1 and f_2. To find these functions [Eqs. (7.43) and (7.44)] in the time-dependent theory, the nonequilibrium contributions must be taken into account. They may be expressed in the form

$$f_1 = f_1^0(\varepsilon) + \delta f_1(\varepsilon), \quad \delta f_1(\varepsilon) = -f_{1,\varepsilon}^0 \frac{R_2}{N_1} \frac{2}{\gamma} \frac{\partial|\Delta|}{\partial t}, \tag{7.108}$$

$$f_2 = -\varphi f_1^0(\varepsilon) + \delta f_2(\varepsilon), \; \delta f_2(\varepsilon) = -2\mu \frac{N_2 \tau_\varepsilon |\Delta|}{N_1 + 2N_2 \tau_\varepsilon |\Delta|} f_{1,\varepsilon}^0. \tag{7.109}$$

The current component due to the function $\delta f_2(\varepsilon)$ in (7.88) is vanishingly small and can be ignored. However, the function $\delta f_1(\varepsilon)$, whose contribution though small in comparison with $\mathbf{j}_s$, is dissipative. In general, this component need not be small in comparison with $\mathbf{j}_n$. The resulting current is given by the following expression in the "local equilibrium approximation":

$$\mathbf{j} = \frac{\pi\sigma_n}{4T} \mathbf{Q} \left(|\Delta|^2 - \frac{\partial|\Delta|^2}{\gamma \partial t} \right)$$
$$+ \sigma_n \mathbf{E} \left\{ 1 + \frac{\sqrt{|\Delta|^2 + \gamma^2}}{2T} \left[\mathrm{K}\left(\frac{|\Delta|}{\sqrt{|\Delta|^2 + \gamma^2}} \right) - \mathrm{E}\left(\frac{|\Delta|}{\sqrt{|\Delta|^2 + \gamma^2}} \right) \right] \right\}. \tag{7.110}$$

This expression should be used in the Ginzburg–Landau equations instead of those presented in Refs. 2–6.

7.2.4. Interference Current in Complete Form

The expression for current in the Ginzburg–Landau regime can be written in the form

$$\mathbf{j} = \mathbf{j}_s + \mathbf{j}_n + \mathbf{j}_{\mathrm{int}}, \tag{7.111}$$

where

$$\mathbf{j}_s = \frac{\pi\sigma_n}{4T}\,\mathbf{Q}\,|\Delta|^2 \tag{7.112}$$

$$\mathbf{j}_n = \sigma_n \mathbf{E}, \tag{7.113}$$

$$\mathbf{j}_{\text{int}} = -\frac{\pi\sigma_n}{4T}\frac{\mathbf{Q}}{\gamma}\frac{\partial|\Delta|^2}{\partial t} + \sigma_n \mathbf{E}\frac{\sqrt{|\Delta|^2+\gamma^2}}{2T}\left[\mathrm{K}\left(\frac{|\Delta|}{\sqrt{|\Delta|^2+\gamma^2}}\right) - \mathrm{E}\left(\frac{|\Delta|}{\sqrt{|\Delta|^2+\gamma^2}}\right)\right]. \tag{7.114}$$

This current (7.111) enters the Maxwell set of equations, which should be supplemented with two equations (for $|\Delta|$ and μ), ensuing from (7.45). We will write down these equations and prove the completeness of the resulting set.

7.2.5. Full Set of Equations

After separating the real and imaginary parts of (7.45) one finds*:

$$-\frac{\pi}{8T_c}\sqrt{1+(2\tau_\varepsilon|\Delta|)^2}\,\frac{\partial|\Delta|}{\partial t} + \frac{\pi}{8T_c}D\,(\nabla^2 - \mathbf{Q}^2)\,|\Delta|$$

$$+\left[\frac{T_c - T}{T_c} - 7\zeta(3)\,\frac{|\Delta|^2+2\mu^2}{8(\pi T_c)^2}\right]|\Delta| = 0, \tag{7.115}$$

$$\frac{2|\Delta|^2}{\sqrt{1+(2\tau_\varepsilon|\Delta|)^2}}\,\mu + D\,\mathrm{div}\,(\mathbf{Q}\,|\Delta|^2) = 0. \tag{7.116}$$

The superfluid momentum $\mathbf{Q}$ enters Eqs. (7.115) and (7.116). It is defined by the relation (7.82) and is connected with the magnetic field strength $\mathbf{H}$ by

$$\mathbf{H} = -\frac{1}{2}\,\mathrm{curl}\,\mathbf{Q}. \tag{7.117}$$

Recalling definition (7.86) of the electric field,

$$\mathbf{E} = \frac{1}{2}\,\dot{\mathbf{Q}} - \nabla\mu, \tag{7.118}$$

it can be easily seen that two of the Maxwell equations

*We also omit the term $P(|\Delta|)$.

$$\operatorname{curl} \mathbf{E} = -\dot{\mathbf{H}}, \quad \operatorname{div} \mathbf{H} = 0, \tag{7.119}$$

are satisfied identically due to (7.117) and (7.118). Note that in the equilibrium Ginzburg–Landau scheme Eq. (7.116) coincides with the continuity equation (because $\mu \equiv 0$, $j \equiv j_s$, and $\dot{\rho} \equiv 0$ in that case). In nonequilibrium conditions, Eq. (7.116) and the continuity equation

$$\operatorname{div} \mathbf{j} + \dot{\rho} = 0 \tag{7.120}$$

are independent. The second pair of the Maxwell equations may be written as

$$\operatorname{curl} \mathbf{H} = 4\pi \mathbf{j} + \frac{\partial \mathbf{D}}{\partial t}, \tag{7.121}$$

$$\operatorname{div} \mathbf{D} = 4\pi\rho, \tag{7.122}$$

where $\mathbf{D} = \varepsilon \mathbf{E}$, and the charge density ρ induced in a nonequilibrium superconductor by the external field is expressed in terms of the gauge-invariant potential μ by (7.52). Thus the charge density, the current, and the electric and magnetic fields may be expressed in terms of μ, $|\Delta|$, $\mathbf{Q}$ and their derivatives. To calculate these (five) quantities, we have two scalar equations [(7.115) and (7.116)] and the vector equation (7.121). The scalar ε (the dielectric susceptibility) entering (7.121) requires one more independent equation, which plays by the continuity equation (7.120) [or, equivalently, Eq. (7.122)].

7.2.6. Boundary Conditions

This set of equations must be supplemented by the boundary conditions, which may differ in various problems. For instance, at the boundary between a superconductor and a normal metal, one can write

$$\left.\frac{\partial \Delta}{\partial \mathbf{n}}\right|_S = \beta \Delta|_S, \tag{7.123}$$

where β is some constant, usually taken as $\beta = (\alpha \xi_0)^{-1}$ ($\alpha \approx 0.81$ is an equilibrium approximation and ξ_0 is the coherence length). In nonequilibrium conditions, α may differ from this value (see Ref. 28), but remains of an order of unity. At the superconductor–vacuum boundary, the following conditions are reasonable:

$$\frac{\partial \Delta}{\partial \mathbf{n}} = 0, \quad \mathbf{Q}_n = 0, \quad \mathbf{E}_n = 0, \tag{7.124}$$

where $\mathbf{n}$ is the vector normal to the superconductor's surface. One should also obtain the continuity of the magnetic field $\mathbf{H}$ and of the tangential component of the electric field $\mathbf{E}$.[29] Some other boundary conditions are discussed in Chap. 9.

We conclude this section by mentioning that μ is not necessarily a continuous function of coordinates and time and may suffer discontinuity, so the solutions of the equations given above may lie in a class of piecewise smooth functions.

7.3. VISCOUS FLOW OF VORTICES

7.3.1. Abrikosov Vortices

As was shown in Chap. 1, in Type II superconductors, the surface energy at the boundary between superconducting and normal phases is negative. This results in the presence of normal domains in Type II superconductors placed in a magnetic field, which penetrates these domains. In isotropic homogeneous superconductors, the domains form a regular structure (a vortex lattice*). Such a vortex state was predicted by Abrikosov[37] (see also Ref. 38) on the basis of the Ginzburg–Landau theory. The magnetic field penetrating into the vortex core is screened by the London currents, so the magnetic induction $\mathbf{B} = 0$ in the intermediate space between vortices. With transport current passing through such a system, the Lorentz force appears and acts on moving charges. In turn, an equal but opposite force acts on the vortex system and pushes the latter into motion. Because the velocity of the vortex lattice cannot increase indefinitely, the flow of vortices must have a viscous character and be accompanied by energy dissipation. If this motion is stopped some way, for example, by the trapping of vortices on imperfections of a crystalline lattice ("pinning"), then the transport current remains superfluid. If pinning does not occur, then ultimately the dissipation energy is eliminated from the kinetic energy of the transport current, which ceases to be superfluid. To maintain this current, an electric field should exist along the current direction. In this manner a resistive current state is formed. We will use the nonstationary Ginzburg–Landau equations to describe vortex motion in superconductors.

The velocity $\mathbf{v}$ of vortex lattice motion is connected to the vectors $\mathbf{E}$ and $\mathbf{B}$ by the relation

$$\mathbf{E} = -\mathbf{v} \times \mathbf{B}. \tag{7.125}$$

We will consider only the weak magnetic fields: $B \ll H_c$, i.e., we will consider the problem of the motion of an isolated vortex.

*In analogy to the case of a crystalline lattice, the vortex lattice can melt. This phenomenon was predicted by Eilenberger[30] (and Fisher[31]). It was demonstrated first in the high-temperature superconductors[32] and afterwards in niobium.[33] The reason it was not noticed earlier in low T_c superconductors is the narrowness of the temperature range of the liquid phase. Theoretical considerations, based on the Born[34] criterion (the vanishing of the shear modulus c_{66} at the melting point) are applicable to vortex melting[35] and allow such tiny features of the phase transition as the lattice premelting to be considered.[36]

7.3.2. Effective Conductivity: Definition

The immediate task is to obtain effectiveconductivity, σ_{eff}, which connects the transport current $\mathbf{j}_{\text{trans}} = \sigma_{\text{eff}}\,\mathbf{E}$ with the electric field **E.** To solve this problem we use the method proposed by Kopnin[39] (see also Ref. 40).

We will apply the time-dependent Ginzburg–Landau equations (7.115) and (7.116) in the form*

$$\frac{\sqrt{1+(2\tau_\varepsilon|\Delta|)^2}}{D}\frac{\partial|\Delta|}{\partial t} + (\nabla^2 - \mathbf{Q}^2)\,|\Delta| + \xi^{-2}\,[1-|\Delta|^2]\,|\Delta| = 0, \tag{7.126}$$

$$\frac{2\,|\Delta|^2}{\sqrt{1+(2\tau_\varepsilon|\Delta|)^2}}\,\mu - D\,\operatorname{div}\,(|\Delta|^2\,\mathbf{Q}) = 0, \tag{7.127}$$

where

$$\mathbf{Q} = \nabla\theta - 2\mathbf{A}, \quad \mu = \frac{1}{2}\dot{\theta} + \varphi, \tag{7.128}$$

θ is the phase of an order parameter $\Delta = |\Delta|\,e^{i\theta}$, and $|\Delta|$ is measured in the units Δ_0 (7.50).

The expression for the current is

$$\mathbf{j} = \lambda_1\mathbf{Q}\,|\Delta|^2 + \sigma_n\mathbf{E} - \lambda_2\mathbf{Q}\frac{\partial|\Delta|^2}{\partial t} + \sigma_n\mathbf{E}\chi\,(\,|\Delta|\,), \tag{7.129}$$

where the coefficients λ_1, λ_2, and the function $\chi(\,|\Delta|\,)$ are obviously defined by comparing (7.111) to (7.114), with (7.129).

7.3.3. Low-Velocity Approximation

If the velocity of vortex motion is small, then the solution of the system (7.126) and (7.127) may be presented as

$$|\Delta| = |\Delta_0\,(\mathbf{r}-\mathbf{v}t)\,| + |\Delta_1(\mathbf{r}-\mathbf{v}t)\,|, \quad \mathbf{Q} = \mathbf{Q}_0\,(\mathbf{r}-\mathbf{v}t) + \mathbf{Q}_1\,(\mathbf{r}-\mathbf{v}t), \tag{7.130}$$

where $\Delta_0\,(\mathbf{r}-\mathbf{v}t)$ and $\mathbf{Q}_0\,(\mathbf{r}-\mathbf{v}t)$ are the Galilean transformed static solutions[37] and Δ_1 and Q_1 are the corrections, which are proportional to **v** and arise as a result of deformation of the vortex structure during the motion. The static solutions are (we use here the cylindrical frame of reference $\{\mathbf{l}_\varphi, \mathbf{l}_\rho, \mathbf{l}_z\}$):

*We ignore here the nonequilibrium phonon field, omitting also in (7.45) the term μ^2, which is quadratic in **E.**

$$\mathbf{Q}_0 = -\frac{\mathbf{l}_\varphi}{\rho}, \quad |\Delta_0| \approx \frac{\rho}{\sqrt{1+\rho^2}}. \tag{7.131}$$

The approximate expression (7.131) for the order parameter modulus follows from the equation

$$(\nabla^2 - \mathbf{Q}_0^2)\,|\Delta_0| + \xi^{-2}\,[1 - |\Delta_0|^2] = 0. \tag{7.132}$$

In analogy to (7.130) we have the expression for the current

$$\mathbf{j} = \mathbf{j}_0(\mathbf{r} - \mathbf{v}t) + \mathbf{j}_1(\mathbf{r} - \mathbf{v}t), \tag{7.133}$$

where

$$\mathbf{j}_0(\mathbf{r}) = \lambda_1 \mathbf{Q}_0\,|\Delta_0|^2, \tag{7.134}$$

$$\mathbf{j}_1 = \mathbf{j}_{s1} + \mathbf{E}\sigma_n\,[1 + \chi(|\Delta|)] + \lambda_2 \mathbf{Q}\,(\mathbf{v}\cdot\nabla\,|\Delta|), \tag{7.135}$$

and $\mathbf{j}_{s1}$ is the correction to the superconducting current $\mathbf{j}_s = \lambda_1 \mathbf{Q}\,|\Delta|^2$. For large distances from the vortex core, the correction $\mathbf{j}_{s1\infty}$ represents the transport current flowing in the superconductor, and determines the effective conductivity σ_{eff}. Note that strictly speaking, the contributions of normal and interference currents in (7.135) should also be taken into account. However, these contributions are small, because $\sigma_n << \sigma_{\text{eff}}$. As to the value of $\lambda_2 \mathbf{Q}\,(\mathbf{v}\cdot\nabla\,|\Delta|)$, it decreases as $1/\rho^3$ when $\rho \to \infty$. Because the corrections to $\mathbf{j}_s$ are needed only at the distances $\rho_0 >> \xi$, it is not necessary to have the exact expressions for the quantities $|\Delta_1|$ and $\mathbf{Q}_1$. Instead, we will use a method[39] that allows us to express the solution $\mathbf{j}_{S1\infty}$ in terms of static solution. One can easily verify the equality

$$\pi L \mathbf{d}\cdot[\mathbf{j}_{s1\infty}\times\mathbf{l}_z] = -\int d^3\mathbf{r}\,\mathrm{div}\,[\mathbf{j}_{s1}\,(\mathbf{d}\cdot\nabla)\,\varphi], \tag{7.136}$$

where the integration (in the cylindrical frame of reference) is restricted by the region $-L/2 \le z \le L/2$; $0 \le \varphi \le 2\pi$; $0 \le \rho \le \rho_0$, and the polar radius ρ_0 obeys the inequality $\lambda_L << \rho_0$ .The vector d is as yet arbitrary. The right side of (7.136), using the expression $\mathbf{Q}_0$ (7.131) and Eq. (7.127), can be transformed to

$$-\int d^3\mathbf{r}\,\mathrm{div}\,(\mathbf{j}_{S1\infty}\,(\mathbf{d}\cdot\nabla)\,\varphi) = \int d^3\mathbf{r}\,(\mathbf{j}_{s1}\,(\mathbf{d}\cdot\nabla)\,\mathbf{Q}_0 - \mathbf{Q}_1\,(\mathbf{d}\cdot\nabla)\,\mathbf{j}_0)$$

$$+\frac{2\lambda_1}{D}\int d^3\mathbf{r}\frac{(\mathbf{d}\cdot\mathbf{l}_\varphi)}{\rho}\frac{|\Delta_0|^2\mu}{\sqrt{1+(2\tau_\varepsilon|\Delta_0|)^2}}. \tag{7.137}$$

We have added a term $\int \mathbf{Q}_1\,(\mathbf{d}\cdot\nabla)\,\mathbf{j}_0 d^3\mathbf{r}$ into (7.137), which disappears upon integration. Indeed, from the definition in Eq. (7.128), it follows that $\mathbf{Q} = \nabla\theta$ (dropping the vector potential **A**). Thus:

$$\int d^3\mathbf{r}\,\mathbf{Q}_1\,(\mathbf{d}\cdot\boldsymbol{\nabla})\,\mathbf{j}_0 = \int d^3\mathbf{r}\,\mathrm{div}\,[\theta_1\,(\mathbf{d}\cdot\boldsymbol{\nabla})\,\mathbf{j}_0] - \int d^3\mathbf{r}\,\theta_1\mathbf{d}\cdot\boldsymbol{\nabla}\,\mathrm{div}\,\mathbf{j}_0. \qquad (7.138)$$

The second term on the right side of Eq. (7.138) vanishes owing to the electroneutrality condition $\mathrm{div}\,\mathbf{j}_0 = 0$. As for the first term, it transforms into a surface integral, which is small in parameter, $1/\rho_0 \ll 1$.

7.3.4. Linearized Equations

On the basis of Eqs. (7.126) and (7.132) we can transform the first integral on the right side of (7.137). From Eq. (7.126) it follows that the quantities $|\Delta_1|$ and $\mathbf{Q}_1$ obey the linearized equation

$$-\frac{\sqrt{1+(2\tau_\varepsilon|\Delta_0|)^2}}{D}\,\mathbf{v}\cdot\boldsymbol{\nabla}\,|\Delta_0| + \nabla^2\,|\Delta_1|$$

$$-\mathbf{Q}_0^2\,|\Delta_1| - 2\mathbf{Q}_0\cdot\mathbf{Q}_1\,|\Delta_0| + \xi^{-2}\,(1-3\,|\Delta_0|^2)\,|\Delta_1| = 0. \qquad (7.139)$$

Taking into account that the functions $|\Delta_0(\mathbf{r}-\mathbf{d})|$ and $\mathbf{Q}_0(\mathbf{r}-\mathbf{d})$ are translational invariant and satisfy the stationary equation (7.132), one finds that quantities $\mathbf{d}\cdot\nabla|\Delta_0|$ and $(\mathbf{d}\cdot\boldsymbol{\nabla})\,\mathbf{Q}_0$ must satisfy the linearized static equation

$$\nabla^2(\mathbf{d}\cdot\boldsymbol{\nabla}\,|\Delta_0|) - \mathbf{Q}_0^2(\mathbf{d}\cdot\boldsymbol{\nabla}\,|\Delta_0|) - 2\mathbf{Q}_0|\Delta_0|\,(\mathbf{d}\cdot\boldsymbol{\nabla})\,\mathbf{Q}_0$$

$$+\xi^{-2}\,(1-3\,|\Delta_0|^2)\,(\mathbf{d}\cdot\boldsymbol{\nabla}\,|\Delta_0|) = 0 \qquad (7.140)$$

(the vector $\mathbf{d}$ is now assumed to be small). Multiplying Eq. (7.139) by $\lambda_1(\mathbf{d}\cdot\nabla)\,|\Delta|$, and Eq. (7.140) by $\lambda_1|\Delta_1|$, subtracting the first from the second, we obtain

$$\lambda_1 D\,[\Delta_1\nabla^2(\mathbf{d}\cdot\boldsymbol{\nabla}\,|\Delta_0|) - (\mathbf{d}\cdot\boldsymbol{\nabla}\,|\Delta_0|)\,\nabla^2\,|\Delta_1|]$$

$$+\lambda_1\sqrt{1+(2\tau_\varepsilon|\Delta_0|)^2}\,(\mathbf{v}\cdot\boldsymbol{\nabla}\,|\Delta_0|)\,(\mathbf{d}\cdot\boldsymbol{\nabla}\,|\Delta_0|)$$

$$= 2\lambda_1 D\,|\Delta_0|\,\mathbf{Q}_0\,[\,|\Delta_1|\,(\mathbf{d}\cdot\boldsymbol{\nabla})\,\mathbf{Q}_0 - \mathbf{Q}_1\,(\mathbf{d}\cdot\boldsymbol{\nabla})\,|\Delta_0|]. \qquad (7.141)$$

One can see now that the right side of Eq. (7.141) is equal to $D\,[\mathbf{j}_{s1}\,(\mathbf{d}\cdot\boldsymbol{\nabla})\,\mathbf{Q}_0 - \mathbf{Q}_1(\mathbf{d}\cdot\boldsymbol{\nabla})\,\mathbf{j}_0]$. Thus, from the relations (7.136), (7.137), and (7.141) it follows that:

$$\pi L\mathbf{d}\cdot[\mathbf{j}_{s1\infty}\times\mathbf{l}_z] = \lambda_1\int d^3\mathbf{r}\,\frac{\sqrt{1+(2\tau_\varepsilon|\Delta_0|)^2}}{D}\,(\mathbf{v}\cdot\boldsymbol{\nabla}\,|\Delta_0|)\,(\mathbf{d}\cdot\boldsymbol{\nabla}\,|\Delta_0|)$$

$$+\frac{2\lambda_1}{D}\int d^3\mathbf{r}\,\frac{(\mathbf{d}\cdot\mathbf{l}_\varphi)}{\rho}\,\frac{|\Delta_0|^2\mu}{\sqrt{1+(2\tau_\varepsilon|\Delta_0|)^2}}. \qquad (7.142)$$

In deriving Eq. (7.142) the relation

$$\int d\mathbf{r}\,[\Delta_1 \nabla^2 (\mathbf{d}\cdot\boldsymbol{\nabla}|\Delta_0|) - (\mathbf{d}\cdot\boldsymbol{\nabla}|\Delta_0|)\nabla^2|\Delta_1|\,] = 0 \tag{7.143}$$

was used. The quantity μ may be written in the form $\mu = (\mathbf{v}\cdot\mathbf{l}_\varphi)\,\tilde{\mu}$, where $\tilde{\mu}$ is governed by (7.127) and by the electroneutrality condition div $\mathbf{j} = 0$, from which

$$\sigma_n[1+\chi(|\Delta|)]\frac{\partial}{\rho\partial\rho}\rho\frac{\partial\tilde{\mu}}{\partial\rho} + \sigma_n\frac{\partial\chi(|\Delta|)}{\partial\rho}\frac{\partial\tilde{\mu}}{\partial\rho}$$

$$-\left[\frac{\sigma_n[1+\chi(|\Delta|)]}{\rho^2} + \frac{2\lambda_1|\Delta_0|^2}{D\sqrt{1+(2\tau_\varepsilon|\Delta_0|)^2}}\right]\tilde{\mu} = 0. \tag{7.144}$$

Calculating in (7.142) the angle integrals, we arrive at

$$\mathbf{d}\cdot[\mathbf{j}_{s1\infty}\times\mathbf{l}_z] = \lambda_1\mathbf{d}\cdot\mathbf{v}\left\{\int_0^\infty \rho\,d\rho\left(\frac{\partial|\Delta_0|}{\partial\rho}\right)^2 \frac{\sqrt{1+(2\tau_\varepsilon|\Delta_0|)^2}}{D}\right.$$

$$\left. -\int_0^\infty d\rho\,\frac{2|\Delta_0|^2\tilde{\mu}}{\sqrt{1+(2\tau_\varepsilon|\Delta_0|)^2}}\right\}. \tag{7.145}$$

7.3.5. *Effective Conductivity: Results*

Finally, the effective conductivity follows from (7.145) and (7.125):

$$\sigma_{\text{eff}} = \frac{\lambda_1}{B}\left\{\int_0^\infty \rho\,d\rho\left(\frac{\partial|\Delta_0|}{\partial\rho}\right)^2 \frac{\sqrt{1+(2\tau_\varepsilon|\Delta_0|)^2}}{D} + \int_0^\infty d\rho\,\frac{2|\Delta_0|^2\tilde{\mu}}{\sqrt{1+(2\tau_\varepsilon|\Delta_0|)^2}}\right\} \tag{7.146}$$

where

$$\frac{\lambda_1}{B} = \frac{\pi\sigma_n}{4TB}\Delta_{\text{GL}}^2 = \frac{\pi\sigma_n}{4T}\frac{D\pi^3 T_c}{7\zeta(3)}\frac{\xi^{-2}}{B} = \frac{H_{c_2}}{B}\frac{D\pi^4}{28\zeta(3)}\frac{T_c - T}{T_c}. \tag{7.147}$$

Neglecting in (7.144) the small second integral, we get

$$\frac{\sigma_{\text{eff}}}{\sigma_n} = \frac{H_{c_2}}{B}\frac{\pi^5 2^{3/2}}{(7\zeta(3))^{3/2}}\tau_\varepsilon T_c\left(1-\frac{T}{T_c}\right)^{1/2}. \tag{7.148}$$

This result coincides exactly with that of Larkin and Ovchinnikov,[12] obtained by direct solution of the generalized kinetic equation (7.1). Besides its self-sufficient

value, the example considered demonstrates the possibility of using TDGL equations to describe nonequilibrium phenomena in superconductors.

7.4. FLUCTUATIONS

We will consider here some characteristic features of fluctuational corrections to self-consistent treatments of superconductivity, such as GL or BCS theory. This reveals the applicability limits of the self-consistent approach.

7.4.1. Ginzburg's Number

To elucidate the role of fluctuations, we will go back to the free energy functional considered in Sect. 1.2. For simplicity we will perform calculations at $T \gtrsim T_c$ for the normal phase, where the equilibrium value is $\Psi_0 \equiv 0$. Then it is convenient to denote the fluctuating value of the order parameter as Ψ. The fluctuation probability is governed by the expression

$$W \propto \exp(-\delta\mathcal{F}/T), \tag{7.149}$$

where $\delta\mathcal{F}$ is defined by Eqs. (1.46), (1.45), and (1.31), with $F_n^0 = 0$. Since we expect the fluctuations to be small, it is sufficient to keep the second-order expansion terms in the free energy functional:

$$\delta\mathcal{F} = \int_{V_0} \left\{ \alpha|\Psi|^2 + \frac{\hbar^2}{2m_*} \left| \frac{\partial\Psi}{\partial\mathbf{r}} \right|^2 \right\} d^3\mathbf{r}. \tag{7.150}$$

Both terms are positive in (7.150), since $T > T_c$.

Let us now make a Fourier expansion of the fluctuating quantities in the volume V_0 (for simplicity we will take $V_0 \equiv 1$ below):

$$|\Psi(\mathbf{r})| = \sum_{\mathbf{k}} \Psi_{\mathbf{k}} e^{i\mathbf{k}\cdot\mathbf{r}}, \quad \left| \frac{\partial\Psi}{\partial\mathbf{r}} \right| = \sum_{\mathbf{k}} i\mathbf{k}\Psi_{\mathbf{k}} e^{i\mathbf{k}\cdot\mathbf{r}}. \tag{7.151}$$

Since $|\Psi(\mathbf{r})|$ is real, $\Psi_{-\mathbf{k}} = \Psi_{\mathbf{k}}^*$. Substituting (7.151) into (7.150) and integrating over the volume, we find ($\varepsilon_{\mathbf{k}} \equiv \hbar^2\mathbf{k}^2/2m_*$):

$$\delta\mathcal{F} = \sum_{\mathbf{k}} (\alpha + \varepsilon_{\mathbf{k}}) |\Psi_{\mathbf{k}}|^2 \equiv \sum_{\mathbf{k}} \delta\mathcal{F}_{\mathbf{k}}. \tag{7.152}$$

As follows from (7.152), (7.149), and (7.152), fluctuations with different values of $\mathbf{k}$ are statistically independent.

Let us consider now the sum over states (a "partition function") caused by the fluctuations:

$$Z^{fl} = \sum_{\Psi_k} \exp(-\delta\mathcal{F}/T). \tag{7.153}$$

This yields the fluctuational contribution to the free energy of the system:

$$\mathcal{F}^{fl} = -T \ln Z^{fl} = -T \ln \sum_{\Psi_k} \exp\left[\frac{-\sum_k (\alpha + \varepsilon_k) |\Psi_k|^2}{T}\right]. \tag{7.154}$$

Performing straightforward transformations, we obtain:

$$\mathcal{F}^{fl} = -T \ln \prod_k \int_0^\infty \exp\left[-\frac{(\alpha + \varepsilon_k) |\Psi_k|^2}{T}\right] d \operatorname{Im} \Psi_k \, d \operatorname{Re} \Psi_k$$

$$= -T \sum_k \ln \left\{\pi \int_0^\infty \exp\left[-\frac{(\alpha + \varepsilon_k) |\Psi_k|^2}{T}\right] d|\Psi_k|^2\right\}$$

$$= -T \sum_k \ln \frac{\pi T}{(\alpha + \varepsilon_k)} \tag{7.155}$$

[in writing Eq. (7.155) we took into account the relation $\iint d \operatorname{Im} \Psi_k \, d \operatorname{Re} \Psi_k = 2\pi \int |\Psi_k| \, d \, |\Psi_k|$]. To evaluate the role of the order parameter fluctuations, one can calculate the fluctuational contribution to the heat capacity C^{fl}, which is defined via the general relation

$$C = -T (\partial^2 \mathcal{F}/\partial T^2). \tag{7.156}$$

Since in (7.155) in a variation of T the most important contribution comes from the temperature dependence of α, one can write:

$$C^{fl} \approx -T_c \left(\frac{\partial \alpha}{\partial T}\right)_{T_c}^2 \frac{\partial^2 \mathcal{F}^{fl}}{\partial \alpha^2}, \tag{7.157}$$

or, taking into account (7.155):

$$C^{fl} \approx \left[T_c \left(\frac{\partial \alpha}{\partial T} \right)_{T_c} \right]^2 \sum_{\mathbf{k}} \frac{1}{(\alpha + \varepsilon_{\mathbf{k}})^2} = \frac{[T_c(\partial\alpha/\partial T)_{T_c}]^2}{(2\pi)^3} \int \frac{d^3\mathbf{k}}{(\alpha + \varepsilon_{\mathbf{k}})^2}$$

$$= \text{const} \frac{[T_c(\partial\alpha/\partial T)_{T_c}]^{3/2}}{(\hbar^2/2m_{*)}^{3/2}} |\varepsilon|^{-1/2}, \varepsilon \equiv \left(\frac{T - T_c}{T_c} \right), \tag{7.158}$$

where the constant is a number ~ 1. [One should note that the long-wavelength fluctuations play the most important role in (7.158). Also, hereafter we will use the absolute values of $\delta T \to |T - T_c|$. The symmetry of the behavior of fluctuating quantities within this Ornstein–Zernicke description can be confirmed by direct calculations at $T \lesssim T_c$.]

We can now compare C^{fl} with some characteristic equilibrium value, such as the jump in heat capacity $\delta C = C_S - C_N$ at the transition point from a superconducting to a normal state. Using (7.156), (1.40), and (1.46), one can calculate

$$\delta C = \frac{2[T_c(\partial\alpha/\partial T)_{T_c}]^2}{\beta T_c}. \tag{7.159}$$

Thus the fluctuations are small if

$$Gi \equiv \frac{C^{fl}}{\delta C} \simeq \frac{m^3\beta^2 T_c}{\hbar^6(\partial\alpha/\partial T)_{T_c}} << |\varepsilon| << 1. \tag{7.160}$$

As follows from (7.160), the mean-field theory has an applicability range only at small values of the parameter *Gi* (usually called the *Ginzburg number).* Fortunately, the *Gi* number is very small for conventional, low temperature superconductors, and thus the mean-field theory is well applicable even very close to T_c. Indeed, using for "clean" superconductors the values of $(\partial\alpha/\partial T)_{T_c}$ and β, which follow from (1.183) and (1.188), we find

$$Gi_{\text{clean}} \simeq \left(\frac{T_c}{\varepsilon_F} \right)^4 \tag{7.161}$$

[in writing (7.161) we used (1.188), in which the density N of electrons may be expressed as $N = 2[(4/3)\pi p_F^3]/(2\pi\hbar)^3 = p_F^3/3\pi^2\hbar^3$].Usually $(T_c/\varepsilon_F) \sim 10^{-3}$,so that Ginzburg's number is incredibly small for superconductors. To estimate *Gi* in the case of "dirty" superconductors, we again need the microscopic values of phenomenological parameters (1.36) and (1.38). For these values we will compare Eqs. (1.48) and (1.51) with (7.45) and (7.102), respectively. It follows then [for completeness we also provide here the relationship between Ψ and Δ, which is analogous to (1.187) for the "dirty" case] that:

$$\left(\frac{\partial\alpha}{\partial T}\right)_{T_c} = \frac{6}{\pi}\frac{\hbar}{\tau_{\text{imp}}}\frac{m}{p_F^2} = \frac{2\hbar}{\pi m D}, \tag{7.162}$$

$$\frac{(\partial\alpha/\partial T)_{T_c}}{\beta} = \frac{2\pi^2}{7\varsigma(3)}\frac{\tau_{\text{imp}}}{\hbar}N, \tag{7.163}$$

$$\Psi(\mathbf{r}) = (\pi/4)^{1/2}(N\tau_{\text{imp}}/\hbar T_c)^{1/2}\Delta(\mathbf{r}), \tag{7.164}$$

and for *Gi* we obtain

$$Gi_{\text{dirty}} \simeq \left(\frac{\hbar}{\tau_{\text{imp}}}\right)^3 \frac{T_c}{\varepsilon_F^4}, \tag{7.165}$$

which is also very small, so that usually the range of temperature fluctuations is not of practical importance. It is worth mentioning once again that the smallness of the *Gi* parameter permits us to apply the Ginzburg–Landau-type approach to the description of superconductors. At the same time, it is wrong to conclude that the smallness of *Gi* rules out the possibility of experimental observation of fluctuational phenomena in superconductors: fluctuations may reveal themselves in one- or two-dimensional samples.[41–43] We will treat different mechanisms of resistivity fluctuations in the next section.

7.4.2. Paraconductivity

Let us suppose that $T \gtrsim T_c$ and there is a constant electric field **E** applied to the metal. One can expect then that spontaneous fluctuations of the order parameter create droplets of finite superfluid density, which will be accelerated by the electric field, raising the normal conductivity σ_n. Actually, the change of the conductivity is small: $\delta\sigma << \sigma_n$, but the temperature dependence $\delta\sigma(T)$ is peculiar and thus could be detected. Fluctuations of the order parameters may lead also to the specific temperature dependence of the heat capacity in small superconducting particles.[44]

Following Schmid,[45] we first treat the average (in thermodynamic sense) current, coupled to the applied field, via the relation:

$$\langle \mathbf{j} \rangle = \sigma_S \mathbf{E}, \tag{7.166}$$

where (still hypothetical) conductivity equals

$$\sigma_S = \frac{e_*^2 N_S \tau^0}{m_*}. \tag{7.167}$$

In Eq. (7.167) N_S is the density of electrons fluctuating between normal and superconducting states: $N_S = \langle |\Psi|^2 \rangle$, and τ^0 is the lifetime of electrons in the

superconducting state. As noted, fluctuations at different wavelengths that contribute to the free energy (7.152) are statistically independent. In view of that*:

$$\langle |\Psi_{\mathbf{k}}|^2 \rangle = \frac{\int_0^\infty |\Psi_{\mathbf{k}}|^2 \exp\left[-(\alpha+\varepsilon_{\mathbf{k}})|\Psi_{\mathbf{k}}|^2/T\right] d|\Psi_{\mathbf{k}}|^2}{\int_0^\infty \exp\left[-(\alpha+\varepsilon_{\mathbf{k}})|\Psi_{\mathbf{k}}|^2/T\right] d|\Psi_{\mathbf{k}}|^2} = \frac{T}{(\alpha+\varepsilon_{\mathbf{k}})}. \tag{7.168}$$

To obtain the value of τ^0 one should consider TDGL equation (7.43). In the fluctuational regime, $\tau_\varepsilon |\Delta| << 1$. Thus all the nonlinear terms, including contributions from the vector potential, as well as the phonon term $P(|\Delta|)$, could be neglected, yielding

$$\eta_0\left(\frac{\partial}{\partial t} + i\frac{e_*}{\hbar}\varphi\right)\Psi - \left(\alpha - \frac{\hbar^2}{2m_*}\nabla^2\right)\Psi = 0, \tag{7.169}$$

where $\eta_0 = [T_c(\partial\alpha/\partial T)_T]\,(\pi/8T_c) = (4mD)^{-1}$ for "dirty" superconductors. Since in the linear approximation the relaxation time should not depend on the electric field applied, one can discard the scalar potential φ in (7.169), and obtain for the Fourier component $\Psi_{\mathbf{k}}$ the equation:

$$\eta_0 \frac{\partial}{\partial t}\Psi_{\mathbf{k}} = -(\varepsilon_{\mathbf{k}} + \alpha)\,\Psi_{\mathbf{k}}. \tag{7.170}$$

For the relaxation time of fluctuating components it follows then that:

$$\tau_{\mathbf{k}}^0 = \frac{\eta_0}{\varepsilon_{\mathbf{k}} + \alpha}. \tag{7.171}$$

To find the value of σ_S (7.167), one should compute

$$N_S\tau^0 = \sum_{\mathbf{k}} \langle|\Psi_{\mathbf{k}}|^2\rangle\tau_{\mathbf{k}}^0. \tag{7.172}$$

*Actually, there is a degeneracy in the system described by Eq. (7.152): the states with $\mathbf{k}$ and $-\mathbf{k}$ are physically identical. Thus in expression (7.149) for the fluctuational probability of $|\Psi_{\mathbf{k}}|^2$, the value of $\delta\mathcal{F}$ doubles. This causes the value of amplitude $\langle |\Psi_{\mathbf{k}}|^2 \rangle$ in (7.168) to be two times smaller: $\langle |\Psi_{\mathbf{k}}|^2 \rangle = T/2\,(\alpha + \varepsilon_{\mathbf{k}})$ (cf., e.g., Ref. 38). To use the explicit form (7.168), one should perform in expressions like (7.183) and (7.184) the subsequent integration over $\mathbf{k}$ over a single hemisphere of its values (of. Ref. 46).

As was demonstrated by Aslamasov and Larkin,[47] the result of this summation depends on the sample's dimensionality. Indeed, since the minimal distance (the "unit length") in this scheme of calculation is restricted by the coherence length $\xi(T)$, the values of $\{\mathbf{k}_x, \mathbf{k}_y, \mathbf{k}_z\}$ in (7.172) are restricted by the condition

$$k_i \left(\equiv \frac{2\pi}{L_i} n \right) \lesssim \xi(T)^{-1}, \tag{7.173}$$

(n is an integer) and when the characteristic length L_i along the i-axis is smaller than $\xi(T)$, only the term $n = 0$ contributes substantially ($|\Psi_{\mathbf{k}}|^2$ is homogeneous along that direction). Thus for bulk samples

$$\sigma_S \propto N_S \tau^0 = \int_0^\infty \frac{d^3\mathbf{k}}{(2\pi)^3} \frac{T\gamma_0}{(\alpha + \varepsilon_{\mathbf{k}})^2} \propto |\varepsilon|^{-1/2} \equiv \left| \frac{T_c - T}{T_c} \right|^{-1/2}, \tag{7.174}$$

while for thin films

$$\sigma_S \propto \frac{1}{L} \int_0^\infty \frac{d^2\mathbf{k}}{(2\pi)^2} \frac{T\gamma_0}{(\alpha + \varepsilon_{\mathbf{k}})^2} \propto |\varepsilon|^{-1} \equiv \left| \frac{T_c - T}{T_c} \right|^{-1}, \tag{7.175}$$

so that in samples with smaller dimensionality, the fluctuations near T_c are more pronounced. For the one-dimensional case:

$$\sigma_S \propto |\varepsilon|^{-3/2} \equiv \left| \frac{T_c - T}{T_c} \right|^{-3/2}. \tag{7.176}$$

This phenomenon is called *paraconductivity* and was first described theoretically by Aslamasov and Larkin.[47] The Green's function technique was used and the diagram for the current–current correlation function (shown in Fig. 7.2a) was considered. Later Maki[48,49] and Thompson[50] took into account another diagram (shown in Fig. 7.2b), which yields a different contribution that is dominant in some conditions. We will consider both mechanisms without referring to these slightly mysterious diagrams, but to the much more transparent TDGL scheme.

7.4.3. Aslamasov–Larkin Mechanism

The physics of the fluctuations outlined by Eq. (7.166) is rather transparent. At the same time, an important question still remains open, namely, how to justify Eq. (7.166) itself. The fact is that in thermodynamic equilibrium the superconducting current has a form (1.54), which is associated with the vector $\mathbf{Q} \propto \mathbf{v}_s$ rather than with the vector $\mathbf{E}$. To proceed with this problem one should bear in mind the relation (1.51). In view of the gauge $\mathbf{A} = 0$, adopted earlier for Eq. (7.169), it

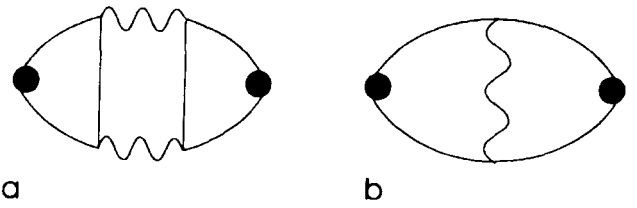

Figure 7.2. Diagrams leading to Aslamasov–Larkin (a) and Maki–Thompson (b) contributions.

becomes clear that both the modulus $|\Psi|$ and the phase θ of the wave function are fluctuating, so that $\langle \nabla\theta \rangle$ is proportional to $\mathbf{E}$.*

One can rewrite Eq. (1.51) in the form:

$$\mathbf{j}_S = -\frac{ie_*\hbar}{2m_*}\langle \Psi^*\nabla\Psi - \Psi\nabla\Psi^* \rangle = \sum_{\mathbf{k}} \frac{e_*\mathbf{k}}{m_*}\langle |\Psi_{\mathbf{k}}|^2 \rangle. \tag{7.177}$$

Following Abrikosov,[38] one can represent $\Psi_{\mathbf{k}}$ in the form

$$\Psi_{\mathbf{k}} = \Psi_{\mathbf{k}}^{(0)} + \Psi_{\mathbf{k}}^{(1)} \tag{7.178}$$

and then use the TDGL equation in the form (7.169) to derive the value of $\Psi_{\mathbf{k}}^{(1)}$ based on the known value of $\Psi_{\mathbf{k}}^{(0)}$ (7.168). For a homogeneous electric field, $\varphi = -\mathbf{E}\cdot\mathbf{r}$. Since the field $\mathbf{E}$ is a static one, only low-frequency fluctuations contribute to the response, so one can omit the time derivative in (7.169). Taking into account that at the Fourier transformation $\mathbf{r}\Psi(\mathbf{r}) \doteq i\,(\partial\Psi_{\mathbf{k}}/\partial\mathbf{k})$, one obtains from (7.169):

$$\Psi_{\mathbf{k}}^{(1)} = -\frac{\gamma_0 e_*}{\alpha + \varepsilon_{\mathbf{k}}}\mathbf{E}\cdot\left(\frac{\partial\Psi_{\mathbf{k}}^{(0)}}{\partial\mathbf{k}}\right), \tag{7.179}$$

so that

$$\mathbf{j} = \frac{T\gamma_0 e_*^2}{m_*^2}\sum_{\mathbf{k}} \mathbf{k}\frac{\mathbf{k}\cdot\mathbf{E}}{(\alpha+\varepsilon_{\mathbf{k}})^3} \equiv \mathbf{E}\sum_{\mathbf{k}}\sigma_{AL}(\mathbf{k}). \tag{7.180}$$

We will focus our attention on the most interesting case of "dirty" superconductors. Considering first the case of bulk samples, one can write

*A good insight into this problem was presented by Abrahams and Woo[51]

$$\sigma_{AL}(3D) = \int \frac{d^3\mathbf{k}}{(2\pi)^3}\,\sigma_{AL}(\mathbf{k}). \tag{7.181}$$

Using the values for α and η_0 (see 7.169, 7.162, and 1.37), we arrive at

$$\sigma_{AL}(\mathbf{k}) = 2\pi e^2\xi^4 k^2 \cos^2\theta / [\,|\varepsilon| + (\xi k)^2]^3, \tag{7.182}$$

where $\xi = (\pi D/8T_c)^{1/2}$, $\hbar \equiv 1$, and θ is the angle between the vectors $\mathbf{k}$ and $\mathbf{E}$. For the bulk sample we obtain

$$\sigma_{AL}(3D) = \int_0^1 d\cos\theta \int \frac{k^2 dk}{4\pi^2}\,\sigma_{AL}(\mathbf{k}) = (e^2/32\xi)\,|\varepsilon|^{-1/2} \tag{7.183}$$

in accordance with Refs. 50 and 52. For thin films, the result is completely independent of the material parameters

$$\sigma_{AL}(2D) = \frac{1}{L}\int \frac{d^2\mathbf{k}}{(2\pi)^2}\,\sigma_{AL}(\mathbf{k}) = \frac{1}{L}\int_0^{\pi} \frac{d\theta}{2\pi}\int \frac{dk^2}{4\pi}\,\sigma_{AL}(\mathbf{k})$$

$$= (e^2/16L)\,|\varepsilon|^{-1} \tag{7.184}$$

and is determined only by the value of the film's thickness and the closeness to the critical temperature.* We should note here the accord between (7.174) and (7.175) and (7.183) and (7.184), respectively. It is interesting to mention that in the two-dimensional case, a consideration[45] based on (7.166) and (7.167) provides the same numerical coefficient as the proper diagrammatic treatment![47]

7.4.4. Maki–Thompson Mechanism

In the preceding consideration of the mechanism of paraconductivity we referred to the superfluid component of the current (7.177), which resulted in a term proportional to $\mathbf{E}$.

Meanwhile,[53] an expression of the same type follows directly from the interference term in the nonequilibrium current (7.114). Indeed, one can rewrite (7.114) in the fluctuational limit $|\Delta| << \gamma$ as

*We refer to the following values of integrals

$$\int_0^{\infty} dx x^4 (1+x^2)^{-3} = (3\pi/16) \text{ and } \int_0^{\infty} dx x (1+x)^{-3} = 1/2,$$

arising in the calculation of (7.183) and (7.184).

$$\mathbf{j}_{\text{int}} = \mathbf{E}\left\{\frac{\gamma}{2T_c}\sigma_n\left[K\left(\frac{|\Delta|}{\sqrt{|\Delta|^2+\gamma^2}}\right) - E\left(\frac{|\Delta|}{\sqrt{|\Delta|^2+\gamma^2}}\right)\right]\right\}$$

$$\cong \mathbf{E}\sigma_n \frac{\pi}{8T_c\gamma}|\Delta|^2. \tag{7.185}$$

The physical meaning of this term is, as discussed in Sect. 7.2, in the interference between normal and superfluid motions of the electrons. As a result of the interference, the normal motion described by the relation $\mathbf{j}_n = \sigma_n\mathbf{E}$, acquires an addition (cf. 7.172):

$$\langle \mathbf{j}_{\text{int}} \rangle = \mathbf{E}\sigma_n \frac{\pi}{8T_c\gamma}\langle|\Delta|^2\rangle = \mathbf{E}\left(\sigma_n \frac{\pi}{8T_c}\right)\sum_{\mathbf{k}} \frac{\langle|\Delta(\mathbf{k})|^2\rangle}{\gamma_{\mathbf{k}}}. \tag{7.186}$$

In accordance with Sect. 7.2, the parameter γ, which smears out the BCS singularity in the single-particle density of states, should be taken as the maximum of possible depairing factors related to $1/2\tau_\varepsilon$, $Dk^2/2$, τ_S^{-1}, etc. Taking $\gamma \simeq Dk^2/2$ (cf. Ref. 4), and using (7.164) for the case of "dirty" superconductors, we arrive at

$$\langle \mathbf{j}_{\text{int}} \rangle = \mathbf{E}\left(\frac{\sigma_n}{DN\tau_{\text{imp}}}\right)\sum_{\mathbf{k}} \frac{\langle|\Psi_{\mathbf{k}}|^2\rangle}{k^2}. \tag{7.187}$$

Substituting (7.167) into (7.187), one can confirm that the resulting expression has exactly the same form*

$$\langle \mathbf{j}_{\text{int}} \rangle = \mathbf{E}\frac{e^2\pi}{2}\sum_{\mathbf{k}} \frac{1}{[\varepsilon + (\xi k)^2]\,k^2}, \tag{7.188}$$

as was used by Thompson.[50] It was pointed out in Ref. 53 that this leads to the Maki–Thompson conductivity σ_{MT}. Moving from (7.188) to integration over all values of $\mathbf{k}$ (as was done in Ref. 50), we will get for the bulk sample:

$$\sigma_{MT}^{\text{dirty}}(3D) = (e^2/8\xi)\,|\varepsilon|^{-1/2}, \tag{7.189}$$

which means that in this case

$$\sigma_{MT}^{\text{dirty}}(3D) = 4\sigma_{AL}^{\text{dirty}}(3D). \tag{7.190}$$

*To make the comparison easier, in expression (19) of Thompson,[50] one should replace the derivative of the digamma function by its numerical value: $\psi'(1/2) = \pi^2/2$.

**In view of the footnote on the degeneracy of the system (Sect. 7.4.2), the values of σ_{MT} should be twice as small as those given for both the 3D and 2D cases.

For the samples of lower dimensionality, the value of $\sigma_{MT}^{\text{dirty}}$, which follows from (7.188), is divergent: for thin films one should deal with expressions of the type

$$\sigma_{MT}(2D) = \frac{e^2}{4L} \int_{k(\to 0)}^{\infty} \frac{dk}{k[(T - T_c)/T_c + (\xi k)^2]}, \tag{7.191}$$

which demands a low-momentum cutoff $k_{\min} = k_0$. In view of this factor, one can obtain[50]:

$$\sigma_{MT}^{\text{dirty}}(2D) = 2\sigma_{AL}^{\text{dirty}}(2D) \ln \{ [\xi^{-2}|\varepsilon| + k_0]/k_0 \}. \tag{7.192}$$

Generally, the cutoff may be caused by internal or external pair breaking, owing for example, to inelastic energy relaxation ($Dk^2/2 \to \tau_\varepsilon^{-1}$), or the influence of the magnetic field [$Dk^2/2 \to (4eDH/c)(n + 1/2)$, $n = 0, \pm 1, \pm 2, \ldots$]. In the case of a small cutoff ($\xi^2 k_0^2 << |T - T_c|/T_c$), the value of (7.191) may exceed (7.183) by an order of magnitude. In the opposite limit of strong pair breaking (or very close to T_c), σ_{MT} tends to zero, as follows from (7.190). One might expect such behavior since in the gapless regime the interference current components disappear in the general TDGL description. It is important to note that the regularization procedure for the case of restricted dimensionality is not trivial, even in absence of external pair breaking: Keller and Korenman[54] and Patton[55] came to the conclusion that the dominant contribution to this cutoff mechanism comes from the nonlinear self-influence of the fluctuations of the pair field. The related scattering of electrons is more effective here than the inelastic single-particle scattering. Later the corresponding process got an analog in localization theory.[56] from where the electron phase relaxation time τ_ϕ (so that $k_0^2 \equiv \pi/8\xi^{-2}T_c\tau_\phi$) migrated into this area. We will not consider this problem in more detail, nor different limiting cases for more complicated physical situations (see, in particular, Refs. 57–91). Instead, we refer the reader to the very interesting discussion presented by Reizer.[92]

References

1. M. P. Kemoklidze and L. P. Pitaevskii, Dynamics of a superfluid Fermi gas at finite temperatures, *Sov. Phys. JETP* **25**(6), 1036–1049 (1967) *[Zh. Eksp. i Teor. Fiz.* **52**(6), 1556–1569 (1967)].
2. A. A. Golub, Dynamic properties of short superconducting filaments, *Sov. Phys. JETP* **44**(1), 178–181 (1976) *[Zh. Eksp. i Teor. Fiz.* **71**[1(7)], 314–347 (1976)].
3. L. Kramer and R. J. Watts-Tobin, Theory of dissipative current-carrying states in superconducting filaments, *Phys. Rev. Lett.* **40**(15), 1041–1043 (1978).
4. G. Schön and V. Ambegaokar, Collective modes and nonequilibrium effect in current-carrying superconductors, *Phys. Rev. B.* **19**(7), 3515–3528 (1979).
5. C.-R. Hu. New set of time-dependent Ginzburg–Landau equations for dirty superconductors, *Phys. Rev. B* **21**(7), 2775–2798 (1980).
6. R. G. Watts-Tobin, Y Krähenbilhl, and L. Kramer, Nonequilibrium theory of dirty, current-carrying superconductors: Phase-slip oscillations in narrow filaments near T_c, *J. Low Temp. Phys.* **42**(5/6), 459–501 (1981).

7. S. N. Artemenko and A. F. Volkov, Electric field and collective oscillations in superconductors, *Sov. Phys. Uspekhi* **22**(5), 295–310 (1979) [*Usp. Fiz. Nauk* **128**(1), 3–30 (1979)].
8. V. F. Elesin and Yu. V. Kopaev, Superconductors with excess quasiparticles, *Sov. Phys. Uspekhi* **24**(2), 116–141 (1981) [*Usp. Fiz. Nauk* **133**(2), 259–307 (1981)].
9. A. Schmid, in *Nonequilibrium Superconductivity, Phonons and Kapitza Boundaries,* K. E. Gray, ed., pp. 423–480, Plenum, New York (1981).
10. J. A. Pals, K. Weiss, P. M. T. van Attekum, R. E. Horstman, and J. Wolter, Nonequilibrium superconductivity in homogeneous thin films, *Phys. Rep.* **80**(4), 323–390 (1982).
11. G. M. Eliashberg, Inelastic electron collisions and nonequilibrium stationary states in superconductors, *Sov. Phys. JETP* **34**(3), 668–676 (1972) [*Zh. Eksp. i Teor. Fiz.* **61** [3(9)], 1254–1272 (1971)].
12. A.I. Larkin, Yu. N. Ovchinnikov, Nonlinear effects during the motion of vortices in superconductors, *Sov. Phys. JETP* **46**(1), 155–162 (1977) *[Zh. Eksp. i Teor. Fiz.* **73**[1(7)], 299–312 (1977)].
13. I. E. Bulyzhenkov and B. I. Ivlev, Nonequilibrium phenomena in superconductor junctions, *Sov. Phys. JETP* **47**(1), 115–120 (1978) *[Zh. Eksp. i Teor. Fiz.* **74**(1), 224–235 (1978)].
14. V. G. Valeev, G. F. Zharkov, and Yu. A. Kukharenko, in *Nonequilibrium superconductivity,* V. L. Ginzburg, ed., pp. 203–282, Nova Science, New York (1988).
15. V. P. Galaiko, Microscopic theory of resistive current states in superconducting channels, *Sov. Phys. JETP* **41**(1), 108–114 (1975) [*Zh. Eksp. i Teor. Fiz.* **68**(1), 223–237 (1975)].
16. V. P. Galayko, Features of the volt-ampere characteristics and oscillations of the electric potential in superconducting channels, *Sov. Phys. JETP* **44**(1), 141–148 (1976) [*Zh. Eksp. i Teor. Fiz.* **71**[1(7)], 273–285 (1976)].
17. U. Eckern, A. Schmid, M. Schmutz, and G. Schon, Stability of superconducting states out of thermal equilibrium, *J. Low Temp. Phys.* **36** (5/6), 643–687 (1979).
18. S. R. De Groot, *Thermodynamics of Irreversible Processes,* pp. 195–207, North–Holland, Amsterdam (1951).
19. J.-J. Chang, in *Nonequilibrium Superconductivity,* D. N. Langenberg and A. I. Larkin, eds., pp. 453–492, North-Holland, Amsterdam (1986).
20. J.-J. Chang and D. J. Scalapino, Kinetic equation approach to nonequilibrium superconductivity, *Phys. Rev. B.* **15**(5), 2651–2670 (1977).
21. K. D. Usadel, Generalized diffusion equation for superconducting alloys, *Phys. Rev. Lett.* **25**(8), 507–508(1970).
22. A. M. Gulian, G. F. Zharkov, and G. M. Sergoyan, Interference current in nonequilibrium superconductors, *Sov. Phys. JETP* **65**(1), 107–111 (1987) [*Zh. Eksp. i Teor. Fiz.* **92**(1), 190–199 (1987)].
23. Yu. N. Ovchinnikov, Properties of thin superconducting films in high-frequency fields, Sov. *Phys. JETP* **32**(1), 72–78 (1971) [*Zh. Eksp. i Teor. Fiz* **59**(7), 128–141 (1970)].
24. Yu. A. Ovchinnikov and A. R. Isahakyan, Electromagnetic field absorption in superconducting films, *Sov. Phys. JETP* **47**(1), 91–94 (1978) [*Zh. Eksp. i Teor. Fiz.* **74**(1), 178–183 (1978)].
25. L. P. Gor'kov and G. M. Eliashberg, The behavior of a superconductor in a variable field, Sov. *Phys. JETP* **28**(4), 1291–1297 (1969) [*Zh. Eksp. i Teor. Fiz.* 56(4), 1297–1308 (1969)].
26. A. G. Aronov, Yu. M. Gal"perin, V. L. Gurevich, and V. I. Kozub, in *Nonequilibrium Superconductivity,* D. N. Langenberg and A. I. Larkin, eds., pp. 325–376, North-Holland, Amsterdam (1986).
27. A. L. Shelankov, Dragging of normal components by the condensate in nonequilibrium superconductors, *Sov. Phys. JETP* **51**(6), 1186–1193 (1980) [*Zh. Eksp. i Teor. Fiz* **78**(6), 2359–2379 (1980)].
28. V. F. Elesin, V. A. Kashurnikov, and A. V. Kharlamov, Boundary condition for nonequilibrium superconductors, Sov. *J. Low Temp. Phys.* **12** (7), 392–395 (1986) [*Fiz. Nizk. Temp.* **12**(7), 694–700 (1978)].

29. L. P. Gor'kov and G. M. Eliashberg, Generalization of the Ginzburg–Landau equations for non-stationary problems in the case of alloys with paramagnetic impurities, *Sov. Phys. JETP* **27**(3), 328–334 (1968) [*Zh. Eksp. i Teor. Fiz.* **54**(2), 612–625 (1968)].
30. G. Eilenberger, Thermodynamic fluctuations of the order parameter in type-Il superconductors near the upper critical field H_{c2}, *Phys. Rev.* **164**(20), 628–635 (1967).
31. D. S. Fisher, Flux-lattice melting in thin-film superconductors, *Phys. Rev. B,* **22**(3), 1190–1199 (1980).
32. P. L. Gammel, L. F. Schneemeyer, J. V. Waszczak, and D. J. Bishop, Evidence from mechanical measurements for flux-lattice melting in single-crystal $YBa_2Cu_3O_7$ and $Bi_{2.2}Sr_2Ca_{0.8}Cu_2O_8$, *Phys. Rev. Lett.* **61**(14), 1666–1669(1988).
33. M. F. Schmidt, N. E. Israeloff, and A. M. Goldman, Vortex-lattice melting in Nb, *Phys. Rev. Lett.* **70**(14), 2162–2165 (1993).
34. M. Born, Thermodynamics of crystals and melting, *J. Chem. Phys.* **7**, 591–603 (1939).
35. V. l. Reentovich and S. B. Rutkevich, On melting temperature of the Abrikosov vortex lattice, *Sov. J. Low Temp. Phys.* **17**(4), 266–268 (1966) [*Fiz. Nizk. Temp.* **17**(4), 504–508 (1991)].
36. H. M. Carruzzo and C. C. Yu, First order premelting transition of vortex lattices, *Phil. Mag. B* **77**(4), 1001–1010(1998).
37. A. A. Abrikosov, On the magnetic properties of superconductors of the second group, *Sov. Phys. JETP* **5**(6), 1174–1182 (1957) [*Zh. Eksp. i Teor. Fiz.* **32**(6), 1443–1452 (1957)].
38. A. A. Abrikosov, *Fundamentals of the Theory of Metals,* pp. 407–460, North-Holland, Amsterdam (1988).
39. N. B. Kopnin, Theory of the resistive state of superconductors (Thesis Sov. Doct. Degree, Chernogolovka, 1983).
40. N. B. Kopnin and L. P. Gor'kov, Vortex motion and resistivity of type-11 superconductors in a magnetic field, *Sov. Phys. Uspekhi* **18**(7), 496–513 (1975) [*Usp. Fiz. Nauk* **116**(3), 413–448 (1975)].
41. J. S. Shier and D. M. Ginzberg, Superconducting transitions of amorphous bismuth alloys, *Phys. Rev.* **147**(1), 384–391 (1966).
42. R. E. Glower, Ideal resistive transition of a superconductor, *Phys. Lett. A* **25**(7), 542–544 (1967).
43. M. Strongin, O. F. Kramer, J. Crow, R. S. Thompson, and H. L. Fine, "Curie-Weiss" behavior and fluctuation phenomena in the resistive transitions of dirty superconductors, *Phys. Rev. Lett.* **20**(17), 922–925(1968).
44. V. V. Shmidt, Phase transition in superconductors of small size, *JETP Lett.* **3**(3), 91–93 (1966) [*Pis'ma v Zh. Eksp. i Teor. Fiz.* **3**(3), 141–145 (1966)].
45. A. Schmid, The resistivity of a superconductor in its normal state, Z *Phys.* **215**, 210–212 (1968).
46. E. M. Lifshitz and L. P. Pitaevskii, *Statistical Physics,* Part 1, pp. 471–478, Pergamon, Oxford (1980).
47. L. G. Aslamasov and A. I. Larkin, Effect of fluctuations on the properties of a superconductor above the critical temperature, Sov. *Phys. Solid State* **10**(4), 875–880 (1968) [*Fiz. Tverd. Tela* **10**(4), 1104–1111 (1968)].
48. K. Maki, The critical fluctuation of the order parameter in type-II superconductors, *Progr. Theor. Phys.* ***39(4),*** 897–911 (1968).
49. K. Maki, Critical fluctuation of the order parameter in a superconductor, *Progr. Theor. Phys.* **40**(2), 193–200(1968).
50. R. S. Thompson, Microwave, flux flow, and fluctuation resistance of dirty type-II superconductors, *Phys. Rev. B* **1**(1), 327–333 (1970).
51. E. Abrahams and J. W. Woo, Phenomenological theory of the rounding of the resistive transition of superconductors, *Phys. Lett. A* **27** (2), 117–118 (1968).
52. H. Schmidt, The onset of superconductivity in the time–dependent Ginzburg–Landau theory, *Z. Phys.* **216**, 336–345(1968).

53. A. M. Gulian, Time-dependent Ginzburg–Landau equations for finite-gap superconductors and the problem of paraconductivity, *Phys. Lett. A* **200**, 201–204 (1995).
54. J. Keller and V. Korenman, Fluctuation-induced conductivity of superconductors above the transition temperature: Regularization of the Maki diagram, *Phys. Rev. B* **5**(11), 4367–4375 (1972).
55. B. E. Patton, Fluctuation theory of the superconducting transition in restricted dimensionality, *Phys. Rev. Lett.* **27**(19), 1273–1276 (1971).
56. P. A. Lee and T. V. Ramakrishnan, Disordered electric systems, *Rev. Mod. Phys.* **57**(2) 287–337 (1985).
57. C. Caroli and K. Maki, Fluctuations of the order parameter in type-II superconductors. I. Dirty limit. *Phys. Rev.* **159**, 306–315 (1967).
58. C. Caroli and K. Maki, Fluctuations of the order parameter in type-II superconductors. II. Pure limit. *Phys. Rev.* **159**, 316–326 (1967).
59. K. D. Usadel, The influence of a static magnetic field on the fluctuation superconductivity, *Z. Phys.* **227**, 260–270(1969).
60. K. D. Usadel, Fluctuations in superconductors above T_c in the high field region, *Phys. Lett. A* **29**(9), 501–502(1969).
61. G. Bergman, Superconducting fluctuations in a magnetic field, Z *Phys.* **225**, 430–443 (1969).
62. E. Abrahams, M. Redi, and J. W. Woo, Effect of fluctuations on electric properties above the superconducting transition, *Phys. Rev. B* **1** (1), 208–213 (1970).
63. K. Kajimura and N. Mikoshiba, Fluctuations in the resistive transition in aluminum films, *J. Law Temp. Phys.* **4**(3), 331–348 (1971).
64. E. Abrahams, R. E. Prange, and M. J. Stephen, Effect of a magnetic field on fluctuations above T_c, *Physica* **55**, 230–233 (1971).
65. R. S. Thompson, The influence of magnetic fields on the paraconductivity due to fluctuations in thin films, *Physica* **55**, 296–302 (1971).
66. R. A. Craven, G. A. Thomas, and R. D. Parks, Fluctuation induced conductivity of a superconductor above the transition temperature, *Phys. Rev. B* **7**(7), 157–165 (1973).
67. K. Maki, Thermoelectric power above superconducting transition, *J. Low Temp. Phys.* **14**(5/6), 419–432(1974).
68. L. G. Aslamasov and A. A. Varlamov, Fluctuation conductivity in intercalated superconductors, *J. Low Temp. Phys.* **38**(2), 223–241 (1980).
69. A. I. Larkin, Reluctance of two-dimensional systems, *JETP Lett.* **31**(4), 219–223 (1980) [*Pis'ma Zh. Eksp. i Teor. Fiz.* **31**(4), 239–243(1980)].
70. S. Hikami and A. I. Larkin, Magnetoresistance of high-temperature superconductors, *Mod. Phys. Lett. B* **2**(5) 693–698 (1988).
71. A. G. Aronov, S. Hikami, and A. I. Larkin, Zeeman effect on magnetoresistance in high-temperature superconductors, *Phys. Rev. Lett.* **62**(8), 965–968 (1989).
72. K. Maki and S. Thompson, Fluctuation conductivity of high-temperature superconductors, *Phys. Rev. B* **39**(4), 2767–2774 (1989).
73. V. V. Gridin, T. W. Krause, and W. R. Datars, Two-dimensional paraconductivity in superconducting $Bi_{1.6}Pb_{0.4}Sr_2Ca_2Cu_3O_y$, *J. Appl. Phys.* **68**, 675–678 (1990).
74. S.-K. Yip, Fluctuations in an impure unconventional superconductor, *Phys. Rev. B* **41**(13), 2612–2615(1990).
75. A. G. Aronov and H. S. Hikami, Skew-scattering effect on the Hall–conductance fluctuation in high-temperature superconductors, *Phys. Rev. B* **41**, 9548–9550 (1990).
76. Q. Y. Ying and H. S. Kwok, Kosterlitz–Thouless transition and conductivity fluctuations in Y–Ba–Cu–0 thin films, *Phys. Rev. B* **42**, 2242–2245 (1990).
77. S. Ullah and A. T. Dorsey, Critical fluctuations in high–temperature superconductors and the Ettingshausen effect, *Phys. Rev. Lett.* ***65*** (16), 2066–2069 (1990).

78. J. B. Bieri, K. Maki, and R. S. Thompson, Non-local effect in magnetoconductivity of high-T_c superconductors, *Phys. Rev. B* **44**(9), 4709–4711 (1991).
79. V. A. Gasparov, Berezinskii–Kosterlitz–Thouless transition and fluctuation paraconductivity in $Y_1Ba_2Cu_3O_7$ single crystal films. *Physica C* **178,** (1991) 449–455.
80. J. B. Bieri and K. Maki, Magnetoresistance of high-T_c superconductors in the fluctuation regime, *Phys. Rev. B* **42**(7), 4854–4856 (1990).
81. R. Hopfengärtner, B. Hensel, and G. Saeman-Ischenko, Analysis of the fluctuation-induced excess conductivity of epitaxial $YBa_2Cu_3O_7$ films: Influence of a short-wavelength cutoff in the fluctuation spectrum, *Phys. Rev. B* **44**(2), 741–749 (1991).
82. S. Ullah and A. T. Dorsey, Effect of fluctuations on the transport, *Phys. Rev. B* **44**(1) 262–273 (1991).
83. M. Ausloos, F. Gillet, Ch. Laurent, and P. Clippe, High-temperature crossover in paraconductivity of granular $Y_1Ba_2Cu_3O_{7-x}$, *Z. Phys. B* **84,** 13–16(1991).
84. A. B. Kaiser and G. Mountjoy, Consistency with anomalous electron–phonon interactions of the thermopower of high-T_c superconductors, *Phys. Rev. B* **43**(7), 6266–6269 (1991).
85. M. Anderson and Ö, Rapp, Magnetoresistance measurements on polycrystalline $YBa_2Cu_3O_{7-\delta}$, *Phys. Rev. B* **44**(14), 7722–7725 (1991).
86. A. A. Varlamov and D. V. Livanov, The effect of fluctuations on the Hall-effect in high T_c superconductors, *Phys. Lett. A* **157**(8/9), 519–522 (1991).
87. A. A. Varlamov and D. V. Livanov, The effect of fluctuations on thermomagnetic phenomena in high T_c superconductors, *Phys. Lett. A* **157**(8/9), 523–526 (1991).
88. K. Semba, T. Ishii, and A. Matsuda, Absence of the Zeeman effect on the Maki–Thompson fluctuation in magnetoresistance of $YBa_2Cu_3O_7$ single crystals, *Phys. Rev. Lett.* **67**(6), 769–772 (1991).
89. B. N. Narozhny, Fluctuation conductivity in strong-coupling superconductors, *Sov. Phys. JETP,* **77**(2), 301–306 (1993) [*Zh. Eksp. i Teor. Fiz.,* **104**(2), 2825–2837 (1993)].
90. W. Holm, Yu. Eltsev, and Ö. Rapp, Paraconductivity along the *a* and *b* axes in $YBa_2Cu_3O_{7-\delta}$ single crystals, *Phys. Rev. B* **51**(17), 11992–11995 (1995).
91. J. Axnäs, W. Holm, Yu. Eltsev, and Ö, Rapp, Sign change of *c*-axis magnetoconductivity in $YBa_2Cu_3O_{7-\delta}$ single crystals, *Phys. Rev. Lett.* **77**(11), 2280–2283 (1996).
92. M. Yu. Reizer, Fluctuation conductivity above the superconducting transition: Regularization of the Maki–Thompson term, *Phys. Rev. B* **45**(22), 12949–12958 (1992).

8

A Longitudinal Electric Field and Collective Modes

8.1. LONGITUDINAL ELECTRIC FIELD

The appearance of new physical quantity μ introduces a new characteristic length into the theory of nonequilibrium superconductivity. Recall that in Chap. 1, in discussing the static description of superconductors, two characteristic lengths were mentioned—the penetration length of the magnetic field λ_L, and the coherence length $\xi(T)$, which characterize the spatial variation of the order parameter modulus. A new characteristic value related to the presence of μ determines the penetration length of the longitudinal electric field $\mathbf{E}$ in a nonequilibrium superconductor. We emphasize that the field $\mathbf{E}$ is not incorporated in the equilibrium theory, so such a feature does not arise there.

8.1.1. Tinkham Expression for the Gauge-Invariant Potential

As was shown in Section 3.3, the Fourier transform of the charge density in superconductors has the form* (here $e = 1$):

$$\rho_\omega(\mathbf{k}) = -N(0)\left[2\varphi_\omega(\mathbf{k}) + \frac{1}{2}\,\mathrm{Tr}\int_{-\infty}^{\infty}\frac{d\varepsilon}{4\pi}\,\frac{d\Omega_p}{4\pi}\,\hat{g}_{\varepsilon\varepsilon-\omega}(\mathbf{p},\mathbf{k})\right]. \tag{8.1}$$

Using the expressions for spectral functions given here, one can obtain a formula in the quasi-classical limit

*To avoid misunderstanding, we emphasize the difference between notations for the Fourier component of the charge density $\rho_\omega(\mathbf{k})$ and the function $\rho(\omega_k)$ related to the photon density of states.

$$\rho = -2N(0)\left\{\varphi + \frac{1}{4}\int_{-\infty}^{\infty} d\varepsilon\left[N_1(f_1+f_2) + \overline{N}_1(f_1-f_2)\right]\right\} \tag{8.2}$$

which is explicitly gauge invariant. We recall now the gauge-invariant potential μ:

$$\mu = \varphi + \frac{\dot{\theta}}{2}, \tag{8.3}$$

where 0 is the phase of the complex order parameter

$$\Delta = |\Delta|\exp(i\theta). \tag{8.4}$$

In the gauge transformation (1.140), θ transforms as $\theta \to \theta + \chi$. The condition of the superconductor's charge neutrality taking into account (8.2) provides the relation (in the first order in $|\Delta|\varepsilon_F$):

$$\varphi = -\frac{1}{4}\int_{-\infty} d\varepsilon\left[N_1(f_1+f_2) + \overline{N}_1(f_1-f_2)\right]. \tag{8.5}$$

Writing (8.5) in the gauge $\theta = 0$, using the relation (8.3) and iterating over φ, one finds in the first approximation

$$\mu = -\int_{|\Delta|}^{\infty} (n_\varepsilon - n_{-\varepsilon})\, d\varepsilon. \tag{8.6}$$

This is a familiar expression for the experimentally observed potential μ, introduced by Tinkham.[1] This formula, as is clear from its derivation, is only the first approximation to more general equations of the theory.* At the same time, treating $(-\dot{\theta}/2)$ in the expression (8.3) as the chemical potential of the paired electrons and referring to φ as the chemical potential of normal electrons, one can interpret μ, in general, as the difference between the potentials of the normal and superfluid components of the electron liquid.

8.1.2. Normal Metal—Superconductor Interface

As in the cases of lengths λ_L and $\xi(T)$, we turn to the Ginzburg–Landau equations (generalized for nonstationary problems) and study the process of current

*Using the substitution $\xi = \sqrt{\varepsilon^2 - |\Delta|^2}\,\mathrm{sign}\varepsilon$, expression (8.6) may be presented in the form $\mu = -\int_0^\infty d\xi(n_\varepsilon - n_{-\varepsilon})\xi/\varepsilon$.. Because the value of ξ/ε is commonly identified with the excitation's charge in superconductors (see Sec. 1.1), usually the gauge-invariant potential is related to the charge imbalance.[2]

flow across the boundary between the superconductor and a normal metal (this problem was considered by Rieger et al.[3]).

We will consider first the case of a gapless superconductor. The equation for an order parameter in this case has the form (see Sect. 2.3):

$$-12\tau_0\left(\frac{\partial}{\partial t}+2i\varphi\right)\Delta+\xi^2(T)\nabla^2\Delta+\left(1-\frac{|\Delta|^2}{\Delta_0^2}\right)\Delta=0, \tag{8.7}$$

where

$$\tau_0=(2\tau_{\text{„}}\Delta_0^2)^{-1}, \quad \Delta_0^2=2\pi^2(T_c^2-T^2). \tag{8.8}$$

Let the superconductor occupy the region $x>0$, and the normal metal $x<0$ (Fig. 8.1). The equation for $|\Delta|$ in the stationary case of interest coincides with the static Ginzburg–Landau equation:

$$\xi^2(T)\frac{\partial^2|\Delta(x)|}{\partial x^2}+|\Delta(x)|\left[1-\frac{|\Delta(x)|^2}{\Delta_0^2}\right]=0. \tag{8.9}$$

Its solution, obeying the boundary condition $|\Delta(x=0)|=0$, is the function

$$|\Delta(x)|=\Delta_\infty\tanh\frac{x}{\sqrt{2}\,\xi(T)}, \tag{8.10}$$

where Δ_∞ is the value of the order parameter modulus $|\Delta(x)|$ at $x=\infty$. The imaginary part of Eq. (8.7) coincides with the continuity equation, which has the form

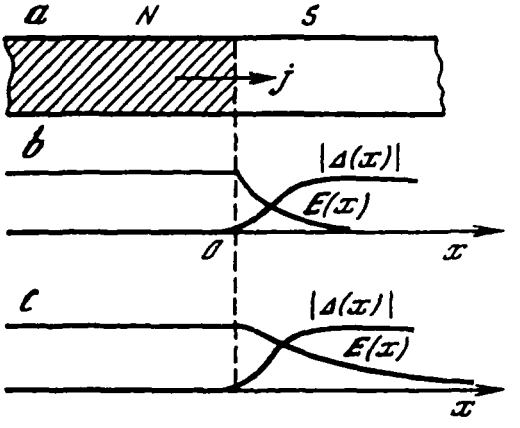

Figure 8. 1. The *NS*-junction investigated, (a) Current flowing across the *NS*-boundary; (b) the electric field **E** and the order parameter modulus $|\Delta|$ as functions of the *x-coordinate* for the current flow in the gapless superconductors; and (c) the same for finite-gap superconductors.

$$12\sigma\mu \frac{|\Delta(x)|^2}{\Delta_0^2} = \xi^2(T) \frac{\partial j_s}{\partial x} = -\xi^2(T) \frac{\partial j_n}{\partial x} \tag{8.11}$$

in the gauge $\dot{\theta} = 0$ [in this gauge, according to Eq. (8.3), $\mu = \varphi$]. In deriving (8.11), the expression for total current density in a superconductor was used:

$$j = j_n + j_s, \tag{8.12}$$

subject to (2.121):

$$j_s = \frac{\sigma_n}{4ie\tau_0\Delta_0^2}\left(\Delta^* \frac{\partial \Delta}{\partial x} - \Delta \frac{\partial \Delta^*}{\partial x}\right). \tag{8.13}$$

Using now the relation (2.121) for j_n:

$$j_n = \sigma_n E = -\sigma_n \frac{\partial \varphi}{\partial x} = -\sigma_n \frac{\partial \mu}{\partial x} \tag{8.14}$$

and the dependence (8.10) for $|\Delta(x)|$, one finds at $x > 0$ the equation for the potential μ:

$$12 \tanh^2\left[\frac{x}{\xi(T)\sqrt{2}}\right]\mu = \xi^2(T) \frac{\partial^2 \mu}{\partial x^2}. \tag{8.15}$$

We will not seek the explicit solutions of Eq. (8.15).* The form of this equation itself shows that the potential μ and the related electric field **E** descend at a distance an order of $\xi(E)$. Hence the characteristic descendence length of the electric field (usually denoted as l_E) for gapless superconductors is of the order

$$l_E \sim \xi(T). \tag{8.16}$$

8.1.3. New Characteristic Length in Superconductors

We will estimate now l_E for finite-gap superconductors. To tackle this problem, we have to use the set of dynamic Ginzburg–Landau-type equations for pure superconductors, which are derived in Sect. 7.1. Separating in (7.45) the real and imaginary parts in analogy with (8.9) and (8.11), one obtains:

$$-\frac{\pi}{8T_c}\sqrt{1 + (2\tau_\varepsilon|\Delta|)^2}\,\frac{\partial|\Delta|}{\partial t} + \frac{\pi}{8T_c} D(\nabla^2 - \mathbf{Q}^2)|\Delta|$$

*This solution is described by a hypergeometric function.[4]

$$+\left[\frac{T_c - T}{T_c} - 7\zeta(3)\frac{(|\Delta|^2 + 2\mu^2)}{8(\pi T_c)^2}\right]|\Delta| = 0, \tag{8.17}$$

$$\frac{2|\Delta|^2}{\sqrt{1 + (2\tau_\varepsilon|\Delta|)^2}}\mu - D\,\mathrm{div}(|\Delta|^2\mathbf{Q}) = 0. \tag{8.18}$$

We emphasize that in the present case the continuity equation

$$\mathrm{div}\,\mathbf{j} + \dot{\rho} = 0 \tag{8.19}$$

and Eq. (8.18) are independent. Also, using the expressions (7.111) to (7.114) for the current $\mathbf{j}$, and considering the stationary case, when $\partial|\Delta|/\partial t \equiv 0$, one finds an equation for the potential μ in the form*

$$\frac{2|\Delta|^2}{\sqrt{1 + (2\tau_\varepsilon|\Delta|)^2}}\mu - D\frac{4T}{\pi}\frac{\partial^2\mu}{\partial x^2} = 0. \tag{8.20}$$

Because we are interested in the case of finite-gap superconductors, we can put in (8.20)

$$\tau_\varepsilon|\Delta| >> 1. \tag{8.21}$$

(Recall that τ_ε^{-1} in 8.20 is the energy damping of single-electron excitations, which in the case of interest must be significantly less than the gap $|\Delta|$ in the electron energy spectrum.) Thus (8.20) may be presented in the form

$$l_E^2\frac{\partial^2\mu}{\partial x^2} = \mu, \tag{8.22}$$

where

$$l_E = \sqrt{D\tau_\varepsilon\frac{4T}{\pi|\Delta|}}. \tag{8.23}$$

Hence the penetration depth of an electric field into the superconductor l_E in the vicinity of T_c exceeds the length of the energy relaxation of electron excitations,

$$l_E >> l_\varepsilon\ (\equiv\sqrt{D\tau_\varepsilon}), \tag{8.24}$$

which in its turn may be substantially larger than $\xi(T)$ and λ_L (Fig. 8.1).**

*We neglect here the contribution provided by the interference current, since the parameter $|\Delta|/T$ is considered small.

**For example, in aluminum $\tau_\varepsilon \sim 10^{-8}$ s (see Table 10.1 in Sect. 10.2) and thus in a pure metal $l_E \sim 1$mm.

Because Eq. (8.23) contains $|\Delta(T)|$ in the denominator, $r_E \to \infty$ at $T \to T_c$, and hence the electric field penetrates further and further into the bulk superconductor. Thus a natural transition from a superconducting to a normal state occurs at $T = T_c$.

Concluding this section, we would like to emphasize that in accordance with definition (8.3), which is the basic one for the value μ, both the single-particle electron excitations and the Cooper condensate contribute to the creation of the electric field in superconductors. It would be wrong to state that the potential μ arises as a consequence of the branch population imbalance only, as would follow from Eq. (8.6). This expression was derived in a fixed gauge and is a consequence of the assumptions made in Sect. 8.1. Note also that in thermodynamic equilibrium $\mu = 0$—this value corresponds to the absolute minimum of the free energy.

8.2. CARLSON–GOLDMAN MODES

8.2.1. Damping of Collective Oscillations

The existence of weakly decaying collective excitations in superconductors came under discussion immediately after the appearance of the BCS microscopic theory. In particular, the weakly damping oscillations of the order parameter, which have a soundlike spectrum in a neutral Fermi liquid, were discussed by Bogoljubov (see, e.g., Ref. 5) and Anderson.[6,7] Later it was realized that these oscillations are connected with the longitudinal vibrations of electron density. So it became necessary to account for the Coulomb interaction. The Coulomb interaction shifts these oscillations into the range of plasma frequency. Consequently, the specific superconducting characteristics cannot be important to these oscillations, because the scale of superconducting energies is much less than the plasma one.

In the two-fluid hydrodynamics of superfluid helium, certain kinds of weakly damping collective excitations are known.[8] Among them the first, second, and fourth sounds represent three-dimensional oscillations with soundlike spectra.

In superfluid helium, the first sound is connected with the density oscillations of normal and superfluid components. In the charged superfluid system, the frequency of these oscillations, along with the Bogoljubov–Anderson modes, would be displaced toward the plasma frequency region. The same occurs with the fourth sound, which is connected with the oscillations of the superfluid component. The second sound represents the oscillations of temperature (entropy), not the density oscillations of the electron liquid and, in principle, might be detected in superconductors. However, as the investigations of Ginzburg[9] and Bardeen[10] have shown, the damping of the second sound, is very large in practically any real experimental conditions.

The appearance of the potential μ (and of the related electric field) in superconductors brings into existence a new type of sound mode that has no analogy in

superfluid helium. Such collective oscillations, reported first by Carlson and Goldman,[11] reveal themselves in the high-frequency range

$$\omega >> \tau_\varepsilon^{-1}. \tag{8.25}$$

During such oscillations the total current density equals zero, i.e., the normal and superconducting currents are oppositely directed. The zero value of the total current and hence of the magnetic field, makes it possible for these oscillations to exist in the depth of a superconductor, because there are now no restrictions related to the Meissner effect. With the Carlson–Goldman oscillations, the longitudinal electric field

$$\mathbf{E} = -\nabla\mu + \frac{\partial \mathbf{Q}}{\partial t}, \tag{8.26}$$

appears in the superconductor, although the value of $|\mathbf{E}|$ is small: $E << |\nabla\mu|$; this ensures the weak damping of oscillations.

8.2.2. Dispersion of the Charge-Imbalance Mode

A simple description of the Carlson–Goldman oscillating mode, which is based on the generalized dynamic equation (8.18), was introduced by Schmid[12] and Schön.[13] We will reproduce this approach in some detail. In the limit of finite-gap superconductors, Eq. (8.18) takes the form

$$-\frac{1}{\tau_\varepsilon}\mu + \frac{1}{|\Delta|} D \operatorname{div}(|\Delta|^2 \mathbf{Q}) = 0. \tag{8.27}$$

The dynamic equation (8.27) was obtained on the assumption of small characteristic frequencies

$$\omega\tau_\varepsilon << 1. \tag{8.28}$$

In the opposite to the (8.28) limit, it may be rewritten as

$$-\frac{\partial \mu}{\partial t} + \frac{1}{|\Delta|} D \operatorname{div}(|\Delta|^2 \mathbf{Q}) = 0. \tag{8.29}$$

As before, we assume the condition $\omega << |\Delta|$, which was used in deriving (8.27). Taking into account expressions (7.113) for $\mathbf{j}_s$ and (7.114) for $\mathbf{j}_n$, and also the above-mentioned relation

$$\mathbf{j}_s + \mathbf{j}_n = 0, \tag{8.30}$$

we find from (8.29) a dispersion equation[12,13] for the Carlson–Goldman mode

$$\omega_q = -\frac{1}{2} i\Gamma \pm \sqrt{a^2 q^2 - \Gamma^2/4}, \tag{8.31}$$

which corresponds to propagation of the longitudinal wave $\exp\{-i(\omega_q t - qx)\}$ with the velocity a and the damping Γ:

$$a^2 = \frac{N_s}{N} \frac{4T}{\pi|\Delta|} \frac{v_F^2}{3}, \qquad \Gamma = \frac{N_s}{N} \frac{1}{\tau_{\text{imp}}}. \tag{8.32}$$

We note that the velocity of propagation of the Carlson–Goldman mode is greater than the velocity of the second sound by the factor $(4T/\pi|\Delta|)^{1/2}$.

8.3. STABILITY AND BREAKING OF COOPER PAIRS

We will consider now the instabilities that may occur in superconductors, driven by the external perturbation from equilibrium, assuming that the possible instabilities rise so fast that any inelastic scattering process could be neglected. In the instability time domain, the distribution function may then be considered as a stationary one, so that the main evolution takes place in the system of paired electrons.

8.3.1. Collisionless Dynamics for Spatially Homogeneous Modes

Since Cooper pairs of a superconductor constitute a bound state of two fermions having identical masses, the diagram technique of Bethe and Salpeter,[14] developed in 1951 for relativistic quantum field theory, is an effective tool for describing the excited Cooper pair field. The original method[14] considers the two-particle Green's function, which describes the spectrum of collective oscillations in the case of a two-particle system (e.g., the energy spectrum of positronium in quantum field theory[15]). A very similar approach was used by Vdovin in the case of triplet pairing[16] and later by Aronov and Gurevich,[17] who considered the two-particle Green's function for a system of singlet pairs. In the latter case attention was focused on the vertex function

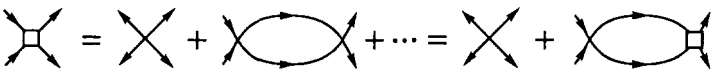

(8.33)

in the pairing channel on the basis of the effective four-fermion BCS Hamiltonian (1.104).

An alternative although simpler approach was carried out by Gal'perin et al.,[18,19] who used the generalized kinetic equations in the collisionless limit. We

will develop the latter approach, starting from the technique of energy-integrated Green's functions accepted in this book.

In a collisionless regime, when the characteristic frequencies of the system's evolution are much higher than the reciprocal time of the energy relaxation of electrons:

$$\omega >> \tau_{\varepsilon}^{-1}, \tag{8.34}$$

one can omit the terms K_{ij} in (7.15) that correspond to inelastic collisions. In this limit Eq. (4.1), which describes spatially homogeneous cases, can be rewritten in the form

$$\begin{pmatrix} \omega g & (2\varepsilon - \omega) f \\ (2\varepsilon - \omega) f^{+} & -\omega \bar{g} \end{pmatrix}_{\varepsilon\varepsilon-\omega} = \begin{pmatrix} (-f\Delta^{*} + \Delta f^{+}) & (g\Delta - \Delta \bar{g}) \\ (-\bar{g}\Delta^{*} + \Delta^{*} g) & (-f^{+}\Delta - \Delta^{*} f) \end{pmatrix}_{\varepsilon\varepsilon-\omega}. \tag{8.35}$$

We are discussing here the time-dependent problem, which can involve the branch-imbalance potential μ (8.6) due to the asymmetry between n_{ε} and $n_{-\varepsilon}$. As was argued by Schmid,[12] it is simpler to solve spatially homogeneous time-dependent problems in the ξ- rather than in ε-representation. To take an advantage of the ξ-representation* we will multiply both parts of (8.35) by $\delta(\varepsilon - \xi)$ with a subsequent integration over ε. Multiplying the result by $\exp(-i\omega t)$, integrating over ω (which brings up the time variable t), and using the relations (4.56) to (4.58), we can rewrite the system of equations in (8.35) in a very simple form

$$i \frac{\partial g(\xi, t)}{\partial t} + 2\,\mathrm{Re}[\Delta^{*}(t) f(\xi, t)] = 0, \tag{8.36}$$

$$\left(i \frac{\partial}{\partial t} - 2\xi \right) f(\xi, t) + 2\Delta(t) g(\xi, t) = 0, \tag{8.37}$$

which coincides with Gal'perin et al.[18,19] The self-consistency equation (7.14) for $\Delta(t)$ acquires the form

$$\Delta(t) = \frac{\lambda}{4\pi i} \int_{-\omega_D}^{\omega_D} d\xi f(\xi, t). \tag{8.38}$$

The collisionless equations (8.36) to (8.38) were originally derived by Volkov and Kogan[22] to discuss quantum relaxation of the order parameter. Since we have omitted the $\hat{H}_1$-term in (8.35), which in the supposed case of $\mathbf{v}_s = 0$ is equivalent to

*In principle, one can investigate collective modes of nonequilibrium superconductors in ε-representation, as was demonstrated for the case of superfluid ^{3}He.[20,21]

the gauge $\varphi \equiv 0$, the time derivative of the steady-state value of the phase equals $\dot{\theta}_0 = 2\mu$ (cf. 8.3), so that the proper function $f(\xi, t)$, as well as $\Delta(t)$, will acquire an additional time-dependent factor $\{\exp(2i\mu t)\}$. For our purpose it is not necessary to keep these factors explicitly, and we will remove them. The influence of external fields (e.g., related to the action of $\hat{H}_1$ or tunneling) is taken into account by considering the function $n_{\pm\varepsilon}$ as nonequilibrium.

8.3.2. Dispersion Equation

We will denote the steady-state solutions of (8.36) to (8.38) as $g(\xi), f(\xi)$, and Δ. In view of (8.38), it is meaningful to introduce the function $\aleph(\xi)$:

$$f(\xi) \equiv i\Delta\aleph(\xi). \tag{8.39}$$

As follows from (8.36), $\aleph(\xi)^* = \aleph(\xi)$. For the function $g(\xi)$ we have from (8.37):

$$g(\xi) = i\xi\aleph(\xi). \tag{8.40}$$

Provided the self-consistency equation (8.38) has the usual form (see, e.g., 1.153) in equilibrium, the function $\aleph(\xi)$ should obey the relation:

$$\aleph(\xi)^{(eq)} = 2\pi \frac{\tanh(\varepsilon_{\mathbf{p}}/2T)}{\varepsilon_{\mathbf{p}}}, \tag{8.41}$$

where $\varepsilon_{\mathbf{p}} = (\xi^2 + |\Delta|^2)^{1/2}$. The generalization of (8.41) for a nonequilibrium steady-state is straightforward:

$$\aleph(\xi) = 2\pi \frac{(1 - 2n_{\mathbf{p}})}{\varepsilon_{\mathbf{p}}}. \tag{8.42}$$

To confirm (8.42), one can refer to the definition of propagators (3.91) and (3.92) and directly integrate $G(\varepsilon, \mathbf{p}) = G_{11}^{+-} + G_{11}^{-+}$ over the frequency variable ε. For the states with $n_{\mathbf{p}} = n_{-\mathbf{p}}$ (e.g., for isotropic distributions) this results in (8.40) and (8.42) up to the sign.*

We will now look for the solutions of Eqs. (8.36) to (8.38) in the form:

$$g(\xi, t) = g(\xi) + \delta g(\xi, t), \tag{8.43}$$

$$f(\xi, t) = f(\xi) + \delta f(\xi, t), \tag{8.44}$$

$$\Delta(t) = \Delta + \delta\Delta(t). \tag{8.45}$$

*In Sect. 4.3 we noted the sign difference between the Eliashberg and Keldysh definitions of these functions.

One can consider Δ in (8.45) as a real value function, so that Re $g(\xi)$ = Re $f(\xi) = 0$. From (8.36) and (8.43) it follows also that Re $\delta g(\xi, t) \equiv 0$. Thus, using the notation ($'$) and ($''$) for real and imaginary parts of the functions [e.g., $\Delta^*(t) = \Delta'(t) - i\Delta''(t)$], we can write

$$\frac{\partial(\delta g'')}{\partial t} + 2\Delta\aleph(\delta\Delta'') - 2\Delta(\delta f') = 0, \tag{8.46}$$

$$\frac{\partial(\delta f')}{\partial t} - 2\xi(\delta f'') - 2\xi\aleph(\delta\Delta') + 2\Delta(\delta g'') = 0, \tag{8.47}$$

$$\frac{\partial(\delta f'')}{\partial t} + 2\xi(\delta f') - 2\xi\aleph(\delta\Delta'') = 0, \tag{8.48}$$

Equation (8.38) for $\Delta(t)$ reduces to

$$\delta\Delta' = -\frac{\lambda}{4\pi i}\int_{-\omega_D}^{\omega_D} d\xi(\delta f''), \tag{8.49}$$

$$\delta\Delta'' = \frac{\lambda}{4\pi i}\int_{-\omega_D}^{\omega_D} d\xi(\delta f'). \tag{8.50}$$

After simple algebra one can obtain from (8.46) to (8.48) for the Fourier components $(\delta f')_\omega$ and $(\delta f'')_\omega$:

$$(4\varepsilon^2 - \omega^2)(\delta f')_\omega - 4\varepsilon^2\aleph(\delta\Delta'')_\omega - 2i\omega\xi\aleph(\delta\Delta')_\omega = 0, \tag{8.51}$$

$$(4\varepsilon^2 - \omega^2)(\delta f'')_\omega + 4\xi^2\aleph(\delta\Delta')_\omega - 2i\omega\xi\aleph(\delta\Delta'')_\omega = 0. \tag{8.52}$$

Substitution of (8.51) and (8.52) into the Fourier transforms of (8.49) and (8.50), respectively, yields a coupled system of homogeneous equations. Setting the determinant to zero, we obtain the dispersion equation for oscillating modes in the form:

$$\left(\frac{\lambda}{4\pi}\int_{-\omega_D}^{\omega_D} d\xi\,\frac{2\omega\xi}{\omega^2 - 4\varepsilon^2}\,\aleph\right)^2 =$$

$$\left(k + \frac{\lambda}{4\pi}\int_{-\omega_D}^{\omega_D} d\xi\,\frac{\omega^2}{\omega^2 - 4\varepsilon^2}\,\aleph\right)\left(k + \frac{\lambda}{4\pi}\int_{-\omega_D}^{\omega_D} d\xi\,\frac{\omega^2 - 4\Delta^2}{\omega^2 - 4\varepsilon^2}\,\aleph\right), \tag{8.53}$$

where

$$k = 1 - \frac{\lambda}{4\pi} \int_{-\omega_D}^{\omega_D} d\xi \aleph. \tag{8.54}$$

In the case of particle-hole symmetry, the left-hand side of (8.53) vanishes, and we arrive at the equation first obtained in Ref. 17. It should be noted that the equation

$$k = 0 = 1 - \frac{\lambda}{2} \int_{-\omega_D}^{\omega_D} d\xi \frac{1 - 2n_p}{\sqrt{\xi^2 + \Delta^2}}, \tag{8.55}$$

coincides with the self-consistency equation for the gap Δ [later in this section we assume Δ is a real parameter, determined for the nonequilibrium steady-state case via Eq. (8.55)].

8.3.3. *Stability Analysis for Particle-Hole Symmetry*

Consider first the case of a normal metal. At $\Delta = 0$, the dispersion equation (8.53) for $n(\xi)$ reduces to

$$1 = -\lambda \int d\xi \frac{1 - 2n(\xi)}{\omega - 2\xi}. \tag{8.56}$$

For a given function $n(\xi)$ Eq. (8.56) has complex roots: $\omega = \omega' + i\omega''$. If the roots are located in the lower half-plane, then the state is stable. At the action of the external fields the function $n(\xi)$ varies, so that at certain values of external parameters the root may shift from one half-plane to another (which corresponds to the change of sign of ω''). The boundary of stability is determined by its crossing of the real axis. This occurs when the root becomes real. Separating the imaginary part of (8.56), using the relation ($\mathcal{P}$ indicates the principal part)

$$\frac{1}{x + i0} = \frac{\mathcal{P}}{x} - i\pi\delta(x), \tag{8.57}$$

we obtain the condition that regulates the change of the sign of the imaginary part of (8.56):

$$n\left(\frac{\omega'}{2}\right) = \frac{1}{2}. \tag{8.58}$$

If the energy ξ is counted from the reference point at which $n(\xi) = \frac{1}{2}$, one obtains from (8.58) an unstable mode $\omega = 0$. The real part of Eq. (8.56) transforms correspondingly to the equation

$$1 = \lambda \int_{-\omega_D}^{\omega_D} \frac{d\xi}{\xi} [1 - 2n(\xi)], \tag{8.59}$$

which coincides in equilibrium with the equation determining the critical temperature T_c [cf. (1.154) and (1.156)], or, in more general terms, the stability boundary of the nonequilibrium state.

To consider the superconducting state in the case of symmetry between the electron-hole branches, we will rewrite Eq. (8.53) (with the left-hand side equal to zero) in the form:

$$[k + (4\Delta^2 - \omega^2)\kappa]\,[k - \omega^2\kappa] = 0, \tag{8.60}$$

where the functions k and κ are defined by the relations

$$\kappa(\omega) = -\lambda \int_{\Delta}^{\infty} \frac{1 - n_\varepsilon - n_{-\varepsilon}}{\sqrt{\varepsilon^2 - \Delta^2}} \frac{d\varepsilon}{\omega^2 - 4\varepsilon^2}, \tag{8.61}$$

$$k = 1 - \lambda \int_{\Delta}^{\omega_D} \frac{d\varepsilon}{\sqrt{\varepsilon^2 - \Delta^2}} [1 - n_\varepsilon - n_{-\varepsilon}]. \tag{8.62}$$

As mentioned, the equation $k = 0$ coincides with the equation for stationary values of the nonequilibrium gap. Substituting $k = 0$ into (8.60), we see that this equation may be decomposed into several co-factors. Two ofthem yield the roots $\omega = 0$, $\omega = \pm 2\Delta$, and two others lead to the equation

$$\kappa(\omega) = 0. \tag{8.63}$$

Hence the stability boundary may be determined by Eq. (8.63). As in the case of normal metal, we will substitute $\omega \to \omega' + i\omega''$ in this equation, and then the stability boundary is determined by the change of the sign of ω''. Separating the imaginary part in (8.63) [using Eq. (8.57)], one finds that the stability boundary is determined by either one of the equations:

$$\omega' = 0, \tag{8.64}$$

$$n\left(\frac{\omega'}{2}\right) = \frac{1}{2}. \tag{8.65}$$

The real part of Eq. (8.63) [together with the condition (8.64) or (8.658)] determines the values of the external parameters at which the instability in the nonequilibrium state occurs. In case of (8.64) this equation has the form

$$\int_{\Delta}^{\infty} d\varepsilon \frac{(1 - n_{\varepsilon} - n_{-\varepsilon})}{\varepsilon^2\sqrt{\varepsilon^2 - \Delta^2}} = 0, \tag{8.66}$$

while in (8.65) it follows from (8.63) and (8.61) that:

$$\int_{\Delta}^{\infty} d\varepsilon \frac{1}{\sqrt{\varepsilon^2 - \Delta^2}} \frac{1 - n_{\varepsilon} - n_{-\varepsilon}}{4\varepsilon^2 - \omega_i'^2} = 0 \tag{8.67}$$

[the index i in (8.67) enumerates the solutions of Eq. (8.65)]. For Eqs. (8.66) and (8.67) to have solutions, the function $1 - n_{\varepsilon} - n_{-\varepsilon}$ must be of a variable sign. If in the function $(n_{\varepsilon} + n_{-\varepsilon})$ in the substantial for integration range does not exceed the value 1 then the superconducting state is stable.

If the function $1 - n_{\varepsilon} - n_{-\varepsilon}$ changes its sign only once, then Eq. (8.67) has no solution. The stability boundary is determined by Eq. (8.66). In this region of stability, nondamping collective modes with frequencies $\omega^2 < 4\Delta^2$ may exist in the system. They are defined by the following dispersion equation

$$\int_{\Delta}^{\infty} d\varepsilon \frac{1}{\sqrt{\varepsilon^2 - \Delta^2}} \frac{1 - n_{\varepsilon} - n_{-\varepsilon}}{4\varepsilon^2 - \omega'^2} = 0, \tag{8.68}$$

which determines the frequency of undamped modes ($\omega' < 2\Delta$). This instability, as seen from (8.66) and (8.68), is connected with the vanishing of the frequency of one of these collective modes.

If the function $1 - n_{\varepsilon} - n_{-\varepsilon}$ changes sign more than once, then solutions of (8.67) may also appear. In such a case, the stability boundary is defined, naturally, by the mode of the largest increment.

8.3.4. *Instability at Branch Imbalance*

Let us now consider the case of $n_{\varepsilon} \neq n_{-\varepsilon}$. In this case the left-hand side of Eq. (8.53) is nonzero:

$$\int_{-\omega_D}^{\omega_D} d\xi \frac{2\omega\xi}{\omega^2 - 4\varepsilon^2} \aleph = -\int_{\Delta}^{\omega_D} d\varepsilon \frac{2\omega}{\omega^2 - 4\varepsilon^2} (n_{\varepsilon} - n_{-\varepsilon}) \neq 0, \tag{8.69}$$

as is the value of μ (8.6). Applying Eq. (8.55) twice to (8.53), one can reduce the latter to the form

$$1 - \frac{\lambda}{2}\int_{-\omega_D}^{\omega_D} d\xi \frac{1 - 2n_p}{\tilde{\xi} \pm [(\omega/2)^2 - \Delta^2]^{1/2}} \frac{\tilde{\xi}}{\varepsilon} = 0, \tag{8.70}$$

which is valid for both superconducting and normal states. In writing down this equation we took into account the fact that the presence of the potential μ in the system of normal excitations shifts the reference origin according to*

$$\tilde{\xi} \equiv \tilde{\xi}_p = \xi + \mu, \tag{8.71}$$

so that

$$\varepsilon \equiv \varepsilon_p = \sqrt{\tilde{\xi}^2 + \Delta^2}. \tag{8.72}$$

Separating, as earlier, the imaginary part of (8.70), one can obtain at the instability point (the vanishing value of ω'') the equation:

$$n\left\{\tilde{\xi} = \mp[(\omega')^2/4 - \Delta^2]^{1/2}\right\} = 1/2, \tag{8.73}$$

determining the frequency ω'. For the function

$$n_p = \left(\exp\frac{\varepsilon_p - \mu\,\mathrm{sign}\tilde{\xi}_p}{T} + 1\right)^{-1} \tag{8.74}$$

it follows that:

$$\omega' = \mp 2\mu, \tag{8.75}$$

$$\omega'' = \frac{2}{\pi}[(T - T_c) - \Delta(\mu)]. \tag{8.76}$$

Substituting (8.73) into (8.55) and expanding in terms of small quantities Δ/T and μ/T, one can obtain:

$$\Delta^2 = \Delta_{eq}^2 - 2\mu^2, \tag{8.77}$$

where Δ_{eq} is the equilibrium value of the gap at the temperature T. Near T_c for this quantity one can find either from (7.115) for "dirty" superconductors or (in agreement with Anderson's theorem) from (1.39), (1.183), (1.187), and (1.188) for the "pure" case the same value:

$$\Delta_{eq}(T) = \left[\frac{8\pi^2 T_c}{7\zeta(3)}\right]^{1/2}[T_c(T - T_c)]^{1/2} \approx 3.09\,[T_c(T - T_c)]^{1/2}. \tag{8.78}$$

As follows from (8.77), at the maximum value of μ**:

$$\mu_{max} = \Delta_{eq}/\sqrt{2} \tag{8.79}$$

*Actually, the quantities ξ and ε are related via the integral relation[12]: $\xi = \int_0^\infty d\varepsilon' N_1(\varepsilon') - \mu$, which in the case of negligible pair breaking yields $\varepsilon = [\mathrm{sign}(\xi + \mu)]\sqrt{(\xi + \mu)^2 + \Delta^2}$ [our definition of $\mu = -\int_{-\infty}^{\infty} d\xi(\xi/\varepsilon)n_p$ differs from that in Ref. 12 by sign].

**The same value for μ follows from TDGL equation (7.45).

one has $\Delta = 0$, and according to (8.76), the increment of instability has a finite value. This means that instability starts at values of μ somewhat smaller than (8.79) when ω'' (8.76) equals zero. Since at this instability point

$$\Delta_c = \Delta_{eq}^2/9T_c << \Delta_{eq}, \tag{8.80}$$

the instability-causing, threshold value of μ is:

$$\mu_c \cong \mu_{max} - \frac{\Delta_c^2}{2^{3/2}\Delta_{eq}}. \tag{8.81}$$

There was an attempt[19] to use this mechanism to explain nonequilibrium phenomena in tunnel junctions. In Ref. 23 it was suggested that this instability should be exploited to elaborate the new principle of a three-terminal (transistor) device. We will not consider these practical implications in more detail here.

References

1. M. Tinkham, Tunneling generation, relaxation and tunneling detection of hole-electron imbalance in superconductors, *Phys. Rev. B* **6**(5), 1747–1756 (1972).
2. G. J. Pethick and H. Smith, Charge imbalance in nonequilibrium superconductors, *J. Phys. C: Solid State Phys.* **13**, 6313–6347 (1980).
3. T. J. Rieger, D. J. Scalapino, and J. E. Mercereau, Charge conservation and chemical potentials in time-dependent Ginzburg–Landau theory, *Phys. Rev. Lett.* **27**(26), 1787–1790 (1971).
4. A. F. Volkov, Theory of the current-voltage characteristics of one-dimensional S-N-S and S-N-junctions, *Sov. Phys. JETP* **39**(*2*), 366–369 (1974) [*Zh. Eksp. i Teor. Fiz.* **66**(2), 758–765 (1974)].
5. N. N. Bogolyubov, V. V. Tolmachov, and D. V. Shirkov, *A New Method in the Theory of Superconductivity*, pp. 31–99, Consultants Bureau, New York (1959).
6. P. W. Anderson, Coherent excited states in the theory of superconductivity: Gauge invariance and the Meissner effect, *Phys. Rev.* **110**(4), 827–835 (1958).
7. P. W. Anderson, Random-phase approximation in the theory of superconductivity, *Phys. Rev.* **112**(6), 1900–1916(1958).
8. I. M. Khalatnikov, *An Introduction to the Theory of Superfluidity,* pp. 72–77, W. A. Benjamin, New York (1965).
9. V. L. Ginzburg, Second sound, the convective heat transfer mechanism, and exciton excitations in superconductors, *Sov. Phys. JETP* **14**(3), 594–598 (1962) [*Zh. Eksp. i Teor. Fiz.* **41**[3(9)], 828–834 (1961)].
10. J. Bardeen, Two-fluid model of superconductivity, *Phys. Rev. Lett.* **1**(2), 399–402 (1958).
11. A. V. Carlson and A. M. Goldman, Superconducting order parameter fluctuations below T_c, *Phys. Rev. Lett.* **31**(5), 880–882 (1973).
12. A. Schmid, in *Nonequilibrium Superconductivity, Phonons and Kapitza Boundaries*, K. E. Gray, ed., pp. 423–480, Plenum, New York (1981).
13. G. Schön, in *Nonequilibrium Superconductivity*, D. N. Langenberg and A. I. Larkin, eds., pp. 589–641, North-Holland, Amsterdam (1985).
14. E. E. Salpeter and H. A. Bethe, A relativistic equation for the bound state problem, *Phys. Rev.* **84**(6), 1232–1242(1951).
15. V. B. Berestezkii, E. M. Lifshitz, and L. P. Pitaevskii, *Quantum Electrodynamics,* pp. 317–454, Pergamon, Oxford (1982).

16. Yu. A. Vdovin, in *Application of Quantum Field Theory Methods to Many-Body Problems* pp. 94–109, Gosatomizdat, Moscow (1963) (in Russian).
17. A. G. Aronov and V. L. Gurevich, Stability of nonequilibrium Fermi distributions with respect to Cooper pairing, *Sov. Phys. JETP* **38**(3), 550–556 (1974) [*Zh. Eksp. i Teor. Fiz.* **65**[3(9)], 1111–1124 (1973)].
18. Yu. M. Gal'perin, V. I. Kozub, and B. Z. Spivak, Stability of nonequilibrium states of a superconductor with a finite difference between the populations of electron- and hole-like spectral branches, *Sov. Phys. JETP* **54**(6), 1126–1129 (1981) [*Zh. Eksp. i Teor. Fiz.* **81** [6(12)], 2118–2125 (1981)].
19. Yu. M. Gal'perin, V. I. Kozub, and B. Z. Spivak, Tunnel injection and tunnel stimulation of superconductivity: The role of branch imbalance, *J. Low Temp. Phys.* **50**(3/4), 185–199 (1983).
20. R. S. Fishman and J. A. Sauls, Response functions and collective modes of superfluid ^{3}He-B in strong magnetic fields, *Phys. Rev. B* **33**(4), 6068–6068 (1986).
21. J. W. Serene and D. Rainer, The quasiclassical approach to superfluid ^{3}He, *Phys. Rep.* **101**(4), 221–311 (1983).
22. A. F. Volkov and Sh. M. Kogan, Collisionless relaxation of the energy gap in superconductors, *Sov. Phys. JETP* **38**(5), 1018–1021 (1974) [*Zh. Eksp. i Teor. Fiz.* **65**(5), 2038–2046 (1973)].
23. A. M. Gulian and D. Van Vechten, Possible three terminal HTS transistor device, *IEEE Trans. Appl. Supercond* **7**(2), 3096–3098 (1997).

9

Phase-Slip Centers

Time-dependent Ginzburg–Landau equations provide a rather deep understanding of the nature of resistive states arising in narrow superconductive filaments. If a dc current passes through such a filament, then, according to the thermodynamic equilibrium GL theory (Sect. 1.2), the filament should pass into its normal state when the current achieves the critical value (Fig. 9.1). But in reality, other types of curves have been registered.[1] Moreover, electromagnetic radiation was detected,[2] which resembles the Josephson effect. These facts demonstrate directly that the resistive state in narrow superconducting filaments is of a nonequilibrium and nonstationary nature.

9.1. ONE-DIMENSIONAL APPROACH

Because in reality the filament is narrow [its cross-sectional dimensions should be less than $\lambda_L(T)$, $\xi(T)$] the resistive state cannot be explained by the motion of Abrikosov's vortices (in distinction to the situation in wide films in Sect. 7.3). The search for new mechanisms that can adequately describe the resistive state has become necessary.

9.1.1. Phase Slippage

Probably, Little was the first to use the idea of a "phase slippage" while analyzing the stability problem of electric current in quasi-one-dimensional structures.* This idea was developed further in a number of papers, particularly by Langer and Ambegaokar,[5] McCumber and Halperin,[6] Skochpol et al.,[2] and others (a detailed bibliography, that can be used to reconstruct the history of the problem is contained in the reviews in Refs. 7–9).

*The expression "phase slippage" was introduced earlier in the theory of superfluids by Anderson.[4]

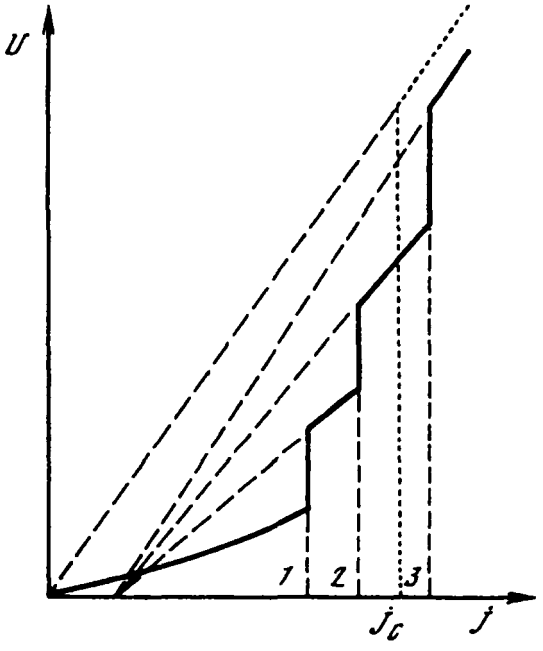

Figure 9.1. Current-voltage characteristic (CVC) of a narrow superconducting filament in the resistive state. Dotted curve, CVC according to the equilibrium theory (j_c is the critical Ginzburg–Landau current); solid line, experimental CVC; the points 1, 2, 3 mark the values of the current at which the jumps take place in the CVC.

To clarify this idea, let us consider two points, x_1 and x_2, of a superconducting filament (Fig. 9.2) with a potential V applied between them. Ignoring for a moment nonequilibrium effects, we conclude that the phase difference of the superconducting order parameter between the points x_1 and x_2 increases linearly in time [according to Eq. (8.9), if in equilibrium $\mu = 0$, then $\varphi \propto \theta$]. This indicates the thickening in time of the spiral shown in Fig. 9.2. But such a thickening cannot occur for too long a time, because the phase gradient determines the velocity of the superfluid motion of electrons, which is restricted by the critical value. To decrease the number of loops, the order parameter modulus should vanish at certain moments of time. At such moments the phase can dump the excessive 2π as it is shown in Fig. 9.2.

The behavior of phase-slip centers (PSCs) was investigated rather extensively on the basis of the Ginzburg–Landau-type dynamic equations (see in particular Refs. 10–18). It was found that in the region of a PSC the order parameter modulus oscillates, periodically turning to zero. In the time-averaged picture, the order

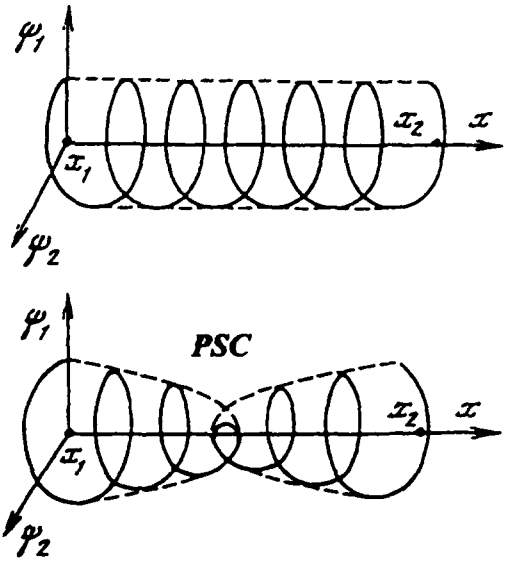

Figure 9.2. Creation of phase-slip centers in a superconducting filament directed along the x-axis; ψ_1 and ψ_2 are real and imaginary parts of the superconducting order parameter.

parameter modulus in the region of a PSC effectively decreases. Something like a "weak link" arises between superconducting "banks" and the situation as a whole resembles the nonstationary picture in weakly coupled superconductors, where the Josephson oscillations appear if a voltage is applied between the banks.

In the next section we present the numerical solutions of dynamic equations, which illustrate in detail the behavior of all physical quantities of interest (such as the order parameter modulus and phase, superconducting and normal currents, superconducting velocity, the scalar and gauge-invariant potentials Φ and μ, the charge ρ appearing in the filament, the current-voltage characteristics, and the periods of the stable oscillations). The results will also illustrate the influence of the interference current component (Chap. 7) on the solutions of the dynamic equations. The spectral characteristics of phonon fluxes emitted from a superconductor in a resistive state will also be discussed.

9.1.2. Initial Dimensionless Equations

Equations (7.45), (7.52), and (7.111) to (7.114) may be written in a convenient compact form introducing dimensionless variables [in (9.1) they are underlined]

$$x = \xi \underline{x}, \quad t = t_0 \underline{t}, \quad \varphi = \varphi_0 \underline{\varphi}, \quad \Delta = \Delta_0 \underline{\Psi}, \quad \mathbf{A} = \xi^{-1} \underline{\mathbf{A}},$$

$$\mathbf{j} = j_0 \underline{\mathbf{j}}, \quad \mu = \varphi_0 \underline{\mu}, \quad \rho = \rho_0 \underline{\rho}, \quad \underline{\Gamma} = 2\tau_\varepsilon \Delta_0. \tag{9.1}$$

Here

$$\xi = \left[\frac{\pi D}{8(T_c - T)} \right]^{1/2}, \quad t_0 = \frac{\pi}{8(T_c - T)\, u_0}, \quad \varphi_0 = \frac{1}{t_0},$$

$$\Delta_0 = \left[\left(\frac{T_c - T}{T_c} \right) \left(\frac{8\pi^2 (T_c)^2}{7\zeta(3)} \right) \right]^{1/2}, \quad j_0 = \frac{\pi \sigma \Delta_0^2}{4 T_c \xi},$$

$$u_0 = \frac{\pi^4}{14\zeta(3)} \approx 5.79, \quad \rho_0 = j \frac{t_0}{\xi(T)}. \tag{9.2}$$

In a dimensionless notation, Eq. (7.45) takes the form* [we will deal further with dimensionless quantities only, dropping the underlines below the symbols in (9.1)]:

$$\frac{u_0}{\sqrt{1 + \Gamma^2 |\Psi|^2}} \left[\frac{\partial}{\partial t} + i\varphi + \frac{1}{2} \Gamma^2 \frac{\partial |\Psi|^2}{\partial t} \right] \Psi$$

$$= (\nabla - i\mathbf{A})^2 \Psi + \left[1 - |\Psi|^2 - 8u_0 \left(1 - \frac{T}{T_c} \right) \mu^2 \right] \Psi. \tag{9.3}$$

Note that φ and μ in this chapter relate to the charge $e_* = 2e$ and differ from quantities μ and φ introduced earlier (which relate to the electron charge e) by a factor of 2. Representing the complex parameter Ψ in the form $\Psi = \psi e^{i\theta}$, where ψ is the modulus and θ is the phase of the order parameter, we find separately the real and imaginary parts of Eq. (9.3)**

$$u_0 \sqrt{1 + \Gamma^2 \psi^2} \frac{\partial \psi}{\partial t} = \nabla^2 \psi + (1 - \psi^2 - \mathbf{Q}^2)\, \psi, \tag{9.4}$$

$$\frac{u_0 \psi^2}{\sqrt{1 + \Gamma^2 \psi^2}} \mu = \operatorname{div} \mathbf{j}_s, \tag{9.5}$$

where

$$\mu = \varphi + \dot{\theta}, \tag{9.6}$$

*The term $P(|\Delta|)$ in Eq. (7.45) is neglected in the derivation of (9.3). Correspondingly, the equation for the inequilibrium phonon subsystem is not used.

**We drop the term with μ^2 in Eq. (9.3).

$$\mathbf{Q} = \nabla\theta - \mathbf{A}, \tag{9.7}$$

$$\mathbf{j} = \mathbf{j}_s + \mathbf{j}_n + \mathbf{j}_{\text{int}}, \mathbf{j}_s = \mathbf{Q}\psi^2, \quad \mathbf{j}_n = \dot{\mathbf{Q}} - \nabla\mu, \tag{9.8}$$

$$\mathbf{j}_{\text{int}} = -\mathbf{Q}\left\{\Gamma\left(\frac{u_0(T_c - T)}{4T_c}\right)^{1/2}\frac{\partial\psi^2}{\partial t}\right\} + (\dot{\mathbf{Q}} - \nabla\mu)\left(\frac{T_c - T}{T_c}\frac{2\pi}{7\zeta(3)}\right)^{1/2}\psi \ln(\psi\Gamma + 1),$$

while the expression for the charge (7.52) takes the form

$$\rho = \frac{2u_0\Gamma\psi^2}{\sqrt{1 + \Gamma^2\psi^2}}\left(u_0\frac{T_c - T}{T}\right)^{1/2}\mu. \tag{9.9}$$

Before attempting to solve Eqs. (9.4) and (9.5), we will make one remark about method. Equations (9.4) and (9.5) [as well as (9.3)] are gauge invariant, i.e., they do not change under the transformation

$$\mathbf{A} \to \mathbf{A} + \nabla\chi, \quad \varphi \to \varphi - \dot{\chi}, \quad \theta \to \theta + \chi, \tag{9.10}$$

where $\chi(\mathbf{r},t)$ is an arbitrary gauge function. Usually the following method of handling Eq. (9.3) is applied. One considers the "current state" and chooses the specific gauge of the vector potential in Eq. (9.3), putting $\mathbf{A} = 0$ and thus neglecting the magnetic field in a narrow superconducting filament. The phase 6 now acquires the meaning of the superconducting velocity potential, $\mathbf{Q} = \nabla\theta$. Solving then Eq. (9.3) [or (9.4) and (9.5)] relative to ψ and θ, one arrives at the usual picture of the resistive state, where the order parameter modulus oscillates in time and the phase suffers jumps (more properly, it "slips," see the following discussion). As mentioned, such active regions are named the *phase-slip centers.*

This procedure, however, is not completely satisfactory. Indeed, the gauge leading to $\mathbf{A} = 0$, strictly speaking, does not exist, wherever there exist a current $\mathbf{j}$ and magnetic field $\mathbf{H} = \text{curl}\,\mathbf{A}$ in the system. Besides, as one can see from (9.10), the superconducting phase θ depends on the choice of gauge and, consequently, the physical quantities cannot depend on θ. In fact, Eqs. (9.4) and (9.5) written in terms of the invariant variables μ, ψ, and $\mathbf{Q}$ do not depend on θ. In particular, these equations conserve their form in the case $\theta = 0$ also, i.e., in the case of a real order parameter. The question then arises of how one should interpret the expression "phase-slip center" if the phase everywhere is identical to zero.

To answer this question, we will split the vector potential into longitudinal and transverse components:

$$\mathbf{A} = \mathbf{A}_l + \mathbf{A}_t, \quad \mathbf{A}_l = \nabla\alpha, \quad \mathbf{A}_t = \text{curl}\,\mathbf{a}, \tag{9.11}$$

where α is some scalar function and $\mathbf{a}$ is a vector function. Under the gauge transformation (9.10), only the longitudinal component $\mathbf{A}_l$ is transformed, but the transverse part $\mathbf{A}_t$ remains unchanged. Introducing into (9.3) instead of $\underline{\Psi}$ the invariant complex function $\Psi = \underline{\Psi} e^{-i\alpha} = \psi e^{i\Theta}$, where $\Theta = \theta - \alpha$ is the invariant superconducting phase, we can rewrite (9.3) in terms of invariant variables

$$\frac{u_0}{(1+\Gamma^2\psi^2)^{1/2}}\left[\frac{\partial}{\partial t} + i\Phi + \frac{1}{2}\Gamma^2\frac{\partial\psi^2}{\partial t}\right]\Psi = (\nabla - i\mathbf{A}_t)^2\Psi + (1-\psi^2)\Psi. \quad (9.12)$$

The superconducting velocity $\mathbf{Q}$ and potential μ (9.6) can be written now in the form

$$\mathbf{Q} = \nabla\Theta - \mathbf{A}_t, \quad \mu = \Phi + \dot{\Theta}, \quad \Theta = \theta - \alpha, \quad \Phi = \varphi + \dot{\alpha}, \quad (9.13)$$

where the values Θ and Φ are invariant under the transformations of (9.10). Considering a narrow superconducting filament and neglecting within it the magnetic field $\mathbf{H} = \text{curl } \mathbf{A}$, we will put $\mathbf{A}_t = 0$.* The invariant quantity Θ has a meaning of the potential part of the superfluid velocity $\mathbf{Q} = \nabla\Theta$, and Φ is the invariant potential of normal motion. Indeed, the electric field E in dimensionless units has the form $\mathbf{E} = -\nabla\varphi - \dot{\mathbf{A}} = -\nabla\Phi$, and the normal current is $\mathbf{j}_n = \mathbf{E} = -\nabla\Phi$.

Equation (9.12) has the same form as (9.3), if we use $\mathbf{A} = \mathbf{A}_t = 0$. However the invariant potential Φ rather than the gauge-variant quantity φ enters into (9.12), and the invariant phase Θ instead of the gauge-variant superconducting phase θ. In particular, Eq. (9.12) is valid also at $\theta = 0$. In further analysis we will use the equation in the form (9.12), assuming $\mathbf{A}_t = 0$. This form coincides in fact with the commonly used one.

9.1.3. Boundary Conditions

Several types of boundary conditions for Eqs.(9.12) and (9.8) may be formulated, depending on the physical state assumed at the ends of the superconducting filament. If a superconducting filament having a length L connects two (identical, for simplicity) bulk superconductors, one can use the following boundary conditions (at the points $x = 0$ and $x = L$):

$$\psi(0) = \psi(L) = \psi_0, \quad \mu(0) = \mu(L) = 0, \quad (9.14)$$

where ψ_0 is some constant characterizing the bulk banks. The boundary condition $\mu = 0$ at the ends corresponds to the value $\mu = 0$ of the bulk superconductor in equilibrium (such boundary conditions were considered in Refs. 12 and 13). The

*The specifics of the spatial one-dimensional case emerge here. In general, it is necessary to use the full system of Maxwell equations [(7.119) to (7.122)] to calculate the transverse component $\mathbf{A}_t$.

condition $\mu = 0$ at the filament end is equivalent to the condition $j_s' = 0$ at $x = 0$ and $x = L$.

One can also choose different boundary conditions

$$\psi(0) = \psi(L) = \psi_0, \quad j_s(0) = j_s(L) = j, \tag{9.15}$$

accepting that in a bulk superconductor the total charge is transported by the superconducting current. (The condition 9.15 for j_s is equivalent to the condition $j_n = 0$ at the ends.) The boundary condition for ψ can be written in a more general form

$$\psi(0) = \beta\psi'(0), \quad \psi(L) = \beta\psi'(L), \tag{9.16}$$

where β is some constant (see Sect. 7.2).

In the case of a long superconducting filament, when the phase-slip centers are created evenly along the filament's length, one can use the cyclic boundary conditions

$$\psi'(0) = \psi'(L) = 0, \quad \mu(0) = \mu(L) = 0. \tag{9.17}$$

Here the points $x = 0$ and $x = L$ correspond to the positions of the neighboring extrema of $\psi(x)$ (which can coincide with the phase-slip centers or lie between them). Because the extrema of the superconducting current and of ψ should coincide, then on these points we evidently have $j_S' = 0$ and $\mu = 0$. If the superconducting filament connects two normal banks, the following boundary conditions are possible

$$\psi(0) = \psi(L) = 0, \quad j_n(0) = j_n(L) = j, \tag{9.18}$$

in accordance with the depression of the order parameter at the ends of the filament due to the proximity effect, so that near the ends the total charge is transferred by the normal current. We will use mainly the boundary conditions (9.14) and (9.15), though the results will not depend substantially on the character of boundary conditions.

9.2. CALCULATIONS PROCEDURE

9.2.1. Nonsingular Representation

The solutions of Eqs. (9.4) and (9.5) or (9.11) are singular and their numerical evaluation demands certain precautions. We present in this section a rather full description of the calculation scheme.

The singularity of Eqs. (9.4) and (9.5) written in terms of the invariant variables ψ and $\mathbf{Q}$, is due to the $\mathbf{Q}^2$ term, which hampers the calculations by turning infinite

at the moments when ψ vanishes. A more convenient form of these equations is attained by using a complex function $\Psi = \psi e^{i\Theta}$:

$$u\left[\dot{\Psi} + i\Phi\Psi + \frac{1}{2}\Gamma^2\Psi\frac{\partial\psi^2}{\partial t}\right] = \Psi'' + \Psi - \psi^2\Psi, \quad u = \frac{u_0}{\sqrt{1+\Gamma^2\psi^2}}. \tag{9.19}$$

Introducing the real and imaginary parts of Ψ by the relation $\Psi = R + iI$, substituting this in Eq. (9.19), and solving the resulting system of equations with respect to $\dot{R}$ and $\dot{I}$, we find

$$\dot{R} = \kappa_1 R'' - \frac{\Gamma^2}{u_1} IRI'' + \frac{R(1-\psi^2)}{u_1} + \Phi I, \tag{9.20}$$

$$\dot{I} = \kappa_4 I'' - \frac{\Gamma^2}{u_1} IRR'' + \frac{I(1-\psi^2)}{u_1} - \Phi R, \tag{9.21}$$

where

$$u_1 = u_0/\sqrt{1+\Gamma^2\psi^2}, \quad \psi^2 = R^2 + I^2, \quad \kappa_1 = (1+\Gamma^2 I^2)/u_1,$$

$$\kappa_4 = (1+\Gamma^2 R^2)/u_1, \quad \Phi(x) = -\int_0^x j_n\,dx + \frac{1}{2}\int_0^L j_n\,dx,$$

$$j_n = j - j_s - j_{\text{int}}. \tag{9.22}$$

The integration constant in (9.22) is chosen from symmetry considerations to ensure that $\Phi(x = L/2) = 0$ (the solution does not depend on the value of this constant). Equations (9.20) and (9.21), written in terms of the Cartesian variables $\Psi = R + iI$, differ advantageously from the representation in Eq. (9.12) of the polar variables $\Psi = \psi e^{i\Theta}$, in that the point $R = I = \psi = 0$ is no longer singular and the process of its intersecting the phase trajectory $\{R, I\}$ can be calculated normally.[12]

9.2.2. Matrix Representation for "Sweeping" Method

We present the system (9.20) and (9.21) in a matrix form

$$\left(\hat{1}\frac{\partial}{\partial t} - \hat{K}\frac{\partial^2}{\partial x^2}\right)\hat{\Psi} = \frac{1-\psi^2}{u_1}\hat{\Psi} + \Phi\hat{\sigma}_y\hat{\Psi}, \tag{9.23}$$

where

$$\hat{\Psi} = \begin{pmatrix} R \\ I \end{pmatrix}, \quad \hat{K} = \hat{\kappa} - \frac{\Gamma^2}{u_1} IR\hat{\tau}_1, \quad \hat{\kappa} = \begin{pmatrix} \kappa_1 & 0 \\ 0 & \kappa_4 \end{pmatrix}. \tag{9.24}$$

and replace the time derivative by the finite difference

$$\frac{\partial \hat{\Psi}}{\partial t} \to \frac{\hat{\Psi}^{\tau} - \hat{\Psi}^{0}}{\tau}, \tag{9.25}$$

here τ is the step in time and $\hat{\Psi}^0$ and $\hat{\Psi}^{\tau}$ are the values of Ψ in the initial and subsequent time layers.

We divide the interval $0 \le x \le L$ into n parts, h being the space step and $\hat{\Psi}^{\tau}$ and $\hat{\Psi}^0$ denoting the value of Ψ in discrete point j, $1 \le j \le N$. Replacing the coordinate derivative by the finite difference

$$\frac{\partial^2 \hat{\Psi}}{\partial x^2} \to \frac{\hat{\Phi}_{j+1} - 2\hat{\Psi}_j + \hat{\Psi}_{j-1}}{h^2}, \tag{9.26}$$

we rewrite Eq. (9.23) in a lattice form

$$\hat{A}_j \hat{\Psi}_{j-1} + \hat{B}_j \hat{\Psi}_j + \hat{C}_j \hat{\Psi}_{j+1} = \hat{F}_j, \quad 2 \le j \le N-1, \tag{9.27}$$

where

$$\hat{A}_j = \hat{C}_j = -\hat{K}_j \frac{\tau}{h^2}, \quad \hat{F} = \hat{\Psi}_j^0, \quad \hat{B}_j = \left[\hat{1} + \hat{K} \frac{2\tau}{h^2} - \left(\frac{1 - \psi^2}{u_1} \hat{1} + \Phi \hat{\sigma}_2 \right) \right]_j. \tag{9.28}$$

The indices $2 \le j \le N-1$ in Eq. (9.27) numerate the interior points of the computation interval where Eq. (9.23) is valid. The values at the current moment τ must be found (the upper index τ is omitted). The coefficients $\hat{A}_j$, $\hat{B}_j$, $\hat{C}_j$, $\hat{F}_j$ depend on Ψ_j^0 at the preceding moment and are assumed to be known.

The boundary conditions of the type (9.14) and (9.15) may be written in a form analogous to (9.27):

$$\hat{B}_1 \hat{\Psi}_1 + \hat{C}_1 \hat{\Psi}_2 = \hat{F}_1, \quad j = 1, \tag{9.29}$$

$$\hat{A}_n \hat{\Psi}_{N-1} + \hat{B}_N \hat{\Psi}_N = \hat{F}_N, \quad j = N, \tag{9.30}$$

where the points $j = 1$ and $j = N$ correspond to the limits of the computation interval.

9.2.3. Recurrence Relations

We seek the solution of the system (9.27) in the form

$$\hat{\Psi}_{j+1} = \hat{X}_j \hat{\Psi}_j + \hat{Y}_j, \tag{9.31}$$

where the matrices $\hat{X}_j$ and $\hat{Y}_j$ are to be found. Inserting (9.31) twice into (9.27), one finds the recurrent relations

$$\hat{X}_{j-1} = -(\hat{B}_j + \hat{C}_j \hat{X}_j)^{-1} \hat{A}_j, \tag{9.32}$$

$$\hat{Y}_{j-1} = (\hat{B}_j + \hat{C}_j \hat{X}_j)^{-1} (\hat{F}_j - \hat{C}_j \hat{Y}_j). \tag{9.33}$$

Expressions (9.31) to (9.33) provide the matrix generalization of the standard sweep method[19,20] in solving the differential equations.

9.2.4. Solution Procedure

The successive steps of finding the solutions are as follows. First we find from the boundary conditions the matrices

$$\hat{X}_{N-1} = -\hat{B}_N^{-1} \hat{A}_n, \quad \hat{Y}_{N-1} = \hat{B}_N^{-1} \hat{F}_N, \quad j = N. \tag{9.34}$$

The remaining matrices $\hat{X}_{j-1}$ and $\hat{Y}_j$ (for $1 \le j \le N-1$) are found further, taking into account that $\hat{A}_1 = 0$. Afterward, the functions Ψ_j $(1 \le j \le N)$ are determined from (9.31). Using the newly found values of Ψ_j one can calculate $\hat{A}_j$, $\hat{B}_j$, $\hat{C}_j$, $\hat{F}_j$ and also the potential $\Phi(x)$ from (9.22). Having determined $\Phi(x)$, one can calculate a new boundary value of the phase Θ^τ $(x = 0)$ from the relation $\mu = \Phi + \Theta$:

$$\Theta^\tau_{x=0} = \Theta^0_{x=0} + (\mu - \Phi)^0_{x=0} \tau, \tag{9.35}$$

where the superscript zero denotes the preceding moment of time. (From symmetry considerations we have $\Theta_{x=L} = -\Theta_{x=0}$.) In the case of boundary condition (9.14) we always have $\mu(0) = \mu(L) = 0$. In the case of boundary condition (9.15), one should use the relation $\mu = j_s'/(u\psi^2)$ [see (9.5)] to find the values of $\mu(0)$ and $\mu(L)$ where the current $j_s = RI' - IR'$ is found in terms of R and I, which is known from the preceding step. A new value of the phase $\Theta^\tau_{x=0}$ determined in this way can be used in the boundary conditions (9.14) and (9.15), which are equivalent to

$$R(x = 0) = \psi_0 \cos \Theta_0 \quad I(x = 0) = \psi_0 \sin \Theta_0, \tag{9.36}$$

$$R(x = L) = \psi_0 \cos \Theta_L \quad I(x = L) = \psi_0 \sin \Theta_L. \tag{9.37}$$

Writing down these conditions in a matrix form [(9.29) and (9.30)], one can repeat the procedure described above once again to find the solution on a new time layer, and so on. If $R(x)$ and $I(x)$ are known, one can calculate the values of $j_s(x)$, $\Phi(x)$ (9.22), $\mu(x) = j_s'(x)/[u\psi^2(x)]$, $Q(x) = j_s(x)/\psi^2(x)$, $\rho(x) = 2\Gamma\sqrt{u_0(1 - T/T_c)}\, j_s'(x)$. $\Theta(x) = \arctan(I/R)$ at any moment of time.

In the case of the boundary conditions (9.17), some complication arises owing to the presence of the derivatives

$$\frac{\partial \psi}{\partial x} = \frac{1}{2\psi}\left(R\frac{\partial R}{\partial x} + I\frac{\partial I}{\partial x}\right), \quad \psi = \sqrt{R^2 + I^2}. \tag{9.38}$$

If the derivatives are represented as a finite difference: $\partial R/\partial x = (R_j - R_{j-1})/h$, then at $j = 1$ (i.e., $x = 0$) the unknown value R_0 appears. To overcome this difficulty, the count interval $1 \le j \le N$ is extended by introducing a subsidiary point $j = 0$. The condition (9.17) (i.e., $RR' + II' = 0$ at $x = 0$) may be written in the form

$$R_0 = R_1 + \alpha_0(I_1 - I_0), \quad \alpha_0 = I_1/R_1 = \tan \Theta_1 \tag{9.39}$$

(the lower indices denote the values $j = 0$ and $j = 1$). One finds from this

$$R_1 = \frac{R_0 + \alpha_0 I_0}{1 + \alpha_0^2}, \quad I_1 = \alpha_0 R_1, \tag{9.40}$$

i.e., the values R_1 and I_1 are expressed in terms of the as-yet unknown values R_0 and I_0 and the known (from the preceding step) value Θ_1^0. One more relation between $\hat{\Psi}_1$ and $\hat{\Psi}_0$ is provided by the recurrence formula (9.41)

$$\hat{\Psi}_1 = \hat{X}_0 \hat{\Psi}_0 + \hat{Y}_0. \tag{9.41}$$

The subsidiary value $\hat{\Psi}_0$ is easily excluded from (9.40) and (9.41), and the value $\hat{\Psi}_1$ may be determined. After that, the sweep procedure of (9.27) to (9.35) is applied to find the remaining values $\hat{\Psi}_j$.

To guarantee the equivalence of both left and right halves of the calculation interval, the left and right runs were alternated and the solution's symmetry was maintained at every step.

To secure the convergence of solutions and to attain a stable oscillation regime, the calculations were carried out using mainly the space step about $h \approx 10^{-1} - 10^{-2}$ and the time step about $\tau \approx 10^{-3}$. The oscillation periods were found to the accuracy of three meaningful numbers. The phase increase for one oscillation period with the same accuracy was found to be π (relative to one PSC). Several hundred oscillations were sometimes performed before reaching the stable oscillation regime, thus making evident the presence of long-lived and weakly damping oscillation modes in the system.

9.3. ANALYSIS OF RESULTS

A numerical analysis shows that if the values of the transport current j along the filament are small enough, then there exist only static solutions of Eq. (9.12) with $\Phi = \mu = 0, j = j_s$. When j is increased, the solutions start to depend on time, the electric field $\mathbf{E} = -\nabla\Phi$ and normal current $\mathbf{j}_n = \mathbf{E}$ appear in a superconducting filament. All the parameters describing the superconductor ($\psi, j_s, j_n, Q, \mu, \Phi, \rho, \Theta$) begin to oscillate in the vicinity of certain active points (PSC). After a sufficiently long time, these oscillations reach a stable regime, and only such stable oscillations are considered in the following section. To elucidate the characteristic features of

these processes, let us consider first a short superconducting filament with only one active center.

9.3.1. Single Active Center

Figure 9.3 shows the distributions of $\psi(x)$ and $j_s(x)$ at different moments for a filament with the parameters $L = 1$, $\Gamma = 0$, $j = 1.5$ for the boundary conditions (9.14). Figure 9.4 depicts the time dependence of $\psi_l = \psi(t)$ and $j_{sl} = j_s(t)$ at the PSC point $x = l = L/2$. The numerals 1–6 at the curve denote the characteristic moments, which correspond to the consecutive stages of an oscillation cycle (see Fig. 9.4). At the moment 5,6 the momentum Q and the potential μ suffer discontinuity, and the derivative of Θ suffers a jump (see later discussion). The numeral 5 denotes the moment just preceding and 6 just after the jump.

A detailed analysis of the numerical solutions has shown that the order parameter ψ_l and the superconducting current j_{sl} vanish simultaneously at the instant of the jump (Fig. 9.4), but the superfluid momentum $Q_l = j_{sl}/\psi_l^2$ behaves singularly, turning to $\pm\infty$ when $j \to \pm 0$. This shows that the current j_s in the vicinity of PSC at some moments is negative. (An analogy with the vortex currents in Type II superconductors and Josephson junctions is evident here.) Such characteristic behavior is common to all time-dependent solutions of Eq. (9.11) investigated by us and does not depend on the type of the boundary condition or the parameters involved. (Negative values of j_s were reported earlier, e.g., in Ref. 14). The gauge-invariant potential $\mu = j_s/(u\psi^2)$ also behaves singularly, taking values $\pm\infty$ on both sides of PSC at the moment of the jump (Fig. 9.5).

Figure 9.6 shows the behavior of the invariant Coulomb potential Φ and of the normal current $j_n = -\Phi' = j - j_s$. As one can see, $j_n > 0$ and $\Phi_0 = \Phi(x = 0) > 0$ at all times.

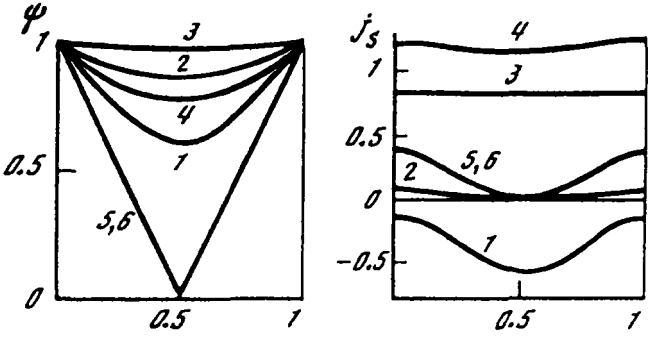

Figure 9.3. Spatial distribution of $\psi(x)$ and $j_s(x)$ at various moments of time for $L = 1$, $\Gamma = 0$, $j = 1.5$. Boundary conditions: $\psi = 1$, $\mu = 0$. The moments of time 1–6 are specified in Fig. 9.4.

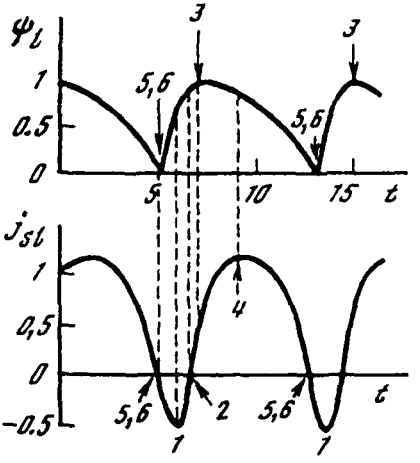

Figure 9.4. Values of ψ and j_s at the point $l = L/2$ (PSC) as the functions of time for the parameters shown in Fig. 9.3. The moment 1, minimum of j_{sl}; 2, the moment when $j_{sl} = 0$; 3, maximum of ψ; 4, maximum of j_{sl}; 5, 6 the moment when ψ and j_{sl} vanish simultaneously, while at the moment 5 $j_{sl} \to +0$, and at the moment 6 $j_{sl} \to -0$.

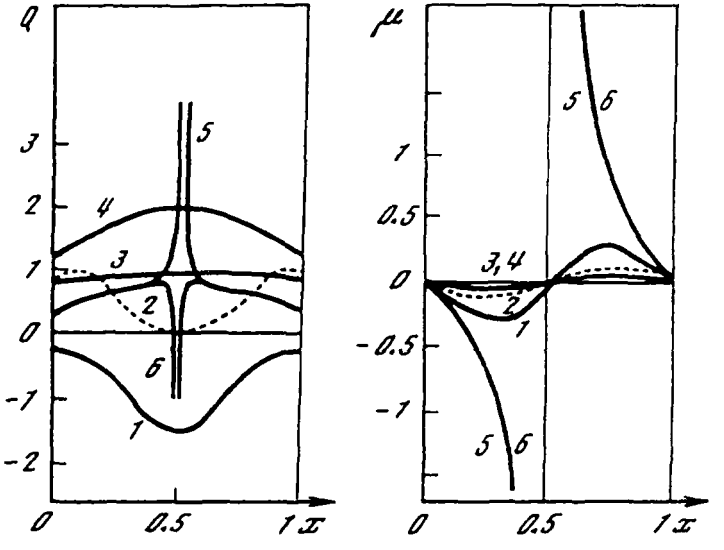

Figure 9.5. Spatial distribution of $Q(x)$ and $\mu(x)$ at various moments of time for parameters shown in Fig. 9.3. At the moment 5 the value $Q = +\infty$; at the moment 6 $Q = -\infty$; at these moments μ is $\pm\infty$.

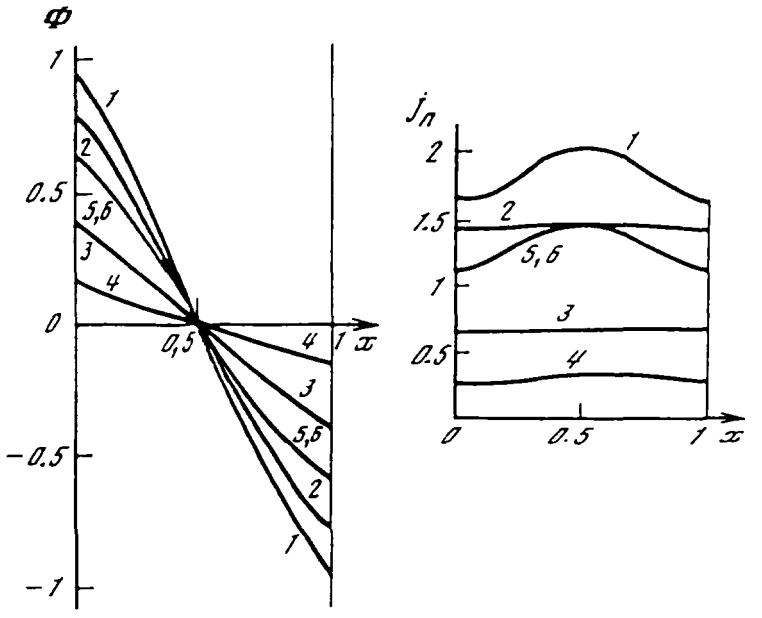

Figure 9.6. Spatial distribution of the invariant Coulomb potential Φ and the normal current j_n at various moments of time for $L = 1$, $\Gamma = 0$, $j = 1.5$ ($\mu_{0,L} = 0$, $\psi_{0,L} = 1$).

Averaging the electric field $E = -\Phi'$ relative to the coordinate x, we find a voltage drop V at the filament ends

$$\langle E \rangle = \frac{1}{L}\int_0^L E dx = \frac{V}{L}, \quad V = \Phi_0 - \Phi_L. \tag{9.42}$$

Here V is a function of time only. Using the relation $\mu = \Phi - \Theta$, one finds the potential drop averaged over the period of oscillations:

$$\overline{V} = \frac{1}{t_p}\int_0^{t_p} V\, dt = \overline{\mu}(0) - \overline{\mu}(L) + \frac{\delta(\Theta_L - \Theta_0)}{t_p}, \tag{9.43}$$

where $\overline{\mu}(0)$ and $\overline{\mu}(L)$ are time-averaged values of μ at the ends of filament and $\delta(\Theta_L - \Theta_0)$ is the phase difference gain between these points for one oscillation period t_p.

In the case of the boundary condition (9.14) we have $\mu(0) = \mu(L) = 0$ and

$$\bar{V} = \frac{\delta(\Theta_L - \Theta_0)}{t_p}. \tag{9.44}$$

Our calculations show that the phase difference gain during the period of steady oscillations is 2π (related to one PSC), and consequently

$$\bar{V} = \frac{2\pi}{t_p}. \tag{9.45}$$

(For unsteady oscillations this gain generally is not equal to 2π.)

9.3.2. Oscillation Frequency

The expression (9.45) for the oscillation frequency at the phase-slip center may be also derived analytically from topological considerations, as was demonstrated by Ivlev and Kopnin.[21] Assuming the oscillation process is stable and the positions of PSC are equidistant along the coordinate x, one obtains in the two-dimensional space-time $\{x, ct\}$ the periodic lattice of points at which the modulus of the order parameter Ψ vanishes (Fig. 9.7). Consider the two-dimensional vectors

$$\mathbf{r} = \{x, t\}, \quad \mathbf{q} = \{Q_x, -\mu\}, \quad \mathbf{p} = \{A_x, -\varphi\} \tag{9.46}$$

in this space-time. Using a relation between the vectors (9.46):

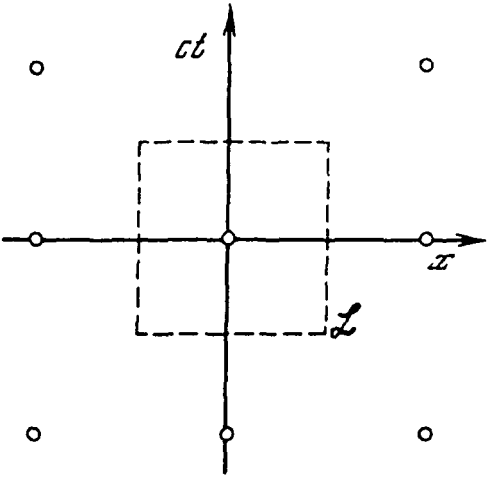

Figure 9.7. Phase-slip centers in the space $[x, ct]$. The elementary cell is denoted by a dashed line $\mathcal{L}$. The order parameter's phase changes by $2\pi n$ in going around the center in space $[x, ct]$.

$$\mathbf{q} = \mathbf{p} - \frac{\hbar c}{2e}\frac{\partial \theta}{\partial \mathbf{r}}, \tag{9.47}$$

which follows from the definitions in (7.82) and (7.85), and integrating (9.45) over the closed contour going around PSC, we have

$$\oint \mathbf{q} \cdot d\mathbf{r} = \oint \mathbf{p} \cdot d\mathbf{r} - \frac{\hbar c}{2e}\oint \frac{\partial \theta}{\partial \mathbf{r}} \cdot d\mathbf{r}. \tag{9.48}$$

The integral on the left side of (9.48) vanishes if the integration contour is chosen along the "elementary cell," denoted by $\mathcal{L}$ in Fig. 9.7 [in the case of a single PSC this contour must be stretched over x to $\pm\infty$ subject to the condition $\mu(\pm\infty) = 0$]. The first integral on the right side of (9.48) may be expressed by Stocks theorem through the integral of curl $\mathbf{p}$ over the area S, restricted by the contours $\mathcal{L}$, so

$$(\text{curl } \mathbf{p})_3 = -\frac{1}{c}\frac{\partial \mathbf{A}}{\partial t} - \frac{\partial \varphi}{\partial x} = \mathbf{E}. \tag{9.49}$$

Taking into account that the last integral in (9.48) provides a phase gain equal to $2\pi n$ (n is an integer) in going around the PSC, one has

$$0 = \int_{\mathcal{L}} E\, dx\, c\, dt - \frac{2\pi\hbar c}{2e}\, n \tag{9.50}$$

and, accordingly,

$$\int_{-t_p/2}^{t_p/2}\int_{-L/2}^{L/2} E\, dt\, dx = \frac{\phi_0 n}{c}, \tag{9.51}$$

where $\phi_0 = \hbar c/2e$ is the flux quantum (see Sect. 1.2). If $\mathbf{E}$ is a static quantity, then the Josephson relation follows from (9.51) at $n = 1$:

$$\omega_j = \frac{2e}{\hbar} V, \tag{9.52}$$

in which $\omega_j = 2\pi/t_p$. Introducing the space and time-averaged value E:

$$\langle E \rangle = \frac{1}{Lt_p}\int E\, dt\, dx, \tag{9.53}$$

we present (9.52) in the form:

$$n\hbar\omega_j = 2e\langle E \rangle L, \tag{9.54}$$

which is a generalization of the Josephson relation (9.52).

9.3.3. Temporal Behavior of the Phase Difference

In Fig. 9.8a the phase difference across the filament ends $\delta\Theta = \Theta_L - \Theta_0$ is depicted as a function of time; the moments 1–6 are marked to correspond to the notations in Fig. 9.4. The phase difference $\delta\Theta$ grows monotonically in time. Such growth is a consequence, in particular, of the boundary condition $\mu(0) = 0$, from which it follows that $\Theta_0 = -\Phi(0) < 0$ (see Fig. 9.8b), i.e., Θ_0 monotonically decreases and, analogously, Θ_L monotonically increases in time. The superconducting current $j_s = \psi^2\nabla\Theta$ always stays finite, i.e., in all regular points ($\psi(x) \neq 0$) the phase gradient is finite. However, the gradient of the continuous function cannot remain limited if the function difference at the ends of the interval grows unlimitedly in time. It follows then that $\Theta(x)$ should suffer a discontinuity at some point to preserve the finite gradient at all other points.

Figure 9.8b shows the behavior of $\Theta(x)$ at different moments. For symmetry reasons $\Theta(x)$ is an odd function relative to the middle point of the interval. If the

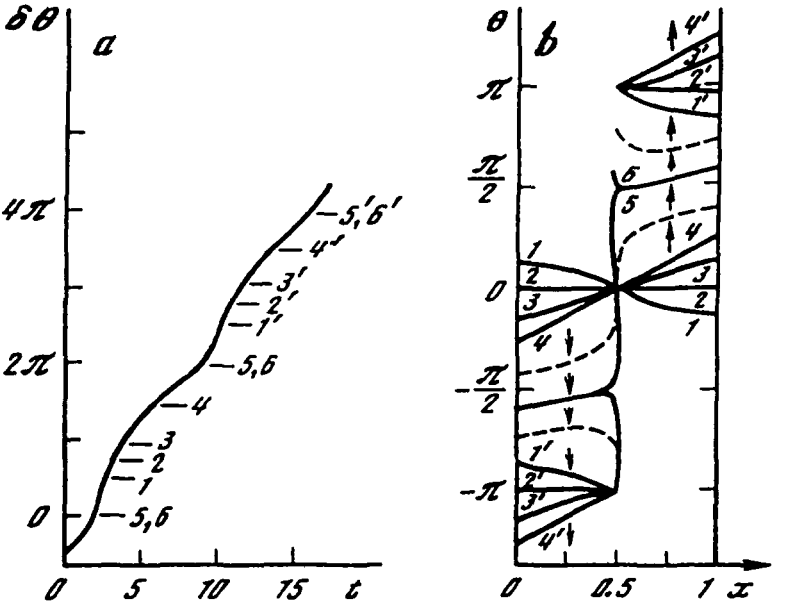

Figure 9.8. The space-time behavior of the phase $\Theta(x, t)$. (a) The phase difference at the ends of a superconducting filament as a function of time; and (b) the behavior of the phase $\Theta(x)$ at various moments of time. At the moments 5,6 (see Fig. 9.4) the derivative $d\Theta/dx$ reverses its sign (changing from $+\infty$ to $-\infty$); ($L = 1$, $\Gamma = 0$, $j = 1.5$; $\psi_{0,L} = 1$, $\mu_{0,L} = 0$).

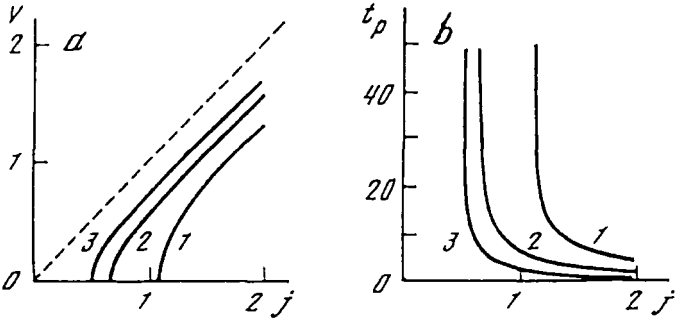

Figure 9.9. Current-voltage characteristics and oscillation periods of PSC. (a) CVC for superconducting filaments with $L = 1,2,3$ ($v = V/L$); and (b) periods of established oscillations for filaments with $L = 1,2,3$ depending on the transport current j; $\Gamma = 0$, $\psi_{0,L} = 1$, $\mu_{0,L} = 0$.

moment 1 corresponds to the minimal current j_s in a system, then the phase $\Theta(x)$ can be represented at this moment as a single-valued continuous function in the interval $0 \le x \le L$. In subsequent moments (2, 3, 4) Θ_0 decreases and the phase gradient increases. Close to the moment of a jump, the phase gradient first turns to $+\infty$ (at the moment 5 immediately before the jump), and then changes to $-\infty$ (at the moment immediately after the jump). At this moment the phase Θ suffers a discontinuity at the location of PSC $x = l = L/2$; the value Θ_l on both sides of PSC being $\Theta(l \pm 0) = \pm\pi/2$, their difference is equal to π at the moment of a jump. After this the two branches of the phase diverge in the directions shown by the arrows, smoothly deforming, and after the moment $1'$ (which corresponds to the subsequent minimum of the current j_s) they take the positions marked by the primed numbers $1'$ on the curves (the phase difference is 2π at this stage). Further on the process is repeated and the two branches of the phase continue to diverge from one another. Because the phase is determined by the relation $\Theta = \arctan(I/R) \pm \pi n$, the resulting picture can always be reduced to the one shown in Fig. 9.8b by shifting it along the ordinate by πn (n is integer).*

The voltage-current characteristics of the short superconducting filaments with the boundary conditions (9.14) are shown in Fig. 9.9a. The ratio of the voltage drop (9.22) to the filament's length ($v = V/L$) is presented as a function of the transport current j through the filament. The dashed straight line corresponds to Ohm's law in a normal filament. The curves corresponding to the resistive state of the

*The multivalued function $\Theta(x)$ can also be represented as a single-valued continuous function on a cylindrical surface ($\pi/2 \le \Theta \le \pi/2$), glued together along the element $\Theta = \pm\pi/2$. The phase difference at the ends of the interval $\delta\Theta = \Theta_l - \Theta_0$ will change by 2π at the moment of a jump, remaining always within the limits $0 \le \delta\Theta \le 2\pi$.

superconducting filament are shifted along the abscissa relative to the normal state Ohm's law by an excess current δj.[12] The phenomenon of excess current was observed experimentally in short superconducting bridges[22–28]; however, we will not discuss this question here in more detail (see Sect. 10.5 and Ref. 29). The periods of stable oscillations t_p, which are related to V by expression (9.45), are shown in Fig. 9.9b in dependence on the transport current j.

9.3.4. Other Boundary Conditions

Figure 9.10 demonstrates the behavior of ψ, j_s, Q, μ, Θ in the case $L = 5$, $\Gamma = 0$, $j = 0.4$ for the boundary condition (9.14) with $\psi_{0,L} = 0.5$, $\mu_{0,L} = 0$. The distributions are presented on one half of the interval $0 \le x \le L/2$ only. For symmetry reasons the functions ψ, j_s, Q^* are even relative to the point $l = L/2$ [i.e., $f(x + l) = f(x)$], and the functions μ and Θ are odd [$f(x + l) = -f(x)$]. The numeration of the curves hereafter corresponds to that used in Fig. 9.4. The voltage-current characteristics for $L = 5$ at $\psi_{0,L} = 0.5$ and $\psi_{0,L} = 1$ ($\mu_{0,L} = 0$) are given in Fig. 9.11.

9.3.5. Finite-Cap Results

The results presented in the preceding section relate to the gapless state ($\Gamma = 0$). For finite-gap superconductors ($\Gamma \neq 0$), the qualitative picture of the processes occurring in the filament does not change significantly. Figures 9.12 and 9.13 depict the voltage-current characteristics for superconducting filaments with $L = 5$, $\Gamma = 10$, and $\Gamma = 100$ for the boundary conditions $\psi_{0,L} = 0.5$ and $\psi_{0,L} = 1$ ($\mu_{0,L} = 0$) (solid lines). The solutions for $L = 5$, $\Gamma = 100$, $\psi_{0,L} = 1$ ($\mu_{0,L} = 0$) at $j = 0.2$ and $j = 0.5$ are shown in Figs. 9.14, and 9.15. For finite-gap superconductors, the space distribution of electric charge arises along the filament driven into the resistive state. The charge ρ is proportional to Γ and has opposite signs to the left and to the right of PSC, so that the total charge is zero. The solutions for $L = 5$, $\Gamma = 100$, $\psi_{0,L} = 1$ ($\mu_{0,L} = 0$) and $j = 0.5$ are shown in Fig. 9.16.

9.3.6. Two Active Centers

For $L = 10$, along with the solution corresponding to one PSC in the middle point, a solution with two phase-slip centers occurs. Figure 9.17 depicts voltage-current dependencies for $L = 10$, $\Gamma = 100$, $\psi_{0,L} = 0.5$, and $\psi_{0,L} = 1$ ($\mu_{0,L} = 0$).

As mentioned at the beginning of this chapter, spontaneous jumps were detected in the experiments registering current-voltage characteristics in the resistive states. These jumps may be explained by the creation of a new PSC and by corresponding transitions from one branch of the solution to another (see Fig. 9.17).

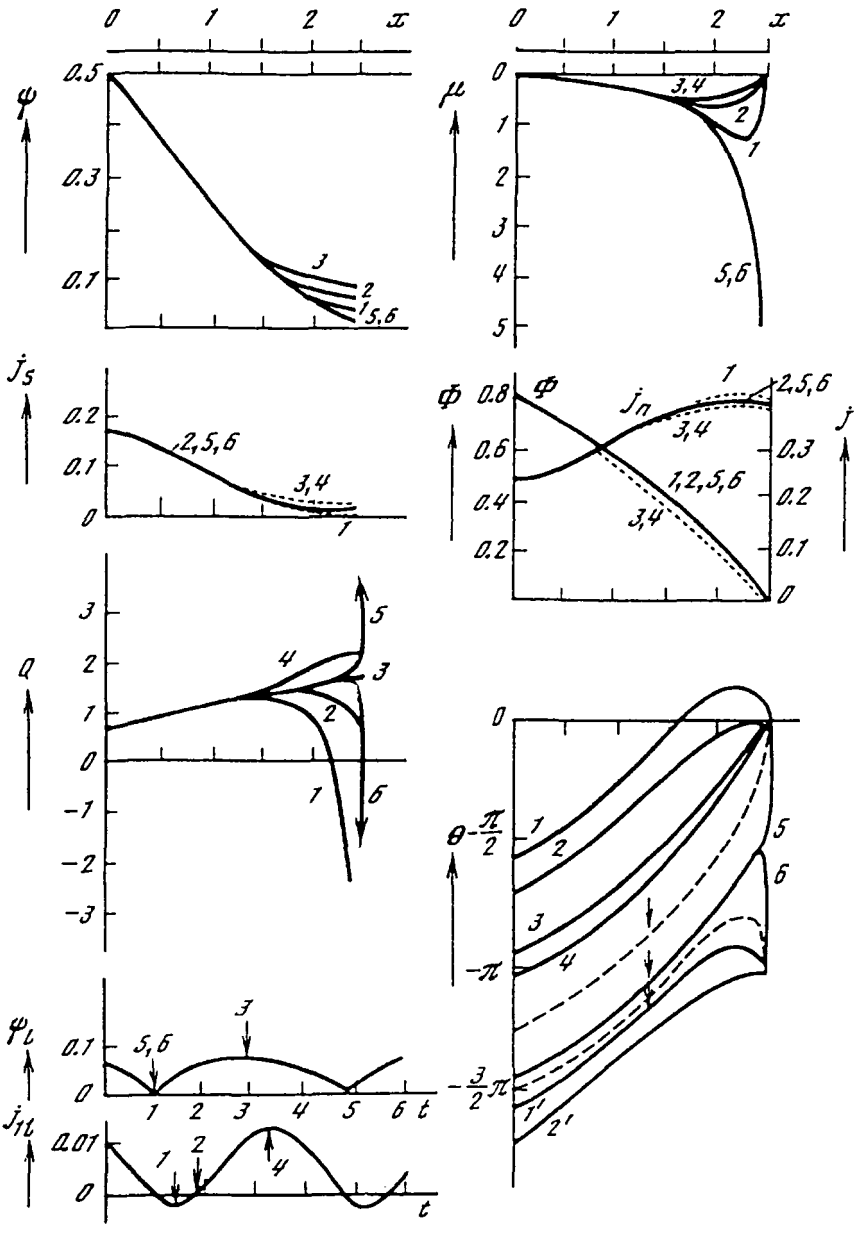

Figure 9.10. Spatial distributions of ψ, j_s, Q, μ, Φ, Θ in various moments of time for $L = 5$, $\Gamma = 0$, $j = 0.4$. The values of Φ_L and j_{sl} at PSC are also shown as functions of time.

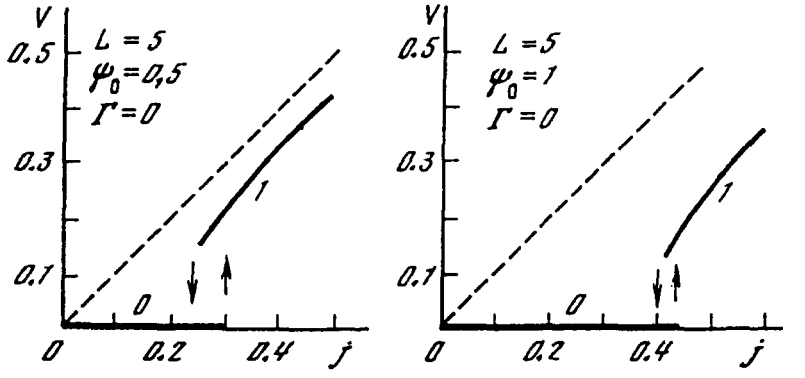

Figure 9.11. Current-voltage characteristics for a filament with $L = 5$, $\Gamma = 0$ (boundary conditions $\psi_0 = 0.5$ and $\psi_0 = 1$; $\mu_0 = 0$). 0, the equilibrium state; 1, the state with a single PSC. Arrows indicate the transitions between branches of solutions (the boundaries of hysteresis); the broken line is Ohm's law in the normal state.

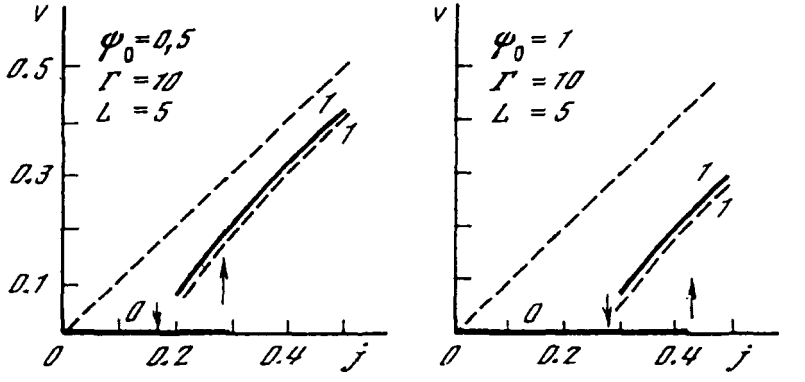

Figure 9.12. Current-voltage characteristics for a filament with $L = 5$, $\Gamma = 10$ ($\psi_0 = 0.5$ and $\psi_0 = 1$; $\mu_0 = 0$). 0,1, the number of PSCs. The dashed line 1 corresponds to the characteristic obtained by taking into account the interference current with the parameter $1 - T/T_c = 0.01$.

9.3.7. Current-Voltage Relations: Galayko Model

It should be pointed out that some features of the current-voltage characteristics (such as those depicted in Fig. 9.1) may be well described by the analytic solutions of the static equations (9.4) to (9.8), or, more properly, by a static version of these equations proposed by Fink et al., and by Galayko et al. (the "static model," see, e.g., Refs. 30–34). The applicability of static equations is connected with the fact

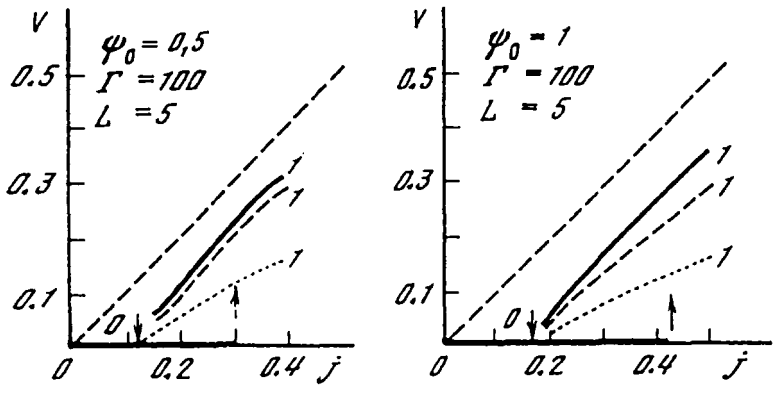

Figure 9.13. Current-voltage characteristics for $L = 5$, $\Gamma = 100$. Solid line, without j_{int}; dashed line, taking into account j_{int} at $1 - T/T_c = 0.01$; dotted line, taking into account j_{int} at $1 - T/T_c = 0.1$.

that the oscillations of physical quantities at PSC are of high frequency, but the current-voltage characteristics are observed on time intervals significantly larger than the oscillation period t_p.

Averaging Eqs. (9.4) and (9.5) over time, keeping only nonzero terms and replacing the mean values of compositions by the compositions of mean (nonzero!) values, one obtains the equations

$$0 = \frac{\partial^2 \psi}{\partial x^2} + (1 - \psi^2 - Q^2)\psi, \tag{9.55}$$

$$\psi^2 \mu = \frac{\partial}{\partial x}(Q\psi^2), \tag{9.56}$$

$$j = Q\psi^2 - \frac{\partial \mu}{\partial x} \tag{9.57}$$

(to simplify the equations we make $\Gamma = 0$, $u = 1$). Using the relation (9.57), we transform (9.56) into the form

$$\frac{1}{\psi^2}\frac{\partial^2 \mu}{\partial x^2} - \mu = 0. \tag{9.58}$$

In thermodynamic equilibrium, $\psi \sim 1$. In the resistive state, the value of ψ diminishes. Thus in the vicinity of PSC one can assume $\psi^2 << 1$ and omit the term $\partial^2\psi/\partial x^2$ in the set of equations (9.55) and (9.58). Then the basic equations of the static model are simplified further and reduced to

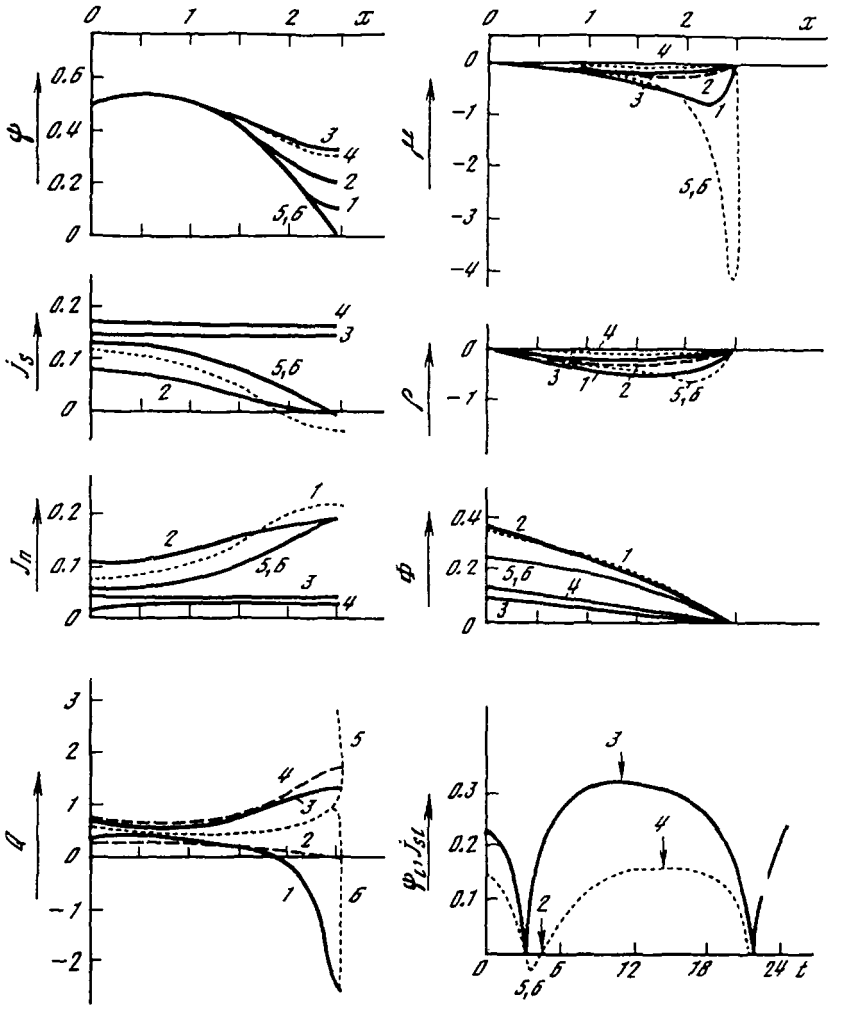

Figure 9.14. Solutions for $L = 5$, $\Gamma = 10$, $j = 0.2$ ($\psi_0 = 0.5$, $\mu_0 = 0$).

$$\frac{\partial^2 \mu}{\partial x^2} - \psi^2 \mu = 0, \tag{9.59}$$

$$\psi^2 + Q^2 = 1, \tag{9.60}$$

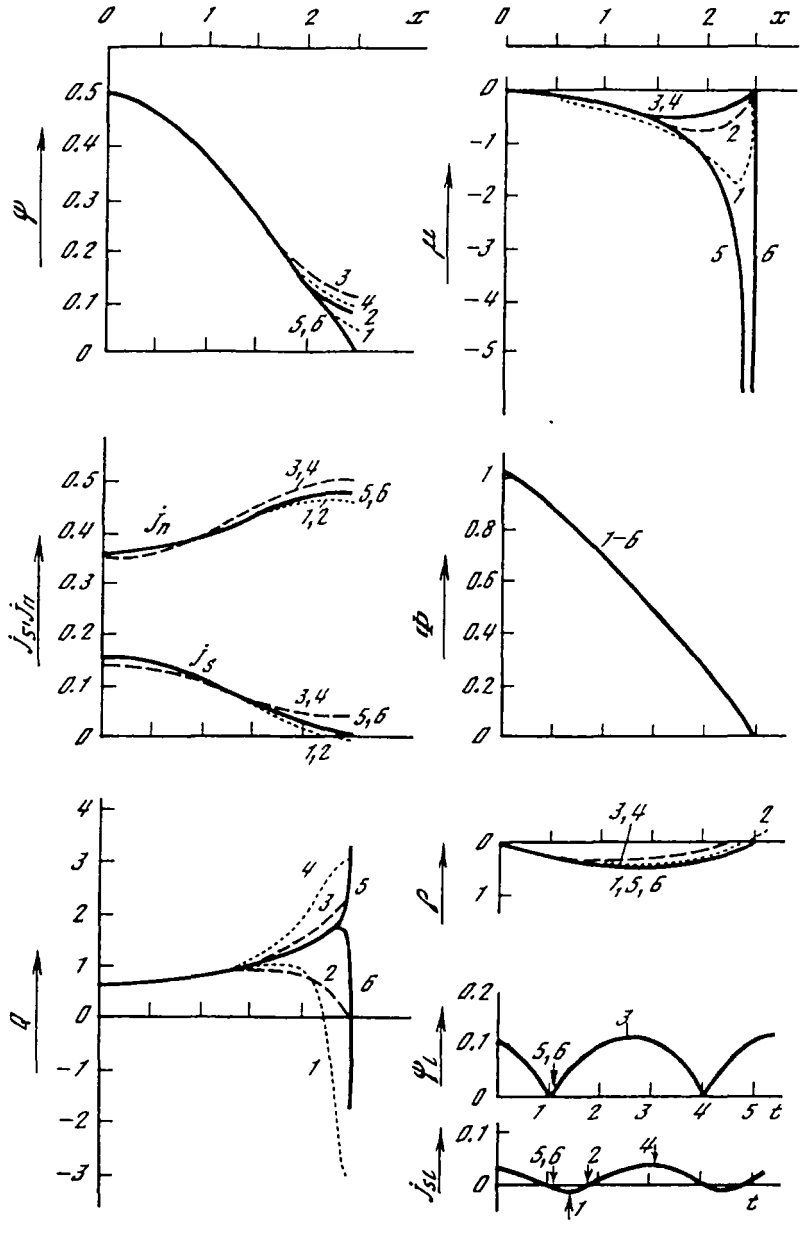

Figure 9.15. Solutions for $L = 5$, $\Gamma = 10$, $j = 0.5$ ($\psi_0 = 0.5$, $\mu_0 = 0$).

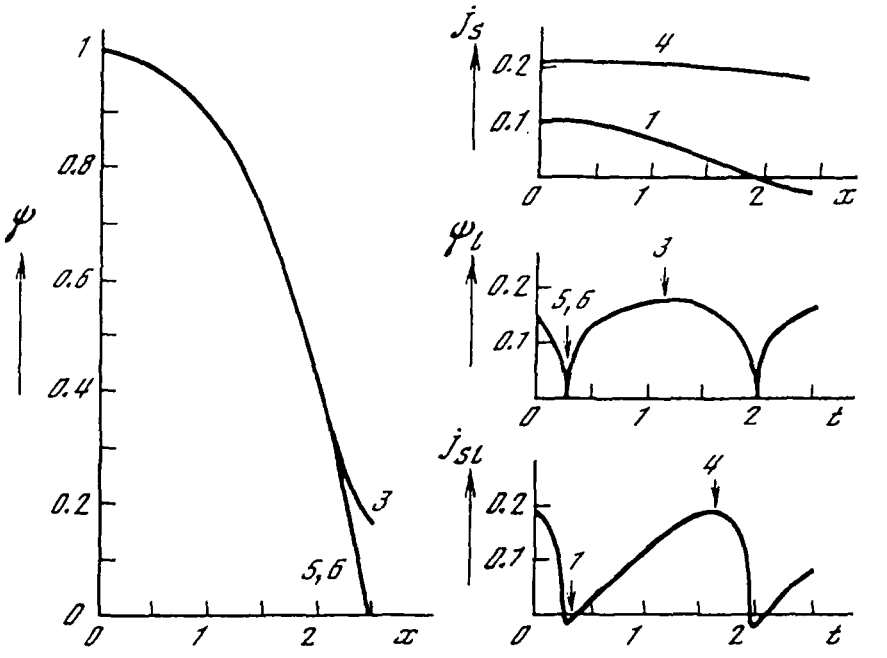

Figure 9.16. Solutions for $L = 5$, $\Gamma = 100$, $j = 0.5$ ($\psi_0 = 1$, $\mu_0 = 0$).

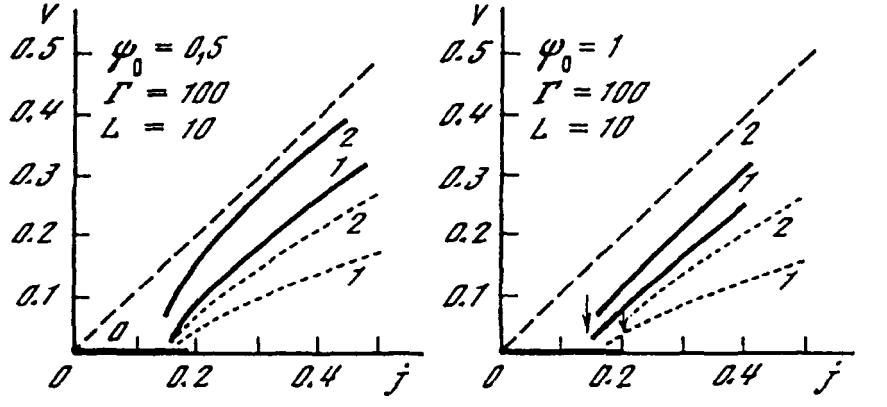

Figure 9.17. Current-voltage characteristics for $L = 10$, $\Gamma = 100$ ($\psi_0 = 0.5$ and $\psi_0 = 1$; $\mu_0 = 0$). 0, 1, 2, the number of PSCs. Solid line, without j_{int}, dotted line, taking into account j_{int} at $1 - T/T_c = 0.1$.

$$j = Q\psi^2 - \frac{\partial \mu}{\partial x}. \tag{9.61}$$

Despite the crudeness of the approximation, the main features of the current-voltage characteristics (as can be seen) are described by Eqs. (9.59) to (9.61). Using the method of solution proposed in Ref. 35, we choose a superconducting current $j_s = Q\psi^2$ as the integration variable. Differentiating Eq. (9.61) over the coordinate x and combining it with (9.59), one finds

$$\frac{\partial x}{\partial j_s} = \frac{1}{\mu\psi^2} \tag{9.62}$$

$$\mu \frac{\partial \mu}{\partial j_s} = -\frac{1}{\psi^2}(j - j_s). \tag{9.63}$$

The boundary conditions for the functions $\mu(j_s)$ and $x(j_s)$must be supplied to these equations. Taking into account the symmetry of the problem and that of $\mu \propto \operatorname{div} j_s$, we have

$$\mu(j_s = 0) = \pm\mu_0 \tag{9.64}$$

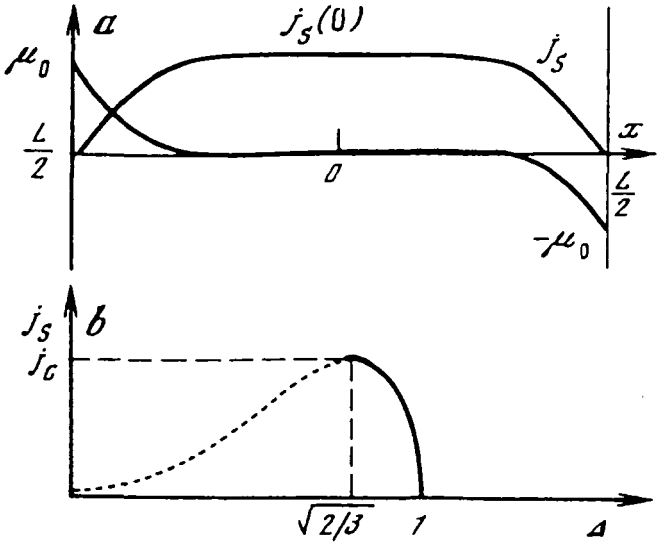

Figure 9.18. Resistive state in a static model: (a) The distribution of superfluid current and of invariant potential and (b) stable (solid line) and unstable (dotted line) branches of solutions of Eq. (9.66).

(the signs + and − refer to the left and right ends of the filament). The second boundary condition is obvious (Fig. 9.18a):

$$x(j_s = 0) = \pm \frac{L}{2}. \tag{9.65}$$

The function $\psi = \psi(j_s)$, appearing in (9.62) and (9.63) is determined by Eq. (9.60), from which (accounting for the expression for j_s) it follows that

$$\psi^2\sqrt{1-\psi^2} = j_s. \tag{9.66}$$

The behavior of the solution of this equation is illustrated in Fig. 9.18b. Because the thermodynamically stable branch of the solution corresponds to the values $\sqrt{2/3} \le \psi \le 1$, one can assume that in the whole range of variation of j_s the function $\psi(j_s)$ varies slowly. This fact simplifies further analysis. Integrating Eq. (9.63) and taking into account that at the center of the filament [where $j_s = j_s(0)$] he value of μ vanishes, we obtain

$$\mu^2(j_s) = 2\int_{j_s}^{j_s(0)} \frac{j - j_s'}{\psi^2(j_s')}\, dj_s'. \tag{9.67}$$

Integration of Eq. (9.62) in the range $x < 0 (\mu > 0)$ aking into account boundary condition (9.65) gives the relation

$$L = 2\int_0^{j_s(0)} \frac{dj_s'}{\mu\psi^2}. \tag{9.68}$$

The value of $j_s(0)$ increases with increasing j. When $j_s(0)$ attains the value j_c, the creation of PSC becomes possible. At the constant length L, this occurs when the total current j reaches a certain critical value $j = j_{max}$. Let us find a relation between j_{max} and L. As mentioned earlier, in the first approximation one can neglect the dependence of ψ on j_s in the expressions (9.67) and (9.68) [assuming $\psi(j_s) \approx \psi(j_c) \equiv \psi = \sqrt{2/3}$] and fulfill the integration in quadratures. Setting $j_s(0) = j_c$, we find from (9.67):

$$\mu^2(j_s) = \frac{1}{\psi^2}\{(j - j_s)^2 - (j - j_c)^2\}. \tag{9.69}$$

Substituting this expression into (9.68) and neglecting the functional dependence $\psi(j_s)$, we obtain the following equation for $j \equiv j_{max}^{(L)}$:

$$L = \frac{2}{\psi}\int_0^j \frac{dj_s}{\sqrt{(j - j_s)^2 - (j - j_c)^2}} = \frac{2}{\psi}\ln\frac{j + \sqrt{(j - j_s)^2 - (j - j_c)^2}}{j - j_c}. \tag{9.70}$$

For a sufficiently long filament (i.e., at $L >> 1$) the relation

$$j = j_c + bj_c \exp\left[-\frac{L}{2}\psi(j_c)\right] \tag{9.71}$$

follows from (9.70), which connects $j_{\max}^{(L)}$ with L [here $b \sim 1$, $\psi(j_c) = \sqrt{2/3}$]. The quantity $j_{\max}^{(L)}$ defines the critical current when the first PSC appears. Because the boundary conditions at the point where the PSC exists coincide with the boundary conditions for the junction of the superconductor and normal metal, for a sufficiently long filament (the distance between PSCs must significantly exceed the penetration depth l_E) we return to the initial problem, but for two consecutively connected segments of the filament. If the current increases further, new PSCs arise, with a critical current

$$j_c^{(n)} = j_c\left(1 + b\exp\left[-\frac{L}{2n}\psi\right]\right) \tag{9.72}$$

corresponding to the creation of the n^{th} PSC. With the appearance of a subsequent PSC, the voltage difference at the filament suffers a jump $2\mu_0$ (which in the first approximation does not depend on j). Taking into account (9.69), one can conclude that between these jumps the current-voltage characteristics have linear sections corresponding to the differential resistivity

$$\frac{dv}{dj} = \frac{2(n+1)}{\mu_0}\int_0^{j_c}\frac{dj_s'}{\psi(j_s')}. \tag{9.73}$$

The length of these sections between jumps (see Fig. 9.1) evolves with n as $\exp[-L\psi/2n]$. In the static model, as we have seen, the creation of a new PSC occurs when the current $j(0)$ attains the value j_c [in dimensionless units $j_c = 2/(3\sqrt{3})$]. In reality (owing to various physical factors) the quantitative criterion of PSC creation may differ from this condition. In principle, a hysteresis is possible at subsequent increases and decreases of the current through the filament. We will not consider these details here.

9.3.8. Shortcomings of the TDGL in the Absence of Relaxation

Returning to the numerical analysis, we note that at large $\Gamma >> 1$ the values of μ and ρ are also large at small distances from PSC and diverge formally at $\Gamma \to \infty$ [see expressions (9.5) and (9.9) for μ and ρ], which is inadmissible for physical reasons. From this limitations also follow on the applicability of the TDGL set of equations for large values of Γ.

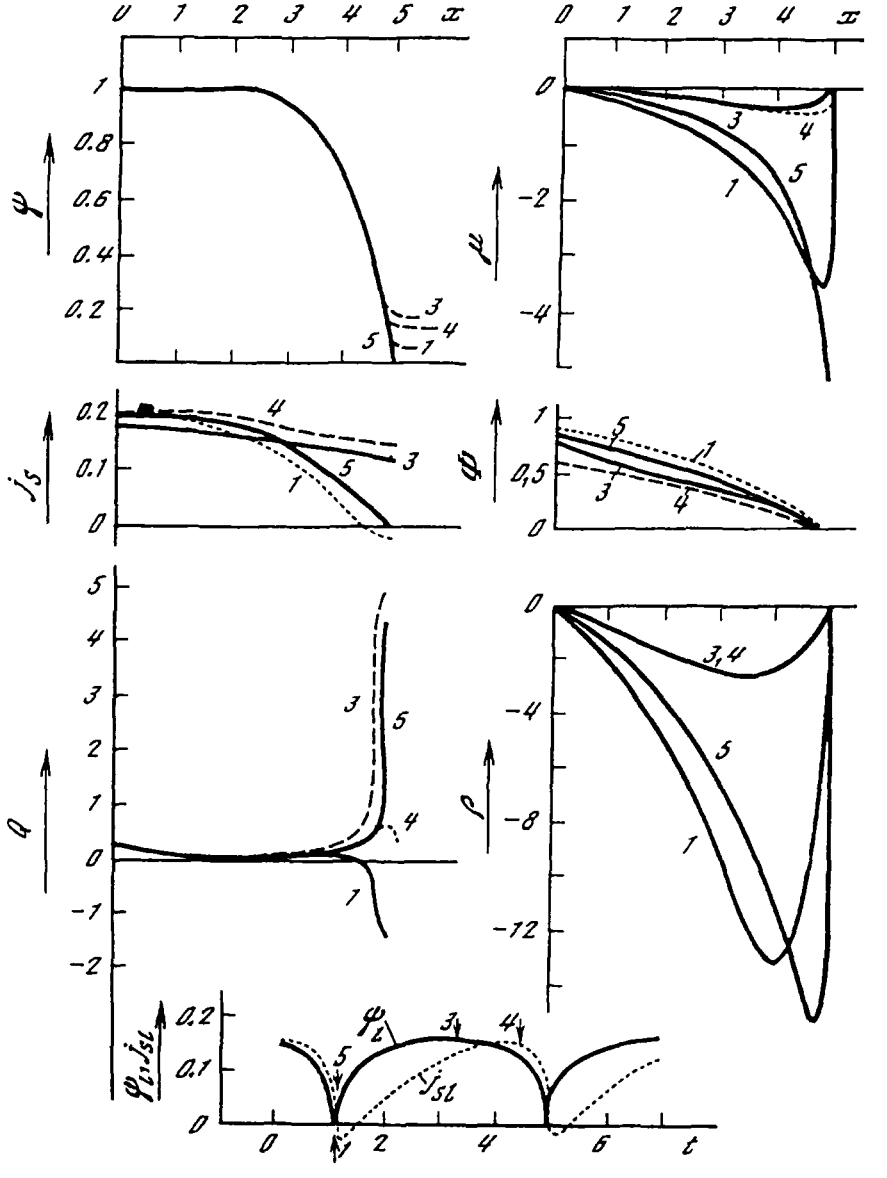

Figure 9.19. Solutions for $L = 10$, $\Gamma = 100$, $j = 0.3$ ($\psi_0 = 1$, $\mu_0 = 0$). There is one PSC in the center of filament.

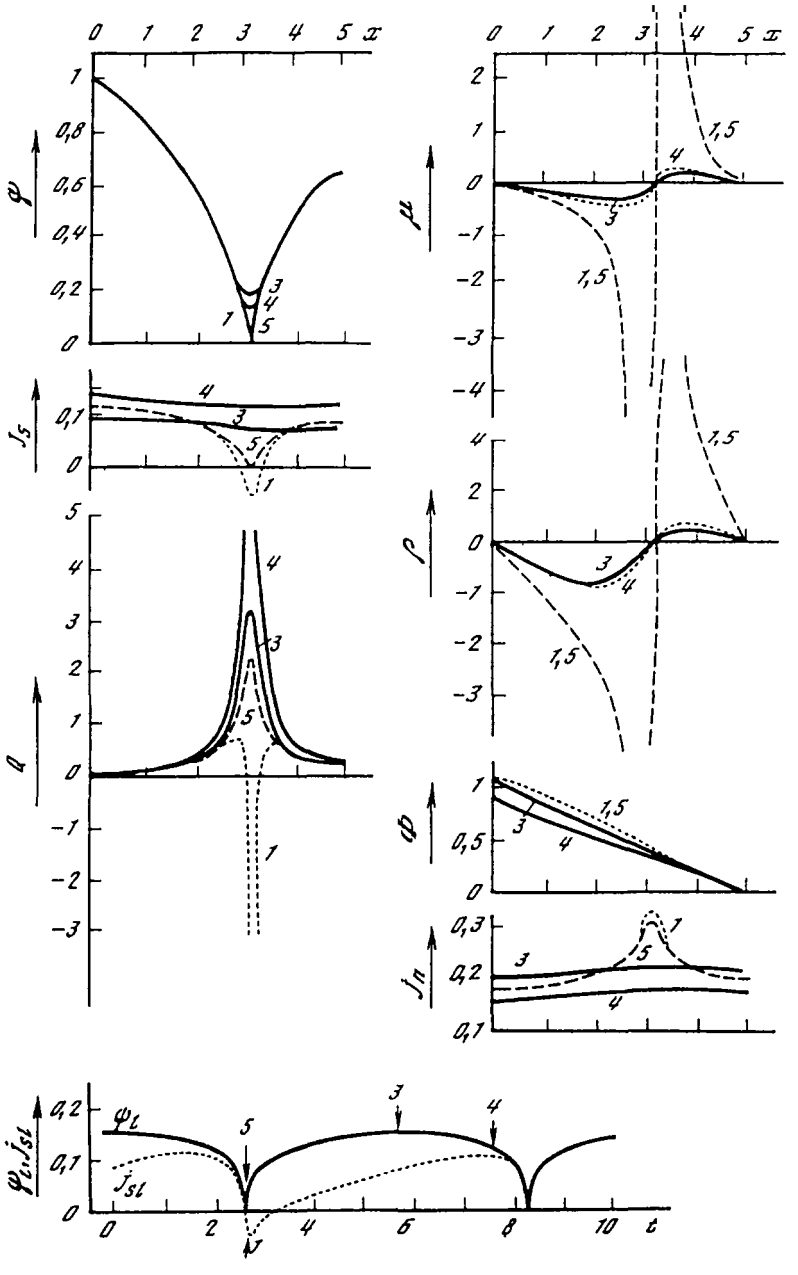

Figure 9.20. Solutions for $L = 10$, $\Gamma = 100$, $j = 0.3$ ($\psi_0 = 1$, $\mu_0 = 0$). Two PSCs are present; the second (not shown) is symmetrically placed relative to the filament's middle point.

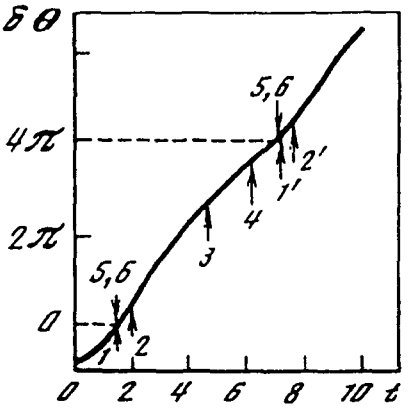

Figure 9.21. Phase difference $\delta\Theta$ between the filament's ends with $L = 10$, $\Gamma = 100$, $j = 0.3$ ($\psi_0 = 1$, $\mu_0 = 0$) in the state with two PSCs as a function of time. During the period of oscillations $\delta\Theta$ increases by 4π. The moments 1–6 are specified in Fig. 9.4.

9.3.9. More Features of Numeric Solutions

The solutions for $L = 10$, $\Gamma = 100$, $\psi_{0.L} = 1$, and $\mu_{0.L} = 0$, $j = 0.3$ are shown in Fig. 9.19 (one PSC) and Fig. 9.20(two PSCs). The phase difference at the filament's ends in the state with two PSCs increases by 4πover the period of stable oscillations (Fig. 9.21). The dynamics of the phase variation along the filament with two PSCs

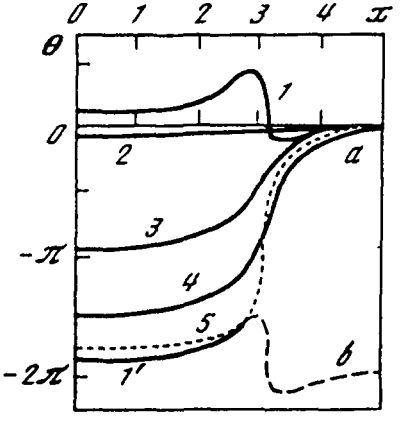

Figure 9.22. Variation of the phase $\Theta(x)$ in time for a filament with $L = 10$, $\Gamma = 100$, $j = 0.3$ ($\psi_0 = 1$, $\mu_0 = 0$) in the state with two PSCs. The behavior of $\Theta(x)$ is shown only on the half-interval ($0 \le x \le L/2$), where there is only one PSC.

is demonstrated in Fig. 9.22. At the moment 5, the phase $\Theta(x)$ has a vertical tangent at the point of PSC (the dotted line). At the next moment (6) the phase at this points breaks and two branches of $\Theta(X)$ on both sides of PSC slip relative one another. The left branch at the moment $1'$ (see Fig. 9.21) remains in the position $1'$, as shown in Fig. 9.22, but the right branch at the moment $1'$ occupies the position *a,* coinciding with the right branch of the curve 1. Because the phase $\Theta(x)$ is a multivalued function $(\Theta(x) = \arctan[I(x)/R(x)])$, the right branch $1'$ can be shifted from the position *a* into position *b* (dashed line). This, however, produces the discontinuity of Θ in the regular point $(x = L/2)$, because the phase is assumed to be antisymmetric relative to the middle of the interval: $\Theta(L/2 + x) = -\Theta(x)$. Figures 9.23–9.26 illustrate the solutions with the boundary condition (9.15) [i.e., $j_s(0) = j$], and Fig. 9.27 corresponds to the cyclic boundary condition (9.17) [$\psi'(0) = 0$].

9.3.10. Role of Interference Current Component

It is of interest to see how the solutions behave if the interference current j_{int} (9.8) is included (we have demonstrated some of the results in the preceding drawings). Figures 9.28–9.31 illustrate the role of the interference current component. One can see from the figures that j_{int} into account does not significantly change the qualitative pattern of the resistive state, although some changes occur. In particular, the oscillation periods and current-voltage characteristics change noticeably (Figs. 9.12, 9.13, and 9.17). The presence of j_{int} is revealed more markedly in the behavior of the potential, in which an anomaly is formed in the vicinity of PSC (Fig. 9.28), which in turn leads to peculiar behavior of the normal component of the current $j_n = -\nabla\Phi$ and also j_{int} (Fjg. 9.30). Such behavior persists also in the case of two PSCs (Figs. 9.29 and 9.31).

With increasing Γ, the magnitude of the anomaly also increases, but at $\Gamma = 0$ the interference contribution disappears. Although the normal current j_n may become rather large when ψ vanishes, there is no anomaly in j_s. Because the total current is kept fixed, $j = j_s + j_n + j_{int} = \text{const}$, the anomaly in j_n is compensated for by a corresponding anomaly in j_{int}. Thus the total current j stays a finite and smooth function.

A remark should be made concerning the anomalies found in j_n and j_{int}. The anomalous behavior of j_n and j_{int} is related to the term $j_{int}^1 Q\partial\psi/\partial t$ in (9.8), which grows when ψ tends to zero and Q becomes infinite. The superconducting current $j_s = \psi^2 Q$ at these moments remains finite. Representing j_{int}^1 in the form $j_{int}^1 \omega\Gamma\psi^2 Q = \omega\Gamma j_s$, it is easy to conclude that enormously large values of $j_{int}^1 >> j_s$ mean $\omega\Gamma >> 1$, i.e., the characteristic frequencies in the vicinity of PSC are greater than the energy damping of electrons. However, in deriving TDGL equations, quasi-classical conditions were assumed, i.e., that the characteristic frequencies should be less than the energy damping [see (7.28)]. In fact, this condition becomes violated in the vicinity of the PSC, which demonstrates a certain

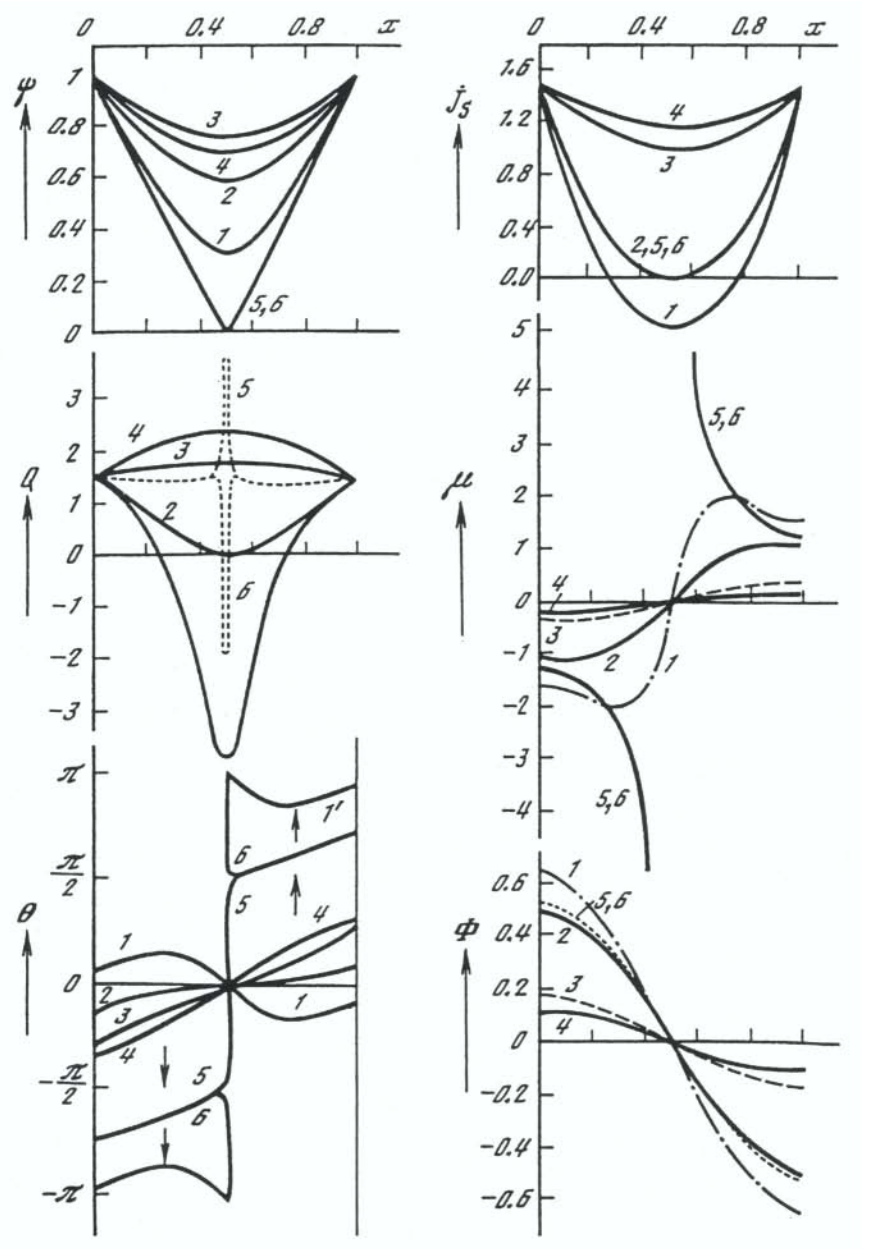

Figure 9.23. Solution for $L = 1$, $\Gamma = 100$, $j = 1.5$ (the boundary values: $\psi_0 = 1$, $j_{n0} = 0$).

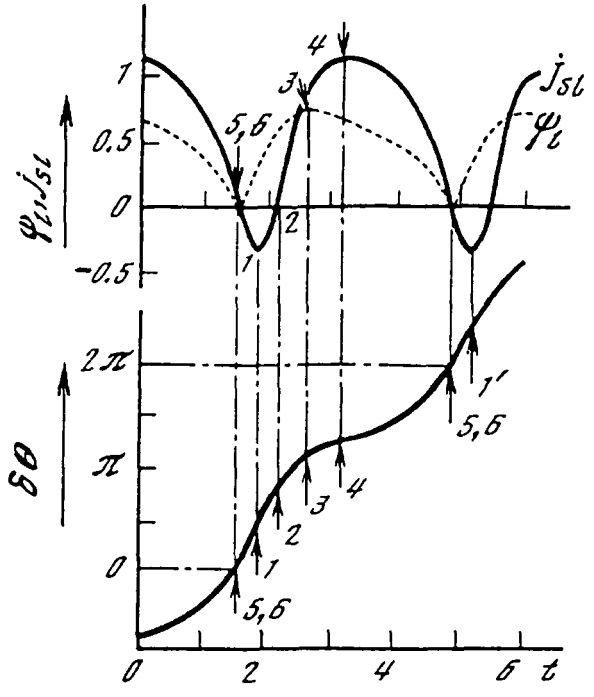

Figure 9.24. The phase difference $\delta\Theta$ at the ends and the values of ψ_l and j_{sl} at the point of the PSC as functions of the time for a filament with $L = 1$, $\Gamma = 0$, $j = 1.5$ (the boundary values: $\psi_0 = 1$, $j_{n0} = 0$).

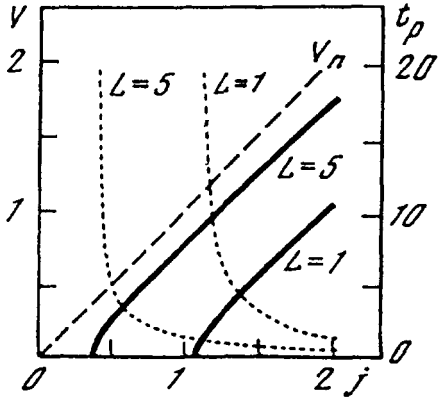

Figure 9.25. Current-voltage characteristics (solid lines) and periods of oscillations (dashed lines) for filaments with $L = 1$ and $L = 5$ (the boundary values $\psi_0 = 1$, $j_{n0} = 0$; $\Gamma = 0$).

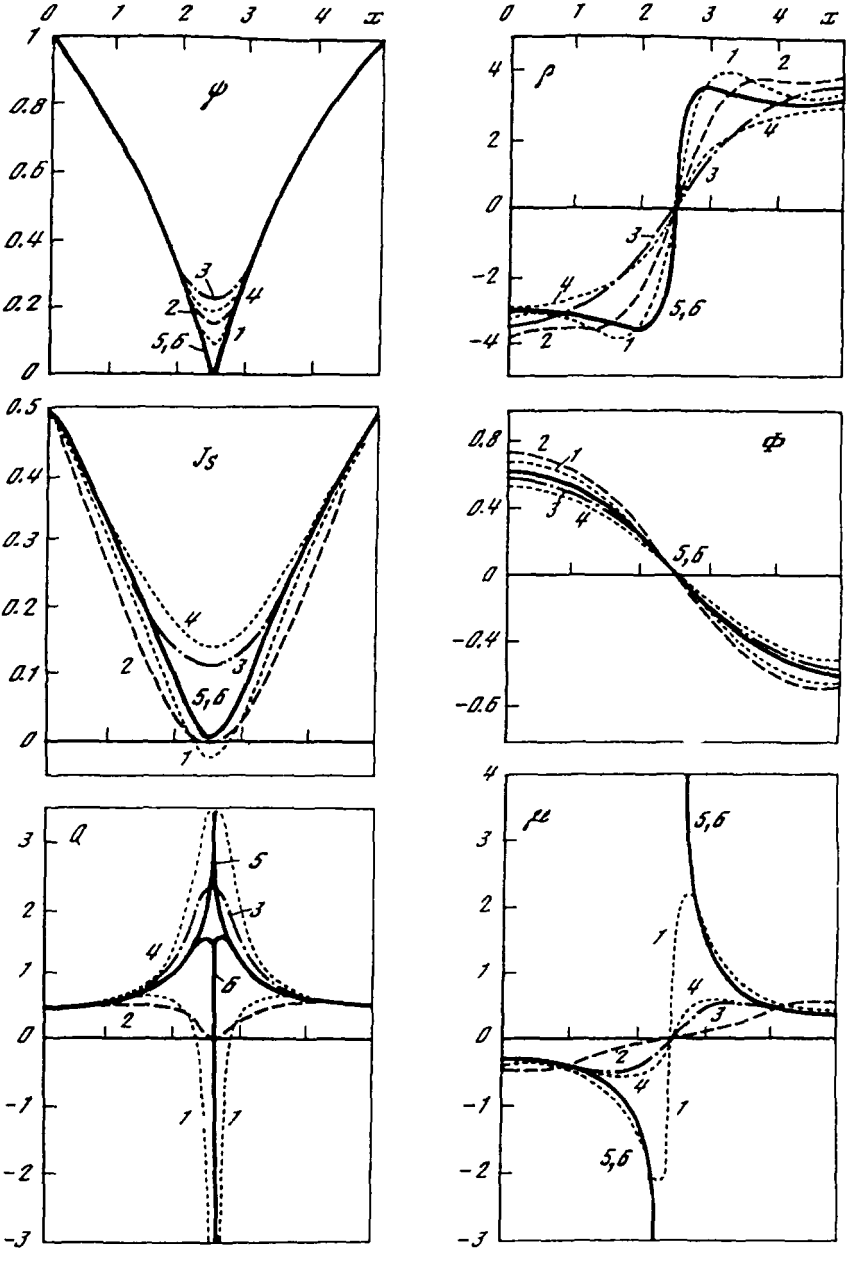

Figure 9.26. Solution for $L = 5$, $\Gamma = 1$, $j = 0.5$ ($\psi_0 = 1$, $j_{n0} = 0$).

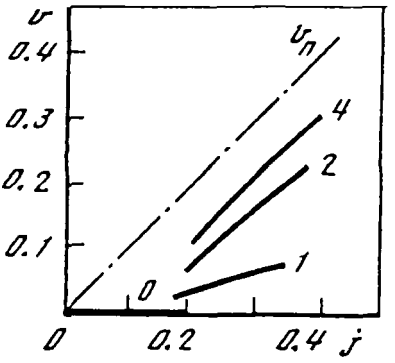

Figure 9.27. Current-voltage characteristics for a filament with $L = 25$, $\Gamma = 100$ for a cyclic boundary condition (9.17). 0, 1, 2, 4, the number of PSCs.

inconsistency in the equations used. It should be noted that this difficulty is inherent to TDGL equations, even with $j_{\text{int}} = 0$. Indeed, the large space and time gradients always arise in the PSC structure, in contradiction to quasi-classical conditions. One possible way to overcome this difficulty might be a consistent accounting for time derivatives of higher order. In such an approach, the inclusion of an additional term proportional to $2\mu^2$ [or to $(\partial/\partial t + 2i\varphi)^2$; see footnote on page 161] in the dynamic equation (7.45) may be reasonable. The inclusion of an interference current component in the set of dynamic equations is in fact a step in this direction.

9.4. EMISSION FROM PHASE-SLIP CENTERS

As shown in the preceding section, the resistive state of a superconducting filament is characterized by periodically placed phase-slip centers. In the vicinity of these centers, having a length scale $\Lambda \sim \xi(T)/[\tau_\varepsilon \Delta_0(T)]^{1/2}$, where Δ_0 is the stationary value of the gap, all the quantities describing the electron system oscillate in time with frequency, which is defined by the voltage drop on the PSC [see expression (9.54)].

9.4.1. Generation of Electromagnetic Radiation

It is natural to suppose that electromagnetic radiation might be generated in these conditions. Indeed, such radiation from narrow thin-film structures was observed,[36] even prior to the creation of the microscopic theory of PSC (a typical level of radiation was 10^{-12} W). As was found further, the picture is complicated: besides the high-frequency radiation (32.13) an emission at low frequencies was also detected.[37] Assuming that this effect may be explained by the motion of the

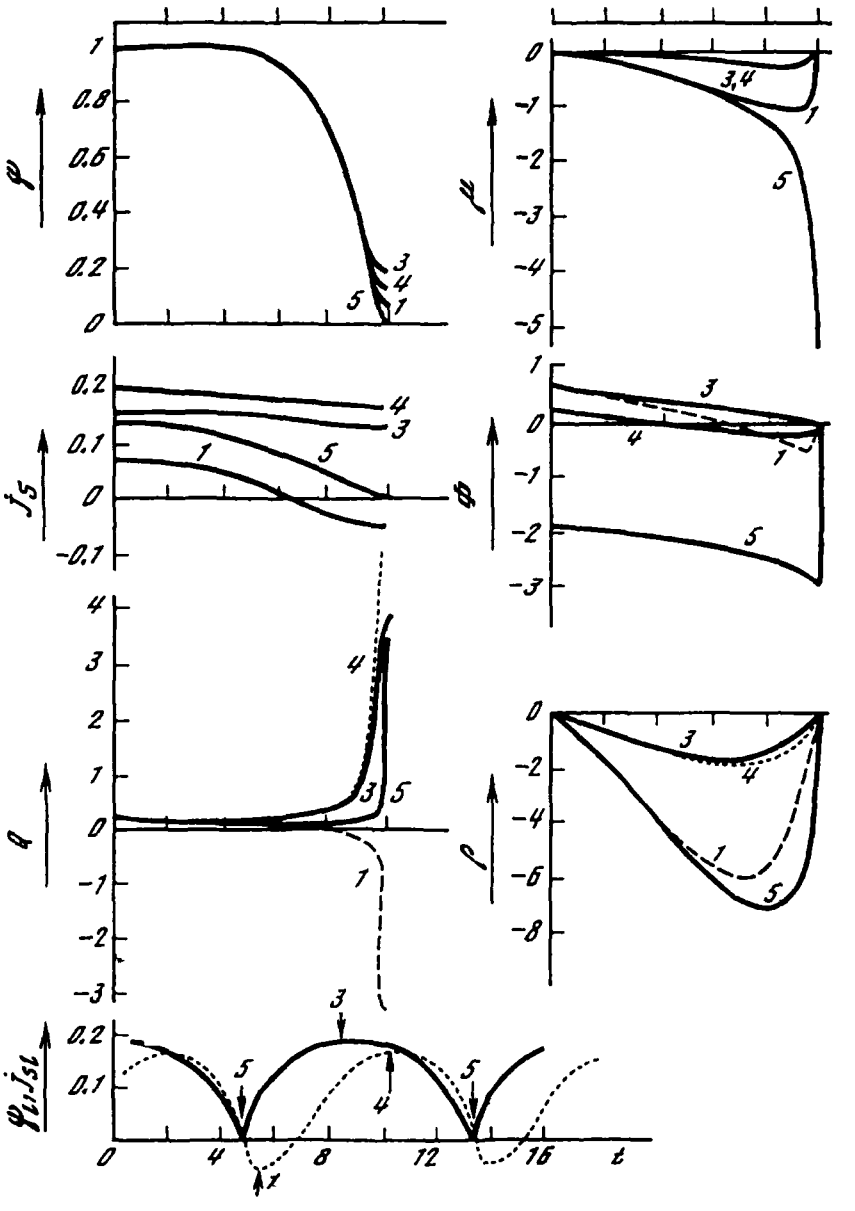

Figure 9.28. Solutions for $L = 10$, $\Gamma = 100$, $j = 0.3$ taking into account j_{int} at $1 - T/T_c = 0.1$ ($\psi_0 = 1$, $\mu_0 = 0$; the state with one PSC).

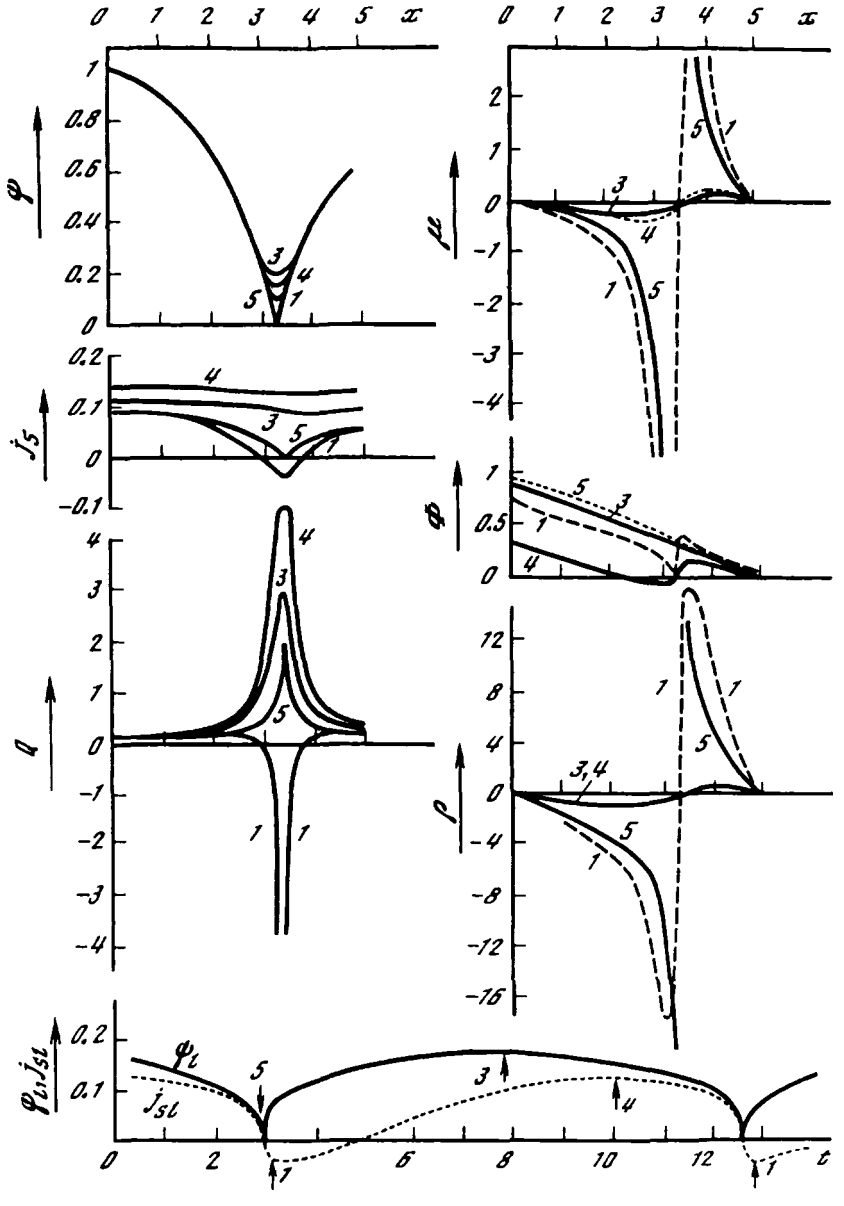

Figure 9.29. Solutions for $L = 10$, $\Gamma = 100$, $j = 0.3$ taking into account j_{int} at $1 - T/T_c = 0.1$ ($\psi_0 = 1$, $\mu_0 = 0$; the state with two PSCs; only one is shown).

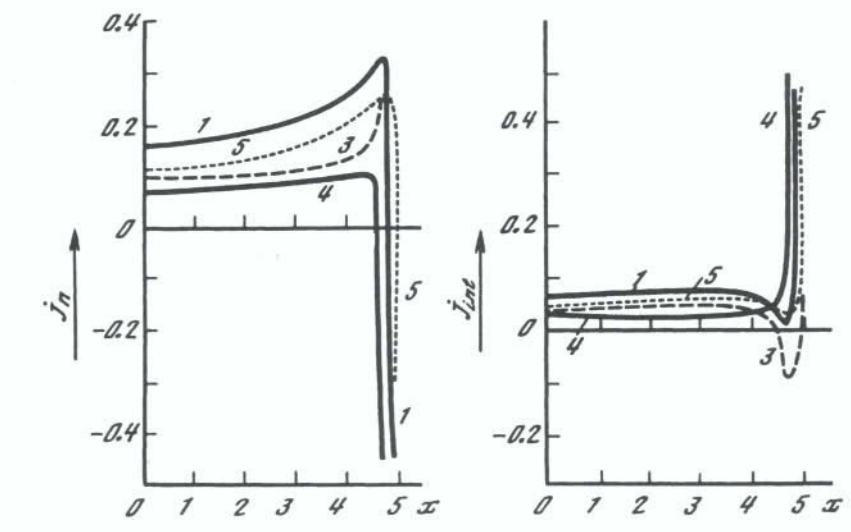

Figure 9.30. Normal and interference currents at different moments of time ($L = 10$, $\Gamma = 100$, $j = 0.3$ $1 - T/T_c = 0.1$; the state with one PSC).

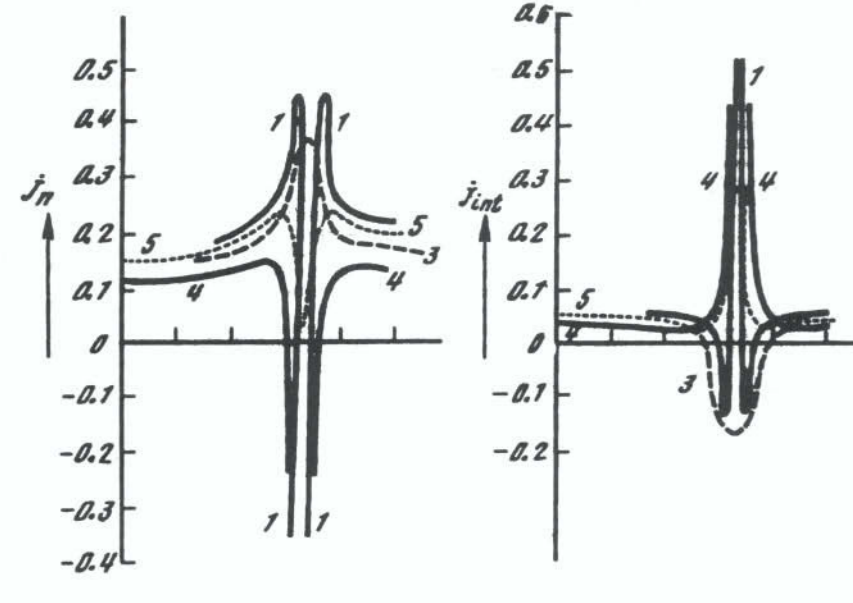

Figure 9.31. Normal and interference currents at different moments of time ($L = 10$, $\Gamma = 100$, $j = 0.3$, $1 - T/T_c = 0.1$; the state with two PSCs).

PSC structure as a whole along the filament, the velocity of the motion was estimated[37] as $10^4 - 10^5$ cm/s. According to this picture, the electric field pulses arise periodically at the ends of the filament, defining the generation frequency. Another explanation of the low-frequency part of the spectrum is that such pulsations are due to small differences in oscillation frequencies of separate phase-slip centers.[38] This difference may be caused by variations in geometrical or physical parameters along the filament. A complete explanation of the mechanism of low-frequency oscillations is yet to be found.

9.4.2. Phonon Radiation

Another interesting consequence of the PSC regime is the possibility of phonon radiation from the PSC. Expressions (7.68) and (7.58) can be used to calculate the spectral dependence $dW/d\omega_q$ of the phonon emission from the phase-slip center for arbitrary moments of time. Since $|\Delta(t)|$ is a periodic function of time, the phonon emission from the active region oscillates and the phonon flux periodically reverses its direction, as is evident from the sign alternations of $\partial|\Delta|/\partial t$ entering into (7.68). [Note that the time-averaged value of the phonon flux is nonzero because of the interdependence of η_1 (7.58) and $|\Delta(t)|$].

The intensity of the phonon flux emitted from the unit volume may be estimated as $w \sim (\omega_D/\varepsilon_F)(\Delta_0^2/\gamma_0)(T^3/u^3)V$. For the voltages $V < \tau_\varepsilon^{-1}$ (e.g., $V \sim 10^2$ nV) we have $w \sim 10^3$ W/cm^3 (at $T \sim 10$ K), which is of the order of Joule's heat $\sim V^2\rho_0\Lambda^2$, where ρ_0 is the specific resistivity of the active region with the length Λ. Thus this kinetic effect,[39] though not observed experimentally as yet, has a noticeable scale.

It is necessary to acknowledge that the sign-alternating pulsating phonon fluxes are not easy to detect. One approach would be to use a high-resolution technique [the detection time of phonons must be shorter than the period of oscillations given by Eq. (9.54)]. Another approach would be to detect the phonon flux by a method that is sensitive to only one direction of the phonon flux (for example, a method based on using the fountain effect in superfluid ^{4}He.)[40]

The detection of the phonon emission, which is spatially modulated and periodically reversed in time, might provide additional confirmation of the validity of current theoretical understanding of the physics of resistive states in "one-dimensional" superconductors. The discovery of phase-slip centers in high-temperature superconductors[41] raises such expectations.

References

1. R. Tidecks, *Current-Induced Nonequilibrium Phenomena in Quasi-One-Dimensional Superconductors,* pp. 1–341, Springer-Verlag, Berlin-New York (1990).
2. W. J. Skochpol, M. B. Beasley, and M. Tinkham, Phase-slip centers and nonequilibrium processes in microbridges, *J. Low. Temp. Phys.* **16** (1/2), 145–167 (1974).

3. W. A. Little, Decay of persistent currents in small superconductors, *Phys. Rev.* **156**(2), 396–403 (1967).
4. P. W. Anderson, Consideration on the flow of superfluid helium, *Rev. Mod. Phys.* **38**(2), 298–310 (1966).
5. J. S. Langer and V. Ambegaokar, Intrinsic resistive transition in narrow superconducting channels, *Phys. Rev.* **164**(2), 498–510 (1967).
6. D. E. McCumber and B. I. Halperin, Time scale of intrinsic resistive fluctuations in thin superconducting wires, *Phys. Rev. B* **1**(3), 1054–1070(1970).
7. B. l. Ivlev and N. B. Kopnin, Theory of current states in narrow superconducting channels, *Sov. Phys. Uspekhi* **27**(3), 206–227 (1984) *[Usp. Fiz. Nauk,* **142**(3), 435–472 (1984)].
8. B. I. Ivlev and N. B. Kopnin, Electric currents and resistive states in thin superconductors, *Adv. Phys.* **33**(1), 47–114 (1984).
9. V. P. Galaiko and N. B. Kopnin, in *Nonequilibrium Superconductivity,* D. N. Langenberg and A. I. Larkin, ed., pp. 543–588, North-Holland, Amsterdam (1985).
10. L. Kramer and R. J. Watts-Tobin, Theory of dissipative current-carrying states in superconducting filaments. *Phys. Rev. Lett.* **40**(15), 1041–1043 (1978).
11. R. J. Watts-Tobin, Y. Krahenbiihl, and L. Kramer, Nonequilibrium theory of dirty, current-carrying superconductors: Phase-slip oscillations in narrow filaments near T_c, *J. Low Temp. Phys.* **42**(5/6), 459–501(1981).
12. K. K. Likharev and L. A. Yakobson, Dynamical properties of superconducting filaments of finite length,Sov. *Phys. JETP* **41** (3), 570–575 (1975) *[Zh. Eksp. i Teor. Fiz.* **68**(3), 1150–1160(1975)].
13. K. K. Likharev, Isothermal domains in quasi-one-dimensional superconductors, *JETP Lett.* **20**(11), 338–339 (1974) *[Pis'ma v Zh. Eksp. i Teor. Fiz.* **20**(11), 730–733 (1975)].
14. L, Kramer and A. Baratoff, Lossless and dissipative current-carrying states in quasi-one-dimensional superconductors, *Phys. Rev. Lett.* **38**(9), 518–521 (1977).
15. L. Kramer and R. Rangel, Structure and properties of the dissipative phase-slip state in narrow superconducting filaments with and without inhomogeneities, *J. Low Temp. Phys.* **57**(3/4), 391–414(1984).
16. R. Rangel and L. Kramer, Theory of periodically driven, current-carrying superconducting filaments. *J. Low Temp. Phys.* **68**(1/2), 85–107 (1987).
17. S. M. Gol'berg, N. B. Kopnin, and M. I. Tribel'skii, Dynamics of the formation and destruction of phase-slip centers in narrow superconducting channels, Sov. *Phys. JETP* **67**(4), 812–820 (1988) *(Zh. Eksp. i Teor. Fiz.* **94**(4), 289–304 (1988)].
18. A. A. Akhmetov, Self-organization of a periodic structure containing phase-slip centers, *Sov. Phys. JETP* **67**(4), 834–838 (1988) *[Zh. Eksp. i Teor. Fiz.* **94**(4), 328–335 (1988)].
19. M. C. Potter, *Mathematical Methods in the Physical Sciences,* pp. 1–466, Prentice-Hall, Englewood Cliffs, NJ(1978).
20. G. I. Marchuk, *Methods of Numerical Mathematics,* pp. 1 –510, Springer-Verlag, Berlin-New York (1982).
21. B. I. Ivlev and N. B. Kopnin, Resistive state of superconductors, *JETP Lett.* **28**(10), 592–595 (1978) [Pis'ma *Zh. Eksp. i Teor. Fiz.* **28**(10), 640–644 (1978)].
22. J. I. Pankove, New effect at superconducting contacts, *Phys. Lett.* **21**(4), 406–407 (1966).
23. A. I. Akimenko, V. S. Solov'ev, and I. K. Yanson, ac Josephson current as a function of voltage, Sov. *J. Low Temp. Phys.* **2**(4), 238–241 (1976) *[Fiz. Nizk. Temp.* **2**(4), 480–485 (1976)].
24. M. Octavio, W. J. Skochpol, and M. Tinkham, Nonequilibrium-enhanced supercurrents in short superconducting weak links, *Phys. Rev. B 17* (1), 159–169 (1978).
25. V, N. Gubankov, V. P. Koshelets, and G. A. Ovsyannikov, Properties of Josephson thin film variable-thickness microbridges, Sov. *Phys. JETP* **46**(4), 755–760 (1977) *[Zh. Eksp. i Teor. Fiz.* **73**[4(10)], 640–644 (1978)].

26. Yu. Ya. Divin and F. Ya. Nad', A model of real superconducting point contacts, *Sov. J. Low Temp. Phys.* **4**(9), 520–525 (1978) *[Fit. Nizk. Temp.* **4**(9), 1105–1114 (1978)].
27. H. A. Notarys and J. E. Mercereau, Proximity effect bridge and superconducting microcircuitry, *J. Appl. Phys.* **44**(4), 1821–1830 (1973).
28. T. M. Klapwijk, M. Sepers, and J. E. Mooij, Regimes in the superconducting microbridges, *Low Temp. Phys.* **27**(5/6), 801–835 (1977).
29. S. N, Artemenko and A. F. Volkov, Electric fields and collective oscillations in superconductors, Sov. *Phys. Uspekhi* **22**(5), 295–310 (1979) *[Usp. Fiz. Nauk* **128**(1), 3–30 (1979)].
30. H. J. Fink, Current transitions of superconducting whiskers, *Phys. Lett. A.* **42**(7), 465–467(1973).
31. H. J. Fink and R. S. Poulsen, Exact solution of a new superconducting state, *Phys. Rev. Lett.* **32**(14), 762–765(1974).
32. H. J. Fink and R. S. Poulsen, Complete solution a new superconducting current state above the critical, *Phys. Rev. B* **11**(5), 1870–1877 (1975).
33. V. P Galaiko, Microscopic theory of resistive current states in superconducting channels, *Sov. Phys. JETP* ***4l(1),*** 108–114 (1975) *[Zh. Eksp. i Teor. Fiz.* **68**(1), 223–237 (1975)].
34. V. P. Galaiko, V. M. Dmitriev, and G. E. Churilov, Resistance current states and the nonstationary properties of superconducting channels, *Sov. J. Low Temp. Phys.* **2**(3), 148–158 (1976) *[Fiz. Nizk. Temp.* **2**(3), 229–316(1976)].
35. E. V. Bezuglyi, E. N. Bratus', and V. P. Galaiko, Voltage jumps in the current-voltage characteristics of superconductive channels, *Sov. J. Low Temp. Phys.* **3**(8), 491–497 (1977) *[Fiz. Nizk. Temp.* **3**(8), 1010–1021 (1977)].
36. G. E. Churilov, V. M. Dmitriev, and A. P. Beskorsyi, Generation of high-frequency oscillations by thin superconducting tin films, *JETP Lett.* **10**(5), 146–147 (1969) *[Pis 'ma v Zh. Eksp. i Teor. Fiz.* **10**(5), 231–233(1969)].
37. G. E. Churilov, V. M. Dmitriev, and V. N. Svetlov, Features in the spectra of electromagnetic oscillations generated in superconducting channels, *Sov. J. Low Temp. Phys.* **9**(5), 250–252 (1983) *[Fiz. Nizk. Temp.* **9**(5), 495–498 (1983)].
38. B.I. Ivlev, N.B. Kopnin, and I.A. Larkin, Low-frequency oscillations in the resistive state of narrow superconductors, *Sov. Phys. JETP* **61**(2), 337–343 (1985) *[Zh. Eksp. i Teor. Fiz.* **88**(2), 575–588(1985)].
39. A. M. Gulyan, G. F. Zharkov, and G. M. Sergoyan, Effect of the order parameter dynamics on the phonon emission in superconductors, *JETP Lett.* **44**(7), 426–429 (1986) *[Pis'ma v Zh. Eksp. i Teor. Fiz.* **44**(7), 331–333 (1986)].
40. H. Schreyer, W. Dietscher, and H. Kinder, Spatial development of multiple gap state in nonequilibrium superconductors, *Phys. Rev. B.* **31**(3), 1334–1337 (1985).
41. R. B. Akopyan and S. G. Gevorgyan, On the observation of phase slip centers in high-temperature superconductors, *JETP Lett.* **52**(12), 674–678 (1990) *[Pis'ma Zh. Eksp. i Teor. Fiz.* **52**(12) 1255–1258(1990)].

10

Josephson Junctions

10.1. TUNNEL SOURCE OF EXCITATIONS

10.1.1. Josephson Effect

Consider a superconductor that occupies all the space, with the current $\mathbf{j}$ flowing along the direction x. In Chap. 1 expression (1.53) was obtained for a superfluid current in an equilibrium superconductor. Because the problem considered here is formally one-dimensional, one can choose a gauge $\mathbf{A} = 0$ and make $\mathbf{j} \propto \nabla\theta$, where θ is the phase of the condensate wave function (1.52). From this expression it follows that the current is defined by the phase difference between the points along the direction of motion. Let now two superconductors occupy two isolated half-spaces and each of them be described by its own wave function. If these superconductors are brought into contact, then a current will flow perpendicular to the boundary because the phases of wave functions in each of superconductors, in general, may differ from each other. Since the states in (1.52) with $\theta + 2\pi n$, where n is an integer, are physically identical the current between superconductors must be a periodic function of the phase difference $\theta_1 - \theta_2$ with the period 2π. In addition, the current must vanish when the phase difference is zero. Hence the functional dependence of the current between superconductors, at least in a first approximation, may be expressed by the relation $j = j_0 \sin(\theta_1 - \theta_2)$; this is the first, or the stationary Josephson effect.[1,2]

If the superconductors occupying the half-spaces are connected by the tunneling barrier, the potential difference $\varphi_1 - \varphi_2$ may appear on the barrier in the current-carrying state. Bearing in mind the relation between the phase of the wave function and the scalar potential (see 8.3), according to which $\theta = -2\varphi$ in equilibrium ($\mu \equiv 0$), we arrive at the conclusion that the current between superconductors oscillates in time: $j = j_0 \sin(\omega_J t)$. The frequency of oscillations is $\omega_J = 2(\varphi_1 - \varphi_2) \equiv 2e(\varphi_1 - \varphi_2)/\hbar$, where we have restored the fundamental constant previously set at unity (the second, or nonstationary Josephson effect).

The phenomena that take place in the Josephson junctions have been studied in numerous papers (see bibliographical review, Ref. 3). Before moving to the description of a nonequilibrium Josephson junction, note that the equilibrium theory of superconductivity (see Sect. 1.2) cannot describe the situation when the potential difference exists at the superconductor's boundary (the potential φ and the normal current do not enter the equilibrium equations at all). In the case considered ($\varphi_1 - \varphi_2 \neq 0$), the boundary between superconductors appears as a nonequilibrium source. In the presence of massive banks, the nonequilibrium carriers may dissipate by diffusion and the nonequilibrium phenomena cannot noticeably change physical properties of the junction, which thus could be considered as equilibrium one. The picture differs for thin-film junctions whose thickness is comparable with the diffusion length of the electron excitations. In this case the junction banks are in a spatially homogeneous nonequilibrium state and, as we will see in this chapter, the nonequilibrium effects become essential.

10.1.2. Tunneling Hamiltonian and Self-Energies

Let the voltage V ($e = \hbar = 1$) be applied to the tunnel junction and this voltage be constant in time. We will describe the tunnel process by the Hamiltonian

$$\hat{H}_T = \sum_{\alpha} \int_{V_1} \int_{V_2} d^3\mathbf{r}_1 d^3\mathbf{r}_2 \{\hat{T}(\mathbf{r}_1,\mathbf{r}_2)\, \Psi^{\dagger}_{1\alpha}(\mathbf{r}_1)\, \Psi_{2\alpha}(\mathbf{r}_2) + H.c.\} \tag{10.1}$$

where the indices 1 and 2 correspond to different banks of the junction and integration is assumed over their volumes. The self-energy parts corresponding to the tunneling in the superconductor–insulator–superconductor junction (SIS′), may be obtained with the help of Hamiltonian (10.1)[4] and in our notations they have the form*

$$(\hat{\Sigma}^{(T)})^{R(A)}(t, t') = \frac{\nu}{\pi} \hat{g}'^{R(A)}(t, t'), \tag{10.2}$$

where ν is the tunneling frequency related to the tunneling operator $\hat{T}(\mathbf{r}_1, \mathbf{r}_2)$, and the function g' corresponds to the superconductor injector.

10.1.3. Derivation of Excitation Source

Taking into account relations (4.13) to (4.15) and (10.2), we find;

*The formal analogy between (10.1) and the Hamiltonian (2.1) describing the scattering of electrons on impurities makes the detailed derivation of Eq. (10.2) excessive [cf. Eq. (2.37)].

$$\{(I_\varepsilon - I_{-\varepsilon}) + u_\varepsilon(I_\varepsilon - I_{-\varepsilon})\}_{\text{eff}} = (2\pi i)^2 \frac{\nu}{\pi} \{[u_\varepsilon \beta_\varepsilon (u_{\varepsilon-V} + u_{\varepsilon+V})$$

$$+ \alpha_\varepsilon(u_{\varepsilon-V} - u_{\varepsilon+V}) - u_\varepsilon(u_{\varepsilon-V}\beta_{\varepsilon-V} + u_{\varepsilon+V}\beta_{\varepsilon+V}) - u_\varepsilon(\alpha_{\varepsilon-V} - \alpha_{\varepsilon+V})$$

$$+ \beta_\varepsilon(u_{\varepsilon-V} - u_{\varepsilon+V}) + (u_{\varepsilon-V} + u_{\varepsilon+V})\, u_\varepsilon\alpha_\varepsilon - u_{\varepsilon-V}\beta_{\varepsilon-V} + u_{\varepsilon+V}\beta_{\varepsilon+V}$$

$$- \alpha_{\varepsilon-V} - \alpha_{\varepsilon+V}] + \cos\theta[-\nu_\varepsilon\nu_{\varepsilon+V}(\beta_\varepsilon - \beta_{\varepsilon+V}) - \nu_\varepsilon\nu_{\varepsilon-V}(\beta_\varepsilon - \beta_{\varepsilon-V})$$

$$- \alpha_\varepsilon\nu_\varepsilon(\nu_{\varepsilon-V} + \nu_{\varepsilon+V})] + \sin\theta[\nu_\varepsilon w_{\varepsilon+V}\beta_\varepsilon + \nu_{\varepsilon+V}w_\varepsilon\beta_{\varepsilon+V} - \nu_\varepsilon w_{\varepsilon-V}\beta_\varepsilon$$

$$- \nu_{\varepsilon-V}w_\varepsilon\beta_{\varepsilon-V} - \alpha_\varepsilon\nu_\varepsilon w_{\varepsilon-V} + \nu_\varepsilon\alpha_\varepsilon w_{\varepsilon+V}]\}, \tag{10.3}$$

where $w_\varepsilon = |\Delta|\theta(|\Delta|^2 - \varepsilon^2)(|\Delta|^2 - \varepsilon^2)^{-1/2}$. Moving to the distribution function n_ε according to (3.84) to (3.88), we find, based on (10.3),

$$(u_\varepsilon \dot{n}_{\pm\varepsilon})^T = \frac{1}{2}\nu\,[Q_1(n_{\pm\varepsilon})\sin\theta + Q_2(n_{\pm\varepsilon})\cos\theta + Q_3(n_{\pm\varepsilon})], \quad \varepsilon \geq \Delta. \tag{10.4}$$

In Eq. (10.4) the dimensionless factors Q_i are defined in the following way:

$$Q_1(n_{\pm\varepsilon}) = \nu_\varepsilon w_{\varepsilon-V}(2n_{\pm\varepsilon} - 1)\theta(|\Delta'| - \varepsilon + V)\theta(|\Delta'| + \varepsilon - V)$$

$$- \nu_\varepsilon w_{\varepsilon+V}(2n_{\pm\varepsilon} - 1)\theta(|\Delta'| - \varepsilon + V)\theta(|\Delta'| - \varepsilon - V), \tag{10.5}$$

$$Q_2(n_{\pm\varepsilon}) = \nu_\varepsilon\nu_{\varepsilon-V}[(n_{\pm\varepsilon} - n_{\varepsilon-V}) + (n_{\pm\varepsilon} - n_{-\varepsilon+V})]\theta(\varepsilon - V - |\Delta'|)$$

$$- \nu_\varepsilon\nu_{\varepsilon+V}[(n_{\varepsilon+V} - n_{\pm\varepsilon}) + (n_{-\varepsilon-V} - n_{\pm\varepsilon})]\theta(\varepsilon + V - |\Delta'|)$$

$$+ \nu_\varepsilon\nu_{V-\varepsilon}[(1 - n_{\pm\varepsilon} - n_{V-\varepsilon}) + (1 - n_{\pm\varepsilon} - n_{-V+\varepsilon})]\theta(V - \varepsilon - |\Delta'|), \tag{10.6}$$

$$Q_3(n_{\pm\varepsilon}) = [(n_{\varepsilon-V} - n_{\pm\varepsilon})(u_\varepsilon u_{\varepsilon-V} \pm u_{\varepsilon-V} + u_\varepsilon \pm 1)$$

$$+ (n_{-\varepsilon+V} - n_{\pm\varepsilon})(u_\varepsilon u_{\varepsilon-V} \pm u_{\varepsilon-V} - u_\varepsilon \mp 1)]\theta(\varepsilon - V - |\Delta'|)$$

$$- [(n_{\pm\varepsilon} - n_{\varepsilon+V})(u_\varepsilon u_{\varepsilon+V} \mp u_{\varepsilon+V} - u_\varepsilon \pm 1)$$

$$+ (n_{\pm\varepsilon} - n_{-\varepsilon-V})(u_\varepsilon u_{\varepsilon+V} \mp u_{\varepsilon+V} + u_\varepsilon \mp 1)]\theta(\varepsilon + V - |\Delta'|)$$

$$+ [(1 - n_{\pm\varepsilon} - n_{V-\varepsilon})(u_\varepsilon u_{V-\varepsilon} \pm u_{V-\varepsilon} - u_\varepsilon \mp 1)$$

$$+ (1 - n_{\pm\varepsilon} - n_{-V+\varepsilon})(u_\varepsilon u_{V-\varepsilon} \pm u_{V-\varepsilon} + u_\varepsilon \pm 1)]\theta(V - \varepsilon - |\Delta'|) \tag{10.7}$$

We emphasize that in these final expressions, which represent the nonequilibrium tunnel source of the Josephson junction,[5] the quantity ε is defined positively. Here

n_ε appears as the electronlike excitation distribution function, while $n_{-\varepsilon}$ denotes the holelike one. [Expression (10.4) without the terms Q_1 and Q_2, i.e., without taking into account the macroscopic phase coherency in the junction, was derived in Ref. 6.]

The tunnel frequency in (10.4) should be expressed in terms of the detectable parameters. To achieve this, it is necessary to have the expression for the current flowing across the Josephson junction in a nonequilibrium state. Naturally, in equilibrium it should transform into the expression obtained by Josephson. We will now derive the expression for this nonequilibrium current.

10.1.4. Expression for Tunnel Current

We start from the 11-component of Eq. (3.63). Integration over ε and subsequent averaging over the angle variables transforms it into a continuity equation. After such a procedure, the terms remaining in (3.63) contain the self-energy parts representing (up to a numeric factor) the divergence of the current density, integrated over the volume V_0 of the nonequilibrium film (the spatial homogeneity of the pattern is assumed). Thus the integral tunnel current acquires the form

$$I = \int j\, ds = J_0 \{I_s \sin\theta + I_{\text{int}} \cos\theta + I_n\}, \quad \theta = 2Vt + \theta_0, \tag{10.8}$$

where $J_0 = \nu V_0 m p_F / 2\pi^2$. For the current amplitude we find the following functionals, (for simplicity the sign of the modulus in quantities Δ and Δ' in these expressions is omitted):

$$I_s = \Delta\Delta' \int_{-\infty}^{\infty} d\varepsilon \left\{ \frac{\theta(\varepsilon^2 - \Delta^2)\theta[\Delta'^2 - (\varepsilon - V)^2]}{\sqrt{\varepsilon^2 - \Delta^2}\sqrt{\Delta'^2 - (\varepsilon - V)^2}} (n_\varepsilon - n_{-\varepsilon} - 1) \right.$$

$$\left. + \frac{\theta[(\varepsilon - V)^2 - \Delta'^2]\theta(\Delta^2 - \varepsilon^2)}{\sqrt{(\varepsilon - V)^2 - \Delta'^2}\sqrt{\Delta^2 - \varepsilon^2}} (n_{\varepsilon - V} - n_{-\varepsilon + V} - 1) \right\}, \tag{10.9}$$

$$I_{\text{int}} = \Delta\Delta' \int_{-\infty}^{\infty} d\varepsilon \left\{ \frac{\theta(\varepsilon^2 - \Delta^2)\theta[(\varepsilon + V)^2 - \Delta'^2]}{\sqrt{\varepsilon^2 - \Delta^2}\sqrt{(\varepsilon + V)^2 - \Delta'^2}} \right.$$

$$\left. \times (1 - n_\varepsilon - n_{-\varepsilon}) \operatorname{sign}(\varepsilon + V) - (1 - n_{\varepsilon + V} - n_{-\varepsilon - V} \operatorname{sign} \varepsilon) \right\}, \tag{10.10}$$

$$I_n = \int_{-\infty}^{\infty} d\varepsilon \left\{ \frac{|\varepsilon|\,|\varepsilon - V|\theta(\varepsilon^2 - \Delta^2)\theta[(\varepsilon - V)^2 - \Delta'^2]}{\sqrt{\varepsilon^2 - \Delta^2}\sqrt{(\varepsilon - V)^2 - \Delta'^2}} \right.$$

$$\left. \times [(1 - n_\varepsilon - n_{-\varepsilon}) \operatorname{sign} \varepsilon - (1 - n_{\varepsilon - V} - n_{-\varepsilon + V}) \operatorname{sign}(\varepsilon - V)] \right.$$

$$- \frac{|\varepsilon - V|\,\theta(\varepsilon^2 - \Delta^2)\theta[(\varepsilon - V)^2 - \Delta'^2]}{\sqrt{(\varepsilon - V)^2 - \Delta'^2}} (n_\varepsilon - n_{-\varepsilon}) \operatorname{sign} \varepsilon$$

$$+ \frac{|\varepsilon|\theta(\varepsilon^2 - \Delta^2)\theta[(\varepsilon - V)^2 - \Delta'^2]}{\sqrt{\varepsilon^2 - \Delta^2}} (n_{\varepsilon - V} - n_{-\varepsilon + V}) \operatorname{sign} (\varepsilon - V) \Bigg\}. \quad (10.11)$$

We stress that the expression derived for the current is not a trivial generalization of the formula figuring in equilibrium theory. The last two terms in (10.11) emerge from the branch imbalance and they characterize solely the nonequilibrium situation. In the equilibrium approximation, $n_\varepsilon \to n_\varepsilon^0(T)$ [where $n_\varepsilon^0(T) = [\exp(|\varepsilon/T|) + 1]^{-1}$], the formulas (10.8) to (10.11) transform to the familiar expressions for the Josephson current.[1,7]

10.1.5. "Tunnel Frequency" Parameter

We will now find the explicit form of ν. Moving to the equilibrium case $n_\varepsilon \to n_\varepsilon^0$ and making the limiting transition in (10.8) to (10.11) to Ohm's law we get $J_0 = 1/2eR$, from which

$$\nu = \frac{1}{4e^2 N(0) S d R}. \quad (10.12)$$

Here S is the junction's cross section, d is the thickness of the S-film, and R is the resistivity of the junction in the normal state (caused by the dielectric interlayer of an area S). For clarity the electron charge e is restored in expression (10.12).

10.1.6. Complete Set of Equations

Nonequilibrium functions n_ε and $n_{-\varepsilon}$ (and also Δ and Δ'), entering the expressions (10.9) to (10.11) are yet to be determined. The following serves the purpose:

$$u_\varepsilon \dot{n}_{\pm\varepsilon} = Q(n_{\pm\varepsilon}) + J^{(e-ph)}(n_{\pm\varepsilon}) + J^{(e-e)}(n_{\pm\varepsilon}). \quad (10.13)$$

At strong deviation from equilibrium, the order parameter modulus Δ (which may be taken as real in spatially homogeneous states) must be determined from the self-consistency equation. The self-consistent value of $|\Delta|$ is determined by formula (4.6), from which it follows (see Sect. 5.2) that

$$1 = \lambda \int_{|\Delta|}^{\infty} \frac{1 - n_\varepsilon - n_{-\varepsilon}}{\sqrt{\varepsilon^2 - |\Delta|^2}} d\varepsilon. \quad (10.14)$$

This relation will be used in conjunction with the kinetic equation (10.13).

Generally, the system of equations (10.13) and (10.14) should also be supplemented by Maxwell's equations, which sometimes dictate the selection among

various solutions of the kinetic problem [since the current through the junction is determined by the relations (10.8)–(10.11)].

10.2. OSCILLATORY PROPERTIES OF A TUNNEL SOURCE

We will now study the kinetics of an electron system of nonequilibrium tunnel Josephson junction. We assume that the Josephson junction consists of two sufficiently thin films with a constant voltage V applied between them. Various applied voltages will be considered: both (1) the supercritical values $V > |\Delta| + |\Delta'|$ when the applied electrical field generates excess quasi-particles from the condensate, and (2) the case of subcritical voltages $(V < |\Delta| + |\Delta'|)$. In the latter case, in addition to the usual Josephson effect, another inherent effect appears: if the electron excitations are out of equilibrium, quantum oscillations arise in the system. We will discuss some manifestations of this effect in more detail.

10.2.1. Clark's Branch Imbalance

As first demonstrated by Clarke,[8] when electrons are injected from a normal metal into a superconducting film (NIS), a potential difference between the Cooper condensate and the excitations appears in the film. Tinkham[9] has shown that this property of the NIS junction was caused by the population imbalance of electron–hole excitation branches in the nonequilibrium superconducting film. We will elucidate the physical meaning of this phenomenon.

Let us consider the tunnel junction SIS′, consisting of films sufficiently thin that the phonons are in equilibrium and the picture in each of the films is homogeneous across their thickness. Let the junction be coupled with a heat bath having a temperature T. We will consider the solutions of Eq. (10.13), assuming arbitrary deviation of the distribution function $n_{\pm\varepsilon}$ from the equilibrium Fermi function $n_\varepsilon^0(T)$. First, however, we will examine some properties of the expression $Q(n_{\pm\varepsilon})$.

1. The typical values of ν (10.12), which determine the injection intensity, are usually significantly smaller than the intensity of relaxation processes (which may be roughly characterized by the damping $\gamma \sim T_c^3/\omega_D^2$, where T_c is the transition temperature, and ω_D is the Debye frequency). In this limiting case $\nu/\gamma << 1$ in (10.4) and we may assume the distribution functions are equilibrium ones: $n_{+\varepsilon} \to n_\varepsilon^0 = [1 - \tanh(|\varepsilon|/2T)]/2$. Assuming also $|\Delta'| = 0$ in (10.5) to (10.7), we obtain the familiar expression[4,9] for the tunnel source of the NIS junction. A remarkable property of this expression is that $Q(\varepsilon) \neq Q(-\varepsilon)$; this finally causes the branch imbalance during the tunneling injection of excitations.
2. One can easily see that the property $Q(\varepsilon) \neq Q(-\varepsilon)$ of the tunnel source holds also in the SIS′ case (even for a symmetrical SIS junction). However,

the source obtained in Ref. 10 and figuring in a number of papers (see Ref. 11) does not possess this property. The relevant expression[10] arises if one drops in Eq. (10.7) all but the $u_\varepsilon u_{\varepsilon+V}$ terms in the corresponding round parentheses, drops also the terms $Q_{1,2}$ in (10.5) and (10.6), and then sets $n_\varepsilon \approx n_{-\varepsilon}$. Such a procedure may be justified only in the case of injection in the range of ε directly above the gap, when the imbalance is insignificant. In the latter case, however, an interesting peculiarity of the tunnel source resulting from the macroscopic phase coherence will be lost.

3. This peculiarity arises from the time-oscillating components $Q_1 \sin 2Vt$, $Q_2 \cos 2Vt$ in (10.4), which are of a quantum nature (they vanish when $\hbar \to 0$). Since the solution of the nonlinear problem (10.13) yields the distribution functions $n_{\pm\varepsilon}$, which are explicitly time dependent, the entire source (including the "stationary" term Q_3) generally "vibrates," and the Fourier spectrum of these oscillations (when the deviation from equilibrium is significant) cannot be represented by the first (Josephson) harmonic only.

10.2.2. Oscillations of the Gauge-Invariant Potential

Thus if the electron injection in the NIS junction leads to the appearance of a nonzero potential μ (see Sect. 8.1.1), in the SIS junction not only does the potential μ appear, but having appeared, it should oscillate in time. At small ν/γ these oscillations would be of small amplitude near the stationary value and have the Josephson frequency. We will now find certain quantitative characteristics of the predicted effects.

Consider a symmetric SIS junction and use in calculations the collision integral (4.119), accepting the electron–phonon collisions as the dominant relaxation mechanism in (10.13). Assuming the deviation from equilibrium to be weak, we present the difference $\delta n_\varepsilon = n_\varepsilon - n_{-\varepsilon}$ in the form

$$\delta n_\varepsilon = \delta n_\varepsilon^0 + \delta n_\varepsilon^1 \sin\theta + \delta n_\varepsilon^2 \cos\theta. \tag{10.15}$$

Substituting (10.15) into (10.13) subject to (4.119) and (10.4), one obtains a coupled system of integral equations for determination of δn_ε:

$$0 = V\frac{V}{2T}\cosh^{-2}\left(\frac{\varepsilon}{2T}\right)(u_{\varepsilon-V} - u_{\varepsilon+V}) - \gamma\left[\delta n_\varepsilon^0 M(\varepsilon) - \hat{M}(\varepsilon\varepsilon')\delta n_\varepsilon^0\right],$$

$$-Vu_\varepsilon \delta n_\varepsilon^2 = \nu\,\delta n_\varepsilon^0 v_\varepsilon v_{\varepsilon-V} - \gamma[\delta n_\varepsilon^1 M(\varepsilon) - \hat{M}(\varepsilon, \varepsilon')\delta n_{\varepsilon'}^1],$$

$$Vu_\varepsilon \delta n_\varepsilon^1 = \nu\delta n_\varepsilon^0 (v_\varepsilon v_{\varepsilon+V} + v_\varepsilon v_{\varepsilon-V}) - \gamma\,[\delta n_\varepsilon^2 M(\varepsilon) - \hat{M}(\varepsilon, \varepsilon')\delta n_{\varepsilon'}^2], \tag{10.16}$$

where the function $M(\varepsilon)$ is

$$M(\varepsilon) = \frac{1}{T_c^3}\left\{\int_{|\Delta|}^{\tilde{\omega}} d\varepsilon'(\varepsilon' - \varepsilon)^2 \,(u_\varepsilon u_{\varepsilon'} - v_\varepsilon v_{\varepsilon'})\,[N_{|\varepsilon'-\varepsilon|} + n_\varepsilon^0\theta(\varepsilon' - \varepsilon)\right.$$

$$\left. - (1 - n_\varepsilon^0)\,\theta\,(\varepsilon - \varepsilon')\,] + \int_{|\Delta|}^{\infty} d\varepsilon'(\varepsilon + \varepsilon')^2\,(u_\varepsilon u_{\varepsilon'} + v_\varepsilon v_{\varepsilon'})\,[N_{\varepsilon+\varepsilon'} + n_\varepsilon^0]\right\}, \qquad (10.17)$$

while the operator $\hat{M}(\varepsilon, \varepsilon')$ is defined as

$$\hat{M}(\varepsilon, \varepsilon')\,X(\varepsilon') = \frac{1}{T_c^3}\left\{\int_{|\Delta|}^{\tilde{\omega}} d\varepsilon'(\varepsilon' - \varepsilon)^2\,[N_{|\varepsilon'-\varepsilon|} + (1 - n_\varepsilon^0)\,\theta(\varepsilon' - \varepsilon)\right.$$

$$\left. + n_\varepsilon^0\theta(\varepsilon - \varepsilon')]\,X(\varepsilon') + \int_{|\Delta|}^{\infty} d\varepsilon'(\varepsilon + \varepsilon')^2\,[N_{\varepsilon+\varepsilon'} + n_\varepsilon^0]\,X(\varepsilon')\right\}. \qquad (10.18)$$

We also denoted here

$$\gamma = \frac{\pi\lambda T_c^3}{2(up_F)^2}, \qquad (10.19)$$

where λ is the dimensionless electron–phonon interaction constant and u is the sound velocity.

Obtaining results of the numerical solution of Eq. (10.16), shown in Fig. 10.1, we may easily calculate the value of the gauge-invariant potential μ, which according to (8.6) equals

$$\mu = \int_{|\Delta|}^{\infty} \delta n_\varepsilon d\varepsilon \equiv \delta\mu^0 - \delta\mu^1 \sin\theta - \delta\mu^2 \cos\theta. \qquad (10.20)$$

Figures 10.2 and 10.3 show the behavior of $\delta\mu^i$ as the functions of V and T, respectively. The stationary value $\delta\mu^0$ of the SIS′ junction, as an examination shows, behaves analogously to that of the NIS junction. At sufficiently small values of v (Fig. 10.2), the dependencies of $\delta\mu^{1,2}$ are analogous to $\delta\mu^0$, although with increasing v the oscillations of $\delta\mu^{1,2}$ reach a maximum and then diminish. At the same time, the stationary part $\delta\mu^0$ increases nearly without bounds (the only limitation is the condition $V < 2|\Delta|$). Another peculiarity of the oscillating terms in the potential μ is their dependence on $|\Delta(T)|$ (i.e., on the temperature; Fig. 10.3). We have $\delta\mu \sim T/|\Delta| \to \infty$ at $T \to T_c$. Despite this, $\delta\mu^{1,2} \to 0$ at $T \to T_c$, because of the structural differences between $Q_{1,2}$ and Q_3 [Eq. (10.4)].

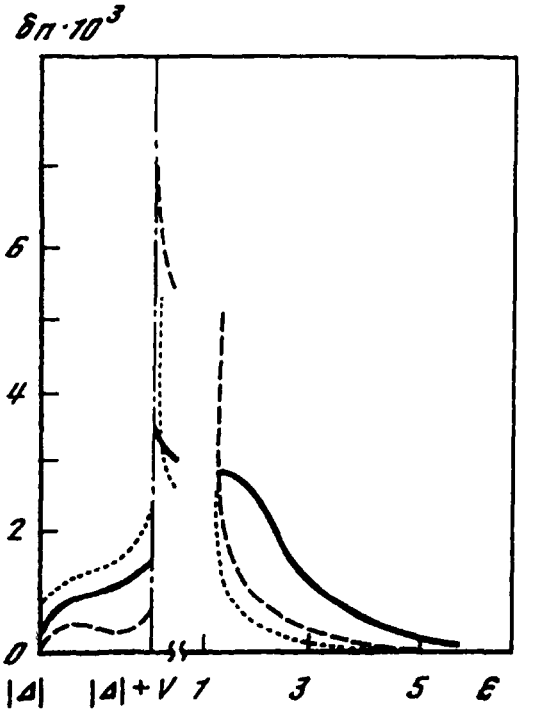

Figure 10.1. The dependence of the stationary function δn^0 (10.15) (solid line, in units ν/γ) and of amplitudes: δ^1 [dashed line, in units $(\nu/\gamma)^2$], δ^2 (dotted line) on ε at injection parameters $\gamma = 0.01$; $T = 0.9$, $\nu = 0.016$, $|\Delta| = 0.98$ (all the parameters in T_c units).

We should note that this examination, strictly speaking, is valid only when $\nu/\gamma \ll 1$ and, for example, at $\nu/\gamma \sim (0.1–0.3)$ $\delta\mu^{1,2}$ may, as is clear from Figs. 10.2 and 10.3, account for 1–10% of $\delta\mu^0$. In the most favorable cases the characteristic values of $\delta\mu^0$ may be on the order of a microvolt, but $\delta\mu^{1,2}$ may be fractions of this value (say, tens or hundreds of nanovolts for low-resistance aluminum junctions). Thus the oscillations of the nonequilibrium gauge-invariant potential may be identified experimentally a detection scheme should be like in Fig. 10.4 with voltmeter replaced by an oscilloscope.

10.2.3. Satellites in Scattered Radiation

The amplitude of oscillations of the gauge-invariant potential μ examined in the previous section is of the second order of smallness in the parameter ν/γ, whereas the potential itself (its time-averaged value) is a first-order effect in ν/γ. The question arises of whether the oscillations of the tunnel source can appear in

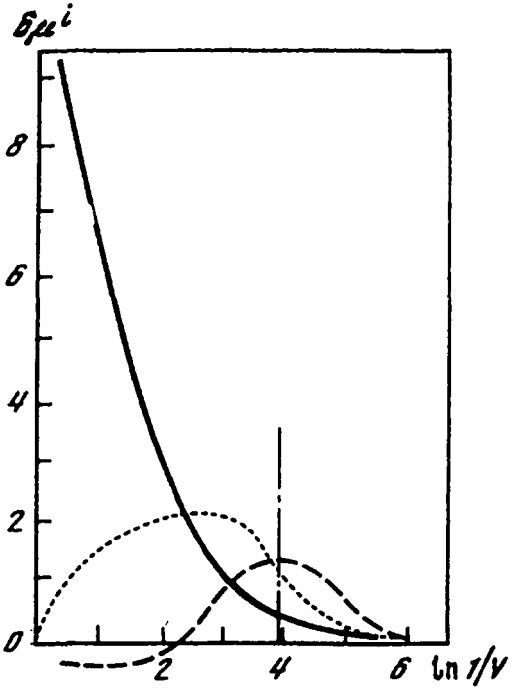

Figure 10.2. The dependence of the stationary value $\delta\mu^0$ and of amplitudes $\delta\mu^1$ and $\delta\mu^2$ on the bias voltage V. Solid line, the amplitude $\delta\mu^0$ (in $T_c\nu$ units); dashed line, the amplitude $\delta\mu^1$ (in 10 $T_c\nu^2$ units); dotted line, the amplitude $\delta\mu^2$ (in 10 $T_c\nu^2$ units). The dashed dotted line corresponds to the situation depicted in Fig. 10.1. The temperature $T = 0.9$, $\nu = 0.01$ (in T_c units).

the first approximation in ν/γ. Such an effect is described in the following paragraphs.

We will focus on the kinetic equation (10.13). In the first approximation over a small parameter ν/γ, the distribution functions $n_{\pm\varepsilon}$ in (10.4) to (10.7) may be taken as equilibrium ones. As a result, one obtains the following expressions for $Q_i(\varepsilon \geq |\Delta|)$:

$$Q_3(\pm\varepsilon) = 2\left\{(u_\varepsilon u_{\varepsilon-V} \pm u_{\varepsilon-V})\left(\tanh\frac{\varepsilon}{2T} - \tanh\frac{\varepsilon - V}{2T}\right)\right.$$
$$\left. - (u_\varepsilon u_{\varepsilon+V} \mp u_{\varepsilon+V})\left(\tanh\frac{\varepsilon + V}{2T} - \tanh\frac{\varepsilon}{2T}\right)\right\}, \qquad (10.21)$$

$$Q_1(\pm\varepsilon) = (v_\varepsilon w_{\varepsilon+V} - v_\varepsilon w_{\varepsilon-V}) \tanh\frac{\varepsilon}{2T}, \qquad (10.22)$$

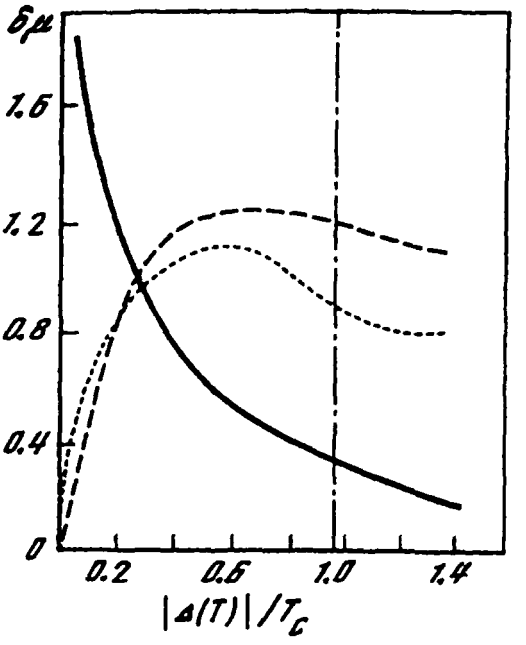

Figure 10.3. The dependence of a stationary value of $\delta\mu^0$ and of amplitudes $\delta\mu^1$ and $\delta\mu^2$ on the gap value $|\Delta(T)|$. The notations and scales are the same as in Fig. 10.2; $V/T_c = 0.016$.

$$Q_2(\pm\varepsilon) = 2\left\{\nu_\varepsilon\nu_{\varepsilon-V}\left(\tanh\frac{\varepsilon - V}{2T} - \tanh\frac{\varepsilon}{2T}\right)\right.$$
$$\left. - \nu_\varepsilon\nu_{\varepsilon+V}\left(\tanh\frac{\varepsilon}{2T} - \tanh\frac{\varepsilon + V}{2T}\right)\right\}. \qquad (10.23)$$

In writing these expressions we have restricted ourselves to the case $V < |\Delta| + |\Delta'|$ (recall that the primed quantities and functions with shifted arguments correspond to the injector). It is easily seen that the functions (10.21) to (10.23) have the properties:

$$Q_3(\varepsilon) \neq Q_3(-\varepsilon), \qquad (10.24)$$

$$Q_1(\varepsilon) = Q_1(-\varepsilon), \quad Q_2(\varepsilon) = Q_2(-\varepsilon) \qquad (10.25)$$

[The property (10.25) is responsible for the oscillating contribution to the potential μ (10.20), being of the second order of smallness in ν/γ]. From (10.25) it follows that the oscillating nonequilibrium contributions to the distribution function of the

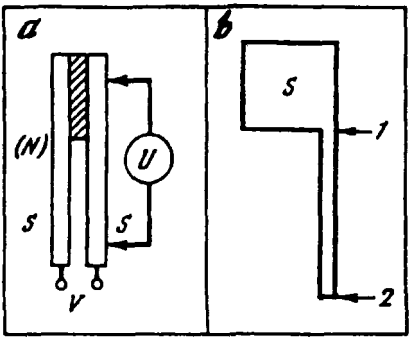

Figure 10.4. Schematic of Josephson junction. (a) The connection of the external circuit V and of voltmeter U for measuring the nonequilibrium gauge-invariant potential; (b) The junction projection is assumed to have the shape shown in the drawing, with the distance between 1 and 2 exceeding the decay length l_E of the electrical field, while the volume of the region 1–2 is much less than the volume of region S, so the diffusion of the quasi-particles into the region 1–2 insignificantly distorts the homogeneous pattern in the main region S (usually the region 1–2 is separated from S by the tunnel barrier).

electron–hole excitations in the first order in ν/γ are symmetric with respect to the sign of ε. We will find these contributions.

Consider the range of temperatures $T > |\Delta(T)|$, so that there is a sufficient number of equilibrium electron excitations. The collision integral $J(n_{\pm\varepsilon})$ in (10.13) may then be linearized in small deviations of the distribution function. The stationary correction to n_ε^0 in this case is determined by the term Q_3 (10.21) and yields an insignificant renormalization of n_ε^0. The asymmetry of Q_3 with respect to ε (property 10.24) causes an imbalance that we will also ignore in view of its additional smallness (as follows from 10.21) and assume further that $\delta n_\varepsilon = \delta n_{-\varepsilon}$. Because the applied voltage $V << T$, the variation δn_ε is localized at energies smaller than T. This means that now we may use in (10.13) the relaxation time approximation for the collision integral $J(n_\varepsilon) \equiv J^{(e-ph)} + J^{(e-e)}$ (we postpone general discussion of the validity of relaxation time approximation until Sect. 11.3):

$$J(n_\varepsilon) \approx -\gamma \frac{\varepsilon}{\sqrt{\varepsilon^2 - |\Delta|^2}} \delta n_\varepsilon, \tag{10.26}$$

where γ is a characteristic energy damping of the nonequilibrium excitations. Substituting (10.21) to (10.23) and (10.26) into (10.13) and carrying out a Fourier expansion of the nonequilibrium addition

$$\delta n_\varepsilon = \delta n_\varepsilon^0 + \delta n_\varepsilon^1 \sin 2Vt + \delta n_\varepsilon^2 \cos 2Vt + \ldots, \tag{10.27}$$

one obtains in the first order in ν/γ the following amplitudes $\delta n_\varepsilon^{1,2}$:

$$\delta n_\varepsilon^1 = \frac{\nu}{2} \frac{Q_2(\varepsilon)\omega_J + \gamma Q_1(\varepsilon)}{u_\varepsilon(\omega_J^2 + \gamma^2)}, \tag{10.28}$$

$$\delta n_\varepsilon^2 = \frac{\nu}{2} \frac{Q_2(\varepsilon)\gamma - \omega_J Q_1(\varepsilon)}{u_\varepsilon(\omega_J^2 + \gamma^2)}, \tag{10.29}$$

where $\omega_J = 2V$. Using these expressions we may now consider the scattering of external electromagnetic radiation by a nonequilibrium tunnel junction.

For a proper description of the scattering process, we must know the generalized susceptibility[12] of the nonequilibrium junction in response to the action of the electromagnetic radiation. For this purpose we will use the photon–electron collision operator. The electron–photon collision operator was derived in the quantum treatment of electromagnetic radiation in Sect. 5.3. Within the same lines one can show that the desired photon–electron operator for "dirty" superconductors has the form (N_{ω_0} corresponds to the occupation number of photons with the frequency ω_0):

$$I^{(\mathrm{pl-e})}(N_{\omega_0}) =$$

$$\pi \int_{|\Delta|}^{\infty} \int_{|\Delta|}^{\infty} d\varepsilon d\varepsilon' [2\delta(\varepsilon - \varepsilon' - \omega_0)\, r_1(\varepsilon, \varepsilon') + \delta(\varepsilon + \varepsilon' - \omega_0)\, r_2(\varepsilon, \varepsilon')], \tag{10.30}$$

$$\begin{aligned} r_1(\varepsilon, \varepsilon') = {} & \{[n_\varepsilon(1 - n_{-\varepsilon'})(1 + N_{\omega_0}) - (1 - n_\varepsilon) n_{-\varepsilon'} N_{\omega_0}] \\ & + [n_{-\varepsilon}(1 - n_{\varepsilon'})(1 + N_{\omega_0}) - (1 - n_{-\varepsilon}) n_{\varepsilon'} N_{\omega_0}]\} (u_\varepsilon u_{\varepsilon'} + v_\varepsilon v_{\varepsilon'} - 1) \\ & + \{[n_\varepsilon(1 - n_{-\varepsilon'})(1 + N_{\omega_0}) - (1 - n_\varepsilon) n_{\varepsilon'} N_{\omega_0}] \\ & + [n_{-\varepsilon}(1 - n_{-\varepsilon'})(1 + N_{\omega_0}) - (1 - n_{-\varepsilon}) n_{-\varepsilon'} N_{\omega_0}]\} (u_\varepsilon u_{\varepsilon'} + v_\varepsilon v_{\varepsilon'} + 1), \end{aligned} \tag{10.31}$$

$$\begin{aligned} r_2(\varepsilon, \varepsilon') = {} & \{[n_\varepsilon n_{-\varepsilon'}(1 + N_{\omega_0}) - (1 - n_\varepsilon)(1 - n_{-\varepsilon'}) N_{\omega_0}] \\ & + [n_{-\varepsilon} n_{\varepsilon'}(1 + N_{\omega_0}) - (1 - n_{-\varepsilon})(1 - n_{\varepsilon'}) N_{\omega_0}]\} (u_\varepsilon u_{\varepsilon'} - v_\varepsilon v_{\varepsilon'} + 1) \\ & + \{[n_\varepsilon n_{-\varepsilon'}(1 + N_{\omega_0}) - (1 - n_\varepsilon)(1 - n_{\varepsilon'}) N_{\omega_0}] \\ & + [n_{-\varepsilon} n_{-\varepsilon'}(1 + N_{\omega_0}) - (1 - n_{-\varepsilon})(1 - n_{-\varepsilon'}) N_{\omega_0}]\} (u_\varepsilon u_{\varepsilon'} - v_\varepsilon v_{\varepsilon'} - 1), \end{aligned} \tag{10.32}$$

where the prefactor n is proportional to the fine structure constant: $n \propto e^2/hc$.

We have written the operator (10.30) in a general form that also accounts for the branch imbalance. We are interested now in the classical limit of (10.30) when $N_{\omega_0} >> 1$. In this case one can carry N_{ω_0} from under the integral signs (henceforth we assume that N_{ω_0} is included in the prefactor n; we will not need the explicit form of this factor and it will be omitted in the following discussion). Retaining only the terms that correspond to the action of a field with frequency $\omega_0 < 2|\Delta|$, one obtains

$$I^{(\mathrm{pt-e})}(N_{\omega_0}) = \Phi_0 + \Phi_1 \sin \omega_J t + \Phi_2 \cos \omega_J t, \tag{10.33}$$

where the functions Φ_i [determined subject to (10.27) to (10.29)] acquire the form

$$\Phi_0(\omega_0, T) = \frac{1}{2}\int_{|\Delta|}^{\infty} d\varepsilon \frac{|\Delta|^2 + \varepsilon(\varepsilon+\omega_0)}{\sqrt{\varepsilon^2 - |\Delta|^2}\sqrt{(\varepsilon+\omega_0)^2 - |\Delta|^2}} \left(\tanh\frac{\varepsilon}{2T} - \tanh\frac{\varepsilon+\omega_0}{2T}\right) \tag{10.34}$$

(the contribution of δn_ε^0 in 10.15 is negligible),

$$\Phi_{1(2)}(\omega_0, T, V, \gamma, |\Delta'|) = |\Delta|\,|\Delta'| \int_{|\Delta|}^{\infty} \frac{d\varepsilon[|\Delta|^2 + \varepsilon(\varepsilon+\omega_0)]}{\sqrt{\varepsilon^2 - |\Delta|^2}\sqrt{(\varepsilon+\omega_0)^2 - |\Delta|^2}}$$

$$\times \left\{ a_{1(2)} \left[\left(\frac{\theta(\varepsilon - V - |\Delta'|)}{(\varepsilon+\omega_0)\sqrt{(\varepsilon - V)^2 - |\Delta'|^2}} \left(\tanh\frac{\varepsilon+\omega_0 - V}{2T} - \tanh\frac{\varepsilon+\omega_0}{2T} \right) \right.\right.\right.$$

$$\left. - \frac{\theta(\varepsilon+\omega_0+V-|\Delta'|)}{(\varepsilon+\omega_0)\sqrt{(\varepsilon+\omega_0+V)^2 - |\Delta'|^2}} \left(\tanh\frac{\varepsilon+\omega_0}{2T} - \tanh\frac{\varepsilon+\omega_0+V}{2T} \right) \right)$$

$$- \left(\frac{\theta(\varepsilon - V - |\Delta'|)}{\varepsilon\sqrt{(\varepsilon - V)^2 - |\Delta'|^2}} \left(\tanh\frac{\varepsilon - V}{2T} - \tanh\frac{\varepsilon}{2T} \right) - \frac{\theta(\varepsilon + V - |\Delta'|)}{\varepsilon\sqrt{(\varepsilon+V)^2 - |\Delta'|^2}} \right.$$

$$\left.\left. \times \left(\tanh\frac{\varepsilon}{2T} - \tanh\frac{\varepsilon+V}{2T} \right) \right) \right] \underset{(-)}{+} a_{2(1)} \left[\frac{1}{2(\varepsilon+\omega_0)} \right.$$

$$\times \tanh\frac{\varepsilon+\omega_0}{2T} \left(\frac{\theta[|\Delta'|^2 - (\varepsilon+\omega_0+V)^2]}{\sqrt{|\Delta'|^2 - (\varepsilon+\omega_0+V)^2}} - \frac{\theta[|\Delta'|^2 - (\varepsilon+\omega_0-V)^2]}{\sqrt{|\Delta'|^2 - (\varepsilon+\omega_0-V)^2}} \right)$$

$$\left. \left. - \frac{1}{2\varepsilon} \tanh\frac{\varepsilon}{2T} \left(\frac{\theta[|\Delta'|^2 - (\varepsilon+V)^2]}{\sqrt{|\Delta'|^2 - (\varepsilon+V)^2}} - \frac{\theta[|\Delta'|^2 - (\varepsilon - V)^2]}{\sqrt{|\Delta'|^2 - (\varepsilon - V)^2}} \right) \right] \right\}. \tag{10.35}$$

The constants a_1 and a_2 are equal to

$$a_1 = \frac{\nu\omega_J}{\omega_J^2 + \gamma^2}, \quad a_2 = \frac{\nu\gamma}{\omega_J^2 + \gamma^2}. \tag{10.36}$$

Before providing the results of the numerical analysis of these integrals, we briefly comment on the physical picture.

According to (10.27) to (10.29), the density of electron excitations in thin superconducting film oscillates with a small amplitude near its steady-state value owing to the existence of macroscopic phase coherence in a system of single-electron excitations. The interaction between the external electromagnetic radiation and the oscillating electron density of states causes the scattering of the electromagnetic wave with the formation of satellites at frequencies $\omega_0 \pm \omega_J$.

The collision operator (10.30) allows one to calculate the response of the nonequilibrium system, for example, to find the relative intensities of the satellites in the reflected radiation. From the point of view of spectroscopic experiments, however, it is easier to deal with the absorption coefficient of the system (specifically, with the imaginary part of the dielectric constant) or, in other words, with characteristics of the wave that passes through the film.

Consider a test wave passing through one of the films of an equilibrium superconducting junction. The absorption coefficient (up to a constant factor) is given by formula (10.34). We assume that the oscillations of the type mentioned earlier occur in the film. Then the absorption coefficient would also oscillate in accordance with (10.33). As a result, the amplitude of the transmitting wave would be modulated (we assume that $2|\Delta| > \omega_0 > \omega_J$) and the satellites would appear. The estimate of their relative intensity is as follows:

$$P \simeq \frac{(\Phi_1^2 + \Phi_2^2)^{1/2}}{2\Phi_0}. \tag{10.37}$$

The presence of a second film in the junction, in which oscillations also occur, somewhat distorts this simple picture. We will return to this question later.

Consider now the results of the numerical analysis of the junction's behavior. The function $P = P(\omega_0, T, V, |\Delta|, |\Delta'|, \gamma, \nu)$* was calculated for three metals: lead, niobium, and tantalum with the parameters shown in Table 10.1 (the data for aluminum will be used later, in further considerations).

The growth of P with a drop in temperature (Fig. 10.5) is due to the reduction in the number of equilibrium excitations, which makes the film effectively more transparent [for convenience Fig. 10.5 shows the dependence $|\Delta(T)|$ in the BCS

*The value of γ was introduced in calculations as a cutoff factor to remove divergence at the integration over ε in (10.35).

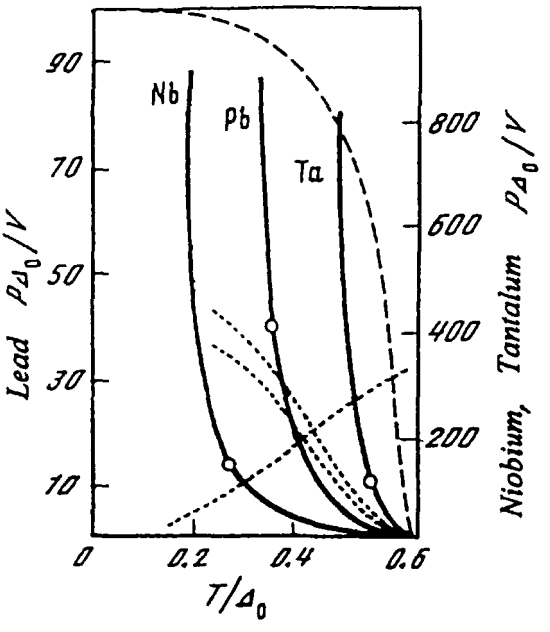

Figure 10.5. The transformation coefficients P for Pb, Nb, and Ta plotted to show their dependence on temperature (at $\omega \approx 300$ GHz for Pb and Nb and $\omega \approx 50$ GHz for Ta; $T_b = 4.2$ K, $|\Delta| = |\Delta'|$). The dashed line shows the $|\Delta(T)|$ dependence in the BCS model; $\Delta_0 = |\Delta(T = 0)|$. The behavior of the amplitudes $|\Phi_i|$ (in arbitrary units) for Pb is represented by the dotted lines; the falling curves (upper and lower) represent $|\Phi_1|$ and $|\Phi_2|$ respectively. The circles indicate the temperature of the helium bath ($T_b = 4.2$ K).

model]. One may become sure of that by direct analysis of the behavior of the Φ_i amplitudes (see the dotted lines in Fig. 10.5).

The presence of a (logarithmic) maximum near $V \sim \gamma$(Fig. 10.6) is a characteristic feature of the dependence of P on the voltage V across the junction. Corresponding voltages are optimal for detection of satellites.

Table 10.1. Some Parameters of Superconductors

Metal	T_c K	$N(0) \times 10^{-21}$ (states/eV)	ω_D (K)	ε_F (eV)	λ	Δ (meV)
Pb	7.2	5.4	105	10.9	1.55	1.45
Nb	9.2	19.9	275	6.2	0.80	1.50
Ta	4.5	25.4	240	18.0	0.70	0.72
Al	1.7	8.1	428	13.5	0.38	0.18

Source: Chang and Scalapino[13] and Otschik et al [14]

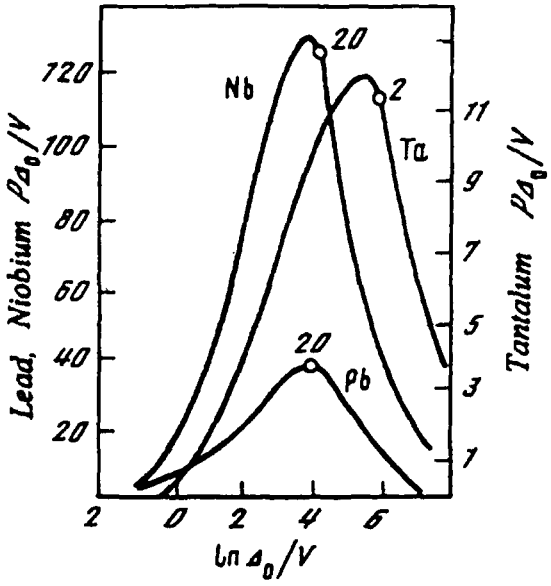

Figure 10.6. The transformation coefficient P plotted as a function of the voltage V across the junction (at the parameters given in Fig. 10.5). The circles indicate the values $V \approx \gamma$ (in microvolts).

The transformation coefficient P is independent of the frequency ω_0 of the test radiation (Fig. 10.7) at sufficiently high frequencies $\omega_0 >> \Delta_0$, but at lower frequencies it increases sharply, which ultimately is due to the singularity in the superconductor's electron density of states (in the calculations this singularity was cut off at energies $\delta\varepsilon \sim \gamma$). The inspection shows that the intensity of the satellites increases with diminishing γ (Fig. 10.8).

The dependence of P on the injector's gap $|\Delta'|$ is a peculiar one (Fig. 10.9). If $|\Delta'| < |\Delta|$ by 1% (this numeric value corresponds to $\gamma = 10^{-2}|\Delta|$, adopted in calculations), P drops by an order of magnitude. However, if $|\Delta'| > |\Delta|$ by 1%, P increases noticeably, but diminishes with further increases in $|\Delta'|$. This circumstance may be of use in the detection of satellites. Indeed, as noted earlier, the estimate (10.37) was obtained for the response of a single film, and, generally speaking, is not valid for a real Josephson junction, shown schematically in Fig. 10.8. However, in asymmetric junctions, the oscillations of the electron excitation's density manifest themselves only in a film with a smaller gap. (The difference between $|\Delta|$ and $|\Delta'|$ must be quite small, about 1%; such a difference $\sim\gamma/|\Delta|$ may exist for films of identical metals owing to some difference in deposition conditions, thickness, etc.) In these cases the estimate of (10.37) may be used directly.

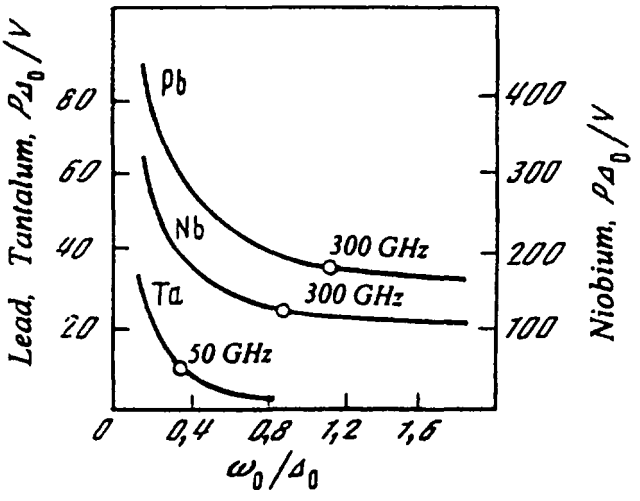

Figure 10.7. The transformation coefficient P plotted as a function of the test radiation frequency $\omega(T_b = 4.2\ K, |\Delta| = |\Delta'|, V \approx \gamma)$.

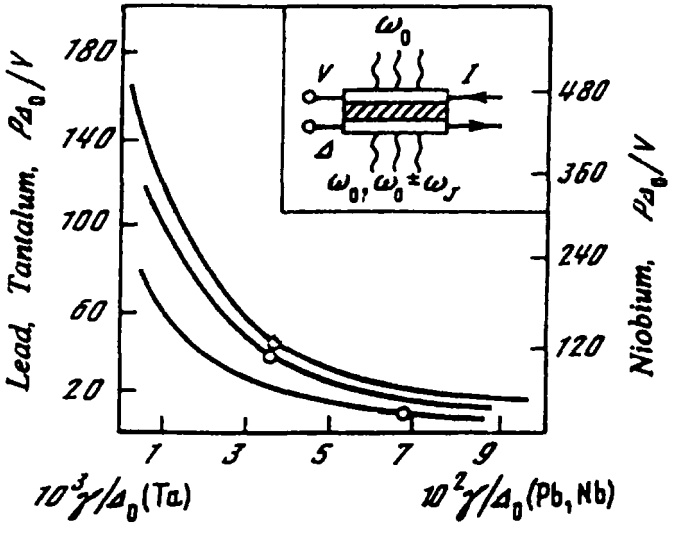

Figure 10.8. The transformation coefficient P plotted as a function of the electron excitation energy damping γ. The circles mark the tabulated values of γ. The inset shows the Josephson junction schematically.

For a lead film with $d \approx 10^3$ Å and $RS \approx 10^{-5}\Omega$ cm^2 we have $\nu/\Delta_0 \sim 2.6 \times 10^{-5}$ and $P \sim 10^{-3}$ at $T = 4.2$ K. Values of the same order were obtained for niobium and tantalum. Such values can be easily measured spectroscopically. For metals with low T_c (and large ω_D, such as aluminum) ν/Δ_0 is relatively large ($\sim 10^{-4}$), while γ is small ($\nu/\gamma \sim 0.1$) and hence $P \sim 0.1$. In such junctions, the level of nonequilibrium excursion is quite high and other interesting effects may also be observed (satellites with multiple frequencies, etc.).

Note the following. In principle, the appearance of satellites in an electromagnetic wave scattered by the Josephson junction may be explained within the usual electrodynamics by accounting for the interference between the ac current induced by the external field and the Josephson current. The proper functional dependencies (similar to those shown in Figs. 10.5–10.9) may obviously be different. It is also important to emphasize the fundamental difference between these effects (the kinetic and electrodynamic one). The "kinetic effect" holds if we consider scattering of the acoustic wave at the junction, instead of electromagnetic radiation ($\omega_0 \rightarrow \omega_q$). The high-frequency acoustic wave would also generate satellites with frequencies $\omega_q \pm \omega_J$. However, the "electrodynamic effect" cannot occur during the scattering of an acoustic wave. Thus the satellites caused by the oscillations in the excitation's density, in principle, can be singled out and unambiguously interpreted.

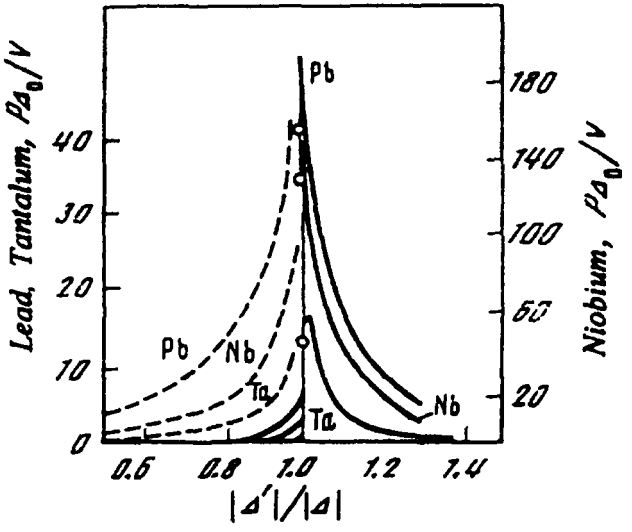

Figure 10.9. The transformation coefficient P as a function of the parameter $|\Delta'|/|\Delta|$. For Pb and Nb, $\omega_0 \approx 300$ GHz, $V \approx 20$ μV; for Ta, $\omega_0 \approx 50$ GHz, $V \approx 1$ μV; $T_b = 4.2$ K. The circles show the case when $|\Delta| = |\Delta'|$. When $|\Delta'| < |\Delta|$, the dashed curves represent the values of $P\Delta_0/V$ on a hundredfold greater scale.

10.3. SELF-CONSISTENT SOLUTION OF KINETIC EQUATIONS

10.3.1. Analytic Solution with a Branch Imbalance

Now we will consider the voltages when

$$V \sim |\Delta| + |\Delta'|. \tag{10.38}$$

In the entire superconducting temperature range, except for a very small vicinity of the transition point, the scale of the inverse frequencies corresponding to (10.38) is small compared to the time intervals that characterize the kinetics of single-particle excitations. Hence at the voltages of Eq. (10.38), the coherent effects in the excitation system are negligible (the results presented in the preceding sections implicitly confirm this).

In spite of the reduced role of quantum oscillations, the range of voltages in Eq. (10.38) is interesting, because the applied electric field is capable of pair breaking during pair tunneling. This breaking process is a resonant one and the resulting degree of nonequilibrium may be quite high.

In general one must consider (10.13) and (10.14) simultaneously with the analogous equations for the injector, so the number of coupled equations doubles. Indeed, the function (10.7) entering into (10.4) (it is enough to consider only its contribution) contains the distribution functions of both superconductors. In two limiting cases—symmetric and highly asymmetric junctions—the situation simplifies. In this chapter we consider the case of a symmetric SIS junction. Then in the force of the symmetry the following identities hold:

$$n_\varepsilon = n'_{-\varepsilon}, \quad n_{-\varepsilon} = n'_\varepsilon, \quad \varepsilon \geq |\Delta|. \tag{10.39}$$

Accounting for (10.39), we represent (10.13) as

$$n_\varepsilon a_{11}(\varepsilon) + n_{V-\varepsilon} a_{13}(\varepsilon) + n_{-V+\varepsilon} a_{14}(\varepsilon) = c_1(\varepsilon), \tag{10.40}$$

$$n_{-\varepsilon} a_{22}(\varepsilon) + n_{V-\varepsilon} a_{23}(\varepsilon) + n_{-V+\varepsilon} a_{24}(\varepsilon) = c_2(\varepsilon), \tag{10.41}$$

where all distribution functions correspond to the test superconductor. We will not provide explicit expressions for the quantities a_{ik} and c_j to save space. These expressions are obvious from a comparison of (10.40) and (10.41) with (10.13).

In representations (10.40) and (10.41), one may explicitly identify terms related to resonant pair breaking. This representation is convenient, because it allows exact accounting for these processes. For this purpose we will move to new arguments in (10.40) and (10.41), making the transposition $V - \varepsilon \to \varepsilon$. We get thus two additional equations defined in the same energy region $(\Delta, V - \Delta)$:

$$n_\varepsilon a_{31}(\varepsilon) + n_{-\varepsilon} a_{32}(\varepsilon) + n_{V-\varepsilon} a_{33}(\varepsilon) = c_3(\varepsilon), \tag{10.42}$$

$$n_\varepsilon a_{41}(\varepsilon) + n_{-\varepsilon} a_{42}(\varepsilon) + n_{-V+\varepsilon} a_{44}(\varepsilon) = c_4(\varepsilon), \tag{10.43}$$

with the determinant

$$\det a_{ik} = \begin{vmatrix} a_{11} & 0 & a_{13} & a_{14} \\ 0 & a_{22} & a_{23} & a_{24} \\ a_{31} & a_{32} & a_{33} & 0 \\ a_{41} & a_{42} & 0 & a_{44} \end{vmatrix} \equiv \det, \tag{10.44}$$

which is nonzero in the region

$$|\Delta| \le \varepsilon \le V - |\Delta|, \tag{10.45}$$

where subject to (10.39)

$$\begin{aligned} a_{33}(\varepsilon) &= a_{11}(V-\varepsilon), \quad a_{44}(\varepsilon) = a_{22}(V-\varepsilon), \\ a_{31}(\varepsilon) &= a_{13}(V-\varepsilon), \quad a_{41}(\varepsilon) = a_{23}(V-\varepsilon), \\ a_{32}(\varepsilon) &= a_{14}(V-\varepsilon), \quad a_{42}(\varepsilon) = a_{24}(V-\varepsilon), \\ c_3 &= c_1(V-\varepsilon), \qquad c_4 = c_2(V-\varepsilon). \end{aligned} \tag{10.46}$$

Composing now the determinants $\det_1$ and $\det_2$ for a system of four equations, one finds in the usual manner in the region (10.45):

$$n_\varepsilon = \frac{\det_1}{\det}, \quad n_{-\varepsilon} = \frac{\det_2}{\det}. \tag{10.47}$$

At low temperatures ($T \ll |\Delta|$) the "tail" of the distribution function at $\varepsilon \gtrsim V - |\Delta|$ is small. Neglecting this tail, as well as the tunneling redistribution of excitations and the relaxation processes, one obtains the solution that generalizes (accounting for the population imbalance) the expression derived by Aronov and Spivak[15] for the case of ultra high frequency (UHF) pumping. The iterations of the solution prove that accounting for the "tail" produces small changes in the resulting picture.

10.3.2. *Inclusion of Self-Consistency Equation*

The procedure for finding the solutions is not entirely reduced to simple iterations. Note that the nonequilibrium gap $|\Delta|$ enters the kinetic equation for $n_{\pm\varepsilon}$; this gap itself depends on the form of $n_{\pm\varepsilon}$. It may be shown that when $|\Delta| \ll \omega_D$, Eq. (10.14) is equivalent to the system

$$|\Delta| = \Delta_0 \exp(-\bar{n}_+ - \bar{n}_-), \quad \bar{n}_\pm = \int_{|\Delta|}^{\infty} \frac{n_{\pm\varepsilon}}{\sqrt{\varepsilon^2 - |\Delta|^2}}\, d\varepsilon. \tag{10.48}$$

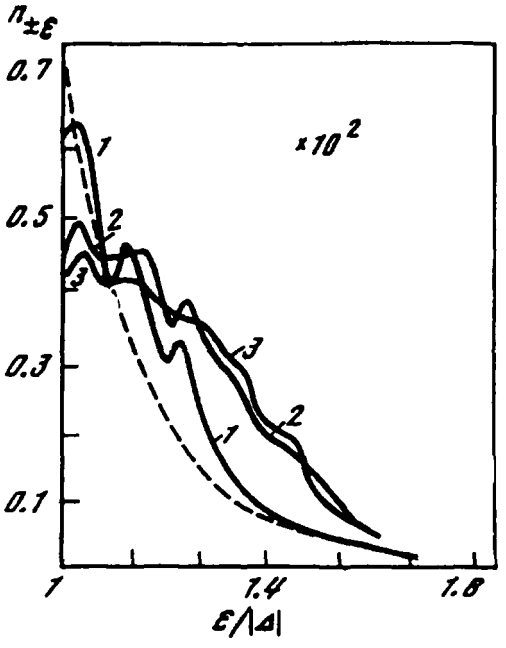

Figure 10.10. The distribution function of the electron excitation n_ε for various values of the parameter ν. Temperature $T = 0.2\Delta_0$; the bias voltage $V = 0.1\Delta_0$; the dashed line represents the Fermi distribution.

This system was included in the general iteration scheme that also utilizes (10.47) at $V > 2|\Delta|$.

The behavior of the excitation distribution function is illustrated in Figs. 10.10–10.14. Note the imbalance between the electronlike (n_ε) and the holelike $(n_{-\varepsilon})$ excitations, which occurs in both the subthreshold $(V < 2|\Delta|)$ and superthreshold $(V > 2|\Delta|)$ regimes.

10.3.3. Analysis of Numerical Solutions: Subthreshold Voltages

In the subthreshold case, in addition to the appearance of "spike," the distribution function shows a tendency for a global displacement toward higher energies (Fig. 10.10), which ultimately stimulates superconductivity (see Sect. 5.2) and creates a phonon deficit (see the following discussion). As the temperature drops, the nonequilibrium features become more pronounced: a larger number of spikes appear, which are separated by a distance V in the energy space (cf. Figs. 10.11 and 10.12). At very low temperatures, the distribution function acquires a "sawtooth" shape and is nonzero even in the range where the equilibrium Fermi "tail" is

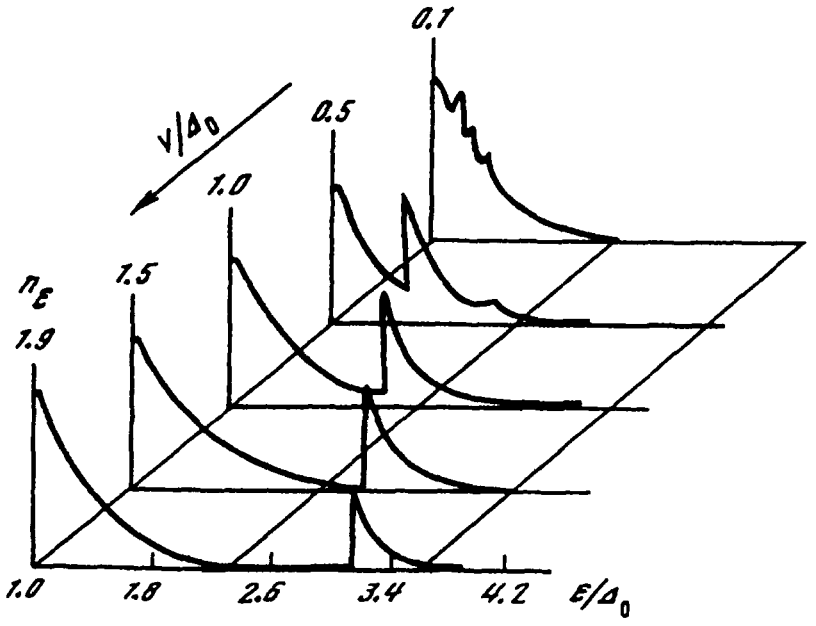

Figure 10.11. The evolution of the distribution function of the electron excitation n_ε with an increase of the bias voltage (for $T = 0.3\Delta_0$, $\nu = 0.1\gamma$).

negligible. Note that the number of observed spikes increases with a drop in voltage (Fig. 10.13).

10.3.4. Analysis of Numerical Solutions: Superthreshold Voltages

In the superthreshold range, virtually all the excess excitations are concentrated in the region above the gap and, as Fig. 10.14 shows, the "tail" adjacent to this region is negligible. Hence we may speak of a "quasi-local" distribution of nonequilibrium quasi-particles. The behavior of the nonequilibrium gauge-invariant potential μ is illustrated in Fig. 10.15.

Note two characteristic features of the behavior of the nonequilibrium gap $|\Delta|$. First, there is a range of V where subthreshold and superthreshold values coexist (compare curves 1 and 2 in Fig. 10.16). This produces the hysteresis in the current-voltage characteristics (see Fig. 10.17). Second, at $T \sim T_c$, with an increase in voltage V the curve $|\Delta(T,V)|$ increases insignificantly, rapidly saturating. Here we have the familiar phenomenon of superconductivity enhancement due to the tunneling absorption of excitations.[17]

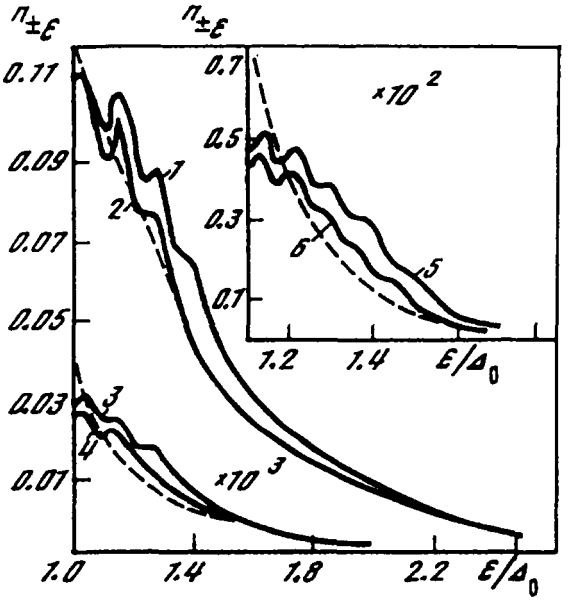

Figure 10.12. The distribution functions of the electron n_ε (upper curves) and hole $n_{-\varepsilon}$ (lower curves) excitations for various temperatures: 1, 2, for $T = 0.4\Delta_0$; 3, 4, for $T = 0.2\Delta_0$. In all cases $\nu/\gamma = 0.1$; $V/\Delta_0 = 0.1$. The dashed line represents the Fermi distribution.

10.4. PHONON EMISSION FROM A TUNNEL JUNCTION

Using the electron-hole distribution function found in the preceding section, one can calculate the spectrum of phonons emitted from the tunnel junction (analogously to the electromagnetic field, considered in Chap. 6).

10.4.1. Phonon Deficit in a Subthreshold Regime

The spectrum of phonons emitted from a nonequilibrium film is shown in Fig. 10.18. The dip in the spectrum at $\omega_q \geq 2|\Delta|$ reflects the presence of the phonon deficit effect. The same effect, though caused by the action of the UHF field, was discussed in Chap. 6. Since the essence of the effect remains the same in the present case, we will not provide a detailed commentary.

One small difference in the present case is that there are now two (rather than one) relaxation peaks* (see Fig. 10.18, curve 1). Their origin is related to the

*Such peaks would most likely occur under UHF pumping also (cf. Chap. 5), if one could perform the calculations with the appropriate accuracy.

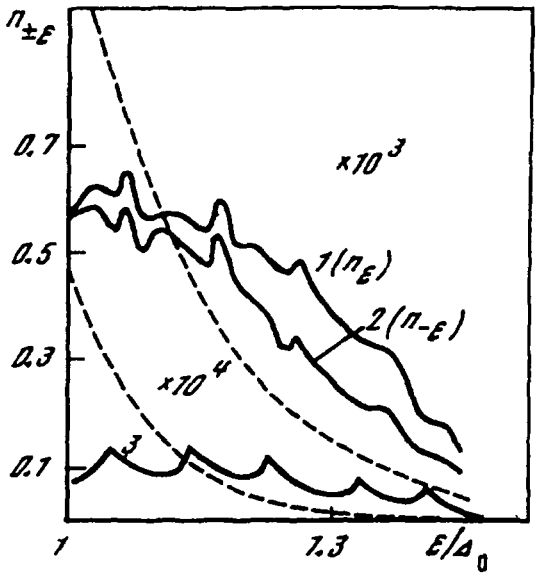

Figure 10.13. The distribution functions of electron n_ε (upper curve) and hole $n_{-\varepsilon}$ (lower curve) excitations for various temperatures: 1,2, at $T \approx 0.15\Delta_0$; 3, at $T = 0.1\Delta_0$. (In the last case, the behavior of the electron and hole excitation branches is virtually identical.)

sawtooth shape of the excitation distribution function (see the inset to Fig. 10.18). In some cases the peaks are indistinguishable at the scale used (Fig. 10.18, curve 2).

10.4.2. Superthreshold Regime: Preconditions of Deficit

The behavior of the phonon emission spectra in the superthreshold regime (Figs. 10.19 and 10.20) is peculiar. Note that curves similar to those in Fig. 10.20 (curve 1) were first obtained by Chang and Scalapino[13] (in a simplified model ignoring imbalance). However, they did not mention that at small values of ω_q the phonon fluxes became negative: this is illustrated in Fig. 10.20 (curve 3).

The phonon deficit effect when the excess quasi-particles are generated by the field from the condensate is not a trivial one. Evidently it is due to the strong localization of excess excitations near the gap edge in the energy space (see Fig. 10.14). As a result, in the scattering of phonons by electrons, the emission of phonons with frequencies higher than the boundary value is forbidden. At the same time, scattering with the absorption of phonons is possible: at high energies ε there is no energy gap. Hence the scattering mechanism causes a phonon deficit in a certain spectral range. A question arises in connection with this: Doesn't the deficit

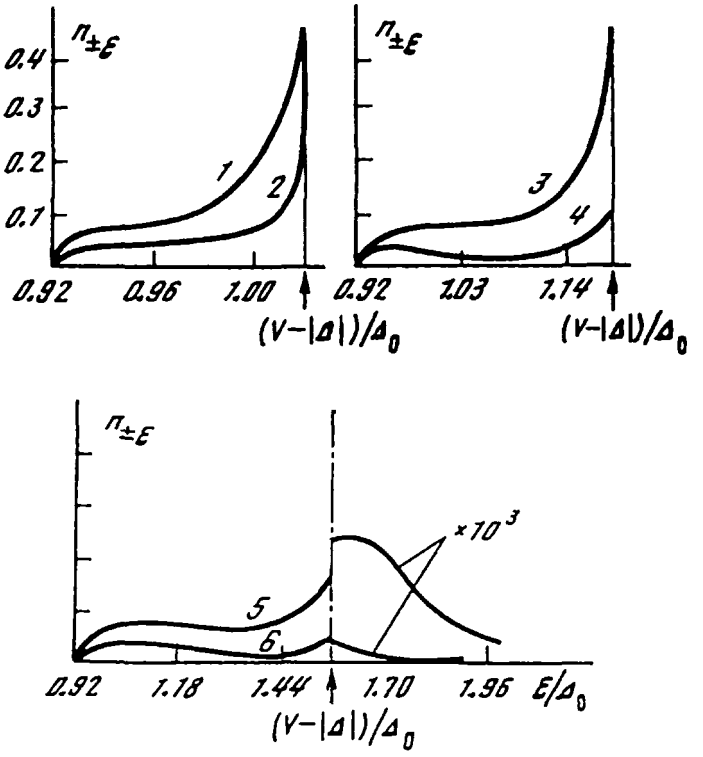

Figure 10.14. The distribution function of excess electronlike (upper curves) and holelike (lower curves) excitations in the above-threshold regime ($T = 0.1\Delta_0$, $\nu = 0.01\gamma$). 1,2, $V = 1.9\Delta_0$; 3,4, $V = 2.01\Delta_0$; 5,6, $V = 2.5\Delta_0$ (in the last case, the small "tail" of the distribution is also shown). As the voltage increases from the threshold value ($V = 2|\Delta| \approx 1.84\Delta_0$), the degree of imbalance increases. The distribution of equilibrium excitations is not shown: in these conditions the Fermi function is exponentially small.

reflect the phonon instability at the relaxation frequencies (i.e., the sign reversal of the phonon absorption coefficient)? As the calculations show (Fig. 10.20, curve 3), the sign of the absorption coefficient does not change. An inspection of the collision integral (4.128) shows that the small (equilibrium) "tail" of the excitation distribution function does not contribute to the nonequilibrium emission of phonons, while it does contribute to the absorption coefficient, compensating for the small dip that results from nonequilibrium.

Note that effects of the type presented in Figs. 10.19 and 10.20 hold for a broad range of junction parameters. We will not dwell here on further quantitative analysis.

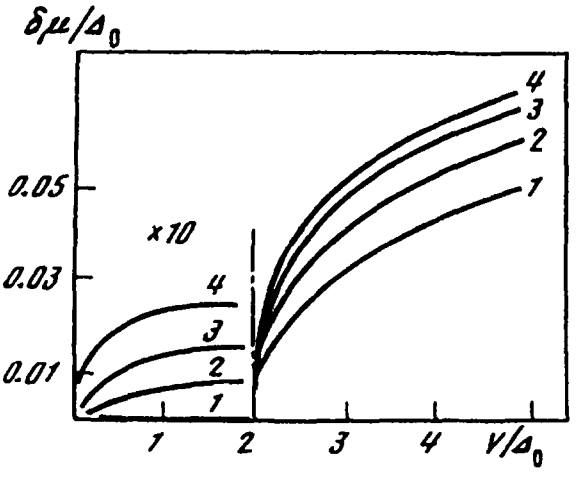

Figure 10.15. The nonequilibrium potential μ plotted as a function of applied voltage V at $\nu = 0.01\gamma$: 1, $T = 04\Delta_0$; 2, $T = 0.3\Delta_0$; 3, $T = 0.2\Delta_0$; 4, $T = 0.1\Delta_0$.

In conclusion, we wish to make a remark concerning the difference between phonon emission from the tunnel junction and that from a film under UHF pumping. As described in Sect. 10.1, the nonequilibrium tunnel source contains terms that oscillate in time. These oscillations may reveal themselves in a system of single-electron excitations, and modulate with the Josephson frequency the phonon

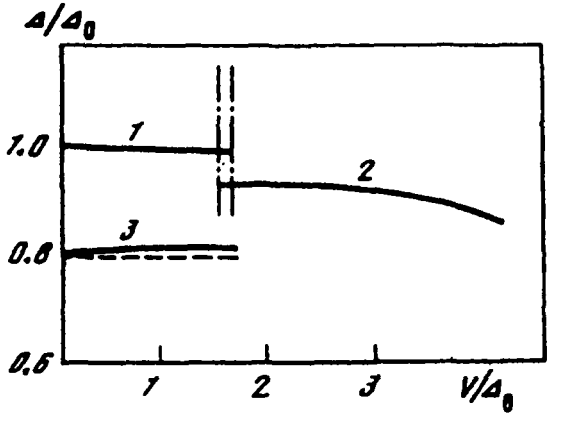

Figure 10.16. The nonequilibrium gap $|\Delta|$ versus the voltage V: 1, 2, at $T/\Delta_0 = 0.1$ (the same at $T/\Delta_0 = 0.2$), $\nu = 0.01\gamma$; 3, at $T/\Delta_0 = 0.4$, $\nu = 0.01\gamma$. The dashed line represents the equilibrium value.

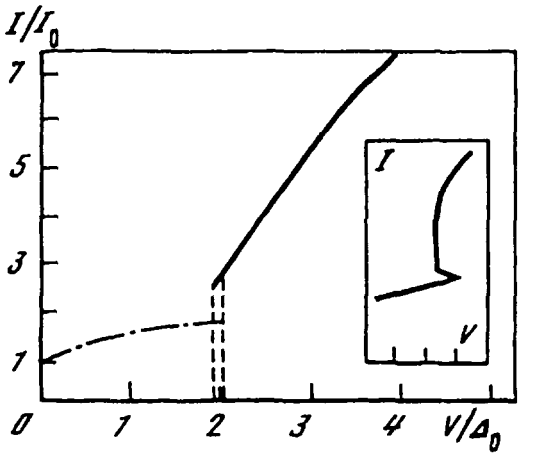

Figure 10.17. The I-V characteristic with hysteresis ($T = 0.22\Delta_0$; $\nu = 0.01\gamma$). The experimental curve[16] is shown in the inset.

radiation emitted by the tunnel junction. The amplitude of this modulation however, is small (at sufficiently large voltage V, it is proportional to γ/V), and that allows us to ignore this dynamic effect. Much more pronounced phenomena of this kind exist in the phase-slip centers, as we saw in Chap. 9.

10.4.3. Microrefrigeration

Is it possible to use the phonon deficit effect to achieve refrigeration by having the negative phonon fluxes yield a cooling effect? In the symmetric SIS junction considered earlier, the answer is most likely "no," since the negative fluxes are more than compensated for by the positive ones. [Bear in mind that to consider the fluxes in terms of energy, it is necessary to multiply the value of the phonon source in (6.4) and (6.7) by the phonon density of the states ($\propto \omega^2$ in the Debye model) and the energy factor ($\propto \omega$), which strongly (as ω^3) enhances the relative contribution of the positive "tail."] Parmenter[18] was the first who argued the benefit of using an SIS′ IS structure (the extraction of electron excitations from a smaller gap, thin-film superconductor S′ by tunneling into the larger gap "banks" S) for electron cooling in S′. This work pioneered the theory of order-parameter enhancement in conditions of nonequilibrium superconductivity (see Chap. 5). It has also initiated subsequent studies on the possibility of tunnel junction refrigeration,[19] which resulted in practical realization of the effect.[20–24]

Initially microrefrigeration studies focused mainly on the effective electronic temperature of the smaller gap superconductor. (Note that in the ultimate case of the smallest gap $S' \to N$, one deals with the most effective SINIS structure.) These

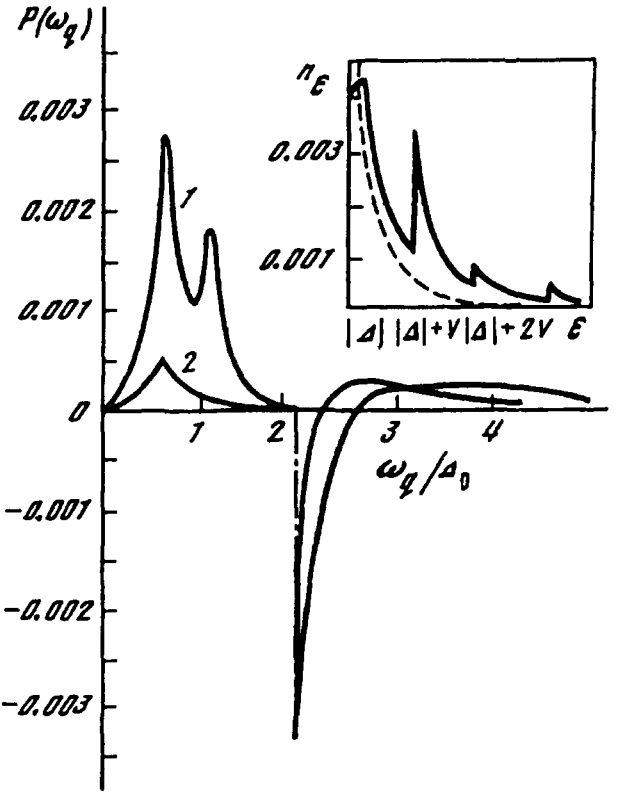

Figure 10.18. The spectral dependence of phonon emission in a subthreshold regime. 1, at $T = 0.2\Delta_0$, $V = 0.5\Delta_0$, $\nu = 0.2\gamma$; 2, same as above, but $V = 0.1\Delta_0$. The electron excitation distribution function that corresponds to case 1 is shown in the inset.

studies were related to the order-parameter enhancement effect, which is based on the effective cooling of the electrons (see Chap. 5). This intrinsic electron cooling can have "on-chip" practical applications.[21] A wider application range is possible when cooling also involves the crystalline lattice. In this case it will be possible to refrigerate external objects. Consideration of the crystalline lattice must take into account the phonon deficit effect, which counteracts Joule heating.[25] For SIS junctions, both mechanisms are proportional to V^2, where V is the voltage across the junction, and the heating is typically stronger than the cooling power of the phonon-deficit mechanism. For asymmetric SIS′ junctions, the cooling power

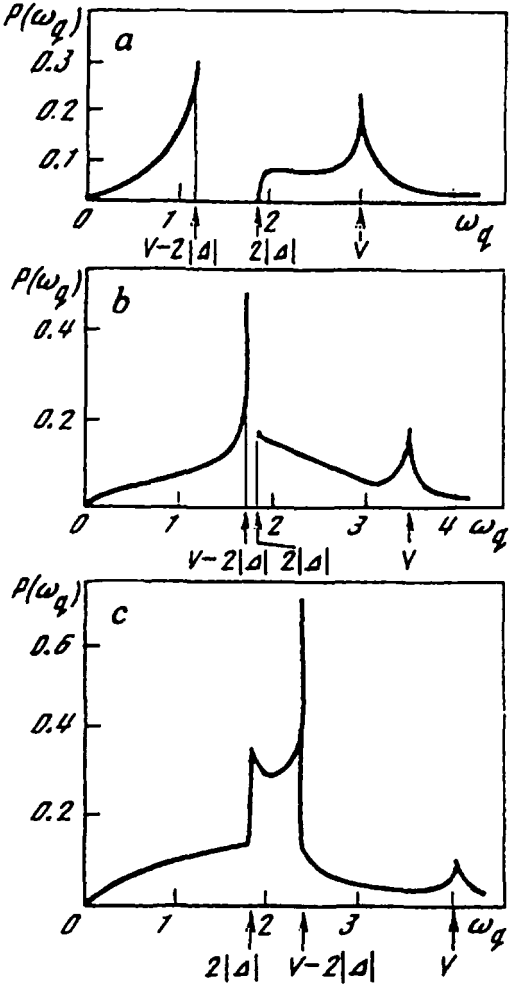

Figure 10.19. The phonon emission spectrum in a superthreshold regime ($T = 0.1\Delta_0$; $\nu = 0.01\gamma$). The x-axis is in Δ_0 units. The voltage V equals: (a) $3\Delta_0$, (b) $3.5\Delta_0$, (c) $4\Delta_0$.

becomes a slower function of V (linear in some range of values), so that for sufficiently small voltages the net difference may result in cooling.*

*There is a close analogy here with the Peltier effect at thermoelectric cooling, where one has competition between the cooling mechanism, which is proportional to the current **j**, and Joule heating, which is proportional to $\mathbf{j}^2$. At low values of **j** one has a net cooling.

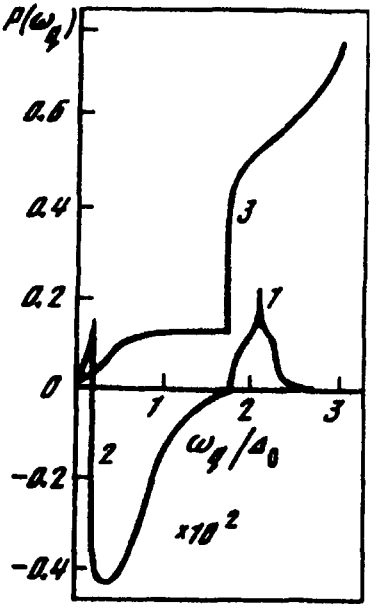

Figure 10.20. The phonon deficit effect in a superthreshold regime ($V = 2.05\Delta_0$, $T = 0.2\Delta_0$, $\nu = 0.01\gamma$). 1, the recombination peak; 2, a relaxation downfall (increased one hundredfold); 3, the spectral dependence of the absorption coefficient (in arbitrary units).

10.5. WEAKLY COUPLED BRIDGES

10.5.1. Modified Aslamasov–Larkin Model

We will consider now the resistive state arising in weakly coupled superconductors. To describe it, we will exploit the Aslamasov–Larkin model,[26] according to which the order parameter within the weak link can be written in the form

$$\Delta(x, t) = \frac{1}{2}\Delta_0 \left\{ \left(1 - \frac{x}{a}\right) e^{i\theta_1} + \left(1 + \frac{x}{a}\right) e^{i\theta_2} \right\}. \tag{10.49}$$

We consider a one-dimensional problem; the coordinate x along the weak link varies from $-a$ to a; $\Delta_0 = \text{const}$ is the order parameter modulus of the bulk superconductor; θ_1 and θ_2 are, respectively, the time-dependent values of the order parameter phase on the left and right "banks."

Since we consider the one-dimensional case, it is sufficient to calculate the current at the point $x = 0$. It follows from (10.49) (in the gauge $\mathbf{A}_x = 0$ and at $x = 0$) that

$$|\Delta|^2 = \Delta_0^2 \cos^2\left(\frac{\theta_1 - \theta_2}{2}\right), \tag{10.50}$$

$$|\Delta|^2 Q = -|\Delta|^2 \nabla\theta = \mathrm{Im}\,(\Delta^* \nabla \Delta) = \frac{\Delta_0}{2a} \sin(\theta_2 - \theta_1). \tag{10.51}$$

In the bulk "bank," one can set $\mu = 0$; assuming $a << \xi(T)$, we find from (7.85) and (7.86)

$$\dot{\theta}_{1(2)} = 2\varphi_{1(2)}, \mathbf{E} \to E_x = -\frac{\partial\varphi}{\partial x} \approx \frac{V}{2a}, V = \varphi_1 - \varphi_2. \tag{10.52}$$

The condition $a << \xi(T)$ indicate that an analysis based on an equation of the Ginzburg-Landau type (7.45) (which assumes that the spatial derivatives are small) cannot be applied. Nevertheless, the expression for the current in the form (7.98) can still be used, since $f_1(\varepsilon)$ in (7.88) may be taken as an equilibrium function, owing to the rapid diffusive dissipation of nonequilibrium excitations toward the bulk superconductive banks. Substituting (10.50) to (10.52) into (7.101) subject to (7.106), one finds

$$j = j_s + j_n + j_{int}, \quad j_s = j_0 \sin(2Vt + \theta_0), \quad j_n + \sigma_n V/2a,$$

$$j_{int} = \frac{\sigma_n V}{2a}\frac{\Delta_0}{2T}\,|\cos(Vt + \theta_0/2)|\ln\frac{4\Delta_0|\cos(Vt + \theta_0/2)| + \gamma}{\gamma}, \tag{10.53}$$

where θ_0 is some constant phase difference and $j_0 = \pi\sigma_n\Delta_0^2/(8aT)$.

In the region of the weak link, there exist a number of "captured" nonequilibrium excitations with energies $\varepsilon < \Delta_0$.[27] As Schmid and Tinkham showed,[28] the presence of these excitations at voltages $V << \gamma$ produces a current contribution $\delta j = j_0 P_1[(\theta_2 - \theta_1)/2]V/\gamma$, where $P_1(x)$ is some non-negative even function of period π with a maximum value of 2/5. The magnitude of the same dissipative phase-dependent structure could also be obtained formally by substitution of (10.51) and an equilibrium distribution function into the second term in (7.88). The interference term arising in this approach is not small in comparison with j_n in (10.53)($\delta j \sim j|\Delta|^2/\gamma T$). As mentioned earlier, there should be no "local equilibrium" contributions to the current in the case of short bridges [$a << \xi(T)$] because of the fast diffusion processes toward the banks. In other cases, however, these terms may be important.

10.5.2. *Cos φ-Term Paradox*

The interference current may determine qualitative features of the dynamic characteristics of nonequilibrium superconducting bridges. In particular, it mani-

fests itself in a so-called "cos φ-term paradox" (see, e.g., Ref. 29). For weak-link bridges, this paradox arises when one attempts to interpret the experimental data on the basis of the standard expression for the current, found by the method of the tunneling Hamiltonian.[1] It is expedient to reconsider this problem.

Let us examine, for example, the interpretation of the experiment by Falco et al.,[30] who measured the fluctuating value of the derivative of the voltage with respect to current. A theoretical analysis of that quantity is based on the Fokker–Planck equation,[31] which can be written for fluctuations in weak-coupling superconductors in analogy with the motion of a Brownian particle in an external potential field.[32] As a result, the expression for the quantity $(\partial \bar{V}/\partial X)_{X=0}$ was found to be

$$\left.\frac{\partial \bar{V}(Y)}{\partial X}\right|_{X=0} = 4\pi^2 \left\{ \int_0^{2\pi} f(\theta)\, d\theta \int_0^{2\pi} \frac{d\theta'}{f(\theta')} \left[1 + \alpha_1 \cos\theta' + \alpha_2 \left|\cos\frac{\theta'}{2}\right| + \alpha_3 P_1\left(\frac{\theta'}{2}\right)\right]\right\}^{-1}. \tag{10.54}$$

Here $\bar{V} = V/(jSR)$, $X = j/j_0$, $f(\theta) = \exp(1/2Y\cos\theta)$, $Y = j_0 S/T$; S is the cross section of the weak link and R is its normal state resistance; the parameters α_i are:*

$$\alpha_1 \approx \frac{\Delta_0^2}{T} \approx 0, \quad \alpha_2 \approx \frac{\Delta_0}{2T} \ln\frac{4\Delta_0}{\gamma}, \quad \alpha_3 = \frac{\pi\Delta_0^2}{4T\gamma}. \tag{10.55}$$

In comparing the theory with experiment, Falco et al.[30] used the ordinary Josephson expression for the current [in the latter case we should set $\alpha_1 = 1$, $\alpha_2 = \alpha_3 = 0$ in (10.54)]. The experimental data were found to lie well below the theoretical curve (they were close to the curve with $\alpha_1 = -1$), and this result was considered a paradox (see Fig. 10.21). If instead one compares the experimental data with the expression (10.54) for $\alpha_2, \alpha_3 \neq 0$, one would find that the theoretical curve of Eq. (10.54) runs well below the one found when $\alpha_1 = 1$, $\alpha_2 = \alpha_3 = 0$. To demonstrate this, consider the behavior of (10.54) in more detail, setting for a moment $\alpha_2 = \alpha_3 = 0$. We thus arrive at

*The value for α_1 may be found if one retains in (10.53) the contribution to the current, which follows from the last term in (7.83) and is approximately equal to $-j_0 VT^{-1}\cos(2Vt + \theta_0)$. Since incorporation of this term into the expression for the current would involve going beyond the accuracy of our treatment, there could be other contributions to α_1 of the same order of smallness, which are effectively negligible.

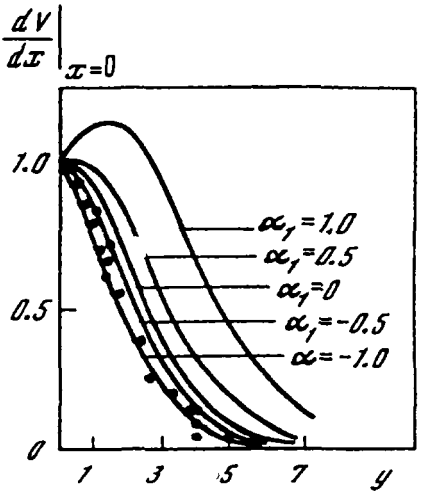

Figure 10.21. Comparison of a theoretical curve (10.54) (at $\alpha_2 = \alpha_3 = 0$) with experimental data[30] (points).

$$K(\alpha_1) = \left.\frac{\partial \bar{V}(Y)}{\partial X}\right|_{X=0} = 4\pi^2 \left\{ \int_0^{2\pi} f(\theta)\, d\theta \int_0^{2\pi} \frac{d\theta'}{f(\theta')} (1 + \alpha_1 \cos\theta') \right\}^{-1}. \qquad (10.56)$$

We look for the dependence of (10.56) on α_1. Only the second integral in the denominator of (10.56) depends on α_1. It may be decomposed into two terms, as is illustrated in Fig. 10.3 (it is convenient to make $Y = 2$). The first term is proportional to the area bounded by the solid line (dashed in Fig. 10.3). The second term is proportional (up to the same multiple) to the area restricted by the line obtained after multiplication of the solid and broken lines. At $0 < \alpha_1 \leq 1$, as one may see from Fig. 10.3, the second term is negative (and has a smaller absolute value than the first term). For this reason, the denominator in (10.56) decreases though remaining positive, and at positive $\alpha_1 > 0$, the value of $K(0)$ is smaller than $K(\alpha_1)$. For a negative α_1, the contribution of the second term is always positive (because the dashed curve in Fig. 10.22 should be reflected relative to the abscissa) and for a given y we have $K(\alpha_1) < K(0)$. In the same manner one can see that the terms containing α_2 and α_3 diminish the values of (10.54). Thus probably the paradox mentioned above might be explained in this particular case. It would be premature to make a detailed comparison of theory and experiment because of insufficient knowledge of the parameters that determine the voltage-

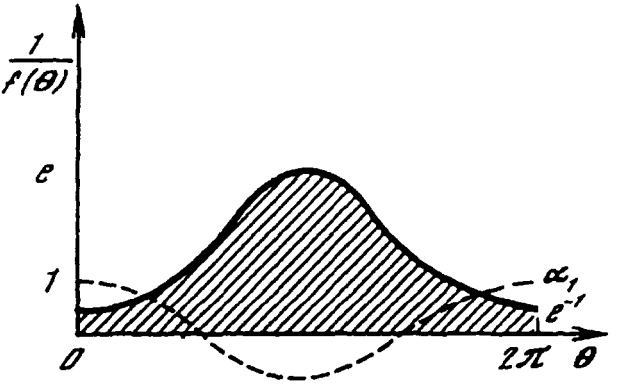

Figure 10.22. The function $1/f(\theta)$. The dashed line corresponds to $\alpha_1 \cos\theta$ (here e is the base of the natural logarithm).

current characteristic of the weak link. For example, the relation between γ and the measured voltage in Ref. 30 is not known; this is an important question,[33] since it determines the dominant term in (10.56).

10.5.3. Excess Current

Excess current has been observed in all the types of weakly coupled superconductors,[34–40] except Josephson junctions. Likharev and Jacobson[41] proposed a model to account for the relaxation of the order parameter in the region of a weak link. They tried to apply a simple generalization of the Ginzburg–Landau equations to the nonstationary case. Though such a generalization may be justified for the gapless superconductors only, nevertheless it was the first successful explanation of the excess current. The problem was treated more precisely by Artemenko et al.[42] They have explained this phenomenon using the model of short bridges. The results obtained in Ref. 42 were confirmed by experiments both at low $(T << |\Delta|)$ and at sufficiently high $T \approx T_c$ temperatures and at arbitrary bias voltages.[34–40] For a bridge "superconductor–constriction–superconductor" at arbitrary temperatures and $V >> |\Delta|$, the result of Artemenko et al. may be written as

$$\sigma_* = \sigma_n \left\{ 1 + \frac{\Delta_0}{V} \left(\frac{\pi^2}{4} - 1 \right) \tanh \frac{V}{2T} \right\}. \tag{10.57}$$

At $V << T \approx T_c$ this result may be rewritten as

$$\sigma_* = \sigma_n \left\{ 1 + \frac{\Delta_0}{2T} \left(\frac{\pi^2}{4} - 1 \right) \right\}, \tag{10.58}$$

where Δ_0 is the BCS value of the gap.

An expression of the same type follows from the formulas of Sect. 7.2, which utilize the idea of interference current [see Eq. (7.104)]. For illustration we will use the results obtained with the Aslamasov–Larkin model. From expression (10.53) it follows that the time-averaged value of the interference current is not zero. Substituting into (7.104) the time-averaged value $|\Delta| = 2\Delta_0/\pi$, we have

$$\sigma_* = \sigma_n \left(1 + \frac{\Delta_0}{\pi T} \left[\ln \frac{8\Delta_0}{\pi\gamma} - 1 \right] \right). \tag{10.59}$$

For ordinary superconductors

$$\frac{1}{\pi} \left[\ln \frac{8\Delta_0}{\pi\gamma} - 1 \right] \approx \frac{1}{2} \left(\frac{\pi^2}{4} - 1 \right), \tag{10.60}$$

so one can omit the logarithmic dependence on T [keeping only the dependence on T via $\Delta = \Delta_0(T)$] in the expression (10.59). Thus we arrive at a qualitative and even quantitative coincidence of the results obtained by rather different techniques (though in the vicinity of T_c only). In particular, the temperature dependence is essentially the same. In addition, some new aspects of this phenomenon emerge: first, the excess current is periodic in time, as can be seen from (10.53). Furthermore, while previously it was thought[42] that the excess current arises in the weak link bridges because of the presence of massive banks (i.e., manifests itself as a boundary effect), from the analysis presented here it follows that as a result of interference between normal and superfluid motions, the excess current may reveal itself in bulk samples also.*

References

1. B. D. Josephson, Possible new effects in superconductive tunneling, *Phys. Lett.* **1**(7), 251–253 (1962).
2. B. D. Josephson, in *Superconductivity.* R. D. Parks, ed., Vol. 1, p. 423, Marcel Dekker, New York (1969).
3. A. I. Golovashkin, V. G. Eleonskii, and K. K. Likharev, *Josephson Effect and Its Applications: Bibliography,* 1962–1980, pp. 1–222, Nauka, Moscow (1983) (in Russian).

*Note that according to (10.59), the experiments on excess conductivity allow us to estimate (with a logarithmic accuracy) the energy relaxation time $\tau_\varepsilon = (2\gamma)^{-1}$ of single-particle excitations in superconductors.

4. A. F. Volkov, Nonequilibrium states in superconducting tunnel structures, *Sov. Phys. JETP* **41**(2), 376–380 (1975) *[Zh. Eksp. i Tear. Fiz,* **68**(2), 756–765 (1975)].
5. A. M. Gulyan and G. F. Zharkov, Electron and phonon kinetics in a nonequilibrium Josephson junction, Sov. *Phys. JETP* 62(1), 89–97 (1985) *[Zh. Eksp. i Teor. Fiz.* **89**(7), 156–171 (1985)].
6. B. I. Ivlev, Resistive states in superconductor junctions, *Sov. Phys. JETP* **48**(5) 893–896 (1978) *[Zh. Eksp. i Teor. Fiz.* 75[5(11)], 1771–1777 (1978)].
7. A. I. Larkin and Yu. N. Ovchinnikov, Tunnel effect between superconductors in an alternating field, *Sov. Phys. JETP* **24**(11), 1035–1040 (1967) *[Zh. Eksp. i Tear. Fiz.* **51**[5(11)], 1535–1543 (1966)].
8. J. Clarke, Experimental observation of pair-quasiparticle difference in nonequilibrium superconductors, *Phys. Rev. Lett.* **28**(21), 1363–1366 (1972).
9. M. Tinkham, Tunneling generation, relaxation and tunneling detection of hole-electron imbalance in superconductors, *Phys. Rev. B.* **7**(5), 1747–1756 (1972).
10. I. K. Kirichenko and V. P. Seminozhenko, Distribution of nonequilibrium excitations and phonon generation in superconducting tunnel junctions, *Sov. J. Low Temp. Phys.* **3**(8), 479–486 (1977) *[Fiz. Nizk. Temp.* **3**(8), 986–1000 (1977)].
11. V. F. Elesin and Yu. V. Kopaev, Superconductors with excess quasiparticles, *Sov. Phys. Uspekhi* **24**(2), 116–141 (1981) *[Usp. Fiz. Nauk* **133**(2), 259–307 (1981)].
12. L. D. Landau and E. M. Lifshitz, *Electrodynamics of Continuous Media,* pp. 313–343, Pergamon, Oxford (1960).
13. J.-J. Chang and D. J. Scalapino, Nonequilibrium superconductivity, *J. Low Temp. Phys.* **31**(1/2), 1–32(1978).
14. P. Otschik, H. Eschrig, and F. Lange, Sound wave amplification in superconductors, *J. Low Temp. Phys.* **43**(3/4), 397–408 (1981).
15. A. G. Aronov and B. Z. Spivak, Properties of superconductors with nonequilibrium excitations, *Sov. Phys. Solid State* **18**(2), 312–320 (1976) [Fiz. *Tverd. Tela* **18**(2), 541–553 (1976)].
16. K. E. Gray and H. W. Willemsen, Inhomogeneous state of superconductors induced by intense tunnel injection in superconducting lead films, *J. Low Temp. Phys.* **31**(5/6), 911–925 (1978).
17. J. A. Pals, K. Weiss, P. M. T. van Attekum, R. E. Horstman, and J. Wolter, Nonequilibrium superconductivity in homogeneous thin films, *Phys. Rep.* **80**(4), 323–390 (1982).
18. R. H. Parmenter, Enhancement of superconductivity by extraction of normal carriers, *Phys. Rev. Lett.* **7**(7), 274–277 (1961).
19. R. G. Melton, J. L. Paterson, and S. B. Kaplan, Superconducting tunnel junction refrigereator, *Phys. Rev. B.* **21**(5), 1858–1867 (1980).
20. M. Nahum, T. M. Eiles, and J. M. Martinis, Electronic microrefrigeration based on a normal metal-insulator-superconductor tunnel junction, *Appl. Phys. Lett.* **65**(24), 3123–3125 (1994).
21. P. A. Fisher, J. N. Ullom, and M. Nahum, Design of a novel on-chip electronic refrigerator based on a normal-insulator-superconductor tunnel junction, *J. Low Temp. Phys.* **101**(3/4), 561–565 (1995).
22. A. Bardas and D. Averin, Peltier effect in normal-metal-superconductor microcontacts, *Phys. Rev.* B, **52**(17), 12873–12877(1995).
23. M. M. Leivo, J. P. Pekola, and D. V. Averin, Efficient Peltier refrigeration by a pair of normal metal/insulator/superconductorjunctions, Appl. *Phys. Lett.* **68**(14), 1996–1998(1996).
24. A. J. Manninen, M. M. Leivo, and J. P. Pekola, Refrigereation of a dielectric membrane by superconductor/insulator/normal-metal/insulator/superconductor tunneling, *Appl. Phys. Lett.* **60**(14), 1885–1887(1997).
25. A. M. Gulyan, G. F. Zharkov, and G. M. Sergoyan, Thermal balance in the tunnel contact of a superconductor, *Sov. Phys. Lebedev Inst. Reports,* **10**, 38–42 (1984) *[Kratk. Soobsch. poFiz, FIAN,* **10**, 33–36(1985)].

26. L. G. Aslamasov and A.I. Larkin, Josephson effect in superconducting point contacts, *JETP Lett.* **9**, 87–91 (1969) *[Pis 'ma v Zh. Eksp. i Teor. Fiz.* **9**, 150–154 (1968)].
27. L. G. Aslamasov and A. I. Larkin, Superconducting contacts with a nonequilibrium electron distribution function, *Sov. Phys. JETP* **43**(4), 698–703 (1976) *[Zh. Eksp. i Tear. Fiz* **70**(4), 1340–1347 (1976)].
28. A. Schmid, G. Schön, and M. Tinkham, Dynamic properties of superconducting weak links, *Phys. Rev. B* **21**(11), 5076–5086 (1980).
29. A. Barone and G. Paternò, Physics and Applications of the Josephson Effect, pp. 47–49, Wiley, New York (1982).
30. C. M. Falco, W. H. Parker, and S. E. Trullinger, Observation of a phase modulated quasiparticle current in superconducting weak links, *Phys. Rev. Lett.* **31**(15), 933–936 (1973).
31. V. Ambegaokar and B. I. Halperin, Voltage due to thermal noise in the Josephson effect, *Phys. Rev. Lett.* **22**(25), 1364–1366(1969).
32. H. A. Kramers, Brownian motion in a field of force and the diffusion model of chemical reactions, *Physica* **7**(4), 284–304 (1940).
33. A. V. Zorin, I. O Kulik, K. K. Likharev and J. R. Schrieffer, The sign of the interference current component in superconducting junctions, *Sov. J. Low Temp. Phys.* **5**(10), 537–546 (1979) [*Fiz. Nizk. Temp.* **5**(10), 1138–1157 (1979)].
34. J. 1. Pankove, New effect at superconducting contacts, *Phys. Lett.* **21**(4), 406–407 (1966).
35. A. I. Akimenko, V. S. Solov'ev, and I. K. Yanson, ac Josephson current as a function of voltage, *Sov. J. Low Temp. Phys.* **2**(4), 238–241 (1976) *[Fiz.* Mat. *Temp.* **2**(4), 480–485 (1976)].
36. M. Octavio, W. J. Skochpol, and M. Tinkham, Nonequilibrium-enhanced supercurrents in short superconducting weak links, *Phys. Rev. B* **17**(1), 159–169 (1978).
37. V. N. Gubankov, V. P. Koshelets, and G. A. Ovsyannikov, Properties of Josephson thin film variable-thickness microbridges, *Sov. Phys. JETP* **46**(4), 755–760 (1977) *[Zh. Eksp. i Teor. Fiz.* **73**[4(10)], 1435–1444(1977)].
38. Yu. Ya. Divin and F Ya. Nad', A model of real superconducting point contacts, *Sov. J. Low Temp. Phys.* **4**(9), 520–525 (1978) [*Fiz. Nizk. Temp.* **4**(9), 1105–1114 (1978)].
39. H. A. Notarys and J. E. Mercereau, Proximity effect bridge and superconducting microcircuitry, *J. Appl. Phys.* **44**(4), 1821–1830 (1973).
40. T. M. Klapwijk, M. Sepers, and J. E. Mooij, Regimes in the superconducting microbridges, *J. Low. Temp. Phys.* **27**(5/6), 801–835 (1977).
41. K. K. Likharev and L. A. Yakobson, Dynamical properties of superconducting filaments of finite length, *Sov. Phys. JETP* **41**(3), 570–576 (1975) *[Zh. Eksp. i Tear. Fiz.* **68**(3), 1150–1160 (1975)].
42. S. N. Artemenko, A. F. Volkov, and A. V. Zaitzev, On the excess current in microbridges S-C-S and S-C-N, *Solid State Commun.* **30**(12), 771–773 (1979).

11

Influence of Laser Radiation

It is not surprising that a nonequilibrium state is created when photons of energy much larger than the pairing energy are absorbed by the superconductor. What is surprising is how strongly the behavior of this still superconducting state depends on the "tiny features" of the superconducting state.

11.1 ELESIN APPROACH TO QUASI-PARTICLE DISTRIBUTIONS

Consider a thin superconducting film irradiated homogeneously by an electromagnetic field. The frequency ω_0 of the radiation is supposed to be substantially higher than the value of the gap*: $\omega_0 >> \Delta$, so the excess quasi-particles in the electron system are created by the field in the energy range $\Delta \le \varepsilon \le \omega_0$. As a consequence, the source "density" $Q(\varepsilon)$ in the kinetic equation for electrons [Eq. (5.21)] is small and the shape of the electron excitation distribution function n_ε is formed mainly by the inelastic collision operators. For simplicity we will consider only inelastic electron-phonon collisions (4.119), assuming that the phonons are in equilibrium as a result of coupling with the heat-bath.

11.1.1. Spectral Function of Electron–Phonon Interaction

We will start with the case of temperature $T = 0$. Denoting $\xi = \sqrt{\varepsilon^2 - \Delta^2}$, $n(\xi') = n'$, one can write the kinetic equation (5.21) for the quasi-stationary state in the form:

$$0 = \left\{ (1 - n) \int_{\xi}^{\omega_D} n' \left(1 - \frac{\Delta^2}{\varepsilon\varepsilon'} \right) \alpha^2 (\varepsilon' - \varepsilon)\, F(\varepsilon' - \varepsilon)\, d\xi' \right.$$

*In this chapter a gauge with the real order parameter Δ will only be used.

$$-n\int_0^{\xi}(1-n')\left(1-\frac{\Delta^2}{\varepsilon\varepsilon'}\right)\alpha^2(\varepsilon-\varepsilon')\,F(\varepsilon-\varepsilon')\,d\xi'$$

$$-n\int_0^{\omega_D}n'\left(1+\frac{\Delta^2}{\varepsilon\varepsilon'}\right)\alpha^2(\varepsilon+\varepsilon')\,F(\varepsilon+\varepsilon')\,d\xi'\Bigg\}+Q(\varepsilon)\quad . \tag{11.1}$$

In Eq. (11.1) the electron-phonon interaction function $\alpha^2(\omega_q)\,F(\omega_q)$ is introduced. The approximation

$$\alpha^2(\omega_q)\,F(\omega_q)=\frac{\pi\lambda}{2\omega_D^{k+1}}\,\omega_q^{k+1} \tag{11.2}$$

corresponds to the cases considered in the previous chapters. In (11.2), the dependence of the electron-phonon interaction matrix element on the wave vector **q** is taken into account ($k = 1$ for ionic crystals). Note that in the adopted notations, the nonequilibrium source $Q(\varepsilon)$ in (11.1) differs by the factor ε/ξ from the canonical form (5.59).

11.1.2. Excess Quasi-particles: Normalization Condition

The concentration of excess quasi-particles is determined by the integral form of Eq. (11.1). The normalization condition[1]

$$\int_0^{\infty}d\xi\int_0^{\infty}d\xi'\,nn'\left(1+\frac{\Delta^2}{\varepsilon\varepsilon'}\right)\alpha^2(\varepsilon+\varepsilon')\,F(\varepsilon+\varepsilon')\,d\xi'=\int_0^{\infty}d\xi\,Q(\varepsilon) \tag{11.3}$$

is obtained by integrating Eq. (11.1) over ξ; the relaxation terms disappear on doing so. The explicit expression for $Q(\varepsilon)$ may be significantly simplified using the condition $\omega_0 >> \Delta$. Omitting the U-factors in (5.59) [i.e., ignoring in Eq. (11.1) the redistribution of excess quasi-particles by electromagnetic radiation—these factors cancel each other in Eq. (11.3)] and simplifying the term that corresponds to the creation of the excess quasi-particles from the condensate by the photon, one can write [cf. Eq. (5.54)]:

$$Q=2\alpha\theta(\omega_0-\varepsilon). \tag{11.4}$$

11.1.3. Separation of "Coherent" Contributions

For $\alpha^2(\omega_q)\,F(\omega_q) \equiv \text{const}$ [i.e., for $k = -1$ in Eq. (11.2)], the kinetic equation (11.1) can be solved analytically.[1] We will analyze only this model case, when Eqs. (11.1) and (11.3) acquire the forms:

$$-(1-n)\int_{\xi}^{\omega_D} d\xi'\, n'\left(1-\frac{\Delta^2}{\varepsilon\varepsilon'}\right)+n\int_{0}^{\xi} d\xi'\,(1-n')\left(1-\frac{\Delta^2}{\varepsilon\varepsilon'}\right)$$

$$+n\int_{0}^{\omega_D} d\xi'\, n'\left(1+\frac{\Delta^2}{\varepsilon\varepsilon'}\right)=0, \tag{11.5}$$

$$\frac{1}{\Delta_0^2}\int_0^{\infty} d\xi\int_0^{\infty} d\xi'\, nn'\left(1+\frac{\Delta^2}{\varepsilon\varepsilon'}\right)=\beta_0,\quad \beta_0=\frac{4\alpha\omega_0}{\pi\lambda\Delta_0^2}. \tag{11.6}$$

In this case, as can be seen from (11.5) and (11.6), the solution $n(\xi)$ depends explicitly on the order parameter through the coherence factors $(1 \pm \Delta^2/\varepsilon\varepsilon')$.

11.1.4. Analytic Solution for $\Delta = 0$

Assuming $\Delta = 0$ in these equations, we will neglect for the moment the "coherent" contribution to the function $n(\xi)$. We will denote the solution of (11.5) with $\Delta = 0$ by $n_0(\xi)$. To define this function, one has the equation

$$-(1-n_0)\int_{\xi}^{\omega_D} d\xi'\, n_0'+n_0\int_{0}^{\xi} d\xi'\,(1-n_0')+\int_{0}^{\infty} d\xi'\, n_0'=0. \tag{11.7}$$

It is useful to introduce the function

$$y(\xi)=\int_{0}^{\xi}(1-n_0')\,d\xi', \tag{11.8}$$

which obeys the nonlinear differential equation, following from (11.7):

$$\frac{dy}{d\xi}(2y-\xi+a)=y+\frac{a}{2}, \tag{11.9}$$

$$a=\int_{-\infty}^{\infty} n_0(\xi)\,d\xi=2\int_{0}^{\infty} n_0(\xi)\,d\xi. \tag{11.10}$$

Introducing further $z = 2y + a - \xi$, one finds from (11.9) the equation:

$$z\frac{dz}{d\xi}=\xi \tag{11.11}$$

from which

$$z=\pm\sqrt{\xi^2+C}, \tag{11.12}$$

or, returning to the original function y,

$$y = \frac{\xi}{2} \pm \sqrt{\frac{\xi^2}{2} + C} - \frac{a}{2}. \tag{11.13}$$

Only the solution with a positive sign before the square root satisfies the boundary condition $y(0) = 0$ [see (11.8)], and thus the integration constant is defined as $C = a^2/4$. So we have obtained for the function n_0:

$$n_0 = 1 - \frac{dy}{d\xi} = \frac{1}{2}\left\{1 - \frac{\xi}{\sqrt{\xi^2 + a^2}}\right\}. \tag{11.14}$$

The characteristic parameter a determines the behavior of the solution $n_0(\xi)$. To obtain this quantity, we rewrite the normalization condition in the form:

$$\frac{a^2}{4} + a\int_0^\infty d\xi\, n_1 + \Delta^2\left(\int_0^\infty d\xi\, n_0/\varepsilon\right)^2 = \Delta\beta_0^2, \tag{11.15}$$

from which it follows* [neglecting corrections of the order of $(\Delta/\Delta_0)^2$]:

$$a = 2\Delta_0\sqrt{\beta}. \tag{11.16}$$

Thus the maximum value of the function $n_0(\xi)$ is 1/2 at $\xi = 0$. If ξ increases, the function n_0 decreases and becomes small at $\xi > a$. As mentioned earlier, the function $n_0(\xi)$ does not depend on A. Thus one can conclude that $n_0(\xi) \le 1/2$ at optical pumping.[1] We will now examine the "coherent" contributions to the function $n(\xi)$.

11.2. ORDER-PARAMETER AMBIGUITY

11.2.1. First-Order "Coherent" Correction

Assuming that $n_1 = n - n_0 << 1$, one finds from (11.5) the equation

$$n_1\left\{2\int_0^{\omega_D} n_0'\, d\xi' + \int_0^{\xi}(1 - 2n_0')\, d\xi'\right\} - (1 - 2n_0')\int_{\xi}^{\omega_D} n_1' d\xi'$$

$$= -\frac{\Delta^2}{\varepsilon}\left[\int_{\xi}^{\omega_D} d\xi' \frac{n_0'}{\varepsilon'} - \int_0^{\xi} d\xi' \frac{1 - 2n_0'}{\varepsilon'}\right]. \tag{11.17}$$

*Δ_0 is small when $\beta \sim 1$, which is of interest here.

Taking into account that the term (11.17), containing n_1 in the integral form, is small, one obtains to the first order in Δ^2/Δ_0^2:

$$n_1 \approx -\frac{\Delta^2}{2\varepsilon\sqrt{\xi^2+a^2}} \ln\frac{a}{\xi+\varepsilon}. \tag{11.18}$$

Note that this function is negative at $\xi \sim \Delta$. Taking into account zero-order solutions, the self-consistency equation [of the type (10.14) that follows from (7.14)] can be presented in the form

$$\begin{aligned}\frac{1}{\lambda}\Delta &= \Delta\int_0^{\omega_D} d\xi\,\frac{1-2n_\xi}{\varepsilon} = \Delta\int_0^{\omega_D}\frac{d\xi}{\sqrt{\Delta_0^2+\xi^2}}\\ &= \Delta\int_0^{\omega_D} d\xi\,\frac{1-2n_0}{\varepsilon} - 2\Delta\int_0^{\omega_D} d\xi\,\frac{n_1}{\varepsilon}\\ &= \Delta\int_0^{\omega_D}\frac{\xi d\xi}{\sqrt{\xi^2+a^2}\sqrt{\xi^2+\Delta^2}} + \Delta^3\int_0^{\omega_D}\frac{d\xi}{\varepsilon^2\sqrt{\xi^2+a^2}}\ln\frac{a}{\xi+\varepsilon},\end{aligned} \tag{11.19}$$

or, after simple transformations, as

$$\Delta\ln\frac{\Delta+a}{\Delta_0} = \Delta^3\int_0^{\omega_D} d\xi\frac{1}{\varepsilon^2\sqrt{\xi^2+a^2}}\ln\frac{a}{\xi+\varepsilon}. \tag{11.20}$$

11.2.2. Critical Pumping Intensity

The parameter a in (11.20) depends on the pumping intensity β through the relation (11.16). The critical value $\beta = \beta_c$, at which Δ vanishes, may be determined from (11.20):

$$a_c = \Delta_0, \tag{11.21}$$

or

$$\beta_c = 1/4. \tag{11.22}$$

11.2.3. Multiple-Order-Parameter Solutions

As mentioned in Ref. 2, the solution $\Delta = 0$ at intensities $\beta \approx \beta_c$ is not a unique one. Indeed, if the coherent contribution n_1 is neglected, the right side of Eq. (11.20) vanishes. So at $a \approx a_c$ (when $\Delta \ll \Delta_0$), it follows from (11.20):

$$\frac{\Delta^2}{\Delta_0} = \Delta \frac{a_c - a}{a_c} = \Delta \left[1 - \left(\frac{\beta}{\beta_c} \right)^{1/2} \right]. \tag{11.23}$$

Thus at $\beta \to \beta_c$ the gap tends to zero monotonically and no nontrivial solutions of Eq. (11.23) exist at $\beta > \beta_c$. If the right side of Eq. (11.20) is taken into account, Eq. (11.23) acquires additional terms:

$$\frac{\Delta^2}{\Delta_0} \left\{ \frac{\pi}{2} \ln \frac{\Delta_0}{\Delta} - 2G - 1 \right\} = \Delta \left[\left(\frac{\beta}{\beta_c} \right)^{1/2} - 1 \right] \equiv \Delta\delta, \tag{11.24}$$

where $G = 0.915\ldots$ is the Katalan constant. In Fig. 11.1 the dependence of δ on the order parameter is plotted according to Eq. (11.24). The above-mentioned trivial solution $\Delta = 0$ (at $\beta > \beta_c$, normal state) also exists for any $\delta > 0$. This state might be realized if one approaches the superconducting state from the normal metal state by decreasing the pumping intensity. Thus at $0 < \delta < \delta_n$ there exist three solutions of the self-consistency equation (11.19). Two nonzero branches $\delta(\beta)$ merge at $\Delta = \Delta_n$, as one can see from Eq. (11.24). In this case

$$\ln \frac{\Delta_n}{\Delta_0} = -\frac{2}{\pi} \left(2G + 1 + \frac{\pi}{2} \right), \quad \delta_n = \frac{\pi}{2} \frac{\Delta_n}{\Delta_0}. \tag{11.25}$$

11.2.4. Stability of Solutions

We will consider now the stability problem of various branches of the solution of Eq. (11.24) relative to spatially homogeneous perturbations:

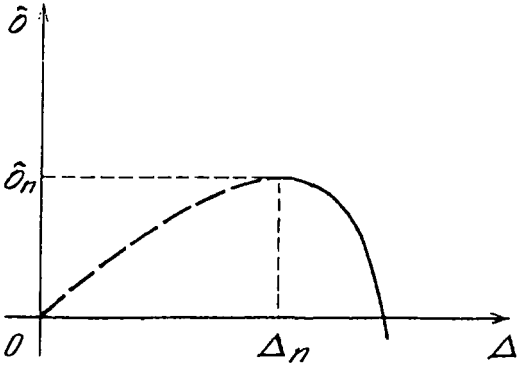

Figure 11.1. Stable (solid lines) and unstable (dashed line) solutions for $\Delta(\delta)$.

$$\delta n(t) = n(t) - n, \quad \delta\Delta(t) = \Delta(t) - \Delta. \tag{11.26}$$

As above, neglecting $Q(\varepsilon)$ in Eq. (11.1), restoring on the left side the time derivative, varying the right side over n and Δ, and omitting the small contribution due to the term with δn in the integrand, one obtains the equation

$$\frac{2}{\lambda}\frac{\partial}{\partial t}(\delta n) = -\delta n\left[\int_0^{\omega_D} d\xi'\, n' + \int_0^{\xi} d\xi'\,(1-2n')\right]$$
$$-\delta\Delta\left\{\frac{2\Delta}{\varepsilon}\left[\int_{\xi}^{\omega_D}\frac{d\xi' n'}{\varepsilon'}\left(1-\frac{\Delta^2}{2\varepsilon'^2}-\frac{\Delta^2}{2\varepsilon^2}\right)\right.\right.$$
$$\left.\left.-\,n\int_0^{\xi}\frac{d\xi'(1-2n')}{\varepsilon'}\left(1-\frac{\Delta^2}{2\varepsilon^2}-\frac{\Delta^2}{2\varepsilon'^2}\right)\right]\right\} \equiv -\delta n a_1(\xi) + \frac{\Delta}{\varepsilon}\delta\Delta a_2(\xi). \tag{11.27}$$

Varying (11.19), one gets

$$2\int_0^{\infty}\frac{\delta n}{\varepsilon}\,d\xi = -\Delta\delta\Delta\int_0^{\infty}\frac{1-2n}{\varepsilon^3}\,d\xi. \tag{11.28}$$

Assuming, as usual,

$$\delta n = \tilde{n}e^{\gamma t}, \quad \delta\Delta = \tilde{\Delta}e^{\gamma t}, \tag{11.29}$$

we obtain from (11.19)

$$\tilde{n} = \frac{(\Delta/\varepsilon)a_2(\xi)}{\gamma_0 + a_1(\xi)}\tilde{\Delta}, \tag{11.30}$$

where $\gamma_0 = 2\gamma/\pi\lambda$. Substituting Eqs. (11.29) and (11.30) into (11.28), we get

$$2\int_0^{\infty} d\xi\,\frac{a_2(\xi)}{\varepsilon^2[\gamma_0 + a_1(\xi)]} = 2\int_0^{\infty} d\xi\,\frac{1-2n}{\varepsilon^3}. \tag{11.31}$$

Noting that the main contributions to the integrals come from small $\xi \sim \Delta$, Eq. (11.31) may be transformed to

$$\frac{2a_2(0)}{\gamma_0 + a_1(0)}\frac{\pi}{2} \approx -\int_0^{\infty} d\xi\,\frac{1-2n}{\varepsilon^3}. \tag{11.32}$$

Substituting $n = n_1 + n_0$ into (11.27) and (11.32), one can obtain:

$$\gamma_0 \approx 2\left(\frac{\pi}{2}\ln\frac{\Delta_0}{\Delta} - 2G - 1 - \frac{\pi}{2}\right) \Big/ \left(\frac{\pi}{2}\ln\frac{\Delta_0}{\Delta} - 2G + 3\right). \tag{11.33}$$

11.2.5. Physics of Coherent Instability

As follows from (11.33), the parameter $\gamma > 0$ at $\Delta > \Delta_n$ so that the corresponding solution is unstable [here Δ_n is the root of the equation $\gamma = 0$, which coincides with (11.25)]. This means that the states of the system, indicated by the dotted line in Fig. 11.1, are unstable against the transition to the normal state or to the state with $\Delta_2 > \Delta_n$. The region of instability coincides with the region of ambiguity of $\Delta(\beta)$. This ambiguity arises, as mentioned earlier, from the coherence factors in the kinetic equation, which reveal the physical cause of instability.[2] Indeed, let the gap at $\Delta < \Delta_n$ be decreased slightly due to a fluctuation. Then the probability of excess quasi-particle recombination decreases owing to the coherence factors. This increases the number of excess quasi-particles and leads to a further decrease in Δ, etc. The reverse conclusions are also valid. As a result, from the intermediate values of Δ_1 the solution passes to the branch $\Delta_0 = 0$ or to the branch $\Delta_2 > \Delta_n$. This leads to the "coherent" instability.

11.3. FINITE TEMPERATURES

11.3.1. Inclusion of Thermal Phonons

As before, we will consider the kinetic equation (5.21), with a collision integral of the form

$$J^{(\mathrm{e-ph})}(n_\varepsilon) = \int_\xi^{\omega_D} d\xi' \left(1 - \frac{\Delta}{\varepsilon\varepsilon'}\right) \alpha^2(\varepsilon' - \varepsilon)\, F(\varepsilon' - \varepsilon)\, [\,(1 - n_\varepsilon)\, n_{\varepsilon'}\, (N_{\varepsilon-\varepsilon'} + 1)$$

$$- n_\varepsilon (1 - n_{\varepsilon'})\, N_{\varepsilon'-\varepsilon}] + \int_0^\xi d\xi' \left(1 - \frac{\Delta}{\varepsilon\varepsilon'}\right) \alpha^2(\varepsilon - \varepsilon')\, F(\varepsilon - \varepsilon')\, [(1 - n_\varepsilon)\, n_{\varepsilon'}\, N_{\varepsilon-\varepsilon'}$$

$$- n_\varepsilon (1 - n_{\varepsilon'})\, (N_{\varepsilon-\varepsilon'} + 1)] + \int_0^{\omega_D} d\xi' \left(1 + \frac{\Delta}{\varepsilon\varepsilon'}\right) \alpha^2(\varepsilon + \varepsilon')\, F(\varepsilon + \varepsilon')$$

$$\times [(1 - n_\varepsilon)\, (1 - n_{\varepsilon'})\, N_{\varepsilon+\varepsilon'} - n_\varepsilon n_{\varepsilon'} (1 + N_{\varepsilon+\varepsilon'})]. \tag{11.34}$$

The phonon distribution function in (11.34) remains in equilibrium: $N_\omega = N_\omega^0$.

11.3.2. τ-Approximation

The deviation of the electron distribution function from its equilibrium value $\delta n_\varepsilon = n_\varepsilon - n_\varepsilon^0$ is assumed to be small and localized in an energy range much smaller than the temperature scale. In such a case, the terms containing δn_ε in the integrands are small compared with the terms containing δn_ε as multipliers. Omitting these integral terms and noting that the terms in square brackets in Eq. (11.34) vanish for the equilibrium substitutions n_ε^0 and N_ω^0, one can write:

$$J^{(\mathrm{e-ph})}(n_\varepsilon) = \left\{ \int_\xi^{\omega_D} d\xi' \left(1 - \frac{\Delta}{\varepsilon\varepsilon'}\right) \alpha^2(\varepsilon' - \varepsilon)\, F(\varepsilon' - \varepsilon)\, (N^0_{\varepsilon'-\varepsilon} + n^0_{\varepsilon'}) \right.$$

$$+ \int_0^{\xi} d\xi' \left(1 - \frac{\Delta}{\varepsilon\varepsilon'}\right) \alpha^2(\varepsilon - \varepsilon')\, F(\varepsilon - \varepsilon')\, (N^0_{\varepsilon-\varepsilon'} + 1 - n^0_{\varepsilon'})$$

$$\left. + \int_0^{\omega_D} d\xi' \left(1 + \frac{\Delta}{\varepsilon\varepsilon'}\right) \alpha^2(\varepsilon + \varepsilon')\, F(\varepsilon + \varepsilon')\, (N^0_{\varepsilon+\varepsilon'} + n^0_{\varepsilon'}) \right\} \equiv -\frac{\delta n_\varepsilon}{\tau_\varepsilon}. \quad (11.35)$$

After algebraic manipulations, taking into account the expressions for n_ε^0 and N_ω^0, one finds

$$\frac{1}{\tau_\varepsilon} = \frac{1}{2} \sum_{\eta=\pm 1} \int_0^\infty d\xi' \left(1 + \eta \frac{\Delta^2}{\varepsilon\varepsilon'}\right) \alpha^2(|\varepsilon + \eta\varepsilon'|)\, F(|\varepsilon + \eta\varepsilon'|)$$

$$\times \cosh\frac{\varepsilon}{2T} \sinh^{-1}\frac{|\varepsilon + \eta\varepsilon'|}{2T} \cosh^{-1}\frac{\varepsilon'}{2T}. \quad (11.36)$$

Because the essential range of integration in (11.36) is $\xi \sim T$, one can consider τ_ε^{-1} at $\varepsilon << T$ as a constant:

$$\frac{1}{\tau_\varepsilon} \approx \int_0^\infty d\xi'\, \alpha^2(\xi')\, F(\xi') \sinh^{-1}\frac{\xi'}{2T} \cosh^{-1}\frac{\xi'}{2T}, \quad (11.37)$$

which in the Debye model [$k = 1$ in (11.2)] is equivalent to

$$\frac{1}{\tau_\varepsilon} = \frac{\pi\lambda}{4\omega_D^2} \int_0^\infty d\xi'\, (\xi')^2 \sinh^{-1}\frac{\xi'}{T} = \frac{7\zeta(3)\pi\lambda T^3}{2\omega_D^2}. \quad (11.38)$$

Note that this expression for τ_ε, as well as the collision integral in the relaxation-time approximation, was used in previous chapters.

11.3.3. Iterative Solution Procedure

Continue now the examination of the collision operator (11.34), removing the restriction for δn_ε to be localized, but assuming it is small in magnitude. The only simplification now follows from neglecting the quadratic in δn_ε terms. Taking into account the identities

$$2(1 - n_\varepsilon^0 + N_{\varepsilon'-\varepsilon}^0) = \cosh\frac{\varepsilon'}{2T}\cosh^{-1}\frac{\varepsilon}{2T}\sinh^{-1}\frac{\varepsilon'-\varepsilon}{2T}, \tag{11.39}$$

$$2(n_\varepsilon^0 + N_{\varepsilon-\varepsilon'}^0) = \cosh\frac{\varepsilon'}{2T}\cosh^{-1}\frac{\varepsilon}{2T}\sinh^{-1}\frac{\varepsilon-\varepsilon'}{2T}, \tag{11.40}$$

one can rewrite (11.34) in the form:

$$J^{(e-ph)}(n_\varepsilon) \approx -\frac{\delta n_\varepsilon}{\tau_\varepsilon} - \frac{1}{2}\sum_{\eta=\pm1}\int_0^\infty d\xi'\,\alpha^2(|\varepsilon+\eta\varepsilon'|)\,F(|\varepsilon+\eta\varepsilon'|)\left(1+\frac{\Delta^2}{\varepsilon\varepsilon'}\right)$$

$$\times\cosh\frac{\varepsilon'}{2T}\cosh^{-1}\frac{\varepsilon}{2T}\sinh^{-1}\frac{|\varepsilon+\eta\varepsilon'|}{2T}\,\delta n_{\varepsilon'}, \tag{11.41}$$

where τ_ε is given by Eq. (11.37). As in Sect. 11.1, the shape of the distribution function is governed by the condition $J^{(e-ph)}(n_\varepsilon) = 0$, which implies:

$$\delta n_\varepsilon = -\frac{\tau_\varepsilon}{2}\sum_{\eta=\pm1}\int_0^\infty d\xi'\,\alpha^2(|\varepsilon+\eta\varepsilon'|)\,F(|\varepsilon+\eta\varepsilon'|)\left(1+\frac{\Delta^2}{\varepsilon\varepsilon'}\right)$$

$$\times\cosh\frac{\varepsilon'}{2T}\cosh^{-1}\frac{\varepsilon}{2T}\sinh^{-1}\frac{|\varepsilon+\eta\varepsilon'|}{2T}\,\delta n_{\varepsilon'}. \tag{11.42}$$

11.3.4. Solution for $\Delta = 0$

Let us initially put $\Delta = 0$. Then from (11.42) it follows that δn_ε varies within the energy range of the order of the temperature scale, decaying exponentially at $\varepsilon << T$. In our case $\delta n_\varepsilon = 0$ at $\varepsilon = 0$ and increases linearly with ε. So:

$$\delta n_\varepsilon(\Delta = 0) \approx \begin{cases} B\varepsilon/T, & \varepsilon \le T; \\ 0, & \varepsilon > T. \end{cases} \tag{11.43}$$

The coefficient B may be estimated from the normalization condition, which is analogous to (11.3):

$$2\alpha\omega_0 = \int_0^\infty d\xi \int_0^\infty d\xi'\, \alpha^2(\varepsilon+\varepsilon')\, F(\varepsilon+\varepsilon')\, \delta n_\varepsilon \cosh\frac{\varepsilon'}{2T} \cosh^{-1}\frac{\varepsilon}{2T} \sinh^{-1}\frac{|\varepsilon+\eta\varepsilon'|}{2T}. \quad (11.44)$$

Using the approximation (11.2) with $k = 1$, one finds (by the order of magnitude)

$$B \approx \frac{\alpha\omega_0\tau_\varepsilon}{T}. \quad (11.45)$$

11.3.5. Coherent Contribution

To estimate the contribution proportional to $(\Delta/T)^2$, one can use an iteration procedure based on (11.42). Substituting (11.43) into (11.42) and taking into account (11.2) and (11.37), one can find the desired correction (up to the factor $1/\pi$, cf. Ref. 3):

$$\delta n_\varepsilon = -\frac{\tau_\varepsilon\Delta^2}{\varepsilon}\int_0^T d\xi' \frac{\alpha^2(\xi')\, F(\xi')}{\varepsilon} \cosh\frac{\varepsilon'}{2T}\, \delta n_{\varepsilon'}(\Delta = 0) \approx -\frac{B\Delta^2}{\varepsilon T}. \quad (11.46)$$

In deriving Eq. (11.46) it was taken into account that the "coherent" correction δn_ε should be essential in the energy range $\xi \sim \Delta$. The part of δn_ε which does not depend on Δ was omitted, although it renormalizes the function $\delta n(\Delta = 0)$.

11.3.6. Two Branches of a Nonzero-Order Parameter

This function $\delta n(\Delta = 0)$ renormalizes T_c in the self-consistency equation (5.25). One can assume that this renormalization has been made and ignore the explicit dependence on $\delta n(\Delta \approx 0)$ in Eq. (5.25), which in the vicinity of T_c has the form[cf. Eq. (1.182)]:

$$-\left[\frac{T-T_c}{T_c} + \frac{7\zeta(3)}{8\pi^2}\left(\frac{\Delta}{T_c}\right)^2 - \kappa\right]\Delta = 0. \quad (11.47)$$

The anomalous part κ, which sometimes is called the *gap control term* (see Sect. 7.1.7), is defined by the relation

$$\kappa \approx -\int d\xi \frac{1}{\varepsilon}\delta n(\xi) \approx B\frac{\Delta}{T_c}. \quad (11.48)$$

Note that the function (11.46) is negative and this enhances the value of Δ. For a given B, one has two branches of solution for Δ in the temperature range $T_c < T < T_M$:

$$\frac{\Delta}{T_c} = \frac{B}{2} \pm \sqrt{\frac{B^2}{4} - \frac{7\zeta(3)}{8\pi^2}\frac{T - T_c}{T_c}}. \tag{11.49}$$

The quantity T_M is defined by the relation $T_M = T_c[1 + 2\pi^2 B^2/7\zeta(3)]$.Apart from these solutions, there is also a trivial solution, $\Delta = 0$. Thus the situation at finite temperatures is analogous to the zero temperature case. In the next section we will consider in more detail some consequences of this ambiguous behavior of the nonequilibrium gap Δ.

11.4. DISSIPATIVE PHASE TRANSITION

11.4.1. Stationary Solutions for Time-Dependent Problems

We will use in our analysis the time-dependent Ginzburg–Landau equation (7.115) for a real order parameter, adding to (7.115) the contribution from the gap control term caused by the action of an electromagnetic field:

$$\frac{\pi}{8T_c}\sqrt{1 + (2\tau_\varepsilon\Delta)^2}\,\frac{\partial\Delta}{\partial t} = -\left[\frac{T - T_c}{T_c} - \xi^2(0)\nabla^2 + \frac{7\zeta(3)}{8\pi^2}\left(\frac{\Delta}{T_c}\right)^2 - B\frac{\Delta}{T_c}\right]\Delta, \tag{11.50}$$

where $\xi^2(0) = \pi D/8T_c$. Introducing the potential function $U(\Delta)$

$$U(\Delta) = -\frac{1}{2}\left[\frac{T - T_c}{T_c} + \frac{7\zeta(3)}{16\pi^2}\left(\frac{\Delta}{T_c}\right)^2 - \frac{2}{3}B\frac{\Delta}{T_c}\right]\Delta^2, \tag{11.51}$$

one finds from Eq. (11.50) that the stationary solutions ($\dot{\Delta} = 0$) must obey the equation

$$\xi^2(0)\Delta(r)'' = -\frac{\partial U[\Delta(r)]}{\partial\Delta(r)} \tag{11.52}$$

(we consider the one-dimensional case $r \equiv x$, omitting below the argument r). As was pointed out in Ref. 3, this equation is analogous to that describing the motion of a particle with the mass $\xi^2(0)$ in the potential $U(\Delta)$: instead of time we have the space coordinate x, and instead of a space coordinate, the value of Δ. The first integral of (11.52) has the form:

$$\frac{1}{2}\xi^2(0)(\Delta')^2 + U = C \tag{11.53}$$

(the "mechanical" analogy to the constant C is the energy of the system). Note the following properties of solutions $\Delta(x)$: the symmetry with respect to the coordinate

reflection and the invariance at an arbitrary shift of the "coordinate" Δ (the mechanical analogy is the time reversal and space translation).[3]

Among the solutions generated by the potential $U(\Delta)$ (Fig. 11.2a) there are three constants:

$$\Delta_i = \text{const}, \quad i = 0, 1, 2, \tag{11.54}$$

which correspond to the extrema of $U(\Delta)$: in these cases we have $C_i = U_i(\Delta_i)$, $\partial U(\Delta_i)/\partial \Delta_i = 0$. The restricted solutions for Δ exist (if $C \geq U$) in the region between the boundary extrema of $U(\Delta)$ (Fig. 11.2a). Generally these bounded solutions are periodic in space (Fig. 11.2c). As follows from (11.52), the curvature in the extrema of periodic solutions is equal to $\{-[1/\xi^2(0)]\partial U/\partial \Delta\}$ at the turning points $U(\Delta) = C$. The periodic solutions degenerate to solitons (localized objects, Fig. 11.2c) whenever one of these curvatures vanishes, e.g., if $C = U_0 = U(\Delta = 0) = 0$. If for some reasons (e.g., at some level of external pumping) $U_0 = U_2$, then there is a possibility of further degeneration of the soliton to the wall-like solution at $C = U_0 = U_2$ (Fig. 11.2d).

11.4.2. Local Stability Against Space-Time Fluctuations

Now we will inspect, following Eckern et al.,[3] the local stability of these solutions against small space–time fluctuations. To do this we will analyze the dynamics of $\Delta(x, t)$ in the vicinity of stationary solutions $\Delta(x)$. Linearizing (11.50) in the vicinity of $\Delta(x)$, and assuming (without any loss of generality) that the prefactor at $\dot{\Delta}$ is equal to 1, one obtains for $U(x, t) = \Delta(x, t) - \Delta(x)$ the equation:

$$\dot{U} = \left.\frac{\partial^2 U}{\partial \Delta^2}\right|_{\Delta=\Delta(x)} U + \xi^2(0)\, U''. \tag{11.55}$$

Presenting $U(x, t)$ in the form $U(x, t) = \exp(-\omega_n t) u_n(x)$, one obtains from (11.55) the one-dimensional analogy of the "Schrödinger" equation:

$$-\xi^2(0)\, u_n'' = \left.\frac{\partial^2 U}{\partial \Delta^2}\right|_{\Delta=\Delta(x)} u_n = \omega_n u_n, \tag{11.56}$$

where ω_n has the meaning of an "energy." As follows from (11.56), spatially homogeneous solutions corresponding to the maxima of $U(\Delta)$ are stable: $\partial^2 U/\partial \Delta^2 < 0$ at these points. On the contrary, the intermediate values of Δ are not stable. To analyze the stability of spatially periodic stationary solutions, one should differentiate (11.52), resulting in:

$$\frac{\partial^2 U}{\partial \Delta^2} = -\xi^2(0)\, \frac{\Delta'''}{\Delta'}. \tag{11.57}$$

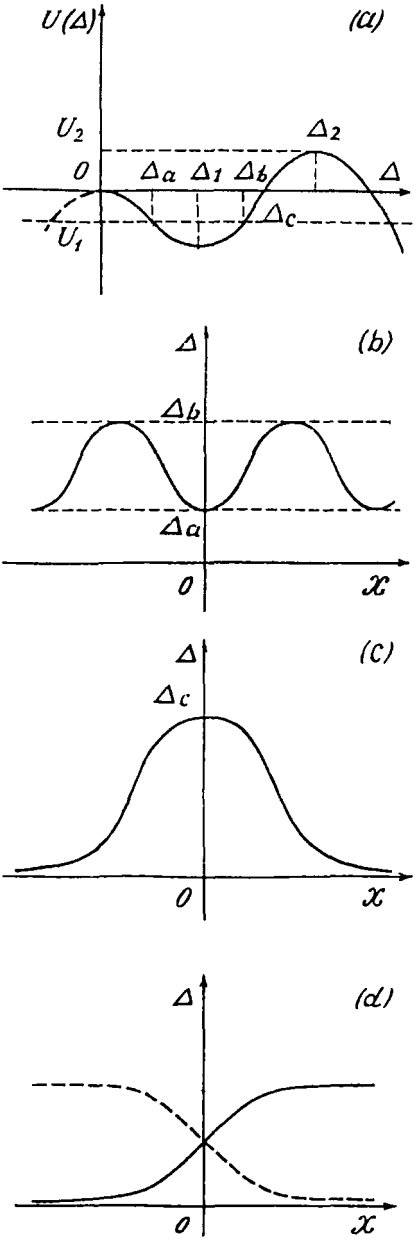

Figure 11.2. (a) Various types of spatially inhomogeneous stationary solutions corresponding to the potential $U(\Delta)$; (b) periodic solution: $U_1 < U < 0$; (c) soliton ($C = 0$); (d) wall-like solution: $C = 0 = U(\Delta_2)$.

Using (11.56) and (11.57), one can establish that the eigenfunction $u_0(x) = \Delta'$ is the only one that corresponds to the eigenvalue $\omega_0 = 0$. For periodic solutions, $u_0(x)$ has an infinite number of nodes. Hence there are functions with a finite number of nodes that correspond to the lower values of "energy": $\omega_n < 0$. So the periodic solutions are not stable. The soliton function $u_0(x)$ has a single node; consequently there is one eigenfunction $u_1(x)$ corresponding to the smaller value of "energy": $\omega_1 < 0$ (the "ground state"). Thus the solitons are not stable either. The wall-like solution $u_0(x)$ has no nodes; this solution is stable against small perturbations.

11.4.3. Coexistence of Normal and Superconducting States

As mentioned earlier, the wall-like solution corresponds to

$$C = U(0) = U(\Delta_2) = 0. \tag{11.58}$$

Taking into account (11.51), it can be found from Eq. (11.58) that the wall-like solution corresponds to the temperature

$$T_K = T_c[1 + 16\pi^2 B^2/63\xi(3)] < T_M. \tag{11.59}$$

The general situation is illustrated in Fig. 11.3. At $T = T_K$, the free energies of superconducting and normal phases are equal: these phases may coexist. At higher temperatures, the normal phase is energetically favorable and the wall moves toward the superconducting region. At lower temperatures, the superconducting state is more favorable and the superconducting phase should expand to fill the space.

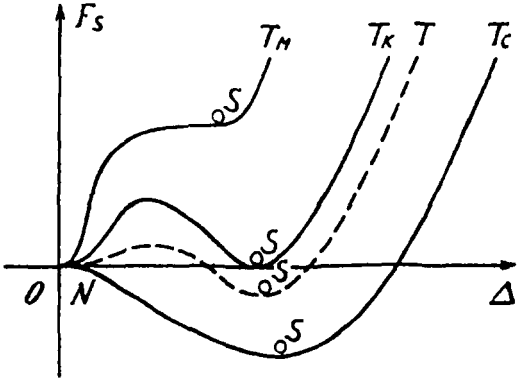

Figure 11.3. Free-energy functional corresponding to spatially homogeneous states at different temperatures $T_c < T < T_K < T_M$. At $T_M > T > T_K$, the superheated superconducting state is possible, whereas at $T_K > T > T_c$, the supercooled normal state may be expected.

11.4.4. Velocity of Phase-Boundary Motion

To obtain the velocity v of NS boundary motion at $\delta T = T - T_K \neq 0$, one can use (cf. Ref. 4) Eq. (11.50). Suppose the motion is stationary and the solution

$$\Delta(x, t) = \Delta(x - vt) \tag{11.60}$$

obeys Eq. (11.52) at $T = T_K$. On account of (11.60) and the condition $v = \text{const}$, Eq. (11.50) transforms at $T = T_K + \delta T$ into

$$\frac{\pi}{8T_c}\sqrt{1 + (2\tau_\varepsilon\Delta)^2}\, v\frac{\partial\Delta}{\partial x} = \frac{\delta T}{T_c}\Delta. \tag{11.61}$$

Using (11.53) at $C = 0$, one obtains

$$-2\left(\frac{\pi}{8T_c}\right)^2 [1 + (2\tau_\varepsilon\Delta)^2]\,[v/\xi(0)]^2 U(\Delta) = \frac{(\delta T)^2\Delta^2}{T_c^2}. \tag{11.62}$$

Integrating expression (11.51) for $U(\Delta)$ along the trajectory of motion within the limits $[\Delta_0, \Delta_2]$, taking into account Eq. (11.59) and

$$\Delta(T = T_K) = \frac{16\pi^2}{21\zeta(3)} BT_c, \tag{11.63}$$

one finds (for $\tau_\varepsilon\Delta_2 >> 1$) the following expression for the motion of the wall (i.e., the NS boundary):

$$v = \bar{c}\frac{\xi(0)}{\tau_\varepsilon}\frac{T - T_K}{T_c} B^4, \tag{11.64}$$

where $\bar{c}^2 = 180\,[21\zeta(3)/8\pi^2]^3/\pi^2 \sim 1$.

Because the spatially homogeneous solutions are locally stable, superheated and supercooled states are possible. The transitions between different phases should be analogous to the first-order phase transitions. The dynamics of these dissipative phase transitions were discussed earlier.

11.5. MAGNETIC PROPERTIES

11.5.1. Equilibrium Diamagnetic Response

The response of a superconductor to a slowly varying magnetic field is determined by the dependence of the superconducting current on the vector potential. This dependence is contained in the first term of Eq. (7.88) ($e = 1$):

$$\mathbf{j}_s = \sigma_n \mathbf{Q} \int_{-\infty}^{\infty} d\varepsilon\, R_2 N_2 f_1 = 2m\mathbf{v}_s \sigma \int_{-\infty}^{\infty} d\varepsilon\, R_2 N_2 (1 - 2n_\varepsilon)\, \mathrm{sign}\varepsilon \equiv \mathbf{v}_s N_s, \tag{11.65}$$

where

$$N_s = 2m\sigma_n \int_{-\infty}^{\infty} d\varepsilon\, R_2 N_2 (1 - 2n_\varepsilon)\, \mathrm{sign}\varepsilon = \pi m \sigma_n \Delta (1 - 2n_{\varepsilon=\Delta}). \tag{11.66}$$

Positive values of N_s in thermodynamic equilibrium

$$N_s = \pi m \sigma_n \Delta^2 2T, \quad T \to T_c, \tag{11.67}$$

$$N_s = \pi m \sigma_n \Delta, \quad T = 0 \tag{11.68}$$

lead to a diamagnetic response. In a nonequilibrium state, as follows from (11.66), N_s may become negative (at $n_\varepsilon > 1/2$), which corresponds to the paramagnetic response.

11.5.2. Paramagnetic Instability

The superconducting paramagnetic state may become unstable against fluctuations of superfluid velocity $\mathbf{v}_s$.[5,6] Indeed, from the Maxwell equation

$$\nabla^2 \mathbf{A} = -\frac{4\pi}{c} (\mathbf{j}_s + \mathbf{j}_n) \tag{11.69}$$

the dispersion relation

$$i\omega = \frac{c^2}{4\pi\sigma_n} \left(q^2 + \frac{1}{\lambda^2} \right) \tag{11.70}$$

follows for small values of $\mathbf{q}$ and ω subject to (11.65). Here $\lambda^{-2} = (N_s/N)\lambda_L^{-2}$ and N is the charge carrier density in the normal metal. Evidently for $\lambda^2 < 0$ the Fourier component of the field with $q < |\lambda|^{-1}$ grows exponentially in time.

11.5.3. Role of Boundary Conditions

Thus the perturbations moving perpendicular to the boundary would be damped out in a film of thickness $d < |\lambda|$, while the perturbations moving along the film would amplify. Note that such amplification may not occur if the film is deposited on a massive superconductor S'.[7] In this case, one must consider three equations: $\nabla^2 \mathbf{A} = 0$ for the half-space $z > 0$, Eq. (11.69) for the film S, and the equation $\nabla^2 \mathbf{A} = (\lambda_L')^{-2} \mathbf{A}$ for the half-space occupied by a superconductor S'. These

equations are linked by the boundary conditions expressing the continuity of the vector potential **A**. The dispersion relations

$$\frac{q+q'\tanh q'd}{q'+q\tanh q'd}=\frac{\sqrt{q^2+(\lambda')^{-2}}}{q'}, \tag{11.71}$$

$$(q')^2=q^2+\lambda^{-2}-\frac{4\pi i\omega\sigma_n}{c^2} \tag{11.72}$$

follow for the solution, which should vanish at $z=\pm\infty$. Because small values of momenta are of interest, one can put $q=0$ and $q'd<<1$, obtaining thus from (11.71) and (11.72):

$$i\omega=\frac{c^2}{4\pi\sigma_n}\left(\frac{1}{\lambda^2}+\frac{1}{\lambda' d}\right). \tag{11.73}$$

At $\lambda^{-2}<0$, the system is stable if

$$d\lambda'<|\lambda|^2. \tag{11.74}$$

If $T=0$, the substitution of (11.14) into (11.66) gives the value $N_s=0$. Consequently, the sign of N_s is defined mainly by the sign of the "coherent" addition. As follows from (11.18), in the case we have considered, $N_s\propto\Delta$ and is positive. Using (11.8), (11.14), (11.65), and (11.66), one finds

$$\mathbf{j}_s\approx\mathbf{v}_s\frac{\pi\sigma\Delta^2}{2a}\ln\frac{a}{\Delta},\quad T=0. \tag{11.75}$$

In the model considered in Sect. 11.4, at finite temperatures one has

$$\mathbf{j}_s\approx\mathbf{v}_s\frac{\pi\sigma\Delta^2}{2T}(1+2B),\quad T\sim T_c, \tag{11.76}$$

i.e., N_s is also positive.

11.5.4. Superheated States at External Pumping

Concluding this section, we will discuss some peculiarities of the dissipative phase transition in a magnetic field.[3,8,9] Suppose a thin film of thickness d (under the action of laser radiation) is placed in a magnetic field H. In this stationary state, $\Delta=\text{const}$ and Eq. (11.65) is modified to

$$0=-\left[\frac{T-T_c}{T_c}+(2m\mathbf{v}_s)^2\xi^2(0)+\frac{7\zeta(3)}{8\pi^2}\left(\frac{\Delta}{T_c}\right)^2-B\frac{\Delta}{T_c}\right]\Delta. \tag{11.77}$$

It was shown in Sect. 1.2 that the average value of $\mathbf{v}_s$ in the film is zero, although $\overline{\mathbf{v}_s^2}\neq 0$. It could be evaluated as

$$\overline{\mathbf{v}_s^2} = \frac{a_1}{m^2\xi^2(0)}\left(\frac{H}{H_c}\right)^2, \tag{11.78}$$

where a_1^2 is a factor that is approximately equal to $(d/\lambda)^2$ (up to the numerical constant). From Eq. (11.77) one can see that the magnetic field renormalizes the temperature. Making the substitution

$$T_* = T + a_1\left(\frac{H}{H_c}\right)^2 T_c, \tag{11.79}$$

one can restate for T_* all the results found in Sect. 11.3 for the original temperature T. Thus, at "temperatures" T_* obeying the relation

$$T_c < T_* < T_M \tag{11.80}$$

the same ambiguity of Δ arises in a thin film. As may be seen from Eqs. (11.80) and (11.79), at $\mathbf{H} \neq 0$ the actual temperature $T < T_c$. Correspondingly, the original values of T_M and T_K are also shifted. At fixed values of T, the superheated or supercooled states may be created by varying the magnetic field. (In close analogy with the first-order phase transition, considered in Sect. 1.2 for the Type I superconductors, one can expect superheating and supercooling in the Type II superconductors.) In this case the first-order phase transition in the Type II superconductors is related to the external deviation from thermal equilibrium.

11.6. BRANCH IMBALANCE INITIATED BY ABSORPTION OF HIGH-ENERGY QUANTA

11.6.1. Finite Curvature of the Fermi Surface

During laser pumping or high-energy particle cascade events, the branch imbalance in superconductors is usually considered negligible. The reason is the symmetry property

$$Q(\varepsilon) = Q(-\varepsilon) \tag{11.81}$$

which the nonequilibrium source (5.12) [as well as its quantum generalization (5.54)] possesses. The property (11.81) yields the solutions of the kinetic equations of (3.63), which are symmetric over the electron and hole branches:

$$n_\varepsilon = n_{-\varepsilon}. \tag{11.82}$$

At the same time, there exists a mechanism that can yield the asymmetric population of electron-hole excitations, even under the action of electromagnetic radiation.[10] The physical source of this asymmetry is the finite curvature of the Fermi surface.

Namely, the density of electron levels has a large-scale dependence on the excitation energy

$$N(\xi) \propto \sqrt{\xi + \varepsilon_F}. \tag{11.83}$$

This dependence was neglected in all the above calculations, since the relation

$$N(\xi) \approx N(0) \left(\equiv \frac{mp_F}{2\pi^2} \right) \tag{11.84}$$

was universally adopted. One can correct the dependence (11.84) by taking into account the relation (11.83):

$$N(\varepsilon) \approx N(0) \left[1 + \operatorname{sign} \varepsilon \frac{\sqrt{\varepsilon^2 - |\Delta|^2}}{2\varepsilon_F} \right]. \tag{11.85}$$

Consequently, the collision integral of electrons with photons may be rewritten in the form*

$$J^{(e-pt)}\,[n_{\pm\varepsilon}(\pm\mathbf{p})] = \left(\frac{e^2 p_F}{2mc^2} \right) \int_{|\Delta|}^{\infty} \frac{d\varepsilon'}{2\pi} \left[1 \pm \frac{\sqrt{\varepsilon'^2 - |\Delta|^2}}{2\varepsilon_F} \right]$$

$$\times \int \frac{d\Omega_{\mathbf{p}'}}{4\pi} \int \rho(\omega_{\mathbf{k}})\, d^3\mathbf{k}\, [q_1 \delta(\mathbf{p}' - \mathbf{p} - \mathbf{k}) + q_2 \delta(\mathbf{p} - \mathbf{p}' - \mathbf{k}) + q_3 \delta(\mathbf{p} + \mathbf{p}' - \mathbf{k})] \tag{11.86}$$

where the factors q_1, q_2, q_3, and $\rho(\omega_{\mathbf{k}})$ were defined in Sect. 5.3.

Thus the interaction of electromagnetic radiation with the electrons in a superconductor (as in a normal metal) "resolves" the electronlike $(\varepsilon > 0)$ and holelike $\varepsilon < 0$ excitations (see Figs. 11.4 and 11.5). As a result, a photoinduced potential must arise. We now consider this effect in more detail.

11.6.2. Photoinduced Potential and Owen–Scalapino μ^* Model

We consider the stationary state that arises in a thin superconducting film, which is analogous to the case considered in Chap. 5. Instead of (5.41), one deals with (11.86), which provides, in the manner described in Sect. 5.3, the following linearized nonequilibrium source:

*We should note that the previously exploited powerful tool for the description of nonequilibrium superconductivity, the energy-integrated Green's function technique, is not rigorously applicable here. This technique is appropriate only for describing processes taking place in the momentum space not far from the Fermi surface. Nevertheless, the Boltzmann-like kinetic equations could be appropriately corrected to include the most important part of the branch imbalance effect resulting from high-energy quanta absorption.

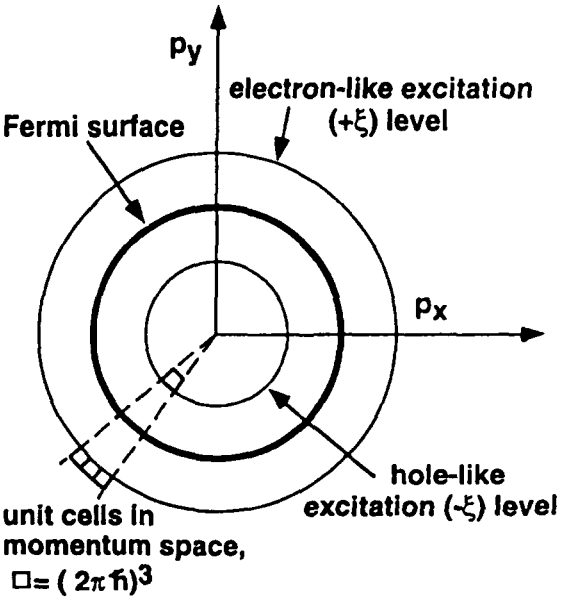

Figure 11.4. Geometrical illustration of the difference in the density of states $N(\pm\xi)$ for electronlike and holelike excitation branches in a normal metal. The difference is caused by the finite curvature of the Fermi surface from which the electrons $(+\xi)$ and holes $(-\xi)$ are equally distanced.

$$
\begin{aligned}
Q(\pm\varepsilon) = \alpha\{ & \nu_{\pm(\varepsilon-\omega_0)}[(n^0_{\varepsilon-\omega_0} - n^0_{\varepsilon})\,(u_\varepsilon u_{\varepsilon-\omega_0} + v_\varepsilon v_{\varepsilon-\omega_0})]\theta(\varepsilon - \omega_0 - \Delta) \\
& - \nu_{\pm(\varepsilon+\omega_0)}\,[(n^0_{\varepsilon} - n^0_{\varepsilon+\omega_0})\,(u_\varepsilon u_{\varepsilon+\omega_0} + v_\varepsilon v_{\varepsilon+\omega_0})]\theta(\varepsilon + \omega_0 - \Delta) \\
& + \nu_{\pm(\omega_0-\varepsilon)}\,[(1 - n^0_{\varepsilon} - n^0_{\varepsilon-\omega_0})\,(u_\varepsilon u_{\omega_0-\varepsilon} + v_\varepsilon v_{\omega_0-\varepsilon})]\theta(\omega_0 - \varepsilon - \Delta)\}
\end{aligned}
\tag{11.87}
$$

where α is defined by (5.60),

$$
\nu_{\pm\varepsilon} = \frac{N(\pm\varepsilon)}{N(0)} = \left[\frac{\varepsilon_F \pm \varepsilon}{\varepsilon_F}\right]^{1/2}, \tag{11.88}
$$

and the substitution of the equilibrium function, $n_{\pm\varepsilon} \to n^0_\varepsilon$ was made in (11.87).

Owing to the presence of $\nu_{\pm\varepsilon}$, Eq. (11.87) implies the property:

$$
Q(\varepsilon) \neq Q(-\varepsilon), \tag{11.89}
$$

which may be regarded as yielding a branch imbalance. Figure 11.5 illustrates the situation clearly.

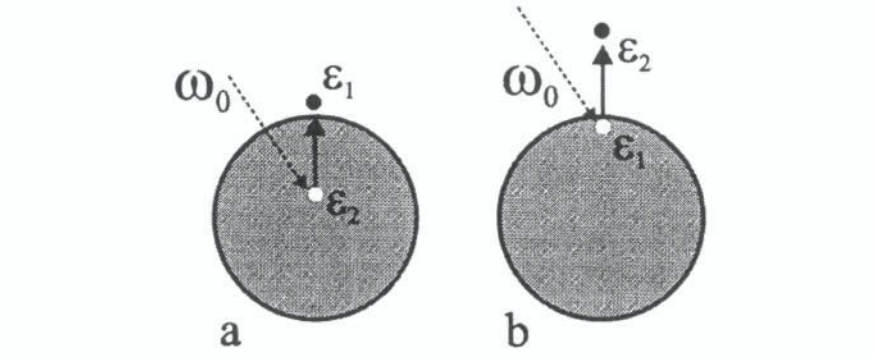

Figure 11.5. Two channels creating electron-hole pairs via photon absorption have different probabilities: channel (b) is of a higher probability.

The steady-state nonequilibrium solutions for electron-hole distribution functions n_ε and $n_{-\varepsilon}$ in the spatially homogeneous case may be found by using the kinetic equation

$$u_\varepsilon \frac{dn_{\pm\varepsilon}}{d\varepsilon} = 0 = Q(\pm\varepsilon) + J^{(e-ph)}(n_{\pm\varepsilon}). \tag{11.90}$$

For the sake of brevity we will consider the case where the bias temperature is absolute zero, and the electromagnetic field is "wide," $\omega_0 >> \Delta$, as everywhere in this chapter. As in Sect. 11.1, we will set $\alpha^2(\omega_q)F(\omega_q) \equiv \text{const}$, and present (11.90) in the form [cf. (11.7)]:

$$(1 - n_{\pm\varepsilon}) \int_{\varepsilon}^{\omega_D+\varepsilon} d\varepsilon'\, n'_{\pm\varepsilon} - n_{\pm\varepsilon} \int_{\max(\alpha,\varepsilon-\omega_D)}^{\varepsilon} d\varepsilon'\,(1 - n'_{\pm\varepsilon}) - \int_{0}^{\omega_D-\varepsilon} d\varepsilon'\, n'_{\pm\varepsilon} = 0. \tag{11.91}$$

In writing (11.91), we focus on the energy dependence of the distribution function on an energy scale that is small compared with ω_D and large compared with the nonequilibrium value of Δ. This value of Δ may be much smaller than the equilibrium value Δ_0 owing to the external pumping. Assuming this to be the case, we set $\Delta \approx 0$ in (11.91). The presence of a superconducting state is revealed in two aspects of the branch-imbalance solutions: they are physically allowed, and they are stable against fluctuations.

By analogy to (11.10), let us denote

$$a_\pm = \int_0^\infty d\varepsilon\, n_{\pm\varepsilon}, \tag{11.92}$$

and assume $a_+ \neq a_-$ on grounds of the phase-space volume. Proceeding as in the derivation of (11.14), we obtain in this case:

$$n_\varepsilon = \frac{1}{2}\left\{1 - \frac{\varepsilon}{\sqrt{(\varepsilon + a_+ - a_-)^2 + 4a_+a_-}}\right\}, \tag{11.93}$$

$$n_{-\varepsilon} = \frac{1}{2}\left\{1 - \frac{\varepsilon}{\sqrt{(\varepsilon - a_+ + a_-)^2 + 4a_+a_-}}\right\}. \tag{11.94}$$

In the absence of imbalance, the value $a = a_+ = a_-$ was obtained from normalization condition (11.3). In the case of imbalance

$$\int_0^\infty d\xi\, Q(\pm\varepsilon) = Q_\pm, \tag{11.95}$$

where $Q_+ \neq Q_-$. Consequently, $a_+ \neq a_-$.

Actually, $a_+ - a_- = -\mu$, where μ is the gauge-invariant potential (8.6), representing the difference between the potentials of the normal and superfluid components of the electron liquid. On somewhat different grounds, this potential was first introduced by Owen and Scalapino[11] (the so-called μ^*-*model).* Despite the existence of a nonzero μ potential following laser pumping of superconductors, it has not yet been experimentally confirmed. A while ago the pioneering work of Testardi[12] initiated interest in the states generated by the influence of electromagnetic radiation on superconductors. This problem continues to attract the attention of a lot of experimentalists (see, e.g., Refs. 13–17). Thus one can expect that branch imbalance will be eventually registered and exploited in practice.

References

1. V. F. Elesin, Nonequilibrium state of superconductors with optical excitation of quasiparticles, *Sov. Phys. JETP* ***39***(*5*), 862–866 (1974) [*Zh. Eksp. i Teor. Fiz.* **66**(5), 1755–1761 (1974)].
2. V. F. Elesin, Features of the phase transition in nonequilibrium superconductors with optical pumping, *Sov. Phys. JETP* **44**(4), 780–786 (1976) [*Zh. Eksp. i Teor. Fiz.* **71**[4(10)], 1490–1502 (1976)].
3. V. Eckern, A. Schmid, M. Schmutz, and G. Schön, Stability of superconducting states out of thermal equilibrium, *J. Low Temp. Phys.* **36**(5/6), 643–687.
4. V. F. Elesin, Nonstationary "intermediate" state of nonequilibrium superconductors, *Sov. Phys. JETP* **46**(1), 185–191 (1977) [*Zh. Eksp. i Teor. Fiz.* **73**(1), 355–364 (1977)].
5. V. G. Baru and A. A. Sukhanov, New types of instabilities in nonequilibrium excitation of a superconductor, *JETP Lett.* **21**(4), 93–94 (1975) [*Pis'ma v Zh. Eksp. i Tear. Fiz.* **21**(4), 209–212 (1975)].
6. A. G. Aronov, Paramagnetic effects in superconductors, *JETP Lett.* **18**(6), 228–229 (1973) [*Pis'ma v Zh. Eksp. i Teor. Fiz.* **18**(6), 387–390 (1973)].
7. V. M. Genkin and A. P. Protogenov, Nonequilibrium states resulting from tunneling in superconductors, *Sov. Phys. Solid State* **18**(1), 13–17 (1976) [*Fiz. Tverd. Tela* **18**(1), 24–32 (1976)].

8. V. F. Elesin, Phase transition in a superconductor with excess quasiparticles in an external magnetic field, *Sov. Phys. Solid State* 22(10), 1808-1809 (1980) [Fiz. *Tverd. Tela* **22**, 3097–3099 (1980)].
9. V. F. Elesin and Yu. V. Kopaev, Superconductors with excess quasiparticles, *Sov. Phys. Uspekhi* **24**(2), 116–141 (1981) [*Usp. Fiz. Nauk* **133**(2), 259-307 (1981)].
10. A. M. Gulian and D. Van Vechten, Electron-hole branch imbalance in superconductors initiated by absorption of high-energy quanta, *Mod. Phys. Lett. B*, **10**(8), 329-338 (1996).
11. C. S. Owen and D. J. Scalapino, Superconducting state under the influence of external dynamic pair breaking, *Phys. Rev. Lett.* **28**(24), 1559-1561 (1972).
12. L. R. Testardi, Destruction of superconductivity by laser light, *Phys. Rev. B* **4**(7), 2189–2196 (1971).
13. J. T. C. Yen and D. N. Langenberg, Light-induced superconducting weak links, *Appl. Phys. Lett.* 32(3), 191–192(1978).
14. Y. S. Lai, Y. Q. Liu, W. L. Cao, and C. H. Lee, Picosecond optical response of $Tl_2Ba_2CaCu_2O_8$ and $Tl_{0.5}Pb_{0.5}Sr_2(Ca_{0.8}Y_{0.2})Cu_2O_7$ high T_c superconductor films, *Appl. Phys. Lett.* **66**(9), 1135-1137(1995).
15. F. A. Hegmann, D. Jacobs-Perkins, C.-C. Wang, S. H. Moffat, R. A. Hughes, J. S. Preston, M. Currie, P. M. Fauchet, T. Y. Hsiang, and R. Sobolewski, Electro-optic sampling of 1.5-ps photoresponse signal from $YBa_2Cu_3O_{7-\delta}$ thin films, *Appl. Phys. Lett.* **67**(2), 285-287 (1995).
16. B. J. Feenstra, J. Schützmann, D. van der Marel, R. P. Pinaya, and M. Decroux, Nonequilibrium superconductivity and quasiparticle dynamics studied by photoinduced activation of mm-wave absorption, *Phys. Rev. Lett.* **79**(24), 4890–4893 (1997).
17. D. Van Vechten, K. S. Wood, G. G. Fritz, J. S. Horwitz, G. M. Daly, J. B. Thrasher, D. M. Photiadis, J. Ding, J. F. Pinto, M. G. Blamire, G. Burnell, A. L. Gyulamiryan, V. H. Vartanyan, R. B. Akopyan, and A. M. Gulian, Voltage responses to optical pulses of unbiased normal and superconducting samples, *Appl. Phys. Lett.* **71**(10), 1415-1417 (1997).

12

Inverse Population Instabilities

We will refer to the inverse population state as the state with the excitation distribution function n_ε satisfying the condition*

$$n_\varepsilon > 1/2 \tag{12.1}$$

in a finite-energy region above the gap edge $|\varepsilon| \geq \Delta$. Comparing (12.1) with the thermodynamic equilibrium function

$$n_\varepsilon^0 = \frac{1}{\exp(|\varepsilon|/T) + 1}, \tag{12.2}$$

one can call the inversely populated state a "negative temperature" state,[1] since at $T < 0$ Eq. (12.2) would satisfy (12.1).

The possibility of inverse population in superconductors challenged investigators for a long time. Despite many theoretical indications of its feasibility, and very unusual and exciting implications (see, e.g., Refs. 2–16), this state has not yet been realized experimentally. Depending on the frequency of external radiation, two characteristic situations are usually considered: the case of "wide" source pumping and the case of "narrow" source pumping.

12.1. "WIDE" PUMPING SOURCE

In wide source pumping, the distribution function n_ε is formed by the counterplay of relaxation and recombination processes within the electron–phonon system, so the detailed properties of $Q(\varepsilon)$ may be neglected. Thus in the following section we will focus our attention on electromagnetic pumping. The generalization of results to tunnel injection is straightforward.

*In this chapter we assume Δ to be a real quantity and ignore the branch imbalance, setting $n_\varepsilon = n_{-\varepsilon}$ in all the expressions.

12.1.1. Elesin Theorem

Suppose a thin superconducting film of thickness d is deposited on a substrate, and a monochromatic electromagnetic field is incident on the film, driving the superconducting electron system out of equilibrium. Suppose also that the main mechanism responsible for relaxation of the electron system toward equilibrium is provided by inelastic collisions of electrons with phonons. The model of a "phonon heat bath," which was used extensively in previous chapters, simplifies the analysis. We will consider mainly the ordinary superconductors at $T = 0$, assuming that a spatially homogeneous state emerges in the film under electromagnetic pumping.

The kinetic equation for electrons may be written in the form:

$$J(n_\varepsilon) + Q(n_\varepsilon) = 0, \tag{12.3}$$

where $Q(\varepsilon)$ is the nonequilibrium source of quasi-particles (5.21) and (5.54), and $J = J^{(e-ph)}(n_\varepsilon) + J^{(e-e)}(n_\varepsilon)$, where $J^{(e-ph)}(n_\varepsilon)$ is the electron–phonon collision integral (4.119), which we will write in a somewhat more general form [cf. Eq. (11.34)]:

$$J^{(e-ph)}(n_\varepsilon) = \int_\Delta^\infty d\varepsilon' \frac{\varepsilon'\varepsilon d\varepsilon'}{\sqrt{\varepsilon^2-\Delta^2}\sqrt{\varepsilon'^2-\Delta^2}} \int_\Delta^{\omega_D} \alpha^2(\omega_q)F(\omega_q)d\omega_q$$
$$\times \left\{ \left(1 - \frac{\Delta^2}{\varepsilon\varepsilon'}\right)[n'(1-n)\delta(\varepsilon' - \varepsilon - \omega_q) - n(1-n')\delta(\varepsilon - \varepsilon' - \omega_q)] \right.$$
$$\left. - nn' \left(1 + \frac{\Delta^2}{\varepsilon\varepsilon'}\right)\delta(\varepsilon + \varepsilon' - \omega_q) \right\}. \tag{12.4}$$

The quantity $\alpha^2(\omega)F(\omega)$ in Eq. (12.2) is the spectral function of the electron-phonon interaction. As noted above, we will not consider in this section inelastic electron–electron collisions, so that the term $J^{(e-e)}(n_\varepsilon)$ will be ignored. To find a proper self-consistent solution of nonlinear kinetic equations, the equation

$$1 = \lambda \int_\Delta^\infty \frac{1 - 2n_\varepsilon}{\sqrt{\varepsilon^2 - \Delta^2}} d\varepsilon \tag{12.5}$$

must be coupled with Eq. (12.1).

We will consider first the isotropic model of metals with the Debye spectrum of phonons, following Elesin.[17] Eq. (12.1) may be rewritten in the form:

$$-(1 - n_\varepsilon)S^+(\varepsilon) + n_\varepsilon S^-(\varepsilon) + n_\varepsilon S^R(\varepsilon) = Q(\varepsilon), \tag{12.6}$$

where

$$\begin{pmatrix} S^+ \\ S^- \\ S^R \end{pmatrix} = \int_\Delta^\infty d\varepsilon' \int_0^{\omega_D} \frac{d\omega_q \varepsilon\varepsilon' \alpha^2(\omega_q) F(\omega_q)}{\sqrt{\varepsilon^2 - \Delta^2}\sqrt{\varepsilon'^2 - \Delta^2}} \begin{cases} n_{\varepsilon'} \delta(\varepsilon' - \varepsilon - \omega_q)\left(1 - \dfrac{\Delta^2}{\varepsilon\varepsilon'}\right) \\ (1 - n_{\varepsilon'})\delta(\varepsilon - \varepsilon' - \omega_q)\left(1 - \dfrac{\Delta^2}{\varepsilon\varepsilon'}\right) \\ n_{\varepsilon'} \delta(\varepsilon' + \varepsilon - \omega_q)\left(1 + \dfrac{\Delta^2}{\varepsilon\varepsilon'}\right) \end{cases}, \tag{12.7}$$

and the quantities S^+, S^-, S^R correspond to the "in" and "out" relaxation scattering of quasi-particles, and, correspondingly, to recombination via the phonon emission. Using (12.6), one can present n_ε as a functional fraction:

$$n_\varepsilon = \frac{S^+(\varepsilon) + Q(\varepsilon)}{S^+(\varepsilon) + S^-(\varepsilon) + S^R(\varepsilon)}. \tag{12.8}$$

In the case of optical pumping, when the frequency ω_0 greatly exceeds the value of Δ, the source $Q(\varepsilon)$ creates nonequilibrium quasi-particles in the wide range of $\Delta \le \varepsilon \lesssim \omega_0$, and inequalities

$$Q(\varepsilon) << (S^R, S^+, S_\varepsilon^-) \tag{12.9}$$

take place in the region $\varepsilon \ge \Delta$ at any practically achievable intensity of optical pumping. This gives us grounds to rewrite (12.8) as

$$n_\varepsilon \approx \frac{S^+(\varepsilon)}{S^R(\varepsilon) + S^-(\varepsilon) + S^+(\varepsilon)}. \tag{12.10}$$

For further analysis, the function $\alpha^2(\omega)F(\omega)$ in (12.7) was chosen[17,18] in the form

$$\alpha^2(\omega)F(\omega) = \pi\lambda\omega_q^{k+1}/2\omega_D^{k+1} \tag{12.11}$$

and the values of $k = 0, \pm 1$ were studied. In all of these cases one can estimate the values of the functionals S^+, S^- and S^R, using for the approximation

$$n_\varepsilon = \begin{cases} 1, & \varepsilon \le \varepsilon_0 \\ 0, & \varepsilon \ge \varepsilon_0 \end{cases}. \tag{12.12}$$

This allows us to find the inequalities

$$S^+(\varepsilon) << S^R(\varepsilon), \qquad S^-(\varepsilon) << S^R(\varepsilon), \tag{12.13}$$

and thus to establish $n_\varepsilon << 1$ (the *Elesin theorem*) from (12.8).

A principal difference between the kinetics of superconductors and semiconductors now becomes clear: the processes of recombination in superconductors have a single-phonon character, while in semiconductors the single-phonon processes of recombination are forbidden (because $E_g > \omega_D$). For superconductors, the role of the semiconductor gap E_g is performed by 2Δ, which does not exceed the phonon boundary frequency ω_D in all known superconductors. Moreover, the relation $\omega_D >> 2\Delta$ holds for traditional superconductors. At the same time, in recently discovered high-temperature superconductors, ω_D is comparable with 2Δ. In this case it is necessary to revise the earlier results.

12.1.2. "Two-Peak" Approximation for $\alpha^2(\omega)F(\omega)$

Such an attempt was made in Ref. 19. A simple "two-peak" approximation for the spectral function was adopted in this work:

$$\alpha^2(\omega_q)F(\omega_q) = a_1\delta(\omega_q - \omega_1) + a_2\delta(\omega_q - \omega_2), \tag{12.14}$$

where ω_1 and ω_2 are characteristic frequencies of phonons in superconductors, and the coefficients a_1 and a_2 include the interaction constants of electrons with these phonon modes and are also proportional to the spectral weights of these modes. For the case

$$\omega_1 << \Delta << \omega_2 \tag{12.15}$$

the problem permits an analytic solution, which can be presented in the form

$$n_\varepsilon \approx \left\{ \frac{(1 - n_{\varepsilon-\omega_1})\,[\varepsilon(\varepsilon - \omega_1) - \Delta^2]\,\sqrt{(\varepsilon + \omega_1)^2 - \Delta^2}\;\theta(\varepsilon - \omega_1 - \Delta)}{n_{\varepsilon+\omega_1}\,[\varepsilon(\varepsilon + \omega_1) - \Delta^2]\,\sqrt{(\varepsilon - \omega_1)^2 - \Delta^2}} + 1 \right\}^{-1}. \tag{12.16}$$

As an analysis of this formula shows, $n_\varepsilon \approx 1$ for a narrow energy range $\Delta \le \varepsilon \le \Delta + \omega_1$. The physical reasons for this result are related to the presence of two groups of phonons, with the frequencies ω_1 and ω_2 obeying the relation (12.13), which causes some peculiarities in the electron kinetics. Indeed, the recombination takes place by the participation of ω_2 phonons only. But this channel turns out to be noneffective, because the quasi-particles in the vicinity of the gap edge (with the energy $\varepsilon \approx \Delta$) are to recombine with the quasi-particles removed far from the gap edge ($\varepsilon \approx \omega_2 - \Delta$). The concentration of these high-energy quasi-particles is rather low. That is why, contrary to the model used in Ref. 17, the recombination processes are not effective in this case, and the term S^R may be neglected in (12.8). With respect to the interplay between factors S^+ and S^- in (12.8), it may be noted that at $T = 0$ (when only spontaneous emission of phonons in a relaxation channel may take place) outscattering of electrons from the states lower than the level $\varepsilon = \Delta + \omega_1$ is impossible [this causes $S^-(\varepsilon) \equiv 0$ at $\varepsilon < \Delta + \omega_1$). A

unique rule—the Pauli principle—thus regulates the filling of states lower than the "energy horizon" $\varepsilon_0 = \Delta + \omega_1$, yielding (12.12).

12.1.3. Numerical Analysis for Realistic Spectral Function

Approximation (12.14) has relevance for some classes of superconductors, such as alloys of transition metals[20,21] and high-temperature superconductors.[22,23] At the same time, more detailed information may be obtained by numerical analysis of Eq. (12.4) subject to (12.5).

In this case it is useful to start with a model approximation for the spectral function $\alpha^2(\omega_q)F(\omega_q)$, plotted in Fig. 12.1,a, and change the parameters x_1, x_2, y_1, y_2, h_1, h_2, z_1, and z_2. The results of numerical analysis for the case of $T = 0$ are shown in Figs. 12.2–12.8. They are different for longitudinal and transverse phonon fields.

First we will discuss the case of longitudinal phonons. As is seen from these results, the distribution function of quasi-particles may be inverted for certain choices of parameters.

Changing the boundary values x_i and y_i, one finds that the most radical variation in the shape of function n_ε (a decrease) takes place when the value of x_2 exceeds 2Δ (Fig. 12.2); this change is caused by the "switching on" of intermediate energy ($\omega_q \lesssim 2\Delta$) phonons in the kinetic processes. We would like to mention here an

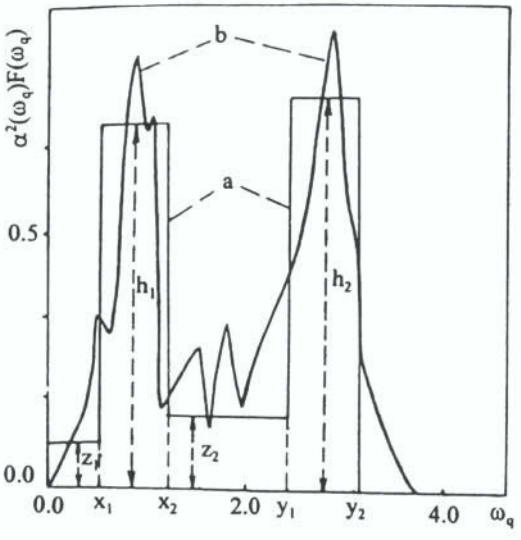

Figure 12.1. a, Model function $\alpha^2(\omega)F(\omega)$ used for numerical calculations; b, experimental curve for 1-2-3 superconductors.[22,23] The axis ω_q is in Δ units.

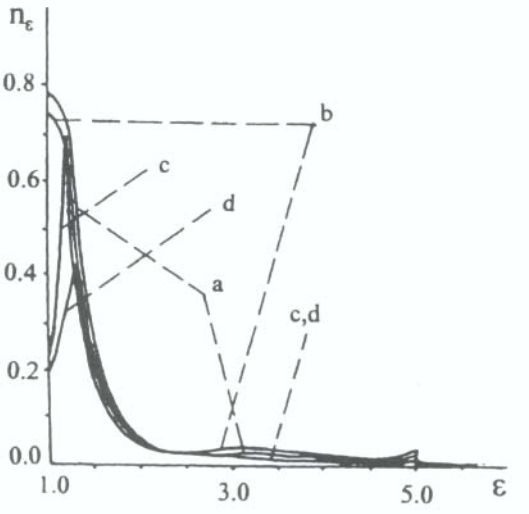

Figure 12.2. Nonequilibrium distribution function of electron excitations n_ε in electromagnetic pumping at frequency ω, coupling parameter $\alpha_0 = 0.005$ [$\alpha_0 = 2D(e/c)^2\ |A_\omega|^2$], and model spectral function $\alpha^2(\omega)F(\omega)$ (see Fig. 12.1a) with the following parameters: a, $x_1 = 0.2$, $x_2 = 1.9$, $y_1 = 3.2$, $y_2 = 4$, $h_1 = h_2 = 1$, $z_1 = z_2 = 0$; b, $x_2 = 1.5$; c, $x_2 = 2.2$; d, $x_2 = 2.3$; other parameters coincide with curve a. All the energy parameters are in Δ units.

interesting feature: shifting of the maximum of n_ε when x_2 exceeds 2Δ (Fig. 12.2,d). The value of n_ε decreases noticeably when the value of z_2 increases (Fig. 12.3).

The change of localization boundaries of high-energy phonons also may strongly influence the formation of function n_ε (Fig. 12.4). When the boundary y_1 is near the critical value 2Δ, the distribution function n_ε is substantially depressed (Fig. 12.4,a), and, in contrast, n_ε strongly increases when the group of high-energy phonons is situated far from 2Δ. With respect to the parameters h_1 and h_2, it may be shown (Fig. 12.5) that the maximum of n_ε increases (being restricted by 1) when the ratio h_1/h_2 increases.

The role of phonons of the lowest energies (described by the parameter z_1) is negligible, as Fig. 12.6 illustrates. It is interesting to note that setting $z_1 = z_2 = h_1 = h_2 (= 1)$, one arrives at (Fig. 12.2,c) the results obtained in Refs. 17 and 18 (for $k = -1$).

Let us consider now the case of a transverse phonon field. For such phonons a very significant sign reversal

$$\left(1 \pm \frac{\Delta^2}{\varepsilon\varepsilon'}\right) \Leftrightarrow \left(1 \mp \frac{\Delta^2}{\varepsilon\varepsilon'}\right) \tag{12.17}$$

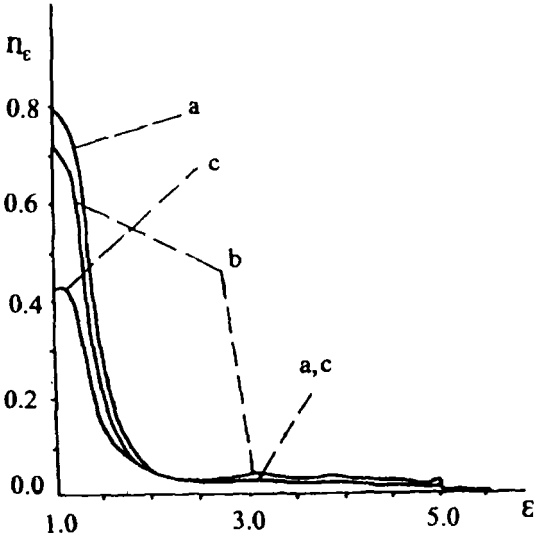

Figure 12.3. The same as in Fig. 12.2 with the following parameters: a, $x_1 = 0.2$, $x_2 = 1.9$, $y_1 = 3.2$, $y_2 = 4$, $h_1 = h_2 = 1$, $z_1 = z_2 = 0$; b, $z_2 = 0.05$; c, $z_2 = 0.1$; other parameters coincide with curve a.

occurs in the coherence factors of the collision integral (12.2). Such an exchange raises the intensity of relaxation processes (S^+ and S^-) and diminishes the intensity of recombination processes (S^R), as may be demonstrated from (12.5). In accordance with (12.6), this must yield an increase in n_ε. Figure 12.7 illustrates such a conclusion. As may be found by a comparison of corresponding curves from Fig. 12.7 and Figs. 12.2-12.6, the function n_ε is indeed greater in the case of transverse phonons than in the case of longitudinal phonons.

In real crystals, both longitudinal and transverse phonon modes are always present. Two limiting curves corresponding to the cases of purely transverse and purely longitudinal phonons are depicted in Fig. 12.8 (taken from Ref. 12). The shape of the function $\alpha^2(\omega_q)F(\omega_q)$ was chosen to correspond to the data obtained for high-temperature superconductors (in particular, $YBa_2Cu_3O_{6.9}$).*

*These superconductors as well as other representatives of high-T_c families are highly anisotropic and this raises the probability of transverse phonon field participation in electron–phonon interactions. Dealing with this class of superconductors, one should bear in mind that there may be additional interactions (e.g., paramagnon exchange), which can mediate the process of energy relaxation of quasi-particles and change the whole picture.[24] Undoubtedly for more precise predictions, the mechanism of superconductivity itself must become better known.

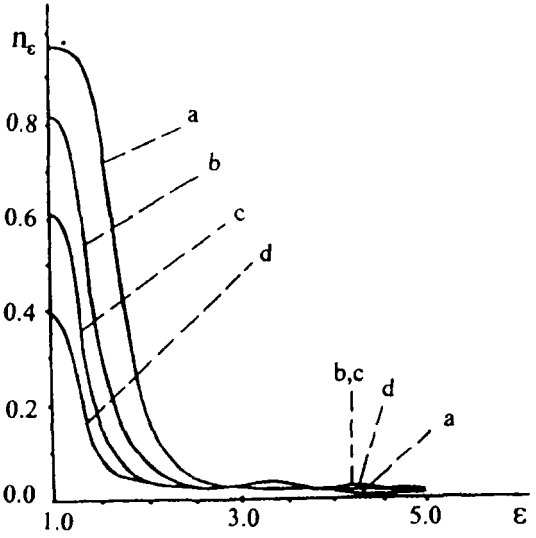

Figure 12.4. The same as in Figs. 12.2 and 12.3 with the following parameters: a, $x_1 = 0.2$, $x_2 = 1.9$, $y_1 = 3.8$, $y_2 = 4$, $h_1 = h_2 = 1$, $z_1 = z_2 = 0$; b, $y_1 = 3.4$; c, $y_1 = 3$; d, $y_1 = 2.6$; other parameters coincide with curve a.

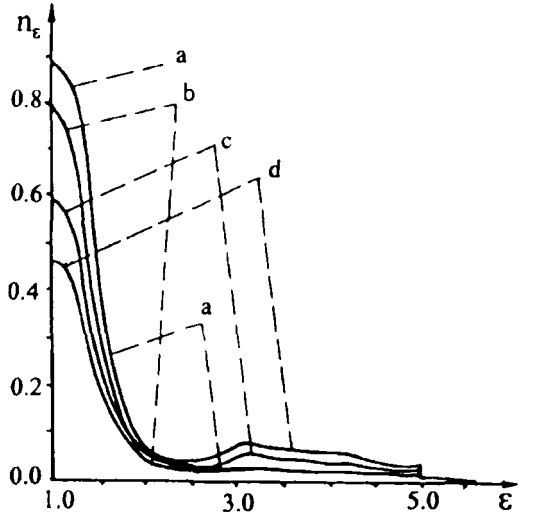

Figure 12.5. The same as Figs. 12.2 to 12.4 with the following parameters: a, $x_1 = 0.2$, $x_2 = 1.9$, $y_1 = 3.2$, $y_2 = 4$, $h_1/h_2 = 2$, $z_1 = z_2 = 0$; b, $h_1/h_2 = 1$; c, $h_1/h_2 = 0.5$; d, $h_1/h_2 = 0.3$; other parameters coincide with curve a.

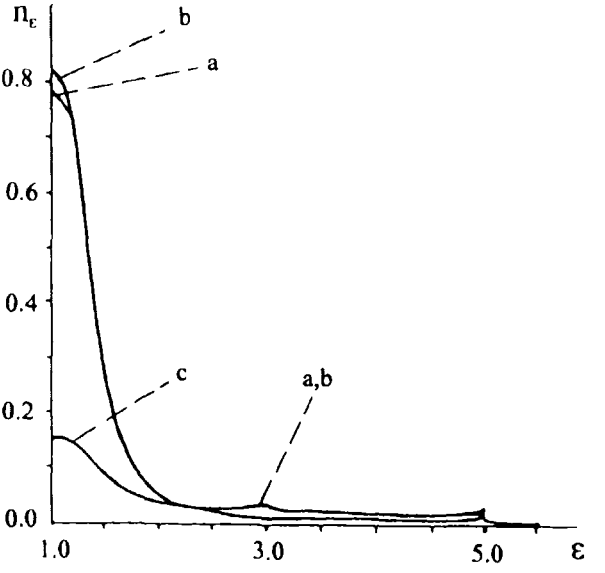

Figure 12.6. The same as Figs. 12.2 to 12.5 with the following parameters: a, $x_1 = 0.2$, $x_2 = 1.9$, $y_1 = 3.2$, $y_2 = 4$, $h_1 = h_2 = 1$, $z_1 = z_2 = 0$; b, $z_1 = 1$; distribution function n_ε calculated with parameters taken from Ref. 25.

12.2. "NARROW" PUMPING

In "narrow" pumping, the pumping source may be regarded as having a resonant action on the system of electrons. Thus the term $Q(\varepsilon)$ in (12.4) can no longer be omitted. Taking this into account, the functional fraction (12.6) can be presented in the form

$$n_\varepsilon = \frac{Q(\varepsilon)}{S^R(\varepsilon)}. \tag{12.18}$$

On pumping by a electromagnetic field with the frequency

$$(\omega_0 - 2\Delta) << \Delta, \tag{12.19}$$

the quasi-particles will be created mainly in the narrow region $\bar{\varepsilon} << \Delta$ above the gap.

12.2.1. Analytic Solution for Resonant Pumping Case

We will start our discussion with the case of relatively weak fields (cf. Chap. 5):

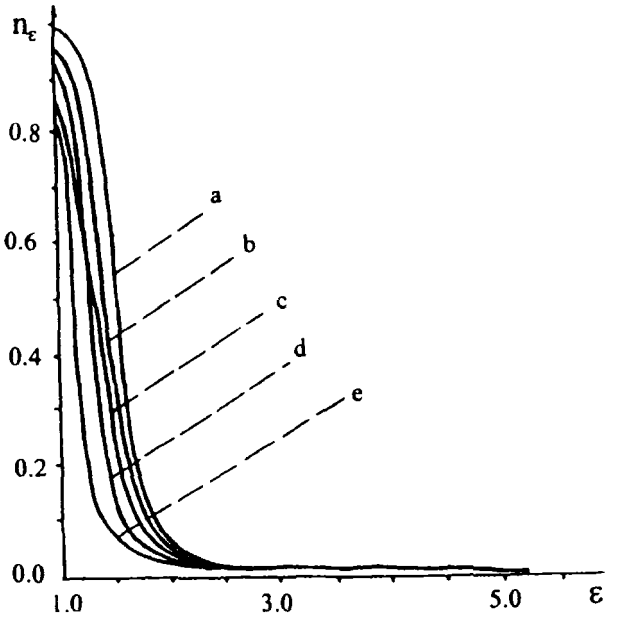

Figure 12.7. The same as Figs. 12.2 to 12.6 but for transverse phonons with the following parameters: a, $x_1 = 0.2$, $x_2 = 1.9$, $y_1 = 3.2$, $y_2 = 4$, $h_1 = h_2 = 1$, $z_1 = z_2 = 0$; b, $z_2 = 0.1$; c, $y_1 = 2.6$; d, $x_2 = 2.3$; in curves b–d, other parameters coincide with curve a; e, distribution function n_ε, calculated with parameters taken from Ref. 25.

$$\alpha << \gamma. \tag{12.20}$$

Dropping the components that are proportional to U-factors in the field term of (5.21), Aronov and Spivak[11,26] found an analytic solution for n_ε(these factors are responsible for the redistribution in the energy space of excess quasi-particles, created by the electromagnetic field). Using the relaxation-time approximation for the collision integral in (12.3), one can ascertain that under these conditions the electron excitation's distribution function has the form[11,26]:

$$n_z = \sqrt{\frac{\Gamma}{\pi}} \frac{\sqrt{z}\theta(z)\theta(1-z)}{\sqrt{z}\sqrt{1-z} + \sqrt{\frac{\Gamma}{\pi}}\,(\sqrt{z} + \sqrt{1-z})}, \tag{12.21}$$

where

$$z = \frac{\varepsilon - \Delta}{\delta}, \qquad \delta = \omega_0 - 2\Delta, \qquad \Gamma = \frac{\alpha}{\gamma}. \tag{12.22}$$

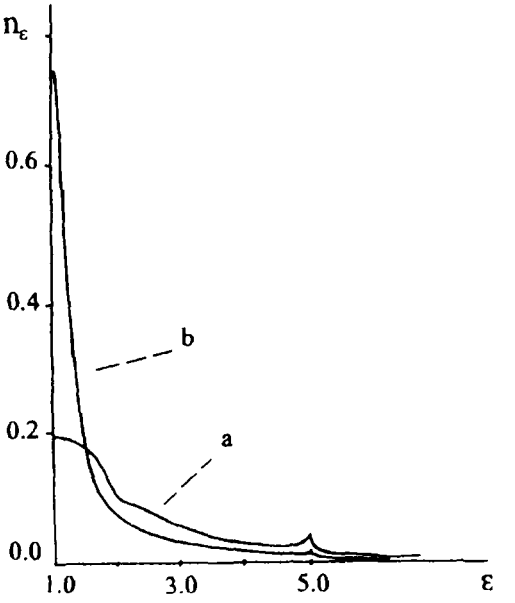

Figure 12.8. Nonequilibrium distribution function n_ε in electromagnetic pumping (with frequency $\omega = 6$, coupling parameter $\alpha_0 = 0.005$), calculated with the experimental curve plotted in Fig. 12.1,b assuming the phonon field is a, longitudinal and b, transverse. All the energy parameters are in Δ units. (From Gulian et al.[12])

The function n_ε at various values of α and ω_0 is plotted in Fig. 12.9.* The result (12.21) indicates that the distribution function of the excess quasi-particles in a superconductor pumped by an external electromagnetic field not only can exceed the value 1/2 but can even attain the maximum value of $n_\varepsilon = 1$. This is connected with the singularity in the superconductor's density of states. Owing to this, the value $n_\varepsilon = 1$ may be attained at $\omega_0 > 2\Delta$ even for exceedingly weak pumping, i.e., even when $\alpha \to 0$ (as is clear from 12.21). This result may be formulated in the following manner: at $T = 0$, the ground state of the superconductor (i.e., the state without electron quasi-particles) is unstable with respect to the transition to the nonequilibrium steady state, in which the value $n_\varepsilon = 1$ is attained, if a weak external electromagnetic field with a frequency in resonance with the threshold frequency is applied. We will consider the possible implications of this result in Sect. 12.3.

*Here we ignore the insignificant "tail" of the excess quasi-particle distribution function at $\varepsilon >> \Delta$ (cf. Refs. 11 and 26).

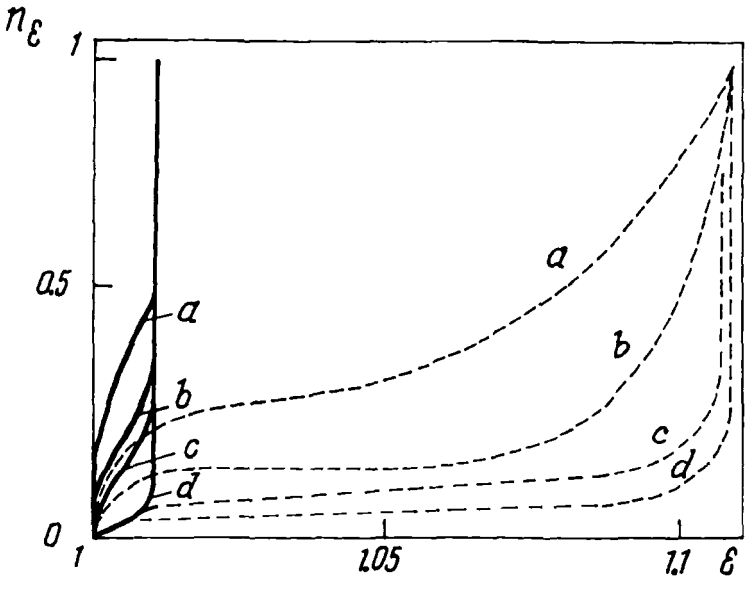

Figure 12.9. Distribution functions of nonequilibrium quasi-particles at frequencies $\omega = 2.01$ (solid lines) and $\omega = 2.1$ (dashed lines) (ω and ε are in Δ units); $\Gamma = \alpha/\gamma$. a, $\Gamma = 1$; b, $\Gamma = 0.1$; c, $\Gamma = 0.01$; and d, $\Gamma = 0.001$.

12.2.2. *Tunnel Injection of Electrons*

Even stronger deviation from equilibrium is possible by tunnel injection of quasi-particles at voltages $V \approx \Delta + \Delta'$. At such voltages one can neglect the terms Q_1 and Q_2 in (10.4): their influence average out. Because of that, the general equations (12.3) and (12.5) may be significantly simplified. We will make these simplifications assuming $n_\varepsilon = n_{-\varepsilon}$. To make a more thorough analysis, we will add to (12.4) the electron-electron collision term (4.36) in the form (below $n_\varepsilon = n_{-\varepsilon}$ is assumed):

$$J^{(e-e)}(\varepsilon) = \frac{1}{2\varepsilon_F} \int_\Delta^\infty \int_\Delta^\infty \int_\Delta^\infty \frac{d\varepsilon_1 d\varepsilon_2 d\varepsilon_3}{\sqrt{\varepsilon^2 - \Delta^2}\sqrt{\varepsilon_1^2 - \Delta^2}\sqrt{\varepsilon_2^2 - \Delta^2}\sqrt{\varepsilon_3^2 - \Delta^2}}$$

$$\times \{M_1 [(1-n)n_1 n_2 n_3 - n(1-n_1)(1-n_2)(1-n_3)]\, \delta(\varepsilon - \varepsilon_1 - \varepsilon_2 - \varepsilon_3)$$

$$+ 3M_2 [n_1 n_2 (1-n)(1-n_3) - n n_3 (1-n_1)(1-n_2)]\, \delta(\varepsilon + \varepsilon_3 - \varepsilon_1 - \varepsilon_2)$$

$$+ 3M_3 [n_1 (1-n)(1-n_2)(1-n_3) - (1-n_1) n n_2 n_3]\, \delta(\varepsilon + \varepsilon_2 + \varepsilon_3 - \varepsilon_1)\},$$

$$M_1 = a(\varepsilon_1\varepsilon_2\varepsilon_3\varepsilon - \Delta^4) - \frac{1}{3}b(-\varepsilon^2 + \varepsilon_1\varepsilon_2 + \varepsilon_1\varepsilon_3 + \varepsilon_2\varepsilon_3)\Delta^2,$$

$$M_2 = -M_1(-\varepsilon_3),\ M_3 = M_1(-\varepsilon_2, -\varepsilon_3). \tag{12.23}$$

The quantity Δ entering expressions (12.18) to (12.23) should be determined from the self-consistency equation (12.5). The self-consistent system of Eqs. (12.18) to (12.23) is highly nonlinear. However, the assumption of a "narrow" energy distribution of the electron excitations makes it possible to effectively find the solution, even taking into account (12.23).

12.2.3. Simplifications for "Narrow" Distributions

Introducing the variables $\delta = \bar{\varepsilon}_{max} - \Delta$ and $z = (\varepsilon - \Delta)/\delta$, $\delta > 0$, and denoting

$$\bar{n} = \int_{\Delta}^{\infty} \frac{n_\varepsilon d\varepsilon}{\sqrt{\varepsilon^2 - \Delta^2}} = \sqrt{\frac{\delta}{2\Delta}} \int_0^1 \frac{n_z dz}{\sqrt{z}}, \tag{12.24}$$

we present Eq. (12.24) in the form

$$\ln\left(\frac{\Delta}{\Delta_0}\right) = -2\bar{n}, \tag{12.25}$$

where Δ_0 is the gap at $T = 0$ in the absence of external perturbation. The "narrow" distribution results [as is seen from (12.25)] in a small value of $\bar{n}$ and hence

$$\Delta \cong \Delta_0(1 - 2\bar{n}). \tag{12.26}$$

Consider now the collision integrals. If the function $n_\varepsilon \sim 1$ and is still concentrated in the region immediately above the gap, the relaxation terms in (12.23) are small in comparison with the recombination terms, and $J^{(e-ph)}$ may be simplified:

$$J^{(e-ph)}(\varepsilon) \cong -\frac{4\pi\lambda\Delta^4}{(up_F)^2}\bar{n}\frac{n_\varepsilon}{\sqrt{\varepsilon^2 - \Delta^2}}. \tag{12.27}$$

The electron–electron collisions may cause a significant change in the distribution function if they are efficient. In our case, when the quasi-particles are concentrated in a narrow layer near the Fermi surface and $n_\varepsilon \approx 1$ in this layer, we must first account for the "collision pairing" processes [the second term in the M_3 component of the collision integral $J^{(e-e)}(\varepsilon)$], when three colliding electron excitations with energies $\varepsilon \geq \Delta$ create a bound state (a Cooper pair) and a free quasi-particle with the energy $\varepsilon \geq 3\Delta$. The opposite "collision breeding" processes in this case are not efficient and hence $J^{(e-e)}(\varepsilon)$ may be reduced to the form

$$J^{(e-e)}(\varepsilon) \equiv -\frac{3}{2\sqrt{2}}(a+b)\frac{\Delta^3}{\varepsilon_F}\bar{n}^2\frac{n_\varepsilon}{\sqrt{\varepsilon^2-\Delta^2}}. \tag{12.28}$$

Comparing (12.27) and (12.28), one may ascertain that the electron-electron collisions are not important if the following parameter:

$$c = c_0\frac{\bar{n}\Delta_0}{\Delta}, \qquad c_0 = \frac{3(a+b)}{8\sqrt{2}\pi\lambda}\frac{\omega_D^2}{\varepsilon_F\Delta_0} \tag{12.29}$$

is small (we set $\omega_D \approx up_F$). For metals with relatively large Debye frequencies (such as Al, see Table 10.1 in Sect. 10.2), the value of c_0 might be insufficiently small, so it becomes necessary to account for (12.28). Unfortunately, the factors a and b in (12.29) are not yet well established experimentally (as mentioned in Ref. 27), so in the next section we consider the values $c_0 = 0;1;10$ to cover the limiting cases.

12.2.4. Analytic Solution for Symmetric Junctions

In the case of an SIS-junction, the quasi-particle source (10.4) has the form (ignoring imbalance):

$$Q(\varepsilon) = \nu[U_-(n_{\varepsilon-V} - n_\varepsilon) + U_+(n_\varepsilon - n_{\varepsilon+V}) - U_0(1 - n_\varepsilon - n_{V-\varepsilon})], \tag{12.30}$$

$$U_\pm = \frac{\varepsilon(\varepsilon \pm V)}{\sqrt{\varepsilon^2-\Delta^2}}\frac{\theta(\varepsilon \pm V - \Delta)}{\sqrt{(\varepsilon \pm V)^2-\Delta^2}}, \; U_0 = \frac{\varepsilon(V-\varepsilon)}{\sqrt{\varepsilon^2-\Delta^2}}\frac{\theta(V-\varepsilon-\Delta)}{\sqrt{(V-\varepsilon)^2-\Delta^2}}. \tag{12.31}$$

The analysis of kinetic equations proceeds in the same manner as for the case of a UHF field. The nonequilibrium electron distribution function is given by the expression

$$n_z = \frac{A\sqrt{z}\theta(1-z)}{A(\sqrt{z}+\sqrt{1-z})+\sqrt{z}\sqrt{1-z}}, \quad z \geq 0 \tag{12.32}$$

$$A = \begin{cases} \Gamma\Delta/2\delta, & \Gamma >> \delta/\Delta \\ \sqrt{\Gamma\Delta/(\pi\delta)}, & \Gamma << \delta/\Delta;\ \delta = \nu - 2\Delta << \Delta. \end{cases} \tag{12.33}$$

Even though we assumed $\Gamma \sim \nu/\gamma$ to be small, the narrow injection source may drive the distribution function to saturation

$$n_z = \frac{\sqrt{z}\theta(1-z)}{\sqrt{z}+\sqrt{1-z}}, \quad z \geq 0, \tag{12.34}$$

if $\Gamma >> \delta/\Delta$. We will consider the implications of (12.34) in Sect. 12.3.

12.2.5. Injection from Bulk Sample to a Thin Film

Let us consider now the case of SIS′ junctions. The latter case was first examined by Genkin and Protogenov,[8] who found that the function n_ε may be close to unity for ε lying above the gap. Because the analysis in Ref. 8 was not completely exhaustive,* we provide here a solution of Eqs. (12.18) to (12.29) in a more accurate approximation. As follows from the results of Chap. 10, the initial equations for the SIS′ junction are analogous to the case of a symmetric SIS junction; the only difference is that the distribution function entering Eq. (12.30) for the source $Q(\varepsilon)$ with shifted arguments, relates to a bulk superconductor, while the factors $U_\pm$ and U_0 are

$$U_\pm = \frac{\varepsilon(\varepsilon \pm V)\ \ \theta(\varepsilon \pm V - \Delta')}{\sqrt{\varepsilon^2 - \Delta^2}\sqrt{(\varepsilon \pm V)^2 - \Delta'^2}}, \qquad U_0 = \frac{\varepsilon(V-\varepsilon)\ \ \theta(V - \varepsilon - \Delta')}{\sqrt{\varepsilon^2 - \Delta^2}\sqrt{(V-\varepsilon)^2 - \Delta'^2}} \tag{12.35}$$

(Δ' is the gap of the bulk injector).

If the thickness of the injector is much greater than the thickness of the film, which in turn does not exceed the diffusion length for the quasi-particles, then the electron system of the bulk superconductor may be considered to be unperturbed, even if the thin film is driven significantly out of equilibrium. Assuming that the resulting highly nonequilibrium ($n_\varepsilon \simeq 1$) distribution of quasi-particles at $T = 0$ is "narrow," the solution of Eqs. (12.3) to (12.5) subject to (12.25), (12.27), and (12.28) can be represented as

$$n_z = \frac{B\theta(1-z)}{B + \sqrt{1-z}}, \tag{12.36}$$

where

$$B = \frac{A}{\bar{n}(1+c)}, \quad A = \sqrt{\frac{\Delta'}{2\delta}}\,\Gamma, \quad \Gamma = \frac{\Gamma_0}{\Delta^3},$$

$$\Gamma_0 = \frac{\nu\omega_D^2}{4\pi\lambda}, \quad \Delta = \Delta_0 \exp(-2\bar{n}), \tag{12.37}$$

while the parameter $\bar{n}$ should be determined from the equation

$$\bar{n} = \sqrt{\frac{\delta}{2\Delta}}\, A \int_0^1 \frac{dz}{\sqrt{z}\,[A + \sqrt{1-z} - (1+c)\bar{n}]}. \tag{12.38}$$

*Unfortunately, in Ref. 8 no detailed analysis was given of the kinetic equations taking into account the self-consistency equation, and the related ambiguity of the solutions of the kinetic equations was not revealed. Such an approach is insufficient for our purposes.

We recall here that the quantities Δ, δ, c, and A in (12.37) depend on $\bar{n}$ and Eq. (12.39) determines the values B for fixed injection parameters. It is expedient to write Eq. (12.39) in the form

$$\bar{n}\left(\frac{\Delta}{2\delta}\right)^{1/2} = B\frac{\pi}{2} - \frac{B^2}{\sqrt{1-B^2}} \begin{cases} \ln\dfrac{1+B+\sqrt{1+B^2}}{1+B-\sqrt{1-B^2}}, & B<1 \\ 2\arctan\dfrac{B-1}{B+1}, & B>1 \end{cases} . \tag{12.39}$$

Equation (12.39) allows further analytic investigation in several limiting cases [for simplicity in (12.37) we put $c = 0$ for the time being].

1. Assume the external parameters V and Γ_0 are such that the self-consistent value of $\bar{n}$ leads to $B << 1$. Then Eq. (12.39) subject to (12.37) reduces to the form

$$\bar{n}\exp(-7\bar{n}) = \frac{\pi}{2}\sqrt{\frac{\Delta'}{\Delta_0}}\frac{\Gamma_0}{\Delta_0^3}. \tag{12.40}$$

Note that the roots of Eq. (12.40) do not depend on the parameter δ, though the range of applicability of Eq. (12.40) does, because $B << 1$ and the steady-state solution should satisfy the inequality

$$\Gamma_0 << \sqrt{\frac{2\delta}{\Delta'}}\,\Delta^3\bar{n}. \tag{12.41}$$

The left-hand side of Eq. (12.40) has a maximum at $\bar{n} = 2/7$. This value of $\bar{n}$ is a root, if

$$\Gamma_0 = \Gamma_0^* = \left(\frac{2}{7e}\right)^2 \frac{\Delta_0^3}{\pi}\sqrt{\frac{\Delta_0}{\Delta'}} \tag{12.42}$$

(here e is the base of the natural logarithm). For larger Γ_0 there is no solution with small B, while for smaller Γ_0 there are two roots. The smaller root behaves as

$$\bar{n} \approx \left[\frac{\pi}{2}\sqrt{\frac{\Delta'}{\Delta_0}}\frac{\Gamma_0}{\Delta_0^3}\right]^{1/2}, \tag{12.43}$$

while the second one increases rather rapidly, finally leaving the range of applicability of our approach (recall that the value of $\bar{n}$ was assumed to be small). In the vicinity of the characteristic value $\Gamma_0 \approx \Gamma_0^*$, one has the following condition for the parameter δ:

$$\left(\frac{\delta}{\Delta_0}\right)^{1/2} >> 10^{-2}. \tag{12.44}$$

Thus, for $\Gamma_0 \approx \Gamma_0^*$, the self-consistent kinetic equations always have two solutions with $B \ll 1$, since condition (12.44) can only be satisfied for a δ_0 that is not too small (δ_0 is the initial voltage displacement above the threshold level, $\delta_0 = V - \Delta' - \Delta_0$; for small $\bar{n}$ we have $\delta - \delta_0 \approx 2\bar{n}$).

2. In the opposite limiting case of $B \gg 1$, the right-hand side of Eq. (12.39) is approximately unity and hence (12.39) has a small root only for small values of δ. Using the relation (12.26) we obtain from (12.39) the following expression for the smallest root

$$\bar{n} \approx 2\left[1 - \sqrt{1 + \frac{1}{2}\frac{\delta_0}{\Delta_0}}\right], \tag{12.45}$$

which becomes meaningless when $\delta_0 > 0$. Thus the self-consistent system of equations with negative initial displacement ($\delta_0 < 0$) has a solution with

$$\bar{n} \approx -\frac{1}{2}\delta_0; \tag{12.46}$$

here $B \gg 1$ if $|\delta_0|$ is sufficiently small.

3. Of the greatest interest is the intermediate case $B \sim 1$, since for such values of B phonon instability (see Sect. 12.3) can be achieved. In this case the right-hand side of Eq. (12.26) is equal to $(\pi/2 - 1)$ and for the small root we again obtain the value (12.46). Thus the roots of interest in cases (2) and (3) coincide; they differ only by the values B, which are determined by the external parameters δ_0 and Γ_0.

A numerical analysis of the transcendental equation (12.39) confirms the reasonings outlined above. Thus, for the parameters $\Gamma_0 = 10^{-3}$, $\delta_0 = 0.02$, $c_0 = 0$, $\Delta' = 2$ (in Δ_0 units), three roots of Eq. (12.38) exist: $\bar{n}_1 = 0.01$ ($B \approx 14$), $\bar{n}_2 \approx 0.05$ ($B \approx 0.1$); and $\bar{n}_3 \approx 0.95$ ($B \approx 0.3$). When $c_0 = 0$ and $\Gamma_0 > \Gamma_0^*$ (for example, $\Gamma_0 = 0.05$), we have (with $\delta_0 = -0.3$, $\Delta' = 0.5$) only a single solution $\bar{n}_1 \approx 0.2$ (here $B \approx 2.9$; $\delta \approx 0.02$; $\Delta \approx 0.67$). With increasing c_0, the value of B decreases ($B \approx 1.9$ when $c_0 = 1$), and for sufficiently large c_0 (for example, $c_0 = 10$), there are no roots at all. Thus the behavior of the tunnel SIS′ junction is very sensitive to the initial injection parameters and to those of the junction itself.

In addition to the solutions ($\bar{n}_{1-3}$) obtained at $\delta_0 < 0$, there also exists a solution $\bar{n}_0 = 0$, which corresponds to the situation with no excess quasi-particles, as well as the solution that corresponds to the normal state ($\Delta = 0$). Setting aside the solutions with large values of $\bar{n}$,* we conclude that in general there are three solutions for $\bar{n}$, the intermediate one corresponding to $B \sim 1$. Keeping in mind the discussion in Chap.

*To consider large values of $\bar{n}$, we should go beyond the approximations used earlier. It is important to note that slates with a larger $\bar{n}$ are separated from states with a smaller $\bar{n}$ by a high energy barrier, and transitions between them are very improbable.[28]

11, one may expect that the latter solution is unstable, while the current-voltage characteristic of the SIS′junction is S-shaped, and the spatially inhomogeneous state is realized in the superconducting film. However, we will not scrutinize this possibility since (as was mentioned earlier) when $\Gamma_0 > \Gamma_0^*$ and $\delta < 0$ (see in particular the case when $\Gamma_0 = 0.05$) there exists only one solution. This solution corresponds to a superconducting state with excess electron excitations, so that the possibility of S-shaping disappears.

The vanishing of the S-shape as Γ_0 increases (i.e., as the nonequilibrium level in the tunnel junction grows) suggests an analogy between the nonlinear behavior

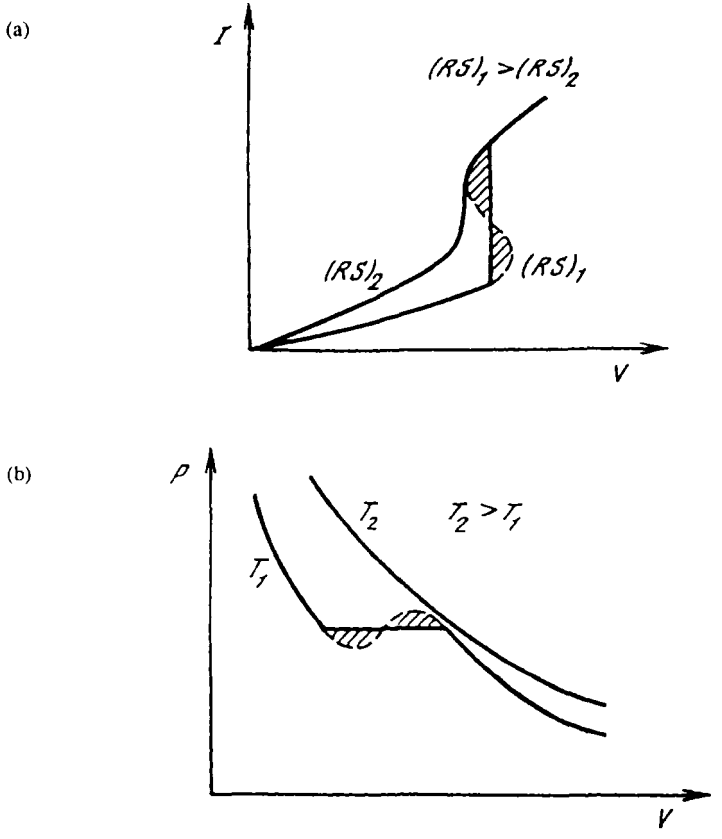

Figure 12.10. (a) Current-voltage characteristic of SIS′ junction and (b) an isotherm of the van der Waals gas. The rise of the nonequilibrium level in the film *S* is physically equivalent to the increase in temperature of a nonideal gas. This leads to a single-valued dependence of $I(V)$. This makes phase stratification in a nonequilibrium superconductor impossible.

of a nonequilibrium superconductor and the behavior of nonideal van der Waals gases. Namely, the increase in the junction's nonequilibrium level is analogous to the increase in the temperature of a nonideal gas, which causes the van der Waals isotherm to acquire a monotonic shape (Fig. 12.10).

12.3. PHONON INSTABILITY

We have accumulated enough results to discuss the possibility of phonon instability in nonequilibrium superconductors. Phonon instability is characterized by the reversal of the sign of the sound absorption coefficient of the nonequilibrium electron system. In the case of positive feedback, such an instability may cause a generation regime, in which phonon emission from the nonequilibrium superconducting film is coherent and monochromatic. More detailed formulation of this problem is given in the following sections.

12.3.1. Decoupling of Electron–Phonon Kinetics

To study the dynamics of the phonon system of a nonequilibrium superconductor, we must, in general, go beyond the phonon heat-bath model. In doing so we should consider a coupled system of kinetic equations of the general form

$$\dot{n}_\varepsilon = Q(n_\varepsilon) + J^{(\mathrm{e-ph})}(n_\varepsilon, N_{\omega_q}), \tag{12.47}$$

$$\dot{N}_{\omega_q} = I^{(\mathrm{ph-e})}(n_\varepsilon, N_{\omega_q}) + L(N_{\omega_q}), \tag{12.48}$$

where Q is the external nonequilibrium source, L is the operator describing the phonon's interaction with the external heat-bath, and I is the phonon–electron collision operator. [We disregard within (12.47) and (12.48) the pair condensate dynamics.] In the presence of feedback, some part of the nonequilibrium phonons emitted by the electron system is reabsorbed by electrons and exerts a reverse influence on the electron system. If the absorption coefficient for any phonon mode is negative, the number of such phonons in the system will grow exponentially, leading to instability, and finally the dynamic state will emerge.

A self-consistent solution for dynamic equations (12.47) and (12.48) is an independent problem, which is not yet resolved (although there have been preliminary attempts to address it: see, e.g., Ref. 29). However, we do not need the full solution because we will investigate only the possibility of getting to the threshold regime of instability. In this case one may consider the following kinetic scheme:

$$\dot{n}_\varepsilon = Q(n_\varepsilon) + J^{(\mathrm{e-ph})}(n_\varepsilon, N^{(i)}_{\omega_q}), \tag{12.49}$$

$$\dot{N}^{(i)}_{\omega_q} = I^{(\mathrm{ph-e})}(n_\varepsilon, N^{(i)}_{\omega_q}) + L(N^{(i)}_{\omega_q}), \tag{12.50}$$

$$\dot{N}^{(e)}_{\omega_q} = I^{(\mathrm{ph-e})}(n_\varepsilon, N^{(e)}_{\omega_q}). \tag{12.51}$$

Here $N^{(i)}_{\omega_q}$ is the superconductor's internal phonon field and $N^{(e)}_{\omega_q}$ corresponds to the external phonon flux whose linear response will be studied. The operators $I^{(\mathrm{ph-e})}$ in (12.50) and (12.51) are of identical structure. In the subthreshold regime we can use the model of the phonon heat-bath (it is applicable at least in the absence of phonon instability). In this case a so-called dissipative steady state establishes: $\dot{n}_\varepsilon = 0$, $\dot{N}^{(i)}_{\omega_q} = 0$, and

$$I^{(\mathrm{ph-e})}(n_\varepsilon, N^{(i)}_{\omega_q}) = -L(N^{(i)}_{\omega_q}). \tag{12.52}$$

Hence, Eqs. (12.49) to (12.51) become ungrouped; the function $N^{(i)}_{\omega_q}$ in (12.49) is equal to its equilibrium value $N^{(0)}_{\omega_q}$, Eq. (12.50) is an identity, while (12.51) will be used to calculate the linear response (i.e., to analyze phonon instability).

We will assume that under the action of external factors the electron system of a superconductor (which is coupled to an external heat-bath) deviates from equilibrium and a dissipative steady state is achieved in which the nonequilibrium electron excitations are characterized by the distribution function n_ε (henceforth it will be assumed that n_ε is an even function and is also spatially homogeneous and isotropic, like the order parameter Δ).

Consider the influence of the external phonon flux on the electron system; this flux is characterized by the occupation numbers N_{ω_q} (we assume $N_{\omega_q} \gg 1$). In nonequilibrium superconductors (as clarified in Sect. 6.2), the phonons may be absorbed (or emitted) both in pair-breaking (or, correspondingly, recombination) and in relaxation processes. If the deviation from equilibrium is significantly large, the recombination processes in superconductors are much more rapid than the relaxation processes, so that in this case it is necessary to consider the stability relative to the recombinational emission of phonons.

12.3.2. Phonon Absorption and Inverse Population

The number of phonons absorbed per unit of time in the volume V_0 at frequency ω_q in the interval $d\omega_q$ is given by the expression (cf. Sect. 6.2):

$$d\dot{N}_{\omega_q} = \rho_0(\omega_q) I(\omega_q) d\omega_q, \tag{12.53}$$

where $I(\omega_q)$ is the electron–phonon collision operator (4.128) and $\rho_0(\omega_q) = V_0\omega_q^2/(2\pi^2 u^3)$. In the case of interest it acquires the form:

$$I(\omega_q) = \int_{\Delta}^{\infty}\int_{\Delta}^{\infty} d\varepsilon_1 d\varepsilon_2 L(\varepsilon_1, \varepsilon_{2)}$$

$$\times \left\{ [(1 - n_{\varepsilon_1})(1 - n_{\varepsilon_2}) - n_{\varepsilon_1} n_{\varepsilon_2}] \left(1 + \frac{\Delta^2}{\varepsilon_1 \varepsilon_2} \right) \delta(\varepsilon_1 + \varepsilon_2 - \omega_q) \right.$$

$$\left. - 2[n_{\varepsilon_1}(1 - n_{\varepsilon_2}) - (1 - n_{\varepsilon_1}) n_{\varepsilon_2}] \left(1 - \frac{\Delta^2}{\varepsilon_1 \varepsilon_2} \right) \delta(\varepsilon_2 - \varepsilon_1 + \omega_q) \right\},$$

$$L(\varepsilon_1, \varepsilon_2) = N_{\omega_q} \frac{\pi\lambda}{2} \frac{\omega_D}{\varepsilon_F} \frac{\varepsilon_1 \theta(\varepsilon_1^2 - \Delta^2)}{\sqrt{\varepsilon_1^2 - \Delta^2}} \frac{\varepsilon_2 \theta(\varepsilon_2^2 - \Delta^2)}{\sqrt{\varepsilon_2^2 - \Delta^2}} \tag{12.54}$$

(recall that for $N_{\omega_q} >> 1$ the external phonon field may be assumed to be classical). The recombination part of the collision integral (12.54) may be written as

$$I(\omega_q)^{(\mathrm{rec})} = \int_{\Delta}^{\omega_q - \Delta} (\varepsilon, \omega_q - \varepsilon) \left(1 + \frac{\Delta^2}{\varepsilon(\omega_q - \varepsilon)} \right) (1 - 2n_\varepsilon)\, d\varepsilon, \tag{12.55}$$

while the relaxation part may be written as

$$I(\omega_q)^{(\mathrm{rel})} = 2 \int_{\Delta}^{\infty} L(\varepsilon\varepsilon + \omega_q) \left(1 - \frac{\Delta^2}{\varepsilon(\omega_q + \varepsilon)} \right) (n_\varepsilon - n_{\varepsilon + \omega_q})\, d\varepsilon. \tag{12.56}$$

As follows from expressions (12.55) and (12.56), phonon instability $[I(\omega_q) < 0]$ due to recombination processes (at frequencies $\omega_q > 2\Delta$) may exist only when the condition (12.1) is satisfied. Note that the distribution n_ε in superconductors is not necessarily a monotonic function. Hence the mode $\omega_q = 2\Delta$ could be not the most unstable and, moreover, the instability condition $n_\Delta > 1/2$ (mentioned in Ref. 9) in general is not the necessary condition. The necessary one is only the weaker condition (12.1).[10]

12.3.3. *Phonon Field Amplification in "Narrow" Electron Distributions*

Assuming the quasi-particle distribution is "narrow," we can simplify expressions (12.55) and (12.56) and present the "sufficient" condition of instability at frequencies $\omega_q \geq 2\Delta$ in the form

$$I(\omega_q) = \frac{\pi\omega_D}{2\varepsilon_F} N_{\omega_q} \Delta \left\{ \int_{\Delta}^{\omega_q - \Delta} \frac{(1 - 2n_\varepsilon)\, d\varepsilon}{\sqrt{\varepsilon - \Delta}\sqrt{\omega_q - \varepsilon - \Delta}} + \frac{1}{\sqrt{\Delta}} \int_{\Delta}^{\bar{\varepsilon}_{\max}} \frac{n_\varepsilon\, d\varepsilon}{\sqrt{\varepsilon - \Delta}} \right\} < 0. \tag{12.57}$$

An analysis of expression (12.57) shows that this condition may be satisfied if the deviation from equilibrium is sufficiently large: $n_{\bar{\varepsilon}} \sim 1, \bar{\varepsilon} < \bar{\varepsilon}_{max}$. Indeed, in this case for frequencies $\omega_q \approx \varepsilon_{max} + 2\Delta$, the first integral in the curly braces is equal to $-\pi$, and the second integral, which does not exceed the value $2\sqrt{(\bar{\varepsilon}_{max}/\Delta) - 1}$, is small, because the electron distribution is "narrow." Thus, instead of absorption of the acoustic wave we have an amplification in this case. The equality sign in the condition

$$I(\omega_q) \leq 0 \tag{12.58}$$

for some value of ω_q determines (ignoring all losses) the threshold of phonon instability (at the given frequency ω_q).

In view of (12.58), the spectral dependence of the absorption coefficient $I(\omega_q)$ is of primary interest. The dependence $I(\omega_q)$ may be obtained for a "narrow" source of electromagnetic pumping by substituting expression (12.21) into (12.57). The resulting integral may be easily evaluated numerically. The corresponding curves are shown in Fig. 12.11. An analysis of these results shows that the absorption coefficient has a sharp minimum at $\omega_q = \omega_0$. With the growth of the field's amplitude, the minimal value of $I(\omega_q)$ diminishes but does not completely vanish, even in the case of very intense fields ($\alpha > \gamma$) where solution (12.21), strictly speaking, is no longer valid.

The absorption coefficient has a dip on the order of the coefficient itself, indicating that at electromagnetic pumping it is possible to at least come close to

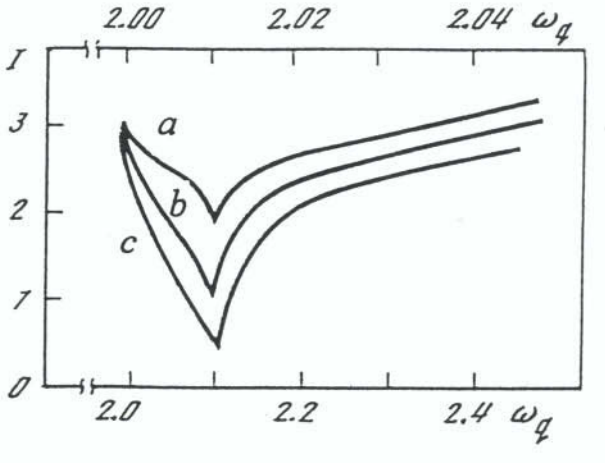

Figure 12.11. Spectral dependence of the phonon absorption coefficient (in relative units) at frequencies $\omega_0 = 2.1$ and $\omega_0 = 2.01$ of the external field (ω_0 are in Δ units) for: a, $\Gamma = 0.1$; b, $\Gamma = 1$; and c, $\Gamma = 10$.

the threshold of coherent phonon generation. Nevertheless, condition (12.58) cannot be satisfied, at least for fields with sufficiently low amplitude.

The case of a "narrow" high-intensity source requires special analysis.[30] However, we will not go in that direction since the tunnel injection of quasi-particles provides a higher level of excursion from equilibrium. In a symmetric junction, the highest achievable level of nonequilibrium distribution function is (12.34), which coincides with the saturation regime at electromagnetic pumping, but in this case without entering the saturation regime. As noted earlier, even in the saturation regime phonon instability does not arise. It is possible to confirm that the inclusion of electron–electron inelastic collisions [in effective approximation (12.27)] does not change this result.

Thus the nonsymmetric SIS′ junction turns out to be regarded as a unique possibility for satisfying all the necessary conditions of phonon instability. Indeed, the solution (12.36), discussed in Sect. 12.2, in case (3), with $B \sim 1$, will provide the threshold regime of acoustic quantum generation. To confirm this it is enough to substitute (12.36) (see Fig. 12.12) into (12.57). As follows from the discussion in Sect. 12.2, when $B \sim 1$, phonon instability could be achieved in a spatially homogeneous and steady-state approach. We will now discuss to what extent the competing instabilities could affect this conclusion.

12.3.4. Stability Against Order-Parameter Fluctuations

In nonequilibrium superconductors there are many factors that influence the stability of the steady state (including, e.g., fluctuations in the superfluid velocity,[7] high-frequency fluctuations of the order parameter,[31] and fluctuations of the elec-

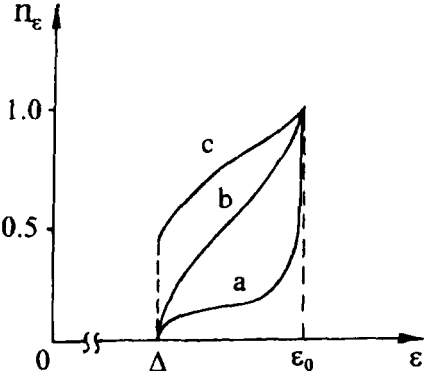

Figure 12.12. Nonequilibrium distribution of electron excitations n_ε at "narrow" pumping by electromagnetic radiation, a, and tunnel injections, b, c. Curve b illustrates saturation in symmetric junctions. Parameter ε_0 is equal to $\omega-\Delta$ for electromagnetic radiation, to $V-\Delta$ for a symmetric tunnel junction, b, and to $V-\Delta'$ for nonsymmetric one, c.

tromagnetic field[11]). We begin with a stability analysis of the inversely populated state related to the high-frequency fluctuations of Δ. The corresponding criterion of instability was considered in Chap. 8. We recall here that the extremal steady-state value of Δ is determined by the sign reversal of the expression

$$P_i(\Delta) = \int_{\Delta}^{\infty} \frac{(1 - 2n_\varepsilon)d\varepsilon}{\sqrt{\varepsilon^2 - \Delta^2}\sqrt{\varepsilon^2 - \omega_i^2/4}}, \tag{12.59}$$

where the frequency of the i-mode can be found from the equation

$$n\left(\frac{\omega_i}{2}\right) = \frac{1}{2}. \tag{12.60}$$

The mode $\omega_0 = 0$ may also be unstable. For a narrow injection source corresponding to the case $B \sim 1$ (which is important in our case), expression (12.59) may be rewritten in the form*

$$P_0(\Delta) = \frac{1 - 2\bar{n}}{\Delta^2} \tag{12.61}$$

and, consequently, the rapid "breakdown" of the Cooper pairs may occur only if $\bar{n} \geq 1/2$. Thus, for small values of $\bar{n}$ this competing instability cannot arise.

12.3.5. Fluctuations of Superfluid Velocity

We will now consider the instability related to the fluctuations of the superfluid velocity $\mathbf{v}_s$. In this case the response of a nonequilibrium superconductor to an external magnetic field becomes paramagnetic (see Sect. 11.5) and the "density of the superfluid component" N_s may change sign:

$$N_s = 1 + 2\int_{\Delta}^{\infty} \frac{\partial n}{\partial \varepsilon} \frac{\varepsilon}{\sqrt{\varepsilon^2 - \Delta^2}} d\varepsilon = 1 + \sqrt{\frac{2\Delta}{\delta}} \int_0^1 \frac{\partial n}{\partial z} \frac{dz}{\sqrt{z}}. \tag{12.62}$$

As follows from (12.62), at small δ and $B \sim 1$ the density N_s may indeed change its sign.

It is important to recognize that phonon instability occurs before N_s becomes negative. In the case $\delta << \Delta$, this may be ascertained directly. One may disregard the constant 1 in Eq. (12.62) and the second of the integrals in (12.57), putting $\omega_q = V$ in the first one (this is the least stable mode). Then, using expression (12.36) for n_z and recognizing that the corresponding integrals could be evaluated in

*For $B > 1$ and $i \neq 0$, the instability does not occur.

quadratures, one may see that N_s changes its sign at $B \geq 1$, while phonon instability is expected at $B > 0.54$. Thus, for the appropriate choice of parameters, the instability related to the sign reversal of N_s might not be destructive. For this reason we will not study the problem of the superfluid velocity fluctuations in detail. Note only that the sign reversal of N_s, if any, does not necessarily indicate the development of instability. The interface between the film and the bulk superconductor can electrodynamically stabilize the situation in a thin film if $\lambda' d < |\lambda^2|$ (cf. Sect. 11.5). Here λ and λ' are the magnetic field penetration depths connected to the London penetration depth by the relation

$$\lambda^{-2} = \lambda_L^2 N_s. \tag{12.63}$$

In the presence of competing processes it is highly important that for a certain choice of parameters the self-consistent kinetic equations allow only one solution with a small $\bar{n}$ [see Eq. (12.46) and Fig. 12.10]. Otherwise, in the case of multiple solutions, a spatially inhomogeneous state of the superconductor may arise (see Chap. 11 and Sect. 12.2), which would complicate the situation.

Note that the longitudinal electric field in superconductors (which is related to the branch imbalance in the electron excitation spectrum) might also fluctuate (cf. Sect. 8.4). However, in our case ($T = 0$ and "narrow" distributions) the imbalance is expected to be small and no instability is likely to be developed as a result of the fluctuations of the longitudinal field. The problem of the stability of the pattern arising relative to the high-frequency fluctuations of a transverse electromagnetic field (photons) will be considered in Sect. 12.4.

12.3.6. Estimated Gain

We now provide some numerical values for parameters relevant to the acoustic quantum generation regime. From the viewpoint of possible experiments, the nonequilibrium state can be efficiently realized in aluminum films as a result of the relatively long lifetime of the electron excitations in this material. Characteristic values of γ for aluminum are estimated to be $\gamma \sim 10^7 - 10^8\ \mathrm{s}^{-1}$ (see Table 10.1 in Sect. 10.2), and if $\nu \sim 0.01\gamma$, then for aluminum at $d \sim 10^{-4}$ cm we have from (10.12) $RS \sim 10^{-5}\ \Omega\ \mathrm{cm}^2$. Such low-resistance junctions may be implemented in practice (see, e.g., Refs. 32 and 33). The necessity to satisfy the inequality $\lambda' d < |\lambda^2|$ imposes additional restraints on both metals comprising the SIS′ junction.

Note that the velocity of sound in a superconductor is significantly less than the speed of light, while the dimensionless electron–phonon interaction constant exceeds the corresponding constant of electromagnetic interaction. Because of that, the gain of the acoustic quantum generation could be quite high. Using (12.53) we may obtain the following expression for the amplification factor (i.e., the gain):

$$K(\omega_q) = \frac{\pi\lambda}{2}\frac{\omega_D}{\varepsilon_F}\frac{\Delta}{u} I^0(\omega_q), \tag{12.64}$$

where $I^0(\omega_q)$ is the quantity in braces in (12.57), and for characteristic metals (see Table 10.1 in Sect. 10.2) we have from (12.64) $K(\omega_q) \sim 10^3\ \mathrm{cm}^{-1}$ during pumping, which corresponds to $I^0(\omega_q) \sim 1$. This is higher than the working gain of gaseous, solid-state, and semiconductor lasers.*

12.4. PHOTON INSTABILITY

Photons represent a Bose field, which has a lot of analogy with the phonon field. At the same time there are major distinctions, which makes the case of photon instability worth a separate discussion.

12.4.1. Two Channels of Electron–Photon Interaction

Consider a photon of frequency $\omega_0 > 2\Delta$ propagating through a superconductor with a nonequilibrium electron population. We assume that the distribution function n_ε is isotropic in the momentum space. As mentioned earlier, a photon can participate (in a first approximation) in two types of processes, which are shown in Fig. 12.13. They can be described by the collision operators (cf. Sect. 5.3):

$$I_{\mathrm{rec}}^{(\mathrm{pt-e})}(N_{\omega_0}) \approx N_{\omega_0}\pi_0 \int_\Delta^\infty \int_\Delta^\infty \frac{\varepsilon_1\varepsilon_2\, d\varepsilon_1 d\varepsilon_2}{\sqrt{\varepsilon^2-\Delta^2}\sqrt{\varepsilon^2-\Delta^2}}\left(1-\frac{\Delta^2}{\varepsilon_1\varepsilon_2}\right)$$
$$\times [(1-n_{\varepsilon_1})(1-n_{\varepsilon_2}) - n_{\varepsilon_1} n_{\varepsilon_2}]\, \delta(\varepsilon_1+\varepsilon_2-\omega_0), \tag{12.65}$$

$$I_{\mathrm{rel}}^{(\mathrm{pt-e})}(N_{\omega_0}) \approx 2N_{\omega_0}\pi_0 \int_\Delta^\infty \int_\Delta^\infty \frac{\varepsilon_1\varepsilon_2\, d\varepsilon_1 d\varepsilon_2}{\sqrt{\varepsilon^2-\Delta^2}\sqrt{\varepsilon^2-\Delta^2}}\left(1-\frac{\Delta^2}{\varepsilon_1\varepsilon_2}\right)$$
$$\times [(n_{\varepsilon_1})(1-n_{\varepsilon_2}) - (1-n_{\varepsilon_1})n_{\varepsilon_2}]\, \delta(\varepsilon_1+\varepsilon_2+\omega_0) \tag{12.66}$$

(these operators are written in the limit of large photon numbers $N_{\omega_0} >> 1$, assuming the absence of branch imbalance: $n_\varepsilon \equiv n_{-\varepsilon}$). Here π_0 is a (positive) constant proportional to the interaction cross section of the photon with an electron quasi-particle.

*Hence the acoustic quantum generation, in principle, might be achieved without using a resonator (superluminescence), with the coherent phonon flux propagating along the thin film. Moreover, because the phonons suffer total internal reflection at the metal–liquid helium interface, it seems expedient to try to implement a ring generator scheme.

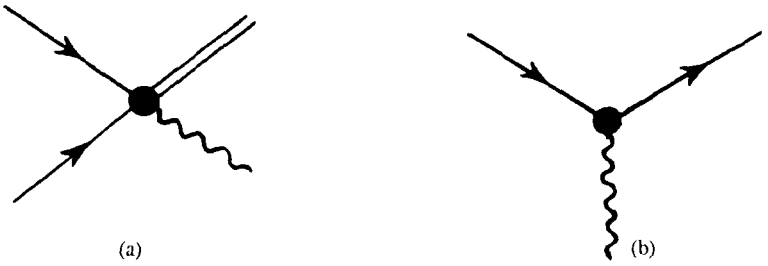

Figure 12.13. Diagrams corresponding to single-quantum processes of recombination (a) and relaxation (b) of electron excitation in superconductors. The wavy line corresponds to a Bose field (photon or phonon) quantum; the double line indicates the Cooper pair.

(these operators are written in the limit of large photon numbers $N_{\omega_0} >> 1$, assuming the absence of branch imbalance: $n_\varepsilon \equiv n_{-\varepsilon}$). Here π_0 is a (positive) constant proportional to the interaction cross section of the photon with an electron quasi-particle.

12.4.2. Photons Versus Phonons

Taking into account that

$$\frac{dN_{\omega_0}}{dt} = I_{\rm rec}^{\rm (pt-e)}(N_{\omega_0}) + I_{\rm rel}^{\rm (pt-e)}(N_{\omega_0}) \equiv -P_{\rm rec}(\omega_0)N_{\omega_0} - P_{\rm rel}(\omega_0)N_{\omega_0}, \qquad (12.67)$$

and integrating in (12.65) and (12.66) with the help of δ-functions, one obtains for the photon absorption coefficients $P_{\rm rec}(\omega_0)$ and $P_{\rm rel}(\omega_0)$ in recombination and relaxation channels, respectively, the following relations:

$$P_{\rm rec}(\omega_0) = \pi_0 \int_\Delta^{\omega_0-\Delta} d\varepsilon \, \frac{\varepsilon(\omega_0-\varepsilon)-\Delta^2}{\sqrt{\varepsilon^2-\Delta^2}\,\sqrt{(\omega_0-\varepsilon)^2-\Delta^2}} (1 - n_\varepsilon - n_{\omega_0-\varepsilon}), \qquad (12.68)$$

$$P_{\rm rel}(\omega_0) = 2\pi_0 \int_\Delta^{\infty} d\varepsilon \, \frac{\varepsilon(\varepsilon+\omega_0)+\Delta^2}{\sqrt{\varepsilon^2-\Delta^2}\,\sqrt{(\varepsilon+\omega_0)^2-\Delta^2}} (n_\varepsilon - n_{\varepsilon+\omega_0}). \qquad (12.69)$$

Interchanging the variables ε and ω_0 – epsilon in the integrand of (12.68), one can rewrite it in the form (the same procedure was applied in Sect. 12.3 to get 12.55):

$$P_{\rm rec}(\omega_0) = \pi_0 \int_\Delta^{\omega_0-\Delta} d\varepsilon \, \frac{\varepsilon(\omega_0-\varepsilon)-\Delta^2}{\sqrt{\varepsilon^2-\Delta^2}\,\sqrt{(\omega_0-\varepsilon)^2-\Delta^2}} (1 - 2n_\varepsilon). \qquad (12.70)$$

$$P^{\mathrm{rel}}(\omega_0) > 4\Delta \sqrt{\frac{\varepsilon_0}{\Delta} - 1}\,\pi_0, \tag{12.72}$$

and thus

$$|P^{\mathrm{rec}}(\omega_0)| < P^{\mathrm{rel}}(\omega_0). \tag{12.73}$$

According to Eq. (12.73) one cannot expect to obtain any amplification of electromagnetic waves at frequencies $\omega_0 \geq 2\Delta$ because the gain in the recombination channel is completely suppressed by the relaxation losses. This is a major difference in the behavior of photon and phonon fields in nonequilibrium superconductors. The physical reason* is in the transverse nature of the photon field as opposed to the interaction of longitudinal phonons within an isotropic metal.

12.4.3. "Clean" Limit Kinematic Restrictions

The result (12.73) is based on Eqs. (12.65) and (12.66), which could be violated in the limit of perfect crystals (i.e., in specimens with a small concentration of elastic scatterers; cf. Chap. 5). In this limit the relaxation process of the type

$$n(1 - n')N \leftrightarrow (1 - n)n'(N + 1), \tag{12.74}$$

which is described by the collision operator (12.65), is forbidden owing to the energy-momentum conservation law subject to the condition $v_F < c$, where v_F is the Fermi velocity and c is the speed of light in the medium. In fact, the last inequality (the Cherenkov condition) suppresses the relaxational channel (Fig. 5.1) while leaving the recombinational channel active. This suppression effect was treated in detail in Sect. 5.4. Hence in this particular case of perfect crystalline samples one can expect a negative absorption coefficient for photons at $\omega_0 \geq 2\Delta$.[34]

12.4.4. Experimental Feasibility

The detection of stimulated emission of electromagnetic radiation from a nonequilibrium point microjunction NIS was reported in Refs. 35–37 (the scheme of the experiment is depicted in Fig. 12.14). The nonequilibrium population was created by excess quasi-particles injected by the current flowing from a normal metal to the superconductor. The recombination of two quasi-particles across the gap (see Fig. 12.13a) creates a new pair, which is added to the Cooper condensate. A pair-binding energy 2Δ was assumed to be emitted in the form of millimeter-range electromagnetic quanta, corresponding to the value 2Δ of superconducting tanta-

*To confirm this conclusion, one should bear in mind that the conductivity has a large imaginary part, which stabilizes electromagnetic fluctuations.[11]

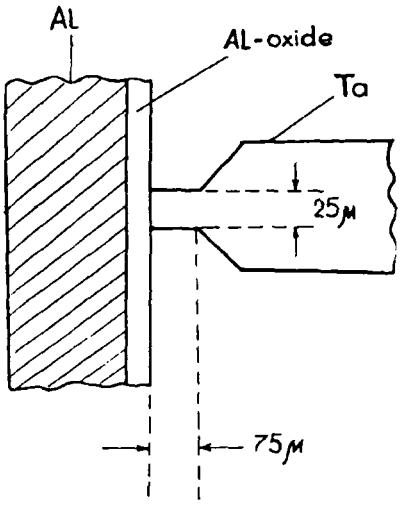

Figure 12.14. Point microjunction for the normal metal–insulator–superconductor used in Refs. 35–37 to generate electromagnetic radiation.

lum, used in the experiments in Refs. 35–37. The power of the emitted coherent radiation was reported to be about 10^{-7} W.

Unfortunately, this result has remained unconfirmed by other authors. Moreover, in a subsequent work,[38] critical arguments were put forward to prove the impossibility of "laser" action. As was pointed out, the relaxation loss channel (see Fig. 12.13b) is very important in superconductors and it overdamps the recombinational gain channel. To have a gain, it is necessary to pay special attention to the crystallinity of the sample. Also, it is necessary to use an injection scheme that guarantees (at least theoretically) the possibility of an inverse population at the operational regime.

As shown in this chapter, the most promising results might be obtained by tunnel injection in nonsymmetric SIS′ junctions, which seems quite appropriate for the creation of an inverse population in the "narrow" pumping case (Fig. 12.12). The deviation from equilibrium is higher when the injector has a larger gap. Recalling the results discussed, it seems evident that with a normal-metal injector (used in Refs. 35–37), one cannot expect to fulfill the necessary conditions for quantum generation.

From the experimental point of view, serious difficulties could arise even in the case of an SIS′ junction. Indeed, as mentioned in Sect. 12.3, the favorable values of the parameter B should be about 1. This means that the RS value of the junction must be less than $10^{-5}\ \Omega\ \text{cm}^2$. Such junctions, with an exceedingly high transparency of the tunneling barrier, are very sensitive to the processes of degradation and

breakdown. This is probably why the inverse population has not been observed experimentally so far.

Possibilities for creating inversely populated states in superconductors exist also in the wide pumping discussed in Sect. 12.1. Some factors could favor this conclusion. Among them are sufficiently high quality of the crystalline structure of the superconducting specimen, the non-Debye character of the phonon spectrum, sufficiently large values of the Cooper gap compared with the characteristic phonon frequencies, and significant participation of transverse phonon modes in the electron relaxation processes.

The fulfillment of the last condition is rather probable in superconductors with an anisotropic crystalline structure, particularly in high-temperature superconductors. To make more strict predictions, one needs to analyze the problem from first principles, using the partial functions $\alpha_\nu^2(\omega_q)F_\nu(\omega_q)$ for all the phonon modes ν. The polarizations of these modes must be known. For numerical calculations, it is necessary also to know the energy band structure of electrons in the normal state as well as the properties of the superconducting state. The positioning of phonon peaks relative to the frequency $\omega_q = 2\Delta$ plays a major role in the shape formation of the function n_ε, as the discussion in Sect. 12.2 revealed.

It must be acknowledged that only the main points of the superconductor-based quantum generation have been outlined in this chapter. Among the omitted questions is the competition between phonon and photon instabilities. Both regimes of instability have practical implications. To some extent, the result of competition is determined by external factors, such as the design of the resonator, or, in a more general sense, the nature of the feedback. This competition becomes of practical importance when the instability threshold is crossed. Investigating beyond this threshold is then a task for future theoretical work.

References

1. E. M. Lifshitz and L. P. Pitaevskii, *Statistical Physics,* Part 1, pp. 221–224, Pergamon, Oxford (1980).
2. D. A. Kirzhnits and Yu. V. Kopaev, Superconductivity in a non-equilibrium with repulsion between particles, *JETP Lett.* **17**(7), 270–273 *[Pis'ma* v *Zh. Eksp. i Teor. Fiz.* **17**(7), 379–382 (1973)].
3. V. M. Galitzkii, V. F. Elesin, and Yu. V. Kopaev, Feasibility of high-temperature superconductivity in nonequilibrium systems with repulsion, *JETP Lett.* **18**(1), 27–29 (1973) *[Pis 'ma v Zh. Eksp. i Teor. Fiz.* **18**(1), 50–53 (1973)].
4. A. G. Aronov, Paramagnetic effects in superconductors, *JETP Lett.* **18**(6), 228–229 (1973) [*Pis 'ma v Zh. Eksp. i Teor. Fiz.* **18**(6), 387–390 (1973)].
5. J.-J. Chang and D. J. Scalapino, Transport properties of nonequilibrium superconductors, *Phys. Rev. B* **9**(11) 4769–4774 (1974).
6. J.-J. Chang and D. J. Scalapino, New instabilities in superconductors under external dynamic pair breaking, *Phys. Rev. B* **10**(9), 4047–4057 (1974).
7. V. G. Baru and A. A. Sukhanov, New types of instabilities in nonequilibrium excitation of a superconductor, *JETP Lett.* **21**(4), 93–94 (1975) *[Pis'ma* v *Zh. Eksp. i Teor. Fiz.* **21**(4), 209–212 (1975)1.

8. V. M. Genkin and A. P. Protogenov, Nonequilibrium states resulting from tunneling in superconductors, *Sov. Phys. Solid State* **18**(1), 13–17 (1976) [Fiz. *Tverd. Tela* **18**(1), 24–32 (1976)].
9. P. Otschick, H. Eschrig, and F. Lange, Sound wave amplification in superconductors, *J. Low Temp. Phys.* **43**(3/4), 397–408 (1981).
10. A. M. Gulyan and G. F. Zharkov, Contribution to the theory of acoustic quantum generators based on nonequilibrium superconductors, *Sov. Phys. JETP* **57**(5), 1059–1065 (1983) *[Zh. Eksp. i Teor. Fiz.* **84**(5), 1817–1829 (1983)].
11. A. G. Aronov and B. Z. Spivak, Nonequilibrium distributions in superconductors, *Sov. Journ. Low Temp. Phys.* **4**(11), 641–660 (1978) [*Fiz. Nizk. Temp.* **4**(11), 1305–1342 (1978)].
12. A. M. Gulian, O. N. Nersesyan, and S.V. Paturyan, On distributions of nonequilibrium electron quasi-particles in anisotropic superconductors with non-Debye phonon spectrum, *Phys. Lett. A* **184**, 218–222(1993).
13. I. E. Bulyzhenkov, Hypersound amplification in nonequilibrium superconductors, *Sov. J. Low Temp. Phys.* **5**(12), 653–655 (1979) [*Fiz. Nizk. Temp.* **5**(12) 1386–1390 (1979)].
14. A. M. Gulian and G. F. Zharkov, in *Thermodynamics and Electrodynamics of Superconductors,* V. L. Ginzburg, ed., pp. 111–182, Nova Science, New York (1988).
15. A. M. Gulian and G. F. Zharkov, in *Nonequilibrium Superconductivity,* V. L. Ginzburg, ed., pp. 1–56, Nova Science, New York (1988).
16. A. M. Gulian, Superconducting tunnel junction as possible source of coherent photon and phonon generation, *Appl. Supercond.* **2**(10–12), 721–728 (1994).
17. V. F. Elesin, Nonequilibrium state of superconductors with optical excitation of quasi-particles, *Sov. Phys. JETP* **39**(5), 862–866 (1974) [*Zh. Eksp. i Teor. Fiz.* **66**(5), 1755–1761 (1974)].
18. V. F. Elesin and Yu. V. Kopaev, Superconductors with excess quasi-particles, *Sov. Phys. Uspekhi* **24**(2), 116–141 (1981) *[Usp. Fiz. Nauk* **133**(2), 259–307 (1981)].
19. A. M. Gulyan, On the inverse population in the nonequilibrium state of superconductors under optical pumping, *Sov. Journ. Low Temp. Phys.* **18**(10), 817–818 (1992) [*Fiz. Nizk. Temp.* **18**(10), 1164–1167(1992)].
20. G. Gladstone, M. A. Jensen, and J. R. Schrieffer, in *Superconductivity,* R. D. Parks, ed., pp. 665–816, Marcel Dekker, New York (1969).
21. S. V. Vonsovskii, Yu. A. Izyumov, and E. Z. Kurmaev, *Superconductivity of Transition Metals, Their Alloys and Compounds,* pp. 179–230, Springer-Verlag, Berlin (1982).
22. W. E. Pickett, Electronic structure of the high-temperature oxide superconductors, *Rev. Mod. Phys.* **61**(2), 433–512 (1989).
23. J. P. Carbotte, Properties of boson-exchange superconductors, *Rev. Mod. Phys.* **62**(4), 1027–1157 (1990).
24. O. N. Nersesyan and S. V. Paturyan, Kinetics and nonequilibrium distributions of quasi-particles in superconductors with strong magnetic correlations, *Sov. J. Low Temp. Phys.* **19**(8), 658–660 (1993) [*Fiz. Nizk. Temp.* **19**(8), 924–927, (1993)].
25. V. F. Elesin, V. E. Kondrashov, and A. S. Sukhikh, Kinetic theory of nonequilibrium superconductors with a wide-band source of quasi-particles, *Sov. Phys. Sol. State* **21**(11), 1861–1866 (1979) [*Fiz. Tverd. Tela* **21**(11), 3225–3234 (1979)].
26. A. G. Aronov and B. Z. Spivak, Properties of superconductors with nonequilibrium excitations, *Sov. Phys. Sol. State* **18**(2), 312–320 (1976) *[Fiz. Tverd. Tela* **18**(2), 541–553 (1976)].
27. A. G. Aronov and B. Z. Spivak, On the role of electron-electron collisions in the formation of nonequilibrium distributions in superconductors, Sov. *Phys. JETP* **50**(2), 328–329 (1979) [*Zh. Eksp. i Teor. Phys.* **77**[2(8)], 652–655, 1979].
28. V. Eckern, A. Schmid, M. Schmutz, and G. Schön, Stability of superconducting states out of thermal equilibrium, *J. Low Temp. Phys.* **36**(5/6), 643–687 (1979).
29. A. N. Oraevskii, Stimulated emission and phase transitions, *Sov. Phys. JETP* **62**(2), 349–354 (1985) *[Zh. Eksp. i Teor. Fiz.* **89**[2(8)], 608–617 (1985)].

30. A. M. Gulian and G. F. Zharkov, Nonequilibrium kinetics of electrons and phonons in superconductors in intense UHF-fields, 7. *Low Temp. Phys.* **48**(1/2), 125–150 (1982).
31. A. G. Aronov and V. L. Gurevich, Stability of nonequilibrium Fermi distributions with respect to Cooper pairing, *Sov. Phys. JETP* **38**(3), 550–556 (1974) [*Zh. Eksp. i Teor. Fiz.* **65**[3(9)], 1111–1124 (1973)].
32. J. A. Pals, K. Weiss, P. M. T. van Attekum, R. E. Horstman, and J. Wolter, Nonequilibrium superconductivity in homogeneous thin films, *Phys. Rep.* **80**(4), 323–390 (1982).
33. H. Schreyer, W. Dietscher, and H. Kinder, Spatial development of multigap states in nonequilibrium superconductors, *Phys. Rev. B* **31**(3), 1334–1337 (1985).
34. A. M. Gulyan, H. N. Nersesyan, and G. M. Sergoyan, Possible "photon" instability of high-temperature non-equilibrium superconductor, *Sov. Phys. Doklady* **34**(2), 153–154 (1989) [*Dokl. Akad. Nauk SSSR* **304**(6), 1347–1350(1989)].
35. W. D. Gregory, L. Leopold, O. Repici, and J. Bostock, Radiative emission at the Ta energy gap frequency in Ta-Al point contacts, *Phys. Lett. A* **29**(1), 13–44 (1969).
36. L. Leopold, W. D. Gregory, O. Repici, and R. T. Averell, Frequency measurement of radiation from normal to superconducting point contact junctions, *Phys. Lett. A* **30**(9), 507–508 (1969).
37. W. D. Gregory, L. Leopold, and O. Repici, Observation of stimulated radiative emission from normal to superconducting metal junctions, *Canad. J. Phys.* **47**, 1171–1176 (1969).
38. A. A. Fife and S. Gygax, Superconductivity maser: A critical reexamination, *Appl. Phys. Lett.* **20**(4), 152–153(1972).

13

Thermoelectric Phenomena

13.1. LINEAR RESPONSE TO THERMAL GRADIENT

Thermoelectric effects in charged Fermi liquids are small owing to the approximate symmetry between particle and hole branches of elementary excitations. In thermal equilibrium, some weak asymmetry in the properties of these excitations results only from a nonzero curvature of the Fermi surface.

13.1.1. Thermopower of Normal Fermi Liquids

We will use for this analysis the general expressions for current obtained in Sect. 7.2, and consider first the case of a normal metal. For this case Eq. (7.83) may be represented as*

$$\mathbf{j} \equiv \mathbf{j}_n^{(n)} = \int_{-\infty}^{\infty} d\varepsilon \, \frac{\sigma_n}{2} \, \nabla f_2. \tag{13.1}$$

Substituting the normal-metal limit ($\Delta \equiv 0$), we arrive at

$$\mathbf{j}_n^{(n)} = -\int_{-\infty}^{\infty} d\varepsilon \, \{\sigma_n \operatorname{sign} \varepsilon \, \nabla n_\varepsilon\}. \tag{13.2}$$

In the case of a linear response we have

$$\nabla n_\varepsilon = -\frac{\varepsilon}{T} n_\varepsilon^0 \, \nabla T, \tag{13.3}$$

where $n_\varepsilon^0 = \{\exp[|\varepsilon|/T] + 1\}^{-1}$ so (13.2) takes the form:

*Both a derivation and a discussion of this basic relation for thermoelectricity in normal metals may be found elsewhere (see, e.g., Refs. 1 and 2).

$$\mathbf{j}_n^{(n)} = \frac{\nabla T}{T} \int_{-\infty}^{\infty} d\varepsilon \, \{\sigma_n \operatorname{sign} \varepsilon \, \varepsilon n_{,\varepsilon}^0\}. \tag{13.4}$$

Everywhere in this book we treated the conductivity σ_n (7.84) as a constant. To describe thermoelectricity, one must account for the dispersion of σ_n in the energy space.* Keeping only the first two terms in the series expansion for σ_n we have

$$\sigma_n = \sigma_n(\varepsilon) \approx \sigma_0 + \varepsilon \frac{\partial}{\partial \varepsilon_F} \sigma_n, \tag{13.5}$$

where

$$\sigma_0 = \sigma(\varepsilon = \varepsilon_F) = \frac{2}{3} N(0) v_F^2 \tau. \tag{13.6}$$

Thus we obtain

$$\mathbf{j}_n^{(n)} = \frac{2}{3} \frac{\nabla T}{T} \left\{ \left[\tau v_F^2 N(0) \right] \int_0^{\infty} d\varepsilon \, \varepsilon \frac{\partial (n_\varepsilon^0 - n_{-\varepsilon}^0)}{\partial \varepsilon} \right.$$

$$\left. + \frac{\partial}{\partial \varepsilon_F} \left[\tau v_F^2 N(0) \right] \int_0^{\infty} d\varepsilon \, \varepsilon^2 \frac{\partial (n_\varepsilon^0 + n_{-\varepsilon}^0)}{\partial \varepsilon} \right\} \equiv b_n \nabla T. \tag{13.7}$$

At thermodynamic equilibrium in normal metals, a symmetry between electron- and holelike excitations ($n_\varepsilon = n_{-\varepsilon}$) is governed by the electroneutrality condition, and the first integral in (13.7) vanishes. Evaluating the second integral in (13.7), one obtains the differential thermopower of a normal metal (or the Seebeck coefficient 5) in the following form:

$$S^{(n)} \equiv -\frac{b_n}{\sigma_0} = \frac{\pi^2}{3e} \frac{T}{\varepsilon_F} \tag{13.8}$$

(the electron charge is restored).

13.1.2. Response of a Superconductor's Normal Component

For superconductors, the calculations of S should be modified by using the spectral functions (7.16); (7.19) to (7.21) in expression (13.7) for the current:

*Ziman[3] describes $\sigma(\varepsilon)$ as the "electrical conductivity which the metal would have, at absolute zero, if the Fermi level, ξ, came at the energy ε" ($\xi = \varepsilon_F$ in our notation).

$$\mathbf{j}_n^{(s)} = -\int_{-\infty}^{\infty} d\varepsilon \left\{ \sigma_n \frac{N_1^2 + N_2^2}{N_1} \operatorname{sign} \varepsilon \nabla n_\varepsilon \right\} =$$

$$= \frac{2}{3} \frac{\nabla T}{T} \left\{ \left[\tau v_F^2 N(0) \right] \int_0^{\infty} d\varepsilon \frac{N_1^2 + N_2^2}{N_1} \varepsilon \frac{\partial (n_\varepsilon^0 - n_{-\varepsilon}^0)}{\partial \varepsilon} \right.$$

$$\left. + \frac{\partial}{\partial \varepsilon_F} \left[\tau v_F^2 N(0) \right] \int_0^{\infty} d\varepsilon \, \varepsilon^2 \frac{\partial (n_\varepsilon^0 + n_{-\varepsilon}^0)}{\partial \varepsilon} \right\} \equiv b_s \nabla T. \tag{13.9}$$

[The component (13.9) of the total current (7.83) is sometimes denoted as $\mathbf{j}_n$, because it describes the diffusion of "normal" excitations in a superconductor driven by a temperature gradient.] In the BCS limit one gets:

$$S^{(s)} \equiv -\frac{b_s}{\sigma_{0_s}} = \frac{2T}{e\varepsilon_{F_{\Delta/T}}} \int_{\Delta/T}^{\infty} dx \frac{x^2}{\cosh^2 \frac{x}{2}}. \tag{13.10}$$

This expression was derived first in Ref. 4 and, as follows from (13.10), $S^{(s)} \to S^{(n)}$ at $T \to T_c$.

The magnetic field inside a superconductor is governed by the usual Maxwell equation curl $\mathbf{B} = 4\pi c^{-1}\mathbf{j}$, where total current density generally is the sum of two components: $\mathbf{j} = \mathbf{j}_s + \mathbf{j}_n^{(s)}$ (for simplicity we ignore here the presence of the interference component; cf. Sect. 7.2). Here $\mathbf{j}_s$ is the usual superconducting current (7.102) and $\mathbf{j}_n^{(s)}$ is the normal excitation current in superconductors generated by the temperature gradient. Since the magnetic field and total current vanish deep inside the superconductor (owing to the Meissner effect), then $\mathbf{j}_s + \mathbf{j}_n^{(s)} = 0$, i.e., the normal and superconducting currents compensate each other, flowing in opposite directions.

Such a current cancellation effect explains why the early experimental search for thermoelectric phenomena in superconductors produced negative results (see Ref. 5 for details). In fact, very sophisticated experiments were performed in an attempt to observe the resulting thermoelectric current in superconductors. For example, Steiner and Grassman[6] suspended a bimetallic ring on an elastic string in a weak magnetic field and then heated the junction. If a net thermoelectromotive force had existed in the superconducting ring, it would have accelerated the superconducting electrons and produced a current that would increase in time and lead to a torsion of the elastic strings. However, during long observation, no rotating momentum was detected.[6] Also, no evidence was found for the Peltier and Thompson heat transfer effects (see Ref. 7). This led to the belief that all thermoelectric phenomena vanish in the superconducting state.[8] The reason for such a

conclusion is the expected total cancellation of two currents—"normal" and "superconducting"—in the bulk of a superconductor.

Nevertheless, as was noted by Ginzburg[9] in 1944, there is no complete cancellation of currents in the case of a superconducting bimetallic plate in the presence of a temperature gradient. A small residual current remains, which flows around the joint of two metals, causing a small magnetic field at the junction (in the interior of the bulk superconducting system). An analogous situation exists in homogeneous but anisotropic superconductors (see Refs. 9 and 10 for details).

In 1973 Gal'perin et al.[11] and independently Garland and Van Harlingen[12] proposed that imposing a temperature difference across the junctions of a superconducting bimetallic ring should create an unquantized magnetic flux Φ_T through the ring. The anticipated size of the effect was very small:: $\Phi_T \sim 10^{-2}\phi_0 \sim 10^{-9}$ G · cm^2 (ϕ_0 is the flux quantum), which is within the sensitivity limit of the SQUID (i.e., a superconducting quantum interference device) technology. It was later recognized that the effects discussed in Ref. 9 and Refs. 10, 13 are virtually the same as these predicted in Refs. 11, 12, and 14.

13.2. THERMOELECTRIC FLUX IN A SUPERCONDUCTING RING

The origin of thermoelectric flux in an inhomogeneous superconducting ring can be easily understood by considering the Maxwell equation governing the magnetic field inside the superconductor: curl $\mathbf{B} = 4\pi c^{-1}\mathbf{j}$, where the total current density is the sum of two components:

$$\mathbf{j} = \mathbf{j}_s + \mathbf{j}_n^{(s)}, \quad \frac{4\pi}{c}\mathbf{j}_s = \frac{\psi^2}{\lambda^2}\left(\frac{\phi_0}{2\pi}\nabla\theta - \mathbf{A}\right), \quad \mathbf{j}_n^{(s)} = b_s\nabla T. \tag{13.11}$$

The usual superconducting current $\mathbf{j}_s$ is excited by the phase gradient of the order parameter and by the magnetic field potential $\mathbf{A}$. The current $\mathbf{j}_n^{(s)} = b_s\nabla T$ is driven by the temperature gradient, analogously to a normal thermoelectric current, $\mathbf{j}_n^{(n)} = b_n\nabla T$. From Eq. (13.11) it follows that

$$\mathbf{A} = \frac{\phi_0}{2\pi}\nabla\theta - \frac{4\pi}{c}\frac{\lambda^2}{\psi^2}\left(\mathbf{j} - \mathbf{j}_n^{(s)}\right), \tag{13.12}$$

or, after integration along a closed contour C and using the condition $\oint_C \nabla\theta \cdot d\mathbf{l} = 2\pi m$ (m is an integer), one obtains

$$\Phi = \oint_C \mathbf{A} \cdot d\mathbf{l} = m\phi_0 - \frac{4\pi}{c}\oint\frac{\lambda^2}{\psi^2}\left(\mathbf{j} - \mathbf{j}_n^{(s)}\right) \cdot d\mathbf{l}. \tag{13.13}$$

Here Φ is the magnetic flux piercing C.

13.2.1. Meissner Effect and Incomplete Cancellation of Thermoelectricity

In a massive superconducting ring, the current j in the bulk of the metal is zero because of the Meissner effect. In a massive superconducting cylinder, the current j at the outside surface is also zero (in the absence of an external magnetic field). Thus the total magnetic flux confined inside the cylindrical system is

$$\Phi = m\phi_0 + \Phi_T, \quad \Phi_T = \frac{4\pi}{c}\oint_C \frac{\lambda^2}{\psi^2}\mathbf{j}_n^{(s)} \cdot d\mathbf{l}, \tag{13.14}$$

where C embraces the outside surface. The term $m\phi_0$ describes a quantized magnetic flux, captured originally inside the hollow superconducting cylinder (usually one may assume $m = 0$); the term Φ_T is the additional unquantized temperature-dependent thermoelectric contribution.[11,12] The current $\mathbf{j}$ flows near the inside cylinder surface at a distance $\sim \lambda$.

Let both metals be in a normal state with the current density $\mathbf{j}_n^{(n)} = b_n \nabla T$. The total current in the normal system is $I_n = \langle j_n^{(n)} \rangle d$, where $\langle j_n^{(n)} \rangle$ is some averaged value. The magnetic field in the hollow is $H_i = 4\pi c^{-1} I_n$, and the flux in the normal system is $\Phi_n = \pi R^2 H_i$ (neglecting the flux confined in the cylinder walls, if $d << R$). Finding the ratio

$$\frac{\Phi_T}{\Phi_n} = \frac{4\pi}{c}\oint_C \frac{\lambda^2}{\psi^2}\mathbf{j}_n^{(s)} \cdot d\mathbf{l} \Big/ \frac{4\pi}{c}\langle j_n^{(n)} \rangle \pi R^2 d = \left\langle \frac{\lambda^2}{\psi^2 R d}\frac{b_s}{b_n} \right\rangle_{\text{av}} \tag{13.15}$$

(here the proper average is assumed), one notices a very small factor $\sim \lambda^2/Rd$ entering Eq. (13.15). This factor reflects the above-mentioned strong cancellation of two currents in superconductors, which results in a drastic reduction in the magnetic flux Φ_T generated in superconductors, compared with the flux Φ_n generated in normal metals.

To make the numerical estimates of Φ_T, one should know the coefficient b_s in Eq. (13.15). For this reason one can use Eq. (13.10). At small T the coefficient $b_s(T)$ quickly diminishes, which reflects the reduction in the number of "normal" excitations at low temperatures. At temperatures $T \to T_c$, the coefficient $b_s(T) \to b_n(T_c)$, which is natural because $\mathbf{j}_s(T \to T_c) \to 0$ and $\mathbf{j} \to \mathbf{j}_n^{(n)}$. Since thermoelectric experiments are usually made at temperatures T and $T + dT$, in close vicinity to T_c for one of the metals, it seems reasonable to set $b_s(T) \sim b_n(T_c)$ for a rough estimate of Φ_T. Setting in (13.15) $R \sim 1$ cm, $d \sim 1$ mm, $T_c - T_1 \sim 10^{-2}$ K, $1 - T/T_c \sim 10^{-3}$ K, accounting for the temperature dependence $\lambda(T) = \lambda_0\sqrt{1 - T/T_c}$ with $\lambda_0 \sim 10^{-6}$ cm^2, and utilizing the measured coefficients $S^{(n)}$ for typical metals used in experiments (such as Pb, In, Sn), one obtains for the expected flux generated in

a superconducting cylinder the estimate $\Phi_T \sim 10^{-9}$ G · cm$^2 \sim 10^{-2}\,\phi_0$ (see Ref. 10 for details).

13.2.2. "Gigantic" Flux Puzzle

In the first experiments by Zavaritskii[15] (performed using superconducting bimetallic loops), thermoelectric fluxes of only the predicted magnitude $\Phi \sim 10^{-2}\,\phi_0$ were registered; the temperature dependence of the generated flux $\Phi(T) \propto \ln(1 - T/T_c)$ was also in agreement with theoretical predictions. However, in subsequent experiments,[16,17] much larger fluxes (on the scale of 10^2–$10^3\,\phi_0$) were observed; the temperature dependence was also found to disagree with the predictions.

Careful measurements of thermoelectric flux made by Van Harlingen et al. confirmed the existence of such a "gigantic" thermoelectric effect. The experiments[18] were made with hollow bimetallic toroids of lead and indium near the transition temperature of indium ($T_c = 3.4$ K). The rate of the magnetic flux increase $d\Phi/dT$ was found to diverge as the transition temperature was approached, with a $d\Phi/dT \propto (1 - T/T_c)^{-3/2}$ power-law dependence, instead of the expected $d\Phi/dT \propto (1 - T/T_c)^{-1}$ power law. It was recognized also that the effect is sensitive to the geometry of the experiment.[19,20]

The observed "gigantic" thermoelectric flux,[18] which exceeds expectations by several orders of magnitude, is a puzzle that has defied explanation for almost 20 years. To date, there is no commonly accepted explanation of this "gigantic" effect, although several hypotheses have been proposed.

One approach to the explanation of the large effect was based on the anomalous behavior of the induced current $\mathbf{j}_n^{(s)} = b_s \nabla T$ in Eq. (13.12). This hypothesis was explored in a number of papers, where the kinetic theory of thermoelectric phenomena in superconductors was modified to account for transport processes unique to the superconducting state, such as additional superfluid counterflow currents[14,21] and the generation of additional currents driven by a nonequilibrium chemical potential[22] (this question is also considered in the next section). However, the inclusion of such effects does not noticeably change the estimate for the coefficient b_s and cannot remove the large discrepancy between the theory and experiment.

A recent paper[23] contains arguments that the usual formulation of the kinetic theory for superconductors should be radically reconsidered. According to Marinescu and Overhauser,[23] the coefficient b_s (in the presence of a temperature gradient) is five orders greater than b_n (even for $T \approx T_c$), and that would be enough to remove the above-mentioned discrepancy. However, this assertion seems to contradict the measurements made with ordinary "loop"-geometry (see, for instance[15]), where no anomalous increase of thermoelectric effect near T_c was noticed. Thus, the arguments raise serious doubts.

Another assumption[17] was that an additional source of magnetic flux should be introduced in Eq. (13.14), which accounts for the redistribution of the magnetic

fields enclosed in normal and superconducting measuring circuits, thus causing spurious effects. However, carefully controlled experiments[18] have apparently excluded this possibility.

Still another conjecture was[24,25] that the number m of captured flux quanta in Eq. (13.14) is temperature dependent and increases spontaneously with ∇T. According to Arutyunan et al.,[25] the vortex–antivortex pairs are generated by the current $\mathbf{j}_n$ inside the superconductor. The antivortex (i.e., the vortex with the opposite flux direction) is expelled from the system, but the vortex remains inside, thus increasing the captured flux. This hypothesis[24,25] will be discussed in Chap. 14.

13.3. THERMOELECTRICITY AND CHARGE IMBALANCE

We consider now certain thermoelectric phenomena related to the gauge-invariant potential μ, existing only in the superconducting state. First the effect predicted theoretically by Pethick and Smith[26] and demonstrated experimentally by Clark et al.[27] will be considered. These studies have initiated a number of theoretical investigations[28–31] that are partly summarized in Ref. 32.

13.3.1. Pethick–Smith Effect: Qualitative Description

The temperature gradient T shifts the Fermi sphere in the momentum space (see Fig. 13.1a). This leads to an electron-hole branch imbalance in the vicinity of the Fermi sphere. This imbalance has different signs in opposite directions on the Fermi sphere and gives $\mu = 0$ after integration over directions of $\mathbf{p}$ (if $\mathbf{v}_s = 0$). The situation is different, if a nonzero supercurrent ($\mathbf{v}_s \neq 0$) is present. In this case the single-particle spectrum has the form[33]

$$\varepsilon_{\mathbf{p}} = (\xi_p^2 + |\Delta|^2)^{1/2} + \mathbf{p} \cdot \mathbf{v}_s \tag{13.16}$$

and some asymmetry arises (Fig. 13.1b), which leads to a finite value of μ.

13.3.2. Spatially Inhomogeneous Kinetic Equation

To describe this phenomenon quantitatively, we will use the general kinetic equation (3.63), in which the terms proportional to $\mathbf{v} \cdot \mathbf{k}$ and connected with spatial inhomogeneity will be important. Our task is to generalize Eqs. (7.30) and (7.41) for the functions f_1 and f_2.

As earlier, we will use the Usadel approximation (7.70)

$$\check{g} \approx \check{g}_s + \mathbf{v} \cdot \check{\mathbf{g}}, \qquad \check{\mathbf{g}}_{\mathbf{p}} = -\frac{i}{2\pi}\tau\left[\check{g}_s, * \left[\check{\partial}, * \check{g}_s\right]_-\right]_-. \tag{13.17}$$

Representing Eq. (7.6) in the form

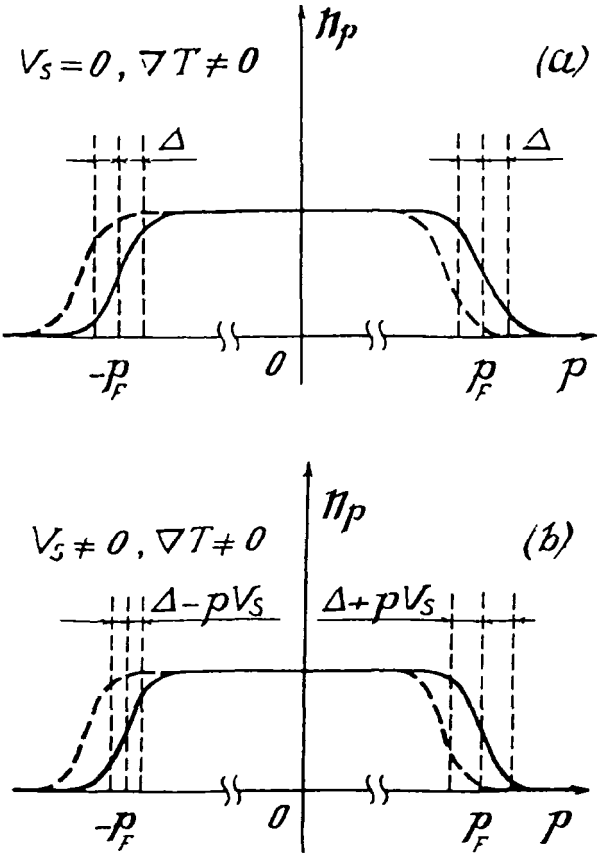

Figure 13.1. The distribution function $n_{\mathbf{p}}$ of electrons and the gap $\Delta + \mathbf{p} \cdot \mathbf{v}_s$ (a) in the absence of superfluid current, and (b) with $\mathbf{v}_s \neq 0$. The direction of $\mathbf{v}_s$ is assumed to be along ∇T.

$$[(\check{\sigma}_z \varepsilon - \check{I}\varphi + i\mathbf{v} \cdot \check{\boldsymbol{\partial}} - \check{\Sigma}), * \check{g}_s]_- = 0 \tag{13.18}$$

and substituting (13.17) into (13.18), we find after angle integration ($D = v_F^2 \tau/3$)

$$\left[\left(\check{\sigma}_z \varepsilon - \check{I}\varphi - (\check{\Sigma} - \check{\Sigma}_{\text{imp}})\right), * \check{g}_s\right]_- + \frac{D}{2\pi}\left[\check{\partial}, * \left[\check{g}_s, * \left[\check{\partial}, * \check{g}_s\right]_-\right]_-\right]_- = 0, \tag{13.19}$$

from which it follows for the "Keldysh component" $\hat{g}_s = \hat{g}$ (cf. Ref. 34; our normalization differs from that of Schmid):

$$\left[\left(\hat{\sigma}_z\varepsilon - \hat{I}\varphi - (\hat{\Sigma} - \hat{\Sigma}_{\text{imp}})\right), * \hat{g}\right]_- + \frac{D}{8\pi}\left\{\left[\hat{\partial}, * \hat{g}^R * \left[\hat{\partial}, * \hat{g}\right]_-\right]_-\right. \tag{13.20}$$

$$\left. + \left[\hat{\partial}, * \hat{g}^R * \left[\hat{\partial}, * \hat{g}^A\right]_-\right]_- - \left[\hat{\partial}, * \left[\hat{\partial}, * \hat{g}^R\right]_- * \hat{g}\right]_- - \left[\hat{\partial}, * \left[\hat{\partial}, * \hat{g}^R\right]_- * \hat{g}^A\right]_-\right\}.$$

Using the relations

$$\hat{g}^R * \hat{g}^R = \hat{g}^A * \hat{g}^A = -\pi^2\hat{I}, \qquad \hat{g}^R * \hat{g} + \hat{g} * \hat{g}^A = 0, \tag{13.21}$$

which follow from the normalization conditions (7.74) and (7.75), one finds by analogy with (7.30) and (7.41) the equations:

$$N_1\dot{f}_1 = D\text{div}\,[(N_1^2 - R_1^2)\nabla f_1] + 2DN_2R_2\mathbf{Q}\cdot(\nabla f_2 - f^0_{1,\varepsilon}\dot{\mathbf{A}})$$

$$-\frac{1}{4\pi}(K_{11} + K_{22}) - f^0_{1,\varepsilon}R_2\frac{\partial|\Delta|}{\partial t}, \tag{13.22}$$

$$N_1\dot{f}_2 = D\text{div}\,[(N_1^2 + N_2^2)(\nabla f_2 - f^0_{1,\varepsilon}\dot{\mathbf{A}})] + 2DN_2R_2\mathbf{Q}\cdot\nabla f_1$$

$$-N_2|\Delta|(2f_2 + f^0_{1,\varepsilon}\dot{\theta}) - \frac{1}{4\pi}\left[K_{11} - K_{22} + \left(-\frac{\Delta^*}{\varepsilon}K_{12} + \frac{\Delta}{\varepsilon}K_{21}\right)\right]. \tag{13.23}$$

In the limiting case $D = 0, \dot{f}_1 = \dot{f}_2 = 0$, these equations transform correspondingly to (7.30) and (7.41); the functions K_{ij} are defined in (7.32) and (7.42). Equations (13.22) and (13.23) were derived originally by Kramer and Watts-Tobin[35] (see also Refs. 34 and 36).

13.3.3. *Influence of Heat Flux*

The interaction of electrons with the heat flux is not taken into account in operators K_{ij}; however, these equations may be used to study thermoelectric effects in superconductors, with some additional assumptions.[30] The main issue is that (in analogy with the normal metal) the temperature gradient creates the gradient of the f_1-function:

$$\nabla f_1 \approx -f^0_{1,\varepsilon}\left(\frac{\varepsilon}{T}\right)\nabla T. \tag{13.24}$$

The functions f_1 and f_2 are generally interdependent, as follows from Eqs. (13.12) and (13.23). Substitution of (13.24) into (13.23) gives the equation for f_2:

$$2DN_2R_2(\mathbf{Q}\cdot\nabla T)\left(\frac{\varepsilon}{T}\right)f^0_{1,\varepsilon} + 2N_2|\Delta|f_2$$

$$+\frac{1}{4\pi}\left[K_{11} - K_{22} - \left(\frac{\Delta^*}{\varepsilon}K_{12} - \frac{\Delta}{\varepsilon}K_{21}\right)\right] = 0. \tag{13.25}$$

The first term in this equation is responsible for the branch imbalance: as may be seen, it is proportional to $(\mathbf{v}_s \cdot \nabla T)$. The second term describes the conversion between the condensate and excitations. The third term represents the electron–phonon collision integral taking into account the nondiagonal channel.

13.3.4. "Mutilated" Collision Operator

In Sect. 7.1 we mentioned that the usual relaxation time approximation for this integral does not conserve the number of particles. The missing term in (7.27) was restored [see (7.44)] using the gauge transformation rules for the functions f_1 and f_2. In this section we will use the "mutilated collision operator" approximation, introduced by Eckern and Schön[37]:

$$K_{11} - K_{22} - \left[\frac{\Delta^*}{\varepsilon} K_{12} + \frac{\Delta}{\varepsilon} K_{21}\right] = \frac{4\pi}{\tau_\varepsilon} N_1 \left[f_2 - \frac{1}{2} f^0_{1,\varepsilon} \int_{-\infty}^{\infty} d\varepsilon' \, N_1 f_2 d\varepsilon'\right]. \qquad (13.26)$$

Along with the "out-scattering" term (7.38), this approximation contains the "in-scattering" term in the integral form. Ignoring the dispersion of τ_ε and N_1 in the vicinity of T_c, one can show that the approximation (13.26) conserves the particle number:

$$\int_{-\infty}^{\infty} \left[K_{11} - K_{22} - \left(\frac{\Delta^*}{\varepsilon} K_{12} + \frac{\Delta}{\varepsilon} K_{21}\right)\right] d\varepsilon = 0, \qquad (13.27)$$

and hence it is compatible with the continuity equation for electrons.

13.3.5. Calculation of Branch Imbalance Potential

Using the expression for the charge density (8.2) and the neutrality condition for a superconductor, one may derive from (8.5) a first approximation in analogy to (8.6):

$$\varphi = -\frac{1}{2} \int_{-\infty}^{\infty} d\varepsilon \, N_1 f_2. \qquad (13.28)$$

Substituting (13.28) into (13.26), we obtain Eq. (7.44); this confirms the correctness of approximation (13.26). Note that in the gauge $\theta = 0$, the quantity φ coincides with μ [cf. (8.6)]. So the equation is valid:

$$2DN_2R_2(\mathbf{Q} \cdot \nabla T)\left(\frac{\varepsilon}{T}\right) f^0_{1,\varepsilon} + \left(2N_2|\Delta| + \frac{N_1}{\tau_\varepsilon}\right) f_2 + \frac{N_1}{\tau_\varepsilon} f^0_{1,\varepsilon} \mu = 0, \qquad (13.29)$$

from which it follows [using (13.28) and the relation $\mu = \varphi$] that:

$$2\mu = \frac{2D(\mathbf{Q}\cdot\nabla T)}{T}\int \frac{N_1N_2R_3\varepsilon\tau_\varepsilon}{2N_2|\Delta|\tau_\varepsilon + N_1} f^0_{1,\varepsilon}\, d\varepsilon + \mu\int \frac{N_1^2 f^0_{1,\varepsilon}}{2N_2|\Delta|\tau_\varepsilon + N_1}\, d\varepsilon. \qquad (13.30)$$

Utilizing expressions (7.16) to (7.21) for spectral functions (with $\gamma = 1/2\tau_\varepsilon$, where τ_ε does not depend on ε, and $|\Delta|\tau_\varepsilon >> 1$), assuming the temperature range $|\Delta| < T$, and putting $f^0_{1,\varepsilon} \approx (1/2T)\cosh^{-2}(|\Delta|/2T)$, one obtains

$$\int_{-\infty}^{\infty} d\varepsilon \frac{N_1N_2R_3\varepsilon\tau_\varepsilon}{2N_2|\Delta|\tau_\varepsilon + N_1} f^0_{1,\varepsilon} \approx \frac{|\Delta|}{4T}\ln(8|\Delta|\tau_\varepsilon)\cosh^{-2}\frac{|\Delta|}{2T}. \qquad (13.31)$$

Thus we finally arrive at the expression for the gauge-invariant potential:

$$\mu = \frac{lp_F}{6}\frac{(\mathbf{v}_s\cdot\nabla T)}{T}\frac{|\Delta|}{T(1-Z)\cosh^2\dfrac{|\Delta|}{2T}}\ln(8|\Delta|\tau_\varepsilon), \qquad (13.32)$$

where $l = v_F\tau$ is the electrons' transport mean-free-path and

$$Z = \frac{1}{2}\int_{-\infty}^{\infty} d\varepsilon \frac{N_1^2 f^0_{1,\varepsilon}}{2N_2|\Delta|\tau_\varepsilon + N_1}\, d\varepsilon. \qquad (13.33)$$

Up to the logarithmic factor, expression (13.32) of Schmid and Schön[29] coincides with that derived by Clarke and Tinkham[28] for pure superconductors with a rather different technique. In the vicinity of T_c it follows that $1 - Z \approx \pi\Delta/4T$ and for fixed values of j_s the temperature dependence of $\mu(T)$ is governed by the temperature dependence of $|\mathbf{v}_s|$:

$$\mu(T) \propto |\mathbf{v}_s(T)| = j_s/N_s(T) \propto \lambda_L^2(T) \propto \left[1 - \left(\frac{T}{T_c}\right)^4\right]^{-1} \simeq \frac{1}{4}\left[1 - \left(\frac{T}{T_c}\right)\right]^{-1}. \qquad (13.34)$$

The estimate for μ agrees with the experiment qualitatively and even quantitatively.[38] The typical values of μ (e.g., for tin[32]) are of on the order of 1 nV at temperature gradients ~ 1 Kcm^{-1} and $T/T_c \simeq 0.9$. This problem is a classic example of spatially homogeneous branch imbalance in nonequilibrium superconductors.

13.3.6. Branch Imbalance and Thermopower

We will demonstrate now that the value of thermopower in the presence of an electron-hole population imbalance changes radically. Let us inspect once again expression (13.7). The influence of external factors may destroy the symmetry of excitation distributions above and below the Fermi surface, so the first term in (13.7)

does not vanish. In normal metals in thermodynamic equilibrium, the symmetry between electron- and holelike distribution functions is maintained by the electroneutrality condition. In nonequilibrium situations (e.g., at the junction interface), the symmetry may be broken. This leads to the appearance of the electric potential, which falls off rapidly from the boundary at distances on the order of the Thomas-Fermi screening length (typically 10^{-7}–10^{-8} cm). Such a short scale excludes the possibility of observing branch imbalance in normal metals. The situation is different in superconductors. In this case there is no problem with electroneutrality: the charge created in a system of normal excitations is compensated by the charge of superfluid electrons. (Because of this, even spatially homogeneous branch imbalance states are possible, as we confirmed in the previous section.) Consider now expression (13.7) for **j**, which is valid not only for normal metals, but also for normal components of current in gapless superconductors. For nonequilibrium distribution functions, the first term in (13.7) does not vanish and gives[39]

$$S^{(\text{noneq})} = \frac{1}{eT}\int_0^\infty (n_\varepsilon - n_{-\varepsilon})\, d\varepsilon = -\frac{\mu}{eT}. \tag{13.35}$$

This expression does not contain the parameter T/ε_F (cf. 13.8, 13.10), which usually implies very small values of S for normal metals in thermodynamic equilibrium.

We should draw attention here to the work[40] (see also[41–43]) which extends the earlier arguments by Pethick and Pines. The conclusion is that the value of b_s, and consequently of $S^{(s)}$ (see 13.10) will be strongly enhanced in superconductors with anisotropic gap. The origin of this enhancement is the asymmetry between relaxation times of electrons and holes, which is caused by their scattering on normal (non-magnetic) impurities. In calculations this effect is seen only beyond the first Born approximation (as for the Kondo-mechanism in case of scattering on magnetic impurities mentioned in Sec. 2.1). The increase in S vanishes at $T = T_c$ and $T = 0$, but is expected to be orders of magnitude larger than usual $S^{(s)}$ at intermediate temperatures $0 < T < T_c$. For isotropic gap superconductors the effect is absent in the BCS model, but should exist, though small, for real superconductors with finite values of imaginary part in superconducting density of states (cf. 7.16, 7.19–7.21 at $\gamma \neq 0$). By the best of our knowledge, the Pethick-Pines mechanism has not yet been confirmed experimentally. One of the possible ways is to investigate the "convective" contribution to the thermal conductance in superconductors (see details in Ref. 43).

13.3.7. Thermopower in Optical Pumping

For finite-gap superconductors, more general formulas of Sect. 13.1 should be used and the kinetic equation must be involved to find the functions n for each problem. For instance, in Sect. 8.1, a thin superconducting film under the action of

electromagnetic radiation was considered. Confining ourselves to the case $\omega_0 < 2\Delta$ (here Δ is the modulus of the order parameter), we obtain [in analogy to (8.17)] the expression:

$$n_\varepsilon - n_{-\varepsilon} \approx \frac{\alpha}{\gamma}\frac{\omega_0}{4T}\left(U_{\varepsilon\varepsilon-\omega_0} - U_{\varepsilon+\omega_0\varepsilon}\right)\frac{\varepsilon^2-\Delta^2}{\varepsilon_F\varepsilon}, \tag{13.36}$$

where $U_{\varepsilon\varepsilon-\omega_0}$ and $U_{\varepsilon+\omega_0\varepsilon}$ are given by (5.22), and α/γ is the same as in (5.28). This result must be substituted into the appropriate term of (13.9). Subject to (13.36), after partial integration in (13.9) and keeping only the most important terms, we find in the BCS limit:

$$S^{(\text{noneq})} \approx -\frac{1}{eT}\int_\Delta^\infty (n_\varepsilon - n_{-\varepsilon})\frac{\varepsilon^2}{(\varepsilon^2-\Delta^2)^{3/2}}\,d\varepsilon$$

$$\approx \frac{1}{2\sqrt{2}}\left(\frac{\Delta}{T}\right)^2\frac{\alpha}{\gamma}\frac{\sqrt{\Delta\omega_0}}{\varepsilon_F}\Delta\int_\Delta^\infty \frac{d\varepsilon}{\varepsilon^2-\Delta^2}. \tag{13.37}$$

Thus electromagnetic radiation leads to a nonequilibrium contribution to differential thermopower, which diverges in the BCS approximation. Removing the divergence by introducing the inelastic scattering rate γ, one obtains[44]

$$S^{(\text{noneq})} \simeq \frac{1}{e}\left(\frac{\Delta}{T}\right)^2\frac{\alpha}{\gamma}\frac{\sqrt{\Delta\omega_0}}{\varepsilon_F}\ln\frac{\Delta}{\gamma}. \tag{13.38}$$

The physical essence of (13.38) is rather transparent. When the temperature gradient is applied to the metal (which was initially in equilibrium), the single-particle excitations diffuse from the hot to the cold end. The approximate similarity of the kinetic characteristics of electron- and holelike excitations having charges of opposite sign leads to effective cancellation of their contributions to thermopower. The external electromagnetic perturbation breaks the symmetry between electron and hole populations, increasing the thermopower.

References

1. S.R. De Groot, *Thermodynamics of Irreversible Processes*, pp. 141–162, North-Holland, Amsterdam (1951).
2. D. K. C. MacDonald, *Thermoelectricity: An Introduction to the Principles,* pp. 1–133, Wiley, New York (1962).
3. J. M. Ziman, The theory of residual resistance of copper, *Proc. Roy. Soc. A* **252**, 63–79 (1959).
4. Yu. M. Gal'perin, V. L. Gurevich, and V. I. Kozub, Thermoelectric effects in superconductors, *Sov. Phys. JETP* **39**(4), 680–685 (1974) *[Zh. Eksp. i Teor. Fiz.* **66**[4(10)], 1387–1397 (1974)].

5. C. M. Falco and J. C. Garland, in: *Nonequilibrium Superconductivity, Phonons and Kapitza Boundaries*, K. E. Gray, ed., pp. 521–540, Plenum, New York (1981).
6. V. K. Steiner and P. Grassmann, Eine obere Grenze der Thermokraft zwischen Supraleiten, *Phys. Z.***36**, 527–528 (1935).
7. R. P. Huebener, in *Solid State Physics,* H. Ehrenreich, F. Seitz, and D. Turnbull, eds., Vol. 27, pp. 64–135, Academic Press, New York (1972).
8. D. Shoenberg, *Superconductivity,* pp. 86–94, Cambridge Univ. Press, Cambridge (1952).
9. V. L. Ginzburg, Thermoelectric phenomena in superconductors, *J. Phys. USSR* **8**, 148–158 (1944) *[Zh. Eksp. i Teor. Fiz.* **14**, 177–187 (1944)].
10. V. L. Ginzburg and G. F. Zharkov, Thermoelectric effects in superconductors, *Sov. Phys. Uspekhi* **21**(5), 381–404 (1978) *[Usp. Fiz. Nauk* **125**(5), 19–69 (1978)].
11. Yu. M. Gal'perin, V. L. Gurevich, and V. I. Kozub, Acoustoelectric and thermoelectric effects in superconductors, *JETP Lett.* **17**(12), 476–477 (1973) *[Pis'ma v Zh. Eksp. i Teor. Fiz.* **17**(12), 687–690 (1973)].
12. J. C. Garland and D. J. Van Harlingen, Thermoelectric generation of flux in a bimetallic superconducting ring, *Phys. Lett. A* **47**(5), 423–424 (1974).
13. V. L. Ginzburg, G. F. Zharkov, and A. A. Sobyanin, Thermoelectric phenomena in superconductors and thermomechanical circulation effect in a superfluid liquid, *JETP Lett.* **20**(3), 97–98 (1974) *[Pis'ma Zh. Eksp. Teor. Fiz.* **20**(3), 223–226 (1974)].
14. A. G. Aronov, Yu. M. Gal'perin, V. L. Gurevich, and V. I. Kozub, The Boltzmann-equation description of transport in superconductors, *Adv. Phys.* **30**(4), 539–592 (1981).
15. N. V. Zavaritskii, Observation of superconducting current excited in a superconductor by heat flow, *JETP Lett.* **19**(4), 126–28 (1974) *[Pis'ma Zh. Eksp. i Teor. Fiz.* **19**(4), 205–208 (1974)].
16. C. M. Falco, Thermally induced magnetic flux in a superconducting ring, *Sol. State Comm.* **19**(7) 623–625 (1976).
17. C. M. Pegrum and A. M. Guenault, Thermoelectric flux effects in superconducting bimetallic loops, *Phys. Lett.* A **59**(5), 393–395 (1976).
18. D. J. Van Harlingen, D. F. Heidel, and J. C. Garland, Experimental study of thermoelectricity in superconducting indium, *Phys. Rev.* B **21**(5), 1842–1857 (1980).
19. R. M. Arutyunyan and G. F. Zharkov, Thermoelectric effect in a superconducting torus, *Phys. Lett.* A **96**(9), 480–482 (1983).
20. V. L. Ginzburg and G. F. Zharkov, Thermoelectric effect in hollow superconducting cylinder, *J. Low Temp. Phys.* **92**(1/2) 25–41 (1993).
21. V. I. Kozub, Surface thermoelectric effects in superconductors, Sov. *Phys. JETP* **47**(1), 178–189 (1978) *[Zh. Eksp. i Teor. Fiz.* **74**(1) 344–362 (1978)].
22. S. N. Artemenko and A. F. Volkov, Electric field and collective oscillations in superconductors, *Sov. Phys. Uspekhi* **22**(5) 295–310 (1979) *[Usp. Fiz. Nauk* **128**(5) 3–30 (1979)].
23. D. C. Marinescu and A. W. Overhauser, Thermoelectric flux in superconducting rings, *Phys. Rev. B* **55**(17), 11637–11645 (1997).
24. R. M. Arutyunyan and G. F. Zharkov, Thermoelectric effect in superconductors, *Sov. Phys. JETP* **56**(30), 632–642 (1982) *[Zh. Eksp. i Teor. Fiz.* **83**(9), 1115–1133 (1982)].
25. R. M. Arutyunyan, V. L. Ginzburg, and G. F. Zharkov, Magnetic vortices and thermoelectric effect in a hollow superconducting cylinder, Sov. *Phys. JETP,* **84**(6) 1186–1196 (1997) *[Zh. Eksp. i Teor. Fiz.* **111**(6), 2175–2193 (1997)].
26. C. J. Pethick and H. Smith, Generation of charge imbalance in a superconductor by a temperature gradient, *Phys. Rev. Lett.* **43**(9), 640–642 (1979).
27. J. Clarke, B. R. Fjordboge, and P. E. Lindelof, Supercurrent induced charge imbalance measured in a superconductor in the presence of a thermal gradient, *Phys. Rev. Lett.* **43**(9), 642–644 (1979).
28. J. Clarke and M. Tinkham, Theory of quasiparticle charge imbalance induced in a superconductor by a supercurrent in the presence of a thermal gradient, *Phys. Rev. Lett.* **44**(2), 106–109 (1980).

29. A. Schmid and G. Schön, Generation of branch imbalance by the interaction between supercurrent and thermal gradient, *Phys. Rev. Lett.* **43**(11), 793–795 (1979).
30. J. B. Nielsen, Y. A. Ono, C. J. Pethick, and H. Smith, The effect of impurity scattering on the thermally induced imbalance in a clean superconductor, *Solid. State Commun.* **33**, 925–928 (1980).
31. O. Entin-Wohlman and R. Orbach, Generation of charge imbalance in a superconductor by a thermal gradient, *Phys. Rev. B* **22**(9), 4271–4279 (1980).
32. B. R. Fjordboge, P. E. Lindelof, and J. Clarke, Charge imbalance in superconducting tin films produced by a supercurrent in the presence of temperature gradient, *J. Low Temp. Phys.* **44**(5/6) 535–551 (1981).
33. A. G. Aronov and V. L. Gurevich, Response of a pure superconductor to slowly varying perturbation, *Sov. Phys. Solid State* **16**(9), 1722–1726 (1974) *[Fiz. Tverd. Tela* **16**(9) 2656–2665 (1974)].
34. A. Schmid, in *Nonequilibrium Superconductivity, Phonons and Kapitza Boundaries,* K. E. Gray, ed., pp. 423–480, Plenum, New York (1981).
35. L. Kramer and R. J. Watts-Tobin, Theory of dissipative current-carrying states in superconductors filaments, *Phys. Rev. Lett.* **40**(15), 1041–1044 (1978).
36. G. Schon and V. Ambegaokar, Collective modes and nonequilibrium effects in current-carrying superconductors, *Phys. Rev. B* **19**(7), 3515–3528 (1979).
37. U. Eckern and G. Schön, Relaxation processes in superconductors, *J. Low Temp. Phys.* **32**(5/6), 821–1178(1978).
38. J. Clarke, in *Nonequilibrium Superconductivity, Phonons and Kapitza Boundaries,* K. E. Gray, ed., pp. 353–422, Plenum, New York (1981).
39. N. A. Galoyan and A. M. Gulian, On thermoelectric effect in superconductors at electron-hole branch imbalance, *Supercond.: Phys. Chem. Technol. (SPCT)* **7**(2), 236–239 (1994) *[Sverkhprovodimost' (KIAE)* **7**(2), 237–240 (1994)].
40. B. Arfi, H. Bahlouli, C. J. Pethick, and D. Pines, Unusual transport effects in anisotropic superconductors, *Phys. Rev. Lett.* **61**(21), 2206–2209 (1998).
41. P. J. Hirschfeld, Thermoelectric effect as a test for exotic superconductivity, *Phys. Rev. B* **37**(16), 9331–9335 (1998).
42. B. Arfi, H. Bahlouli, and C. J. Pethick, Transport properties of anisotropic superconductors: influence of arbitrary electron-impurity phase shifts, *Phys. Rev. B* **39**(13), 8959–8983 (1989).
43. V. L. Ginzburg, On heat transfer (heat conduction) and the thermoelectric effect in the superconducting state, *Phys. Uspekhi* **41**(3), 307–311 (1998) *[Usp. Fit Nauk* **168**(3), 363–368 (1998)].
44. N. A. Galoyan and A. M. Gulian, Thermoelectric power of superconductors in conditions of optically induced branch imbalance, *Mod. Phys. Lett.* B **8**(8/9), 509–515 (1994).

14

Vortices and Thermoelectric Flux

14.1. VORTEX ORIGINATION BY A MAGNETIC FIELD

Consider a superconducting half-space in an external magnetic field $\mathbf{H}_e$, parallel to the interface. With $\mathbf{H}_e$ increasing, the vortices originate at the surface (i.e., the filamentlike region inside the superconductor appears, where the order parameter Ψ is suppressed, with a localized magnetic field and circular currents $\mathbf{j}_s$ flowing around this region). A detailed description of the behavior of vortex line structure is possible by using the complete set of nonlinear Ginzburg–Landau equations. However, the solution of this problem is known at present only for the case $x >> \xi(T)$, where x is the distance from the vortex center to the surface and $\xi(T)$ is the coherence length. We will assume $x \geq \xi(T)$ so that the influence of the surface on the order parameter behavior is negligible; if $x < \xi(T)$, only qualitative estimates are possible.

14.1.1. Bean–Livingston Barrier

The existence of a surface barrier impeding penetration of magnetic vortices into Type II superconductors in an external magnetic field was first analyzed by Bean and Livingston[1] and then investigated in many experimental and theoretical works.[2–6] The behavior of a magnetic flux line near the plane surface of a semi-infinite superconductor in an external magnetic field $\mathbf{H}_e$ parallel to the interface has been studied, and, in particular, an expression for the free energy of a superconductor containing a vortex has been obtained with a view to describing a plane surface barrier. (The problem of a surface barrier for circular flux lines in a hollow superconductor with an azimuthal magnetic field applied has also been addressed recently.[7,8]) We will reproduce the main results presented in Refs. 1–6, but first a more general expression will be derived which describes the surface barrier for a hollow superconducting cylinder of finite thickness in an external magnetic field, taking into account the flux quantization effect.

14.1.2. Hollow Superconducting Cylinder

Let us consider a hollow superconducting cylinder (Fig. 14.1) with an inside radius R_1 and an outside radius R_2, the field outside the cylinder being $\mathbf{H}_e$ and the field inside $\mathbf{H}_i$. There is a magnetic flux line inside the superconductor carrying one flux quantum $\boldsymbol{\mu}\phi_0$, where $\phi_0 = hc/2e$ (the vector $\boldsymbol{\mu}$ is aligned with the z-axis; its z-projection assumes the values $\mu = \pm 1$ and 0; and the fields $\mathbf{H}_i$ and $\mathbf{H}_e$ are also parallel to the z-axis). The flux line $\boldsymbol{\mu}\phi_0$ is at distance x from the cavity surface, with a radius R_1. The field $\mathbf{H}_i$ corresponds to m flux quanta (with direction $\mathbf{m}\phi_0$) trapped in the cavity. In order to describe the process of penetration of vortices from the outer to the inner side of the cylinder, we need to find the Gibbs free energy (or thermodynamic potential) of the system given in Fig. 14.1.

We start with the energy conservation law in a superconductor:

$$\Delta\varepsilon = \Delta Q + \frac{c\Delta t}{4\pi}\int_{\sigma_e}[\mathbf{E}\times\mathbf{H}_e]\cdot d\boldsymbol{\sigma} + \frac{c\Delta t}{4\pi}\int_{\sigma_i}[\mathbf{E}\times\mathbf{H}_i]\cdot d\boldsymbol{\sigma} + \frac{c\Delta t}{4\pi}\int_{\sigma_\mu}[\mathbf{E}\times\mathbf{H}_\mu]\cdot d\boldsymbol{\sigma}, \quad (14.1)$$

when the change in the energy during time Δt is due to the heat ΔQ dissipated in the superconductor and electromagnetic energy transmitted through the inside (σ_i) and outside (σ_e) surfaces of the sample. The vortex has a normal core, which is modeled by a void σ_μ with a radius $r_\mu \to 0$ containing one flux quantum $\boldsymbol{\mu}\phi_0$. The field on the vortex axis is denoted by $\mathbf{H}_\mu(0)$. In the limit $r_\mu \to 0$, the field $\mathbf{H}_\mu(0)$ coincides with the magnetic induction $\mathbf{B}_\mu(0)$, i.e., the real field on the vortex axis.

Using formulas like

$$\mathbf{a}\cdot\operatorname{curl}\mathbf{b} - \mathbf{b}\cdot\operatorname{curl}\mathbf{a} + \operatorname{div}[\mathbf{a}\times\mathbf{b}] = 0 \quad (14.2)$$

and the Gauss theorem

$$\int_V \operatorname{div}[\mathbf{F}(\mathbf{r})]d^3\mathbf{r} = \int_S \mathbf{F}(\mathbf{r})\cdot d\mathbf{S}, \quad (14.3)$$

one can replace the surface integrals in Eq. (14.1) by volume integrals. We also use the Maxwell equations

$$\operatorname{curl}\mathbf{E} = -\frac{1}{c}\frac{\partial\mathbf{B}}{\partial t}, \quad \operatorname{curl}\mathbf{H} = 0, \quad (14.4)$$

where $\mathbf{E}$ and $\mathbf{B}$ are the electric and magnetic fields in the superconductor, and $\mathbf{H}$ (i.e., $\mathbf{H}_e$, $\mathbf{H}_i$, and $\mathbf{H}_\mu$) are the unscreened (unlike the magnetic induction $\mathbf{B}$) magnetic fields in a vacuum. The $\mathbf{H}$ fields in Eq. (14.1) are constant on the surface σ, which applies to all cylindrical surfaces whose cross sections are defined by curves of the second order, not just to the circular cylinder shown in Fig. 14.1.

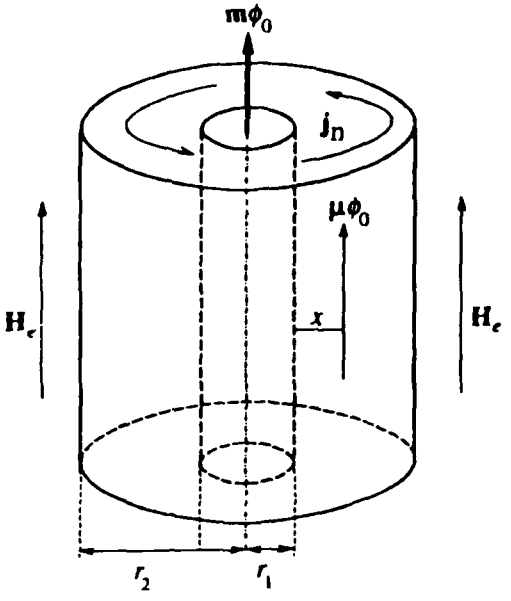

Figure 14.1. Cylinder with radii r_1 and r_2 in the external magnetic field $\mathbf{H}_e$. The internal field is $\mathbf{H}_i = m\phi_0/\pi r_1^2$. The vortex $\mu\phi_0$ is at distance x from the cavity. The thermocurrent $\mathbf{j}_n$ can flow around the inside surface (see Sect. 14.2). We use notations R_1 and R_2 for r_1 and r_2 in the text.

Using the inequality $\Delta Q \le T\Delta S$, where T= const is the sample temperature and S is its entropy, and introducing the superconductor free energy $\mathcal{F}_s = \varepsilon - TS$, we transform Eq. (14.1) to the form $\Delta G \le 0$, where the Gibbs free energy C is expressed by (cf. Refs. 9–11):

$$G = \mathcal{F}_s - \frac{1}{4\pi}\int_V \mathbf{H}_e \cdot \mathbf{B} d^3\mathbf{r} + \frac{H_i^2}{8\pi} V_i. \tag{14.5}$$

Here $V = V_i + V_s$ is the total sample volume, V_i is the interior cavity volume, and V_s is the superconductor volume, while the volume of the normal core of a vortex $V_\mu = 0$. In deriving Eq. (14.5), we have assumed that the external field $\mathbf{H}_e$ is fixed, $\mathbf{H}_e$ = const (i.e., $\partial\mathbf{H}_e/\partial t = 0$), but the field in the cavity is variable (it could depend, for example, on the temperature or on the vortex distance x to the surface; only the number m of trapped magnetic flux quanta in the cavity is fixed, i.e., the magnetic fluxoid is quantized). Thus, any changes in the system lead to a decrease in the Gibbs free energy ($\Delta G \le 0$), provided that T *and* $\mathbf{H}_e$ are maintained constant in time.

The superconductor free energy $\mathcal{F}_s$ is expressed through the standard Ginzburg–Landau functional:

$$\mathcal{F}_s = \mathcal{F}_{n0} + \int_{V_s} \frac{\mathbf{B}^2}{8\pi} d^3\mathbf{r} + \int_{V_s} \left\{ -\alpha|\Psi|^2 + \frac{\beta}{2}|\Psi|^4 + \frac{1}{2m_*} \left| i\hbar\nabla\Psi + \frac{e_*}{c}\mathbf{A}\Psi \right|^2 \right\} d^3\mathbf{r}, \quad (14.6)$$

where $\mathcal{F}_{n0}$ is the free energy of a normal metal in a zero magnetic field; α and β are the temperature-dependent parameters that determine the thermodynamic critical magnetic field of a massive superconductor, $H_c = 4\pi\alpha^2/\beta$; $e_* = 2e$ and $m_* = 2m_e$ are the charge and mass of a Cooper pair; $\Psi = |\Psi|e^{i\theta}$ is the complex order parameter; θ is its phase; and $\mathbf{A}$ is the vector potential of the electromagnetic field.

The variational equation $\delta\mathcal{F}_s/\delta\mathbf{A} = 0$ yields, as usual (cf. Sect. 1.2), the magnetic field in the system:

$$\text{curl}\,\mathbf{B} = \frac{4\pi}{c}\mathbf{j}_s, \quad \mathbf{B} = \text{curl}\,\mathbf{A}, \quad (14.7)$$

$$\mathbf{j}_s = \frac{c}{4\pi\lambda_L^2}\left(\frac{\hbar c}{e_*}\nabla\theta - \mathbf{A}\right), \quad \frac{1}{\lambda_L^2} = \frac{4\pi e_*^2|\Psi|^2}{m_* c^2}. \quad (14.8)$$

The boundary conditions on the inside and outside surfaces of the superconductor are

$$\mathbf{B}|_{\sigma_i} = \mathbf{H}_i, \quad \mathbf{B}|_{\sigma_e} = \mathbf{H}_e, \quad \mathbf{B}|_{\sigma_\mu} = \mathbf{H}_\mu(0), \quad (14.9)$$

where the field $\mathbf{H}_e$ is fixed, and the fields in the cavity, $\mathbf{H}_i$, and on the vortex axis, $\mathbf{H}_\mu(0)$, must be calculated as a function both of the number m of magnetic flux quanta in the cavity and the distance x to the axis of the vortex $\boldsymbol{\mu}$.

14.1.3. General Consideration of Gibbs Free Energy

The system energy is measured with respect to its value in the normal state (when $|\Psi| = 0$). Let us express the Gibbs free energy as $G = G_s + G_n$, where G_n is the free energy of the normal state; in addition, $G_s(|\Psi| = 0) = 0$ and $\mathbf{B}(|\Psi| = 0) = \mathbf{H}_e$. Equation (14.5) can be transformed, using Eqs. (14.6) to (14.8) (see similar calculations in Ref. 11) to

$$G_s = \mathcal{F}_{s0} - \frac{\mathbf{H}_e}{8\pi} \cdot \int_V (\mathbf{B} - \mathbf{H}_e) d^3\mathbf{r} + \frac{\hbar}{2e_*}\int_{V_s} \mathbf{j}_s \cdot \nabla\theta d^3\mathbf{r}, \quad (14.10)$$

$$\mathcal{F}_{s0} = \int_{V_s} \left\{ -\alpha|\Psi|^2 + \frac{\beta}{2}|\Psi|^4 + \frac{\hbar^2}{2m_*}(\nabla|\Psi|)^2 \right\} d^3\mathbf{r}, \quad (14.11)$$

where $\mathcal{F}_{s0}$ corresponds to the condensation energy of the system.

The phase $\theta(\mathbf{r})$ in Eq. (14.10) (unlike that in Ref. 11) has not one but two topological singularities owing to two doubly connected regions, σ_i and σ_μ, shown in Fig. 14.1. In this connection, the phase as a function of a coordinate can be expressed as

$$\theta(\mathbf{r}) = \theta_1(\mathbf{r}_1) + \theta_2(\mathbf{r}_2), \quad \nabla_{\mathbf{r}}\theta = \nabla_{\mathbf{r}_1}\theta_1 + \nabla_{\mathbf{r}_2}\theta_2, \tag{14.12}$$

where $\mathbf{r}$ is the integration point in Eq. (14.10) (we assume that $z = 0$ holds); $\mathbf{r}_1$ is the radius vector connecting the center of the cavity σ_i with the point $\mathbf{r}$; $\mathbf{r}_2$ is the radius vector connecting the vortex center with the point $\mathbf{r}$; θ_1 is the angle at which point $\mathbf{r}$ is seen from the cavity center; and θ_2 is the angle at which this point is seen from the vortex center. The phases in Eq. (14.12) satisfy the following conditions:

$$\oint_{C_1} \nabla\theta_1 \cdot d\mathbf{l} = 2\pi m, \quad \oint_{C_2} \nabla\theta_2 \cdot d\mathbf{l} = 2\pi\mu, \quad \oint_{C_3} \nabla\theta \cdot d\mathbf{l} = 2\pi(m + \mu), \tag{14.13}$$

where m is an integer; $\mu = 0, \pm 1$; C_1 is an arbitrary closed path around the cavity σ_1, but not encircling the vortex σ_μ; C_2 is an arbitrary closed path around the vortex, but not encircling the cavity; and C_3 is a closed path encircling both σ_i and σ_μ.

From $\mathbf{j}_s = (c/4\pi)$ curl $\mathbf{B}$ and the formula curl $\nabla\theta = 0$, which applies to all functions $\theta(\mathbf{r})$ $(\mathbf{r} \neq 0)$, the second integral in Eq. (14.10) can be transformed, using Eqs. (14.2), (14.3), and (14.12), to

$$\frac{\hbar}{2e}\int_{V_s} \mathbf{j}_s \cdot \nabla\theta \, d^3\mathbf{r} =$$

$$\frac{\phi_0}{8\pi} L_z \left\{ \oint_{C_i} [\mathbf{H}_i \times \nabla\theta_1] \cdot d\mathbf{l} + \oint_{C_\mu} [\mathbf{H}_\mu(0) \times \nabla\theta_2] \cdot d\mathbf{l} - \oint_{C_e} [\mathbf{H}_e \times \nabla\theta] \cdot d\mathbf{l} \right\}, \tag{14.14}$$

where L_z is the cylinder height (in what follows, $L_z = 1$); C_i is a closed path on the inside surface σ_i; C_μ is a path encircling the vortex; and C_e is a closed path on the outside cylinder surface.

The field $\mathbf{B}(\mathbf{r})$ in the superconductor, the field $\mathbf{H}_\mu(0)$ on the vortex axis, and the field $\mathbf{H}_i$ in the cavity are functions of the vortex coordinate x. This dependence will be made explicit: $\mathbf{B}(\mathbf{r}, x)$, $\mathbf{H}_\mu(0; x)$, and $\mathbf{H}_i(x)$. As a result, the Gibbs free energy (14.10) is transformed, taking into account Eq. (14.13), to

$$G_s = \mathcal{F}_{s0} - \frac{1}{8\pi}\int_V \mathbf{H}_e \cdot (\mathbf{B}(\mathbf{r}; x) - \mathbf{H}_e) \, d^3\mathbf{r}$$

$$+ \frac{\phi_0}{8\pi} \{ \mathbf{m} \cdot (\mathbf{H}_i(x) - \mathbf{H}_e) + \boldsymbol{\mu} \cdot [\mathbf{H}_\mu(0; x) - \mathbf{H}_e] \}. \tag{14.15}$$

To consider in a unified way all the possibilities of the magnetic flux direction in a vortex $(\mu = 0, \pm 1)$, the number μ in Eq. (14.15) is written formally as a vector $\boldsymbol{\mu}$ that

is directed along the z-axis and that may acquire three values, $0, \pm 1$ (analogously for $\mathbf{m}$ and other vectors).

This equation is universal, since it has been derived from Eqs. (14.1), (14.5), and (14.10) using identities. It is exact if applied to superconductors defined by cylindrical surfaces whose cross sections are second-order curves. Equations (14.1 1) and (14.15) do not demand that $|\Psi(\mathbf{r})| = \text{const}$. If $\boldsymbol{\mu} = 0$ holds, Eq. (14.15) yields the Gibbs free energy of circular[11] and elliptical[12] hollow cylinders, and at $\mathbf{m} = \boldsymbol{\mu} = 0$ it yields the Gibbs free energy of a superconducting plate[9] and of a solid circular cylinder[10] in an external magnetic field $\mathbf{H}_e$.

14.1.4. In-Plate Penetration

The exact equation (14.15) expresses the free energy of a hollow superconductor containing a flux line in terms of the fields $\mathbf{B}(\mathbf{r})$, $\mathbf{H}_i$, and $\mathbf{H}_\mu(0)$. The field $\mathbf{B}(\mathbf{r})$ in the superconductor, the field $\mathbf{H}_i$ in the cavity, and the field $\mathbf{H}_\mu(0)$ on the vortex axis are functions of the vortex position x with respect to the cavity surface. These fields are derived from Eqs. (14.7) and (14.8) with boundary conditions (14.9). This derivation can be done analytically only in the case $|\Psi(\mathbf{r})| = \text{const}$, and this condition is assumed hereafter. This approximation is feasible if the magnetic field is sufficiently weak (the region near the vortex axis is considered separately).

First let us consider an isolated vortex $\boldsymbol{\mu}$ in an infinite superconductor. The field $\mathbf{B}(\boldsymbol{\rho})$ with respect to the vortex axis ($\boldsymbol{\rho} = 0$) is derived from Eq. (14.7) and expressed by the equations [the field around an isolated vortex, $|\mathbf{B}(\boldsymbol{\rho})|$, is denoted by $h(\rho)$[2,3]]

$$h(\rho) = \frac{\phi_0}{2\pi\lambda_L^2} K_0\left(\frac{\rho}{\lambda_L}\right), \quad \frac{dh}{d\rho} = -\frac{\phi_0}{2\pi\lambda_L^3} K_1\left(\frac{\rho}{\lambda_L}\right), \quad \rho \geq \xi, \tag{14.16}$$

where $K_0(y)$ and $K_1(y) = -dK_0/dy$ are modified Bessel functions of the second kind, λ_L is the magnetic field penetration depth, and $\lambda_L^2 = m_* c^2/4\pi e_*^2|\Psi|^2$ (1.59). For $y >> 1$, the function $K_0(y)$ drops exponentially. For $y << 1$, the function $K_0(y)$ has a logarithmic singularity, so Eq. (14.16) does not apply to the field h near the vortex axis ($\rho = 0$).

A more accurate analysis taking into account the equation for the order parameter $|\Psi(\rho)|$ indicates[4,5] that Eq. (14.16) holds for distances down to $\rho \sim \xi$, where ξ is the coherence length, $\lambda_L(T) = \kappa\xi(T)$, and $\kappa >> 1$ is the Ginzburg–Landau parameter for a Type II superconductor. In the range of distances $\rho < \xi(T)$, the amplitude of the order parameter drops; $|\Psi(\rho)| \to 0$ as $\rho \to 0$. As a result, the field $h(0)$ on the vortex axis is finite and equals approximately twice the first critical field H_{c1}, which corresponds to the onset of vortex penetration into the superconductor:

$$h(0) = 2H_{c1} = \frac{\phi_0}{2\pi\lambda_L^2} K_0\left(\frac{1}{\kappa}\right), \quad \left.\frac{dh(\rho)}{d\rho}\right|_{\rho=0} = -\frac{\phi_0}{2\pi\lambda_L^3} K_1\left(\frac{1}{\kappa}\right), \tag{14.17}$$

$$K_0\left(\frac{1}{\kappa}\right) \approx \ln \kappa, \quad K_1\left(\frac{1}{\kappa}\right) \approx \kappa, \quad \kappa >> 1. \tag{14.18}$$

The expression for H_{c1} in Eq. (14.17) holds for $\kappa > 20$, whereas at smaller κ this formula is quite inaccurate.[4] Note that Eq. (14.17) has been derived taking into account the gradient of the order parameter near the vortex axis.[1–6] In the following paragraphs we will use Eq. (14.16) for $\rho \geq \xi$, assuming $\lambda_L = const$ and taking into account Eq. (14.17) for $\rho < \xi$.

The field $\mathbf{B}(\boldsymbol{\rho}; x)$ at some point $\boldsymbol{\rho}$ in a semi-infinite superconductor generated by a vortex at distance x from a plane boundary $x = 0$ is calculated using the mirror-reflection technique as a sum of two solutions of Eq. (14.16) for the vortex $\boldsymbol{\mu}$ at point x and its mirror reflection [the antivortex $(-\boldsymbol{\mu})$] at $(-x)$ with respect to the boundary:

$$\mathbf{B}_\mu(\boldsymbol{\rho}; x) = \boldsymbol{\mu} h(|\boldsymbol{\rho}_1|) - \boldsymbol{\mu} h(|\boldsymbol{\rho}_2|). \tag{14.19}$$

We have added the index μ to the field $\mathbf{B}$ to indicate that this field is generated by the vortex. Here $\boldsymbol{\rho}_1$ is the radius vector connecting the center of the vortex $\boldsymbol{\mu}$ with the observation point $\boldsymbol{\rho}$, and $\boldsymbol{\rho}_2$ is the radius vector connecting the center of the antivortex $(-\boldsymbol{\mu})$ with the observation point $\boldsymbol{\rho}(\boldsymbol{\rho}_2 = 2\mathbf{x} + \boldsymbol{\rho}_1$, where 2x is the vector connecting the centers of the vortex and antivortex and is perpendicular to the superconductor boundary). It may be shown that at any point $\boldsymbol{\rho}$ on the interface between the superconductor and vacuum ($x = 0$) the field satisfies $\mathbf{B}_\mu(\boldsymbol{\rho}; x = 0) = 0$, as follows from Eq. (14.19).

If there is a certain external field $\mathbf{H}_e$ on the interface $x = 0$, an exponentially decaying function $\mathbf{H}_e e^{-x/\lambda_L}$ should be added to Eq. (14.19). In this case, the condition $\mathbf{B}_\mu(0; x) = \mathbf{H}_e$ is satisfied. By setting $\boldsymbol{\rho}_1 = 0$ and $\boldsymbol{\rho}_2 = 2\mathbf{x}$ in Eq. (14.19) (the point $\rho_1 = 0$ is on the vortex axis), we obtain $\mathbf{B}_\mu(0; x)$ at the axis of the vortex at distance x from the interface:

$$\mathbf{B}_\mu(0; x) = \boldsymbol{\mu}[h(0) - h(2x)] + \mathbf{H}_e e^{-x/\lambda_L}. \tag{14.20}$$

For a superconducting plate of a finite thickness d in an external magnetic field $\mathbf{H}_e$, the solution $\mathbf{B}_\mu(0; x)$ is expressed as a sum of repeated mirror reflections from the two interfaces. If $d >> \lambda_L$, one can take into account only the nearest reflections:

$$\mathbf{H}_\mu(0; x) = \boldsymbol{\mu}\{h(0) - h(2x) - h[2(d - x)]\} + \mathbf{H}_e e^{-x/\lambda_L} + \mathbf{H}_e e^{-(d-x)/\lambda_L}. \tag{14.21}$$

[Note that $\mathbf{H}_\mu(0; x) \equiv \mathbf{B}_\mu(0; x)$, since both these functions determine the field on the vortex axis.] The solution (14.21) satisfies Eqs. (14.7) and (14.8), and the boundary conditions

$$\mathbf{H}_\mu(0; x)|_{x=0} = \mathbf{H}_\mu(0; x)|_{x=d} = \mathbf{H}_e; \tag{14.22}$$

moreover, $\mathbf{H}_\mu(0; x)|_{x=d/2} = \boldsymbol{\mu} h(0)$ if $d >> \lambda_L$.

The total magnetic flux $\boldsymbol{\Phi}(x)$ in the system is the sum of two terms:

$$\boldsymbol{\Phi}(x) = \int_S \mathbf{B}(\mathbf{r}; x) \cdot \mathbf{ds} = \boldsymbol{\Phi}_0 + \delta\boldsymbol{\Phi}(x), \quad \boldsymbol{\Phi}_0 = \int_S \mathbf{B}(\mathbf{r}) \cdot \mathbf{ds}, \tag{14.23}$$

where $\boldsymbol{\Phi}_0$ is the flux without a vortex and $\delta\boldsymbol{\Phi}(x)$ is the flux associated with the vortex. The latter decreases as the vortex approaches an interface:

$$\delta\boldsymbol{\Phi}(x) = \boldsymbol{\mu}\phi_0 \left[1 - e^{-x/\lambda_L} - e^{-(d-x)/\lambda_L}\right], \tag{14.24}$$

so the vortex placed on any interface does not contribute to the total flux in a plate, $\delta\boldsymbol{\Phi}(0) = \delta\boldsymbol{\Phi}(d) = 0$ since $d >> \lambda_L$.

The Gibbs free energy of a superconducting plate containing a vortex for $\mathbf{H}_i = \mathbf{H}_e$ (or $m = 0$) is derived from Eq. (14.15):

$$G_s = \mathcal{F}_{s0} - \frac{1}{8\pi}\int_V \mathbf{H}_e \cdot [\mathbf{B}(\mathbf{r}; x) - \mathbf{H}_e]\, d^3\mathbf{r} + \frac{\phi_0}{8\pi}\boldsymbol{\mu} \cdot [\mathbf{H}_\mu(0; x) - \mathbf{H}_e]. \tag{14.25}$$

As a result, we derive from Eq. (14.25), with due account of Eqs. (14.21) and (14.24),

$$G_s = G|_{\mu=0} + \mathcal{G}(x), \quad G|_{\mu=0} = \mathcal{F}_{s0} - \frac{1}{8\pi}\int_V \mathbf{H}_e \cdot [\mathbf{B}(\mathbf{r}) - \mathbf{H}_e]\, d^3\mathbf{r}, \tag{14.26}$$

$$\mathcal{G}(x)/\frac{\phi_0}{8\pi} = \mu^2 \left\{h(0) - h(2x) - h[2(d-x)]\right\} - 2\boldsymbol{\mu} \cdot \mathbf{H}_e \left(1 - e^{-x/\lambda_L} - e^{-(d-x)/\lambda_L}\right), \tag{14.27}$$

where $G|_{\mu=0}$ is the Gibbs free energy of the plate without vortices,[9] and $\mathcal{G}(x)$ is the contribution due to the vortex. Equation (14.26) is a generalization of the result presented in Ref. 1 and 2 for a plate with a finite thickness ($d >> \lambda_L$).

Note that when $x \sim d/2$ and $2H_e = h(0)$, it follows from Eq. (14.26) that $\mathcal{G} = 0$; therefore the equilibrium critical field can be defined as $H_{c1} = h(0)/2$. When $H_e = H_{c1}$ holds, a vortex added to the system does not change the total energy: $\mathcal{G}(x) = 0$ for $d >> \lambda_L$, i.e., the vortex inside the superconductor is in thermodynamic equilibrium.

The behavior of the function $\mathcal{G}(x)$ defined by Eq. (14.26) is illustrated in Fig. 14.2. The surface barrier vanishes when the condition

$$d\mathcal{G}(x)/dx|_{x=0} = 0 \tag{14.28}$$

is fulfilled, from which the threshold field (i.e., the maximum "superheating") is derived using Eqs. (14.16) and (14.17):

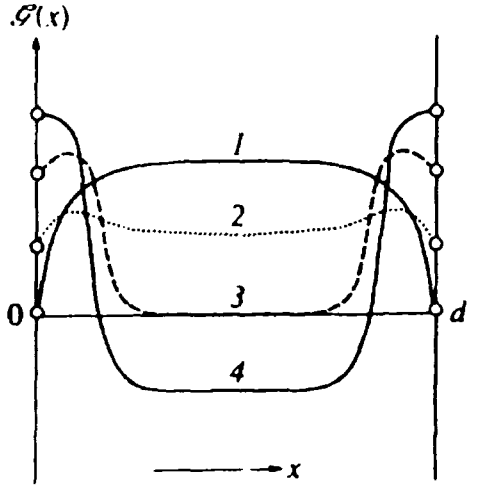

Figure 14.2. The function $\mathcal{G}(x)$ (Eq. 14.26) in different magnetic fields $\mathbf{H}_e$: (1) $\mathbf{H}_e = 0$; (2) $\mathbf{H}_e > 0$; (3) $\mathbf{H}_e = \mathbf{H}_{c1}$; (4) $\mathbf{H}_e = \mathbf{H}_*$.

$$H_* = \frac{\phi_0}{2\pi\lambda_L^2}\kappa = \frac{H_c}{\sqrt{2}}, \tag{14.29}$$

where H_c is the thermodynamic critical field of the superconductor. When $H > H_*$, vortices should move from the interface into the superconductor interior.

14.1.5. Penetration into a Hollow Cylinder

The Gibbs free energy of a hollow cylinder containing a vortex is determined by the general formula (14.15), which requires the total magnetic flux $\mathbf{\Phi}(x)$, the field $\mathbf{H}_i(x)$ in the cavity, and the magnetic field $\mathbf{H}_\mu(0; x)$ on the vortex axis. These parameters are usually determined using the mirror-reflection method, but in the case of a hollow cylinder of arbitrary dimensions it is difficult to find an exact solution like (14.19) because of the surface curvature. In the following paragraphs we consider the case of a circular cylinder characterized by radii R_1 and R_2 with a large cavity radius: $R_1 >> \lambda_L$. This allows us to neglect the effect of the surface curvature and use the formulas for the field generated by a vortex in the case of a plane interface.

When the total magnetic flux is calculated using Eq. (14.23) (the integration is performed over the entire cross section of the sample, including the inner cavity), one should take into account that, unlike the case of Eq. (14.24), the flux associated with a vortex is now

$$\delta\Phi(x) = \mu\phi_0\left[1 - e^{-(d-x)/\lambda_L}\right], \tag{14.30}$$

since only the fraction $\phi_0 e^{-(d-x/\lambda_L)}$ of the flux dissipates into the environment, whereas the other fraction $\phi_0 e^{-x/\lambda_L}$, which also dissipates into the environment in the case of a planar plate, now remains in the inner cavity and contributes to the trapped field.

The field in the cavity $\mathbf{H}_i(x)$ is a sum of the field $\mathbf{H}_{i0}$ in the absence of the vortex and $\delta\,\mathbf{H}_i(x)$ added by the vortex:

$$\mathbf{H}_i(x) = \mathbf{H}_{i0} + \delta\mathbf{H}_i(x), \quad \delta\mathbf{H}_i(x) = \mu\frac{\phi_0}{\pi R_1^2}\, e^{-x/\lambda_L} Z_m. \tag{14.31}$$

The field $\mathbf{H}_{i0}$ corresponds to m flux quanta contained in the cavity and is expressed as follows[11]:

$$\mathbf{H}_{i0} = m\frac{\phi_0}{\pi R_1^2} Z_m + \mathbf{H}_e Z_e, \quad Z_m = \frac{D_0}{D_1}, \quad Z_e = \frac{2}{\rho_1^2 D_1}, \tag{14.32}$$

$$D_0 = K_0(\rho_1)I_0(\rho_2) - I_0(\rho_1)K_0(\rho_2), \quad D_1 = K_2(\rho_1)I_0(\rho_2) - I_2(\rho_1)K_0(\rho_2), \tag{14.33}$$

where $K_n(x)$ and $I_n(x)$ are modified Bessel functions, $\rho_1 = R_1/\lambda_L$, and $\rho_2 = R_2/\lambda_L$. The factors Z_m and Z_e in Eq. (14.32) are functions of temperature and system dimensions, and describe shielding properties of a superconducting cylinder of a finite thickness. In the specific case $[d >> \lambda_L(T), R_1 >> \lambda_L(T)]$, the shielding factor $Z_m \approx 1$ at all realistic temperatures, and the factor Z_e is exponentially small. In the limiting case of a temperature very close to T_c, when $\lambda_L \to \infty$ and $d/\lambda_L \to 0$, the factors $Z_m \to 0$ and $Z_e \to 1$. Thus, the shielding factor Z_m in Eq. (14.32) accounts for the fact that the trapped flux $\Phi_{i0} = \mathbf{H}_{i0}\pi R_1^2 \to 0$ as $\lambda_L \to \infty$, i.e., as the cylinder becomes transparent for a magnetic field, although the number m of trapped flux quanta remains fixed. In this case $\mathbf{H}_i \to \mathbf{H}_e$. We assume that the condition $d >> \lambda_L$ holds, therefore $Z_m = 1$ and $Z_e = 0$.

The additional flux in the system $\delta\Phi(x)$ and the additional field in the cavity $\delta\mathbf{H}_i(x)$ due to the vortex are

$$\delta\Phi(x) = \mu\phi_0\left[1 - e^{-(d-x)/\lambda_L}\right], \quad \delta\mathbf{H}_i(x) = \mu\frac{\phi_0}{\pi R_1^2}\, e^{-x/\lambda_L}, \tag{14.34}$$

respectively.

When using Eq. (14.15), one must know the total flux in the system given by Eq. (14.23), the field $\mathbf{H}_i(x)$ in the cavity given by Eq. (14.31), and the field $\mathbf{H}_\mu(0; x)$ on the vortex axis. Instead of Eq. (14.21), the field on the vortex axis is determined now by the equation [here, as in previous calculations, $\mathbf{H}_\mu(0; x) \equiv \mathbf{B}_\mu(0; x)$]

$$\mathbf{H}_\mu(0; x) = \boldsymbol{\mu}\left\{h(0) - h(2x) - h[2(d-x)]\right\} + \mathbf{H}_i(x)e^{-x/\lambda_L} + \mathbf{H}_e e^{-(d-x)/\lambda_L}. \quad (14.35)$$

Using Eqs. (14.30) to (14.35), let us express the Gibbs free energy (14.15) as $G_s = G(m) + \mathcal{G}(x)$, where $G(m)$ is the system energy in the absence of vortices[11]:

$$G(m) = F_{s0} - \frac{1}{8\pi}\int_V \mathbf{H}_e \cdot (\mathbf{B}(\mathbf{r}) - \mathbf{H}_e)d^3\mathbf{r} + \frac{\phi_0}{8\pi}\mathbf{m} \cdot (\mathbf{H}_{i0} - \mathbf{H}_e), \quad (14.36)$$

and $\mathcal{G}(x)$ is the energy due to the vortex:

$$\mathcal{G}(x)/\frac{\phi_0}{8\pi} = \mu^2\{h(0) - h(2x) - h[2(d-x)]\} - 2\boldsymbol{\mu} \cdot \mathbf{H}_e\left[1 - e^{-(d-x)/\lambda_L}\right]$$

$$+\left(2\boldsymbol{\mu} \cdot \mathbf{m}e^{-x/\lambda_L} + \mu^2 e^{-2x/\lambda_L}\right)\frac{\phi_0}{\pi R_1^2}. \quad (14.37)$$

For $x = d$ we have $\mathcal{G}(d) = 0$, i.e., a vortex placed on the outside surface does not affect the system's energy. If the vortex is placed on the inside surface ($x = 0$), this means, in fact, that the system contains $m + \mu$ quanta in the cavity. Therefore the following condition should hold:

$$G(m) + \mathcal{G}(x)\big|_{x=0} = G(m + \mu), \quad (14.38)$$

where $G(m)$ is the Gibbs free energy of the system without vortices. It can be shown that this condition is satisfied exactly:

$$\mathcal{G}(0) = \frac{\phi_0}{8\pi}\left[-2\boldsymbol{\mu} \cdot \mathbf{H}_e + (2\boldsymbol{\mu} \cdot \mathbf{m} + \mu^2)\frac{\phi_0}{\pi R_1^2}\right] = G(m + \mu) - G(m). \quad (14.39)$$

Note that a vortex placed on the inside surface ($x = 0$) is just a current encircling the cavity and maintaining an additional flux quantum.

The behavior of the function $\mathcal{G}(x)$ given by Eq. (14.37) in the case of a hollow cylinder with a wall thickness d is illustrated by Fig. 14.3a (we consider the case of $\mathbf{H}_e = 0$). The barrier preventing penetration of a vortex from the cavity into the superconductor vanishes when the condition $\mathcal{G}'(0) = \partial\mathcal{G}(x)\partial x|_{x=0} = 0$ is satisfied, i.e., with due account of Eq. (14.17),

$$\mathcal{G}'(0) = \frac{\phi_0}{8\pi^2\lambda_L}\left[\kappa - 2(\boldsymbol{\mu} \cdot \mathbf{m} + \mu^2)\frac{\lambda_L}{R_1^2}\right] = 0, \quad (14.40)$$

for which we determine either the maximum number m_* of flux quanta that can be trapped in the cavity at a given temperature:

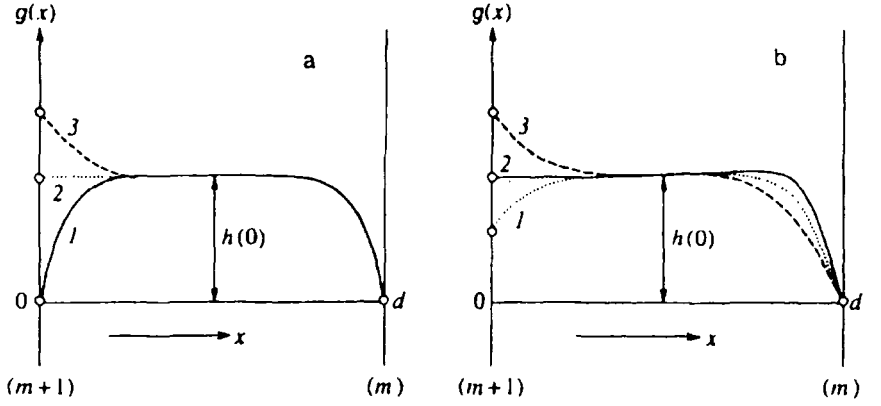

Figure 14.3. The function $g(x) = 8\pi\mathcal{G}(x)/\phi_0$ (Eq. 14.37): (a) at different m ($\mathbf{H}_e = 0$, T = const). Curves $g(x)$ connect the states with the numbers of quanta $m + 1$ and m (the open circles correspond to $x = 0$ and $x = d$). (a) 1, $m = 0$; 2, $m = m_*$; 3, $m > m_*$; (b) at different temperatures T ($\mathbf{H}_e = 0$, $m < m_*$), 1, $T < T_*$; 2, $T = T_*$; 3, $T > T_*$. Here m_* is the maximum number of flux quanta that can be contained in the cavity (Eq. 14.41).

$$m_* = \frac{\kappa}{2}\frac{R_1^2}{\lambda_L^2(T)} - 1, \tag{14.41}$$

or the maximum "overheat" temperature T_* above which a field corresponding to m trapped flux quanta cannot be confined in the cavity:

$$\frac{T_*}{T_c} = 1 - 2\kappa\frac{\xi_0^2}{r_1^2}(\boldsymbol{\mu}\cdot\mathbf{m} + \mu^2). \tag{14.42}$$

At $T > T_*$, a flux quantum should be ejected from the cavity (Fig. 14.3b, curve 3).

14.2. VORTEX ORIGINATION BY THERMOELECTRIC CURRENT

The giant thermoelectric effect observed in hollow bimetallic cylinders[13,14] was investigated previously[15] by solving a model problem of a homogeneous cylinder carrying a normal current $\mathbf{j}_n$ circulating around a cavity to simulate the real thermoelectric current (see Fig. 14.1). We now generalize the formulas of the preceding section to include the thermoelectric current $\mathbf{j}_n$.The energy conservation is expressed in this case (we assume that the external field $\mathbf{H}_e$ is zero) by

$$\Delta\varepsilon = \Delta Q + \frac{c\Delta t}{4\pi}\int_{\sigma_i}[\mathbf{E}\times\mathbf{H}_i]\cdot d\boldsymbol{\sigma} + \frac{c\Delta t}{4\pi}\int_{\sigma_\mu}[\mathbf{E}\times\mathbf{H}_\mu]\cdot d\boldsymbol{\sigma} - \Delta t\int_{V_s}\mathbf{E}\cdot\mathbf{j}_n d^3\mathbf{r}, \tag{14.43}$$

where the last term on the right is the work done by the electric field $\mathbf{E} = -c^{-1}\partial\mathbf{A}/\partial t$ on the given current $\mathbf{j}_n = b\nabla T$. We assume that this current flows in the plane perpendicular to the cylinder axis, $\partial\mathbf{j}_n/\partial t = 0$, $\operatorname{curl}\mathbf{j}_n = 0$, $j_n = Q_0/r$, where $Q_0 = b\Delta T/\pi$. The amplitude of total current around the cavity in the normal state is $I_n = Q_0\ln(R_2/R_1)$, and the related field in the plane $H_n = 4\pi c^{-1}I_n$.

14.2.1. Free Energy Barrier

The Gibbs free energy of the system (provided that $T = \text{const}$ and $\mathbf{j}_n = \text{const}$) is expressed similarly to Eq. (14.5):

$$G = \mathcal{F}_s + \frac{H_i^2}{8\pi}V_i - \frac{1}{c}\int_{V_s}\mathbf{A}\cdot\mathbf{j}_n d^3\mathbf{r}, \tag{14.44}$$

where $\mathcal{F}_s$ is given by Eq. (14.6), and the variation $\delta G/\delta\mathbf{A}$ yields the equation

$$\operatorname{curl}\mathbf{B} = \frac{4\pi}{c}(\mathbf{j}_s + \mathbf{j}_n), \tag{14.45}$$

where $\mathbf{j}_s$ is expressed by Eq. (14.8). Equation (14.44) is easily transformed to a form similar to Eq. (14.10) (recall that $G = G_s + G_n$, $G_s(|\Psi| = 0) = 0$):

$$G_s = \mathcal{F}_{s0} + \frac{\hbar}{2e_*}\int_{V_s}\mathbf{j}_s\cdot\nabla\theta d^3\mathbf{r} - \frac{1}{2c}\int_{V_s}(\mathbf{A} - \mathbf{A}_n)\cdot\mathbf{j}_n d^3\mathbf{r}, \tag{14.46}$$

where $\mathbf{A}_n$ is the vector potential in the normal state, i.e., $\mathbf{A}_n = \mathbf{A}(|\Psi| = 0)$, and, using Eqs. (14.12), (14.13), and (14.45), to the form similar to Eq. (14.15):

$$G_s = \mathcal{F}_{s0} + \frac{\phi_0}{8\pi}\{\mathbf{m}\cdot\mathbf{H}_i(x) + \boldsymbol{\mu}\cdot\mathbf{H}_\mu(0;x)\}$$

$$+ \frac{\phi_0}{4\pi}\mathbf{m}\cdot\mathbf{H}_n - \frac{\phi_0}{4\pi}\boldsymbol{\mu}\cdot\mathbf{H}_n\frac{\mathcal{L}(x)}{\mathcal{L}_0} + \frac{\lambda_L}{4\mathcal{L}_0}\mathbf{H}_n\cdot[\mathbf{H}_i(x) - \mathbf{H}_n], \tag{14.47}$$

where $\mathcal{L}(x) = \ln[R_2/(R_1 + x)]$, $\mathcal{L}_0 = \mathcal{L}(0) = \ln(R_2/R_1)$. Equation (14.47) is exact, but after substituting $\mathbf{H}_i(x)$ and $\mathbf{H}_\mu(0;x)$, one has to use approximate expressions similar to those of the mirror-reflection method.

As a result, we obtain $G_s = G(m) + \mathcal{G}(x)$, where $G(m) \equiv G_s|_{\mu=0}$ is identical to the expression in Ref. 15:

$$G(m) = \mathcal{F}_{s0} + \frac{\phi_0}{8\pi}\mathbf{m}\cdot\mathbf{H}_{i0} - \frac{\phi_0}{4\pi}\mathbf{m}\cdot\mathbf{H}_n + \frac{\lambda_L}{4\mathcal{L}_0}\mathbf{H}_n\cdot(\mathbf{H}_{i0} - \mathbf{H}_n), \tag{14.48}$$

where the field $\mathbf{H}_{i0}$ in the cavity containing m flux quanta is given by[15]

$$\mathbf{H}_{i0} = \mathbf{m}\frac{\phi_0}{\pi R_1^2} Z_m + \mathbf{H}_n Z_{\rm th}, \quad Z_m = \frac{D_0}{D_1}, \quad Z_{\rm th} = \frac{2\lambda_L^2}{R_1^2} Z_m. \tag{14.49}$$

As $\lambda_L \to \infty, Z_{\rm th} \to 1$; for $d >> \lambda_L$ and $r_1 >> \lambda_L$ the shielding factor is $Z_{\rm th} = (2\lambda_L^2/R_1^2)Z_m << Z_m$. By setting $Z_m = 1$ and $Z_{\rm th} = 0$, we obtain

$$\mathbf{H}_i(x) = \mathbf{H}_{i0} + \delta\mathbf{H}_i(x), \quad \delta\mathbf{H}_i(x) = \boldsymbol{\mu}\frac{\phi_0}{\pi R_1^2} e^{-x/\lambda_l}, \tag{14.50}$$

$$\mathbf{H}_\mu(0, x) = \boldsymbol{\mu}\{h(0) - h(2x) - h[2(d-x)]\} + \mathbf{H}_i(x)e^{-x/\lambda_L}. \tag{14.51}$$

The contribution to the Gibbs free energy $\mathcal{G}(x)$ due to the vortex is

$$\mathcal{G}(x)/\frac{\phi_0}{8\pi} = \mu^2\{h(0) - h(2x) - h[2(d-x)]\}$$

$$+ (2\boldsymbol{\mu}\cdot\mathbf{m} + \mu^2 e^{-x/\lambda_L})\frac{\phi_0}{\pi R_1^2} e^{-x/\lambda_L} - 2\boldsymbol{\mu}\cdot\mathbf{H}_n\frac{\mathcal{L}(x)}{\mathcal{L}_0}. \tag{14.52}$$

For $x = d$ we have $\mathcal{G}(d) = 0$, as expected. At $x = 0$ the condition $\mathcal{G}(0) = G(m + \mu) - G(m)$ is satisfied exactly.

The expression for $\mathcal{G}'(0) = \partial\mathcal{G}/(x)\partial x|_{x=0}$ has the form

$$\mathcal{G}'(0) = \frac{\phi_0^2}{8\pi^2\lambda_L^3}\left[\kappa - 2(\boldsymbol{\mu}\cdot\mathbf{m} + \mu^2)\frac{\lambda_L^2}{R_1^2} + 2\boldsymbol{\mu}\cdot\mathbf{H}_n\frac{\pi\lambda_L^3}{\mathcal{L}_0\phi_0 R_1}\right]. \tag{14.53}$$

Comparison with Eq. (14.40) demonstrates that the right-hand side of Eq. (14.53) contains the additional term $\sim \boldsymbol{\mu}\cdot\mathbf{H}_n$, which can be either positive or negative, depending on the direction of current $\mathbf{j}_n$ and field $\mathbf{H}_n$ generated by this current.

The behavior of the Gibbs free energy $\mathcal{G}(x)$ as a function of the thermoelectric current when the cavity contains the largest possible magnetic flux $m_*\phi_0$ (Eq. 14.41) is illustrated by Fig. 14.4. Curve 1 corresponds to the case $j_n = 0$, when $\boldsymbol{\mu}\cdot\mathbf{H}_n = 0$ and the derivative $\mathcal{G}'(0) = 0$ (Eq. 14.40); curves 2 and 3 correspond to $j_n > 0$, when $\boldsymbol{\mu}\cdot\mathbf{H}_n > 0$ and $\mathcal{G}'(0) > 0$; and curve 4 to $j_n < 0$, when $\boldsymbol{\mu}\cdot\mathbf{H}_n < 0$ and $\mathcal{G}'(0) < 0$.

This means that in the presence of a thermoelectric current generating magnetic field $\mathbf{H}_n$ in the same direction as the captured magnetic flux $\mathbf{m}_*\phi_0$ in the cavity (Eq. 14.41), the derivative $\mathcal{G}'(0) > 0$ since $\boldsymbol{\mu}\cdot\mathbf{H}_n > 0$. The force acting on the vortex $F(x) = -\partial\mathcal{G}(x)/\partial x$ is directed toward the cavity at $x = 0$. Thus the thermoelectric current effectively blocks the trapped magnetic flux in the cavity and prevents ejection of magnetic vortices from the superconductor (curve 3 in Fig. 14.4), which would take place at higher temperatures in the absence of the thermoelectric current j_n (Fig. 14.3b).

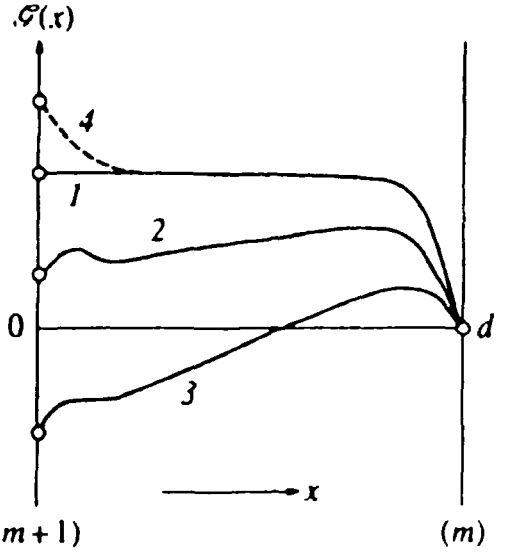

Figure 14.4. Function $\mathcal{G}(x)$ (Eq. 14.52) at different thermocurrents j_n: 1, $j_n = 0$; 2 and 3, $j_n > 0$; 4, $j_n < 0$. Curve 2 has a minimum that disappears at higher j_n (curve 3).

If the current is directed oppositely to $\boldsymbol{\mu} \cdot \mathbf{H}_n < 0$, (curve 4 in Fig. 14.4), then $\mathcal{G}'(0) < 0$, the trapped magnetic flux $m_*\phi_0$ cannot be confined in the cavity; and flux lines should be formed and ejected from the superconductor. Whether this predicted effect really takes place can be determined experimentally.

Note also that the function $\mathcal{G}(x)$ has a minimum at $x \sim (2\text{–}3)\lambda_L$ (curve 2 in Fig. 14.4). This means that a vortex can occupy a metastable position at some distance from the cavity. Here we do not discuss this effect in detail.

14.3. VORTEX–ANTIVORTEX PAIR GENERATION

Now compare the behavior of the vortex and antivortex (i.e., a vortex containing the magnetic flux of the opposite sign) inside a superconductor with a thermoelectric current $\mathbf{j}_n$. It follows from Eqs. (14.52) and (14.53) that $\mathcal{G}(0) < 0$ and $\mathcal{G}'(0) > 0$ in the case of a vortex ($\mu = 1$, $\boldsymbol{\mu} \cdot \mathbf{H}_n > 0$) and in a sufficiently strong thermoelectric field $\mathbf{H}_n$ (curves 3 and 4 in Fig. 14.5a). This means that a force directed toward the cavity acts on a vortex near the inside surface. In the case of an antivortex ($\mu = -1$, $\boldsymbol{\mu} \cdot \mathbf{H}_n < 0$), we have $\mathcal{G}(0) > 0$ and $\mathcal{G}'(0) < 0$, i.e., the driving force is directed from the cavity (curves 3 and 4 in Fig. 14.5b). Thus, if there is a vortex–antivortex couple, its components can be driven apart by thermocurrent $\mathbf{j}_n$

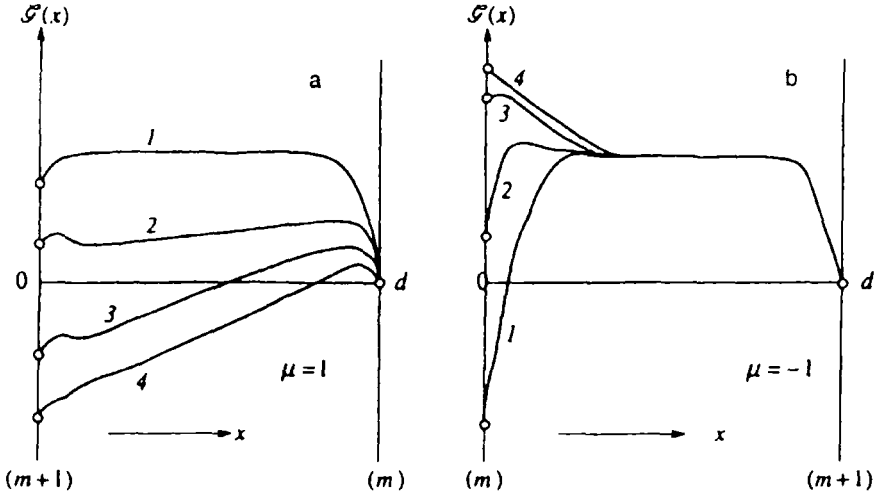

Figure 14.5. Function $\mathcal{G}(x)$ (Eq. 14.52) at different currents j_n in the presence of (a) vortex $\mu = 1$ and (b) antivortex $\mu = -1$. Here $m < m_*$ and 1, $j_n = 0$; 2–4, j_n increases.

under certain conditions. This effect can lead to important consequences, which are discussed in this section.

14.3.1. Two-Vortice Free Energy

Here we calculate the Gibbs free energy when the system shown in Fig. 14.1 contains two vortices, $\boldsymbol{\mu}_1\phi_0$ and $\boldsymbol{\mu}_2\phi_0$, located along the radius at distances x_1 and x_2 from the cavity surface (r_1). Using the same technique as in the preceding section, one easily obtains an exact formula that is a generalization of Eq. (14.47):

$$G_s = \mathcal{F}_{s0} + \frac{\phi_0}{8\pi}\left[\mathbf{m}\cdot\mathbf{H}_i(x_1,x_2) + \boldsymbol{\mu}_1\cdot\mathbf{H}_{\mu_1}(0;x_1,x_2) + \boldsymbol{\mu}_2\cdot\mathbf{H}_{\mu_2}(0;x_1,x_2)\right]$$

$$-\frac{\phi_0}{4\pi}\left[\mathbf{m}\cdot\mathbf{H}_n + \boldsymbol{\mu}_1\cdot\mathbf{H}_n\frac{\mathcal{L}(x_1)}{\mathcal{L}_0} + \boldsymbol{\mu}_2\cdot\mathbf{H}_n\frac{\mathcal{L}(x_2)}{\mathcal{L}_0}\right]$$

$$+\frac{\lambda_L}{4\mathcal{L}_0}\mathbf{H}_n\cdot[\mathbf{H}_i(x_1,x_2) - \mathbf{H}_n]. \qquad (14.54)$$

Magnetic fields on the vortex axes $\boldsymbol{\mu}_1$ and $\boldsymbol{\mu}_2$ are determined using the mirror-reflection technique:

$$\mathbf{H}_{\mu_1}(0;x_1,x_2) = \boldsymbol{\mu}_1 H_{r0} f(x_1) + \boldsymbol{\mu}_2 H_{r0} f(x_1,x_2) + \mathbf{H}_i(x_1,x_2)e^{-x_1/\lambda_L}, \qquad (14.55)$$

$$\mathbf{H}_{\mu_2}(0; x_1, x_2) = \boldsymbol{\mu}_2 H_{c0} f(x_2) + \boldsymbol{\mu}_1 H_{c0} f(x_1, x_2) + \mathbf{H}_i(x_1, x_2) e^{-x_2/\lambda_L}, \quad (14.56)$$

where

$$f(x) = K_0(0) - K_0\left(\frac{2x}{\lambda_L}\right) - K_0\left(\frac{2d-2x}{\lambda_L}\right), \quad (14.57)$$

$$f(x_1, x_2) = K_0\left(\frac{|x_1 - x_2|}{\lambda_L}\right) - K_0\left(\frac{x_1 + x_2}{\lambda_L}\right) - K_0\left(\frac{2d - x_1 - x_2}{\lambda_L}\right). \quad (14.58)$$

The functions $f(x_1)$, $f(x_2)$, and $f(x_1, x_2)$ are introduced to take into account both the intrinsic fields of each vortex and the fields generated by the counterpart vortex, as well as the contributions of the nearest mirror reflections from both interfaces ($x = 0$ and $x = d$). The field around each vortex is described by the Bessel functions $K_0(\rho)$ and $K_1(\rho)$ for $\rho = x/\xi \geq 1$, but at the vortex axis we set $K_0 = \ln \kappa$ and $K_1(0) = \kappa$ in accordance with Eq. (14.17).

For convenience let us write the expressions for all typical fields in the problem:

$$H_{c0} = \frac{\phi_0}{2\pi\lambda_L^2}, \quad H_{c1} = \frac{\phi_0}{4\pi\lambda_L^2} \ln \kappa, \quad H_c = \frac{\phi_0 \kappa}{2\sqrt{2}\,\pi\lambda_L^2}. \quad (14.59)$$

The field inside the cavity is

$$\mathbf{H}_i(x_1, x_2) = \mathbf{H}_{i0} + \delta\mathbf{H}_i(x_1, x_2), \quad (14.60)$$

where $\mathbf{H}_{i0}$ is defined by Eq. (14.32), and the increase in the cavity field due to the vortices $\boldsymbol{\mu}_1$ and $\boldsymbol{\mu}_2$ is

$$\delta\mathbf{H}_i(x_1, x_2) = \boldsymbol{\mu}_1 \frac{\phi_0}{\pi R_1^2} e^{-x_1/\lambda_L} + \boldsymbol{\mu}_2 \frac{\phi_0}{\pi R_2^2} e^{-x_2/\lambda_L} \quad (14.61)$$

(here, as previously, $Z_m = 1$ and $Z_{th} = 0$).

By expressing G_s as $G_s = G(m) + \mathcal{G}(x_1, x_2)$, where $G(m)$ is defined by Eq. (14.48), we obtain an equation for the contribution of the vortices:

$$g(x_1, x_2) = \mathcal{G}(x_1, x_2) / \frac{\phi_0 H_{c0}}{8\pi} = \mu_1^2 f(x_1) + \mu_2^2 f(x_2) + 2\boldsymbol{\mu}_1 \cdot \boldsymbol{\mu}_2 f(x_1, x_2)$$

$$+ 2\frac{\lambda_L^2}{R_1^2}\left[\mu_1^2 e^{-2x_1/\lambda_L} + \mu_2^2 e^{-2x_2/\lambda_L} + 2\boldsymbol{\mu}_1 \cdot \boldsymbol{\mu}_2 e^{-(x_1+x_2)/\lambda_L}\right.$$

$$\left. + 2\boldsymbol{\mu}_1 \cdot \mathbf{m}\ e^{-x_1/\lambda_L} + 2\boldsymbol{\mu}_2 \cdot \mathbf{m}\, e^{-x_2/\lambda_L}\right]$$

$$- a\left[\boldsymbol{\mu}_1 \cdot \mathbf{e}_n \mathcal{L}(x_1) + \boldsymbol{\mu}_2 \cdot \mathbf{e}_n \mathcal{L}(x_2)\right]. \tag{14.62}$$

Here $\mathbf{e}_n = \mathbf{H}_n/H_n$ and $a = 2H_n/\mathcal{L}_0 H_{c0}$.

The free energy (14.62) satisfies the necessary conditions, namely, at $\boldsymbol{\mu}_2 = 0$ the expression for $\mathcal{G}(x_1, x_2)$ coincides with Eq. (14.52), if $\boldsymbol{\mu}_2 = -\boldsymbol{\mu}_1$ (i.e., a vortex and antivortex are contained in the superconductor at the same time), $g(x_1, x_2)|_{x_1 = x_2 = x_0} = 0$ for all $x_0 = x_1 = x_2$. The condition $g(x_0, x_0) = 0$ indicates that nothing happens at this point; that is, the presence of a vortex and antivortex at one point x_0 does not change the system's energy because the fields generated by them cancel out $[(\boldsymbol{\mu}_1 + \boldsymbol{\mu}_2)\phi_0 = 0]$ and therefore do not affect the order parameter of the superconductor. This means that a vortex and antivortex pair can be generated through fluctuations, and this process does not require a supply of energy. But when a vortex and antivortex are being separated, the forces acting on them are directed oppositely. The vortex and antivortex are attracted to each other,[2,3,6] whereas a thermocurrent tends to separate them by driving the vortex to the cavity and the antivortex outside because the two last terms on the right-hand side of Eq. (14.62) have opposite signs for $\boldsymbol{\mu}_2 = -\boldsymbol{\mu}_1$. The function $g(x_1, x_2)$ in Eq. (14.62) reflects the presence of countervailing factors, such as interaction between the vortices and between the vortices and the cavity surface.

14.3.2. Vortex–Antivortex Separation

On analyzing function (14.62), we should determine the point (x_1, x_2) at which the variation $\delta g(x_1, x_2) = 0$, i.e., when the barrier preventing separation of vortices vanishes. One can verify that less energy is needed when a vortex and antivortex pair is generated on the inside surface R_1 (i.e., $x_1 = x_2 = 0$). It is rather obvious that the inside surface is the best place for the beginning of a vortex–antivortex separation since the field $\mathbf{H}_n(x)$ generated by thermocurrent $\mathbf{j}_n$ is largest there and acts on the vortex and antivortex in opposite directions. The resulting antivortex is driven outside and carries away magnetic flux $-\phi_0$, whereas the vortex remains on the cavity surface $(x_1 = 0)$. Thus, if the system previously contained magnetic flux $\Phi_{\text{tot}} = m\phi_0$, where Φ_{tot} is the total magnetic flux inside the circle with radius R_2, then, after the antivortex crosses the outside surface R_2, the system will contain the magnetic flux $\Phi_{\text{tot}} = (m + 1)\,\phi_0$. When the vortex axis crosses the inner boundary R_1, it will transfer all this flux to the inner surface and all its currents will transform to the currents encircling the cavity, i.e., the vortex has turned into an additional current flowing around the cavity. No singularity in the order parameter Φ will remain. The behavior of the function $g(0, x_2)$ at different temperatures is illustrated by Fig. 14.6.

By substituting $\boldsymbol{\mu}_2 = -\boldsymbol{\mu}_1$ and $x_1 = 0$ into Eq. (14.62), we determine the derivative

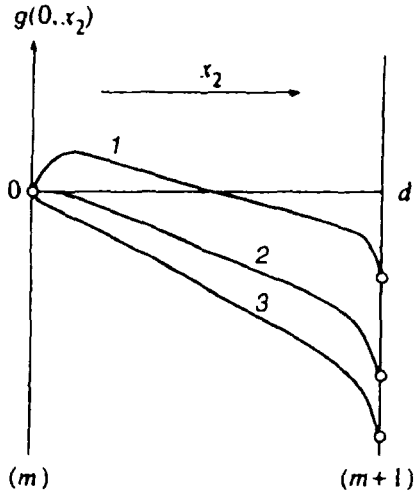

Figure 14.6. The function $g(0, x_2)$ (Eq. 14.62) versus the distance x_2 between the cavity surface and the antivortex at different temperatures: 1, $T < T_*$; 2, $T = T_*$; 3, $T > T_*$. Here T_* is the threshold temperature at which the antivortex is driven from the cavity.

$$g_0' = \left.\frac{\partial g(0, x_2)}{\partial x_2}\right|_{x_2=0} = \frac{2}{\lambda_L}\left[K_1(0) + \frac{2\lambda_L^2}{R_1^2}m - \frac{a}{2}\frac{\lambda_L}{R_1}\right]. \tag{14.63}$$

The parameter a in Eq. (14.46) is a function of temperature and can be expressed in a compact form as

$$a = a_0\frac{t}{1-t}, \quad a_0 = \frac{16\pi}{c}\frac{bT_c\lambda_L^2(0)}{\phi_0}, \quad t = \frac{T-T_1}{T_c-T_1}. \tag{14.64}$$

Here we have used the formulas

$$a = \frac{2H_n}{\mathcal{L}_0 H_{c0}}, \quad H_n = \frac{4\pi}{c}\frac{b\Delta T}{\pi}\mathcal{L}_0, \quad H_{c0} = \frac{\phi_0}{2\pi\lambda_L}, \quad \Delta T = T - T_1, \tag{14.65}$$

$$\lambda_L(T) = \frac{\lambda_L(0)}{1 - T/T_c}, \quad \frac{T-T_1}{T_c} = \left(1 - \frac{T_1}{T_c}\right)t, \quad 1 - \frac{T}{T_c} = \left(1 - \frac{T_1}{T_c}\right)(1-t). \tag{14.66}$$

The reduced temperature t ranges between 0 and 1.

It follows from Eqs. (14.46) and (14.47) that as $T \to T_c$ $(t \to 1)$, the parameter a increases and the condition $g_0' = 0$ can always be satisfied. This condition

determines t_* at which the barrier to separation between the vortex and antivortex vanishes, because at $t = t_*$ the attractive force between the vortex and antivortex equals the force resulting from the thermocurrent driving them apart.

14.3.3. Threshold Temperature of Separation

Taking into account Eq. (14.47), we can write the equation for the threshold temperature t_* as

$$\kappa + 2m\frac{\lambda_1^2}{R_1^2}\frac{1}{1-t} - \frac{a_0}{2}\frac{\lambda_1}{R_1}\frac{t}{(1-t)^{3/2}} = 0, \tag{14.67}$$

where $\lambda_1 = \lambda_1(T = T_1)$. This cubic equation can be solved using the Cardano formulas. In particular, for $m = 0$ we have the temperature of transition from level $m = 0$ to $m = 1$, i.e., the temperature of the first jump in m:

$$t_* = 1 - (A + B), \quad A = \left(\frac{q}{2} + \sqrt{Q}\right)^{1/3}, \quad B = \left(\frac{q}{2} - \sqrt{Q}\right)^{1/3}, \tag{14.68}$$

$$q = \alpha\left(1 - \frac{2}{3}\alpha + \frac{2}{27}\alpha^2\right), \quad Q = \frac{\alpha^2}{4}\left(1 - \frac{4}{27}\alpha\right), \quad \alpha = \left(\frac{a_0}{2\kappa}\frac{\lambda_1}{R_1}\right)^2. \tag{14.69}$$

For $\alpha << 1$ we have $t_* = 1 - \alpha^{1/3}$ or

$$\frac{T_*}{T_c} = 1 - \Delta_1\left(\frac{a_0\lambda_1}{2\kappa R_1}\right)^{2/3}, \quad \Delta_1 = 1 - \frac{T_1}{T_c}. \tag{14.70}$$

The function $m(t)$ can be easily derived from Eq. (14.48) by taking the integral part of m:

$$[m] = \frac{R_1^2}{2\lambda_1^2}\left[\frac{a_0}{2}\frac{\lambda_1}{R_1}\frac{t}{\sqrt{1-t}} - \kappa(1-t)\right], \tag{14.71}$$

i.e., the total magnetic flux in the system $\Phi \equiv \Phi_{tot}(t) = [m]\phi_0$ at point of transitions $m \to m + 1$ has been found as a function of temperature. For the derivative $d\Phi/dt$ we have

$$\frac{d\Phi}{dt} = \phi_0\frac{R_1^2}{2\lambda_L}\left[\frac{a_0}{2}\frac{\lambda_L}{R_1}\left(\frac{1}{\sqrt{1-t}} + \frac{t}{2(1-t)^{3/2}}\right) + \kappa\right]. \tag{14.72}$$

Note that as $t \to 1$, i.e., $T \to T_c$, the asymptotic limit is described by the formula $d\Phi/dt \sim (1-t)^{-3/2} \sim (T_c - T)^{-3/2}$.

14.3.4. Comparison with Experiment and Discussion

As mentioned earlier, Van Harlingen et al.[13,14] discovered that in hollow bimetallic superconducting samples with a temperature gradient, the total magnetic flux was anomalously large—several orders of magnitude higher than theoretical predictions. In fact, Eq. (14.49) indicates that the field in the cavity $\mathbf{H}_i$ is a sum of the field due to the originally trapped magnetic flux $m\phi_0$ and the field $\mathbf{H}_n$ generated by the thermocurrent $\mathbf{j}_n$. In superconductors, the field due to the thermocurrent is suppressed by the factor $Z_{\text{th}} \sim \lambda_L/R_1 d << 1$ in comparison with normal metal, because in a bulk superconductor the normal current and superconducting current cancel each other ($\mathbf{j}_s + \mathbf{j}_n = 0$,),[16] i.e., the Meissner effect occurs (see Ref.17 for details). The resulting magnetic flux should be about $10^{-2}\phi_0$, whereas the measured fluxes[13] were on the order of tens and hundreds of flux quanta ϕ_0. There is no generally accepted interpretation of this "giant" thermoelectric effect. The hypothesis proposed in Ref. 15 and later developed in Refs. 18–23, which suggested that the "giant" effect can be interpreted in terms of jumps in the trapped magnetic flux due to transitions between quantum states with the fluxes $m\phi_0$ and $(m + 1)\phi_0$ induced by the thermocurrent, raised serious objections. Namely, the quantum number m in the hollow superconductor is a topological invariant[24] and can be changed only by introducing an additional vortex $\mu\phi_0$ through the outside sample surface. But if the external field is zero, there exists a barrier to penetration of vortices from the outside interface (Fig. 14.4), and a vortex cannot be generated inside the sample for topological reasons. It was suggested in Ref. 15 on an intuitive basis that there should be some mechanism for increasing the quantum number m without a real transfer of a flux quantum by a vortex, but with the direct generation of additional current around the inner cavity. This hypothesis, however, was not based on solid ground because the corresponding mechanism had not been substantiated. However, the mechanism of a vortex–antivortex pair generation, described in Sect. 14.3, justifies the hypothesis suggested by Arutyunyan and Zharkov[15].

In fact, if a vortex–antivortex pair is generated at some point inside the superconductor, the quantum number m (i.e., the total flux $\Phi_{\text{tot}} = m\phi_0$) of the system does not change, so the topological laws are not violated. If the vortex axis remains on the cavity surface ($x_1 = 0$), the currents associated with the vortex encircle the cavity and contribute to the internal field $\mathbf{H}_i$, i.e., the vortex is converted to a current encircling the cavity. As the antivortex moves away from the cavity surface ($x_2 > 0$), a region with an oppositely directed field is formed near its axis, and $|\Psi| = 0$ holds on its axis x_2. (Note that a detailed description of the field configuration and order parameter near the cavity surface for $x_2 < \xi$ would require detailed calculations of the vortex structure like those discussed in Refs. 4 and 5). As the antivortex moves away from the interface, carrying the negative flux, the field in the cavity gradually increases, which indicates the generation of an additional current encircling the cavity. However, the total magnetic flux in the system remains constant

$\Phi_{tot} = m\phi_0$, and only when the antivortex approaches the outside surface within a distance approximately equal to λ_L and its flux gradually passes to the external space does the total flux become $\Phi_{tot} = (m + 1)\phi_0$. The quantum number m of the system jumps from m to $m + 1$ at the moment when the axis of the antivortex crosses the outside surface (in accordance with topological considerations) and the system would arrive at a state with $(m + 1)\phi_0$ quanta. Thus the proposed mechanism allows the system to transfer to a higher magnetic level through generation of a vortex–antivortex pair and its separation by thermoelectric current. As a result, we have a physical picture that probably describes the "giant" thermoeffect observed experimentally.

Proceeding to a more substantial discussion of experimental results,[14] note that Eq. (14.71) with the total flux in the system $\Phi_{tot} \approx [m]\phi_0$ directly indicates a "giant" effect since the additional flux in the system due to each newborn fluxoid $\mu\phi_0$ is two orders of magnitude higher than the value $\sim 10^{-2}\ \phi_0$ predicted by a simple theory.[17] The total flux measured as a function of temperature[14] is described near T_c by the formula $d\Phi/dt \sim (T_c - T)^{-3/2}$, which is in agreement with Eq. (14.72) for $t \to 1$. For lower t, the right-hand side of Eq. (14.72) is a flatter function of temperature because of the large constant κ. This constant also determines the large height of the barrier for a single vortex introduced in a superconductor in the Bean–Livingston theory.[1] Note, however, that this theory applies only to the case of a superconductor with a mirror-smooth surface (when the mirror-reflection technique can be used). If the surface is rough, the measured threshold field[25] is considerably smaller than the theoretical value,[1] which indicates a smaller contribution of the last term on the right-hand side of Eq. (14.72) and a wider temperature range, in which the law $(T_c - T)^{-3/2}$ holds. Moreover, Fig. 14.5 indicates that the barrier for vortices on the outside surface, where the presence of residual magnetic fields may be important, decreases with increasing j_n (i.e., with the temperature of the hotter junction, $T \to T_c$). Such effects should be also taken into account in comparing the experiment and theory. Note also that the simplified uniform model used above does not allow us to compare quantitatively the calculations of Sect. 14.3 and experimental results[15]; therefore, only qualitative comparison is possible.

First let us estimate the parameter a_0 in Eq. (14.47), which determines the magnitude of the effect. By expressing the coefficient b as α/ρ, where α is the thermoelectric coefficient and ρ is the resistivity, and using published data[26] for the constants α and ρ, we find $a_0 \sim 1$–50 for pure superconductors. Van Harlingen[13] used bimetallic samples of pure In and Pb, but the parameters of the junction (alloy) were not known. This may be an important point, since a vortex–antivortex pair would be generated, most probably in the junction (because it is a weak link in the system) with large κ and λ_L, whereas the thermoelectric current j_n, and hence the parameter a_0, are determined by characteristics of pure bulk superconductors, where κ is usually small. As a result, the choice of the system parameters is somewhat arbitrary. Taking $T_c = 5$ K, $1 - T_1/T_c = 10^{-2}$, $a_0 = 10$, $\kappa = 10$, $R_1 = 0.1$ cm, and $\xi_0 = 10^{-5}$ cm,

we derive from Eq. (14.49) T_* at which the first jump in the total flux occurs, namely $T_*/T_c \simeq 0.99$. An anomalously large flux was detected in experiments[13] at smaller $T_c - T$, but this could have various causes. For example, the samples used in experiments[13] were toroids with rectangular cross sections; therefore the geometric factors affecting the generation of vortices were notably different from the case of an infinite cylinder. Thus, the presence of a sharp angle at the interface of two superconductors may lead to a much smaller effective radius R_1 in Eq. (14.49) and correspondingly diminish T_*/T_c. A smaller κ also produces the same effect and the possibility of vortex generation in Type I superconductors with a small κ cannot be excluded.

The effects of surface roughness and the uncertainty of parameters at the junctions were mentioned earlier. As follows from the analysis reported by Mkrtchyan et al.,[27] the height of the barrier to vortex penetration on an interface between two superconductors with very different λ_L significantly diminishes. Note also that a vortex–antivortex pair can be generated, not in the form of two antiparallel flux lines, but as a closed ring of a finite dimension, like a vortex ring in a superfluid helium,[28,29] which takes less energy (see also Ref. 30). All these factors can have a considerable effect on the height of the barrier to pair formation.

Thus the theory presented have suggested a possible interpretation for the "giant" thermoelectric effect,[13] although additional investigation taking into account real experimental conditions is needed. If the above theory is principally correct, then magnetic hysteresis effects should be observed. Indeed, the vortices are generated when the temperature difference $T_2 - T_1$ increases, thus increasing the number of flux quanta trapped inside the cavity. If the temperature difference diminishes, the number of trapped flux quanta will not change. The experimental search for such a temperature magnetic pump effect seems warranted.

We note in conclusion that the proposed mechanism of magnetic flux generation may be relevant to the problem of the origin of the superhigh magnetic fields around the rotating neutron stars, whose high-density matter may be in a superconducting or superfluid state.[31]

References

1. S. R. Bean and J. D. Livingston, Surface barrier in type-II superconductors, *Phys. Rev. Lett.* **12**(1), 14–16(1964).
2. P. G. De Gennes, *Superconductivity of Metals and Alloys*, pp. 1–280, W.A. Benjamin, New York (1968).
3. M. Tinkham, *Introduction to Superconductivity*, pp. 1–310, McGraw-Hill, New York (1975).
4. D. Saint-James, G. Sarma, and E. Thomas, *Type II Superconductivity*, pp. 1–364, Oxford University Press, Oxford (1969).
5. A. A. Abrikosov, *Fundamentals of the Theory of Metals*, pp. 1–370, North-Holland, Amsterdam (1988).
6. V. V. Shmidt, *Introduction to the Physics of Superconductivity*, pp. 1–238, Nauka, Moscow (1982) (in Russian).

7. E. Altshuler and R. Mulet, Penetration of circular vortices into a superconducting hollow cylinder, *J. Supercond.* **8**(6), 779–780 (1995).
8. Yu. Genenko, Magnetic self-field entry into a current-carrying type-II superconductor, *Phys. Rev. B* **49**(10), 6950–6957(1994).
9. V. L. Ginzburg, Contemporary state of the theory of superconductivity, *Usp. Fiz. Nauk* **48**, 25–118 (1952) (in Russian).
10. V. L. Ginzburg, On the destruction and onset of superconductivity in a magnetic field, *Sov. Phys. JETP*7(1), 78–87 (1958) [*Zh. Eksp. i Teor. Fiz.* **34**[7(10)], 113–125 (1958)].
11. R. M. Arutyunyan and G. F. Zharkov, Penetration of a magnetic field in a thin hollow superconducting cylinder, *Sov. Phys. JETP* **51**(4) 768–774 (1980) [*Zh. Eksp. i Teor. Fiz.* **78**(4), 1530–1541 (1980)].
12. E. A. Demler and G. F. Zharkov, Thermoelectric effect in hollow superconducting elliptical cylinder, *Sverkhprovodimost'(KIAE)* **8**, 276–287 (1995) (in Russian).
13. D. J. Van Harlingen, Thermoelectric effects in superconducting state, *Physica B* **109–110**, 1710–1721 (1982).
14. D. J. Van Harlingen, D. F. Heidel, and J. C. Garland, Experimental study of thermoelectricity in superconducting indium, *Phys. Rev. B* **21**(5), 1842–1857 (1980).
15. R. M. Arutyunyan and G. F. Zharkov, Thermoelectric effect in superconductors, *Sov. Phys. JETP* **56**(3), 632–642 (1982) [*Zh. Eksp. i Teor. Fiz.* **83**[3(9)], 1115–1133 (1982)].
16. V.L.Ginzburg,*Thermoelectric Phenomena in Superconductors,J. Phys. USSR* **8**, 148–156(1944).
17. V. L. Ginzburg and G. F. Zharkov, Thermoelectric effects in superconductors, *Sov. Phys. Uspekhi* **21**(5), 381–404 (1978) [*Usp. Fiz. Nauk* **125** (5), 19–69 (1978)].
18. R. M. Arutyunyan and G. F. Zharkov, Thermoelectric effect in a superconducting torus, *Phys. Lett. A* **96**(9), 480–482(1983).
19. V. L. Ginzburg and G. F. Zharkov, Thermoelectric effect in hollow superconducting cylinders, *J. Low. Temp. Phys.* **92**(1/2), 25–41 (1993).
20. V. L. Ginzburg and G. F. Zharkov, Thermoelectric effects in superconducting state, *Physica C* **235–240**, pp. 3129–3130(1994).
21. E. A. Demler and G. F. Zharkov, Thermoelectric effect in a hollow superconductor in an external magnetic field, *Bull, Lebedev Inst. Phys.* **3–4**, 44–49 (1995) [*Kratk. Soob. po Fiz. FIAN* **3–4**,44–49 (1995)].
22. R. M. Arutyunyan, V. L. Ginzburg, and G. F. Zharkov, Magnetic vortices and thermoelectric effect in hollow superconducting cylinder, *Sov. Phys. JETP* **84**(6), 1186–1196 [*Zh. Eksp. Teor. Fit.* **111**(6), 2175–2193(1997)].
23. R. M. Arutyunyan, V. L. Ginzburg, and G. F. Zharkov, On the "giant" thermoelectric effect in hollow superconducting cylinder, *Sov. Phys. Uspekhi* **63**(4), 435–438 [*Usp. Fiz. Nauk* **167**(4), 457–460(1997)].
24. R. Rajamaran, *Solitons and Instantons. An Introduction to Solitons and Instantons in Quantum Field Theory,* pp. 1–258, North-Holland, Amsterdam (1982).
25. W. Buckel, *Supraleitung Grundlagen und Anwendungen* pp. 1–276, Bergser, Weinheim, (1972) (in German).
26. *Tables of Physical Constants*, I. K. Kikoin, ed., pp. 1–379, Atomizdat, Moscow (1976) (in Russian).
27. G. S. Mkrtchyan, F. R. Shakirzyanova, E. A. Shapoval, and V. V. Shmidt, Interaction between a vortex and the boundary between two superconductors, *Sov. Phys. JETP* **36**(2), 352–353 (1972) [*Zh. Eksp. i Teor. Fiz.* **63**(2), 667–669 (1972)].
28. C. Bauerle, Y. M. Bunkov, S. N. Fisher, H. Godfrin, and G. R. Pickett, Laboratory simulation of cosmic string formation in the early universe using superfluid He-3, *Nature* **382**(6589), 332–334 (1996).
29. V. M. H. Ruutu, V. B. Eltsov, A. J. Gill, T. W. B. Kibble, M. Krusius, Y. G. Makhlin, B. Placais, G. E. Volovik, and W. Xu, Vortex formation in neutron-irradiated superfluid He-3 as an analogue of cosmological defect formation, *Nature* **382**(6589) 334–336 (1996).

30. V. P. Galaiko, Formation of vortex nuclei in superconductors of the second kind, *Sov. Phys. JETP* **23**(5), 878–881 (1966) [*Zh. Eksp. i Teor. Fiz.* **50**[5(11)] 1322 (1966)].
31. A. D. Sedrakian, D. M. Sedrakian, and G. F. Zharkov, Type I superconductivity of protons in neutron stars, *Mon. Not. Roy. Astr. Soc.* **290**(1), 203–207 (1997).

Index